Volcanoes of the Antarctic Plate and Southern Oceans

American Geophysical Union

ANTARCTIC RESEARCH SERIES

Physical Sciences

ANTARCTIC OCEANOLOGY
Joseph L. Reid, *Editor*
ANTARCTIC OCEANOLOGY II: THE AUSTRALIAN-NEW ZEALAND SECTOR
Dennis E. Hayes, *Editor*

ANTARCTIC SNOW AND ICE STUDIES
Malcolm Mellor, *Editor*
ANTARCTIC SNOW AND ICE STUDIES II
A. P. Crary, *Editor*

ANTARCTIC SOILS AND SOIL FORMING PROCESSES
J. C. F. Tedrow, *Editor*
DRY VALLEY DRILLING PROJECT
L. D. McGinnis, *Editor*
GEOLOGICAL INVESTIGATIONS IN NORTHERN VICTORIA LAND
Edmund Stump, *Editor*
GEOLOGY AND PALEONTOLOGY OF THE ANTARCTIC
Jarvis B. Hadley, *Editor*
GEOLOGY OF THE CENTRAL TRANSANTARCTIC MOUNTAINS
Mort D. Turner and John F. Splettstoesser, *Editors*
GEOMAGNETISM AND AERONOMY
A. H. Waynick, *Editor*
METEOROLOGICAL STUDIES AT PLATEAU STATION, ANTARCTICA
Joost A. Businger, *Editor*
OCEANOLOGY OF THE ANTARCTIC CONTINENTAL SHELF
Stanley S. Jacobs, *Editor*
STUDIES IN ANTARCTIC METEOROLOGY
Morton J. Rubin, *Editor*
UPPER ATMOSPHERE RESEARCH IN ANTARCTICA
L. J. Lanzerotti and C.G. Park, *Editors*
THE ROSS ICE SHELF: GLACIOLOGY AND GEOPHYSICS
C. R. Bentley and D. E. Hayes, *Editors*

American Geophysical Union

ANTARCTIC RESEARCH SERIES

Biological and Life Sciences

BIOLOGY OF THE ANTARCTIC SEAS
Milton O. Lee, *Editor*
BIOLOGY OF THE ANTARCTIC SEAS II
George A. Llano, *Editor*
BIOLOGY OF THE ANTARCTIC SEAS III
George A. Llano and Waldo L. Schmitt, *Editors*
BIOLOGY OF THE ANTARCTIC SEAS IV
George A. Llano and I. Eugene Wallen, *Editors*
BIOLOGY OF THE ANTARCTIC SEAS V
David L. Pawson, *Editor*
BIOLOGY OF THE ANTARCTIC SEAS VI
David L. Pawson, *Editor*
BIOLOGY OF THE ANTARCTIC SEAS VII
David L. Pawson, *Editor*
BIOLOGY OF THE ANTARCTIC SEAS VIII
David L. Pawson and Louis S. Kornicker, *Editors*
BIOLOGY OF THE ANTARCTIC SEAS IX
Louis S. Kornicker, *Editor*
BIOLOGY OF THE ANTARCTIC SEAS X
Louis S. Kornicker, *Editor*
BIOLOGY OF THE ANTARCTIC SEAS XI
Louis S. Kornicker, *Editor*
BIOLOGY OF THE ANTARCTIC SEAS XII
David L. Pawson, *Editor*
BIOLOGY OF THE ANTARCTIC SEAS XIII
Louis S. Kornicker, *Editor*
BIOLOGY OF THE ANTARCTIC SEAS XIV
Louis S. Kornicker, *Editor*
BIOLOGY OF THE ANTARCTIC SEAS XV
Louis S. Kornicker, *Editor*
BIOLOGY OF THE ANTARCTIC SEAS XVI
Louis S. Kornicker, *Editor*
BIOLOGY OF THE ANTARCTIC SEAS XVII
Louis S. Kornicker, *Editor*
BIOLOGY OF THE ANTARCTIC SEAS XVIII
Louis S. Kornicker, *Editor*
BIOLOGY OF THE ANTARCTIC SEAS XIX
Louis S. Kornicker, *Editor*

ANTARCTIC TERRESTRIAL BIOLOGY
George A. Llano, *Editor*
TERRESTRIAL BIOLOGY II
Bruce Parker, *Editor*
TERRESTRIAL BIOLOGY III
Bruce Parker, *Editor*

ANTARCTIC ASCIDIACEA
Patricia Kott
ANTARCTIC BIRD STUDIES
Oliver L. Austin, Jr., *Editor*
ANTARCTIC PINNIPEDIA
William Henry Burt, *Editor*
ANTARCTIC CIRRIPEDIA
William A. Newman and Arnold Ross
BIRDS OF THE ANTARCTIC AND SUB-ANTARCTIC
George E. Watson
ENTOMOLOGY OF ANTARCTICA
J. Linsley Gressitt, *Editor*
HUMAN ADAPTABILITY TO ANTARCTIC CONDITIONS
E. K. Eric Gunderson, *Editor*
POLYCHAETA ERRANTIA OF ANTARCTICA
Olga Hartman
POLYCHAETA MYZOSTOMIDAE AND SEDENTIARIA OF ANTARCTICA
Olga Hartman
RECENT ANTARCTIC AND SUBANTARCTIC BRACHIOPODS
Merrill W. Foster

Volume 48

ANTARCTIC
RESEARCH
SERIES

Volcanoes of the Antarctic Plate and Southern Oceans

W.E. LeMasurier and J.W. Thomson, Editors

P.E. Baker, P.R. Kyle, P.D. Rowley, J.L. Smellie, and W.J. Verwoerd, Associate Editors

American Geophysical Union
Washington, D.C.
1990

Volume 48 | ANTARCTIC RESEARCH SERIES

VOLCANOES OF THE ANTARCTIC PLATE AND SOUTHERN OCEANS

W.E. LeMasurier and J.W. Thomson, Editors

P.E. Baker, P.R. Kyle, P.D. Rowley, J.L. Smellie, and W.J. Verwoerd, Associate Editors

Published under the aegis of the
Board of Associate Editors, Antarctic Research Series
Charles R. Bentley, Chairman
Samuel C. Colbeck, David H. Elliot, E. Imre Freidmann,
Dennis E. Hayes, Louis S. Kornicker,
John Meriwether, and Charles R. Stearns

Library of Congress Cataloging in Publication Data

Volcanoes of the Antarctic plate and southern oceans /
editors, W.E. LeMasurier and J.W. Thomson ; associate
editors, P.E. Baker . . . [et al.].

p. cm.—(Antarctic research series ; v. 48)
Includes bibliographical references.
ISBN 0-87590-172-7
1. Volcanoes—Antarctic regions. 2. Volcanoes—South Atlantic Ocean. 3. Volcanoes—South Pacific Ocean. I. LeMasurier, W. E. (Wesley E.) II. Thomson, Janet W. III. Series.
QE538.V65 1989 89-17765
551.2'1'09989—dc20 CIP

ISBN 0-87590-172-7
ISSN 0066-4634

Copyright 1990 by the American Geophysical Union
2000 Florida Avenue, N.W.
Washington, DC 20009

Figures, tables, and short excerpts may be reprinted in scientific books and journals if the source is properly cited.

Authorization to photocopy items for internal or personal use, or the internal or personal use of specific clients, is granted by the American Geophysical Union for libraries and other users registered with the Copyright Clearance Center (CCC) Transactional Reporting Service, provided that the base fee of $1.00 per copy, plus $0.20 per page is paid directly to CCC, 21 Congress St., Salem, MA 01970. 0066-4634/90/$01.00+0.20.

This consent does not extend to other kinds of copying, such as copying for creating new collective works for resale. The reproduction of multiple copies and the use of extracts, including figures and tables, for commercial purposes requires specific permission from AGU.

Published by
American Geophysical Union
With the aid of grant DPP-85-20816 from the
National Science Foundation
May 1990

Printed in the United States of America

CONTRIBUTING AUTHORS

C. J. Adams, Institute of Nuclear Sciences, Department of Scientific and Industrial Research, Wellington, New Zealand

P. E. Baker, University of Nottingham, England

J. Barling, Monash University, Clayton, Victoria, Australia

J. C. Behrendt, U.S. Geological Survey, Denver, Colorado

S. G. Borg, University of California, Berkeley

L. Chevallier, University of Stellenbosch, South Africa

P. J. Ellerman, University of Colorado, Boulder

J. A. Gamble, Victoria University of Wellington, New Zealand

M. J. Hole, British Antarctic Survey, Cambridge, England

Y. Kawachi, University of Otago, Dunedin, New Zealand

K. S. Kellogg, U.S. Geological Survey, Denver, Colorado

P. R. Kyle, New Mexico Institute of Mining and Technology, Socorro

K. E. La Prade, East Texas State University, Commerce

T. S. Laudon, University of Wisconsin, Oshkosh

W. E. LeMasurier, University of Colorado, Denver

W. C. McIntosh, New Mexico Bureau of Mines, Socorro

J. A. Moore, New Mexico Institute of Mining and Technology, Socorro

P. A. Morris, West Australia Department of Mines, Perth, Western Australia

P. Mueller, Bundesanstalt für Geowissenschaften, Hannover, West Germany

M. R. Noll, New Mexico Institute of Mining and Technology, Socorro

J. Nougier, Université d'Avignon, France (now at Conseiller Scientifique auprès Ambassade de France au Canada, Ottawa, Ontario)

J. M. O'Neill, U.S. Geological Survey, Denver, Colorado

D. C. Rex, University of Leeds, England

P. D. Rowley, U.S. Geological Survey, Denver, Colorado

M. Schmidt-Thomé, Bundesanstalt für Geowissenschaften, Hannover, West Germany

M. F. Sheridan, Arizona State University, Tempe

J. L. Smellie, British Antarctic Survey, Cambridge, England

E. Stump, Arizona State University, Tempe

F. Tessensohn, Bundesanstalt für Geowissenschaften, Hannover, West Germany

J. W. Thomson, British Antarctic Survey, Cambridge, England

R. J. Tingey, Bureau of Mineral Resources, Canberra, Australia

R. Varne, University of Tasmania, Hobart, Australia

W. R. Vennum, Sonoma State University, Rohnert Park, California

W. J. Verwoerd, University of Stellenbosch, South Africa

L. Viereck, Hygiene Institut des Ruhrgebiets, Gelsenkirchen, West Germany

F. A. Wade, late of Texas Tech University, Lubbock

A. C. Wright, New Mexico Institute of Mining and Technology, Socorro

G. Wörner, Universität Mainz, West Germany

CONTENTS

The Antarctic Research Series: Statement of Objectives
Board of Associate Editors xv
Preface
W.E. LeMasurier and J.W. Thomson xvii
Late Cenozoic Volcanism on the Antarctic Plate: An Overview
W.E. LeMasurier 1

A. McMURDO VOLCANIC GROUP–WESTERN ROSS EMBAYMENT

Introduction
P.R. Kyle 19

A.I Hallett Volcanic Province
Summary
W.C. McIntosh and P.R. Kyle 26
Individual Volcano Descriptions
A.1 Adare Peninsula
W.C. McIntosh and P.R. Kyle 32
A.2 Hallett Peninsula
W.C. McIntosh and P.R. Kyle 36
A.3 Daniell Peninsula
W.C. McIntosh and P.R. Kyle 40
A.4 Coulman Island
W.C. McIntosh and P.R. Kyle 43
A.5 Possession Islands
W.C. McIntosh and P.R. Kyle 46

A.II Melbourne Volcanic Province
Summary
P.R. Kyle 48
Individual Volcano Descriptions
A.6 Malta Plateau
M. Schmidt-Thomé, P. Mueller, and F. Tessensohn 53
A.7 The Pleiades
P.R. Kyle 60
A.8 Mount Overlord
P.R. Kyle and M.R. Noll 65
A.9 Vulcan Hills
P.R. Kyle 69
A.10 Mount Melbourne
G. Wörner and L. Viereck 72
A.11 Local Suite Basaltic Rocks
P.R. Kyle 79

A.III Erebus Volcanic Province
Summary
P.R. Kyle 81
Individual Volcano Descriptions
A.12 Ross Sea
J.C. Behrendt 89
A.13 Franklin Island
P.J. Ellerman and P.R. Kyle 91
A.14 Beaufort Island
P.J. Ellerman and P.R. Kyle 94
A.15 Mount Bird
A.C. Wright and P.R. Kyle 97
A.16 Mount Terror
A.C. Wright and P.R. Kyle 99
A.17 Mount Erebus
J.A. Moore and P.R. Kyle 103
A.18 Hut Point Peninsula
P.R. Kyle 109
A.19 White Island, Black Island, and Brown Peninsula
A.C. Wright and P.R. Kyle 113
A.20 Minna Bluff
A.C. Wright and P.R. Kyle 117
A.21 Mount Discovery
A.C. Wright and P.R. Kyle 120
A.22 Mount Morning
A.C. Wright and P.R. Kyle 124
A.23 Mason Spur
A.C. Wright and P.R. Kyle 128
A.24 Royal Society Range
A.C. Wright and P.R. Kyle 131
A.25 Taylor and Wright Valleys
A.C. Wright and P.R. Kyle 134

A.IV Southernmost Ross Embayment
Individual Volcano Descriptions
A.26 Sheridan Bluff
E. Stump, S.G. Borg, and M.F. Sheridan 136
A.27 Mount Early
E. Stump, S.G. Borg, and M.F. Sheridan 138
Bibliography 139

B. MARIE BYRD LAND

Summary
W.E. LeMasurier 147
Individual Volcano Descriptions
B.1 Mount Murphy
W.E. LeMasurier, Y. Kawachi, and D.C. Rex 164
B.2 Mount Takahe
W.E. LeMasurier and D.C. Rex 169

B.3 Toney Mountain
W.E. LeMasurier, Y. Kawachi, and D.C. Rex 175
B.4 Crary Mountains
W.E. LeMasurier, Y. Kawachi, and D.C. Rex 180
B.5 Mount Siple
W.E. LeMasurier and D.C. Rex 185
B.6 Mount Hampton
W.E. LeMasurier and Y. Kawachi 189
B.7 Mount Cumming
W.E. LeMasurier and Y. Kawachi 195
B.8 Mount Hartigan
W.E. LeMasurier 199
B.9 Mount Sidley
W.E. LeMasurier 203
B.10 Mount Waesche
W.E. LeMasurier and Y. Kawachi 208
B.11 Mount Flint–Reynolds Ridge
W.E. LeMasurier, Y. Kawachi, and D.C. Rex 212
B.12 Ames Range
W.E. LeMasurier 216
B.13 Mount Bursey
W.E. LeMasurier 221
B.14 Mount Moulton
W.E. LeMasurier and Y. Kawachi 225
B.15 Mount Berlin
W.E. LeMasurier and Y. Kawachi 229
B.16 Satellitic Volcanic Centers 234
B.16A Miocene and Older Centers, Walgreen Coast
W.E. LeMasurier 235
B.16B Miocene-Oligocene Centers, Mount Petras, and Usas Escarpment
W.E. LeMasurier 239
B.16C Miocene-Pliocene Centers, Hobbs Coast
W.E. LeMasurier 244
B.16D Pliocene-Pleistocene Hobbs Coast Volcanoes
W.E. LeMasurier 248
B.16E Fosdick Mountains
W.E. LeMasurier and F.A. Wade 251
Bibliography 253

C. ALEXANDER ISLAND, PALMER LAND, AND ELLSWORTH LAND

Summary
P.D. Rowley, J.W. Thomson, J.L. Smellie, T.S. Laudon, K.E. La Prade, and W.E. LeMasurier 257
Individual Volcano Descriptions
C.1 Rothschild Island
J.W. Thomson, P.D. Rowley, and M.J. Hole 266
C.2 Mount Pinafore–Debussy Heights
M.J. Hole and J.W. Thomson 268
C.3 Hornpipe Heights
M.J. Hole 271
C.4 Beethoven Peninsula
M.J. Hole 273
C.5 Southeastern Alexander Island
P.D. Rowley and J.L. Smellie 277
C.6 Rydberg Peninsula
P.D. Rowley and J.W. Thomson 280
C.7 Snow Nunataks
J.W. Thomson and J.M. O'Neill 283
C.8 Jones Mountains
P.D. Rowley 286
C.9 Hudson Mountains
P.D. Rowley, T.S. Laudon, K.E. La Prade, and W.E. LeMasurier 289
C.10 Henry Nunataks
J.W. Thomson and K.S. Kellogg 294
C.11 Merrick Mountains
P.D. Rowley, W.R. Vennum, and J.L. Smellie 296
Bibliography 299

D. GRAHAM LAND AND SOUTH SHETLAND ISLANDS

Summary
J.L. Smellie 303
Individual Volcano Descriptions
D.1 Bridgeman Island
J.L. Smellie 313
D.2 Deception Island
P.E. Baker 316
D.3 Penguin Island
J.L. Smellie 322
D.4 Melville Peak, King George Island
J.L. Smellie 325
D.5 Kraków Peninsula, King George Island
J.L. Smellie 327
D.6 Northern Livingston and Greenwich Islands
J.L. Smellie 331
D.7 Brabant Island, Anvers Island, and Islands in Southern Bransfield Strait
J.L. Smellie 334
D.8 Paulet Island
J.L. Smellie 337

D.9 Southern Tabarin Peninsula and Islands in Antarctic Sound
J.L. Smellie 339
D.10 Islands in Northern Prince Gustav Channel
J.L. Smellie 342
D.11 Cain and Abel Nunataks, Trinity Peninsula
J.L. Smellie 344
D.12 James Ross Island
J.W. Thomson 345
D.13 Seal Nunataks
J.L. Smellie 349
D.14 Argo Point
J.W. Thomson 352
Bibliography 355

E. SOUTH SANDWICH ISLANDS
Summary
P.E. Baker 361
Individual Volcano Descriptions
E.1 Leskov Island
P.E. Baker 366
E.2 Mount Curry, Zavodovski Island
P.E. Baker 368
E.3 Protector Shoal
P.E. Baker 370
E.4 Mount Hodson, Visokoi Island
P.E. Baker 371
E.5 Vindication Island
P.E. Baker 373
E.6 Candlemas Island
P.E. Baker 376
E.7 Mount Michael, Saunders Island
P.E. Baker 379
E.8 Montagu Island
P.E. Baker 382
E.9 Bristol Island
P.E. Baker 384
E.10 Bellingshausen Island
P.E. Baker 387
E.11 Cook Island
P.E. Baker 390
E.12 Thule Island
P.E. Baker 393
Bibliography 395

F. OCEANIC ISLANDS ON THE ANTARCTIC PLATE
Summary
W.J. Verwoerd, L. Chevallier, and J.W. Thomson 397
Individual Volcano Descriptions
F.1 Bouvetøya
W.J. Verwoerd 405
F.2 Marion Island
W.J. Verwoerd 411
F.3 Prince Edward Island
W.J. Verwoerd 420
F.4 Îles Crozet
J. Nougier and J.W. Thomson 423
F.5 Îles Kerguelen
J. Nougier and J.W. Thomson 429
F.6 Heard and McDonald Islands
J. Barling 435
F.7 Amsterdam and Saint Paul Islands
J. Nougier and J.W. Thomson 442
F.8 Gaussberg
R.J. Tingey 446
F.9 Balleny Islands
A.C. Wright and P.R. Kyle 449
F.10 Scott Island
A.C. Wright and P.R. Kyle 452
F.11 Peter I Island
P.D. Rowley 454
Bibliography 457

G. SUBANTARCTIC VOLCANOES OF THE PACIFIC PLATE
Summary
J.A. Gamble and J.W. Thomson 465
Individual Volcano Descriptions
G.1 Antipodes Islands
J.A. Gamble and C.J. Adams 468
G.2 Auckland Islands
J.A. Gamble and C.J. Adams 470
G.3 Campbell Island
P.A. Morris and J.A. Gamble 474
G.4 Macquarie Island
R. Varne and J.W. Thomson 476
Bibliography 480

INDEX 483

The Antarctic Research Series: STATEMENT OF OBJECTIVES

The Antarctic Research Series, an outgrowth of research done in the Antarctic during the International Geophysical Year, was begun in 1963 with a grant from the National Science Foundation to the American Geophysical Union. It is a book series designed to serve scientists, including graduate students, actively engaged in Antarctic or closely related research, and others versed in the biological or physical sciences. It provides a continuing, authoritative medium for the presentation of extensive and detailed scientific research results from Antarctica, particularly the results of the United States Antarctic Research Program.

Most Antarctic research results are, and will continue to be, published in the standard disciplinary journals. However, the difficulty and expense of conducting experiments in Antarctica make it prudent to publish as fully as possible the methods, data, and results of Antarctic research projects so that the scientific community has maximum opportunity to evaluate these projects and so that full information is permanently and readily available. Thus the coverage of the subjects is expected to be more detailed and extensive than is possible in the journal literature.

The series is designed to complement Antarctic fieldwork, much of which is in cooperative, interdisciplinary projects. The Antarctic Research Series encourages the collection of papers on specific geographic areas within Antarctica (such as the East Antarctic Plateau or the Weddell Sea). In addition, many volumes focus on particular disciplines, including marine biology, oceanology, meteorology, upper atmosphere physics, terrestrial biology, geology, glaciology, human adaptability, engineering, and environmental protection.

Topical volumes in the series are normally devoted to papers in one or two of these areas. Annual volumes, an innovation in 1990 to encourage rapid publication, can contain papers in any discipline. When needed, the series utilizes special formats, such as maps. To reach the most appropriate community, papers approved for the Antarctic Research Series may be published in any of the monographs or serials issued by the American Geophysical Union.

Priorities for publication are set by the Board of Associate Editors. Preference is given to research manuscripts from projects funded by U.S. agencies, long manuscripts, and manuscripts that are not readily publishable elsewhere in journals that reach a suitable reading audience. The series serves to emphasize the U.S. Antarctic Research Program, thus performing much the same function as the more formal expedition reports of most of the other countries with national Antarctic research programs.

The standards of scientific excellence expected for the series are maintained by the review criteria established for the AGU publications program. Each paper is critically reviewed by two or more expert referees. A member of the Board of Associate Editors may serve as editor of a volume, or another appropriate researcher may be appointed. The Board works with the individual editors of each volume and with the AGU staff to assure that the objectives of the series are met, that the best possible papers are presented, and that publication is achieved in a timely manner.

Researchers interested in submitting proposals for volumes or papers for consideration should contact the AGU publication staff at 2000 Florida Avenue, N.W., Washington, D.C. 20009.

BOARD OF ASSOCIATE EDITORS
Antarctic Research Series

2/90

PREFACE

This volume attempts to present both a comprehensive overview of the south polar and subpolar volcanic provinces, and summary data on the status of knowledge of each volcano or volcano group. This broad region, covering roughly 6% of the Earth's surface, is infrequently visited and yet truly international. Its geoscience literature is dispersed in many journals, monographs, symposium volumes, and expedition reports, in many nations, and we hope that this summary will make it more widely available. The preparation of the volume has been a project of the International Association of Volcanology and Chemistry of the Earth's Interior (IAVCEI) through its Working Group on Antarctic Volcanology. It represents a substantial update and expansion of IAVCEI's 1960 *Catalogue of Active Volcanoes* for Antarctica (edited by W.H. Berninghausen and M. Neumann van Padang). The organization and format of the volume, conventions followed, and other items of information are presented below.

Organization. The volume is organized into seven sections covering in a clockwise manner the volcanic provinces of Antarctica and the subantarctic islands. Each section begins with a summary of the region represented and is followed by individual volcano descriptions (IVD's) as numbered subsections. Wherever possible, section coverage was assigned to express petrologic and/or tectonic coherence, and this can readily be seen in most cases. However, the boundary between sections C and D has no clearly defined geologic significance and represents mainly a division of labor and expertise among workers active in this area. All volcanoes that rest on oceanic crust are included in sections E, F, and G, but the plate tectonic setting of each of these sections is different. The continental volcano Gaussberg (see IVD F.8) is included in section F because it lies geographically closer to the volcanoes of the Kerguelen Plateau than to any others, but no petrogenetic relationship is implied.

Format. The IVD format is modeled on the *Catalogue of Active Volcanoes of the World* (CAVW) but is expanded to include more petrologic, chronologic, structural, and historic information than the catalogue. A "date of report" entry is included in the statistics for each IVD because of the long preparation time for the volume. An abbreviated list of references is included with each IVD, with complete reference information given in the section bibliography. The latter is intended to include all the references that the authors could find for each volcano, regardless of whether the reference was cited.

Volcano ages. The age range covered in each section varies, because our intention is to represent the full history of each currently active volcanic province in the Antarctic regions. Thus, among the oceanic islands (section F), the activity of Îles Kerguelen spans the past 39 million years (m.y.) but in the South Sandwich Islands (section E) the oldest exposed rocks date only from 3 million years ago (Ma). The Neogene period embraces all of the alkaline activity in the western Ross Embayment (section A) and nearly all alkaline activity in Marie Byrd Land (section B), while in Graham Land (section D), Neogene time covers the transition from a long period of calc-alkaline magmatism to the alkaline activity of the last 8 m.y. Thus the age range in each section is governed by the rock record, but the Neogene period covers nearly all entries in the volume, and the great majority of volcanic features described are less than 10 m.y. old.

"Activity." The designation of volcanoes in this region as "active," "dormant," or "extinct" is less certain here than for the inhabited and vegetated regions of the Earth, because there is no historical record and no ^{14}C datable material for most volcanoes in the south polar regions. Furthermore, most are remote from commercial shipping lanes and airline routes, and some are remote even from resupply routes to Antarctic field stations. The number of days they have actually been observed may be as few as 10 or 20 days, during a single year or two. In recent years, satellite images have provided indications of possible activity for a few volcanoes (see IVD's B.5,

C.9, and D.2), but these have been difficult to confirm. Rather than attempt new definitions for our specific cases, we have presented the evidence for Holocene activity as objectively as possible in each IVD and in Table I of the overview, which follows, and use the terms "possibly active" or "probably active" where deemed appropriate.

Use of Ma and m.y. Both abbreviations are used in this volume. The North American Stratigraphic Code recommends the use of Ma in reference to a specific date in the geologic past and m.y. as an abbreviation for million years in designating an interval of time or duration of an event. Since this convention is not used outside of North America, it has not been rigorously enforced in this volume out of deference to the many non-American contributors, although some of the latter have adopted it in their contributions.

Documentation. The level of data included in IVD's depends largely on what is available, and it varies greatly from volcano to volcano. The IVD's of the most thoroughly studied volcanoes include representative analyses of major and trace elements, isotopic analyses, microprobe data, modal analyses, and K-Ar ages, but in no case is an IVD intended to present the level of documentation of a journal article. On the other hand, some IVD's include only one or two analyses of major elements. The absence of more data usually means that none are available. Wherever possible, we have included good quality photographs in the IVD's because these are an especially important form of documentation for inaccessible areas.

Classification. At the time when most reports were written, the Le Maitre (1984) version of the International Union of Geological Sciences (IUGS) classification was adopted, and most authors included an alkali versus silica diagram with relevant classification boundaries in their contributions. Subsequently, many made the adjustments to the updated Le Bas et al. (1986) version, but only if it could be done without delaying publication.

Maps. The scale of the region described here has required a hierarchical coverage of its tectonic and geographic features. Thus index maps to all the volcanic regions described in this volume, together with plate boundaries, are presented on the inside front and back covers of the volume. Large tectonic and geographic features within Antarctica are shown in Figures I and VII of the overview, and still smaller scale features are shown on maps that accompany the section summaries and IVD's.

Completeness and originality. A wide range in the extent of knowledge, and in the ratio of original to review material, is represented in the IVD's. Mount Erebus (see IVD A.17) and Deception Island (see IVD D.2), for example, are active volcanoes that have been extensively studied by many scientists from several nations. A continuation of this work, with an ever increasing degree of sophistication, is virtually assured by the close proximity to these volcanoes of several permanent scientific stations. Gaussberg too has been intensively studied. It was mapped in considerable detail in 1901 (see IVD F.8), while the German Imperial Antarctic Expedition was beset in the ice for a year. Later it became the subject of several detailed investigations because of its unique petrologic character. At the other extreme, many volcanoes have been visited only once, with limited opportunity for study. The largest in this category is the Pleistocene-Holocene(?) volcano Mount Siple (see IVD B.5). The "extent of knowledge" section in each IVD serves as a guide to the data and background information that were available for each description.

Many IVD's are original contributions that include previously unpublished maps and analytical data; others are partially or entirely reviews of previously published material. Some IVD's are status reports on work still actively in progress, others are syntheses of larger reports being prepared for publication elsewhere, and still others are compilations of sparse reconnaissance data that have never been published because a return visit to the field area was not possible. There is therefore an unevenness in the amount of detail presented. Nevertheless, the volume offers a comprehensive guide to the volcanoes on the Antarctic plate and on the southern edges of neighboring plates, and it is hoped that it will provide a context and a focus for future studies.

Acknowledgments

The idea of producing an updated and expanded version of the CAVW for Antarctica began with the Working Group on Antarctic Volcanology in the mid 1970s under the leadership of Peter Baker. The subsequent leader (W.E.L.) inherited the project and proposed it to the Antarctic Research Series board in 1978. A great many people have

provided input and support during the intervening years, and it is with some diffidence that we attempt to recall all of them and record our thanks. In more or less chronological order we gratefully acknowledge help and support from the following. First, to IAVCEI for sponsoring the Working Group and its activities, and to Ian Gass, former president of IAVCEI, for his active and constructive involvement with the volume. Charlie Bentley, chairman of the Antarctic Research Series (ARS) board, was instrumental in getting the project off the ground, and David Elliot, a member of the ARS board, provided 9 years of continuous counsel, sound editorial advice, and prompt critical review of the more difficult sections of the volume. W.E.L. thanks the National Science Foundation Division of Polar Programs, and specifically Mort D. Turner, for financial and moral support of this project from its inception. For the opportunity to devote a full year to this project in 1982-1983, W.E.L. is grateful to the University of Colorado for a faculty fellowship and to D.S. Coombs for the hospitality of the Geology Department at the University of Otago, New Zealand. J.W.T. thanks the past and present directors of the British Antarctic Survey (BAS) (R.M. Laws and D.J. Drewry) for their continuing support of her involvement in the project since 1983, and the heads of the Earth Sciences and Geology divisions at BAS (C.W.M. Swithinbank and M.R.A. Thomson, respectively) for their active encouragement and advice. Although they are each individually credited, we (W.E.L. and J.W.T.) must gratefully acknowledge the associate editors for their indispensible role in soliciting, coordinating, and reviewing contributions from scientists in all corners of the globe. Many scientists were invited to contribute but declined because of other commitments; other potential contributors regretfully came to our attention too late to be included. We are very grateful to our panel of external reviewers, J.W. Cole, I.G. Gass, Tom Simkin, and J. Whitford-Stark. Each reviewed the entire volume for consistency and cohesiveness, and each provided a critical scientific review of about one quarter of the volume, for which they are acknowledged in the appropriate sections. The preface and overview were reviewed by each of the above, by all the associate editors, and by Jane Barling, David Elliot, Bill McIntosh, Ian Norton, and Bob Tingey. We regret that we could not adopt all the excellent suggestions that were offered, and we must acknowledge the obvious fact that none of these individuals is responsible for any factual errors, or unevenness of presentation, that remain after their careful and time-consuming efforts.

A number of photographs and diagrams have been reproduced in this volume by courtesy of the original publishers. We would like to express our gratitude to the following for permission to use their material: Australian Academy of Science for Figure F.4.3, reproduced from *Antarctic Earth Science,* edited by R.L. Oliver, P.R. James, and J.B. Jago; Director, British Antarctic Survey for Frontispiece section C, Figures C.2.2, C.3.1, and C.7.2, Frontispiece section D, Figures E.2.1, E.6.1, E.7.2, E.7.3, and E.10.2, reproduced from *British Antarctic Survey Bulletin* number 80 and *British Antarctic Survey Scientific Report* number 91, and the Falkland Islands Dependencies Aerial Survey Expedition photographs reproduced in Figures D.3.2, D.7.2, and D.8.2; Cambridge University Press for Figure A.4.3, reproduced from *Geological Evolution of Antarctica,* edited by M.R.A. Thomson, J.A. Crame, and J.W. Thomson; Geological Society of Australia, Inc., for Figures F.8.2 and F.8.3, reproduced from *Journal of the Geological Society of Australia,* volume 30; National Institute of Polar Research Editorial Board, Japan, for Figures A.17.5 and A.17.6, reproduced from the *Proceedings of the NIPR Symposium on Antarctic Geoscience,* volume 1; Springer-Verlag for Figures B.VI*a* and B.VI*b*, reproduced from *Contributions to Mineralogy and Petrology,* volume 83; University of Wisconsin Press for Figures A.7.1 and F.7.3, reproduced from *Antarctic Geoscience,* edited by C. Craddock; United States Navy for the numerous Trimetragon (TMA) air photographs used in sections A, B, C, and D.

Finally, we gratefully acknowledge the University of Colorado at Denver and the British Antarctic Survey for providing a variety of support services, not the least of which has been a very large bill for postal and telephone services. Patricia Baldwin and Gerry Darr (University of Colorado at Denver) and Gillian Clarke (British Antarctic Survey) devoted enormous blocks of time to typing and word processing, far beyond their normally assigned duties. J.W.T. acknowledges the help of past and present colleagues at BAS, particularly R.W. Burn, A.B. Moyes, and A.D. Saunders for the use of their previously unpublished field notes and chemical analyses, and R.K. Headland for researching early descriptions of some of the historical volcanic eruptions. To our respective spouses (Heather and Mike) we offer our sincere thanks for their patience and moral support throughout the preparation of the volume.

It is no exaggeration to say that the task of producing a volume as comprehensive as this would have been impossible without the cooperation and constructive help of all these contributors, reviewers, and other involved individuals. We hope the reader will be tolerant of the errors that slipped through the cracks, and the differences in style and philosophy of presentation that inevitably result from consensus in a multinational undertaking. We also hope that contributors will forgive the sometimes autocratic manner in which their contributions were molded to form during the final rush to meet a publication deadline.

Wesley E. LeMasurier and Janet W. Thomson

Late Cenozoic Volcanism on the Antarctic Plate:

AN OVERVIEW

W.E. LeMasurier

The Antarctic plate is an unusual part of the world from a tectonic and a climatic point of view, and both characteristics have left an imprint on the products of late Cenozoic volcanism. The plate is encircled by divergent plate boundaries along roughly 95% of its perimeter (see map on the inside front cover) and is broken internally by numerous large rift structures, suggesting a nearly plate-wide extensional tectonic regime. Within this environment the Antarctic plate has evolved into one of the great alkaline volcanic regions of the world, with major alkaline provinces located in several places on the continent as well as in the surrounding ocean basins. Basaltic rocks are dominant among nearly all these provinces, but a highly diverse array of felsic rocks are found in Marie Byrd Land, the western Ross Embayment, and Îles Kerguelen. The only subduction-related volcanoes of Neogene age within or bordering the plate are found in the South Sandwich and South Shetland Islands (see map on the inside front cover). Thus the circum-Pacific "rim of fire" changes its character significantly along its Antarctic sector.

The imprint of climate on the products of volcanism derives from the fact that Antarctica has been covered by a continental ice sheet for most of the last 30 m.y. [*Barrett et al.*, 1989], and many of the surrounding oceanic islands support large permanent ice caps. As a result, hydroclastic rocks are perhaps more abundant and widespread in Antarctic volcanoes than in any other subaerial volcanic environment in the world. From this writer's point of view, the abundances of alkaline rocks and of hydrocalstic rocks are the first-order characteristics of Antarctic volcanism.

We are still in the age of discovery where Antarctic volcanoes are concerned. The subantarctic islands and some coastal volcanoes were discovered by sealers, whalers, and explorers in the mid-1800s (see, for example, section A frontispiece and Figure F.9.2). The inland volcanoes and those along the more ice-bound coasts were discovered in the 1930s, by the Byrd expeditions, and in the mid-1950s, during activities related to the International Geophysical Year. The Ross Sea submarine volcanoes (see

Copyright American Geophysical Union

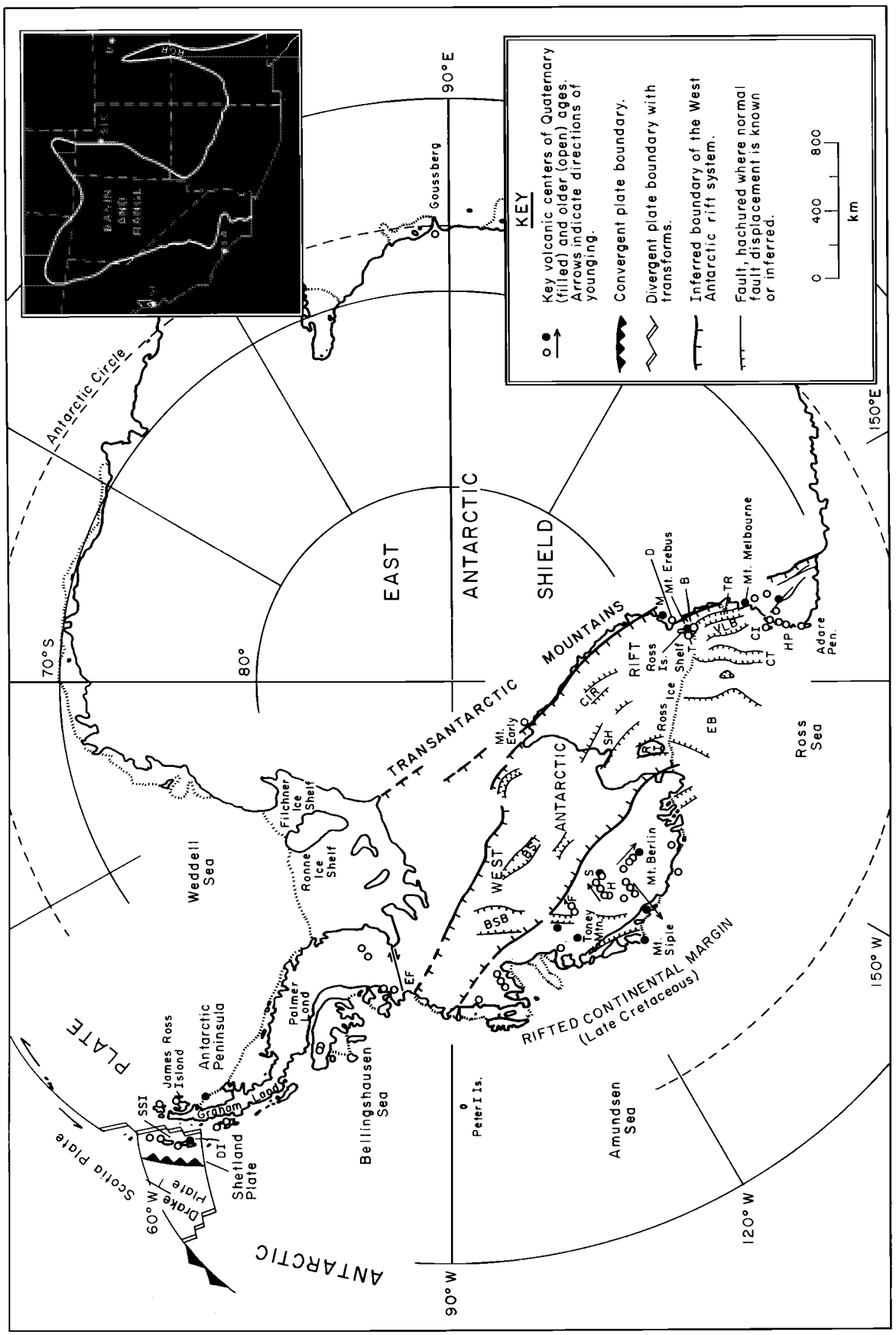

Copyright American Geophysical Union

individual volcano description A.12) were discovered in 1984, barely in time to be included in this volume, and there are likely to be many other volcanoes concealed beneath the ice sheet that will eventually be discovered by geophysical surveys. This should be kept in mind as an important qualifier to the generalizations that follow.

This overview is based as much as possible on contributions within the volume. The intention is to provide a review of the major volcanic features and to guide the reader to specific sections within the volume for more detailed information and a full set of references. Places named in the following paragraphs can be found on the inside front cover (IFC) and inside back cover (IBC) maps and in Figure I.

Physical Volcanology

Distribution. More than 100 volcanoes are described in this volume. There are 95 individual volcano descriptions (IVD's), but many of these describe two, three, or four closely coalesced large volcanoes, and a few others group as many as 50 small monogenetic vents into one IVD. In all, 69 IVD's (in sections A–D and IVD F.8) describe volcanoes on the Antarctic continent, three more (see IVD's G.1–G.3) describe volcanoes on the New Zealand–Campbell Plateau continental block, and 23 IVD's (in sections E and F and IVD G.4) describe volcanoes that rest on oceanic crust (see IFC map). Among the latter, all of the South Sandwich Islands (12 IVD's) are convergent plate margin volcanoes, and Macquarie Island (see IVD G.4) includes the obducted volcanic and plutonic portions of an ophiolite complex at a plate boundary. All the Indian Ocean and South Pacific oceanic islands described in section F (10 IVD's) are alkaline intraplate volcanoes. The Antipodes, Auckland, and Campbell Island volcanoes (see IVD's G.1-G.3) lie on the Campbell Plateau, which is underlain by continental crust that was part of West Antarctica in pre-Cenozoic time.

Size. The sizes of Antarctic volcanoes and volcanic provinces are often difficult to appreciate because of the remoteness of these regions and their gross distortion on most world maps. The West Antarctic rift system, described below, is about 3200 km long and 800 km wide, fully comparable in scale with the East African rift from the Red Sea to Mozambique, or with the Basin and Range from the Snake River plain (United States) to well south of Sonora (Mexico). Figure I includes an inset of the Basin and Range province at the same scale as the map of Antarctica to provide a familiar frame of reference.

The largest of the well-exposed Antarctic volcanoes are Mount Erebus (3795 m), at the southwest extremity of the Ross Sea, and Mount Siple (3110 m), on the coast of Marie Byrd Land (IBC map). Each has an exposed volume of about 1800 km^3 and more than 3000 m of relief. Mount Sidley (4181 m), in Marie Byrd Land (see Figure I and section B frontispiece), is the highest volcano in Antarctica. However, it rises above an ice sheet level of 2000 m elevation, and its base could lie anywhere from a few tens to a few thousands of meters beneath the ice sheet. For example, the base of Toney Mountain (3595 m) is known from seismic data to lie about 2500 m below

Fig. I. (opposite) Interpretive map of Cenozoic volcanic and tectonic features of Antarctica showing the relationship of key volcanic centers to present-day plate boundaries and to the West Antarctic rift system. Abbreviations for volcanic localities are as follows. For the western Ross Sea region: HP, Hallett Peninsula; CI, Coulman Island; M, Mount Morning; D, Mount Discovery; B, Mount Bird; and T, Mount Terror. For Marie Byrd Land: S, Mount Sidley; H, Mount Hampton; and F, Mount Frakes. For the northern Antarctic Peninsula: SSI, South Shetland Islands; and DI, Deception Island. No attempt is made to represent relative sizes of volcanoes. The boundaries of the rift are inferred on the basis of subglacial topography (Figure VI), loci of crustal thinning [*Bentley*, 1973], distribution of isostatic gravity anomalies [*Bentley and Robertson*, 1982], and the positions of flanking volcanic fields. See text for discussion. Individual fault-bounded basins in the Ross Sea are well defined by multichannel seismic data [*Behrendt et al.*, 1987; *Cooper et al.*, 1987]; similar basins shown here under ice-covered regions are interpreted from the detailed subglacial topography of *Drewry* [1982]. Abbreviations for fault-related features are as follows, in clockwise order from 150°E longitude: TR, Terror rift; VLB, Victoria Land Basin; CT, Central Trough; EB, Eastern Basin; CIR, "Crary Ice Rise"; SH, "Steers Head"; RI, Roosevelt Island; BST, Bentley Subglacial Trench; BSB, Byrd Subglacial Basin; and EF, Ellsworth fault. Inset shows the Basin and Range province and Rio Grande rift (RGR), western United States, at the same scale as the map of Antarctica; boundary is from *Eaton* [1979]. Abbreviations for cities are as follows: SF, San Francisco; LA, Los Angeles; SLC, Salt Lake City; and D, Denver.

Copyright American Geophysical Union

sea level (see IVD B.3). A total of 10 volcanoes in Marie Byrd Land have summit elevations above 3000 m (see Table B.I), and in the western Ross Embayment, Mount Terror (3230 m), Mount Melbourne (2732 m), Mount Morning (2723 m), and Mount Discovery (2681 m) are the next highest volcanoes after Mount Erebus (Figure I). James Ross Island (1470 m) and Deception Island (542 m) shield volcanoes, at the northern tip of the Antarctic Peninsula (Figure I), have submerged base diameters of at least 60 km and 30 km, respectively, and are as large in terms of rock volume as some of the higher and steeper felsic volcanoes.

Among the oceanic islands, Big Ben volcano (2745 m), on Heard Island (see ICF map), is the highest of the Indian Ocean volcanoes, and Peter I Island (1640 m) is highest among the Pacific subantarctic volcanoes. The South Sandwich Islands are all less than about 1000 m in elevation, but each has between 1500 and 2000 m of submerged relief and a base diameter of 20–30 km.

Structure. The larger Antarctic volcanoes are either basaltic shield volcanoes or shield-like volcanoes of felsic and intermediate compositions. They are composed of flow rock, a variety of agglutinates, and variable proportions of hydroclastic deposits, but most contain only minor amounts of magmatic ash. Some good examples of large, predominantly basaltic shield volcanoes are found on Campbell and Auckland Islands (see IVD's G.3 and G.2) and Heard Island (IVD F.6), all in the ocean basins (see IFC map), and at James Ross Island (IVD D.12), Mount Murphy (IVD B.1), Mount Siple (?) (IVD B.5), Mount Bird (IVD A.15), and Mount Terror (IVD A.16), all on the continent (Figure I). The large shield volcanoes north and south of Hallett Peninsula (see IVD's A.1–A.4) also appear to be predominantly basalt, with felsic rocks occurring mainly in near-vent areas. Large trachytic and phonolitic volcanoes like Mount Melbourne (IVD A.10), Mount Erebus (IVD A.17), Mount Takahe (IVD B.2), Mount Sidley (IVD B.9), and Mount Berlin (IVD B.15) are described as stratovolcanoes, composite cones, and shield volcanoes, depending on the preference of the writer, but in few cases are they as ash rich as typical stratovolcanoes. Small-scale felsic pyroclastic flow deposits are described from a few of the western Ross Sea volcanoes (e.g., Mount Melbourne, IVD A.10) and from Deception Island (IVD D.2), but Antarctic volcanoes are notable for their lack of large-volume magmatic ash deposits.

The most common pyroclastic rocks (in the broad sense adopted by *Fisher and Schmincke* [1984]) in Antarctic volcanoes appear to be hyaloclastites, autobrecciated lava flows, and agglutinates. Hyaloclastite, sometimes associated with pillow lava, occurs in the basal sections of some large shield volcanoes (e.g., Mount Murphy, IVD B.1; Mount Takahe, IVD B.2; and James Ross Island, IVD D.12) and is the major constituent of tuff cones and table mountains (e.g., Shield Nunatak, IVD A.10; Sheridan Bluff, IVD A.26; Shepard Island and Cruzen Island, IVD B.16D; and Jones Mountains, IVD C.8). These hydroclastic features are found all along the Pacific coast and as far inland as Mount Early (IVD A.27), the southernmost volcano known in the world (Figure I). Field studies and K-Ar dating of these rocks have led to interpretations of glacial history in a large number of volcanic localities in Antarctica. A good example of the scale and complexity of these deposits can be seen by comparing a coastal example, James Ross Island (Figure D.12.2) with one that is 150 km inland, Mount Takahe (Figure B.2.3). Both photographs show large-scale volcanogenic structures that record the transition from a subaerial to an intraglacial environment, but at James Ross Island the plane of transition is horizontal, while at Mount Takahe it is nearly vertical. In the former case the transition is believed to represent a static water level, closely controlled by sea level (see IVD D.12) [*Jones and Nelson*, 1970], while the Mount Takahe transition has apparently been controlled by ice contact in an environment of rapid subglacial drainage that is about 2000 m above sea level (see Figure B.2.3). Many additional occurrences of hydroclastic deposits are described throughout the volume.

Reasons for the apparent absence of large continental ash flow fields in Antarctica are largely a matter of speculation. Assuming that none are concealed beneath the ice sheet, this may be a reflection of generally low magmatic volatile contents and an absence of large-scale crustal melting. The latter is consistent with the small volume of felsic rocks in Antarctica and the lack of geochemical evidence for large-scale crustal involvement in their origin. The scarcity of pyroclastic flow deposits is a notable difference from volcanism in comparable tectonomagmatic settings such as the Rio Grande and

Copyright American Geophysical Union

East African rifts, where large ash flow fields are well known.

Alkaline flood basalts are reported from Îles Kerguelen (see IVD F.5), but flood basalts have not been reported from any other upper Cenozoic locality represented in this volume. They are suspected in eastern Marie Byrd Land (MBL), but exposures of the basal parts of volcanic sections in MBL are not good enough in most places to distinguish a small flood basalt field from a large shield volcano.

Activity. The number of active volcanoes in Antarctic regions is difficult to assess. Most of them are seen very rarely, and then only from a distance. Cloud formations seen at a distance have been mistaken for plumes, a variety of evaporative and wind-blown snow phenomena have been mistaken for plumes and for fumarolic activity (again from a distance), wind-blown ash on the snow surface can mimic a true volcanic ashfall, and conversely, the effects of all but the largest-scale eruptions can be quickly obliterated by blizzards. Reports of eruptions are therefore viewed with caution by those familiar with the Antarctic environment and are not usually accepted until they have been confirmed by subsequent investigations. Table I lists the volcanoes that are known or believed to be active and the criteria

TABLE I. Manifestations of Holocene Activity of Antarctic Plate Volcanoes

Eruption Seen*	Eruption Report Questioned	Ash Layer on Ice	Fresh Cone** or K-Ar <0.1 Ma	Fumarolic Activity	Other Evidence (See Referenced IVD for Explanation)
Mount Erebus (A.17)	Mount Siple (B.5)	Mount Melbourne (A.10)	The Pleiades (A.7)	Mount Melbourne (A.10)	Mount Takahe (B.2)
Deception Island (D.2)	Webber Nunatak (C.9)		Mount Melbourne (A.10)	(?)Mount Kauffman (B.12)	Toney Mountain (B.3)
Zavodovski Island (E.2)	Seal Nunataks (D.13)	Seal Nunataks (D.13)	Local Suite (A.11)	Mount Berlin (B.15)	Mount Waesche (B.10)
Visokoi Island (E.4)	Candlemas Island (E.6)		Mount Morning (A.22)	Bridgeman Island (D.1)	Seal Nunataks (D.13)
Bristol Island (E.9)	Bouvetøya (F.1)	Thule Island (E.12)	Royal Society Range (A.24)	(?) Penguin Island (D.3)	Protector Shoal (E.3)
Marion Island (F.2)	Buckle Island (F.9)		Mount Takahe (B.2)	Seal Nunataks (D.13)	Prince Edward Island (F.3)
Heard Island (F.6)			Mount Siple (B.5)	Leskov Island (E.1)	Île aux Cochons (F.4)
			Mount Waesche (B.10)	Candlemas Island (E.6)	Amsterdam Island (F.7)
			Mount Andrus (B.12)	Saunders Island (E.7)	Peter I Island (F.11)
			Mount Berlin (B.15)	Bellingshausen Island (E.10)	
			Penguin Island (D.3)	Thule Island (E.12)	
			Paulet Island (D.8)	Bouvetøya (F.1)	
			Antipodes Islands (G.1)	Île de la Possession (F.4)	
				Îles Kerguelen (F.5)	
				Saint Paul Island (F.7)	

The volcanoes listed in the first column plus Protector Shoal are the only ones for which Holocene activity is unquestioned.
*Ash layers, fumarolic activity, and fresh cone all found here also.
**Unreliable in most Antarctic environments.

Copyright American Geophysical Union

that have been used in the assessment. In a general way, the reliability of the criteria is believed to decrease to the right in this table, bearing in mind the concerns noted above. Unconfirmed reports, or those without good photographic documentation, are listed in the second column. Fresh cone morphology is not weighted as strongly as it would be in more temperate regions, where precipitation occurs as rainfall, and it should probably be disregarded for volcanoes south of about latitude 70°S. Fumarolic activity could also be considered ambiguous when one considers that there is vigorous fumarolic activity at Yellowstone National Park (United States) but no Holocene lava flows or tephra. However, the largest fumarolic volcanoes in Table I are far smaller than those at Yellowstone. Fumarolic activity may perhaps be a better indicator of recent activity for these Antarctic volcanoes than for very large volcanic systems, but not necessarily a better predictor of future activity.

Altogether there are 40 different volcanoes listed in Table I, but only eight for which Holocene activity is unquestioned. Mount Erebus (IVD A.17) and Deception Island (IVD D.2) have been the most carefully monitored of the active Antarctic volcanoes, followed by Heard Island (IVD F.6). A lava lake is persistently present in the active crater of Mount Erebus, and a lava lake was reported in the summit crater of Big Ben (Heard Island) in 1986.

Chemical Characteristics

The overwhelmingly alkaline character of Antarctic and subantarctic volcanoes is illustrated in Figures II-V. Figure II presents an outline of the International Union of Geological Sciences (IUGS) classification scheme, together with the *Macdonald and Katsura* [1964] and the *Irvine and Baragar* [1971] alkaline-subalkaline boundary lines. Figures III-V reproduce, at a common scale, the compositional ranges of the volcanic provinces described in this volume. Truly subalkaline compositions are found in the South Sandwich Islands (Figure III) and South

Fig. II. The IUGS classification scheme for volcanic rocks [*Le Bas et al.*, 1986]. Dashed line shows the earlier version [*Le Maitre*, 1984], used by some authors in this volume. Dotted line and dot-dashed line show the alkaline/subalkaline field boundaries of *Irvine and Baragar* [1971] and *Macdonald and Katsura* [1964], respectively. Abbreviations are as follows: A, andesite; B, basalt; Ba, basaltic andesite; Bm, benmoreite; Bn, basanite; D, dacite; F, foidite; H, hawaiite; KTb, potassic trachybasalt; L, latite; M, mugearite; P, phonolite; Pc, picrobasalt; Ptp, phonotephrite; R, rhyolite; S, shoshonite; T, trachyte; Tp, tephrite; and Tpp, tephriphonolite.

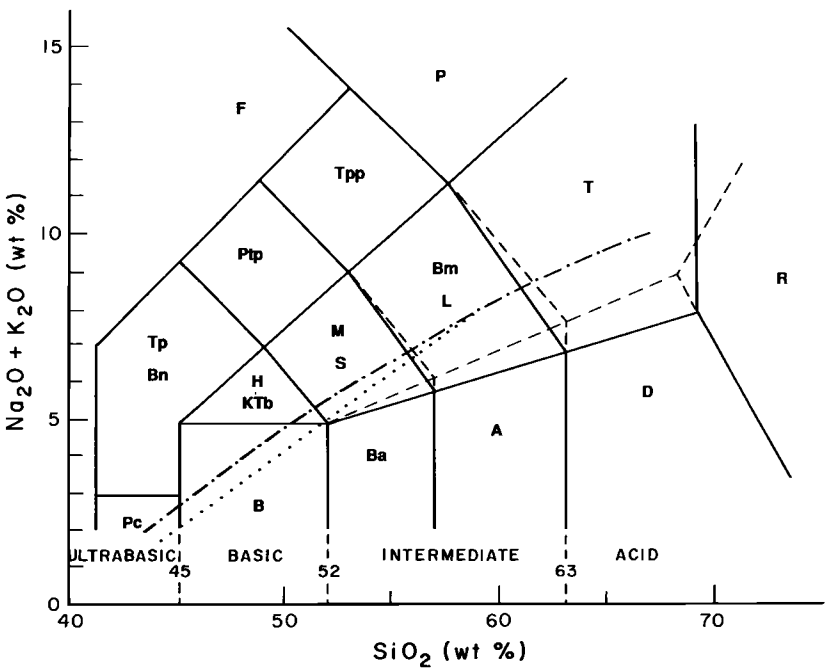

Copyright American Geophysical Union

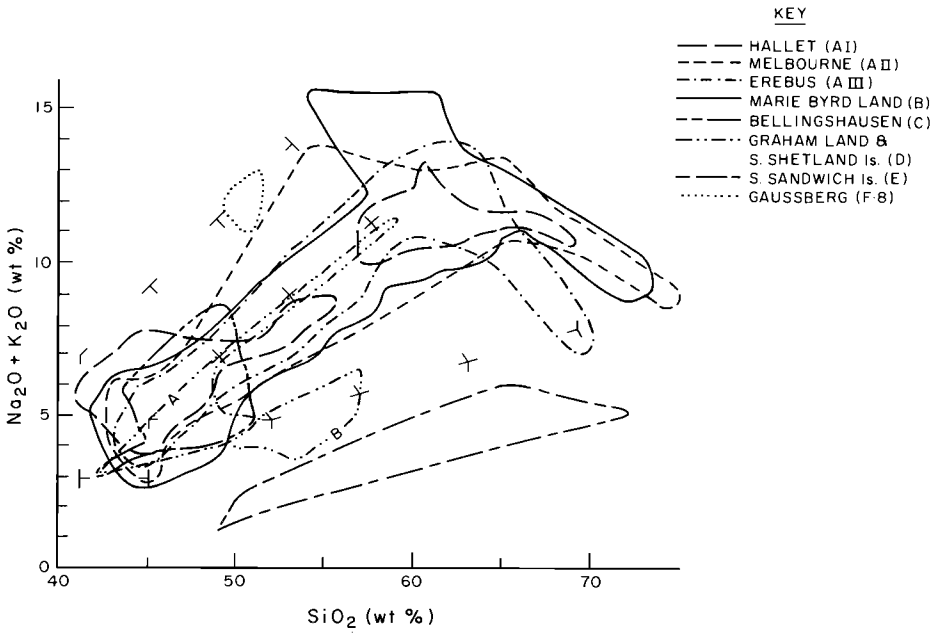

Fig. III. A summary total alkali versus silica diagram showing compositional fields for all volcanic provinces on the Antarctic continent (sections A, B, C, and D and Gaussberg (in IVD F.8)) plus the South Sandwich Islands (section E). The field for Graham Land and the South Shetland Islands has been divided into two parts, one for within-plate settings (A) and the other for arc and back-arc settings (B). Intersections of major fields in the IUGS classification are shown for reference. See inside front cover map for locations.

Fig. IV. Summary total alkali versus silica diagram for South Atlantic and Indian Ocean volcanoes of the Antarctic plate (see section F, IVD's F.1–F.7). Intersections of major fields in the IUGS classification are shown for reference (see Figure II). P.E., Prince Edward Island.

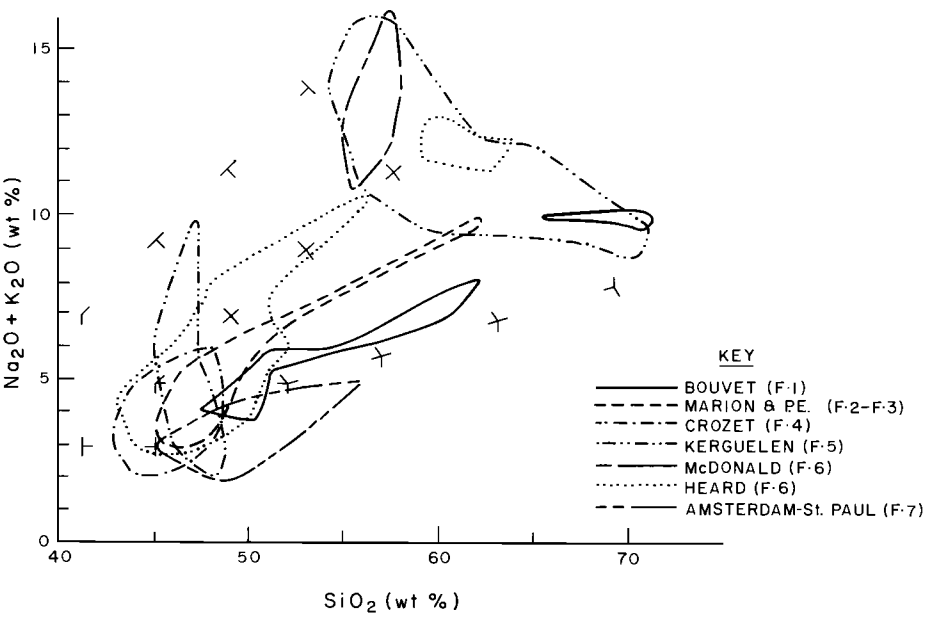

Copyright American Geophysical Union

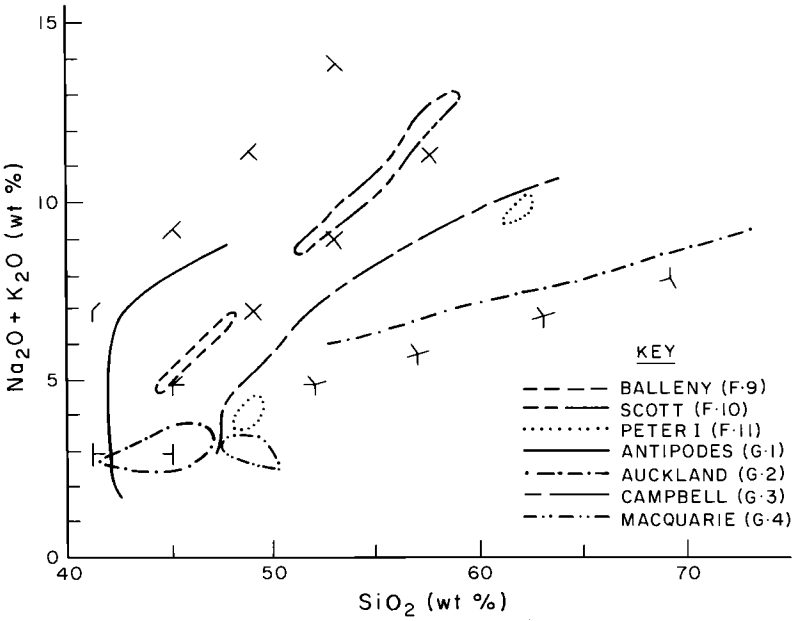

Fig. V. Summary total alkali versus silica diagram for South Pacific Ocean volcanoes of the Antarctic plate and for subantarctic volcanoes of the Pacific plate (see section F, IVD's F.9–F.11, and section G). Intersections of major fields in the IUGS classification are shown for reference (see Figure II).

Shetland Islands (line B in Figure III), Amsterdam and Saint Paul islands (Figure IV), and Macquarie Island (Figure V), while the remaining rock series represent a broad spectrum of alkalinity. Many of the alkaline suites appear to be bimodal in these diagrams, e.g., Hallett Province (Figure III), Bouvetøya, Îles Kerguelen, and Heard Island (Figure IV), Auckland and Peter I islands (Figure V), but no effort was made to screen these suites for inadequate sampling.

Basaltic rocks dominate in nearly all of these volcanic provinces. More than 70% of the total volume of rocks described are basalt, picrobasalt, basanite, tephrite, hawaiite, and potassic trachybasalt (Figure II), hereinafter referred to as basaltic rocks. Most are alkaline and strongly undersaturated (*ne*- and *ol*-normative). The alkaline rocks range from basanite to slightly *hy*-normative basalt transitional to tholeiite. Mantle and crustal xenoliths occur as inclusions in alkali basalt in a large number of the localities described in sections A, B, C, and D.

Basalts in the South Sandwich arc, and in the South Shetland Islands off the Pacific coast of Graham Land, are tholeiitic with calc-alkaline affinities. Both tholeiitic and transitional varieties occur on Amsterdam, Saint Paul, and Macquarie islands. Reviews of the mineralogic, isotopic, major and trace element characteristics of the basaltic rocks and their included xenoliths are given in the section summaries.

Table II lists the occurrences of felsic rock types that are reported in this volume, subdivided into localities found on continental and on oceanic crust. The list includes many localities that are known only from reconnaissance studies, and it should be viewed as a crude approximation of felsic rock distribution (asterisks indicate where more than just a few felsic flows or lava domes are known to occur). Trachytes generally occur with phonolites and rhyolites, and thus the "trachyte only" column lists volcanoes where highly undersaturated or highly oversaturated rocks have not been found. Among the continental provinces, the largest volumes and greatest number of occurrences of felsic rock are in the western Ross Embayment provinces and Marie Byrd Land (see Table II). Phonolitic rocks seem to predominate in the western Ross Embayment, while trachytes and rhyolitic rocks seem to predominate in Marie Byrd Land, but a full spectrum of felsic rocks is found in both these regions. The rhyolitic rocks in the western

Copyright American Geophysical Union

TABLE II. Occurrences of Felsic Rocks

Phonolitic Rocks	Trachyte Only	Oversaturated Rocks**
	Continental Localities	
Adare Peninsula (A.1)	Hallett Peninsula (A.2)	Malta Plateau* (p, c) (A.6)
The Pleiades (A.7)	Coulman Island (A.4)	Mount Overlord (c) (A.8)
Mount Overlord* (A.8)	Vulcan Hills (A.9)	Mount Morning (p) (A.22)
Mount Bird (A.15)	Mount Melbourne* (A.10)	
Mount Terror (A.16)	Mason Spur (A.23)	Toney Mountain* (c) (B.3)
Mount Erebus* (A.17)		Mount Hartigan (c) (B.8)
Hut Point Peninsula (A.18)	Mount Murphy (B.1)	Mount Waesche* (c) (B.10)
White Island (A.19)	Mount Takahe* (B.2)	Mount Andrus* (p) (B.12)
Mount Discovery* (A.21)	Mount Steere (B.4)	Mount Kosciusko* (p) (B.12)
Mount Morning* (A.22)	Mount Flint (B.11)	Mount Moulton (p) (B.14)
	Mount Kauffman (B.12)	
Mount Frakes (B.4)	Mount Bursey* (B.13)	Deception Island (r) (D.2)
Mount Hampton* (B.6)	Mount Berlin* (B.15)	
Mount Sidley* (B.9)	Dorrel Rock (B.16A)	Auckland Islands (r) (G.2)
Mount Moulton (B.14)	Kouperov Peak (B.16C)	Campbell Island (r) (G.3)
	Shepard Island (B.16D)	
Gaussberg* (F.8)		
	James Ross Island (D.12)	
	Oceanic Localities	
Île de la Possession (F.4)	Prince Edward Island (F.3)	Protector Shoal (r) (E.3)
Îles Kerguelen* (F.5)	Heard Island (F.6)	Candlemas Island (d) (E.6)
McDonald Island (F.6)	Peter I Island (F.11)	Cook Island (d) (E.11)
Scott Island* (F.10)		Bouvetøya (c) (F.1)
		Îles Kerguelen* (c) (F.5)
		Saint Paul Island (c) (F.7)

*Major occurrence (see text).
**Rhyolite (r), comendite (c), pantellerite (p), and dacite (d).

Ross Embayment occur only among the oldest (>7–10 Ma) volcanoes, whereas there is no discernible chronologic sequence related to the saturation characteristics of volcanoes in Marie Byrd Land. Felsic rocks are usually concentrated around the summit vent areas of the larger central volcanoes, and in some continental examples they appear to make up a major proportion of the volcano.

Comparing chemical characteristics (Figures IV and V) with locations (IFC map) shows that, among the oceanic islands, those that occur on or near a mid-ocean ridge are composed of saturated or oversaturated rock types (Bouvetøya and Prince Edward, Amsterdam, and Saint Paul islands). The undersaturated suites are found well off the ridge crests (Scott, McDonald, and Possession islands); however, trachytes occur both on and off the ridges, and Îles Kerguelen fit no pattern. Îles Kerguelen are an unusual and anomalous volcanic center in that it has a very high (13%) estimated proportion of felsic rocks, it has substantial proportions of both phonolitic and rhyolitic rock suites (including a 350 km^2 "granito-syenitic" pluton), and it is an exceptionally long-lived center. There was at one time speculation that Îles Kerguelen were a microcontinent underlain by sialic crust, but this has been disproven by geophysical studies and recent drilling (see section F summary and *Wise* [1989]). The Kerguelen Plateau is now believed to be an accumulation of Cretaceous tholeiitic flood basalts extruded along the spreading axis that rifted the Indian subcontinent from Antarctica, and thus its origin may be related to the same flood basalt episode that produced the Rajmahal traps in southeastern India. From this perspective, the

Copyright American Geophysical Union

Îles Kerguelen and Heard Island late Cenozoic volcanoes may represent the relatively late stage residuum from a major mantle plume whose activity was initiated around 118 Ma [*Story et al.*, 1989; *Wise*, 1989].

There appear to be no significant geochemical differences between the continental and oceanic alkaline rocks of the Antarctic plate, except perhaps that the very undersaturated compositions seem more common on the continent (see Figures III-V and section summaries), and there is no oceanic counterpart to the leucitite at Gaussberg noted below. Close geochemical similarity between continental and oceanic occurrences seems to be characteristic of alkaline rocks [*Pearce et al.*, 1977], and this is confirmed by some of the more detailed geochemical descriptions in sections A-G. However, in comparing Figures III-V with Table II, felsic rocks appear to be more abundant and show more complex variation in continental provinces as compared with those in ocean basins. The oceanic islands tend to be characterized by a single felsic rock type, with Îles Kerguelen again the obvious exception. Judging from the available isotopic data, these differences are likely to represent the effects, among continental rocks, of a complicated plumbing system and long residence time in crustal reservoirs, rather than the addition of crustal melt components to mantle-derived magmas.

Antarctica has many unusual alkaline rock types, the best known of which are the felsic rocks at Mount Erebus and Gaussberg. The phonolites at Mount Erebus contain abundant anorthoclase phenocrysts, commonly more than 3 cm long, and resemble the more widely known kenyte of East Africa and rhomb porphyries of the Permian Oslo rift province. Strombolian eruptions of phenocryst-rich anorthoclase phonolite bombs from the summit lava lake are a common event at Mount Erebus (IVD A.17). Similar rocks are found at Mount Sidley (IVD B.9), Mount Hampton (IVD B.6), and Mount Frakes (IVD B.4), in Marie Byrd Land, each of which is a large volcano that seems to be composed predominantly of peralkaline phonolites and related trachytes.

The unusual leucitite lava flows at Gaussberg (IVD F.8) are well known and have been intensively studied. They are the only known example of leucite-bearing rocks among the late Cenozoic volcanoes of Antarctica and the only highly potassic rocks on the continent. They are also, incidentally, the only Cenozoic volcanic rocks known on the East Antarctic shield (Figure I), where the thickest continental crust in Antarctica is found. The only potassic series volcanic rocks that have been reported from the ocean basins in Antarctic regions are on Heard Island, north of Gaussberg, which has led to speculation about a petrogenetic connection related to volcanism along the Kerguelen-Gaussberg aseismic ridge (see IVD F.8). Heard Island lava flows are similar to the more widely known Gough Island suite [*Le Maitre*, 1962].

Tectonic Relationships

The major tectonic features associated with Antarctic volcanism include a stationary plate environment, common to all volcanoes in this volume except those in sections E and G; the West Antarctic rift system, to which the volcanoes in sections A, B, and C are related; and the active plate margin and transitional environments of the northern Antarctic Peninsula (section D) and the South Sandwich island arc (section E). Each of these environments is described below, followed by a brief review of pre-Cenozoic tectonic features and their influence on Cenozoic volcanism.

Stationary plate environment. The Antarctic plate is encircled by mid-ocean ridges and transform faults, broken by a convergent plate boundary only in the segment between South America and the tip of the Antarctic Peninsula (see IFC map). Although the plate boundaries have moved continuously, and mostly northward away from the continent, the plate itself has not moved perceptibly in Neogene time and may not have moved significantly within the past 80 m.y. [*Herron and Tucholke*, 1975; *Weissel et al.*, 1977; *Barron and Harrison*, 1979; *Duncan*, 1981; *Grindley and Oliver*, 1983; *Stock and Molnar*, 1987; *LeMasurier and Rex*, 1989]. Cenozoic tectonic activity on the continent has been characterized mainly by vertical displacements and extension, related to intracontinental rifting [e.g., *Cooper et al.*, 1987; *Kellogg and Rowley*, 1989; *LeMasurier and Rex*, 1989]. Thus the environment of volcanism throughout the plate has been mainly one of tectonic extension coupled with plate immobility. Graham Land, the South Shetland Islands, and the South

Copyright American Geophysical Union

Sandwich Islands (sections D and E) are the exceptions, as noted below.

The immobility of the plate is reflected mainly in the lack of linear hotspot traces among either the continental or the oceanic volcanoes described in this volume. There are numerous aseismic ridges and plateaus surmounted by volcanic islands on the oceanic portions of the plate, but linear migrations of Neogene activity are not unambiguously displayed, even though they have been proposed (see section F summary). On the continent, there are good examples of linear volcanic chains in the Hallett province (section A.I) and in Marie Byrd Land (section B). However, sparse K-Ar data from Hallett provide no evidence for migration of activity there, and the well-documented systematic migrations in Marie Byrd Land are clearly not related to plate motions [*LeMasurier and Rex*, 1989]. Îles Kerguelen (IVD F.5) may provide the most distinctive signature of late Cenozoic volcanism on the Antarctic plate: a 39-m.y. history of nearly continuous, highly localized, intraplate volcanism, representing a fixed hotspot located beneath an immobile plate.

West Antarctic rift system. The scale and regional extent of the West Antarctic rift (Figure I) have been difficult to define precisely, because much of the topography is buried beneath the ice sheet (Figure VI), the continent is very nearly aseismic, geophysical data are sparse, and the Cenozoic volcanic fields are deceptively arranged in a way that suggests a primary relationship to the continental margin. Radio-echo sounding data [*Drewry*, 1982] have refined the generalized subglacial topography shown in Figure VI and demonstrated that there is no continuous sub-sea level topographic low along the Transantarctic Mountain front (Figure I) between the Ross Sea and the Weddell Sea. There is, however, a pronounced trough between the Ross Sea and the Bellingshausen Sea, with maximum depths of –2555 m in the Bentley Subglacial Trench and –2000 m in the Byrd Subglacial Basin.

Seismic data show that crustal thicknesses reach a minimum of 25 km along the whole length of the Ross-Bellingshausen topographic trough, increasing at the flanks of the trough to 32 km beneath the highlands of coastal Marie Byrd Land, 36 km beneath the Ellsworth Mountains block and Transantarctic Mountains (Figure VII), and 40 km beneath East Antarctica [*Bentley*, 1973]. The floor of the trough is further characterized by a broad negative isostatic gravity anomaly (–10 to –20 mGals) and is flanked on both sides by four relatively narrow positive anomalies of +10 to +30 mGals [*Bentley and Robertson*, 1982]. The axis of the trough is nearly devoid of the narrow-width aeromagnetic anomalies found on its flanks, and this has been interpreted as the magnetic signature of sedimentary rock [*Behrendt*, 1964]. These topographic and geophysical characteristics are similiar to those found in large intracontinental rift systems elsewhere in the world, such as the East African rift, the Rio Grande rift, and the Oslo graben [*Girdler*, 1975; *Seager and Morgan*, 1979; *Husebye and Ramberg*, 1978].

All of the exposed Cenozoic volcanoes from the western Ross Embayment to Palmer Land seem to be arrayed along the flanks of the West Antarctic rift, as it is expressed by topography and geophysical characteristics along the Ross-Bellingshausen trough. Volcanoes from the Adare Peninsula to Mount Early (section A) lie on the East Antarctic flank, Marie Byrd Land volcanoes lie on the Pacific flank, and those in Ellsworth Land, Palmer Land, and Alexander Island (section C) seem to lie on both flanks.

The rift system is highly asymmetrical in the distribution of volcanic products and in its overall form and structure. The largest volumes of basaltic and felsic rock, and the longest duration of activity, occur in the western Ross Embayment and Marie Byrd Land provinces. These provinces were clearly active in the Early Miocene (IVD's A.6 and A.22) and Late Oligocene (IVD's B.16A and B.16B), although recent drilling in McMurdo Sound suggests that volcanism may have extended back to Late Eocene time in the western Ross Sea (see section A.III summary). At the eastern end of the rift, around the Bellingshausen Sea, volcanic centers are small, widely scattered, entirely basaltic, and Late Miocene to Recent(?) in age. These generalizations are not evident from Figure I, which shows schematic representations of the localities of Quaternary and pre-Quaternary volcanoes, irrespective of their size and composition. The elevations of pre-Cenozoic basement rock exceed 4000 m in numerous peaks along the Transantarctic Mountains (TAM), descend abruptly across the TAM front to between –2500 m and –4500 m beneath the rift axis [*Bentley and*

Copyright American Geophysical Union

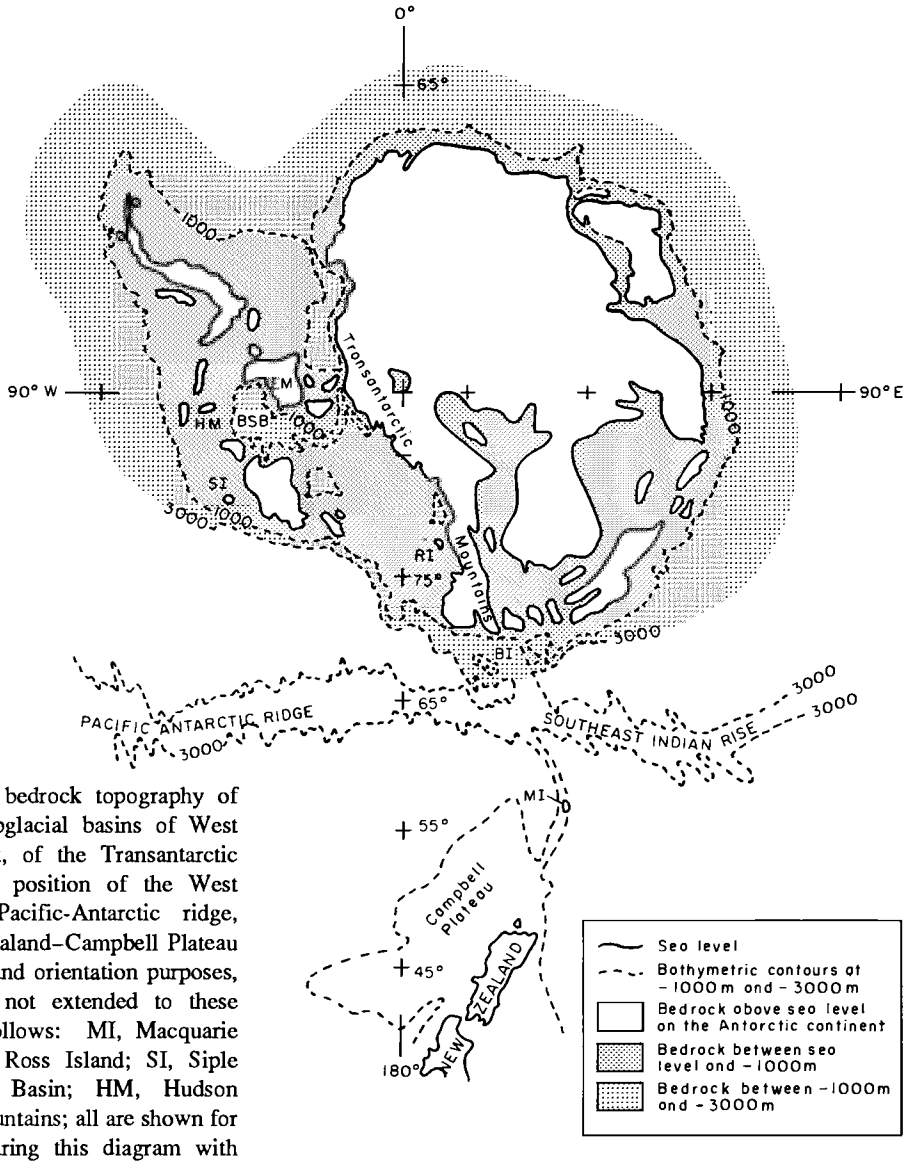

Fig. VI. Generalized subglacial bedrock topography of Antarctica, showing the deep subglacial basins of West Antarctica (the area left, or east, of the Transantarctic Mountains) that help define the position of the West Antarctic rift system. The Pacific-Antarctic ridge, Southeast Indian rise, and New Zealand–Campbell Plateau block are shown for comparative and orientation purposes, but bedrock depth symbols are not extended to these regions. Abbreviations are as follows: MI, Macquarie Island; BI, Balleny Islands; RI, Ross Island; SI, Siple Island; BSB, Byrd Subglacial Basin; HM, Hudson Mountains; and EM, Ellsworth Mountains; all are shown for orientation purposes when comparing this diagram with other diagrams in this volume. Adapted from *American Geographical Society* [1970].

Fig. VII. (opposite) Major tectonic elements of pre-Cenozoic Antarctica. Orogenic belts shown here are the Ross orogen (early Paleozoic) and Andean orogen (late Mesozoic) of *Craddock* [1972], represented here as former active plate margins. The boundary between the two belts is not exposed. Rock assemblages in both belts are dominated by granitoids; the late Mesozoic assemblage is superimposed on middle and late Paleozoic plate margin assemblages, and all three extended into the New Zealand–Campbell Plateau (NZ-CP) block (see *Borg et al.* [1987] for the early Paleozoic and *R.A. Cooper et al.* [1982] for the late Mesozoic). The Jurassic rift system is inferred from the distribution of Jurassic flood basalt, diabase sills and gabbro, from multichannel seismic reflection data in the western Ross Sea, and from Jurassic southern hemisphere continental reconstructions. Boundaries shown here are after *Schmidt and Rowley* [1986]. Tectonic blocks are defined by structural trends, lithologies, and paleomagnetic data; boundaries are determined by topography and aeromagnetic data; Mesozoic and Cenozoic displacements are known for some blocks and inferred for others [*Dalziel and Elliot*, 1982; *Dalziel and Grunow*, 1985; Elliot, personal communication, 1989]. Block names are as follows: MBL, Marie Byrd Land; EWM, Ellsworth-Whitmore Mountains; TI and AP, Thurston Island–Antarctic Peninsula; HN, Haag Nunataks. All boundaries are shown in their present-day positions except the NZ-CP block.

Copyright American Geophysical Union

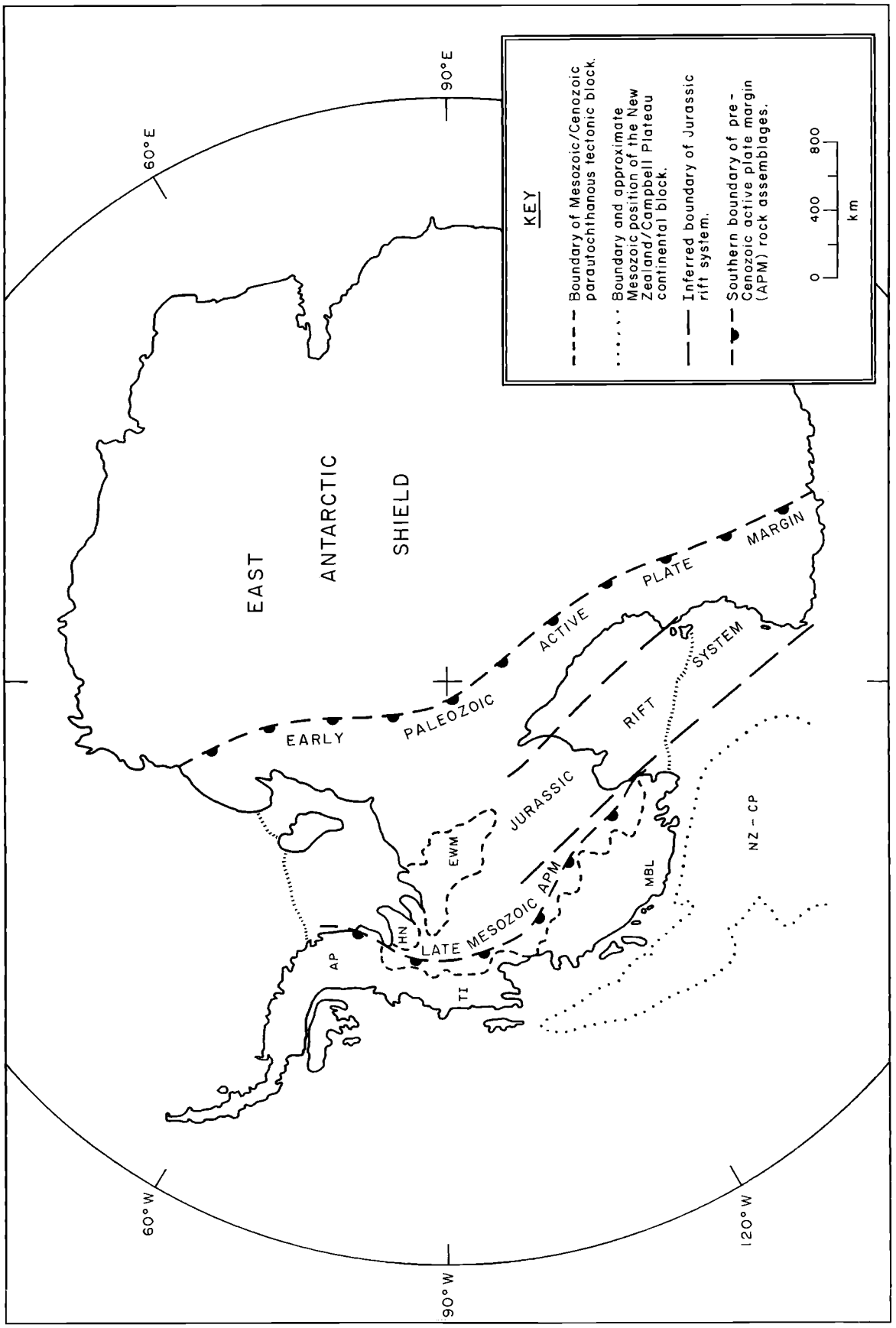

Copyright American Geophysical Union

Clough, 1972; *McGinnis et al.*, 1983], and then vary between −3000 m and +2700 m in the horsts and grabens of Marie Byrd Land.

It has been suggested that glacial ice is the equivalent of basin fill in the deep topographic troughs, and this, plus the ages of flanking volcanic fields and the vertical fault displacements of the early Tertiary erosion surface in Marie Byrd Land, suggests that much of the subglacial topography is a product of late Cenozoic tectonic displacement (see section B summary and *LeMasurier and Rex* [1982]). The inferred boundaries of the rift system shown in Figure I are based on all of the topographic, geophysical, and geologic features described above. A possible branch toward the Weddell Sea is shown dashed, because deep subglacial troughs are the only suggestion of Cenozoic rifting in that area.

Active plate margin and transitional environments. Both the earliest and the latest stages in the evolution of an island arc/subduction system are represented in Antarctic regions. The subduction-related volcanoes in Graham Land and the South Shetland Islands (section D) represent the last remnant of an active plate margin that in Cretaceous time extended along the entire Pacific margin of the combined Antarctic–New Zealand–Campbell Plateau continent [*Cooper et al.*, 1982]. The New Zealand–Campbell Plateau (NZ-CP) block (Figure VII) separated from Marie Byrd Land around 80 Ma, creating the present rifted continental margin (Figure I), and thereafter subduction terminated systematically northeastward toward the tip of the Antarctic Peninsula. This convergent plate boundary disappeared completely about 4 Ma (see section D summary). Thus, arc, back-arc, and within-plate environments all overlapped, spatially, within the past 10 m.y. in the northern Antarctic Peninsula. It is now a slowly developing marginal basin environment, and the transition from subduction-related to rift-related magmatism is well displayed by calc-alkaline, transitional, and alkaline rock suites. The characteristics of the rocks that represent these environments are presented in Table D.I and described in the accompanying text. The pre-Neogene calc-alkaline volcanoes are not described in this volume.

The South Sandwich arc, which adjoins the Antarctic plate (see IFC map), is the only active island arc described in this volume. It is an unusually mafic island arc (70% basalt), and in contrast to the South Shetland Islands, it is believed to represent an early stage in arc evolution (see section E summary and *Baker* [1968]).

Pre-Cenozoic tectonic influences. Figure VII shows the major pre-Cenozoic tectonic elements of Antarctica, to help illustrate the antecedents of present-day tectonic environments. The late Mesozoic active plate margin shown here is the predecessor of the Neogene active plate margin in Graham Land and the South Shetland Islands. Prior to about 80 Ma, it included the NZ-CP block in approximately the position shown [*Cooper et al.*, 1982]. The pronounced difference between this terrane and the early Paleozoic active plate margin assemblage that underlies the western Ross Embayment provinces (section A) is believed to be reflected in isotopic differences between these provinces and those in Marie Byrd Land, Ellsworth Land, Palmer Land, and Alexander Island [*Brewer and Clarkson*, 1989].

The West Antarctic rift system apparently occupies a zone of lithospheric weakness along which volcanism and extensional strain have been repeatedly focused. The location of the Jurassic rift shown in Figure VII is based on the occurrence of Jurassic tholeiites exposed along a large part of the Transantarctic Mountains [*Kyle et al.*, 1981; *Elliot*, 1985; *Schmidt and Rowley*, 1986]. This rift is also parallel to the line along which the NZ-CP block broke away from Marie Byrd Land in the Late Cretaceous. Crustal attenuation in Antarctica and the NZ-CP block and basin filling in the Ross Sea have been postulated for this time, but the chronology is not well documented [*R.A. Cooper et al.*, 1982; *A.K. Cooper et al.*, 1987].

The Mesozoic-Cenozoic tectonic blocks in West Antarctica have been rotated and uplifted, probably by repeated episodes of deformation, but there is no evidence that the locus of late Cenozoic volcanic activity has been influenced by block boundaries (compare Figure I with Figure VII). No major differences in the nature of magma source regions are suspected, other than those that could be attributed mainly to depth of melting or lateral inhomogeneities, because none of the blocks is believed to be an exotic terrane [*Dalziel and Elliot*, 1982; *Dalziel and Grunow*, 1985; Elliot, personal communication,

Copyright American Geophysical Union

1989]. Conversely, however, future work may reveal similarities between the isotopic geochemistry of the Campbell Plateau volcanoes and those in Marie Byrd Land that derive from their lithospheric similarities.

The volcanism at Îles Kerguelen and Heard Island may be relicts of the breakup of Gondwanaland, if the plume model referred to earlier is correct. Similarly, it has been suggested that Îles Crozet volcanism (see IVD F.4) represents a late stage of mantle plume activity that was initiated with the earliest Karoo flood basalt activity (around 193 Ma) and was followed later by Jurassic flood basalt activity in Antarctica which accompanied the separation of Africa from Antarctica [*White and McKenzie,* 1989].

Summary

Most characteristics of Antarctic plate volcanic rocks are related to a stable, extensional plate tectonic environment and, to a lesser extent, to an eruptive environment that was frequently dominated by glacial ice. Major characteristics are itemized below, with references to the sections where they are described in greater depth.

1. The ages of volcanoes described in this volume range from 39 Ma at Îles Kerguelen (IVD F.5) to the almost continuous present-day eruptions at Mount Erebus (IVD A.17). Eight Antarctic and subantarctic volcanoes are known to be active, and 32 others are suspected of Holocene activity. This relatively high level of uncertainty expresses the difficulty of assessing levels of activity in this environment.

2. Antarctic plate volcanoes are dominated by alkaline basaltic rocks. Felsic rocks occur in greatest abundance and diversity on the continent. The largest volumes of felsic rock, and perhaps of basaltic rock too, are in the western Ross Embayment (see section A) and Marie Byrd Land (see section B). Îles Kerguelen (IVD F.5) have the largest proportion (13%) and most diverse assemblage of felsic rocks among the oceanic volcanoes.

3. Subalkaline, arc-related volcanoes are found only in Graham Land (see section D), the South Shetland Islands (see section D), and the South Sandwich Islands (see section E). Volcanoes of the South Sandwich Islands apparently represent the development of a new arc, while those in Graham Land and the South Shetland Islands mark the extinction of an arc system that followed the entire Pacific margin of Antarctica in Mesozoic time. Alkaline volcanism overlapped and finally supplanted the arc-related volcanism in Graham Land and the South Shetland Islands.

4. The most abundant pyroclastic rocks found so far in Antarctic regions are hyaloclastites, autobrecciated lava flows, and a variety of agglutinates. The scarcity of magmatic ash is reflected in the shield-like character of most felsic volcanoes. The abundance of hydroclastic rock results from the persistence of intraglacial and periglacial eruptive environments through much of Neogene time.

5. Aside from the South Sandwich arc, oceanic volcanism has occurred within the plate and has taken place without forming distinctive spatial patterns. There are no well-developed linear chains, and although there is a tendency for volcanoes to be more undersaturated away from ridge crests, this saturation pattern is not strongly expressed.

6. The distribution of volcanoes on the continent is closely related to two major tectonic features. Those that occur from the western Ross Embayment, across Marie Byrd Land, to the base of the Antarctic Peninsula lie along the flanks of the West Antarctic rift system. The present rift lies along a portion of the continent that has been repeatedly attenuated, downfaulted, and flanked by volcanic activity since Jurassic time and is similar in scale to the Basin and Range province of North America and the East African rift system. The Graham Land and South Shetland Island volcanoes represent a second major environment of continental volcanism. They have formed near the margin of the Antarctic plate during a time of rapid change from subduction-related volcanism to back-arc and marginal-basin activity.

7. None of the volcanoes described here has been known for more than 200 years, those on the floor of the Ross Sea (see IVD A.12) were discovered in 1984, and some that have been known of for decades have seldom been visited. There is a high probability that a significant number remain to be found on the floor of the Ross Sea and beneath the ice sheet, especially along the axial part of the West Antarctic rift system. A great deal of new information, and major changes in the generalizations presented here, can be anticipated from future investigations.

Copyright American Geophysical Union

Acknowledgments

I gratefully acknowledge the reviews and helpful suggestions of my co-editor, of each of the associate editors, and of J.W. Cole, I.G. Gass, T. Simkin, J. Whitford-Stark, J. Barling, D.H. Elliot, W.C. McIntosh, I. Norton, and R. J. Tingey. Special thanks to Tom Simkin for suggesting and helping with Table I and to David Elliot and Peter Rowley for reviewing the final draft.

References

American Geographical Society, *Antarctica,* scale 1:5,000,000, New York, 1970.

Baker, P.E., Comparative volcanology and petrology of the Atlantic island-arcs, *Bull. Volcanol., Ser. 2, 32,* 189–206, 1968.

Barrett, P.J., A.R. Pyne, M.J. Hambry, D.B. Harwood, and P.N. Webb, Antarctic glacial history from Ross Sea drilling, *Int. Geol. Congr. Abstr. 28th 1,* 92, 1989.

Barron, E.J., and C.G.A. Harrison, Reconstruction of the Campbell Plateau and the Lord Howe Rise, *Earth Planet. Sci. Lett., 45,* 87–92, 1979.

Behrendt, J.C., Antarctic Peninsula traverse geophysical results relating to glaciological and geological studies, *Res. Rep. 64-1,* 112 pp., University of Wisconsin Geophysical and Polar Research Center, Madison, 1964.

Behrendt, J.C., A.K. Cooper, and A. Yuan, Interpretation of marine magnetometer gradiometer and multichannel seismic-reflection observations over the western Ross Sea shelf, Antarctica, in *The Antarctic Continental Margin: Geology and Geophysics of the Western Ross Sea, CPCEMR Earth Sci. Ser.,* vol. 5B, edited by A.K. Cooper and F.J. Davey, pp. 155–177, Circum-Pacific Council for Energy and Mineral Resources, Houston, Tex., 1987.

Bentley, C.R., Crustal structure of Antarctica, *Tectonophysics, 20,* 229–240, 1973.

Bentley, C.R., and J.W. Clough, Antarctic subglacial structure from seismic refraction measurements, in *Antarctic Geology and Geophysics,* edited by R.J. Adie, pp. 683–691, Universitetsforlaget, Oslo, 1972.

Bentley, C.R., and J.D. Robertson, Isostatic gravity anomalies in West Antarctic, in *Antarctic Geoscience,* edited by C. Craddock, pp. 949–954, University of Wisconsin Press, Madison, 1982.

Borg, S.G., E. Stump, B.W. Chappell, M.T. McCulloch, D. Wyborn, R.L. Armstrong, and J.R. Holloway, Granitoids of northern Victoria Land, Antarctica: Implications of chemical and isotopic variations to regional crustal structure and tectonics, *Am. J. Sci., 287,* 127–169, 1987.

Brewer, T.S., and P.D. Clarkson, Mesozoic magmatism in greater Antarctica: Implications for Precambrian plate tectonics, in *Geologic Evolution of Antarctica,* edited by M.R.A. Thomson, J.A. Crame, and J.W. Thomson, Cambridge University Press, New York, in press, 1989.

Cooper, A.K., F.J. Davey, and J.C. Behrendt, Seismic stratigraphy and structure of the Victoria Land basin, western Ross Sea, Antarctica, in *The Antarctic Continental Margin: Geology and Geophysics of the Western Ross Sea, CPCEMR Earth Sci. Ser.,* vol. 5B, edited by A.K. Cooper and F.J. Davey, pp. 27–66, Circum-Pacific Council for Energy and Mineral Resources, Houston, Tex., 1987.

Cooper, R.A., C.A. Landis, W.E. LeMasurier, and I.G. Speden, Geologic history and regional patterns in New Zealand and West Antarctica—Their paleotectonic and paleogeographic significance, in *Antarctic Geoscience,* edited by C. Craddock, pp. 43–53, University of Wisconsin Press, Madison, 1982.

Craddock, C., Antarctic tectonics, in *Antarctic Geology and Geophysics,* edited by R.J. Adie, pp. 449–455, Universitetsforlaget, Oslo, 1972.

Dalziel, I.W.D., and D.H. Elliot, West Antarctica: Problem child of Gondwanaland, *Tectonics, 1,* 3–19, 1982.

Dalziel, I.W.D., and A.M. Grunow, The Pacific margin of Antarctica: Terranes within terranes within terranes, in *Tectonostratigraphic Terranes of the Circum-Pacific Region, CPCEMR Earth Sci. Ser.,* vol. 1, edited by D.G. Howell, pp. 555–564, Circum-Pacific Council for Energy and Mineral Resources, Houston, Tex., 1985.

Drewry, D.J. (Ed.), *Antarctica: Glaciological and Geophysical Folio,* Scott Polar Research Institute, Cambridge, England, 1982.

Duncan, R.A., Hotspots in the southern oceans—An absolute reference frame for motion of the Gondwana continents, *Tectonophysics, 74,* 29–42, 1981.

Eaton, G.P., A plate tectonic model for late Cenozoic crustal spreading in the western United States, in *Rio Grande Rift: Tectonics and Magmatism,* edited by R.E. Riecker, pp. 7–32, AGU, Washington, D.C., 1979.

Elliot, D.H., Physical geography—Geological evolution, in *Key Environments—Antarctica,* edited by D.W.H. Walton and W.N. Bonner, pp. 39–61, Pergamon, New York, 1985.

Fisher, R.V., and H.-U. Schmincke, *Pyroclastic Rocks,* Springer-Verlag, New York, 1984.

Girdler, R.W., The great negative Bouguer gravity anomaly over Africa, *Eos Trans. AGU, 56,* 516, 1975.

Grindley, G.W., and P.J. Oliver, Palaeomagnetism of Cretaceous volcanic rocks from Marie Byrd Land, Antarctica, in *Antarctic Earth Science,* edited by R.L. Oliver, P.R. James, and J.B. Jago, pp. 573–578, Cambridge University Press, New York, 1983.

Herron, E.M., and B.E. Tucholke, Seafloor magnetic pattern and basement structure in the southeastern Pacific, *Initial Rep. Deep Sea Drill. Proj., 35,* 263–278, 1975.

Husebye, E.S., and I.B. Ramberg, Geophysical Investigation, "The Oslo Paleorift," *Nor. Geol. Unders., 337,* 41–53, 1978.

Copyright American Geophysical Union

Irvine, T.N., and W.R.A. Baragar, A guide to the chemical classification of the common volcanic rocks, *Can. J. Earth Sci., 8*, 523–548, 1971.

Jones, J.G., and P.H.H. Nelson, The flow of basalt lava from air into water—Its structural expression and stratigraphic significance, *Geol. Mag., 107*, 13–19, 1970.

Kellogg, K.S., and P.R. Rowley, Structural geology and tectonics of the Orville Coast region, southern Antarctic Peninsula, Antarctica, *U.S. Geol. Surv. Prof. Pap. 1498*, 25 pp., 1989.

Kyle, P.R., D.H. Elliot, and J.F. Sutter, Jurassic Ferrar Supergroup tholeiites from the Transantarctic Mountains, Antarctica, and their relationship to the initial fragmentation of Gondwana, in *Gondwana V*, edited by M. Cresswell and P. Vella, pp. 283–287, A.A. Balkema, Rotterdam, 1981.

Le Bas, M.J., R.W. Le Maitre, A. Streckeisen, and B. Zanettin, A chemical classification of volcanic rocks based on the total alkali-silica diagram, *J. Petrol., 27*, 745–750, 1986.

Le Maitre, R.W., Petrology of volcanic rocks, Gough Island, South Atlantic, *Geol. Soc. Am. Bull., 73*, 1309–1340, 1962.

Le Maitre, R.W., A proposal by the IUGS Subcommission on the Systematics of Igneous Rocks for a chemical classification of volcanic rocks based on the total alkali silica (TAS) diagram, *Aust. J. Earth Sci., 31*, 243–255, 1984.

LeMasurier, W.E., and D.C. Rex, Volcanic record of Cenozoic glacial history in Marie Byrd Land and western Ellsworth Land: Revised chronology and evaluation of tectonic factors, in *Antarctic Geoscience*, edited by C. Craddock, pp. 725–734, University of Wisconsin Press, Madison, 1982.

LeMasurier, W.E., and D.C. Rex, Evolution of linear volcanic ranges in Marie Byrd Land, West Antarctica, *J. Geophys. Res., 94*, 7223–7236, 1989.

Macdonald, G.A., and T. Katsura, chemical composition of Hawaiian lavas, *J. Petrol., 5*, 82–133, 1964.

McGinnis, L.D., D.D. Wilson, W.J. Burdelik, and T.H. Larson, Crust and upper mantle study of McMurdo Sound, in *Antarctic Earth Science*, edited by R.L. Oliver, P.R. James, and J.B. Jago, pp. 204–208, Cambridge University Press, New York, 1983.

Pearce, T.H., B.E. Gorman, and T.C. Birkett, The relationship between major element chemistry and tectonic environment of basic and intermediate volcanic rocks, *Earth Planet. Sci. Lett., 36*, 121–132, 1977.

Schmidt, D.L., and P.D. Rowley, Continental rifting and transform faulting along the Jurassic Transantarctic rift, Antarctica, *Tectonics, 5*, 279–291, 1986.

Seager, W.R., and P. Morgan, Rio Grande rift in southern New Mexico, west Texas, and northern Chihauhua, in *Rio Grande Rift: Tectonics and Magmatism*, edited by R. Riecker, pp. 87–106, AGU, Washington, D.C., 1979.

Stock, J., and P. Molnar, Revised history of early Tertiary plate motion in the south-west Pacific, *Nature, 325*, 495–499, 1987.

Storey, M., H. Whitechurch, J.H. Sevigny, V.J.M. Salters, and Leg 120 Shipboard Scientific Party, Basement drilling of Kerguelen Plateau by Ocean Drilling Program (Leg 120): Report on shipboard results and work in progress, *Int. Geol. Congr. Abstr. 28th, 3*, 187–188, 1989.

Weissel, J.K., D.E. Hayes, and E.M. Herron, Plate tectonic synthesis: Displacements between Australia, New Zealand and Antarctica since the late Cretaceous, *Mar. Geol., 25*, 231–277, 1977.

White, R., and D. McKenzie, Magmatism at rift zones: The generation of volcanic continental margins and flood basalts, *J. Geophys. Res., 94*, 7685–7729, 1989.

Wise, S.W., Geologic and tectonic evoution of the Kerguelen Plateau as revealed by ODP leg 120 drilling, *Int. Geol. Congr. Abstr. 28th, 3*, 371, 1989.

Copyright American Geophysical Union

A.
McMurdo Volcanic Group
Western Ross Embayment

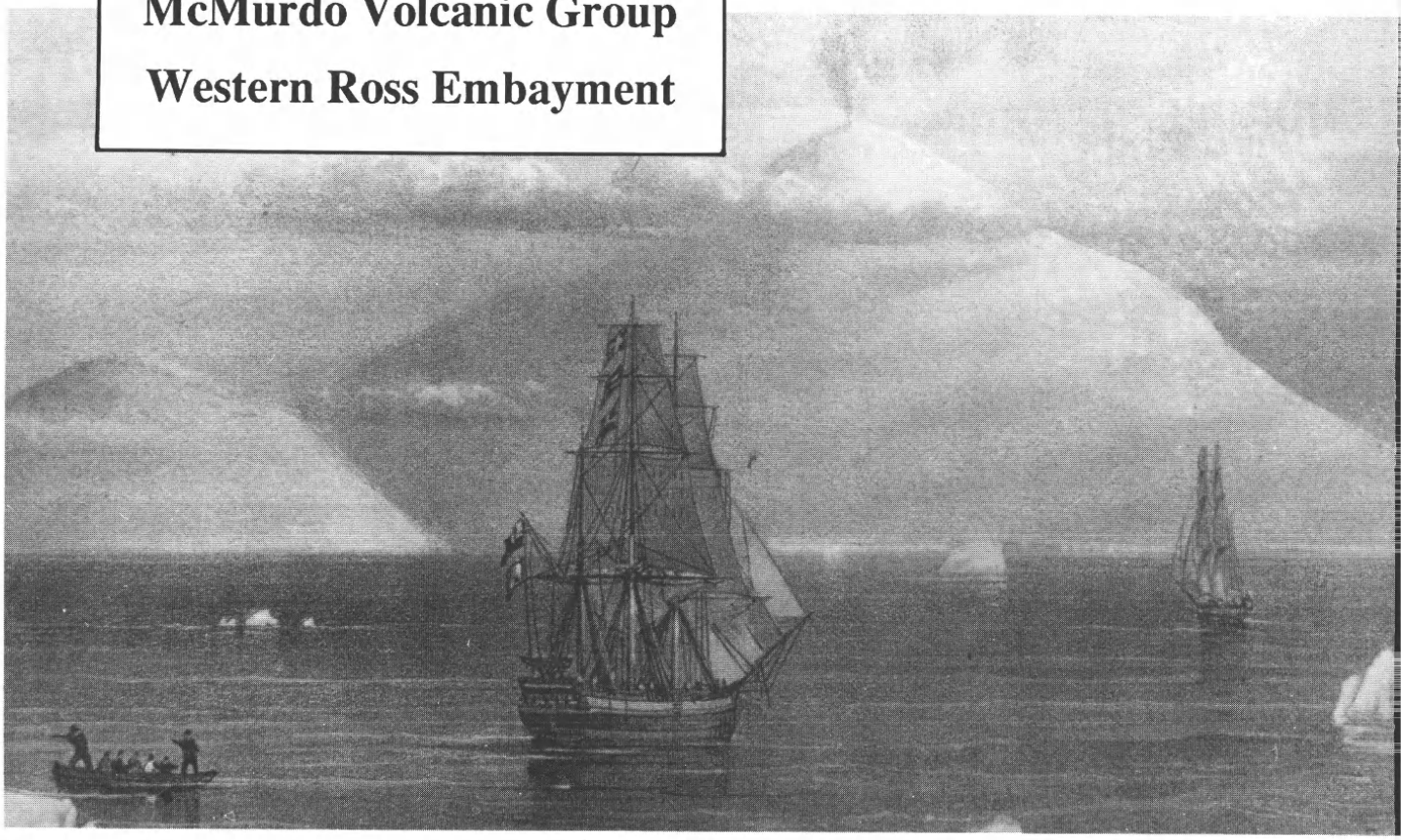

Copyright American Geophysical Union

Introduction

P.R. Kyle

Frontispiece. The discovery of Mount Erebus by Sir James Ross in his two ships *Erebus* and *Terror*. On January 27, 1841, Mount Erebus was described as "emitting flame and smoke in great profusion" and later, on January 28, 1841, "some of the officers believed they could see streams of lava pouring down its sides until lost beneath the snow" [*Ross*, 1847].

All Cenozoic volcanic rocks situated within the western Ross Embayment (Figure A.I), in or adjacent to the Transantarctic Mountains, are here defined as belonging to the McMurdo Volcanic Group (Table A.I). "Ross Embayment" is an informal but widely used designation to describe the combined area covered by the Ross Sea and the Ross Ice Shelf.

They represent one of the most extensive alkali volcanic provinces in the world, comparable in extent to the alkali volcanic rocks in the East African rift systems. The term McMurdo Volcanics (Group) was introduced by *Harrington* [1958] to describe late Cenozoic volcanic rocks of Victoria Land, islands in the western Ross Sea, the Balleny Islands, and Scott Island. This definition excluded Sheridan Bluff and Mount Early, two small volcanic centers situated near Scott Glacier, in the central Transantarctic Mountains. However, the age, setting, and character of the rocks from these two centers are similar to those of the McMurdo Volcanic Group rocks, and here they are included in this stratigraphic unit. The Balleny Islands, on the other hand, are situated on oceanic crust and have no geographic or tectonic relationship to the other McMurdo Volcanic Group rocks, and are here formally excluded from the group. They are described in section F. *Nathan and Schulte* [1968] recommended formal recognition of the McMurdo Volcanic Group, and this usage has generally been followed, although *Hamilton* [1972] used the term Ross Sea petrographic province.

Kyle and Cole [1974] subdivided the McMurdo Volcanic Group into several informal provinces: Hallett, Melbourne, and Erebus (and the now excluded Balleny volcanic province). The provinces were defined on the basis of spatial distribution and tectonic setting. Subsequent work (discussed below) has suggested that petrologic differences may also exist between the provinces.

Volcanic centers within the McMurdo Volcanic Group are diverse in form and structure. They range from small scoria cones and flows covering only a few tens of square meters, to the enormous

Copyright American Geophysical Union

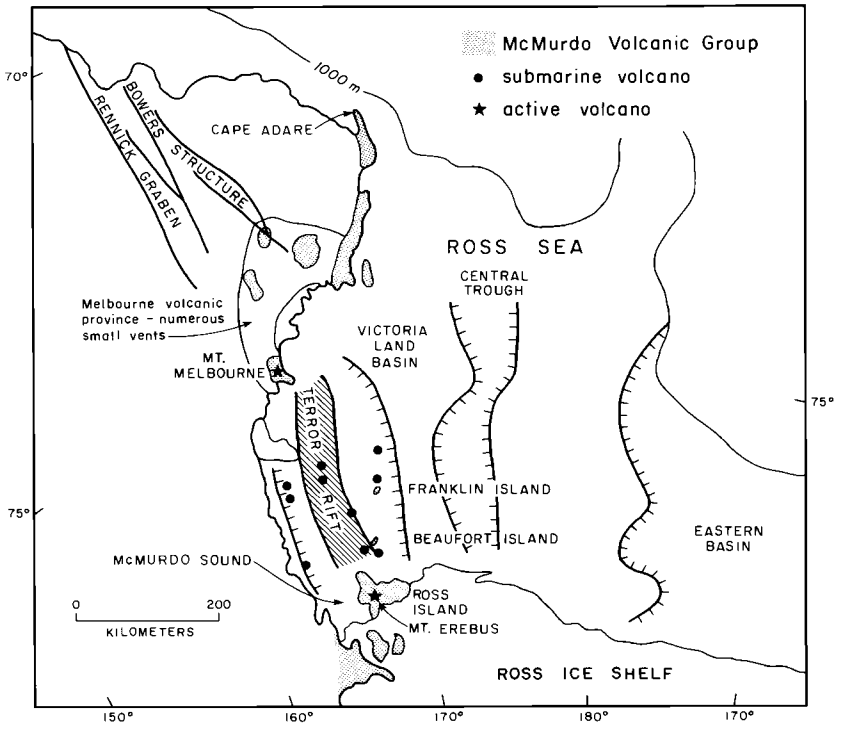

Fig. A.I. Simplified tectonic map of the western Ross Embayment, based on work by *Kyle and Cole* [1974], *Cooper et al.* [1987], *Gair et al.* [1969], *Warren* [1969], and *Wright-Grassham* [1987], showing the distribution of McMurdo Volcanic Group rocks along the western margin of the Ross Embayment.

bulk of Mount Erebus (estimated volume, 1800 km^3 [*Dibble et al.*, 1984]), which dominates Ross Island. Mount Melbourne and Mount Erebus are active volcanoes, and many other centers should be considered dormant.

Mount Erebus, the southernmost active volcano in the world, has a permanent convecting anorthoclase phonolite lava lake in its 3794-m-high summit crater. Small Strombolian eruptions occur frequently every day, but occasionally, as in late 1984, larger, more sustained Strombolian eruptions occur, ejecting bombs up to 10 m long to distances over 1.5 km from the eruptive vent.

In general, three major volcanic forms can be recognized: (1) basaltic shield volcanoes, over 3000 m high; (2) stratovolcanoes, dominantly trachytic or phonolitic in composition; and (3) small, isolated, dominantly basaltic scoria cones and lava flows. In some cases, basaltic volcanoes coalesce along linear fractures to form elongate piles ranging in size from 20 × 4 km (Hut Point Peninsula (see individual volcano description (IVD) A.18)) to 78 × 20 km (Adare Peninsula (see IVD A.1)). Commonly, the basic shields and felsic stratovolcanoes are dotted with late-stage parasitic centers. These range from basaltic scoria cones to endogenous domes of the most evolved compositions, including phonolite, peralkaline trachyte, oversaturated *Q*-trachyte, and peralkaline rhyolite.

Aerial and marine magnetic surveys of the western Ross Sea show numerous magnetic anomalies [*Behrendt et al.*, 1987; *Bosum et al.*, 1989]. The anomalies have a large range in size, from those associated with small recent submarine volcanoes (Ross Sea (see IVD A.12)) to anomalies indicative of large intrusive bodies exceeding 200 × 40 km.

So far, no submarine volcanoes have been recognized south of the Erebus volcanic province, because magnetic surveys have been limited to surface traverses and rare aerial flight lines. Considering the great extent of volcanism between southern McMurdo Sound and Cape Adare in the Hallett volcanic province (Figure A.I) it is likely that other volcanic centers should exist between the Erebus volcanic province and the two isolated centers at Sheridan Bluff (see IVD A.26) and Mount Early (see IVD A.27), near the south pole.

Copyright American Geophysical Union

TABLE A.I*a*. Volcanoes of the Hallett Volcanic Province of the McMurdo Volcanic Group

IVD	Volcano	Volcano Type	Rock Types	Age	Comments
A.1	Adare Peninsula	Elongate complex of overlapping shield volcanoes.	Predominantly alkalic basalts with phonolite and alkali trachyte.	0–13 Ma	Consists of five major vents. Mainly subaerial eruptions. Best studied of Hallett volcanic province volcanoes.
A.2	Hallett Peninsula	Elongate complex of overlapping shield volcanoes.	Predominantly basaltic with trachytes.	<10 Ma	Consists of three major vents. Mainly subaerial flows and pyroclastic rocks.
A.3	Daniell Peninsula	Elongate complex of overlapping shield volcanoes.	Poorly known, probably mainly basaltic.	Unknown	Consists of at least two major shield volcanoes. Poorly studied.
A.4	Coulman Island	Elongate complex of overlapping shield volcanoes.	Mainly basaltic (alkali basalt, basanite, tephrite) with lesser intermediate differentiates and trachyte.	<10 Ma	Consists of at least two major shield volcanoes. One large caldera known. Poorly studied with only one K-Ar date of 7 Ma.
A.5	Possession Islands	Eroded remnants of unknown number of volcanic vents.	Basanite and hawaiite.	Unknown	Consists of nine small islands and stacks.

TABLE A.I*b*. Volcanoes of the Melbourne Volcanic Province of the McMurdo Volcanic Group

IVD	Volcano	Volcano Type	Rock Types	Age	Comments
A.6	Malta Plateau	Felsic lavas and pyroclastic rocks with associated alkaline intrusions.	Peralkaline trachytes and melarhyolites predominant but basaltic rocks common.	6–25 Ma	Major volcanic complex probably consisting of several major explosive silicic vents and numerous basaltic vents.
A.7	The Pleiades	Small stratovolcano with numerous scoria cones, domes, and flows.	Mainly trachytic, often peralkaline. Two differentiation lineages recognized.	<1 Ma	Youngest of the major trachytic centers in the Melbourne volcanic province. May have had Holocene eruptive activity.
A.8	Mount Overlord	Large stratovolcano with numerous parasitic vents.	Mainly felsic lavas and pyroclastics. Two differentiation lineages recognized.	7–8 Ma	Welded fall deposits and ignimbrites around base indicate extensive explosive activity. May be source of ignimbrites.

Copyright American Geophysical Union

TABLE A.*Ib*. (continued)

IVD	Volcano	Volcano Type	Rock Types	Age	Comments
A.9	Vulcan Hills	Eroded high-level sub-volcanic complex.	Gabbro intrusive rocks cut by dikes of hawaiite, mugearite, and trachyte.	Unknown, >10 Ma?	All samples have normative *hy*; evolved rocks contain *Q*.
A.10	Mount Melbourne	Undissected stratovolcano atop a widespread volcanic field of subglacial and subaerial volcanoes.	Wide range comprising three lineages. Includes alkali basalt, basanite, tephrite, hawaiite, trachyte.	Summit lavas, <0.5 Ma; other, <5 Ma	Lavas more saturated, lower in Na_2O and higher in K_2O than other McMurdo Volcanic Group rocks.
A.11	Local Suite Basaltic Rocks	Small basaltic cones, flows, and pyroclastic deposits.	Mainly basaltic.	Unknown, <10 Ma?	These small basaltic vents are widespread throughout northern Victoria Land; over 40 vents are known.

TABLE A.*Ic*. Volcanoes of the Erebus Volcanic Province of the McMurdo Volcanic Group

IVD	Volcano	Volcano Type	Rock Types	Age	Comments
A.12	Ross Sea	Submarine, defined by seismic reflection profiles and magnetic anomalies.	Unknown	Unknown	Eight magnetic anomalies, recognized as volcanic.
A.13	Franklin Island	Island remnant of shield volcano	Basanite	<7 Ma	
A.14	Beaufort Island	Island remnant of stratovolcano.	Tephrite and phonotephrite.	Unknown	
A.15	Mount Bird	Basaltic shield volcano with parasitic cones.	Mainly basaltic with phonolitic and basanitic parasite cones.	3–5 Ma	The shield is poorly exposed. A coastal strip at Cape Bird shows general stratigraphy.
A.16	Mount Terror	Basaltic shield surmounted by parasitic cones and domes.	Mainly basanite with phonolite domes.	<15 Ma	Extensive exposure on the eastern flank has never been examined.
A.17	Mount Erebus	Composite phonolite volcano with parasitic vents.	Predominantly anorthoclase phonolite, but intermediate differentiates and basanites occur.	<1 Ma	Currently active with a persistent convecting lava lake of phonolite magma which undergoes daily Strombolian eruptions. The lavas define the Erebus lineage consisting of a differentiation suite from basanite to phonolite.

Copyright American Geophysical Union

TABLE A.1c. (continued)

IVD	Volcano	Volcano Type	Rock Types	Age	Comments
A.18	Hut Point Peninsula	20-km-long, 4-km-wide peninsula of coalescing basanite scoria cones. One phonolite cone.	Mainly basaltic (basanite, tephrite, hawaiite) but with intermediate differentiates (mugearite, benmoreite) and phonolite.	<2 Ma	Three drill holes drilled by the Dry Valley Drilling Project (DVDP) penetrated 381 m of the section. The DVDP lineage is defined by the suite of lavas ranging from basanite to phonolite.
A.19	White Island, Black Island, Brown Peninsula	Basaltic shield volcanoes and cinder cones, phonolite flows, plugs and domes.	Basanite to phonolite. Rare alkali basalt.	11 Ma, <5 Ma	Black Island had an early eruptive episode at 11.2 Ma, otherwise most activity is <5 Ma.
A.20	Minna Bluff	Peninsula of coalescing basalt shield volcanoes, cinder cones, and lava flows.	Basanite common, also intermediate differentiates and phonolite.	11–7 Ma	Extensive exposure in cliffs has been investigated only in a reconnaissance manner.
A.21	Mount Discovery	Composite central volcano with parasitic vents.	Mainly benmoreite and phonolite with late basanites and hawaiite.	<6 Ma	
A.22	Mount Morning	Eroded trachytic subvolcanic complex overlain by large central volcano with parasitic vents.	Basanite, trachybasalt, phonolite, trachyte, peralkaline trachytes.	<19 Ma	Subvolcanic complex is older (12–19 Ma) and buried in part by central volcano (<2 Ma).
A.23	Mason Spur	Deeply eroded trachytic volcanic complex, overlain by younger scoria cones.	Variable but predominantly peralkaline trachyte, with basanite.	6–13 Ma	Two distinct stratigraphic episodes of volcanism.
A.24	Royal Society Range	Small cinder cones and lava flows.	Mainly basanite.	<3 Ma	Many scattered cones have not been examined in any detail. Contain important xenoliths.
A.25	Taylor and Wright valleys	Small cinder cones and lava flows.	Mainly basanite.	<5 Ma	Important in establishing glacial history of southern Victoria Land.

Copyright American Geophysical Union

TABLE A.I*d*. Other Volcanoes of the McMurdo Volcanic Group in Southernmost Ross Embayment

IVD	Volcano	Volcano Type	Rock Types	Age	Comments
A.26	Sheridan Bluff	Subglacial (?) hyaloclastite overlain by lava flows.	Mildly alkaline basalt and olivine tholeiite.	18 Ma	Only known occurrence of tholeiitic rocks in McMurdo Volcanic Group.
A.27	Mount Early	Subglacial cone.	Alkaline olivine basalt.	16 Ma	Displays elements of moberg stratigraphy found in Icelandic subglacial eruptions.

The McMurdo Volcanic Group is stratigraphically important because it represents the first terrestrial geologic record in the Transantarctic Mountains since the Jurassic Ferrar Supergroup tholeiites were erupted and emplaced [*Kyle et al.*, 1981]. The oldest dated McMurdo Volcanic Group lava sample from Sheridan Bluff (A.26) is 19.8 Ma, with alkaline intrusions in the Melbourne volcanic province ranging back to 25 Ma (e.g., Malta Plateau (see IVD A.6)). Cores from drill holes in McMurdo Sound, however, contain volcanic sand which has been correlated with the McMurdo Volcanic Group [*Barrett and McKelvey*, 1986]. Paleontological data show that this volcanogenic sedimentary rock may be older than 35 Ma, indicating that volcanism commenced much earlier than dated terrestrial samples would suggest [*Barrett et al.*, 1986; *Gamble et al.*, 1986] (see summary A.III for an expanded discussion).

The distribution of the McMurdo Volcanic Group along the western Ross Embayment is tectonically controlled. Two major tectonic elements are present in the area: the Transantarctic Mountains and the Ross Embayment. The Transantarctic Mountains are a major uplifted and block-faulted range which extends over 3000 km across Antarctica. Average uplift rates of 100 m/m.y. have been inferred from fission-track studies [*Gleadow and Fitzgerald*, 1987]. Uplift started at about 50 Ma. A major crustal suture separates the Transantarctic Mountains from the Ross Embayment [*Fitzgerald et al.*, 1986], with displacements which may exceed 12 km. The suture zone is marked by rapid crustal thinning from 40 km beneath the Transantarctic Mountains to less than 25 km beneath McMurdo Sound and Ross Island [*McGinnis et al.*, 1985].

The Ross Sea is composed of three major rift basins. The Victoria Land basin, the westernmost of the three, is well characterized by multichannel seismic data [*Cooper et al.*, 1987]. The younger of the two episodes of extension recognized within this basin is represented by a major graben termed the Terror rift (Figure A.I), at either end of which are the two active volcanoes, Mount Melbourne and Mount Erebus. Timing of extension associated with the Terror rift is poorly constrained, but it could correlate with the onset of volcanism at about 35 Ma, or even earlier. The western Ross Sea is obviously still tectonically active, with marine seismic profiles showing evidence of recent fault traces cutting surface sediments [*Cooper et al.*, 1987]. A major anomaly in the area is its aseismicity [*Johnston*, 1987], especially for tectonic earthquakes with magnitudes greater than 5 on the Richter scale. Microseismic activity is associated with the active volcanism of Mount Erebus [*Dibble et al.*, 1984].

Petrologic details of rocks from the three volcanic provinces are discussed in more detail in the province summaries. However, it is worth highlighting some of the differences which support the initial subdivision of the McMurdo Volcanic Group into the three volcanic provinces.

The Hallett volcanic province is dominated by four large elongate piles of predominantly basaltic rocks. These apparently were erupted from vents or fissures whose distribution is controlled by the

Copyright American Geophysical Union

major crustal suture bounding the Transantarctic Mountains and Ross Embayment. Differentiated lavas occur in the province and appear to be dominated by phonolitic compositions.

The Melbourne volcanic province is situated both on the bounding fault(s) separating the Transantarctic Mountains from the Ross Sea and, predominantly, on the mountains themselves. NE-SW trending faults associated with the Rennick and Bowers grabens may control the distribution of the vents [*Kyle and Cole,* 1974]. Structures bounding the block-faulted Transantarctic Mountains also seem to control the distribution of volcanic rocks in places such as The Pleiades (see IVD A.7), where large stratovolcanoes may be situated at the intersection of major fracture systems. Differentiated lavas, particularly trachytes and peralkaline trachyte/rhyolite, volumetrically exceed the basic rocks, the trachytes forming large stratovolcanoes and possibly caldera complexes. Although basanites occur throughout the Melbourne volcanic province as small isolated scoria cones and lava flows, the degree of undersaturation of the parental basalt for the stratovolcanoes was less. Peralkalinity is better developed in this province than elsewhere in the McMurdo Volcanic Group. The extreme and extensive evolution in magma composition may be a function of the greater crustal thickness, which allowed the development of larger crustal magma chambers.

The Erebus volcanic province is located at the southern end of the Terror rift. The area is marked by a flexure in the trend of the Transantarctic Mountains (Figure A.I), where several fault zones bounding the Transantarctic Mountains may intersect. Volcanic activity is divisible into two phases. From 19 to about 10 Ma, trachytic rocks similar to those found in the Melbourne volcanic province were dominant. However, most activity has occurred in the last 10 m.y. and is almost exclusively basanitic to phonolitic. Overall, basic rocks are dominant in this younger phase, but phonolite forms the bulk of Mount Erebus, the largest, highest, and recently most active volcano in the Ross Sea area.

In summary, the three volcanic provinces described in sections A.I–A.III have their own unique tectonic setting, which controlled the nature and distribution of the volcanoes. Petrologic differences also exist, and these are controlled in part by tectonic setting, crustal thickness, the degree of partial melting of the mantle source for the basalts, and the development of inferred large upper crustal magma chambers where fractionation and crustal interaction occurred. Overall, the whole McMurdo Volcanic Group is alkaline, and the basalts are all undersaturated; the only exception is the occurrence of tholeiitic basalt in the southernmost exposed McMurdo Volcanic Group rocks at Mount Early (see IVD A.27).

Twenty-seven volcanic centers within the McMurdo Volcanic Group are described here. The centers vary from small single vents such as Mount Early (see IVD A.27) to large volcanic fields composed of numerous eruptive vents such as Mount Melbourne (see IVD A.10). The 27 centers have been divided into four sections: the Hallett volcanic province (A.I), the Melbourne volcanic province (A.II), the Erebus volcanic province (A.III), and vents in the southernmost Ross Embayment (A.IV).

Acknowledgments

Jim Cole, David Elliot, and Janet Thomson reviewed the whole McMurdo Volcanic Group section. Their helpful suggestions and constructive criticism are much appreciated. Continuous support from the Division of Polar Programs is gratefully acknowledged.

Copyright American Geophysical Union

[redacted]

[redacted]

[redacted]

[redacted]

Fig. A.1.1. Distribution of McMurdo Volcanic Group rocks in the Hallett volcanic province.

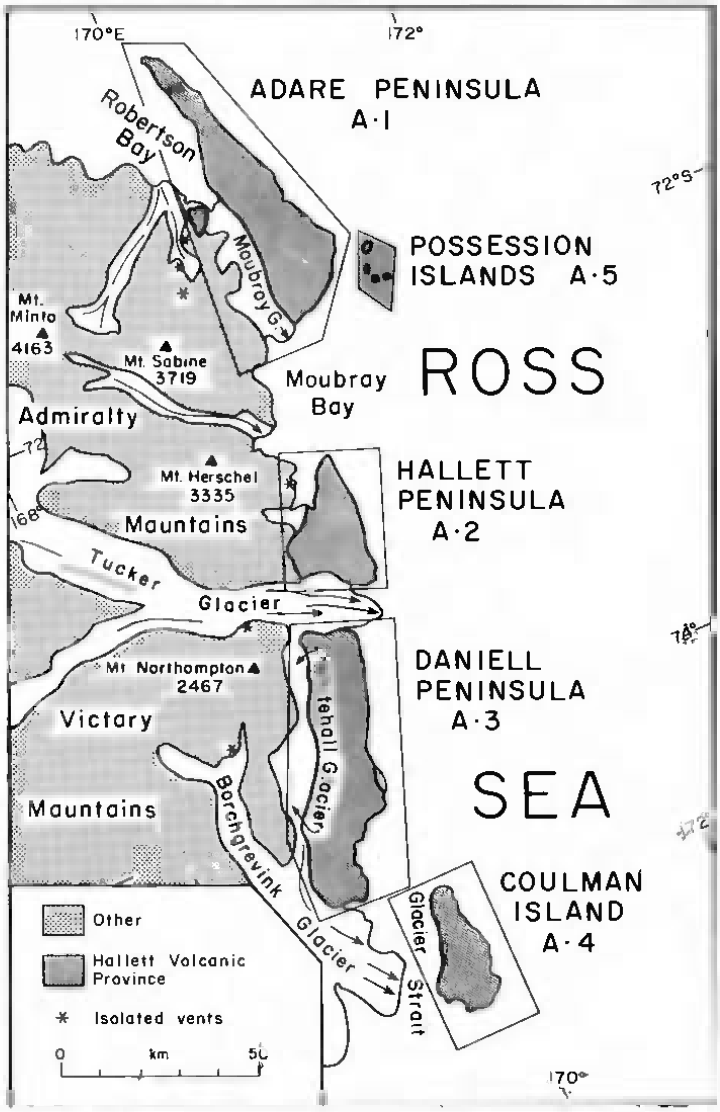

[redacted]

Copyright American Geophysical Union

Copyright American Geophysical Union

ranges, some more than 3000 m high, slope steeply down to the continental shelf upon which the Hallett province volcanic piles are built. Much of this shelf lies about 500 m below sea level, although bedrock rises on the east side of Daniell Peninsula where granodiorite is exposed beneath the volcanic rocks.

The major volcanoes are located at the boundary between the Ross Sea and the Transantarctic Mountains of northern Victoria Land. This boundary has been postulated as being an early Paleozoic suture between convergent plates [*McGinnis et al.*, 1983, 1985]. Large displacement normal faults along it may have provided conduits for the axial fissure zones of the four major volcanic complexes in the Hallett province. *Kyle and Cole* [1974] referred to this fissure zone as the "Hallett Fracture." Seismic work necessary to characterize subsurface faults has not yet been performed, and surficial mapping along the western edges of Hallett and Adare peninsulas has revealed only minor, small displacement faulting [*Jordan*, 1981]. Geophysical studies in south and central Victoria Land have indicated displacements of as much as 12 km along analogous north-south trending normal faults [*Fitzgerald et al.*, 1986; *Cooper et al.*, 1987].

An aeromagnetic survey over the Ross Sea and adjacent Transantarctic Mountains of an area south of Coulman Island was made by the German GANOVEX IV expedition in 1984–1985. Preliminary results were presented at the Fifth Antarctic Earth Sciences Symposium in Cambridge [*Bosum et al.*, 1989], and detailed results will be published in a special issue of *Geologisches Jahrbuch*. Several large and extensive magnetic anomalies, which may be related to older, buried McMurdo Volcanic Group intrusive rocks, occur in the western Ross Sea, bordering the Hallett volcanic province.

Volcanic Geology

Adare, Hallett, and Daniell peninsulas and Coulman Island each consist of two or three overlapping elliptical shield volcanoes erupted along north-south trending central fissures (Figure A.I.2). Each volcanic pile has a smooth, undissected upper surface bounded by cliffs. The degree of erosion varies among the four complexes, and on Adare and Hallett peninsulas the entire western slopes of the shields and portions of the axial crests have been removed. Daniell Peninsula and Coulman Island are much less eroded. The cliffs bounding all four complexes are probably a combination of wave-cut cliffs and cirque headwalls; north-south faulting may also have contributed to their development.

Lava flows (individually 1–200 m thick), related breccias, and subordinate pyroclastic deposits form the bulk of the four shield volcano complexes. The more mafic lavas tend to form regular subhorizontal, breccia-poor sequences of many thin (1–15 m) flows or flow units [*Hamilton*, 1972, Figure 26*b*], whereas more evolved lavas form irregular thick, chaotic, breccia-rich sequences ("marble cake" of *Hamilton* [1972, Figure 26*a*]). Breccias associated with most of the lavas are angular, holocrystalline to glassy, clast supported, and matrix-poor; some have evidence of welding and/or hematitic reddening. Conversely, other flows are associated with glassy, matrix-rich breccias, and a few of them show pillowed bases. Breccias of both types are commonly palagonitized, cemented, or zeolitized, and many appear yellow-brown as a result of marginal alteration of clasts or surficial coatings of secondary minerals.

A variety of pyroclastic deposits are exposed as inclined layers, irregular bodies, cinder cones, and tuff cones. A number of uneroded cinder cones occur near the crests of each of the four major shield complexes, and spectacular cross-sectional exposures of cinder cones and tuff cones buried beneath lava flows are present near the bases of the eastern cliffs of Adare and Hallett peninsulas.

Many of the pyroclastic deposits are distinctive subaerial Hawaiian or Strombolian lapilli tuffs, composed primarily of well-sorted sideromelane droplet lapilli and/or tachylitic cinders. Many of these units show clear evidence of welding or deuteric hematitic oxidation, and some contain reddened, fusiform Strombolian bombs with bread-crust-like surfaces. Palagonitic and zeolitic alteration of these lapilli tuffs is common. Associated with the Hawaiian and Strombolian units are less abundant subaerial or shallow-water Surtseyan deposits composed of poorly sorted, variably bedded tuffs and lapilli tuffs. Some of these deposits contain accretionary lapilli, and one unit on Possession Island (see IVD A.5) also contains beach pebbles, suggesting a littoral eruptive environment. Thick sections of hyaloclastite (glass-rich tuff

Copyright American Geophysical Union

breccia) are rare in the province. Limited amounts of hyaloclastite pillow breccias have been reported from the bases of the lowermost exposed lava flows around Robertson Bay, along the western shoreline of Adare Peninsula [*Jordan*, 1981].

Dikes are common in the province, particularly in cliff exposures beneath vent areas. In some cases, anastomosing dike swarms constitute more than 70% of the exposure. Some intrusions within pyroclastic deposits form irregular to rounded pods, in many cases radially jointed [*Hamilton*, 1972, Figure 30*c*]. The country rock surrounding the intrusions and dense dike swarms is variably discolored by hydrothermal alteration. The alteration obscures the primary volcanic features, such as lava flow boundaries.

Eruptive Environments

There are two conflicting interpretations of the eruptive environments of the volcanoes making up the Hallett volcanic province. *Hamilton* [1972] suggested that they were erupted predominantly into a subglacial environment during a period of expansion of Antarctica's continental ice sheet. He interpreted the large volumes of yellow-brown volcaniclastic deposits in the interiors of the volcanoes as subglacially erupted palagonitic tuff breccias and pillow breccias. Subaerial rocks were believed to be limited to thin outermost carapaces, analogous to the table mountains of Iceland [*Jones*, 1969]. Glacial erratics mantling the northern end of Adare Peninsula were cited as further evidence of a high-standing continental ice sheet.

LeMasurier et al. [1983] and *McIntosh and Gamble* [1989] believed that the volcanoes of the Hallett volcanic province formed under predominantly subaerial conditions. Their evidence included the high proportion of lava flows in most exposed sections of the Hallett volcanic piles and also that most of the yellow-brown volcaniclastic deposits appear to be glass-poor, clast-supported autoclastic breccias cogenetic with unbrecciated lava flows. The character of many of these breccias has been obscured by zeolitization and cementation, but some clearly show welding and/or hematitic reddening, characteristic of subaerial deuteric oxidation. The pillowed bases and glassy, matrix-rich basal breccias of other lavas are interpreted as products of interaction with limited amounts of ice or snow in a periglacial environment.

Many of the pyroclastic deposits in the Hallett province volcanoes are also clearly subaerial. Most are distinctive, subaerially erupted Hawaiian or Strombolian deposits. Others represent Surtseyan tuff-cone deposits erupted and accumulated in subaerial or shallow-water environments.

Significant amounts of characteristic subglacial deposits are limited to the northern end of Adare Peninsula, where pillows and palagonitic pillow breccias form the basal part of the lowest lavas exposed around Robertson Bay [*Jordan*, 1981]. In addition, exposures along the northeasternmost cliffs of Cape Adare reveal an apparent glacial unconformity [*LeMasurier et al.*, 1983] and a tuff breccia containing glacial erratics [*Priestley*, 1923]. These features, together with the erratics which locally mantle the surface, apparently record synvolcanic and postvolcanic advances of a regional ice sheet derived from the west.

Chronology

Chronologic data are lacking from much of the Hallett volcanic province. *Hamilton* [1972] (see *Armstrong* [1978] for revised values) gave K-Ar dates for Hallett Peninsula (5.49 ± 0.12, 6.6 ± 0.4 Ma), Coulman Island (7.2 ± 0.5 Ma), and Adare Peninsula (2.27 ± 0.5 Ma). *Kreuzer et al.* [1981] reported 12 K-Ar dates from a small area on the western slope of the Adare Peninsula. These range from 6.77 to 13.2 Ma, excluding one deviant date of 1.14 Ma (Figure A.I.3).

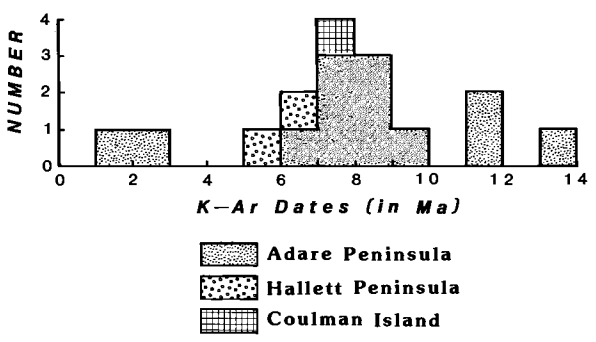

Fig. A.I.3. Histogram showing K-Ar dates from the Hallett volcanic province. See Figures A.1.1, A.2.1, and A.4.1 for sample locations.

Copyright American Geophysical Union

The dates given by *Kreuzer et al.* [1981] show that the duration of volcanism that built up the Adare Peninsula spanned a period of at least 6.5 m.y. Undissected cinder cones along the crests of the major volcanic piles have been interpreted by *Hamilton* [1972] as evidence of Holocene activity. However, youthful-looking scoria cones elsewhere in the McMurdo Volcanic Group have shown a wide range in age.

Petrology and Geochemistry

Petrographic descriptions and geochemical analyses of assorted samples from the Hallett volcanic province are given by *Harrington et al.* [1967] and *Hamilton* [1972]. Additional analytical data have been collected by the authors and are summarized in the individual volcano descriptions. Unfortunately many of the analyzed samples are hydrated and/or altered. In the following discussion, all samples with greater than 2.5 wt % loss on ignition (LOI) or $H_2O^+ + H_2O^- + CO_2$ were eliminated, leaving 54 analyses, which are plotted in Figure A.I.4.

The overall chemical variation in the Hallett volcanic province lavas is surprisingly small considering the 250-km distance over which they are spread and a possible 13-m.y. activity. Ultrabasic ($SiO_2 < 45$ wt %) and basic (SiO_2 45–52 wt %) rocks predominate and are mainly basanite, alkali basalt, and hawaiite (Figure A.I.4). On the Hallett Peninsula there is a well-defined trend of basanite-hawaiite-mugearite-benmoreite-trachyte, suggesting that simple differentiation has occurred. Evolved lava types, namely phonolite and trachyte, occur on the Adare Peninsula.

Hallett volcanic province rocks are sodic. All ultrabasic and basic analyses have a Na_2O/K_2O ratio greater than 2 (Figure A.I.5). The phonolites and trachytes are slightly more potassic, but none have a Na_2O/K_2O ratio less than 1.

Overall, the lavas show well-defined fractionation trends in SiO_2 variation diagrams (Figure A.I.6), which are consistent with evolution by fractional crystallization. Although data are scarce, it does appear as if there is a weakly undersaturated lineage of basanite to trachyte and a strongly undersaturated lineage from basanite to phonolite.

There are insufficient high-quality trace-element data to test the fractionation models. *Hamilton* [1972] gave semiquantitative spectroscopic analyses which indicate considerable scatter in trace-element compositions. There is plenty of scope for detailed petrologic studies in the province, if access to the rocks can be gained.

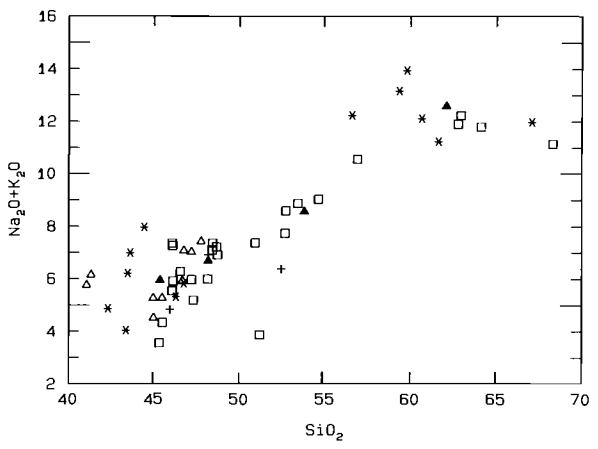

Fig. A.I.4. Summary alkali ($Na_2O + K_2O$) versus silica diagram (in weight percent) for the Hallett volcanic province. All analyses are recalculated to 100% volatile-free. Only samples with <2.5% loss on ignition or $H_2O^+ + H_2O^- + CO_2$ are plotted. Adare Peninsula (asterisks); Hallett Peninsula (squares); Possession Islands (open triangles); Daniell Peninsula (pluses); and Coulman Island (solid triangles).

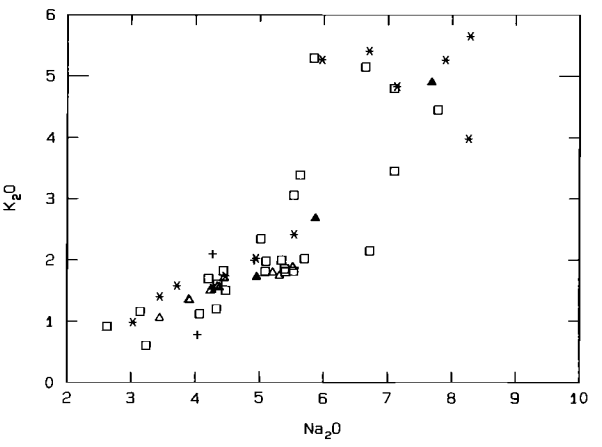

Fig. A.I.5. Summary K_2O versus Na_2O plot (both in weight percent) for the Hallett volcanic province. See Figure A.I.4 caption for symbols and sample selection criteria.

Copyright American Geophysical Union

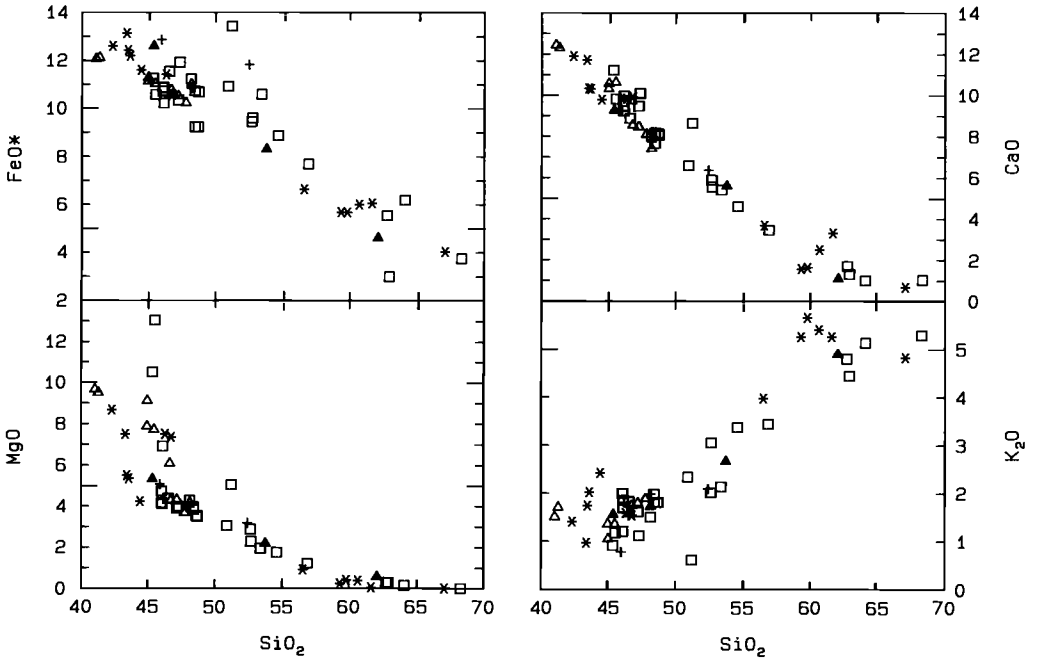

Fig. A.I.6. Representative silica variation diagrams of Hallett volcanic province rocks. All plots are in weight percent. See Figure A.I.4 caption for symbols and sample selection criteria.

Acknowledgments

Fieldwork in the Hallett volcanic province was undertaken from the U.S.C.G. icebreakers *Glacier* and *Polar Sea*. We thank the crews, especially the helicopter pilots, for their efforts. Fieldwork was supported by National Science Foundation, Division of Polar Programs, grants to P.R. Kyle and W.E. LeMasurier. Nick Banks, Pam Ellerman, and Anne Wright assisted in the field. Comments and suggestions from Gerhard Wörner were helpful.

Copyright American Geophysical Union

A.1. Adare Peninsula

Type of volcano: Elongate complex of overlapping shield volcanoes.

Individual volcanoes: Five major vents, more than seven cinder cones, more than five tuff rings.

Location: Northeastern coast of northern Victoria Land (71°37′S, 170°33′E); northernmost of the four major volcanic piles in the Hallett volcanic province.

Height above sea level: 2083 m.

Estimated volume: 550 km^3 above sea level, total of 2000 km^3.

Evidence of Holocene activity: None.

Authors of report: W.C. McIntosh and P.R. Kyle.

Date of report: January 1987.

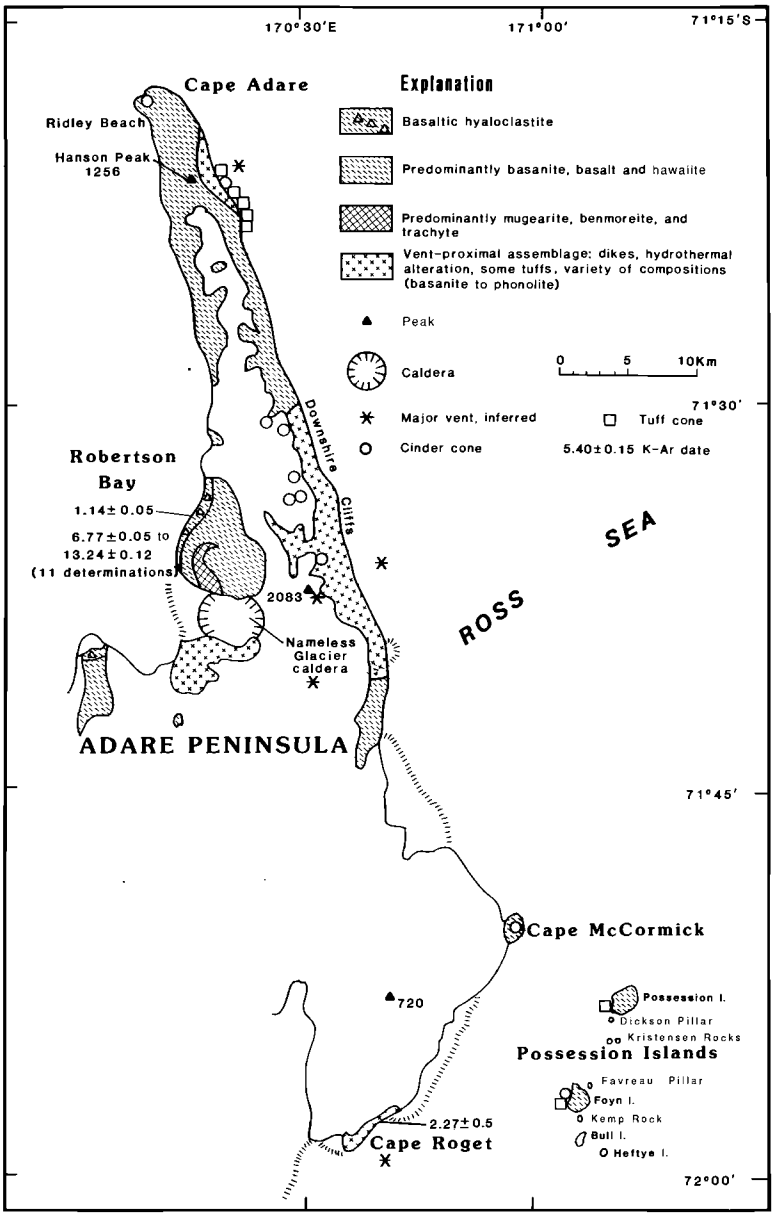

Fig. A.1.1. Generalized reconnaissance geologic map of Adare Peninsula and Possession Islands.

Copyright American Geophysical Union

Fig. A.1.2. Aerial view looking north-northeast across Robertson Bay to the northernmost 50 km of Adare Peninsula. Right of center is the 2083-m-high summit of an unnamed shield volcano. In the middle foreground (right) is the Nameless Glacier caldera (Figure A.1.1), bounded on the north by an extensive area of predominantly basaltic lavas. The caldera is 5 km in diameter. (U.S. Navy photograph, TMA 866 F33 013.)

Fig. A.1.3. Aerial view looking northward, showing the southern end of Adare Peninsula and the Possession Islands. In the left distance is Cape Adare. Cape McCormick and Cape Roget (Figure A.1.1) are slightly right of center. The 2083-m-high shield volcano dominating the southern end of the peninsula is unnamed. (U.S. Navy photograph, TMA 1282 F31 135.)

Form and Structure

Adare Peninsula (Figures A.1.1–A.1.3) consists of a broad domical shield complex in the south, separated by a 500-m-high saddle from a narrow northern extension around Hanson Peak. Its eastern edge is bounded by 600- to 2000-m-high cliffs, but its western margin is less abrupt, and cliffs, where present, do not exceed 1000 m in height. The general shape of Adare Peninsula suggests that it represents the western slope of a formerly larger edifice and that erosion has removed the entire eastern portion and the axial fissure zone. This interpretation is supported by bathymetric data, which show Adare Peninsula to be the westernmost quarter of a 20- to 50-km-wide submarine high.

There is a major volcanic center in the central part of Adare Peninsula, as shown by the topography of the undissected upper constructional surface and by cliff exposures of numerous dikes and associated hydrothermal alteration. This volcanic center probably included at least five distinct vents: a caldera located in the depression now filled by Nameless Glacier, two vents along the present crest of Adare Peninsula, and three eroded vents located east of the peninsula [*Hamilton*, 1972]. A major volcanic center,

Copyright American Geophysical Union

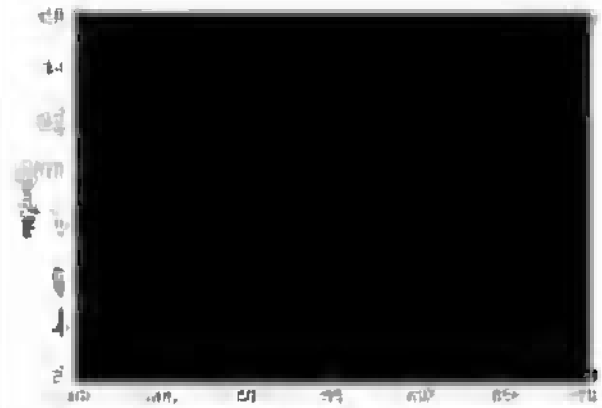

Copyright American Geophysical Union

analytical evidence of alteration (H_2O^+ and CO_2, >2.0%), in agreement with petrographic observations of secondary mineralization and with field observations of secondary discoloration in subvent dike swarm areas.

Chronologic Data

Kreuzer et al. [1981] reported K-Ar dates of 12 samples from the western edge of Adare Peninsula, near the south end of Robertson Bay. With the exception of one grossly deviant date (1.14 ± 0.05 Ma) they ranged from 6.77 ± 0.05 to 13.24 ± 0.12 Ma. *Armstrong* [1978] obtained a K-Ar date of 2.27 ± 0.5 Ma (corrected to new decay constant) from Cape Roget.

TABLE A.1.1. Representative Chemical Analyses of Rocks From Adare Peninsula

	1	2	3
SiO_2	43.06	58.10	65.88
TiO_2	3.43	0.16	0.16
Al_2O_3	15.90	18.57	15.18
Fe_2O_3*	13.67	6.18	4.40
MnO	0.23	0.22	0.13
MgO	5.44	0.24	0.02
CaO	10.22	1.53	0.64
Na_2O	4.43	7.73	7.01
K_2O	1.72	5.16	4.74
P_2O_5	0.92	0.05	0.03
LOI	0.65	1.63	0.86
Total	99.67	99.57	99.05
Ba	614	902	14
Cr	46	5	6
Cu	55	15	13
Ga	21	26	43
Nb	126	235	562
Ni	29	6	12
Pb	2	14	39
Rb	49	179	304
Sr	998	134	11
Th	10	25	56
V	259	2	2
Y	40	38	150
Zn	113	118	265
Zr	351	782	1607

All samples collected by A.C. Wright. XRF analyses by P.R. Kyle. LOI, loss on ignition.

* Total Fe expressed as Fe_2O_3.

1. AW82209. Basanite, Cape Adare.
2. AW82213. Trachyte flow, Cape Adare.
3. AW82211G. Trachyte dike, Cape Adare.

Extent of Knowledge

Adare Peninsula is the best studied of the four major volcanic piles of the Hallett volcanic province. Early explorers wintered at Ridley Beach and studied rocks in the Robertson Bay area [*Prior*, 1902; *Ferrar*, 1907; *Priestley*, 1923; *Smith*, 1959, 1964]. *Smith* [1959] gave detailed petrographic descriptions of samples collected by Priestley and others in 1911; included were chemical analyses of rock samples (Figure A.1.5) and an anorthoclase separated from a sanidinite. *Harrington et al.* [1967] briefly described some features of the geology. *Hamilton*'s [1972] reconnaissance study of the entire Hallett volcanic province included nine sample localities on Adare Peninsula. *LeMasurier et al.* [1983] visited Ridley Beach and two new localities at the base of Downshire Cliffs. *Jordan* [1981] made a relatively detailed study of that part of Adare Peninsula adjacent to southern Robertson Bay.

The best exposed and least studied portions of Adare Peninsula are its east facing cliffs. Access to these cliffs is difficult because of their steepness and height (up to 2000 m). Furthermore, the sea ice below the cliffs breaks up relatively early each season, and safe landing areas for boats or helicopters are limited.

Bibliography

Armstrong, 1978
David et al., 1896
Ferrar, 1907
Hamilton, 1965, 1967*a,b*, 1972
Harrington et al., 1967
Jordan, 1981
Kreuzer et al., 1981
LeMasurier et al., 1983
Priestley, 1914, 1923
Prior, 1902
Rastall and Priestley, 1921
Smith, 1959, 1964
Wilson, 1908

Copyright American Geophysical Union

A.2. Hallett Peninsula

Type of volcano: Elongate complex of overlapping shield volcanoes.

Individual volcanoes: Mount Harcourt, at least three shield volcanoes, three cinder cones, and more than four tuff cones.

Location: Northeastern coast of northern Victoria Land (72°26′S, 170°12′E).

Height above sea level: 1770 m.

Estimated volume: 330 km^3 above sea level, total of 700 km^3.

Evidence of Holocene activity: None.

Authors of report: W.C. McIntosh and P.R. Kyle.

Date of report: January 1987.

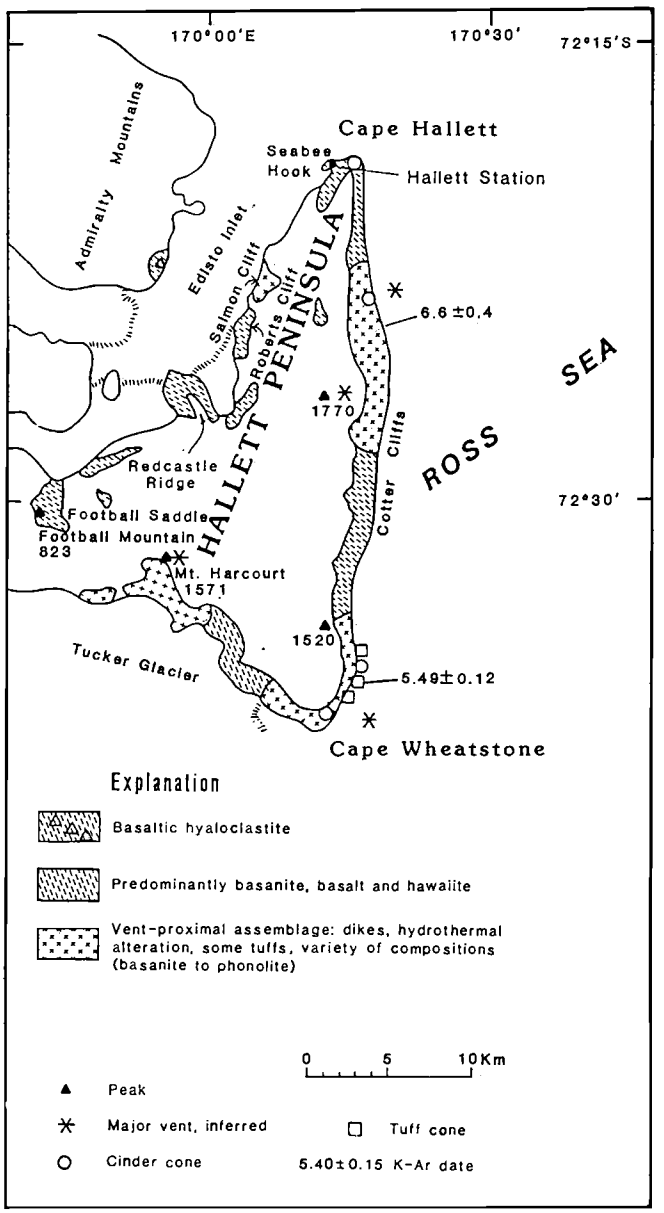

Fig. A.2.1. Generalized reconnaissance geologic map of Hallett Peninsula.

Copyright American Geophysical Union

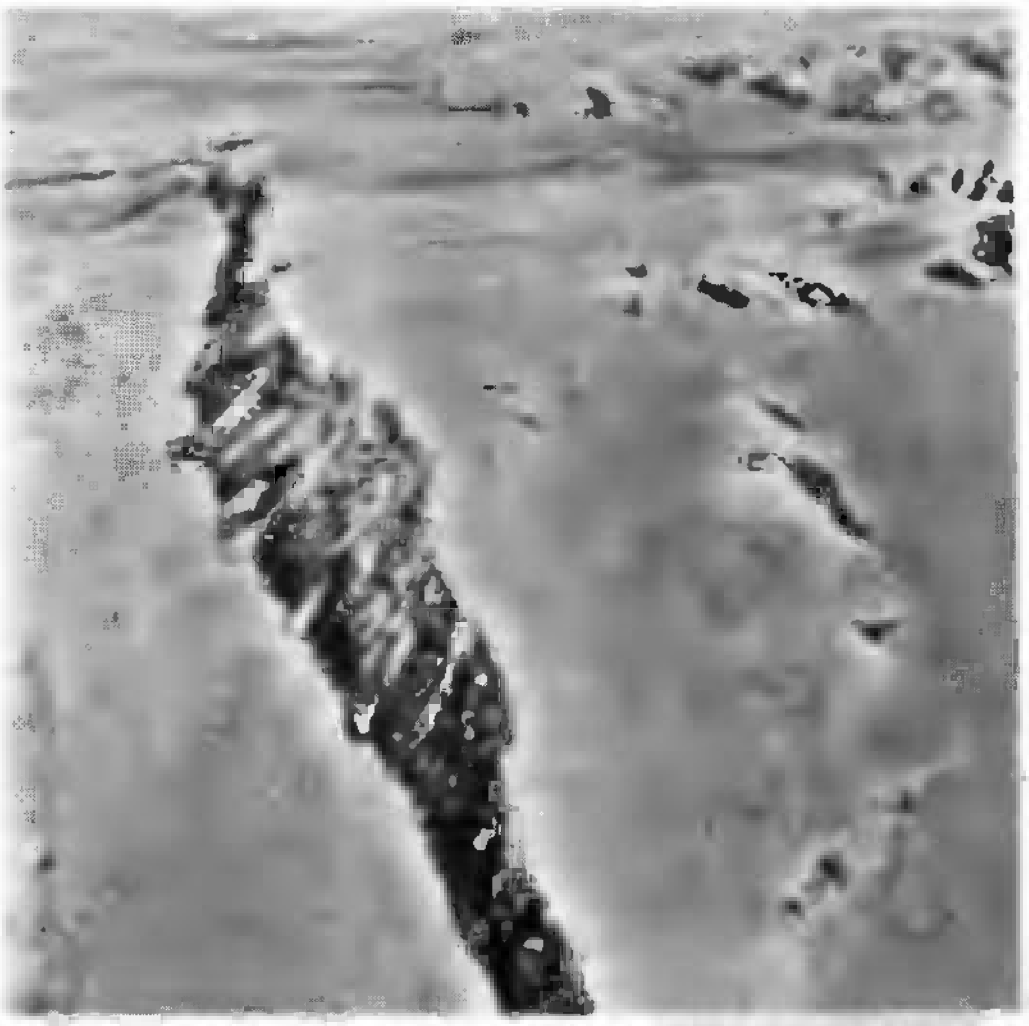

Copyright American Geophysical Union

[redacted]

[redacted]

[redacted]

[redacted]

[redacted]

Copyright American Geophysical Union

Cliffs [*Hamilton,* 1972]. Mount Harcourt is a conical stratovolcano consisting of flows dipping at angles of up to 25°.

At least two cinder cones composed of red and black Strombolian tephra are exposed in the cliffs adjoining Seabee Hook. Several additional cross-sectional exposures of hydrothermally altered cinder cones and tuff cones are present near sea level along Cotter Cliffs, below areas inferred to be major volcanic centers (Figure A.2.1).

The crestal axis of Hallett Peninsula trends along an azimuth of about 5°. Similar-trending small (20 m) displacement faults were found to cut the thin volcanic cover exposed on Football Saddle. Faulting may also have played a part in the development of the east facing Cotter Cliffs.

Petrologic Characteristics

Chemical analyses (Table A.2.1) of 38 samples [*Harrington et al.,* 1967; *Hamilton,* 1972; Kyle and McIntosh, unpublished data, 1988] from Cape Hallett and adjacent areas on the mainland show a wide range of alkali compositions (Figure A.2.4). In general, the analyses show a reasonably well defined evolutionary trend from basanite/tephrite and trachybasalt to trachyte and alkali trachyte. Ten of the samples are altered or hydrated (H_2O or loss on ignition (LOI), >2.00) and account for some of the scatter in the trend (Figure A.2.4). The distribution of the analyzed samples shows that evolved rocks are limited to near-vent areas, where alteration also tends to be more advanced. Evolved rocks probably make up less than 10% of the total volume of the Hallett Peninsula volcanic rocks.

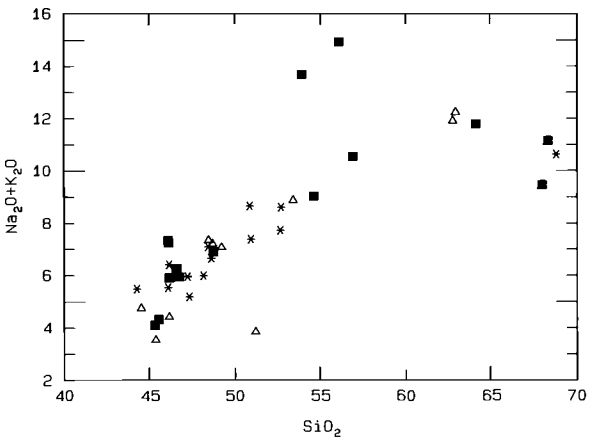

Fig. A.2.4. Alkali versus silica plot for analyzed rocks from Hallett Peninsula and adjacent areas (analyses recalculated to 100% volatile-free). Sources: Kyle and McIntosh (unpublished data, 1988) (asterisks); *Harrington et al.* [1967] (open triangles); and *Hamilton* [1972] (solid squares). Note that much of the scatter in the analyses is due to sample alteration and hydration.

Chronologic Data

Two K-Ar dates obtained by *Armstrong* [1978] are 5.49 ± 0.12 and 6.6 ± 0.4 Ma (recalculated to new decay constants) (Figure A.2.1).

Extent of Knowledge

Hallett Peninsula is one of the better studied of the four volcanic complexes in the province. The presence of the now-abandoned Hallett Station on Seabee Hook (Figure A.2.1) has facilitated access to the area. *Harrington et al.* [1967] gave detailed field and petrographic descriptions and geochemical analyses of volcanic rocks from several localities on Hallett Peninsula and nearby areas. They described a 300-m section of lava flows near Cape Hallett and sections at Roberts Cliff, Salmon Cliff, and Redcastle Ridge. Two formations were named: the Roberts Cliff Tuffite and the Herschel Tuffaceous Moraine. *Hamilton* [1972] visited 10 localities on Hallett Peninsula; *LeMasurier et al.* [1983] revisited four of these localities. *Jordan* [1981] made a detailed study of a small exposure of volcanic rocks near Football Saddle.

Deep dissection and excellent exposures make Hallett Peninsula a good locality for detailed study. Helicopter landing sites are relatively abundant, but easy access from sea ice is limited to the western margin.

Bibliography

Armstrong, 1978
Hamilton, 1972
Harrington et al., 1967
Jordan, 1981
LeMasurier et al., 1983
Turnbull, 1959

Copyright American Geophysical Union

A.3. Daniell Peninsula

Type of volcano: Elongate complex of overlapping shield volcanoes.
Individual volcanoes: Mount Brewster, one unnamed major volcano, more than 10 cinder cones.
Location: Northeastern coast of northern Victoria Land (72°57′S, 169°22′E).
Height above sea level: 2026 m.
Estimated volume: 1100 km^3 above sea level, total of 1900 km^3.
Evidence of Holocene activity: None.
Authors of report: W.C. McIntosh and P.R. Kyle.
Date of report: January 1987.

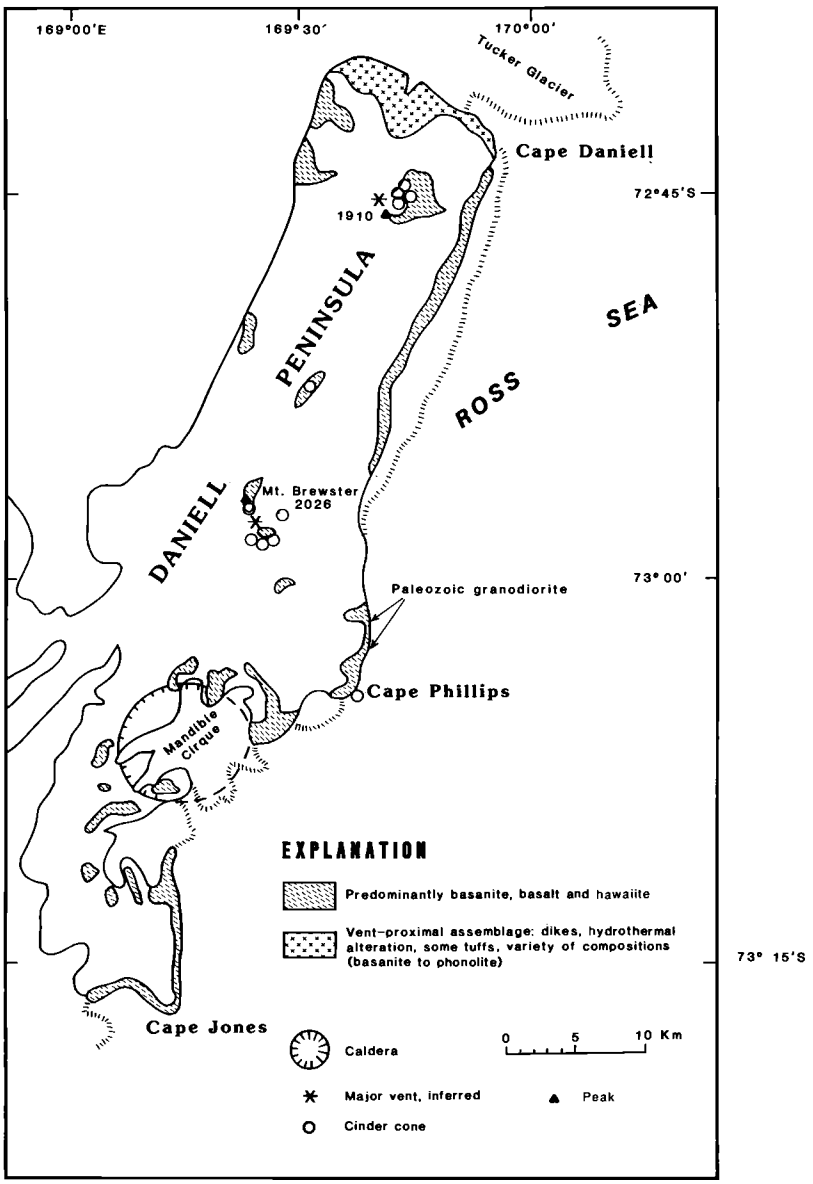

Fig. A.3.1. Geologic sketch map of Daniell Peninsula.

Copyright American Geophysical Union

Form and Structure

The northern part of Daniell Peninsula (Figures A.2.2 and A.3.1) is a broad, parallel-sided shield complex which rises to a height of approximately 1650-2026 m along its crest. Dissection in this part of the peninsula is minimal, but its western edge is bounded by a wave-cut cliff averaging 500 m in height. The 600- to 800-m-high cliffs at its northern end reflect erosion by Tucker Glacier, accompanied by minor cirque erosion. The southern third of Daniell Peninsula is irregular in shape, resulting from deep dissection by cirque glaciers; no undissected constructional surface remains.

The undissected northern part of Daniell Peninsula was probably a product of eruptions from numerous vents along an axial fissure zone. The two broad summits at either end, Mount Brewster (2026 m) and an unnamed peak (1910 m), represent major vents along this fissure. The location of major vents in the southern part of the peninsula is uncertain. *Hamilton* [1972] suggested that the arcuate embayment at Mandible Cirque (Figure A.3.2) represents an eroded caldera. About 10 small cinder cones are exposed along the undissected crest of northern Daniell Peninsula. Excellent cross-sectional exposures of cinder cones, buried beneath 400 m of lava flows, are present in cliffs near sea level at Cape Phillips.

The axial crest and shorelines of Daniell Peninsula are straight and extend along an azimuth of about 28°. Alignment of this trend with Mount Harcourt on Hallett Peninsula (Figures A.2.1 and A.3.2) suggests control by faults that continue beneath Tucker Glacier.

Two outcrops of Paleozoic granodiorite are exposed near sea level on the east side of Daniell Peninsula, 10 km north of Cape Phillips [*Hamilton*, 1972]. These outcrops probably represent an island of basement rock on which the Daniell Peninsula volcanoes were built.

Petrologic Characteristics

Hamilton [1972] published one analysis from Daniell Peninsula (Table A.3.1); two previously unpublished analyses are also listed. On the basis of the classification of

Fig. A.3.2. Aerial view northward along Daniell Peninsula, showing Mandible Cirque caldera (?) in the foreground and the coalesced volcanoes of central and northern Daniell Peninsula. Summit height of the peninsula is about 2000 m. The southern end of Hallett Peninsula (cf. Figure A.2.2) is visible just beyond Tucker Glacier. Paleozoic granodiorite, marking the base of the Daniell Peninsula volcanic pile, is exposed at Cape Phillips (far right, middle ground). (U.S. Navy photograph, TMA 1037 F33 197.)

Copyright American Geophysical Union

Le Bas et al. [1986], the rocks are basanite, alkali basalt, and mugearite (Figure A.3.3).

Chronologic Data

None.

TABLE A.3.1. Representative Chemical Analyses of Volcanic Rocks From Daniell Peninsula

	1	2	3
SiO_2	44.70	47.50	51.30
TiO_2	3.67	2.77	2.49
Al_2O_3	16.17	16.75	14.57
Fe_2O_3	8.10	11.86*	12.84*
FeO	5.22	--	--
MnO	0.19	0.23	0.22
MgO	4.92	3.87	3.10
CaO	8.98	7.60	6.21
Na_2O	3.93	4.85	4.18
K_2O	0.75	1.96	2.05
P_2O_5	0.62	1.18	0.86
H_2O^+	1.17	0.76**	1.71**
H_2O^-	0.68	--	--
Total	99.10	99.33	99.52

Dashes, not determined.
*Total Fe expressed as Fe_2O_3.
**Loss on ignition.

1. 277. Massive alkali basalt lava, east side of Daniell Peninsula [*Hamilton*, 1972].
2. AW82238. Basanite, north end of Daniell Peninsula (collected by A.C. Wright; XRF analysis by P.R. Kyle).
3. AW82246. Mugearite, lava flow breccia, Cape Phillips (collected by A.C. Wright; XRF analysis by P.R. Kyle).

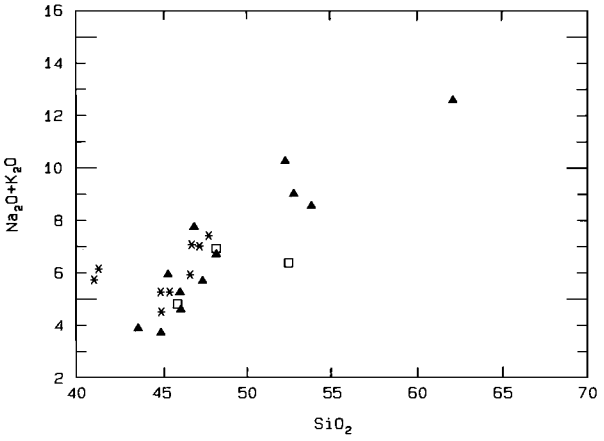

Fig. A.3.3. Alkali versus silica plot for analyzed rocks from Daniell Peninsula (squares), Coulman Island (solid triangles), and Possession Islands (asterisks). Sources: *Hamilton* [1972] and Kyle (unpublished data, 1988) (see Tables A.3.1, A.4.1, and A.5.1).

Extent of Knowledge

Daniell Peninsula is the least studied of the Hallett volcanic province piles. Six localities were visited by *Hamilton* [1972], and two of these were revisited by *LeMasurier et al.* [1983]. *Harrington et al.* [1967] recognized a few volcanic features at the northern end of the peninsula. Although some local areas are well exposed, lack of dissection and heavy snow and ice cover make this the most poorly exposed of the four Hallett volcanic province piles.

Bibliography

Armstrong, 1978
Hamilton, 1972
Harrington et al., 1967
LeMasurier et al., 1983

Copyright American Geophysical Union

A.4. Coulman Island

Type of volcano: Elongate complex of overlapping shield volcanoes.

Individual volcanoes: Coulman caldera, two major vents, numerous cinder cones and tuff rings.

Location: Northeastern coast of northern Victoria Land (73°33′S, 169°37′E); southernmost of the four major Hallett volcanic province piles.

Height above sea level: 1998 m.

Estimated volume: 300 km^3 above sea level, total of 600 km^3.

Evidence of Holocene activity: None.

Authors of report: W.C. McIntosh and P.R. Kyle.

Date of report: June 1987.

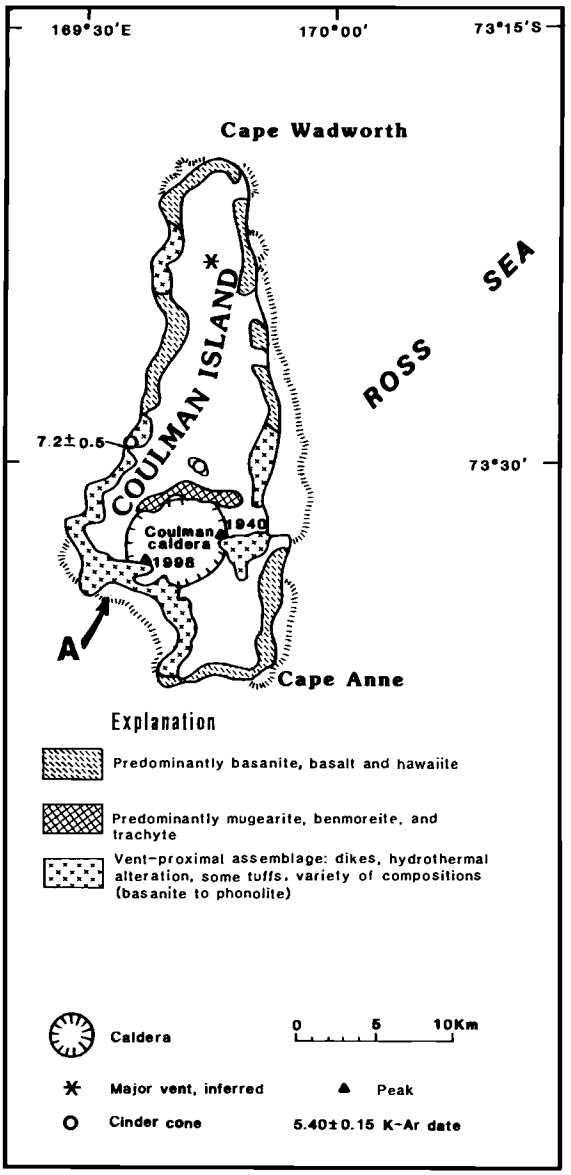

Form and Structure

Coulman Island (Figures A.4.1 and A.4.2) is the smallest of the Hallett volcanic province piles. Much of its surface area is an undissected constructional surface. Erosion is symmetrical with respect to the central eruptive axis, with marginal cliffs generally 600–1000 m high. Coulman caldera [*Hamilton,* 1972], 5 km wide and at least 700 m deep, is prominent at the southwestern end of the island. Dikes and quaquaversally dipping flows exposed in the northwestern and central eastern cliffs indicate two additional major vents in these areas.

A 1386-m stratigraphic section (Figure A.4.3), measured 2 km southwest of Coulman caldera, shows that the volcanic sequence consists predominantly of lavas and related breccias with subordinate (<5%) Strombolian tuffs. The majority of the flow-related breccias are matrix-poor, holocrystalline, and deuterically reddened, characteristic of eruption into a subaerial environment. A few of the lavas show slightly pillowed bases and glassy, matrix-rich basal breccias. These features probably reflect limited interaction with snow and ice in a periglacial environment [*McIntosh and Gamble,* 1989].

Several cinder cones are exposed on the upper surface of the island near its central axis, north of Coulman caldera. Cliff exposures of cones include a bomb-bearing Strombolian cinder-cone deposit near sea level on the west side of Coulman Island [see *Hamilton,* 1972, Figure 27]. Several additional tuff- and cinder-cone deposits are exposed in the eastern cliffs. Minor faulting, possibly related to caldera collapse, is present at the southern end of the island.

An undulatory unconformity of probable glacial origin was observed extending some 2 km along the base of the northern cliffs.

Fig. A.4.1. (opposite) Geologic sketch map of Coulman Island. A, location of the stratigraphic section shown in Figure A.4.3.

Copyright American Geophysical Union

Copyright American Geophysical Union

TABLE A.4.1. Representative Chemical Analyses of Volcanic Rocks From Coulman Island

	1	2	3
SiO_2	43.95	51.05	60.87
TiO_2	3.49	1.99	0.66
Al_2O_3	18.13	17.00	17.37
Fe_2O_3	11.70*	10.42*	3.21
FeO	--	--	1.62
MnO	0.16	0.33	0.23
MgO	4.01	1.80	0.57
CaO	12.07	4.23	1.06
Na_2O	3.08	6.29	7.53
K_2O	0.54	3.72	4.80
P_2O_5	0.55	0.84	0.11
H_2O^+	2.21**	2.22**	1.11
H_2O^-	--	--	0.32
CO_2	--	--	0.19
Cl	--	--	0.08
F	--	--	0.15
Total	99.89	99.89	99.88
As	2	4	--
Ba	336	1079	--
Ce	92	285	--
Cr	20	1	--
Cu	15	24	--
Ga	21	27	--
La	44	161	--
Nb	56	256	--
Ni	14	8	--
Pb	5	6	--
Rb	6.2	94	--
Sc	17	6	--
Sr	1118	569	--
Th	6	18	--
U	<1	1.5	--
V	291	22	--
Y	23	67	--
Zn	71	118	--
Zr	226	660	--

Dashes, not determined.
*Total Fe expressed as Fe_2O_3.
**Loss on ignition.

1. WCM 86040. Alkali basalt, flow, southern end of Coulman Island (collected by W.C. McIntosh; XRF analysis by P.R. Kyle).
2. WCM 86044. Phonotephrite, flow, southern end of Coulman Island (collected by W.C. McIntosh; XRF analysis by P.R. Kyle).
3. 218-1. Trachyte, north rim of Coulman caldera [*Hamilton*, 1972].

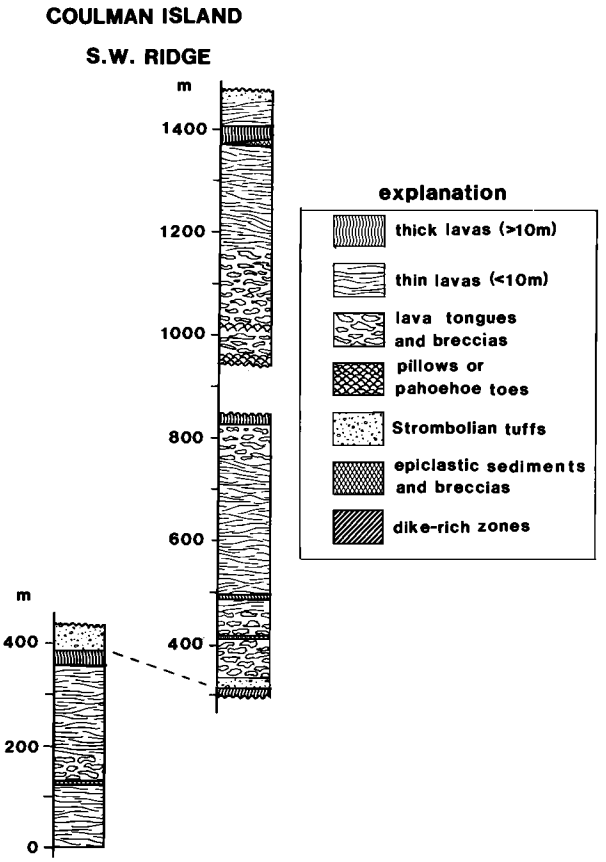

Fig. A.4.3. A measured stratigraphic section at the south end of Coulman Island (see Figure A.4.1 for location) [from *McIntosh and Gamble*, 1989].

Extent of Knowledge

Harrington et al. [1967] briefly described the geology of Coulman Island and included a sketch map showing the main geologic features. *Hamilton* [1972] described the island and also Coulman caldera. Further investigations of the south end of the island were made by W.C. McIntosh in February 1986 [*McIntosh and Gamble*, 1989].

Bibliography

Armstrong, 1978
Hamilton, 1972
Harrington, 1959
Harrington et al., 1967
McIntosh and Gamble, 1989
Prior, 1902

Copyright American Geophysical Union

A.5. Possession Islands

Type of volcano: A group of nine small islands and stacks, each an erosional remnant of basaltic intrusions, flows, and/or tuffs.

Location: 8 km off the southeastern coast of Adare Peninsula, between 71°53′S, 171°14′E and 71°58′S, 171°07′E.

Height above sea level: 101 m (summit of Foyn Island).

Estimated volume: 0.5 km^3 above sea level (for whole island group), total of 60 km^3.

Evidence of Holocene activity: None.

Authors of report: W.C. McIntosh and P.R. Kyle.

Date of report: January 1987.

Form and Structure

Possession Island (2.2 × 1.7 km) and Foyn Island (2.0 × 1.5 km) are the largest islands in the group; the remainder are less than 1 km long, and several are only stacks (see Figures A.1.1 and A.1.3). Erosion has completely removed the constructional surfaces from all the islands.

Foyn Island consists of flows and cinder-cone deposits intruded by a massive basaltic body showing radial columnar jointing. These units are overlain by a post-erosional mantle of basaltic cinders. Possession Island has a similar massive intrusive body, but it has intruded tuff-cone deposits. These contain polished beach pebbles, suggesting that the tuff cone erupted in a littoral environment. An apparently similar intrusive body on Heftye Island was observed from the air. Such intrusive bodies are probably responsible for the erosional resistance of the Possession Islands.

Hamilton [1972] suggested that the Possession Islands might represent the eroded core of a major volcano. However, their basaltic composition and lack of hydrothermal alteration argue against this interpretation. The straight north-south valley which bisects Possession Island may be related to erosion along a fault [*Harrington et al.*, 1967].

Petrologic Characteristics

In spite of their small size, Possession and Foyn islands have been relatively well studied petrologically. Analyses of nine samples [*Hamilton*, 1972; Kyle and McIntosh, unpublished data, 1987] show basanite and hawaiite compositions (see Table A.5.1 for representative analyses

TABLE A.5.1. Representative Chemical Analyses of Volcanic Rocks From Possession Islands

	1	2	3	4	5	6
SiO_2	41.11	44.86	45.12	46.77	47.38	47.47
TiO_2	3.43	2.91	3.01	2.73	2.71	2.48
Al_2O_3	12.90	14.51	15.39	17.49	17.38	17.64
Fe_2O_3*	13.42	12.50	12.40	11.75	11.72	11.28
MnO	0.22	0.19	0.20	0.23	0.22	0.23
MgO	9.66	9.09	7.89	4.26	4.32	3.63
CaO	12.44	10.54	10.34	8.53	8.48	8.03
Na_2O	4.24	3.45	3.92	5.32	5.23	5.49
K_2O	1.50	1.04	1.36	1.74	1.80	1.87
P_2O_5	1.16	0.60	0.68	1.19	1.10	1.21
LOI	<0.00	<0.00	<0.00	<0.00	<0.00	0.41
Total	100.08	99.69	100.31	100.01	100.34	99.74

All samples collected by A.C. Wright. XRF analyses by P.R. Kyle. Many of the samples had negative loss on ignition (LOI) as shown above by <0.00 values. This is due to weight gain during oxidation of iron from FeO to Fe_2O_3.

*Total Fe expressed as Fe_2O_3.

1. AW82214. Basanite, uppermost flow, south end of Possession Island.
2. AW82205. Basalt, intrusive megapillow, Foyn Island.
3. AW82207. Basanite flow, Foyn Island.
4. AW82224. Basanite, volcanic bomb in breccia, Possession Island.
5. AW82215. Basanite, glassy bomb in breccia, Possession Island.
6. AW82219. Basanite, margin of megapillow, Possession Island.

Copyright American Geophysical Union

and Figure A.3.3). These samples are highly undersaturated; normative *ne* ranges from 6.5 to 19.4%. Furthermore, they are among the least altered of all the rocks analyzed from the Hallett volcanic province.

Chronologic Data

None.

Extent of Knowledge

Harrington et al. [1967] briefly discussed possible models for the origin of the island. *Waterhouse* [1965] described helicopter landings on the island made from USCGC *Glacier* in 1964. Further landings were made from *Glacier* in January 1983 [*LeMasurier et al.*, 1983].

Bibliography

Hamilton, 1972
Harrington et al., 1967
LeMasurier et al., 1983
Prior, 1902
Smith, 1959, 1964
Waterhouse, 1965

Copyright American Geophysical Union

A.II. Melbourne Volcanic Province

Summary

P.R. Kyle

Introduction

The Melbourne volcanic province extends northward from Mount Melbourne to the southern and western boundary of the Hallett volcanic province (Figure A.II.1). It can be subdivided into four main subprovinces or volcanic fields (Malta Plateau, The Pleiades, Mount Overlord, and Mount Melbourne) and also includes numerous small, predominantly basaltic vents and poorly known eroded centers. Three of the subprovinces are each dominated by a large stratovolcano of felsic and peralkaline composition. Although

Fig. A.II.1. Melbourne volcanic province of the McMurdo Volcanic Group, showing the distribution of major volcanic centers. Smaller, mainly basaltic vents scattered throughout the area are shown in Figure A.11.1. The boxes and numbers show the location and reference numbers of areas described in the individual volcano descriptions.

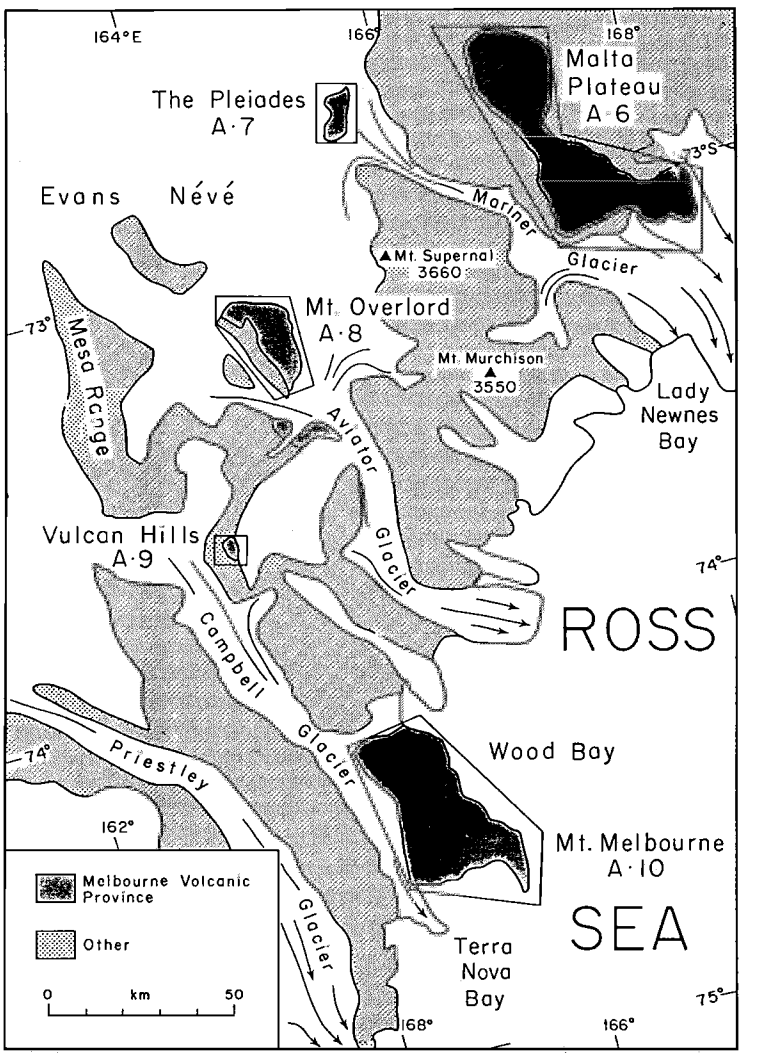

Copyright American Geophysical Union

felsic rocks are also common at Malta Plateau, no single major stratovolcano or caldera has yet been identified there.

The majority of the volcanic vents in this province are located in the Transantarctic Mountains, a feature which distinguishes it from the Erebus and Hallett volcanic provinces, where vents are mainly concentrated along the bounding fault zone between the Transantarctic Mountains and the Ross Embayment.

The Melbourne volcanic province was originally defined by *Kyle and Cole* [1974] to include all late Cenozoic alkali volcanic rocks exposed in an arcuate band extending inland from Mount Melbourne to Mount Overlord, The Pleiades, and Malta Plateau. Recent geologic mapping and geophysical observations have shown that the province is more extensive, both to the north and to the west. Malta Plateau (see IVD A.6) is now known to be largely volcanic, and thick sequences of volcanic rocks occur along the lower Mariner Glacier. Aeromagnetic observations indicate additional intrusive complexes extending inland from the coast between Daniell Peninsula and Mount Melbourne and also offshore [*Bosum et al.*, 1989]. Some of these magnetic anomalies appear to be associated with eroded gabbroic rocks, possibly similar to those at Vulcan Hills (see IVD A.9).

An extensive area between Borchgrevink and Mariner glaciers, including Malta Plateau, consists of mafic and peralkaline lavas and dikes (see IVD A.6). Preliminary mapping by GANOVEX III has resulted in the subdivision of the McMurdo Volcanic Group rocks into two formations, the "Malta Volcanics" and the "Meander Intrusives" [*Mueller et al.*, 1989]. The area apparently has a complex geologic history and a wide range of rock types.

The large stratovolcanoes of Mount Overlord, The Pleiades, and Mount Melbourne are composed of a wide range of intermediate and felsic alkali differentiates which have evolved from alkali basaltic rocks. Basaltic rocks, however, are generally rare and occur as small late-stage parasitic cones and vents. *Nathan and Schulte* [1968] called the rocks associated with the stratovolcanoes the Central Suite. Mount Melbourne overlies, and is surrounded by, an extensive volcanic plateau up to 800 m above sea level, consisting of basaltic to highly differentiated (trachytic) rocks, some of which were erupted subglacially [*Wörner and Viereck*, 1987, 1989].

Isolated basaltic vents are scattered throughout much of the Melbourne volcanic province and include small scoria cones, lava flows, hyaloclastites, and minor pyroclastic deposits. Some of these are discussed in IVD A.11. Such isolated basaltic occurrences were referred to as the Local Suite by *Nathan and Schulte* [1968].

TABLE A.II.1. Summary of K-Ar Dates for Volcanic Rocks From the Melbourne Volcanic Province

Location (IVD no.)	Dates, Ma	Source
Mount Melbourne (A.10)	0.01 ± 0.02	1
	0.26 ± 0.06	1
	0.08 ± 0.015	1
	0.015 ± 0.035	2
Cape Washington (A.10)	0.45 ± 0.05	2
	2.7 ± 0.2	2
Edmonson Point (A.10)	0.05 ± 0.02	2
	0.074 ± 0.11	2
Shield Nunatak (A.10)	0.11 ± 0.07	2
	1.55 ± 0.05	2
Baker Rocks (A.10)	0.74 ± 0.10	1
	0.20 ± 0.04	1
East flank of Mount Melbourne (Willows Nunatak) (A.10)	2.5 ± 0.1	1
Hades Terrace (A.11)	4.4 ± 0.2	1
Nathan Hills (A.11)	18.5 ± 0.7	1
Mount Overlord (A.8)	7.0 ± 0.14	1
	8.3 ± 1.7	1
	7.4 ± 0.14	1
The Pleiades (A.7)	0.01 ± 0.04	1
	0.04 ± 0.05	1
	0.02 ± 0.04	1
	0.003 ± 0.014	1

Sources are 1, *Armstrong* [1978]; 2, Wörner and Kreuzer (unpublished data, 1988). Note that dates given by Armstrong have been adjusted to new decay constants (see Table A.II.2) by using tables by *Dalrymple* [1979]. Additional data are given in Table A.II.2 and the Malta Plateau description (IVD A.6).

Copyright American Geophysical Union

Reconnaissance mapping in northern Victoria Land during the late 1950s and 1960s by various New Zealand expeditions [*Gair*, 1967; *Nathan and Schulte*, 1968; *Riddolls and Hancox*, 1968; *Gair et al.*, 1969] defined the general distribution of the volcanic centers. Subsequent work has included detailed studies of the large stratovolcanoes, but little is known about the smaller isolated basaltic rocks of the Local Suite (see IVD A.11).

Chronology

Radiometric dates are available from a number of localities in the Melbourne volcanic province. *Armstrong* [1978] made 15 conventional K-Ar age determinations (Table A.II.1), and two new conventional K-Ar dates are given in Table A.II.2. Seven K-Ar ages from the Mount Melbourne volcanic field by Wörner and Kreuzer (unpublished data, 1988) are given in Table A.II.1. *Stump et al.* [1983] obtained a two-point whole-rock chlorite Rb-Sr isochron of 9 ± 1 Ma on a granite pluton, and data from *Mueller et al.* [1989] are summarized in the Malta Plateau description (see IVD A.6).

Radiometric dating of rocks from Malta Plateau and the surrounding areas shows them to be the oldest in the McMurdo Volcanic Group. Intrusive rocks from "Eagle's Bluff," on the south side of Mariner Glacier, date mainly from 22–25 Ma, whereas lavas on Malta Plateau date from 6–11 Ma. Peralkaline dikes near Borchgrevink Glacier date from 14–18 Ma, spanning the interval between the lavas and intrusive rocks.

An 18.5-Ma date for Nathan Hills (Table A.II.1) is believed to be anomalously old. However, one of the oldest reliable dates, besides those from Malta Plateau, is a 14.7-Ma date for the hyaloclastite at Parasite Cone (Table A.II.2). This date is significant because it was obtained on a subglacial hyaloclastite cut by a channel containing till in which Beacon Supergroup sedimentary rock clasts predominate. Ice was obviously present at this time, and as there are no nearby mountains or hills, it is inferred that the ice was present as a large névé or ice sheet and not as a small valley glacier.

Mount Overlord (7.2 Ma) is the oldest stratovolcano. There was an apparent 6-m.y. hiatus in Central Suite felsic volcanism until the formation of The Pleiades (all K-Ar dates are less than 0.1 Ma). Dates in the Mount Melbourne volcanic field range from 3 Ma in the surrounding volcanic plateau to less than 0.25 Ma at the Mount Melbourne stratovolcano.

Volcanic Activity

Mount Melbourne is one of two active volcanoes within the McMurdo Volcanic Group. Although no historic eruptions have been witnessed, the presence of fumarolic ice towers and ground heated by geothermal activity attest to the presence of near-surface cooling magma. A major tephra (volcanic ash) layer is well exposed in ice, particularly on the eastern side of Mount Melbourne [*Keys et al.*, 1983; *Wörner and Viereck*, 1989], and has been tentatively dated at 200 years old [*Lyon*, 1986]. Three small nested craters on

TABLE A.II.2. New K-Ar Dates for Basanites From the Melbourne Volcanic Province

Sample	Location and Description	K,%	$^{40}Ar^*$ mol/g × 10^{-11}	Mean Date, Ma
81512B	Whole-rock basanite	0.997	1.276 (39.65)**	
	float, Aviator Glacier	0.993	1.314 (41.63)	
			1.302 (41.63)	7.50 ± 0.14
81501	Whole-rock basanite clast	1.061	2.698 (30.77)	
	from hyaloclastite,	1.063	2.675 (33.71)	
	Parasite Cone	1.033		14.67 ± 0.30

Decay constants used are $^{40}K/K = 1.167 \times 10^{-2}$, $\lambda_\beta = 4.962 \times 10^{-10}$ yr^{-1}, $\lambda_\varepsilon = 0.581 \times 10^{-10}$ yr^{-1}. Quoted error is ±1σ (68% confidence level). Analyses by K. Foland, Ohio State University.

*Radiogenic ^{40}Ar.

**Percent atmospheric ^{40}Ar.

Copyright American Geophysical Union

the south crater rim, having associated geothermal activity (ice towers and steaming ground), were produced by phreatomagmatic eruptions during the waning stages of the last eruption [*Wörner and Viereck*, 1989]. Mount Melbourne should be considered active and capable of producing moderate explosive eruptions which could disperse tephra eastward (the prevailing wind direction) over the western Ross Sea.

The Pleiades have yielded extremely young K-Ar dates, the youngest being 3 ± 14 ka. Age estimates based on the extent of erosion [*Nathan and Schulte*, 1968] proved incorrect when radiometric dates became available [*Armstrong*, 1978]. However, the youthful appearance of The Pleiades suggests that Holocene eruptions may have occurred and the volcanic center is certainly only dormant. Pumice lapilli are common on the surface of Mount Pleiones, at the southern end of The Pleiades, and are taken to indicate a moderate pumice eruption in recent times.

It is possible that some of the small basaltic vents (Local Suite) erupted in Holocene times. A small vent on the south side of Cosmonaut Glacier, about 2 km upstream from Aviator Glacier, erupted when ice levels were higher, probably during the last glacial (Wisconsin time). The flow apparently poured onto and into Cosmonaut Glacier, creating a chaotic deposit of intermixed till, hyaloclastite, and basalt. The deposit caused Cosmonaut Glacier to be slightly diverted.

In summary, there is a high probability of future eruptions in the Melbourne volcanic province, particularly from the active Mount Melbourne and the now dormant Pleiades.

Petrology

Detailed petrologic studies have been made at The Pleiades [*Kyle*, 1976, 1982, 1986*b*], Mount Overlord [*Noll*, 1985], and Mount Melbourne [*Wörner et al.*, 1989]. At all other locations (e.g., Malta Plateau and Vulcan Hills) the published studies must be considered as reconnaissance in nature.

Basaltic rocks are widespread throughout the province but are rare on the large stratovolcanoes. When they occur on stratovolcanoes, such as at Mount Overlord, they form parasitic cones unrelated to the main development of the volcano. The most extensive suite of analyzed basalts from the Mount Melbourne volcanic field (MMVF) [*Wörner et al.*, 1989 (Figures A.II.2 and A.10.3) range widely in alkali contents, and hence their degree of undersaturation, from alkali basalt to basanite. Elsewhere, extrapolation of fractionation trends (Figure A.II.2), as well as a few analyzed specimens, suggests that basanite is the dominant parental magma. Decreasing degrees of partial melting in the mantle source could account for the alkali basalt to basanite range.

Many of the basanites occur as small cones whose locations may be controlled by the presence of faults and crustal fractures. The basalts may reach the surface only in places of inherent crustal weaknesses. Because of the widespread distribution of basaltic vents it is likely that the crust in the whole province is being underplated by basaltic material.

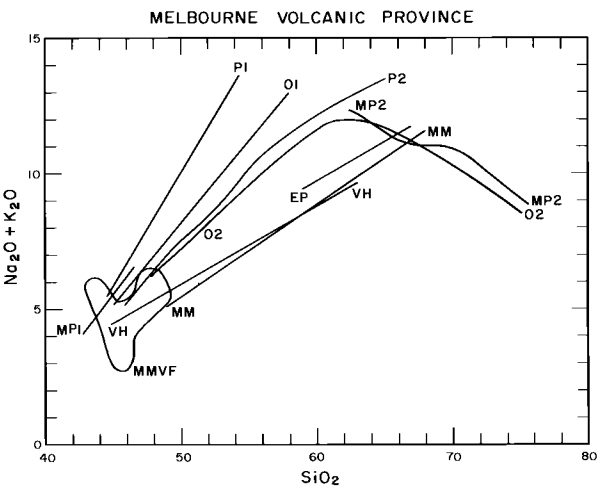

Fig. A.II.2. Total alkali versus silica diagram showing generalized trends for rocks from the main volcanic centers in the Melbourne volcanic province. P1, The Pleiades, sodic, strongly undersaturated basanite to phonolite suite. P2, The Pleiades, weakly undersaturated basanite - trachyte - peralkaline trachyte suite. O1, Mount Overlord, strongly undersaturated basanite to phonolite suite. O2, Mount Overlord, weakly undersaturated hawaiite - trachyte - comendite suite. MP1, Malta Plateau, younger basanites from Mariner Glacier. MP2, Malta Plateau, peralkaline *Q*-trachyte - peralkaline rhyolite - granite suite. VH, Vulcan Hills, hawaiite to trachyte lavas and intrusives. MM, Mount Melbourne, alkali basalt - trachyte suite of the main cone. EP, Edmonson Point, trachytes. MMVF, Mount Melbourne volcanic field basalts showing a range from alkali basalt to basanite.

Copyright American Geophysical Union

When the basaltic magma accumulated in magma chambers in sufficient volume, it differentiated to give the various felsic rocks. The fractionation lineages shown in Figure A.II.2 fan out from the basaltic fields, with an initial slope which depends on the degree of undersaturation of the parental basalt or basanite. The extent of differentiation and the nature of the resulting products depend on the size and depth of the magma chamber, the degree of crustal assimilation (if any), and the physical properties (i.e., temperature, oxygen fugacity, volatile content) of the parental magma.

The fractionation lineages can be grouped into three main types: (1) a strongly undersaturated basanite - phonolite sequence, exemplified by The Pleiades (P1) and Mount Overlord (O1) (Figure A.II.2), (2) a weakly undersaturated basanite - alkali basalt - hawaiite - trachyte - comendite trend, which is most complete at Mount Overlord (O2) (Figure A.II.2), and (3) a potassic, oversaturated alkali basalt - trachyte trend, as seen at Mount Melbourne (MM) (Figure A.II.2).

There is no age control on the trends. The peralkaline trend shown by older (14–25 Ma) intrusive rocks on Malta Plateau is similar to that shown by comenditic welded tuffs, ignimbrites, and lavas from the 7-Ma Mount Overlord. Young lavas (<0.25 Ma) from Mount Melbourne have total alkali-silica trends similar to those of the old eroded lavas and intrusive rocks from Vulcan Hills.

No attempt is made here to examine the fractionation lineages in anything other than total alkali-silica space, or in any detail. Quantitative fractionational crystallization models have been developed for the lineages at The Pleiades [*Kyle*, 1976; *Kyle and Rankin*, 1976; Kyle, unpublished data, 1986] and Mount Overlord [*Noll*, 1985].

Concluding Remarks

The Melbourne volcanic province is the most extensive and oldest in the McMurdo Volcanic Group. Significant erosion along the crest and eastern flank of the Transantarctic Mountains has exposed small gabbroic to syenitic subvolcanic intrusive bodies. Although poorly known, they should provide an important insight into the early development of volcanism in the province. The aeromagnetic survey by GANOVEX IV has shown huge magnetic anomalies which may represent hidden intrusive bodies related to the subvolcanic intrusions. A careful integration of the volcanic record with the geophysical data has the potential of greatly extending our understanding of the geologic and tectonic development of northern Victoria Land [e.g., *Tessensohn and Wörner*, 1989].

Recognition of extensive volcanism in the Malta Plateau area clearly indicates the need for more detailed field studies, such as that undertaken on the Mount Melbourne volcanic field by G. Wörner and colleagues [*Wörner and Viereck*, 1987, 1989; *Wörner et al.* 1989; *Tessensohn and Wörner*, 1989]. The large volumes and long duration of eruption of highly peralkaline rocks in the Malta Plateau area offer important opportunities for laboratory investigations.

Fractionation trends defined by the lavas in the Melbourne volcanic province are the most varied and complete within the McMurdo Volcanic Group. The extreme degree of fractionation is probably a result of accumulation of magma in crustal chambers. The formation of such magma chambers may be aided by the 40-km-thick crust, which could impede magma reaching the earth's surface.

Preliminary geochemical studies have defined the general evolutionary trends of the lava lineages. However, a dearth of isotopic data, apart from limited data at Mount Melbourne [*Wörner et al.*, 1989], have hindered an understanding of crustal involvement in magma genesis. Future laboratory work must include detailed isotopic studies.

Acknowledgments

Gerhard Wörner provided unpublished K-Ar dates from Mount Melbourne and made useful comments on the contents of this section. Ken Foland, with the assistance of Anne Wright-Grassham, made two new K-Ar age determinations. Editorial assistance from Janet Thomson is much appreciated. Assistance in the field from the late Peter Jennings, John Gamble, Bill McIntosh, Harry Keys, and Anne Wright-Grassham is appreciated. Support from the Division of Polar Programs, National Science Foundation, has made it all possible.

Copyright American Geophysical Union

A.6. Malta Plateau

Type of volcano: Felsic lava flows resting on an uplifted plateau of basement rocks; associated alkaline intrusions.

Location: Victory Mountains, northern Victoria Land (72°40′–73°10′S, 167°–168°30′E).

Height above sea level: 2600-m-high plateau with several domelike features rising up to 3000 m; southeastern part almost at sea level.

Estimated volume: 240 km^3.

Evidence of Holocene activity: None.

Authors of report: M. Schmidt-Thomé, P. Mueller, and F. Tessensohn.

Date of report: May 1986.

Form and Structure

Malta Plateau is an ice-covered, north-south trending plateau about 40 km in length and 20 km in width (Figure A.6.1). The high, smooth landform is bounded on the south and west by Mariner Glacier, on the east by tributaries of Borchgrevink Glacier, and on the north by tributaries of Trafalgar Glacier. Icefalls up to 1500 m high drop from the plateau. The bulk of the plateau has a uniform elevation of around 3000 m, but in the southeast it slopes like a ramp down to near sea level (Figure A.6.2). Ice-free ridges on this ramp form the main outcrops, and only cinder cones are exposed on the plateau itself. The volcanic rocks of Malta Plateau straddle a major basement fault separating the Leap Year quartzites of the Bowers Terrane (in the west) from turbidites of the Robertson Bay Terrane (in the east).

Volcanic rocks (termed the "Malta Volcanics" [*Mueller et al.*, 1989]) form lava flows, lapilli and crystal tuffs,

Fig. A.6.1. Geologic map of the Malta Plateau area.

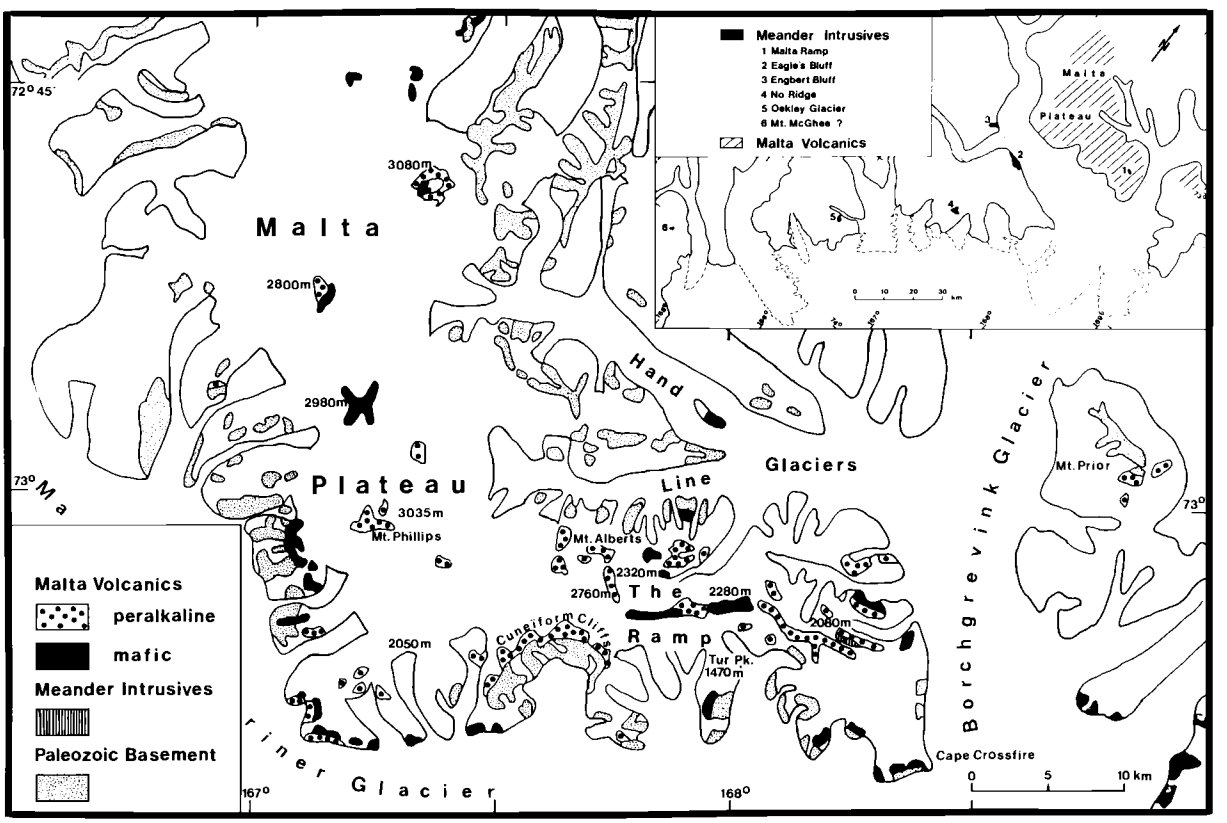

Copyright American Geophysical Union

Copyright American Geophysical Union

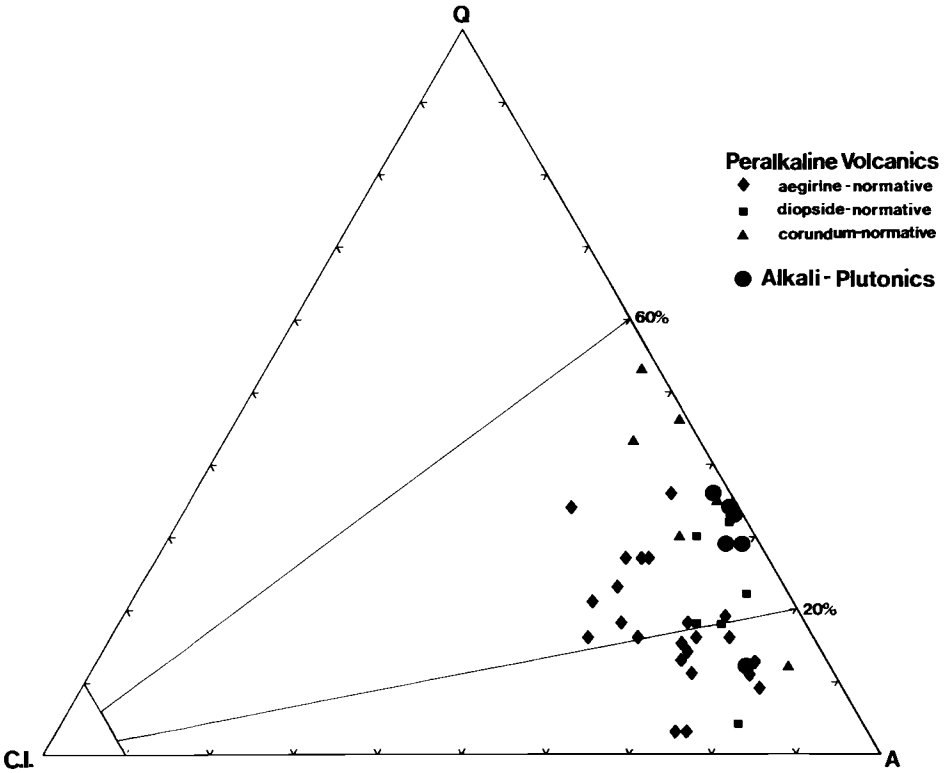

Fig. A.6.3. Plot of representative chemical analyses of volcanic and intrusive rocks from the Malta Plateau area. Modified Streckeisen diagrams are after *Mueller* [1974]. A, alkali feldspar; Q, quartz; C.I., color index.

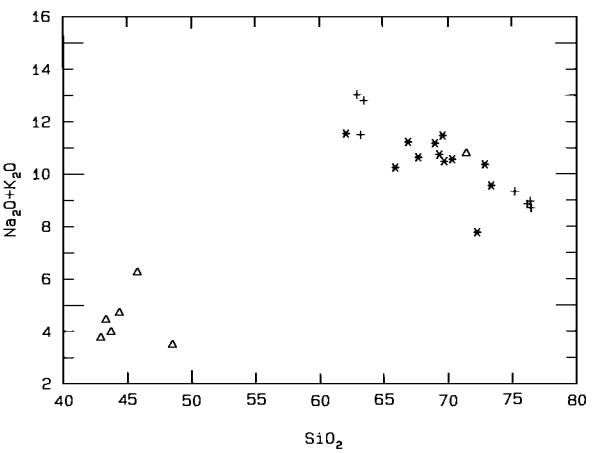

Fig. A.6.4. Alkali versus silica plot of representative analyses of volcanic rocks (Table A.6.1) and intrusive rocks from Malta Plateau area (Table A.6.2). Analyses of volcanic rocks are from *Mueller et al.* [1989] (asterisks) and from Kyle (personal communication, 1987; unpublished data, 1987) (triangles). Analyses of intrusive rocks are from *Mueller et al.* [1989] (pluses). All data are recalculated to 100% volatile-free.

with a well-developed miarolitic texture. There are two varieties of granite: a fine-grained porphyritic rock with dense granophyric intergrowths around phenocrysts of perthitic K-feldspar and quartz, and biotite as the mafic component; and a coarse-grained variety consisting of platy perthitic K-feldspar, minor plagioclase and interstitial quartz, aegirine or aegirine-augite, and aenigmatite. Quartz-poor alkali syenites contain fayalite, as well as colorless clinopyroxene commonly fringed by aegirine-augite and aegirine and sometimes replaced by biotite. Most rocks are miarolitic with open pore spaces containing fluorite, albite growing on perthitic alkali feldspar, and a younger generation of aegirine and arfvedsonite.

Chronologic Data

Radiometric dates obtained from the volcanic and associated intrusive rocks [*Mueller et al.*, 1989] are summarized below:

Peralkaline and silicic lavas of the Malta Plateau proper—K-Ar whole rock: 6.5, 6.7, 8.5, 8.9, 10.7 Ma.

Peralkaline dikes at Mount Prior and Tur Peak—K-Ar whole rock: 14.1, 14.7, 14.8, 14.9, 15.0, 15.2, 15.3, 18.1, 18.2 Ma.

Copyright American Geophysical Union

TABLE A.6.1. Representative Chemical Analyses of Volcanic Rocks From the Malta Plateau Area

	1	2	3	4	5	6	7	8
SiO_2	42.44	44.92	48.73	60.50	63.74	65.95	65.96	67.88
TiO_2	4.51	2.58	2.48	0.75	0.56	0.49	0.34	0.21
Al_2O_3	14.36	15.26	13.87	14.17	12.94	12.87	15.14	14.49
Fe_2O_3*	15.46	12.53	12.34	8.65	7.90	6.75	4.66	3.88
MnO	0.21	0.22	0.17	0.29	0.25	0.16	0.13	0.11
MgO	5.75	6.23	9.41	0.28	0.08	0.00	0.13	0.00
CaO	11.26	9.34	9.63	1.51	1.35	0.85	1.12	0.85
Na_2O	3.34	4.42	2.62	6.24	4.90	5.53	5.96	5.85
K_2O	0.37	1.70	0.87	5.01	5.02	4.83	5.11	5.15
P_2O_5	1.15	0.80	0.31	0.10	0.03	0.04	0.06	0.01
SO_3	--	--	--	0.13	0.30	0.16	0.17	0.17
LOI	1.06	1.97	--	1.75	2.00	1.63	0.25	0.50
Trace	--	--	--	0.21	0.27	0.18	0.29	0.34
Total	99.91	99.97	100.43	99.59	99.34	99.44	99.32	99.44
Ba	--	--	--	242	14	21	307	--
Bi	--	--	--	--	--	--	9	--
Ce	--	--	--	190	271	187	200	463
Co	--	--	--	4	20	9	9	14
Cr	--	--	--	9	18	10	16	14
Cu	--	50	15	17	32	--	12	169
La	--	--	--	93	144	71	111	245
Mo	--	--	--	10	12	8	12	19
Nb	--	99	32	117	157	99	188	181
Ni	--	92	83	9	11	--	8	8
Pb	--	<2	3	5	13	14	150	200
Rb	--	48	22	50	147	96	236	216
Sc	--	--	--	8	--	3	6	--
Sn	--	--	--	22	22	--	25	25
Sr	--	1030	469	24	17	5	66	4
Ta	--	--	--	9	15	9	17	15
Th	--	7	3	8	21	13	33	43
U	--	--	--	3	6	--	9	12
V	--	--	--	7	3	6	16	8
W	--	--	--	--	--	--	--	--
Y	--	33	24	53	89	59	59	74
Zn	--	94	93	207	253	191	152	170
Zr	--	284	177	559	866	566	726	863

Dashes, not determined.
*Total Fe expressed as Fe_2O_3.

1. VC-44. Basanite, lower Mariner Glacier (Kyle, personal communication, 1987, XRF analysis).
2. 82089. Basanite, lower Mariner Glacier (Kyle, personal communication, 1987, XRF analysis).
3. 82107. Basalt, lower Mariner Glacier (Kyle, personal communication, 1987, XRF analysis).
4. 3200. Peralkaline trachyte, southwest corner of Malta Plateau (K-Ar age: 10.7 ± 0.2 Ma) [*Mueller et al.*, 1989].
5. 3204. Aegirine-bearing peralkaline *Q*-trachyte, north of Cape Crossfire (K-Ar age: 14.8 ± 0.4 Ma) [*Mueller et al.*, 1989].
6. 3297. Aegirine-bearing peralkaline *Q*-trachyte, north of Tur Peak (K-Ar age: 14.7 ± 0.4 Ma) [*Mueller et al.*, 1989].
7. 3265. Aegirine-bearing peralkaline *Q*-trachyte, spot height 2900 m, Malta Plateau (K-Ar age: 6.5 ± 0.2 Ma) [*Mueller et al.*, 1989].
8. 3269. Peralkaline rhyolite from crater, spot height 3080 m, Malta Plateau (K-Ar age: 8.9 ± 0.2 Ma) [*Mueller et al.*, 1989].

Copyright American Geophysical Union

TABLE A.6.1. (continued)

	9	10	11	12	13	14	15	16
SiO_2	68.16	68.36	68.51	69.06	69.42	70.52	71.93	72.18
TiO_2	0.41	0.41	0.43	0.24	0.25	0.16	0.33	0.33
Al_2O_3	12.55	12.83	9.86	13.66	9.14	13.63	10.13	10.33
Fe_2O_3*	6.01	5.88	7.71	4.03	9.21	2.94	5.64	5.72
MnO	0.05	0.09	0.21	0.10	0.26	0.06	0.13	0.13
MgO	0.01	0.00	0.00	0.08	0.01	0.02	0.00	0.00
CaO	0.34	0.46	0.40	0.68	0.32	0.74	0.36	0.29
Na_2O	5.26	5.62	6.64	5.62	3.54	4.21	5.50	4.67
K_2O	4.99	4.97	4.66	4.74	3.93	6.44	4.72	4.74
P_2O_5	0.02	0.01	0.02	0.03	0.01	0.01	0.01	0.01
SO_3	0.14	0.13	0.14	0.30	0.17	--	0.17	0.19
LOI	1.50	0.63	0.38	0.50	2.88	0.93	0.13	0.38
Trace	0.28	0.26	0.37	0.33	0.44	--	0.42	0.40
Total	99.72	99.65	99.33	99.37	99.58	99.66	99.47	99.37
Ba	138	123	4	132	--	--	--	--
Bi	--	--	--	--	6	--	--	--
Ce	277	195	362	213	422	--	385	347
Co	11	--	9	18	--	--	10	7
Cr	3	15	10	16	7	--	7	16
Cu	--	20	28	17	7	<10	30	54
La	155	113	172	70	210	--	196	103
Mo	4	4	16	11	17	--	26	9
Nb	147	149	210	267	280	149	247	245
Ni	--	7	8	9	10	--	6	--
Pb	22	13	18	49	38	24	28	32
Rb	142	138	154	358	133	306	259	259
Sc	--	--	--	3	--	--	2	--
Sn	--	24	--	29	42	--	35	30
Sr	7	10	4	33	6	12	7	6
Ta	12	16	19	23	22	--	21	19
Th	19	20	26	47	41	36	38	40
U	5	--	9	14	9	--	12	3
V	--	7	6	9	18	--	7	14
W	--	--	--	8	--	--	6	--
Y	96	51	125	58	133	91	122	84
Zn	269	176	347	194	492	148	281	291
Zr	910	950	1351	1001	1519	719	1512	1518

Dashes, not determined.
*Total Fe expressed as Fe_2O_3.

9. 3214. Peralkaline rhyolite, north of Tur Peak (K-Ar age: 14.1 ± 0.3 Ma) [*Mueller et al.*, 1989].
10. 3213. Peralkaline rhyolite, north of Tur Peak (K-Ar age: 15.0 ± 0.4 Ma) [*Mueller et al.*, 1989].
11. 3199. Peralkaline rhyolite, north of Tur Peak (K-Ar age: 14.9 ± 0.3 Ma) [*Mueller et al.*, 1989].
12. 3264. Peralkaline rhyolite, spot height 2900 m, Malta Plateau (K-Ar age: 6.7 ± 0.2 Ma) [*Mueller et al.*, 1989].
13. 3294. Peralkaline rhyolite, north of Tur Peak (K-Ar age: 15.2 ± 0.4 Ma) [*Mueller et al.*, 1989].
14. 82105. Peralkaline rhyolite, lower Mariner Glacier (Kyle, personal communication, 1987; XRF analysis).
15. 3283. Peralkaline rhyolite (obsidian), Mount Phillips [*Mueller et al.*, 1989].
16. 3285. Peralkaline rhyolite, Mount Phillips (K-Ar age: 8.5 ± 0.2 Ma) [*Mueller et al.*, 1989].

Copyright American Geophysical Union

TABLE A.6.2. Representative Chemical Analyses of Intrusive Rocks From Scattered Outcrops Between Mariner and Aviator Glaciers

	1	2	3	4	5	6	7
SiO_2	61.78	62.49	62.54	74.38	75.44	75.70	75.79
TiO_2	0.55	0.68	0.69	0.10	0.09	0.23	0.12
Al_2O_3	15.37	16.26	16.02	13.22	12.47	12.00	12.45
Fe_2O_3*	6.13	5.70	5.22	1.55	1.36	2.38	1.61
MnO	0.19	0.15	0.18	0.02	0.02	0.06	0.02
MgO	0.29	0.43	0.28	0.04	0.03	0.08	0.05
CaO	0.99	1.65	0.90	0.36	0.48	0.12	0.44
Na_2O	7.74	6.69	7.46	4.38	4.14	4.66	3.88
K_2O	5.05	4.68	5.16	4.85	4.70	4.13	4.74
P_2O_5	0.10	0.15	0.10	0.01	0.01	0.01	0.01
SO_3	0.01	0.02	0.04	0.02	0.03	0.01	0.02
LOI	0.58	0.75	0.79	0.63	0.63	0.44	0.53
Trace	0.13	0.21	0.20	0.10	0.12	0.05	0.11
Total	99.41	99.86	99.58	99.66	99.52	99.87	99.77
As	17	--	--	17	--	14	6
Ba	12	784	35	18	16	4	22
Bi	16	7	7	10	1	11	10
Ce	137	135	224	113	119	64	161
Co	20	--	2	19	12	18	9
Cr	4	--	--	--	--	--	--
Cu	23	54	141	8	8	12	10
La	85	67	113	57	61	33	78
Mo	8	12	7	7	10	8	11
Nb	68	57	111	46	88	16	75
Ni	6	7	1	--	5	5	--
Pb	14	8	55	21	21	12	24
Rb	76	58	83	203	265	49	173
Sc	7	10	3	2	--	2	2
Sn	20	--	22	--	21	--	22
Sr	8	95	13	13	6	4	10
Th	--	--	13	28	32	--	27
U	11	9	13	11	12	6	9
V	--	--	--	5	--	--	10
W	--	--	--	--	--	--	10
Y	43	38	65	44	73	13	61
Zn	104	90	122	24	39	48	61
Zr	343	343	546	166	157	44	135

All analyses from *Mueller et al.* [1989]. Dashes, not determined.
*Total Fe expressed as Fe_2O_3.

1. NR2363. Aegirine syenite, "No Ridge."
2. FT1348. Aegirine arfvedsonite syenite, "No Ridge."
3. FT1353. Aegirine arfvedsonite syenite, "No Ridge."
4. FT1342. Biotite alkali feldspar granite, "Eagle's Bluff."
5. FT1343b. Granophyric biotite alkali feldspar granite, Engberg Bluff.
6. FT1338. Aegirine granite, Oakley Glacier.
7. FT1343a. Granophyric biotite alkali feldspar granite, Engberg Bluff.

Copyright American Geophysical Union

"Eagle's Bluff" Granite—K-Ar biotite: 26/22.1 Ma (two fractions), 22.7 Ma, 25.2 Ma, 22.6/23 Ma (two fractions); Rb-Sr biotite: 18.4, 22.3, 22.9, 24 Ma; Rb-Sr whole-rock isochron: 25 Ma; Rb-Sr chlorite whole-rock isochron [*Stump et al.*, 1983]: 9 Ma.

The intrusives appear to be the oldest igneous rocks on Malta Plateau and also the oldest in the McMurdo Volcanic Group. The dikes are younger (14–18 Ma), and the lavas are between 10 and 6 Ma (the youngest date being obtained from volcanic cones on the plateau top).

Extent of Knowledge

Malta Plateau was first visited in November 1964 [*Crowder*, 1968], during the course of a U.S. helicopter-supported geological reconnaissance based at Hallett Station. It was revisited in 1968 by a New Zealand Geological Survey party [*Riddolls and Hancox*, 1968] that sledged in from the north. U.S. Antarctic Research Program geologists under P.R. Kyle visited and sampled the lower Mariner Glacier area, near Cape Crossfire, and southern Borchgrevink Glacier in January 1982. The present summary is based mainly on helicopter-supported field work by G. Mortimer, M. Schmidt-Thomé, and T.O. Wright, from January 27 to February 13, 1983.

Bibliography

Armstrong, 1978
Crowder, 1968
Dow and Neall, 1972, 1974
Hamilton, 1972
Jordan, 1981
Mortimer et al., 1984
Mueller et al., 1989
Riddolls and Hancox, 1968
Stump et al., 1983
Sturm and Carryer, 1968

Copyright American Geophysical Union

A.7. The Pleiades

Type of volcano: Small trachytic stratovolcano and scoria cones, endogenous domes, and lava flows.

Individual volcanoes: Mount Pleiones, "Taygete Cone," "Aleyone Cone," and numerous small scoria cones.

Location: South end of Evans Névé, northern Victoria Land (72°40′S, 165°30′E).

Height above sea level: ~3040 m.

Evidence of Holocene activity: Young radiometric ages and areas of hydrothermal alteration.

Author of report: P.R. Kyle.

Date of report: November 1986.

Form and Structure

The Pleiades include a small stratovolcano, Mount Pleiones (Figure A.7.1), which rises 500 m above the flat plateau formed by Evans Névé. Extending 13 km in a north-northeast direction from Mount Pleiones are a series of small cones and domes with associated lava flows and pyroclastic rocks (Figure A.7.2). Several small scoria cones (Figure A.7.1, C4 and C5) sit on the flank of Mount Pleiones.

Mount Pleiones consists of three cones, each with a crater (Figure A.7.3), and is composed mainly of tristanite and trachyte [*Kyle*, 1982]. The domes and cones to the northeast of Mount Pleiones appear to be aligned around the

Fig. A.7.1. Sketch map of The Pleiades, showing the distribution of eruptive centers and location of samples [from *Kyle*, 1982]. (VUW, Victoria University of Wellington, New Zealand.)

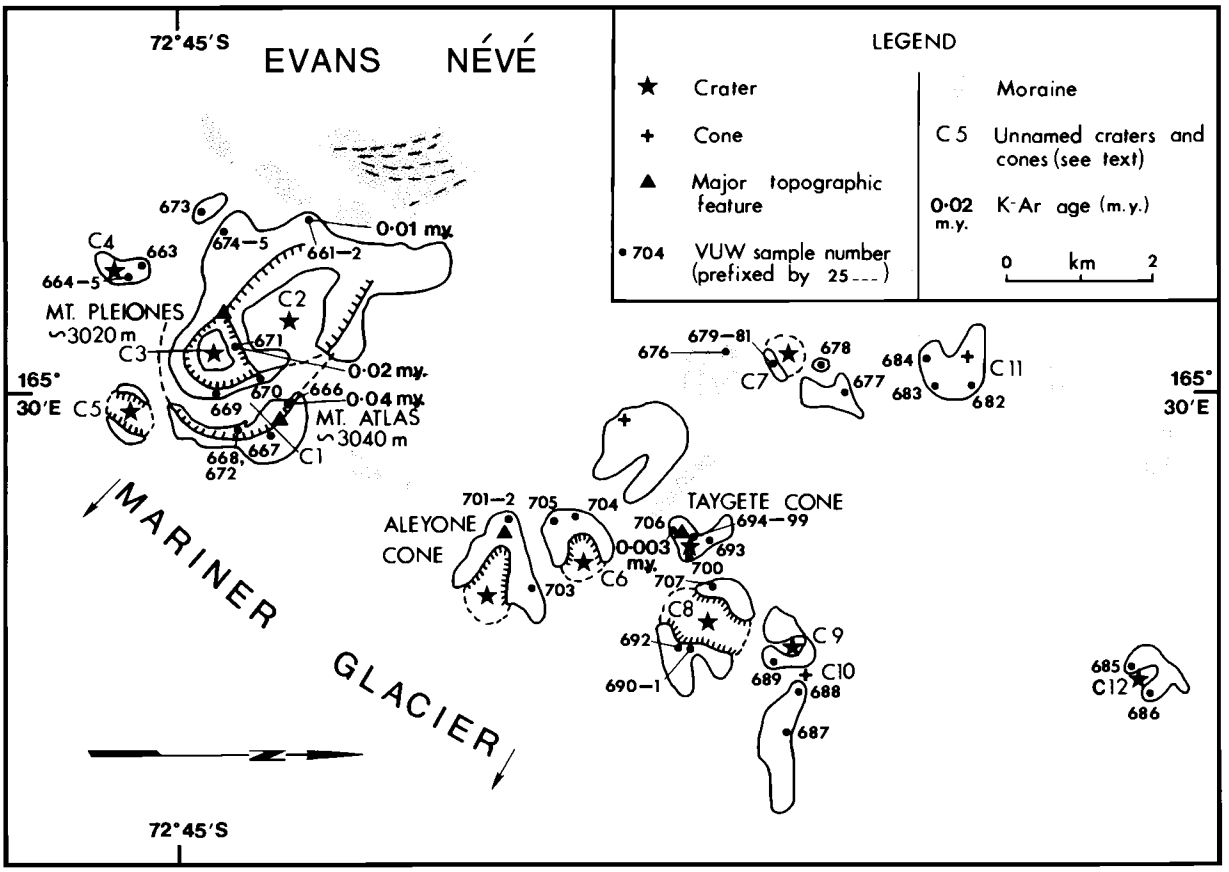

Copyright American Geophysical Union

Fig. A.7.2. Oblique aerial view looking eastward across the northern end of The Pleiades. The high point to the right is "Aleyone Cone" (Figure A.7.1). The eastward flowing Mariner Glacier is behind The Pleiades. (U.S. Navy photograph, TMA 731 F33 031.)

Fig. A.7.3. Vertical air photograph of Mount Pleiones, showing the set of three nested craters, two of which are breached in a northwesterly direction. (U.S. Navy photograph, TMA 1379 F32 279.)

Copyright American Geophysical Union

edge of a snow-covered circular feature, perhaps an older caldera. This circular feature is poorly developed and not easily recognized on the ground, but it is apparent in air photographs. Endogenous domes include the peralkaline K-trachyte dome at "Taygete Cone" and the phonolite dome at crater C11 (Figure A.7.1).

The Pleiades show a linear alignment broadly parallel to the trend of the Transantarctic Mountains. This lineation may indicate that crustal structures (such as block faulting) may have controlled the distribution of the volcanic rocks.

Petrologic Characteristics

Major- and trace-element analyses of 32 samples (Table A.7.1 and Figure A.7.4) have been used [*Kyle*, 1976, 1982, 1986*b*] to divide the lavas into two evolutionary lava lineages: a strongly undersaturated sodic lineage and a weakly oversaturated potassic lineage. Lavas within these lineages have been classified as basanite - *ne*-hawaiite -

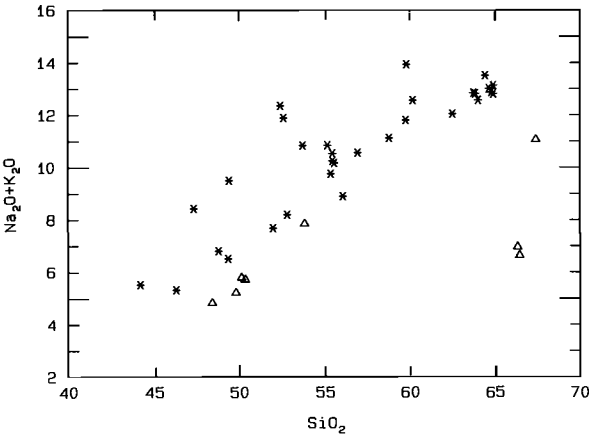

Fig. A.7.4. Alkali versus silica plot for analyzed lavas (asterisks) from The Pleiades; cognate cumulate xenoliths (triangles) are also plotted.

TABLE A.7.1. Representative Chemical Analyses of Volcanic Rocks From The Pleiades

	1	2	3	4	5	6	7	8
SiO_2	44.26	46.11	47.58	48.44	49.26	51.76	52.77	53.74
TiO_2	3.66	2.41	2.96	2.85	2.63	1.15	1.23	1.17
Al_2O_3	14.82	14.35	16.97	16.19	16.10	18.96	19.10	18.23
Fe_2O_3	4.01	3.30	3.53	5.11	4.67	4.39	5.15	5.16
FeO	8.70	8.35	8.08	6.33	6.49	3.86	3.45	4.24
MnO	0.20	0.21	0.24	0.20	0.20	0.25	0.25	0.28
MgO	7.21	8.94	3.51	4.72	5.09	1.22	1.29	1.13
CaO	10.98	10.04	8.15	7.82	8.14	4.58	4.72	4.82
Na_2O	3.80	3.84	5.80	4.41	4.24	8.34	8.03	7.47
K_2O	1.74	1.48	2.67	2.33	2.25	3.85	3.90	3.35
P_2O_5	0.78	0.59	0.99	0.89	0.73	0.39	0.41	0.48
Total	100.16	99.62	100.48	99.29	99.80	98.75	100.30	100.07
Ba	356	416	555	483	396	763	745	794
Cr	194	317	8	32	94	--	--	--
Cu	52	60	21	40	41	12	13	9
Ni	78	190	6	30	45	--	--	--
Rb	40	37	73	62	71	126	126	101
Sr	795	745	1052	873	758	971	988	1050
V	252	185	115	151	156	16	22	6
Zn	96	97	112	104	105	117	101	131

Dashes, not determined.
*Total Fe expressed as Fe_2O_3.
** Includes LOI (loss on ignition) = 1.28 wt %.
1. 25679. Basanite, Cone 7 [*Kyle*, 1982].
2. 25682. Hawaiite, Cone 11 [*Kyle*, 1982].
3. 25685. Phonotephrite, Cone 12 [*Kyle*, 1982].
4. 25664. Hawaiite, Cone 4 [*Kyle*, 1982].
5. 25703. Hawaiite, "Aleyone Cone" [*Kyle*, 1982].
6. 25691. Tephriphonolite, Cone 8 [*Kyle*, 1982].
7. 25690. Tephriphonolite, Cone 8 [*Kyle*, 1982].
8. 25704. Tephriphonolite, Cone 6 [*Kyle*, 1982].

Copyright American Geophysical Union

ne-mugearite - *ne*-benmoreite - phonolite for the sodic lineage and trachyandesite - tristanite - K-trachyte - peralkaline K-trachyte for the potassic lineage. On the basis of the total alkali-silica (TAS) classification of *Le Bas et al.* [1986] the strongly undersaturated rocks are basanite, phonotephrite, tephriphonolite, and phonolite, whereas the rocks of the weakly undersaturated lineage are hawaiite, mugearite, benmoreite, trachyte, and peralkaline trachyte (Figure A.7.4). Classification of The Pleiades lavas into sodic and potassic is probably not justified, as the potassic rocks are not strongly potassic.

Strongly undersaturated sodic lavas are among the final eruptive products and constitute about 1% by volume; they always overlie the potassic lavas. *Kyle* [1982] suggested that sodic lavas represented the outpourings from a single compositionally zoned magma chamber. The evolution of the lava lineages has been examined by using rare earth elements [*Kyle and Rankin,* 1976]. Cognate xenoliths of essexite and syenite, as well as xenoliths of upper crustal granitoids, occur at Mount Pleiones. Microprobe analyses of the phenocryst phases from a suite of selected samples are described by *Kyle* [1986*b*].

Chronologic Data

Four K-Ar date determinations [*Armstrong,* 1978] show that The Pleiades are among the youngest volcanic centers in Antarctica. Dates range from 0.04 ± 0.05 Ma at Mount Pleiones to 0.003 ± 0.014 Ma at "Taygete Cone." Pumice lapilli are scattered over Mount Pleiones. Five areas of hydrothermal alteration near the top of "Taygete Cone" appear youthful and may represent recent hot springs. It is inferred that The Pleiades are extremely young and should be considered dormant.

TABLE A.7.1. (continued)

	9	10	11	12	13	14
SiO_2	55.12	59.79	59.94	62.39	63.84	64.56
TiO_2	1.29	0.21	0.60	0.24	0.29	0.15
Al_2O_3	17.39	18.83	18.19	16.56	16.52	16.95
Fe_2O_3	3.07	3.54	4.03	4.51*	2.00	3.28
FeO	5.66	1.89	1.34	--	2.88	0.74
MnO	0.23	0.20	0.18	0.16	0.17	0.15
MgO	1.65	0.16	0.57	0.25	0.14	0.07
CaO	4.11	1.34	2.13	1.14	1.30	0.94
Na_2O	7.31	8.68	7.29	7.61	7.21	7.81
K_2O	3.52	5.26	5.22	4.96	5.32	5.18
P_2O_5	0.59	0.09	0.17	0.07	0.07	0.02
Total	99.94	99.99	99.66	99.17**	99.74	99.85
Ba	899	633	869	<10	444	26
Cr	5	10	--	--	--	--
Cu	13	8	6	<10	9	--
Ni	5	--	--	<10	--	--
Rb	88	183	224	320	255	315
Sr	643	97	415	73	48	7
V	6	--	8	--	--	--
Zn	110	115	81	192	106	139

9. 25661. Benmoreite, Mount Pleiones [*Kyle,* 1982].
10. 25683. Phonolite, Cone 11 [*Kyle,* 1982].
11. 25687. Trachyte, Cone 10 [*Kyle,* 1982].
12. 82056. Peralkaline trachyte pumice tephra, Mount Pleiones (Kyle, unpublished data, 1984).
13. 25701. Peralkaline trachyte, "Aleyone Cone" [*Kyle,* 1982].
14. 25699. Peralkaline trachyte, "Taygete Cone" [*Kyle,* 1982].

Copyright American Geophysical Union

Extent of Knowledge

Most exposures of volcanic rocks at The Pleiades have been examined by P.R. Kyle and associates during fieldwork in 1971–1972 and 1981–1982. The lack of erosion, and the snow and ice cover, limit exposure. Major- and trace-element analyses [*Kyle*, 1976; *Kyle and Rankin,* 1976; Kyle, unpublished data, 1986] of 32 specimens, and microprobe analyses of mineral phases [*Kyle*, 1986*b*] make The Pleiades reasonably well characterized. A good suite of possibly cognate xenoliths have not been examined in any detail.

Bibliography

Armstrong, 1978
Gair et al., 1969
Kyle, 1976, 1982, 1986*b*
Kyle and Cole, 1974
Kyle and Rankin, 1976
Nathan and Schulte, 1968
Riddolls and Hancox, 1968

Copyright American Geophysical Union

A.8. Mount Overlord

Type of volcano: Stratovolcano with associated pyroclastic deposits and subsidiary vents.
Location: Aviator Glacier, northern Victoria Land (73°10′S, 164°35′E).
Height above sea level: 3396 m.
Evidence of Holocene activity: None.
Authors of report: P.R. Kyle and M.R. Noll.
Date of report: June 1986.

Form and Structure

Mount Overlord forms an asymmetrical cone on the northwest corner of Deception Plateau, overlooking Aviator Glacier (Figures A.8.1–A.8.3). A well-defined caldera, over 800 m across, is surrounded by a largely undissected rim, with reasonable exposure on the western half of the cone. The caldera is breached to the south and northeast. Parasitic cones are found along the northern and western flanks, where exposure is best. On the eastern flank, capping the cliffs above Aviator Glacier, are welded and unwelded tuffs and ignimbrites. Cognate xenoliths are common. Ice cover limits much of the exposure.

Petrologic Characteristics

Mount Overlord is predominantly composed of intermediate and felsic alkaline lavas with volumetrically minor basaltic rocks (Table A.8.1 and Figure A.8.4). The rocks may be divided into two suites, a strongly undersaturated suite (SUS) and a weakly undersaturated suite (WUS) [*Noll*, 1985]. The SUS is composed of a series from

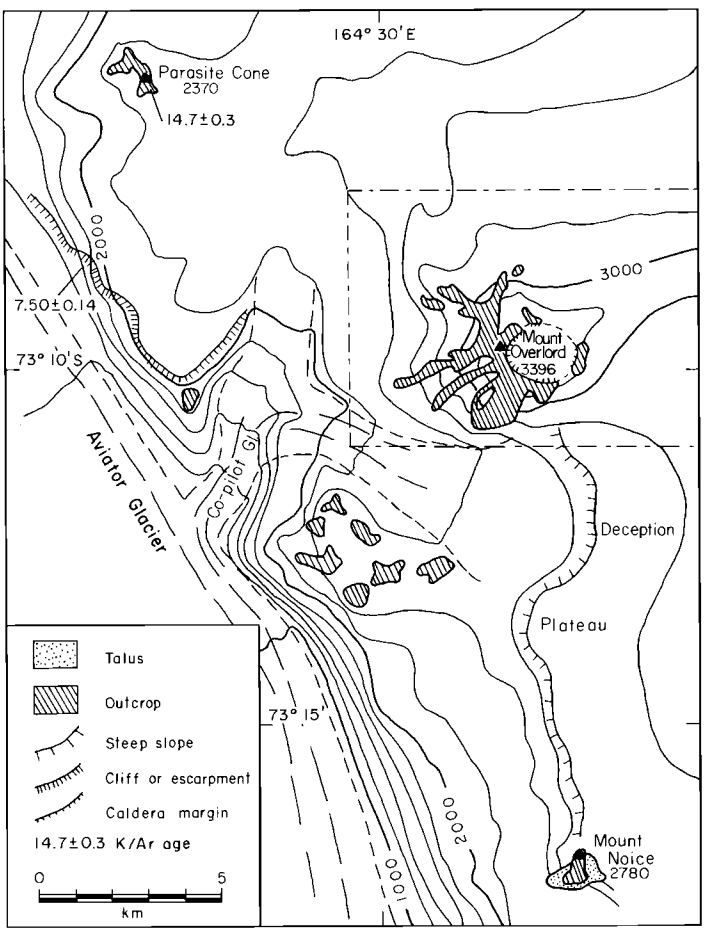

Fig. A.8.1. Sketch map of the upper Aviator Glacier, showing the location of Mount Overlord and the surrounding volcanic vents and the location of analyzed samples.

Copyright American Geophysical Union

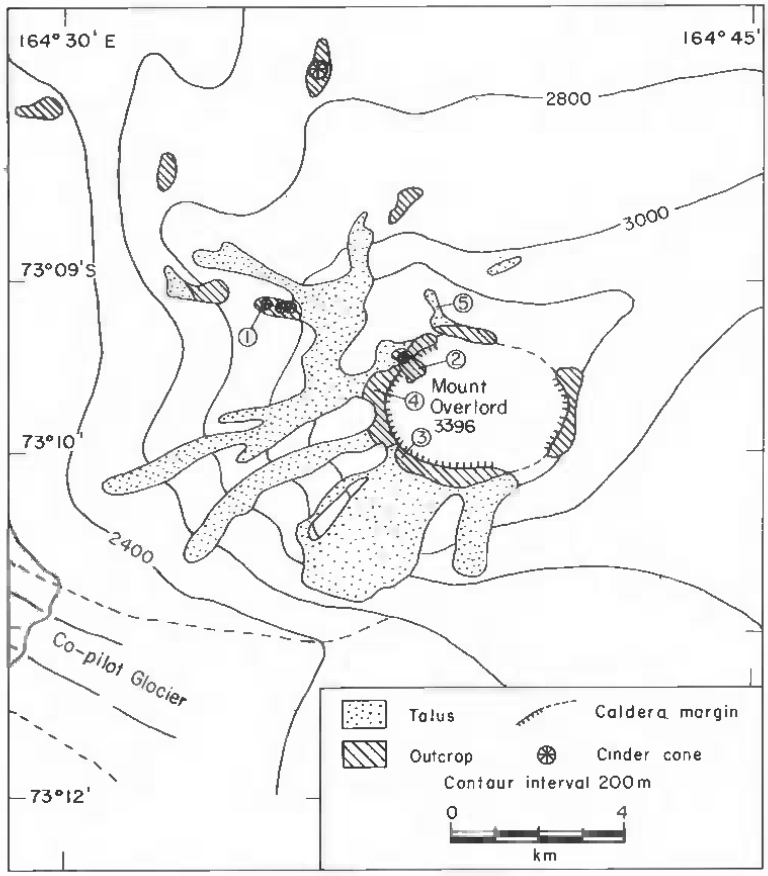

Fig. A.8.2. Sketch map of Mount Overlord, showing the location of analyzed samples.

Fig. A.8.3. Oblique aerial view of Mount Overlord (3396 m) looking northeastward. Small parasitic cones are apparent on the lower flanks of the volcano. On the extreme right in the middle distance is Mount Noice (2780 m). The broad, flat Deception Plateau, which extends behind Mount Overlord, may be due to the presence of ignimbrite erupted from Mount Overlord. Slightly left of center in the distance is Mount Murchison (3501 m), and behind that, to the left, is Coulman Island (see IVD A.4), the southernmost center in the Hallett volcanic province. (U.S. Navy photograph, TMA 710 F31 342.)

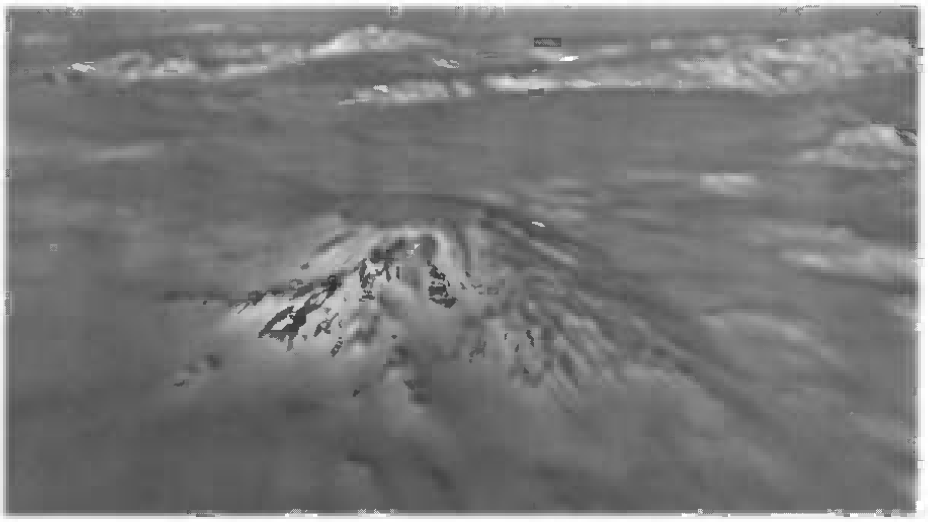

Copyright American Geophysical Union

TABLE A.8.1. Representative Chemical Analyses of Volcanic Rocks From Mount Overlord

	1	2	3	4	5
SiO_2	45.60	52.60	54.78	58.96	75.09
TiO_2	2.53	1.78	1.01	0.68	0.27
Al_2O_3	15.26	18.31	19.03	18.24	11.31
FeO*	11.48	8.22	6.63	5.27	3.21
MnO	0.20	0.20	0.21	0.17	0.08
MgO	8.34	2.73	1.34	0.81	0.06
CaO	9.65	5.32	3.65	2.21	0.38
Na_2O	3.38	6.33	7.72	6.70	5.00
K_2O	1.42	2.97	3.85	4.98	4.71
P_2O_5	0.84	0.66	0.42	0.22	0.02
LOI	-0.07	0.73	0.52	0.91	0.22
Total	98.63	99.85	99.16	99.15	100.35
Ba	524	731	776	545	--
Ce	125	174	217	231	--
Co	46	16	8	4	--
Cr	392	25	3	8	--
Cs	0.5	1.2	2.0	3.0	--
Cu	50	13	<10	<10	<10
Eu	2.9	3.2	2.8	2.1	--
Ga	20	25	27	28	30
Hf	5.8	11	15	19	--
La	63	92	119	128	--
Lu	0.3	0.5	0.7	0.7	--
Nb	93	133	186	238	166
Ni	160	15	<10	<10	<10
Pb	<2	9	14	17	32
Rb	40	73	126	159	247
Sb	0.1	0.2	0.4	0.3	--
Sc	22	25	3.7	4.4	--
Se	0.8	1.2	1.7	2.0	--
Sm	8.8	11	11	13	--
Sr	887	948	750	229	3.4
Ta	5.5	8.9	12	15	--
Tb	1.2	1.3	1.3	1.5	--
Th	7	18	31	32	37
U	1	4	6	6	7
Y	29	37	46	54	89
Yb	2.3	3.8	4.4	5.0	--
Zn	112	121	132	141	168
Zr	294	589	832	943	896

All samples analyzed by XRF and instrumental neutron activation [from *Noll*, 1985]. Dashes, not determined. LOI, loss on ignition.

*Total Fe expressed as FeO.

1. 81510. Basanite.
2. 81422. Mugearite.
3. 81428. Phonolite.
4. 81442. Trachyte.
5. 81435A. Comendite.

Copyright American Geophysical Union

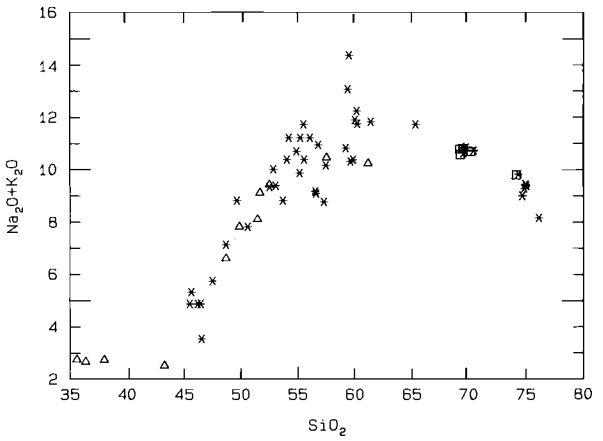

Fig. A.8.4. Alkali versus silica plot of volcanic rocks from Mount Overlord (asterisks), Mount Noice (squares), and cognate cumulate xenoliths included in Mount Overlord lavas (triangles). All analyses are recalculated to 100% volatile-free. Data are from *Noll* [1985].

basanite to *ne*-hawaiite, *ne*-mugearite, *ne*-benmoreite, and phonolite. The WUS consists of alkali basalts, hawaiites, mugearites, benmoreites, trachytes, *Q*-trachytes, and comendites. Welded subaerial fall deposits occur on the caldera rim. Analyses of the cognate xenoliths are given in Table A.8.2.

Rhyolite, which is weakly peralkaline, is common as obsidian and flows at Mount Noice. Chemically, the rhyolite is similar to the welded subaerial fall deposits on Mount Overlord.

Chronologic Data

Four K-Ar dates for Mount Overlord give an average of 7.2 Ma. Three samples [*Armstrong*, 1978] yielded dates of 7.0 ± 0.14 and 8.3 ± 1.7 Ma for intermediate lavas and 7.4 ± 0.14 Ma for a basalt. A new K-Ar date of 7.5 ± 0.14 Ma, on an alkali basalt from Aviator Glacier (Table A.II.2), confirms the age of Mount Overlord. A basanite clast in hyaloclastite at Parasite Cone (Figure A.8.1) has a value of 14.67 ± 0.3 Ma (Table A.II.2).

Extent of Knowledge

Exposed outcrop makes up ~10–20% of the volcano. The best exposure is along its western rim and flanks and in the caldera wall. Current information is based on brief visits by H.S. Gair in 1962–1963 and by S. Nathan and F.J. Schulte in 1966–1967; more extensive work was done by P.R. Kyle, M.R. Noll, and others during the 1981–1982 field season.

Bibliography

Armstrong, 1978
Gair, 1967
Kyle, 1976
Nathan and Schulte, 1968
Noll, 1985

TABLE A.8.2. Representative Chemical Analyses of Cognate Cumulate Xenoliths in Lavas From Mount Overlord

	1	2	3
SiO_2	37.91	50.50	60.37
TiO_2	3.92	1.86	0.75
Al_2O_3	13.66	17.76	17.36
FeO*	16.98	8.70	4.85
MnO	0.23	0.22	0.18
MgO	7.61	2.85	1.22
CaO	13.48	6.12	3.42
Na_2O	2.32	6.27	6.01
K_2O	0.40	2.64	4.08
P_2O_5	2.89	0.77	0.38
LOI	0.00	0.88	0.27
Total	98.70	98.57	98.89
Ba	241	1056	1348
Ce	159	209	231
Co	54	20	4
Cr	81	20	6
Cs	1.7	1.0	1.6
Cu	60	--	--
Eu	4.9	3.9	2.6
Ga	19	--	--
Hf	16	9.5	8.9
La	65	109	119
Lu	0.3	0.5	0.6
Nb	33	147	120
Ni	28	--	--
Pb	--	5	14
Rb	9.2	71	127
Sb	--	0.2	0.2
Sc	19	11	5
Se	0.3	1.8	1.4
Sm	16	14	14
Sr	1658	1139	444
Ta	13	10	7.7
Tb	1.7	1.5	1.6
Th	--	14	28
U	1	4	4
Y	38	43	51
Yb	2.0	4.3	4.3
Zn	112	--	--
Zr	105	450	393

All samples analyzed by XRF and instrumental neutron activation [from *Noll*, 1985]. Dashes, not determined. LOI, loss on ignition.

* Total Fe expressed as FeO.

1. 81473. Essexite.
2. 81476. Anorthosite.
3. 81480. Sodalite syenite.

Copyright American Geophysical Union

A.9. Vulcan Hills

Type of volcano: Eroded stratovolcano, high-level subvolcanic complex.
Location: East of upper Campbell Glacier, northern Victoria Land (73°39′S, 163°40′E).
Height above sea level: 2987 m.
Evidence of Holocene activity: None.
Author of report: P.R. Kyle.
Date of report: February 1987.

TABLE A.9.1. Representative Chemical Analyses of Volcanic and Hypabyssal Intrusive Rocks From Vulcan Hills

	1	2	3	4	5	6	7	8	9	10	11
SiO_2	47.26	49.32	49.37	49.80	51.75	52.56	52.96	58.80	59.79	62.89	64.04
TiO_2	3.49	2.72	2.89	2.22	2.30	2.14	1.63	1.26	0.76	0.33	0.17
Al_2O_3	16.21	14.96	15.52	18.48	17.58	17.06	16.00	15.64	15.11	17.08	16.31
Fe_2O_3*	13.06	12.34	11.66	9.93	10.16	10.78	8.04	8.20	6.22	4.61	4.52
MnO	0.17	0.24	0.20	0.18	0.14	0.19	0.14	0.19	0.12	0.15	0.18
MgO	4.54	5.02	4.45	3.07	3.07	2.95	2.10	1.71	1.03	0.20	0.06
CaO	9.40	7.35	6.91	8.20	7.99	4.30	5.50	3.66	3.70	0.56	0.78
Na_2O	3.61	3.65	3.94	4.12	4.22	4.90	4.05	4.84	5.76	6.57	6.45
K_2O	1.20	1.97	2.15	1.60	1.81	3.30	2.61	3.65	2.62	5.42	4.91
P_2O_5	1.25	0.94	0.62	0.97	0.76	0.87	0.68	0.55	0.23	0.07	0.02
LOI	0.00	0.96	2.10	0.87	0.00	0.73	5.75	1.08	4.41	1.76	1.81
Total	100.19	99.47	99.81	99.44	99.78	99.78	99.46	99.58	99.75	99.64	99.25
*Q***	0.00	0.00	0.00	0.00	0.00	0.00	4.1	5.8	7.1	1.6	5.2
Cu	31	37	28	14	24	10	<10	12	<10	<10	<10
Ga	24	23	25	24	26	29	22	26	25	34	37
Nb	46	81	79	62	49	120	60	94	107	250	321
Ni	17	18	32	9	13	11	<5	<10	<5	<5	<5
Pb	<2	4	<2	4	6	7	12	13	7	16	20
Rb	30	57	54	38	50	78	82	103	39	172	155
Sr	947	742	918	1056	922	815	583	537	318	28	26
Th	<2	7	5	3	6	9	11	12	14	31	34
Y	30	43	38	33	31	46	37	47	48	66	104
Zn	97	304	113	113	99	191	107	138	128	151	228
Zr	157	342	346	259	217	573	311	486	530	1321	1512

All samples analyzed by XRF by P.R. Kyle. LOI, loss on ignition.
*Total Fe expressed as Fe_2O_3.
**Normative quartz.

1. 82042. Basalt (gabbro), main mass of subvolcanic rocks forming south Vulcan Hills.
2. 82040A. Hawaiite, intrusive rocks intermixed with 82040B and intruding 82042, south Vulcan Hills.
3. 82051. Hawaiite, medium-grained irregular dike, north Vulcan Hills.
4. 82020. Hawaiite, lava flow overlying gabbroic rocks, south Vulcan Hills.
5. 82046. Intrusive mugearite, south Vulcan Hills.
6. 82040B. Mugearite, intrusive rock intermixed with 82040A, south Vulcan Hills.
7. 82022. Benmoreite, porphyritic dike intruding Beacon Supergroup sediments, south Vulcan Hills.
8. 82050. Benmoreite, irregular fine-grained dike, north Vulcan Hills.
9. 82039. Trachyte dike, south Vulcan Hills.
10. 82047. Trachyte flow, north Vulcan Hills.
11. 82021. Trachyte dike, south Vulcan Hills.

Copyright American Geophysical Union

Form and Structure

Vulcan Hills (see Figure A.11.1) was referred to as "Surprise Hills" by *Nathan and Schulte* [1968], who visited the area in 1966–1967 and briefly described the geology as low-dipping flows of basaltic and trachytic rocks overlying basalts of the Kirkpatrick Basalt Group. They suggested that the flows represented the dissected remnant of an ancient volcano. During a brief helicopter stop in the 1981–1982 field season, the author collected a number of samples and generally confirmed the interpretation by *Nathan and Schulte* [1968]. Two outcrop areas were visited: north Vulcan Hills (containing the highest point) and south Vulcan Hills (a small nunatak about 2 km to the south). During the later visit, no Kirkpatrick basalts were identified, but gabbroic rocks, believed to be part of the Vulcan Hills sequence, appeared to overlie Beacon Supergroup sedimentary rocks. The gabbroic rocks, which on the basis of the total alkali-silica (TAS) classification [*Le Bas et al.*, 1986] include hawaiite and mugearite, are intruded by numerous dikes of porphyritic benmoreite and trachyte. Trachyte flows were observed in several places. The short duration of the visit did not allow any careful observation of the interrelationships between the various rock units.

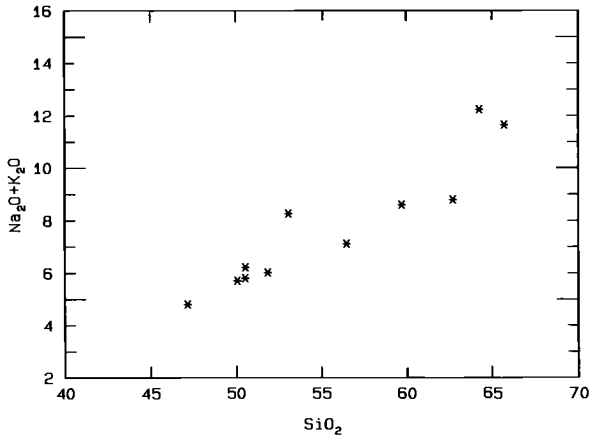

Fig. A.9.1. Alkali versus silica plot for volcanic and high-level intrusive (hypabyssal) rocks from Vulcan Hills.

Petrologic Characteristics

Eleven samples collected by the author in 1981–1982 have been analyzed (Table A.9.1). The samples show varying degrees of alteration but allow preliminary interpretations of the petrologic characteristics. On the basis of the TAS classification [*Le Bas et al.*, 1986] the sample types are alkali basalt (gabbro), hawaiite, mugearite, benmoreite, and trachyte. In the alkali versus silica diagram (Figure A.9.1) the rocks show a wide range in compositions, suggesting that Vulcan Hills may have once been a major stratovolcano with a variety of lava flows. The rocks are all given volcanic terminology, even though many were intrusive (hypabyssal). This allows comparison with other McMurdo Volcanic Group rocks.

Fig. A.9.2. Harker variation diagrams plotted against Zr as an index of fractionation. Trace elements (Zr, Sr, Nb) are in parts per million; major elements (SiO_2, alkalis) are in weight percent after normalization to 100% on a volatile-free basis.

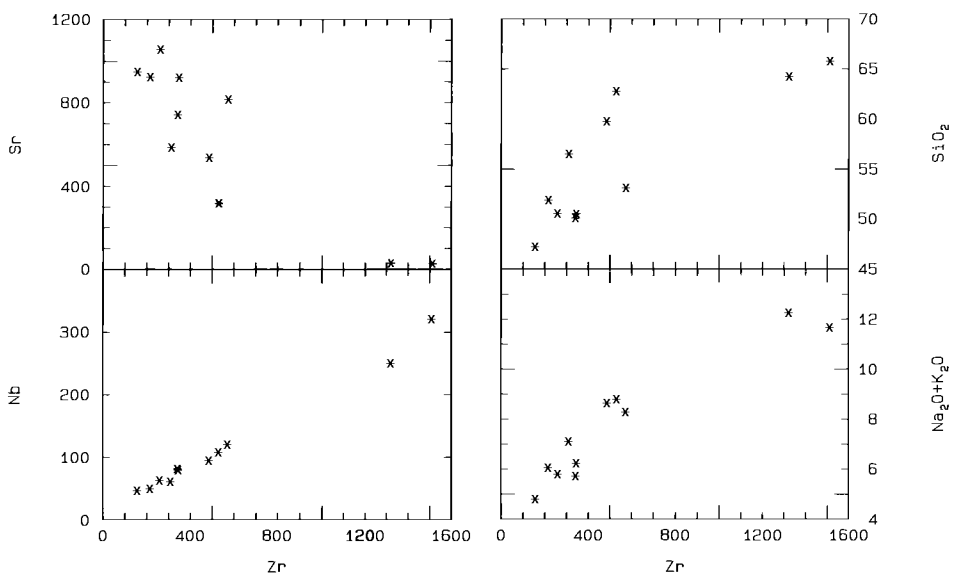

Copyright American Geophysical Union

All analyzed samples contain normative *hy*, whereas the benmoreites and trachytes are oversaturated and have normative *Q* (Table A.9.1). Overall, trace-element plots (e.g., Nb versus Zr (see Figure A.9.2)) suggest that the rocks may have evolved from a single alkali basalt parent. The large gap in Zr content and the break in Sr content suggest that evolution of the evolved trachytes may have involved significant feldspar fractionation.

Chronologic Data

No chronologic data are available. However, the extensive erosion of the rocks suggests formation prior to major ice cover, which effectively reduces erosion. Compared to Mount Overlord, which dates from about 7 Ma and yet does not show significant erosion, Vulcan Hills is likely to be older (probably earlier than 10 Ma).

Extent of Knowledge

The results of the reconnaissance mapping in 1966–1967 [*Nathan and Schulte,* 1968] and 1981–1982 (Kyle, unpublished data, 1986) are tentative. However, they do suggest the existence of older eruptive vents in northern Victoria Land.

Bibliography

Nathan and Schulte, 1968

Copyright American Geophysical Union

A.10. Mount Melbourne

Type of volcano: Large undissected stratovolcano centered in a volcanic field composed of densely spaced subglacial (palagonitized volcaniclastites, pillows, and hyaloclastite mass flows) and subaerial volcanoes (tuff rings, cinder and scoria cones, lava flows).

Location: Between Wood Bay and Campbell Glacier, northern Victoria Land (74°21′S, 164°42′E).

Height above sea level: 0–2732 m, partly submerged below sea level.

Estimated volume: Volcanic field, 250 km^3; central stratovolcano, 180 km^3.

Evidence of Holocene activity: Tephra layers in and on top of ice and overlying recent erosional surface on the eastern and southeastern flanks; fumarolic activity, young K-Ar ages.

Authors of report: G. Wörner and L. Viereck.

Date of report: January 1986.

Form and Structure

The Mount Melbourne volcanic field (MMVF) (Figures A.10.1 and A.10.2) forms a north-south trending peninsula on the Victoria Land coast, between Wood and Terra Nova bays (see Figure A.II.1). The field is characterized by a smooth subglacial morphology, in contrast to the rugged terrain of the surrounding basement intrusive rocks (Figures A.10.1 and A.10.2). The northern limit of the field is marked by steep faults against the Transantarctic Mountains, but the southern and eastern limits are submerged below sea level, and the western boundary is Campbell Glacier. Within the MMVF, all exposed rocks are volcanic, and there are a number of volcanoes scattered over basement rocks in the Random Hills area, to the north and west of Campbell Glacier. These indicate the continuity of the Melbourne volcanic province northward to Mount Overlord and The Pleiades.

Transitions from subglacial to subaerial volcanic rock types are commonly observed in erosional profiles along the coast; volcanic structures are mainly of tabular morphology (e.g., Shield Nunatak). Subglacial volcaniclastites are

Fig. A.10.1. The Mount Melbourne volcanic field (MMVF) of the Melbourne volcanic province. Major individual eruptive centers, morphological ridges, and types of volcano (subglacial/subaerial) are indicated [from *Wörner et al.*, 1989].

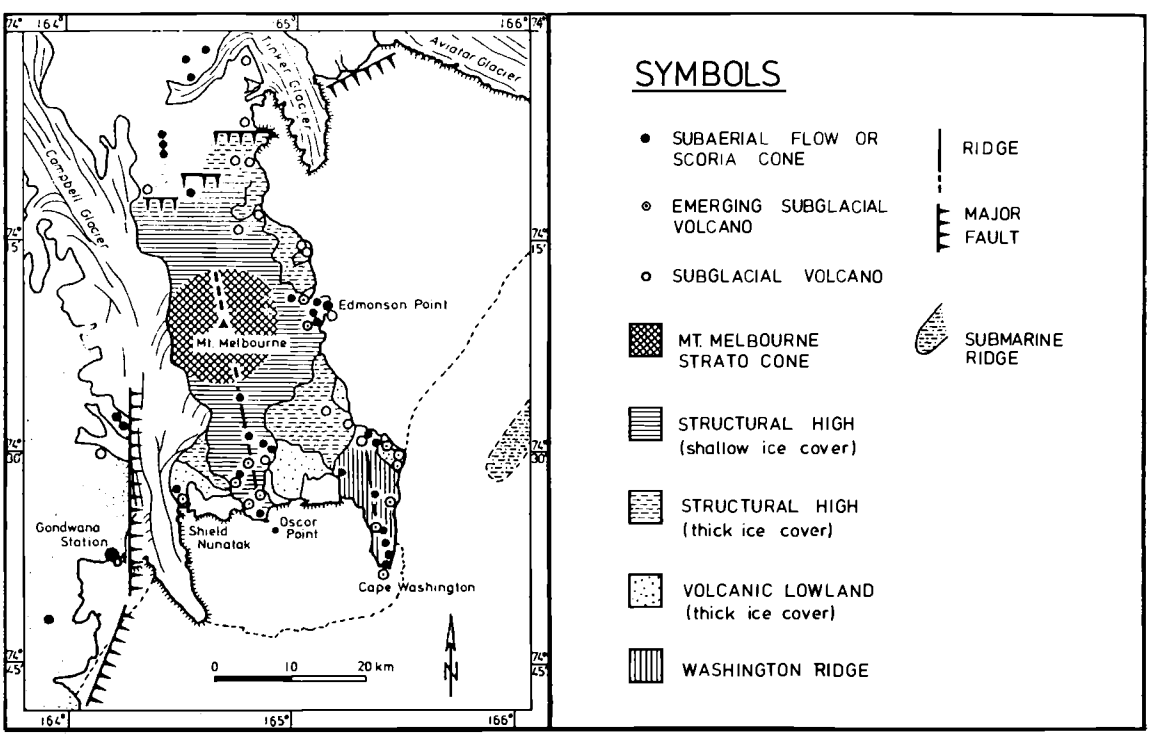

Copyright American Geophysical Union

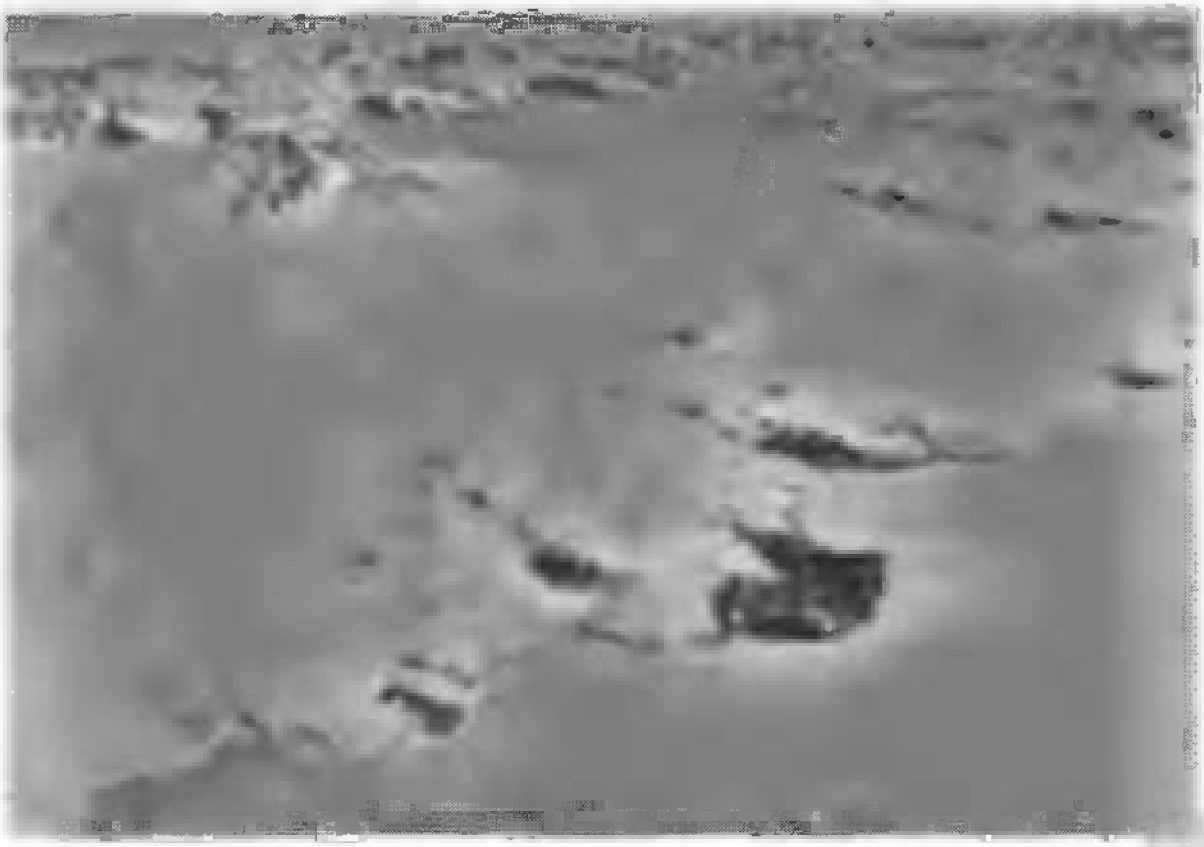

Copyright American Geophysical Union

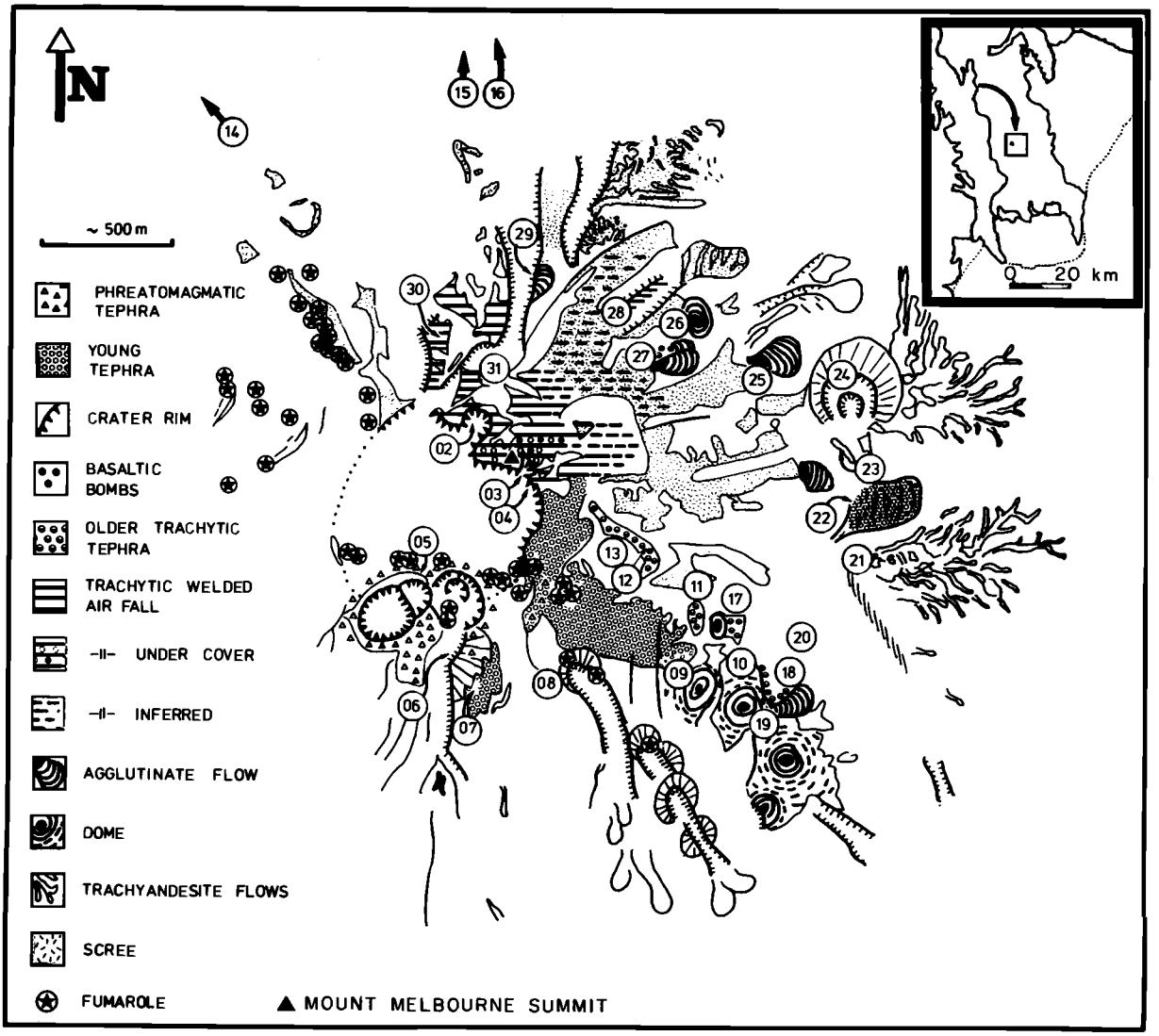

Fig. A.10.3. Map of Mount Melbourne stratovolcano, showing rock type distribution. Note the linear NNW-SSE arrangement of fumaroles and local eruptive centers across the summit [from *Wörner and Viereck,* 1987]. Encircled numbers refer to sample localities.

phreatomagmatic craters. Erosional scars on the eastern and southeastern sides either are local and directly related to eruptive activity (collapse of newly erupted scoria cones on a steep slope) or, alternatively, represent large-scale slumping and partial collapse of the steep eastern flank. From field observations and petrographic and chemical correlations an older trachyte fall deposit and dome phase can be recognized, separated by an erosional unconformity from a younger trachyandesite scoria and lava flow sequence. This in turn is followed by still younger trachytic and basaltic tephra. The most recent eruption of trachyte forms a blanket of pyroclastic fall pumice and scoria around the eastern and southern flanks of the volcano. It is also found in and on top of ice [*Nathan and Schulte,* 1967; *Keys et al.,* 1983; *Wörner and Viereck,* 1989] and is believed to be as young as a few hundred years [*Adamson and Cavaney,* 1967; *Nathan and Schulte,* 1967; *Keys et al.,* 1983; *Lyon,* 1986]. Present-day fumarolic activity is concentrated along a NNE-SSW line which cuts through the summit area and along the line of phreatomagmatic craters at the southern rim of the main summit crater (Figures A.10.3 and A.10.4). Fumarole temperatures are constant, reaching 59°C at 25-cm depth [*Lyon and Giggenbach,* 1974; *Keys et al.,* 1983]. Warm ground supports an abundance of plant life (about a dozen species of algae, one species of moss, and one of liverwort) [*Broady et al.,* 1987].

Copyright American Geophysical Union

Copyright American Geophysical Union

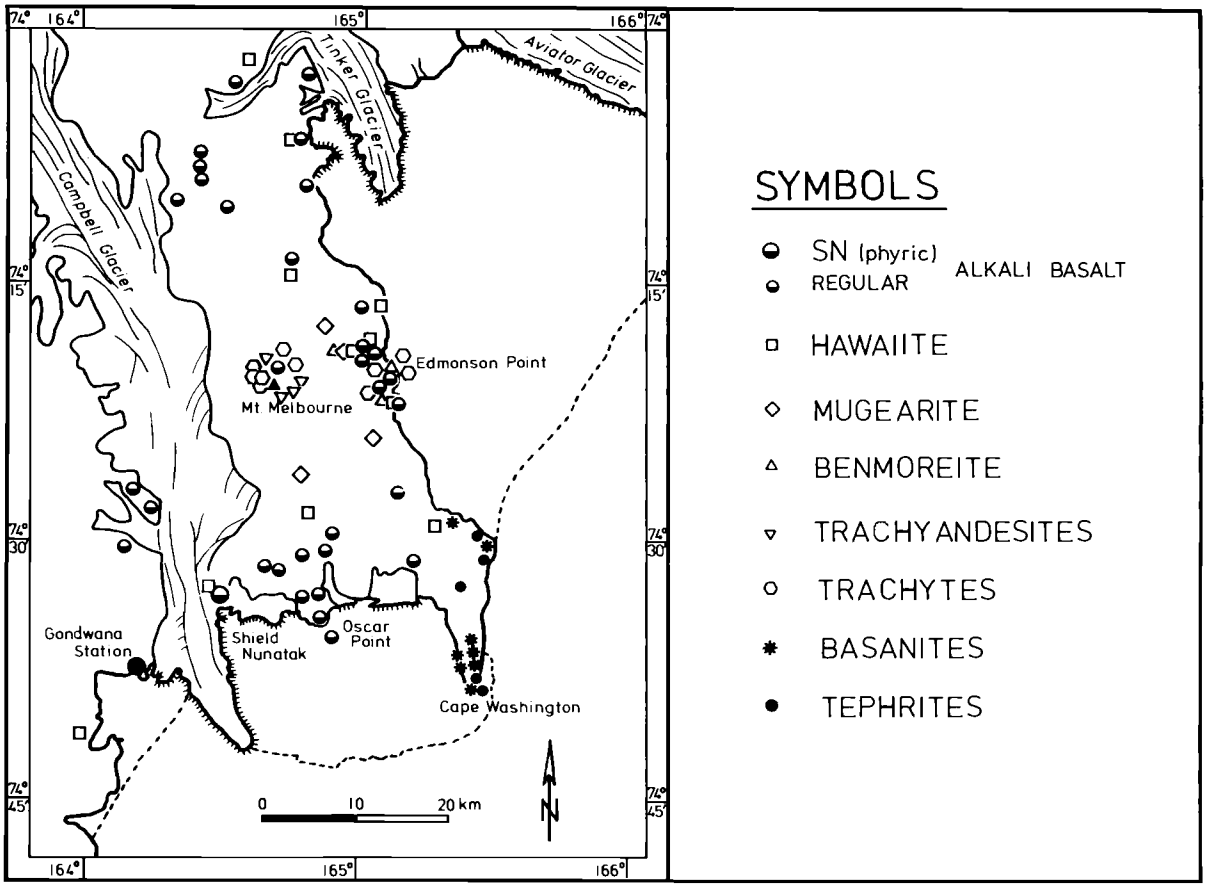

Fig. A.10.5. Distribution of the different rock types in the Mount Melbourne volcanic field. (Nomenclature after *Coombs and Wilkinson* [1969] and *Wörner et al.* [1989].) SN, Shield Nunatak.

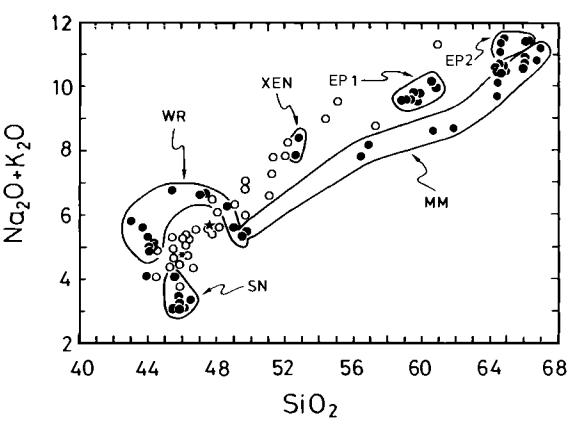

Fig. A.10.6. Alkali versus silica plot for volcanic rocks from Mount Melbourne. Note the low alkali content of the Mount Melbourne summit lavas (MM), and the two distinct types of mafic rocks, i.e., Shield Nunatak alkali basalt (SN) and Cape Washington ridge basanites (WR). EP, Edmonson Point; LIS, local isolated suite [after *Wörner et al.*, 1989].

granulite and tholeiitic cumulate xenoliths as well as spinel lherzolites (+plagioclase) and harzburgite mantle nodules.

Primary magma compositions in groups I and III are rare, and most samples are slightly fractionated, with Mg numbers around 64 (group I) and 58 (group III). Sr isotopic compositions are different in both groups (0.7033 and 0.7029, respectively), indicating the possibility of distinct mantle sources. Degrees of partial melting are implied to be higher for the alkali basalt magmas (group I).

Magmatic differentiation produced continuous major- and trace-element variations, with no compositional gap. Chemical lineages of the mildly alkalic basalts (group I) show, for a number of elements in the more differentiated parts, a trend similar to and partly overlapping with mafic members of the Mount Melbourne summit lavas (group II); therefore, a genetic relationship is likely. However, even the most mafic MM trachybasalt (Table A.10.1, analysis 9) is still distinctly SiO_2 oversaturated, and the MM trachyandesites are invariably lower in Na_2O (see Figure A.10.7). This demonstrates independent magma evolution within the larger Mount Melbourne magmatic system, as compared to

Copyright American Geophysical Union

TABLE A.10.1. Representative Chemical Analyses From the Mount Melbourne Volcanic Field

	1	2	3	4	5	6	7	8	9
SiO_2	42.14	43.80	45.00	46.30	48.90	59.50	63.10	64.00	64.20
TiO_2	3.75	4.47	2.87	3.28	3.39	0.76	0.52	0.38	0.32
Al_2O_3	12.93	15.95	13.34	15.68	15.87	16.24	15.55	14.89	14.11
Fe_2O_3	3.02	3.52	2.63	3.40	5.51	1.26	2.81	2.97	2.41
FeO	10.43	10.09	9.06	9.18	6.23	6.48	3.10	2.66	2.85
MnO	0.21	0.18	0.17	0.20	0.19	0.21	0.15	0.17	0.16
MgO	9.15	6.13	9.86	5.23	3.99	0.60	0.21	0.02	0.04
CaO	9.92	9.47	11.74	7.10	8.73	3.02	1.97	1.55	1.18
Na_2O	3.94	3.16	2.26	4.41	3.65	5.81	5.58	5.74	5.95
K_2O	1.71	0.84	0.73	2.08	1.71	4.16	4.68	4.67	4.80
P_2O_5	0.95	0.84	0.62	1.13	0.62	0.20	0.08	0.05	0.03
H_2O	0.23	0.44	0.21	0.98	0.26	0.25	0.22	0.36	1.25
CO_2	0.02	0.01	0.02	0.05	0.01	0.02	0.03	0.02	0.03
Total	98.37	99.17	98.50	98.89	99.04	98.53	97.96	97.49	97.32
Ba	640	429	297	654	661	1306	1047	1491	184
Co	51	46	49	35	31	3	3	<3	<3
Cr	177	52	432	51	47	16	16	15	15
Cu	55	46	74	32	32	10	15	11	8
Nb	101	47	37	103	68	134	166	157	176
Ni	187	58	178	55	24	4	4	5	5
Rb	51	22	22	50	49	105	152	137	146
Sr	1050	922	621	1134	684	371	186	89	14
Y	37	22	20	38	29	54	64	63	75
Zn	139	108	90	144	121	153	153	160	190
Zr	382	166	141	530	267	556	719	679	755

All samples analyzed by XRF [from *Wörner et al.*, 1989].
1. 13-140. Basanite/tephrite, Cape Washington ridge.
2. 08-034. Basanite/tephrite, Oscar Point ridge.
3. 10-016. Alkali basalt, Shield Nunatak.
4. 01-129. Basanite/tephrite, Cape Washington ridge.
5. 31-253. Hawaiite, Mount Melbourne summit.
6. 02-070. Trachyte, Edmonson Point.
7. 04-173a. Trachyte, Mount Melbourne summit.
8. 09-188. Trachyte, Mount Melbourne summit.
9. 16-231. Trachyte, Mount Melbourne summit.

surrounding local small-volume centers. Evolved *Q*-trachytic MM lavas also have higher Sr isotopic ratios (0.7044), suggesting an increasing role of crustal contamination.

Mount Melbourne apparently represented the focus of magmatic activity for less alkaline (i.e., larger degree of partial melting), more contaminated, and more differentiated lavas.

Cape Washington ridge basanites (group III) compare with the undersaturated sodic lineage of The Pleiades [*Kyle and Rankin,* 1976] and Mount Overlord [*Noll,* 1985], both of which are volcanic fields in the Melbourne volcanic province [*Kyle and Cole,* 1974]. Phonolites are absent in the MMVF, and rocks more evolved than *Q*-trachytes have not been erupted. This probably relates to the rather recent age of the MM magmatic system. Rhyolitic lavas, such as those at Mount Overlord and Malta Plateau, are to be expected in the geologic future.

In general, MMVF group I and group II lavas are distinctly more saturated and lower in Na_2O than any other McMurdo Volcanic Group rocks [*Wörner et al.,* 1989; *Nathan and Schulte,* 1968] (Figure A.10.7). Tectonic control at the intersection of the Rennick tectonic lineament and the prominent fault along the front of the Transantarctic Mountains apparently plays an important role in magma genesis in the MMVF.

Copyright American Geophysical Union

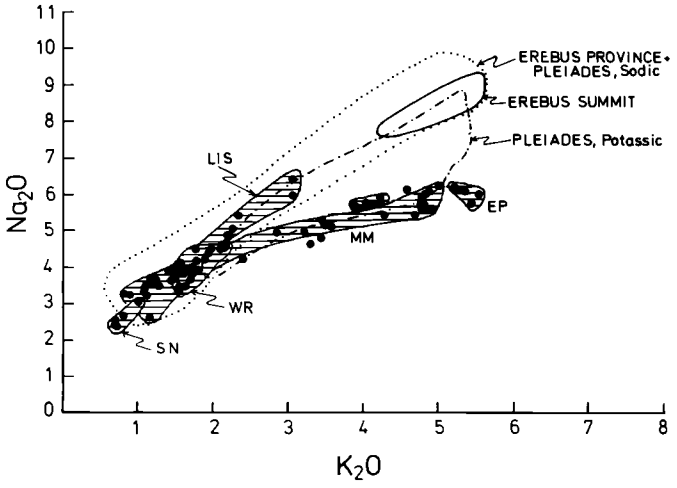

Fig. A.10.7. A Na_2O versus K_2O plot showing the comparison of Mount Melbourne lava lineages with other McMurdo Volcanic Group rocks [*Kyle,* 1977, 1982]. Note the low Na_2O content of Mount Melbourne summit lavas (MM). LIS, local isolated suite; see Figure A.10.6 for other symbols [from *Wörner et al.,* 1989].

Chronologic Data

Fumaroles, warm and dry ground, as well as the occurrence of primary tephra layers in and on top of glaciers, document the very recent age of the last eruption [*Adamson and Cavaney,* 1967; *Nathan and Schulte,* 1967; *Lyon and Giggenbach,* 1974; *Keys et al.,* 1983; *Wörner and Viereck,* 1989]. K-Ar age determinations for Mount Melbourne summit lavas range from 0.01 to 0.26 Ma. Additional dates on more mafic rock in the surrounding area indicate that some of the lavas may be significantly older than the stratocone. Deep glacial erosion and evidence for an older moraine deposit were observed at Edmonson Point and Baker Rocks. Subaerial lava flows underlying the subglacial Shield Nunatak, and a glacial erosion surface, may also belong to an older volcanic phase (pre-"Older Drift"?). This phase is overlain by a younger one, which has preserved primary tuff-ring morphology and may be as young as the last major phase of glaciation.

Extent of Knowledge

Early accounts of the geology of the Mount Melbourne area were concerned with its fumarolic activity. *Nathan and Schulte* [1968] and *Kyle* [1976] gave brief descriptions of the area, concentrating on Mount Melbourne summit and its rock types. *Armstrong* [1978] dated six samples by K-Ar methods. An extensive mapping and sampling program was completed by the present authors during GANOVEX IV in 1984–1985. A total of 69 samples from the MMVF and 19 additional MM summit lavas have been analyzed by XRF, and a representative suite of rocks also by instrumental neutron activation analysis (INAA) and for radiogenic isotopes (Sr, Nd) [*Wörner and Viereck,* 1989]. Geochemical, petrologic, and fluid inclusion studies on cumulate and mantle xenoliths are in progress.

A comprehensive aeromagnetic survey of this and other parts of Victoria Land and the Ross Sea basin was carried out during GANOVEX IV in 1984–1985. A map summarizing the results and interpretations will be given in a special volume of *Geologisches Jahrbuch.*

Bibliography

Adamson and Cavaney, 1967
Armstrong, 1978
Broady et al., 1987
Denton and Hughes, 1981
Keys et al., 1983
Kyle, 1976, 1982
Kyle and Cole, 1974
Kyle and Rankin, 1976
Lyon, 1986
Lyon and Giggenbach, 1974
Nathan and Schulte, 1967, 1968
Noll, 1985
Tessensohn and Wörner, 1989
Wörner and Viereck, 1987, 1989
Wörner et al., 1989

Copyright American Geophysical Union

A.11. Local Suite Basaltic Rocks

Type of volcano: Small basaltic scoria cones and flows with minor assorted pyroclastic deposits.
Location: Isolated occurrences throughout northern Victoria Land.
Height above sea level: Various, up to 3000 m.
Evidence of Holocene activity: None.
Author of report: P.R. Kyle.
Date of report: January 1987.

Fig. A.11.1. Map of northern Victoria Land, showing the location of small isolated and mainly basaltic vents not associated with the major volcanic centers and older gabbroic intrusions, namely the "Meander Intrusives" [after *Mueller et al.*, 1989]. Data were compiled from *Gair et al.* [1969], *Nathan and Schulte* [1968], *Riddolls and Hancox* [1968], and Figures A.6.1 and A.10.1.

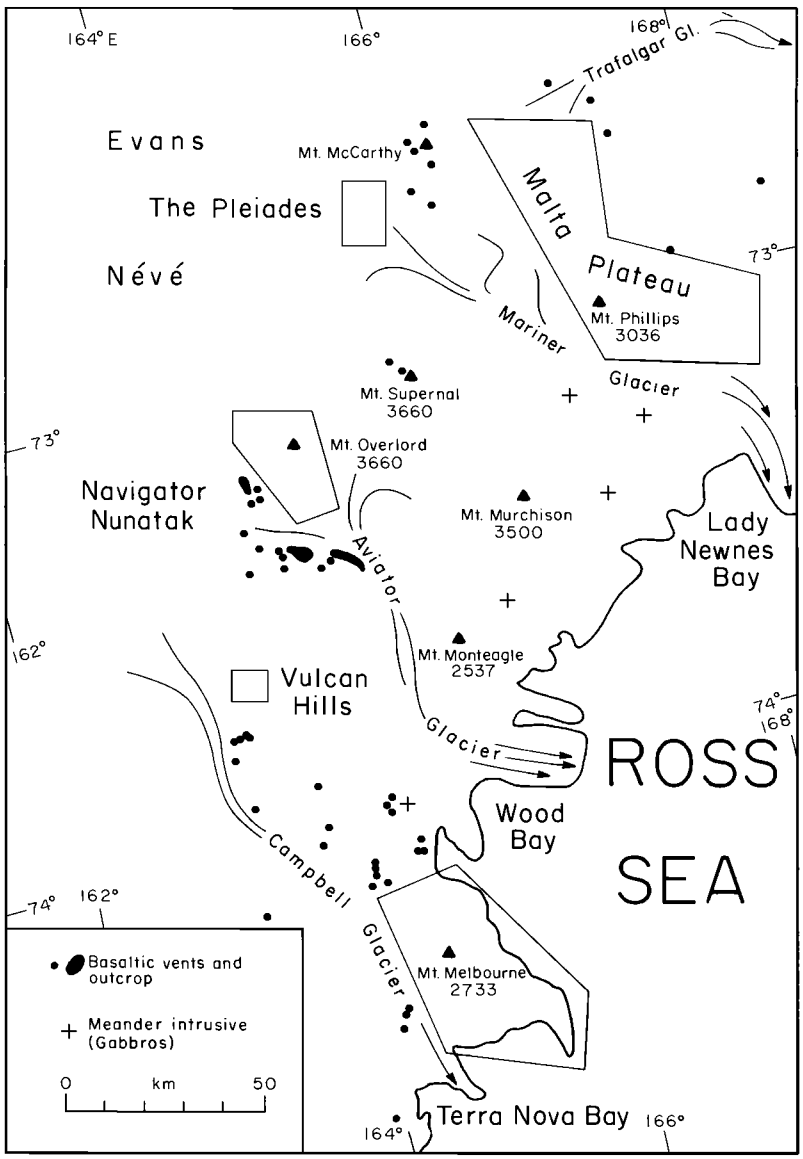

Copyright American Geophysical Union

Form and Structure

Small scoria cones consisting of welded Hawaiian/ Strombolian deposits, pyroclastic breccias, minor hyaloclastites, and rare lava flows are scattered throughout northern Victoria Land (Figure A.11.1). Most have not been visited, and it is difficult to generalize about their morphology. From limited observations these small isolated vents are often associated with minor faults.

Petrologic Characteristics

No detailed petrologic data are available on these rocks. Most are basaltic and are dominantly olivine and clinopyroxene bearing. Often they contain assorted xenoliths ranging from dunite to upper crustal granitoids. Typically, the lavas are multicolored as a result of strong oxidation. A representative analysis of a basanite is given in Table A.11.1.

Chronologic Data

Two K-Ar dates have been obtained for these rocks (Table A.II.1). A sample from Hades Terrace is dated at 4.4 ± 0.2 Ma, and a Nathan Hills sample gives 18.5 ± 0.7 Ma. Nathan (personal communication, 1976) considers the latter date to be anomalous and geologically unreasonable. A young flow spilling onto Cosmonaut Glacier has diverted it but has not yet been removed by erosion. It is inferred to be young [*Nathan and Schulte,* 1968], not more than 50,000 years.

Extent of Knowledge

No systematic attempt has been made to examine these small scattered occurrences of basaltic rocks. The exact number and locations are unknown. Brief descriptions are given by *Nathan and Schulte* [1968], who introduced the term "Local Suite."

Bibliography

Gair et al., 1969
Mueller et al., 1989
Nathan and Schulte, 1968
Riddolls and Hancox, 1968
Wörner et al., 1989

TABLE A.11.1. Chemical Analyses of Local Suite Volcanic Rocks

	1	2	3	4
SiO_2	41.37	44.76	45.85	47.21
TiO_2	3.55	3.09	3.39	2.24
Al_2O_3	14.18	15.28	16.78	15.95
Fe_2O_3	3.02	13.21*	13.65*	12.23*
FeO	9.10	0.00	0.00	0.00
MnO	0.19	0.20	0.20	0.19
MgO	8.52	8.37	5.45	8.01
CaO	10.80	9.70	8.41	9.55
Na_2O	3.55	3.79	4.25	3.65
K_2O	1.91	1.66	1.34	1.31
P_2O_5	0.67	0.79	0.61	0.52
LOI	--	-0.78	0.80	0.11
Total	97.06	100.07	100.73	100.96
Ba	397	--	--	--
Cr	204	--	--	--
Cu	59	52	--	--
Ga	--	20	--	--
Nb	--	82	--	--
Ni	124	144	--	--
Pb	--	5	--	--
Rb	44	42	--	--
Sr	772	831	--	--
Th	--	6	--	--
V	276	--	--	--
Y	--	31	--	--
Zn	97	102	--	--
Zr	--	238	--	--

All samples analyzed by P.R. Kyle using XRF techniques. Dashes, not determined. LOI, loss on ignition.

*Total Fe expressed as Fe_2O_3.

1. 25708. Basanite scoria cone, Webb Névé, northern Victoria Land.
2. 82132. Basanite scoria cone, northern side of Mount McCarthy, northern Victoria Land.
3. 81513A. Basanite scoria cone, Cosmonaut Glacier.
4. 81514. Trachybasalt scoria cone, Cosmonaut Glacier.

Copyright American Geophysical Union

A.III. Erebus Volcanic Province

Summary

P.R. Kyle

Introduction

Extensive studies have been made in the Erebus volcanic province, making it geologically the best known of the three volcanic provinces within the McMurdo Volcanic Group. Many areas have been mapped, at least on a reconnaissance basis, and a large mineralogical and geochemical data base is available. Radiometric age determinations are numerous and have been used to reconstruct the paleogeography of the volcanic rocks in the area [*Kyle*, 1981*c*].

Mount Erebus is an active volcano (Figures A.III.1 and A.III.2) and contains a persistent convecting lava lake of anorthoclase phonolite magma. Small Strombolian eruptions occur on a daily basis [*Kyle*, 1982; *Dibble et al.*, 1984], often ejecting anorthoclase phonolite bombs onto the crater rim [*Kyle*, 1977]. From September to December 1984, larger Strombolian eruptions occurred more frequently, ejecting bombs up to 2 km from the crater and sending small eruption columns to over 2 km high. Emissions of sulfur dioxide and particulate material have been measured from the lava lake [*Rose et al.*, 1985; *Chuan et al.*, 1986]. A detailed study of the seismicity of Mount Erebus was made as part of the International Mount Erebus Seismic Study (IMESS) [*Dibble et al.*, 1984]. Observations of the lava lake by a permanently mounted video camera are providing data on the timing and mechanisms of eruptions from the lava lake. Knowing the origin times of an eruption and the resulting earthquakes has allowed seismic data to place better constraints on the seismic velocity within Mount Erebus, which in turn allows better location of deep earthquakes [*Dibble et al.*, 1989; *S.J.D. Barrett*, 1987].

Much of the recent work in the Erebus volcanic province has been undertaken by graduate students [*Muncy*, 1979; *Kirsch*, 1981; *Moore*, 1986; and

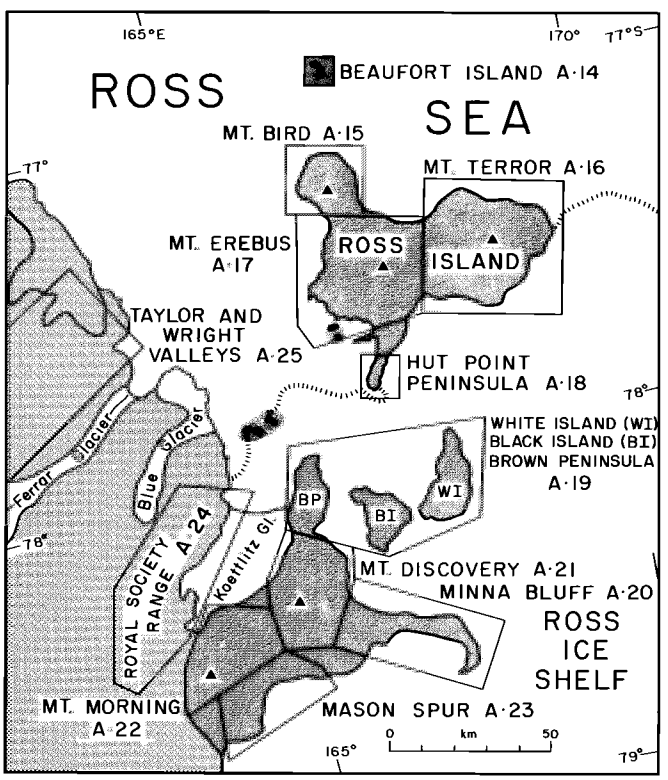

Fig. A.III.1. Generalized distribution of volcanic rocks in Erebus volcanic province, showing the location of the individual volcanic centers described, as indicated, by name and IVD number.

Copyright American Geophysical Union

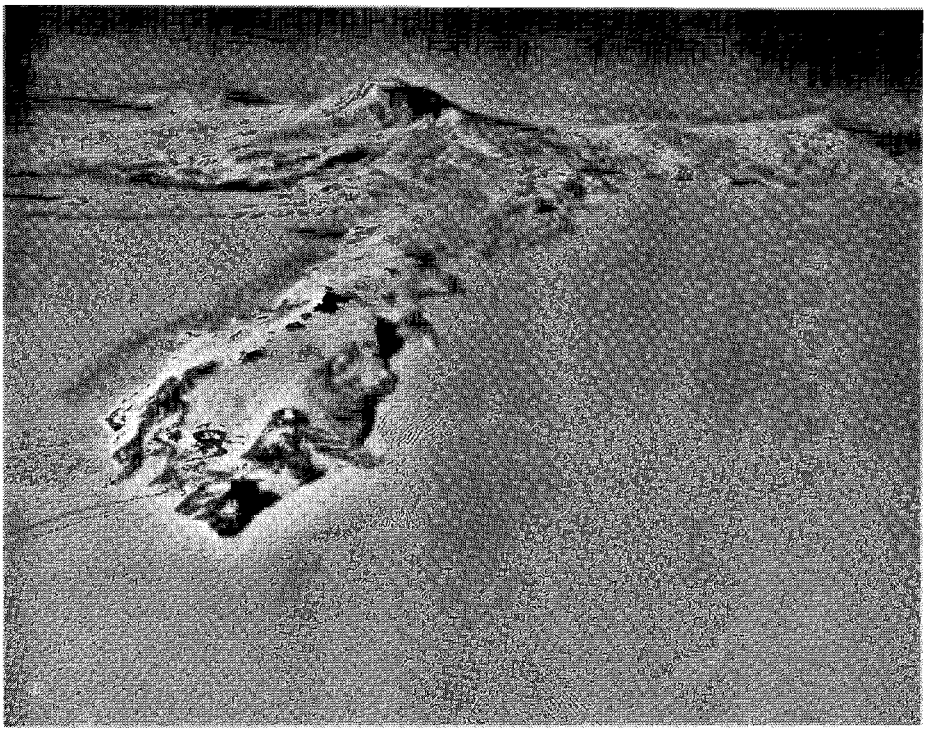

Fig. A.III.2. Aerial view looking north of Ross Island. In the foreground is Hut Point Peninsula, the site of McMurdo Station (left-center tip of the peninsula), the main base for the United States Antarctic Program, and Scott Base (on the prominent rock outcrop extending to the right and bounded by pressure ridges of the Ross Ice Shelf), the main base for the New Zealand Antarctic Research Programme. In the middle distance (slightly left of center) is the 3794-m-high active volcano Mount Erebus. A small volcano plume can be seen rising from the summit crater. Mount Terror (to the right of Mount Erebus) has a more shield-like appearance, with lower slope angles than the steep-sided, predominantly phonolitic Mount Erebus. Behind and to the left of Mount Erebus is Mount Bird, with Cape Bird, an area of reasonable exposure which extends along the eastern (left) flank of the volcano. (U.S. Navy photograph, TMA 550 F33 216.)

Fig. A.III.3. Aerial view looking southwest of the major volcanic centers in the southern part of McMurdo Sound. On the left is Black Island and behind it the long peninsula of Minna Bluff. Right of Black Island is Brown Peninsula, which is bounded to the west (right) by Koettlitz Glacier and to the east by moraine-covered ("dirty") ice of the Ross Ice Shelf. Mount Discovery is the prominent volcano behind and to the left of Brown Peninsula. The steep-sided dome-like top to Mount Discovery is composed mainly of felsic rocks, chiefly phonolite. Mount Morning is behind and to the right of Mount Discovery. Two broad bands of exposed rock extend up the slopes of Mount Morning, nearly reaching the summit caldera. (U.S. Navy photograph, TMA 549 F33 206.)

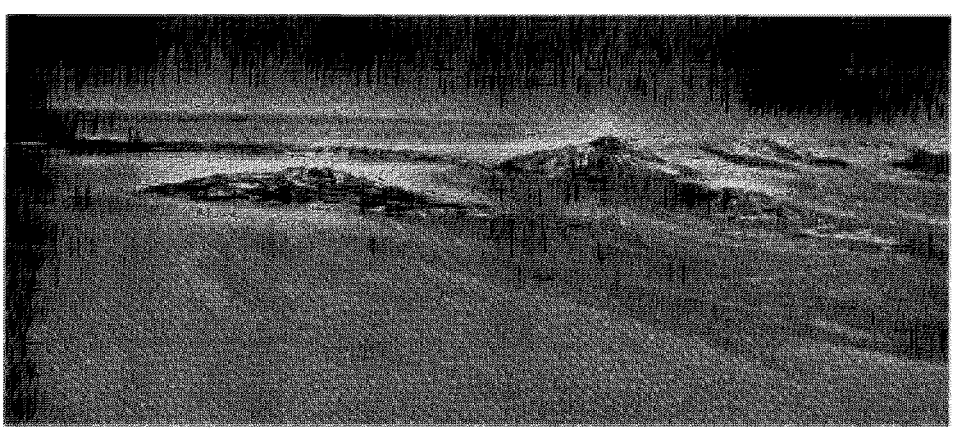

Copyright American Geophysical Union

Wright-Grassham, 1987]. The data from their theses are summarized here and in the accompanying individual volcanic descriptions.

Most volcanism in the Erebus volcanic province occurs in the Ross Island (Figures A.III.1 and A.III.2) and the Discovery subprovinces (Figures A.III.1 and A.III.3). Volcanism also occurs in the Ross Sea south of Franklin Island, and in the Dry Valley region.

Marine and airborne magnetic surveys, in combination with shipboard seismic profiling, have revealed extensive areas of volcanic rocks in the Ross Sea [*Behrendt et al.*, 1987; *Cooper et al.*, 1987]. Numerous volcanoes have been identified (see IVD A.12), and some of these may have been recently active [*Behrendt et al.*, 1987]. Volcanism is obviously widespread throughout much of the western Ross Sea, especially close to major structural features such as the Terror rift within the Victoria Land basin [*Cooper et al.*, 1987].

Tectonic Setting

The majority of the volcanic vents within the Erebus volcanic province are situated on thinned crust within the Ross Embayment. In the western Ross Sea the Victoria Land basin contains over 12 km of sediment and extends from Ross Island to Cape Washington (Figure A.III.4). Within the basin the younger Terror rift is divided into the Discovery graben and the Lee arch. The southern extension of

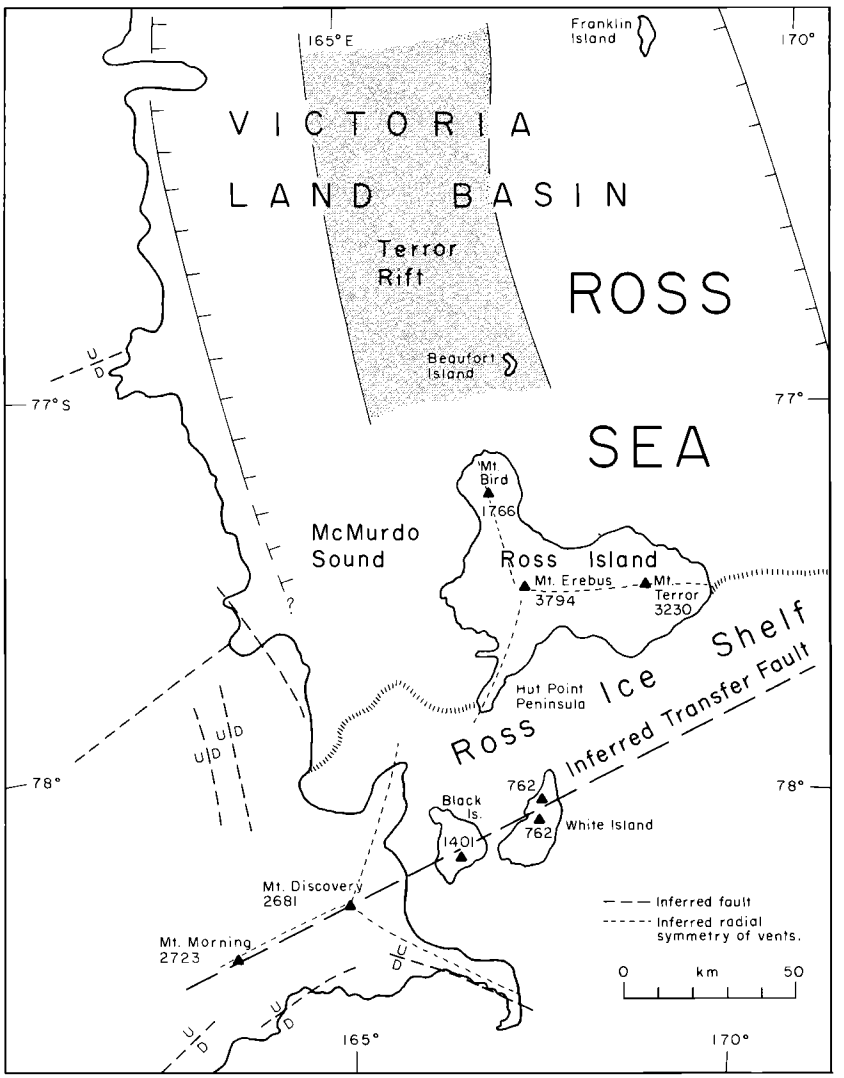

Fig. A.III.4. Generalized tectonic map of Erebus volcanic province, compiled from *Warren* [1969], *Cooper et al.* [1987], *Wright-Grassham* [1987], and Kyle (unpublished observations, 1987).

Copyright American Geophysical Union

the Terror rift is unknown. On the basis of a seismic profile [*McGinnis et al.*, 1985] from Hut Point Peninsula to the Victoria Land coast, the Terror rift is inferred to extend at least beneath Ross Island. It is significant that the active volcanoes, Mount Melbourne and Mount Erebus, lie at either end of the rift.

The distribution of major volcanic centers within the Erebus volcanic province was discussed by *Kyle and Cole* [1974]. They considered that major centers at Mount Bird, Mount Terror, and Hut Point Peninsula on Ross Island were radially distributed about Mount Erebus at 120° angles. It was suggested that crustal doming created the radial fractures. Petrologically, lavas at Mount Erebus differ from those at the three surrounding centers (see discussion below). *Kyle et al.* [1989] has suggested that to account for the volume of phonolite at Mount Erebus, it is necessary to invoke significant mantle upwelling as a mantle plume or hot spot. Initiation of the plume may have caused crustal doming and the formation of the radial symmetry. Subsequent loading of the crust by the Ross Island volcanic pile has depressed the crust, resulting in a moat surrounding the island.

Mount Discovery shows a radial distribution of vents about it, similar to Mount Erebus. Minna Bluff, Brown Peninsula, and Mount Morning are at 120° angles about Mount Discovery [*Kyle and Cole*, 1974]. This distribution could be an early expression of the hotspot now underlying Mount Erebus.

Wright-Grassham [1987] believed that some vents in the Discovery subprovince lie on a major lineament defined by Mount Morning, Mount Discovery, Black Island, and White Island (Figure A.III.4). The lineament may represent a transfer or transform fault which terminates the Terror rift.

Geochronology

Numerous radiometric age determinations have been made on surface samples from the Erebus volcanic province, mainly by *Armstrong* [1978] and *Wright-Grassham* [1987] using the conventional K-Ar method. Three samples have been dated from Mason Spur (see IVD A.23) by the incremental $^{40}Ar/^{39}Ar$ method.

Although the oldest surface samples from the Erebus volcanic province are 19 m.y. old, drill cores collected in McMurdo Sound record a period of volcanism and erosion extending back to early Oligocene time (about 40 Ma).

Sand-sized volcanic glass occurs throughout much of the 702-m-deep CIROS-1 drill hole [*P.J. Barrett*, 1987; George, unpublished data, 1988]. Microfossil evidence suggests an early Oligocene age at the bottom of the hole. Geochemical analyses show significant and increasing influxes of McMurdo volcanic material above 300 m in CIROS-1 drill core (Roser and Pyne, unpublished data, 1988). This correlates with the base of MSSTS-1 [*P.J. Barrett*, 1987] and suggests an age of at least 30 Ma. In the lower 25 m of the 227-m-deep MSSTS-1 drill core, volcanic sands correlated with McMurdo Volcanic Group exceed 30% of the total sand fraction [*Barrett et al.*, 1986]. An age of 28–30 Ma has been assigned to this interval by using microfossil data. Basaltic clasts from 213 m give K-Ar ages of 13.7 and 24.3 Ma [*Gamble et al.*, 1986]. Variable argon loss from the basalt may explain the discordance between the radiometric and paleontologic age determinations. Extensive volcanic debris, dated as early Miocene (21 Ma) by microfossil data, appears at 60 m in MSSTS-1 and occurs almost continuously to the top of the core. Volcanic sand is generally absent in the MSSTS-1 drill core between 60- and 200-m depth. It is unlikely that the source of the volcanic sediment in the drill cores is exposed on land, but it could be buried beneath sediments in the Ross Sea. Seismic records within the western Ross Sea indicate older igneous rocks interbedded within the sedimentary record [*Cooper et al.*, 1987].

K-Ar dating of volcanic rocks has been used to establish the age of glaciation in the McMurdo Sound area. Basalts dated as over 4 Ma from the Taylor and Wright valleys established a minimum age for the formation of the Dry Valleys [*Armstrong et al.*, 1968; *Fleck et al.*, 1972]. Numerous K-Ar dates have been made on samples from the foothills of the Royal Society Range (see IVD A.24) [*Armstrong*, 1978], with most less than 3 Ma. Although interbedded within glacial deposits, no major attempt has been made to use these to date the various glaciations that occurred in the area.

Ages for the main volcanic centers are shown in Figure A.III.5. Within each volcanic center, volcanic activity appears in general to span periods of only 1–2 m.y., although longer periods have been observed in

Copyright American Geophysical Union

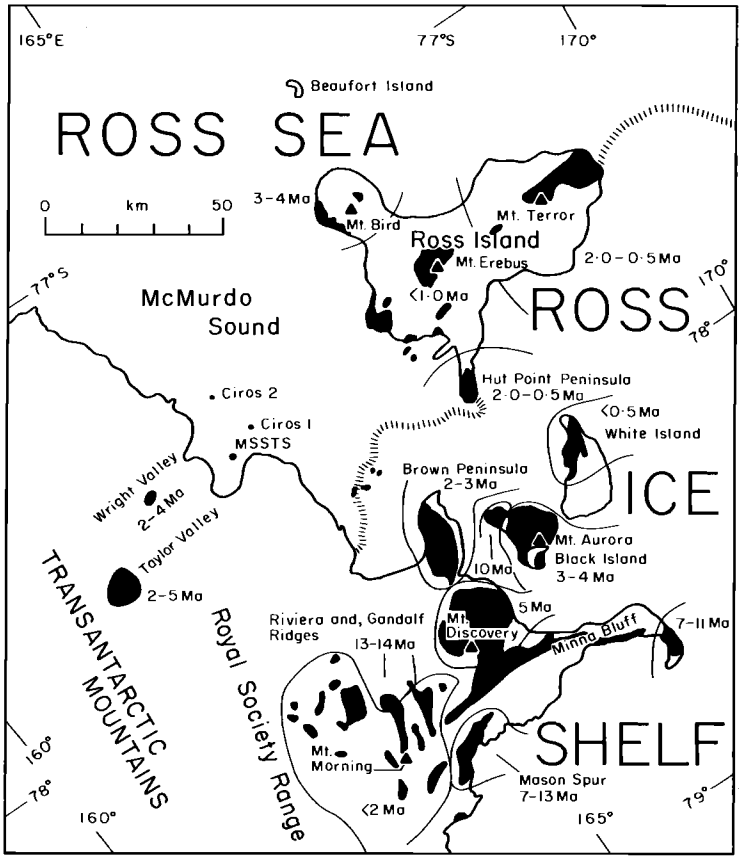

Fig. A.III.5. Generalized ages for the major volcanic centers within the Erebus volcanic province, based mainly on K-Ar age determinations of surficial samples listed in the individual volcano descriptions.

some areas. The oldest centers are situated around the base of Mount Morning in the Discovery subprovince. Three deeply eroded, predominantly trachytic centers occur at "Gandalf Ridge" (18.7–15.5 Ma), "Riviera Ridge" (15.2–13.0 Ma), and Mason Spur (13.5–12.4 Ma). It is likely that Mount Morning has buried other older volcanic centers.

At about 11 Ma a major petrologic change to a basanite/phonolite association developed with eruptions at the eastern tip of Minna Bluff (11.0–9.0 Ma) and the northern end of Black Island (10.9 Ma). Volcanic activity then appears to have migrated northwestward to central Minna Bluff (8.3–7.3 Ma) and Mount Discovery (5.3–4.4 Ma).

Volcanism became more extensive and widespread at about 4 Ma. Ross Island was built up progressively, first with the formation of Mount Bird (4–3 Ma), followed by that of Mount Terror (2–0.6 Ma), Hut Point Peninsula (1.8–0.4 Ma), and finally Mount Erebus, which is younger than 1 Ma. In the Discovery subprovince there were eruptions at Black Island (3.8–3.4 Ma), Brown Peninsula (2.8–2.0 Ma), Mount Morning (<2 Ma), and White Island (0.2 Ma).

Stratigraphy

Reconnaissance geologic mapping has been undertaken in many areas of the Erebus volcanic province. In early field mapping, *Cole and Ewart* [1968] defined four lithostratigraphic formations: three on Black Island and the fourth at Cape Bird. The formations were then correlated to Brown Peninsula and Cape Bird and later by *Cole et al.* [1971] also to Cape Crozier, White Island, and Hut Point Peninsula. As each of these volcanic centers is different in age, it was recommended by *Kyle et al.* [1979] that the use of these formations be discontinued. Each volcanic center erupts independently, and so correlation of lithostratigraphic units is incorrect.

Informal lithostratigraphic units at centers in the Discovery subprovince were given an initial (e.g., MB, Minna Bluff) and numbered from oldest to

Copyright American Geophysical Union

youngest [*Wright-Grassham*, 1987]. Detailed mapping in this area has resulted in the recognition of many informal stratigraphic units; at Mason Spur, for example, there are nine stratigraphic units (MS1 to MS9). If all these units were defined formally, it would result in an unnecessary proliferation of stratigraphic names.

There have been suggestions [*Treves*, 1967; *Goldich et al.*, 1975] that the major volcanic centers go through similar eruptive episodes. The first eruptive products were basanite, followed by phonolite and then a younger basanite. Detailed mapping with associated radiometric age determinations shows that such a generalization cannot be upheld.

Paleomagnetism

A limited number of sites have been sampled and measured for paleomagnetism in the Erebus volcanic province. The earliest study [*Cox*, 1966; *Mankinen and Cox*, 1988] shows that many of the vents had reversed magnetism and therefore predated the Brunhes/Matuyama boundary at 0.73 Ma.

At Hut Point Peninsula, paleomagnetic studies, combined with radiometric age determinations of drill core from Dry Valley Drilling Project (DVDP) holes 1, 2, and 3 and surface samples, show about 1 m.y. of eruptive activity [*Kyle and Treves*, 1974; *McMahon and Spall*, 1974*a*, *b*; *Funaki*, 1979, 1983, 1984]. Using basic magnetic properties, *Funaki* [1984] deduced that Erebus volcanic province lavas have a stable component of natural remanent magnetization.

Mineralogy

Mineralogical investigations have been made of a number of suites of Erebus volcanic province rocks. These include microprobe analyses of the main mineral phases in lavas from Hut Point Peninsula [*Kyle*, 1981*b*], Mount Erebus [*Kyle*, 1977; *Moore*, 1986; *Kyle et al.*, 1989], and several centers in the Discovery subprovince [*Wright-Grassham*, 1987]. The mineral analyses have been used mainly to model magmatic evolution of the petrologic suites.

Large anorthoclase phenocrysts in the phonolite from Mount Erebus have attracted numerous investigations [*Mountain*, 1925; *Carmichael*, 1962, 1963, 1967; *Carmichael and MacKenzie*, 1964; *Boudette and Ford*, 1966; *Berlin and Henderson*, 1969; *Mason et al.*, 1982].

Within the basic and ultrabasic rocks, clinopyroxene is ubiquitous and is usually accompanied by olivine, various spinels, apatite, plagioclase, and kaersutite. Rhonite, a rare Ti-rich silicate, is common in some lavas from Hut Point Peninsula [*Kyle and Price*, 1975]. The felsic differentiates have ubiquitous feldspar ranging form oligoclase to sanidine; anorthoclase is the most abundant feldspar. Mafic phases are usually green clinopyroxene, kaersutite, or aenigmatite. Alkali amphiboles and micas are uncommon. Fayalitic olivine occurs in phonolite from Mount Erebus and a few other localities. Apatite and titanomagnetite are common accessory phases. Feldspathoids are seldom observed optically in any lava, even though normative compositions of the rocks are strongly undersaturated. Nepheline is an incipient groundmass phase which is best distinguished by microprobe techniques.

Petrology

Extensive petrographic studies of volcanic rocks mainly from Ross Island were stimulated by collections made in the early 1900s by geologists on expeditions led by Scott and Shackleton. This work is summarized in monographs by *Smith* [1954, 1959].

In modern times a number of classification schemes have been used to describe the volcanic rocks. Field-based studies generally termed dark-colored mafic rocks as basalt, and lighter-colored felsic varieties as trachyte [*Cole and Ewart*, 1968; *Cole et al.*, 1971]. These were often subdivided using phenocryst contents (e.g., olivine basalt, pyroxene trachyte).

With the advent of rapid geochemical analysis, subsequent classifications have been based on geochemical criteria. *Kyle et al.* [1979] generally used the classification proposed by *Coombs and Wilkinson* [1969]. In this classification, most lavas within the Erebus volcanic province fall into basanite, phonolite, and trachyte fields, with minor amounts of intermediate compositions, i.e., *ne*-hawaiite, *ne*-mugearite, and *ne*-benmoreite. Goldich and associates [*Goldich et al.*, 1975, 1981; *Sun and Hanson*, 1975, 1976; *Stuckless and Ericksen*, 1976; *Stuckless et al.*, 1981; *Weiblen et al.*, 1981] used an unconventional classification and termed all the intermediate rocks

Copyright American Geophysical Union

trachybasalts; these were then subdivided into low- and high-Si varieties. They referred to the basic rocks as basanitoids because they lacked modal nepheline. *Kyle et al.* [1979] preferred the term basanite, which implies modal nepheline, because they often detected nepheline as a groundmass phase.

Although *Wright-Grassham* [1987] used the total alkali-silica (TAS) classification of *Le Bas et al.* [1986] in her study of the Discovery subprovince, the classification of *Kyle et al.* [1979] was used in most of the individual volcano descriptions in this section.

Geochemical data have been used to define a number of evolutionary trends or lava lineages within the Erebus volcanic province. Rocks younger than about 11 Ma mainly belong to a basanite/tephrite-phonolite association. These have been subdivided into the DVDP lineage [*Kyle*, 1981*b*] and the Erebus lineage [*Kyle*, 1976, 1981*b*; *Moore*, 1986; *Kyle et al.*, 1989]. The Erebus lineage formed by fractional crystallization of a basanite parent with removal of olivine, clinopyroxene, feldspar, nepheline, apatite, and spinel. For the DVDP lineage the mineral phases fractionated were olivine, clinopyroxene, kaersutite, feldspar, apatite, and spinel. The principal difference between the two lineages is the presence or absence of kaersutite. Kaersutite is unstable at temperatures exceeding 1050°C [*Yagi et al.*, 1975], so it may be differences in temperature and volatile contents which control the two lava lineages. *Wright-Grassham* [1987] recognized an additional basanite-phonolite lineage from Minna Bluff. Although the chemistry of the lavas resembles that of the lavas from Mount Erebus, mass balance models show that kaersutite was an important phase that was fractionated. In this respect it resembles the DVDP lineage. On Mount Erebus there are minor occurrences of benmoreite and

Fig. A.III.6. Generalized alkali-silica trends for the various suites of volcanic rocks from the Erebus volcanic province: (1) Hut Point Peninsula; the trend has been referred to as the DVDP lineage [*Kyle*, 1981*b*]. (2) Brown Peninsula [*Kyle et al.*, 1979]. (3) Minna Bluff; a basanite to phonolite sequence shown by the youngest lavas. (4) Mount Discovery; younger lavas from the volcanic field surrounding the main central volcano, and parasitic vents on the volcano. (5) Mount Erebus; the trend has been referred to as the Erebus lineage [*Kyle*, 1976]. (6) Mount Discovery; evolved lavas forming the main stratovolcano, older than lavas shown as trend 4. (7) Minna Bluff; compositions shown by lavas stratigraphically underlying those portrayed in trend 3. (8) "Riviera Ridge" and "Gandalf Ridge" on the northern slopes of Mount Morning; rocks stratigraphically overlying those shown by trend 11a and field 11b, yet older than 10 Ma. (9) Black Island; older lavas (>10 Ma). (10) Mason Spur; sequences of lavas older than 10 Ma, yet stratigraphically overlying trachytes shown by field 12. (11) "Riviera Ridge" and "Gandalf Ridge"; trend of basic rocks indicated as 11a and the field for trachytes indicated as 11b. These stratigraphically underlie rocks shown by trend 8. (12) Mason Spur; field for trachytes which stratigraphically underlie those shown by trend 10.

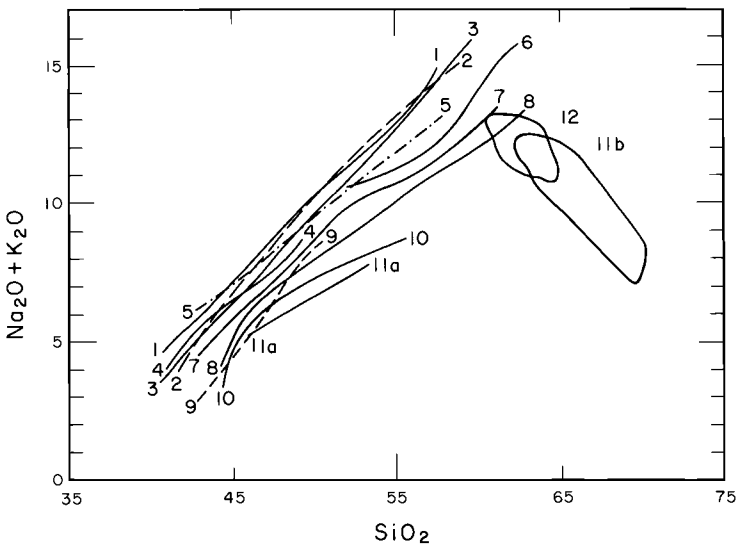

Copyright American Geophysical Union

trachyte which are obviously unrelated to the Erebus lineage. *Moore* [1986] called these the enriched iron series. Volumetrically they are insignificant.

Lavas older than 11 Ma are dominantly trachytic, usually peralkaline. They occur at Mason Spur and in the vicinity of Mount Morning, at "Riviera Ridge" and "Gandalf Ridge," (Figure A.III.1). They define fractionation trends, but these are poorly constrained because of the lack of basic rocks. *Wright-Grassham* [1987] believed that fractional crystallization was important in their formation but also suggested that other open system processes, such as crustal contamination, may have operated.

In alkali versus silica plots (Figure A.III.6) the older trachytic rocks have lower total alkalis and are less undersaturated than rocks younger than 11 Ma.

Xenoliths

Xenoliths are common in Erebus volcanic province rocks [*Kyle et al.*, 1987]. In some instances they have been examined in considerable detail to constrain the composition of the lithosphere and processes which have affected it [*Gamble and Kyle*, 1987; *Kalamarides et al.*, 1987; *Berg et al.*, 1989; *Gamble et al.*, 1988; *Kalamarides and Berg*, 1989; *McGibbon*, 1989].

Xenoliths include assorted supracrustral material, mafic and felsic granulites, and a wide range of mafic and ultramafic types. Xenoliths from "Foster Crater," a small basanite vent situated on the foothills of the Royal Society Range (see IVD A.24), are diverse. Included are a suite of xenoliths showing varying degrees of metasomatism [*Gamble et al.*, 1988] and infiltration of basaltic melts [*Gamble and Kyle*, 1987]. Mineralogical and geochemical analyses of granulite xenoliths show that the composition of the lower crust in the Transantarctic Mountains is significantly different from that under the Ross Embayment [*Kalamarides et al.*, 1987; *Kalamarides and Berg*, 1989].

Many xenolith localities remain to be studied in detail. Intensive isotopic investigations currently under way [*McGibbon*, 1989] should constrain the age of the xenoliths and the processes which have modified them.

Acknowledgments

Greatest thanks are extended to Bill McIntosh for his continued support in the field and for numerous discussions, comments, and criticism of this and other contributions in this section. To all the graduate students and friends who have contributed in the field and laboratory, thanks. Continuous support over the last 10 years from the Division of Polar Programs has made it all possible. Jim Cole and David Elliot reviewed this summary and the individual volcano descriptions which follow. Thanks to Wes LeMasurier and Janet Thomson for their patience, help, and encouragement.

Copyright American Geophysical Union

A.12. Ross Sea

Type of volcano: Submarine; defined by multichannel seismic reflection profiles showing penetration of sedimentary sections, and as short-wavelength magnetic anomalies.

Location: Western Ross Sea.

Height above sea level: All are below sea level.

Evidence of Holocene activity: None.

Author of report: J.C. Behrendt.

Date of report: May 1987.

Form and Structure

Eight short-wavelength, seismically defined penetrative structures having associated 1- to 5-km-wide magnetic anomalies (Table A.12.1) in the western Ross Sea (Figure A.12.1) are interpreted as volcanic in origin. Modeled anomalies fitted to the observed data and constrained by 24-fold seismic reflection profiles support the interpretation of these submarine volcanoes.

Anomaly a (Figure A.12.1) is interpreted as a submarine caldera with an associated volcanic dome and is underlain by magma or rock above the Curie temperature [*Behrendt et al.*, 1987].

Petrologic Characteristics

Unknown.

Chronologic Data

None. Anomaly c is located on smooth topography, suggesting partial glacial erosion (i.e., pre-20,000 years

TABLE A.12.1. Summary of Magnetic Anomalies Observed in the Western Ross Sea

Anomaly	Description of Anomaly	Depth below Sea Level, m	Relief, m	Comments
a (Barrett)	300 nT, complex, positive and negative	370	100	4 km wide
b	no data			
c (Kyle)	200 nT, 300 nT, both positive	560 690	160 100	smooth surface, probably glaciated
d (Hamilton)	1400 nT, complex	200	600	rugged bathymetry suggests post-glacial
e (Tessensohn)	60 nT, 75 nT	435	180	
f (Davey)	60 nT, 75 nT	480	150	
g (LeMasurier)	complex, 4 peaks, 100–300 nT	180	100	
h (Cooper)	100 nT	345	100	

Copyright American Geophysical Union

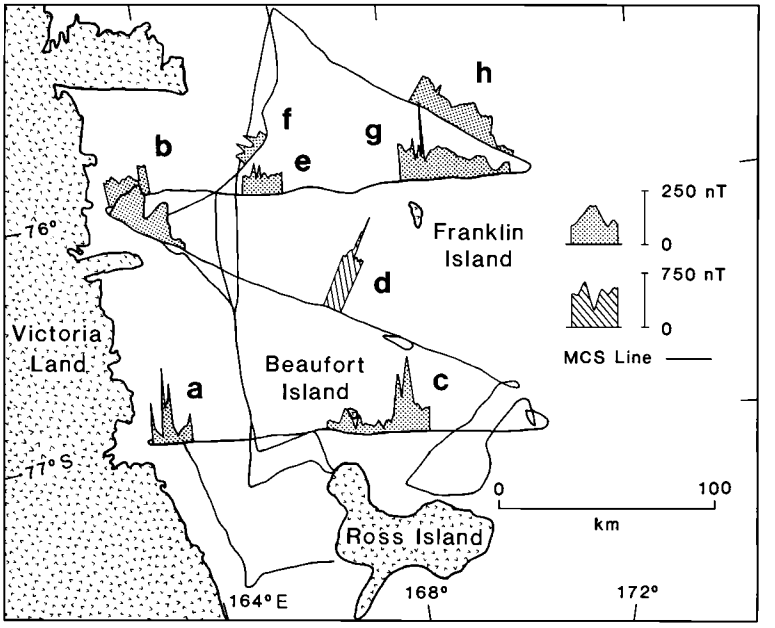

Fig. A.12.1. Map of western Ross Sea. Short-wavelength magnetic anomalies along S.P. *Lee* ship track over the western Ross Sea continental shelf. Numbered track lines also have 24-fold seismic reflection data. Anomalies a–h are caused by submarine volcanoes and subvolcanic intrusions throughout the Victoria Land basin. Anomaly d (about 1400 nT) is at the 0- to 750-nT scale. MCS, multichannel seismic line.

B.P.). Anomaly d has a rugged bathymetric form and negative central magnetic anomaly, implying young postglacial age.

Extent of Knowledge

Discovered by S.P. *Lee* geophysical survey in February 1984.

Bibliography

Behrendt et al., 1987
Cooper et al., 1987

Copyright American Geophysical Union

A.13. Franklin Island

Type of volcano: Island remnant of a shield volcano.
Location: Ross Sea, 115 km north-northeast of Cape Bird, Ross Island (76°10′S, 168°23′E).
Height above sea level: 247 m.
Evidence of Holocene activity: None.
Authors of report: P.J. Ellerman and P.R. Kyle.
Date of report: March 1987.

Form and Structure

Franklin Island, approximately 7.6 km in length and 2 km in width (Figure A.13.1), is a remnant of a shield volcano whose primary vent was located to the east. Bedrock is exposed in steep cliffs beneath an ice cap along the eastern, southern, and southwestern coasts. A beach on the southwest side of the island is composed of gently dipping interbedded lavas and tuffs. Lavas are thicker and more lobate toward the base of the section, becoming thin and sheet-like toward the top. Dips commonly have a westward component, but locally attitudes are chaotic, especially where interbedded tuffs are abundant. Tuffs range from poorly bedded and sorted material to cross-bedded, moderately well sorted deposits. Both are well exposed in the cliffs above the penguin rookery. North of Bernacchi Head the bedded tuff dips eastward into the vent of a probable parasitic cone [*Waterhouse,* 1965]. One vertical dike was observed, cutting tuffs cropping out above the southeastern beach.

A representative vertical section from the southeast side of the island consists of approximately 80 m of thick, poddy

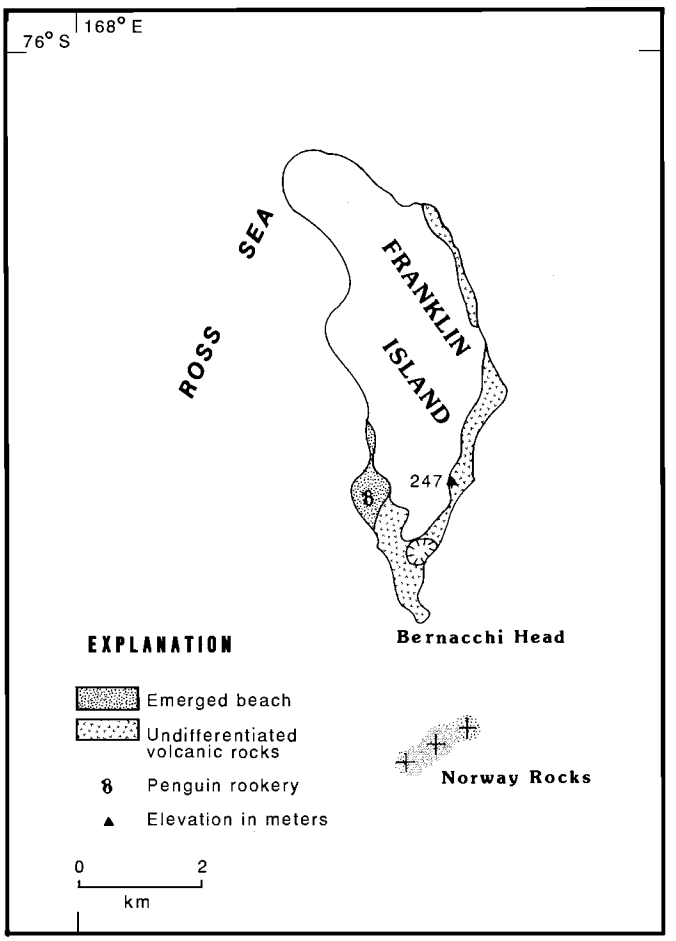

Fig. A.13.1. Geologic sketch map of Franklin Island. (Geology by P.J. Ellerman.)

Copyright American Geophysical Union

lava overlain by 70 m of nearly horizontal lava flows, followed by 30 m of yellow, bedded tuff. Twenty meters of thin, sheet-like flows cap the section. Cliffs of highly chaotic interbedded tuff and lava commonly form the bulk of the lower section along the coastal exposures. Bedded cinders appear to overlie the upper flows.

Glacial erratics occur up to within 20 m of the summit of Franklin Island. At the northern end of the west facing beach, emerged beach ridges are exposed; the highest of these is 7 m above sea level [*Denton et al.*, 1975].

TABLE A.13.1. Representative Chemical Analyses of Volcanic Rocks From Franklin Island

	1	2	3
SiO_2	43.82	44.03	44.09
TiO_2	2.15	2.16	2.23
Al_2O_3	13.74	13.93	13.80
Fe_2O_3*	11.92	11.95	12.93
MnO	0.27	0.26	0.22
MgO	7.52	7.31	9.20
CaO	9.77	9.74	9.96
Na_2O	5.93	6.51	4.66
K_2O	2.09	2.36	1.66
P_2O_5	0.88	0.89	0.63
LOI	1.20	0.97	0.30
Total	99.29	100.11	99.69
Ba	899	922	--
Cr	384	329	--
Cu	45	46	54
Ga	20	20	21
Nb	177	176	104
Ni	128	123	184
Pb	3	--	2
Rb	82	84	59
Sr	1281	1283	885
Th	15	17	9
V	152	146	--
Y	47	47	35
Zn	121	118	105
Zr	451	457	275

XRF analyses by P.R. Kyle. Dashes, not determined. LOI, loss on ignition.

* Total Fe expressed as Fe_2O_3.

1. AW82278. Basanite, pahoehoe flow toe, headland at south end of penguin rookery beach (collected by A.C. Wright).
2. AW82280. Basanite, massive flow overlying AW82278 (collected by A.C. Wright).
3. HC-FRI-2. Basanite, lava flow with olivine nodules (collected by P.J. Ellerman).

Petrologic Characteristics

Four analyzed samples from Franklin Island (see Table A.13.1 for representative analyses) are all basanites (Figure A.13.2). Euhedral to subhedral olivine is the primary phenocryst phase, although plagioclase phenocrysts were noted in a few samples; olivine also occurs in the groundmass along with clinopyroxene, plagioclase, and opaque minerals. Lherzolite nodules up to 12 cm in diameter are abundant in dark gray basanite boulders on the penguin rookery beach, increasing in number toward the exposed southern summit ridge. These nodules are composed of anhedral olivine, orthopyroxene, and chrome diopside. Clinopyroxene reaction rims have formed where the orthopyroxene is in contact with the basanite. Tuffaceous rocks collected above the beach just south of the penguin rookery appear to reflect varying degrees of water interaction. Glass vesicularity ranges from highly vesicular sideromelane at one poorly bedded outcrop to angular, almost completely nonvesicular fragments in a cross-bedded sequence. Reconnaissance sampling suggests that vesicularity increases upward in the section. All samples are vitric tuffs composed primarily of sideromelane and subsidiary tachylite. The slightly palagonitized glass contains euhedral to subhedral olivine phenocrysts and, occasionally, crystallites of clinopyroxene and plagioclase. Xenocrysts of anhedral olivine and orthopyroxene, similar to those described from the lherzolite nodules, are seen in some tuff samples. Tuffs are porous and uncompacted, containing patchy carbonate cement. Void-filling zeolites are less common.

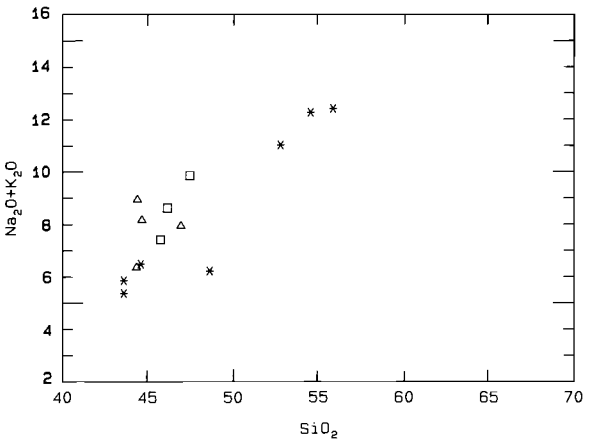

Fig. A.13.2. Alkali versus silica plot for analyzed samples from Franklin Island (triangles), Beaufort Island (squares), and Mount Bird (asterisks). All analyses recalculated to 100% volatile-free, with total Fe expressed as FeO. Sources: Tables A.13.1, A.14.1, and A.15.1; *Goldich et al.* [1975], *Cole and Ewart* [1968], *Jensen* [1916], and *Prior* [1899].

Copyright American Geophysical Union

Chronologic Data

A date of 4.8 ± 2.0 Ma for a sample described as an olivine basalt was reported by *Armstrong* [1978].

Extent of Knowledge

A party from the 1841 expedition of Sir James Ross landed on the island [*Ross,* 1847] and collected a sample, which was described by *Prior* [1899]. Landings were made by ski-equipped fixed-wing aircraft of the GANOVEX IV expedition in 1984–1985.

The present report is based on visits in 1965 [*Waterhouse,* 1965] and 1983 by science parties supported by the icebreaker USCGC *Glacier*. The eastern cliffs were described during a reconnaissance helicopter flight. Helicopter landing is possible on the penguin rookery beach.

Bibliography

Armstrong, 1978
Broadie, 1959
Denton et al., 1975
LeMasurier et al., 1983
Prior, 1899, 1902
Ross, 1847
Waterhouse, 1965

Copyright American Geophysical Union

A.14. Beaufort Island

Type of volcano: Island remnant of a stratovolcano.
Location: Ross Sea, 20 km north of Cape Bird (76°59′S, 167°01′E).
Height above sea level: 740 m.
Evidence of Holocene activity: None.
Authors of report: P.J. Ellerman and P.R. Kyle.
Date of report: March 1987.

Form and Structure

Beaufort Island (Figures A.III.1, A.14.1, and A.14.2) is a remnant of a near-vent portion of an alkaline stratovolcano, most of which has been removed by erosion. The island is composed of interbedded lavas, breccias, and tuffs which have been extensively altered by the numerous dikes which intrude them. For the most part, both lavas and tuffs are laterally discontinuous. Along the eastern cliffs the generalized sequence consists of massive, pale-colored tuff at the base of the section overlain by thick, discontinuous lava pods and interbedded tuffs. Lavas become thinner, sheet-like, and more laterally extensive toward the top of the section. The rocks dip to the west and northwest, with dip angles up to 30° exposed in the southern cliffs. *Harrington* [1958] considered the locally contorted interbedded tuffs,

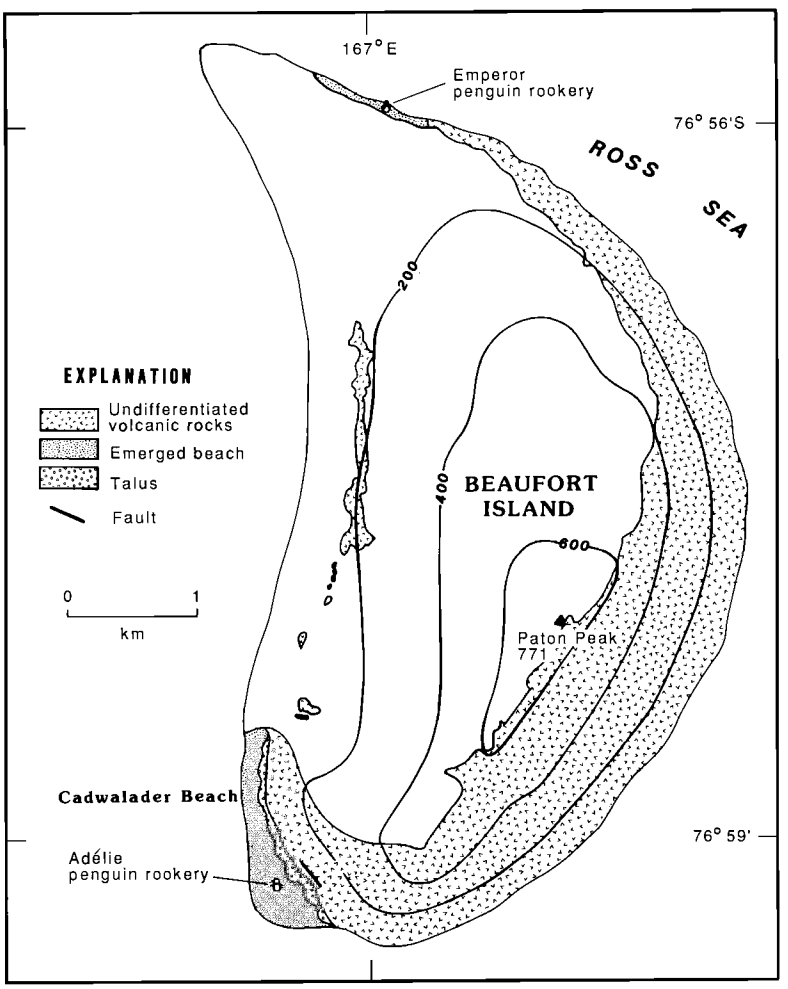

Fig. A.14.1. Geologic sketch map of Beaufort Island. (Geology by P.J. Ellerman.)

Copyright American Geophysical Union

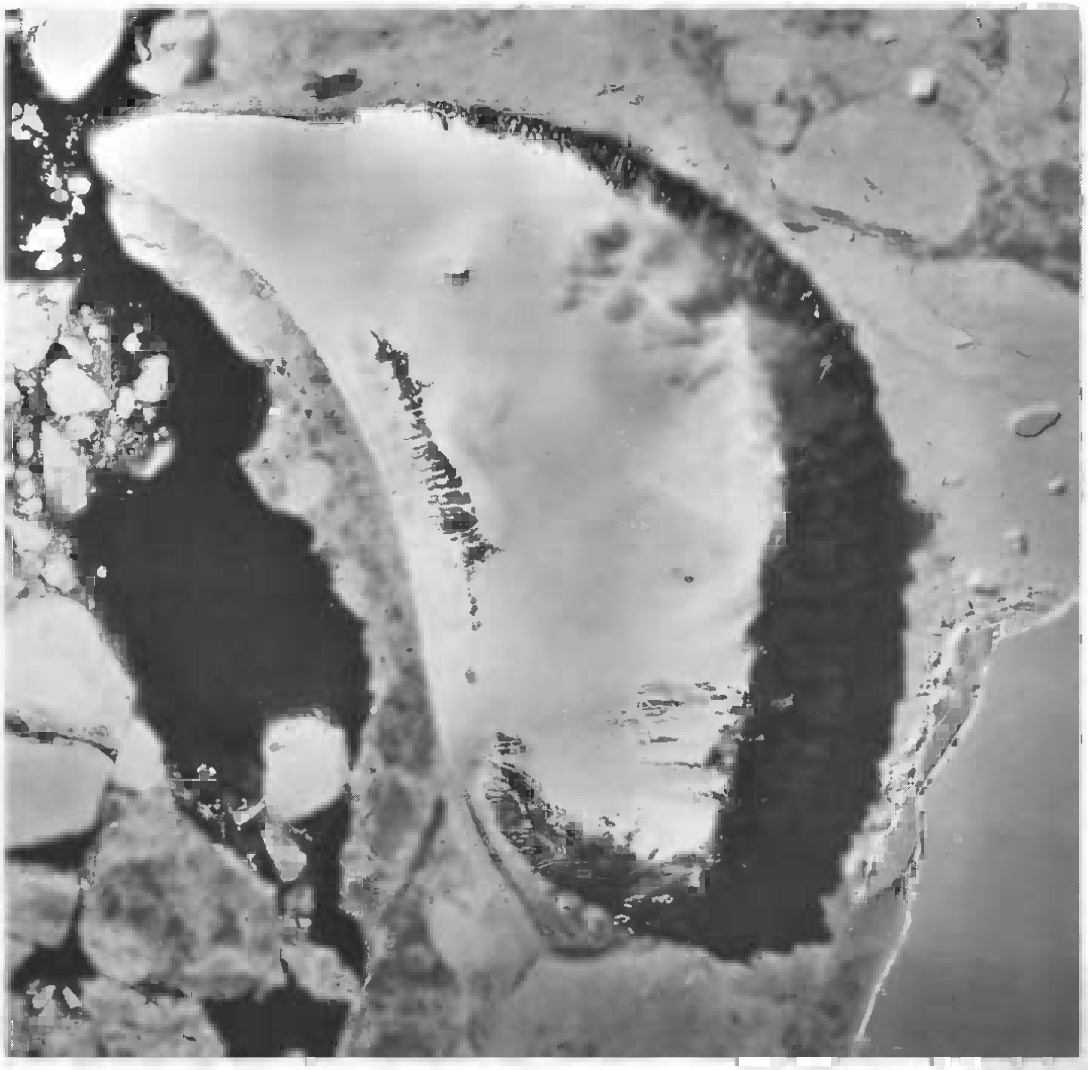

Copyright American Geophysical Union

TABLE A.14.1. Representative Chemical Analyses of Volcanic Rocks From Beaufort Island

	1	2	3
SiO_2	45.00	45.79	46.53
TiO_2	3.30	3.12	2.49
Al_2O_3	16.60	16.89	17.47
Fe_2O_3	5.65	11.53*	10.44*
FeO	5.85	--	--
MnO	0.11	0.21	0.24
MgO	4.90	4.03	3.06
CaO	9.25	8.14	7.28
Na_2O	5.00	5.65	6.57
K_2O	2.30	2.91	3.09
P_2O_5	0.40	0.91	0.88
H_2O^+	1.06	0.34**	1.40**
H_2O^-	0.84	--	--
Total	100.26	99.53	99.45
Ba	--	905	--
Cr	--	55	--
Cu	--	46	26
Ga	--	23	27
Nb	--	144	187
Ni	--	26	10
Pb	--	<5	<5
Rb	--	89	96
Sr	--	1209	1376
Th	--	5	11
V	--	133	--
Y	--	40	48
Zn	--	116	132
Zr	--	478	593

Dashes, not determined.
*Total Fe expressed as Fe_2O_3.
**Loss on ignition at 1000°C.

1. P23006. Tephrite, cliff at north end of penguin rookery (collected by H.J. Harrington, New Zealand Geological Survey Antarctic Expedition, 1958–1959; wet chemical analysis made by Chemistry Division, Department of Scientific and Industrial Research, New Zealand).
2. AW82284. Phonotephrite, cliff behind penguin rookery (collected by A.C. Wright; XRF analysis by P.R. Kyle).
3. HC-BI-5. Phonotephrite, flow-banded dike (XRF analysis made by P.R. Kyle).

subhedral glomeroporphyritic titanaugite crystals occasionally rimmed by kaersutite phenocrysts. Nepheline occurs as a groundmass mineral; apatite is a common accessory phase. Tuffs and breccias sampled from this section are massive, unsorted, and impersistent units, mostly composed of vesicular sideromelane shards, trachytic lithic fragments, titanaugite, kaersutite, and apatite crystals. Heterolithic tuffs are common and may represent slumping of the volcanic pile, or debris flows. Most of the rocks have been pervasively altered, with analcime, zeolites, and carbonate being abundant.

Chronologic Data

Harrington [1958] estimated the age of the island on the basis of its morphology and degree of erosion, agreeing with *David and Priestley* [1914] that the island had been at least partly overridden by glacial ice, possibly from an expanded Ross Ice Shelf. This interpretation is supported by *Denton et al.* [1975].

Extent of Knowledge

The exposed southeastern cliffs are accessible from Cadwalader Beach, where both boat and helicopter landings are possible. There are several early descriptions of Beaufort Island [*Ferrar*, 1907; *Debenham*, 1923]. H.J. Harrington was able to observe the island from the icebreaker USCGC *Glacier* in 1957, and he described the geology [*Harrington*, 1958]. In 1965, New Zealand geologists, also supported by the USCGC *Glacier*, landed on Cadwalader Beach [*Waterhouse*, 1965]. During the 1983 Science Cruise I of the USCGC *Glacier*, United States and New Zealand geologists visited Beaufort Island, also landing on Cadwalader Beach [*LeMasurier et al.*, 1983].

Cadwalader Beach is the site of an Adélie penguin rookery. An Emperor penguin rookery is located on a raised beach or bench [*Harrington*, 1958] on the north end of the island. Beaufort Island has been designated a Specially Protected Area.

Bibliography

David and Priestley, 1914
Debenham, 1923
Denton et al., 1975
Ferrar, 1907
Harrington, 1958
LeMasurier et al., 1983
Waterhouse, 1965

Copyright American Geophysical Union

A.15. Mount Bird

Type of volcano: Basaltic shield volcano with basaltic and phonolitic parasitic cones.
Location: Northern Ross Island (77°10′–77°22′S, 166°20′–167°06′E).
Height above sea level: 0–1800 m.
Evidence of Holocene activity: None.
Authors of report: A.C. Wright and P.R. Kyle.
Date of report: January 1986.

Form and Structure

Mount Bird is a basaltic shield volcano forming the northern part of Ross Island. It rises from below sea level to an elevation of 1800 m, with an average slope of 11° [*Kyle*, 1976]. The main cone is formed of a thick sequence of basaltic flows which are best exposed in the coastal cliffs. Numerous parasitic basaltic scoria cones and phonolite cones and domes are scattered over the slopes of the mountain; these are poorly exposed, except for a 30-km-long strip along the western shore (Figures A.15.1 and A.15.2).

Cole and Ewart [1968] mapped a 20-km strip along the west coast south of Cape Bird hut (Figure A.15.1). In this area the volcanic stratigraphy consists of an older olivine basalt - basalt - hornblende basalt - trachyte sequence [*Treves*, 1967]. Hyaloclastite tuff crops out below the snout of Shell Glacier. *Cole and Ewart* [1968] correlated this volcanic sequence with three formations erected by them on Black Island. A fourth formation, Trachyte Hill Formation, was named from the Mount Bird area. The correlation of these formations away from their type locality is now considered invalid. *Kyle et al.* [1979] recommended that the use of Trachyte Hill Formation should be discontinued.

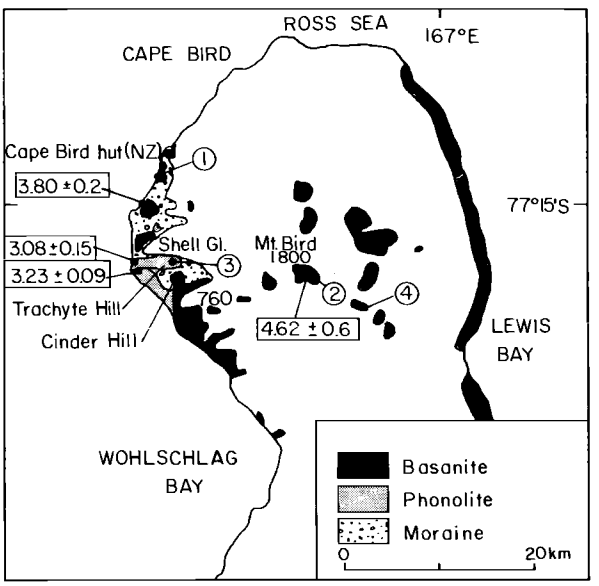

Fig. A.15.1. Sketch map showing the volcanic geology of the Mount Bird area [from *Cole and Ewart*, 1968]. Encircled numbers refer to the location of samples for which geochemical analyses are given in Table A.15.1; boxed numbers refer to K-Ar ages in millions of years.

Petrologic Characteristics

Phenocryst phases in the basanitic lavas contain various combinations of olivine, clinopyroxene, kaersutite, and plagioclase. Kaersutite and pyroxene are the principal phenocrysts in the phonolites. The basaltic lavas of the main cone are basanite in composition, and the lavas from the parasitic cones are basanitic and phonolitic (Table A.15.1 and Figure A.13.2); intermediate compositions are uncommon. Olivine nodules are present in some basanite lavas from the scoria cones, e.g., at Cinder Hill, a locality from which peridot is also recorded [*Wilson et al.*, 1974].

Basanites from Cape Bird have yielded $^{87}Sr/^{86}Sr$ ratios of 0.7044 and 0.7045 [*Jones and Walker*, 1972], and a phonolite from near the summit of Mount Bird [*Stuckless and Ericksen*, 1976] has a ratio of 0.7033.

Chronologic Data

K-Ar age determinations on four samples from Mount Bird indicate that the main cone was active between 3.8 and 4.6 Ma (Figure A.15.1). Younger phonolitic volcanism has been dated at 3.23 and 3.08 Ma [*Armstrong*, 1978].

Seven of eight paleomagnetic determinations made on samples from the ice-free west coast area indicate reversed polarity [*Kyle*, 1976]. Within the range of one standard deviation of the K-Ar age the polarity of three samples dated also by K-Ar methods is consistent with the *McDougall and Rahman* [1972] paleomagnetic time scale.

Extent of Knowledge

The ice-free coastal strip extending 20 km south from Cape Bird hut is the only part of Mount Bird which has been geologically mapped [*Cole and Ewart*, 1968]. *Cole and Ewart* [1968] presented modal analyses for 22 rocks from this area. Seven geochemical analyses have been

Copyright American Geophysical Union

Copyright American Geophysical Union

A.16. Mount Terror

Type of volcano: Large shield volcano surmounted by numerous parasitic cones.
Location: Eastern Ross Island, southern Ross Sea (77°22′–77°42′S, 167°43′–169°23′E).
Height above sea level: 0–3230 m.
Evidence of Holocene activity: None.
Authors of report: A.C. Wright and P.R. Kyle.
Date of report: January 1986.

Form and Structure

Mount Terror is a large basaltic shield volcano forming the eastern portion of Ross Island (Figures A.16.1–A.16.3). It rises from sea level to 3230 m, with an average slope of 9° [*Kyle*, 1976]. Numerous parasitic basaltic and trachytic cones and domes are scattered over the slopes of the mountain, including Mount Terra Nova (2130 m), a large basaltic cone on the western flank.

Most of the geology of Mount Terror is obscured by snow and ice. At Cape Crozier, interbedded basanite flows and pyroclastic breccias, originating from the flanks of Mount Terror, are overlain by parasitic vents which produced basaltic cinder cones and lava flows, and phonolitic endogenous domes. The sequence is intruded by dikes. A stratigraphy and correlation of these rocks with formations established elsewhere in the McMurdo Sound area [*Cole and Ewart*, 1968] is no longer valid [*Kyle et al.*, 1979].

Petrologic Characteristics

Samples from the Cape Crozier area range from basanite to phonolite [*Prior*, 1907; *Goldich et al.*, 1975; *Kyle*,

Fig. A.16.1. Sketch map showing the volcanic geology of Cape Crozier [from *Kyle*, 1976]. Encircled numbers refer to the location of samples for which geochemical analyses are given in Table A.16.1; boxed numbers refer to K-Ar ages in millions of years.

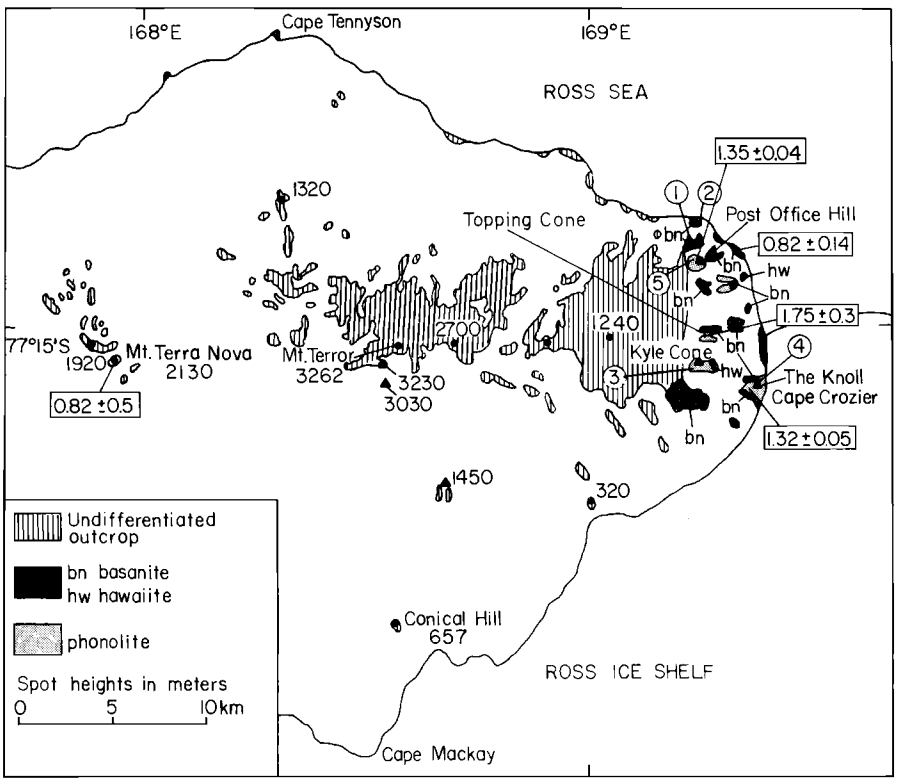

Copyright American Geophysical Union

Fig. A.16.2. Distant aerial view looking southward to Mount Terror. Cape Crozier is on the extreme left. (U.S. Navy photograph, TMA 431 F31 063.)

Fig. A.16.3. Aerial view of Mount Terror looking southward. Extensive areas of exposed rock occur on the northern and eastern flanks of Mount Terror, but these have never been examined. Reconnaissance mapping of Cape Crozier (at left) is shown in Figure A.16.1. (U.S. Navy photograph, TMA 730 F31 028.)

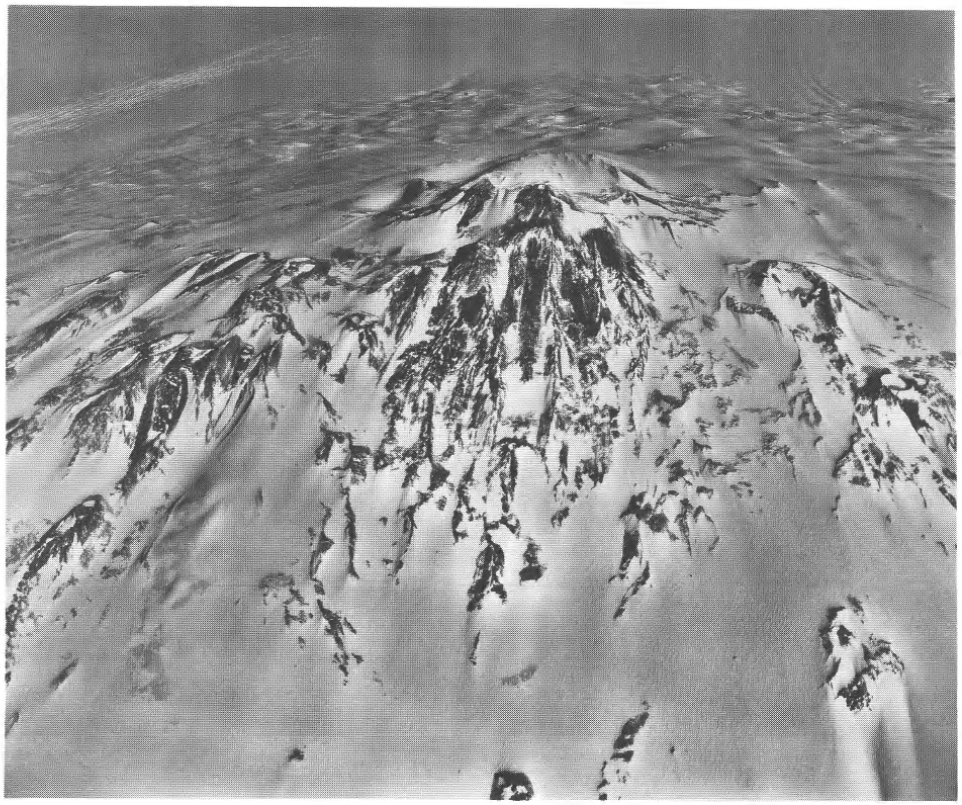

Copyright American Geophysical Union

1976], and despite the lack of detailed work elsewhere, this area is considered to be representative of the flanks of Mount Terror [*Kyle*, 1976]. Basalt and phonolite are reported from Mount Terra Nova [*Treves*, 1970], and geochemical analyses [*Goldich et al.*, 1975] indicate the presence of phonotephrite.

A differentiation sequence, ranging from olivine-augite basanite through phonotephrite to kaersutite phonolite, is exposed at Topping Cone, Cape Crozier. Nearby pyroxene phonolite is exposed on The Knoll. Total phenocryst content is variable, ranging up to 16% [*Cole et al.*, 1971], but it is apparently independent of composition.

Geochemical analyses of representative samples from the Cape Crozier area are given in Table A.16.1 and plotted in Figure A.16.4. $^{87}Sr/^{86}Sr$ ratios of 0.7040 and 0.7045 have been determined on "olivine basalt" samples from Cape Crozier [*Jones and Walker*, 1972].

Chronologic Data

K-Ar age determinations on three phonolite cones at Cape Crozier fall in the range 1.32–1.75 Ma [*Kyle*, 1976; *Armstrong*, 1978], giving a minimum age for the underlying basanite sequence forming the lower slopes of Mount Terror. An age of 0.82 Ma is recorded for a basanite flow exposed in the sea cliffs 2 km northeast of Post Office Hill. There is a single, imprecise date of 0.8 Ma from the summit of Mount Terra Nova.

TABLE A.16.1. Representative Chemical Analyses of Volcanic Rocks From Cape Crozier

	1	2	3	4	5
SiO_2	43.47	44.00	46.38	57.40	58.27
TiO_2	3.28	2.83	3.18	0.29	0.42
Al_2O_3	12.85	14.20	17.09	19.92	19.38
Fe_2O_3	3.18	3.12	6.67	3.60	3.67
FeO	9.67	7.38	4.63	1.30	1.78
MnO	0.19	0.19	0.23	0.20	0.22
MgO	11.78	10.80	4.38	0.17	0.41
CaO	10.60	10.50	8.97	1.57	1.95
Na_2O	2.93	4.38	4.65	8.50	8.10
K_2O	1.09	1.77	2.36	5.83	5.15
P_2O_5	0.58	0.65	1.05	0.05	0.12
H_2O	0.07	0.30	--	--	--
CO_2	0.09	0.02	--	--	--
F	0.02	--	--	--	--
LOI	--	--	--	0.63	0.46
Total	99.80	100.14	99.59	99.46	99.93
Ba	280	510	530	593	928
Cr	760	430	56	<5	<5
Cu	57	44	26	<7	<7
Ni	210	170	26	<5	<5
Rb	26	56	51	142	134
Sr	840	950	1426	143	481
V	280	210	206	<5	<5
Y	31	31	--	--	--
Zn	112	78	110	104	105
Zr	290	330	385	781	789

Dashes, not determined. LOI, loss on ignition.

1. Basanite, younger sequence, Cape Crozier [*Goldich et al.*, 1975].
2. Basanite, older sequence, Cape Crozier [*Goldich et al.*, 1975].
3. Phonotephrite, western base of Kyle Cone [*Kyle*, 1976].
4. Pyroxene phonolite, top of crater rim, north side of The Knoll [*Kyle*, 1976].
5. Kaersutite phonolite, southeast of Post Office Hill [*Kyle*, 1976].

Copyright American Geophysical Union

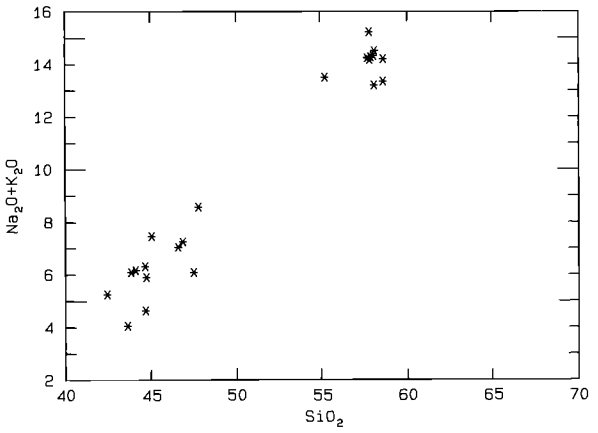

Fig. A.16.4. Alkali versus silica plot for analyzed samples of volcanic rocks from Mount Terror (most samples are from Cape Crozier). All analyses are recalculated to 100% volatile-free, with total Fe expressed as FeO. Sources: *Goldich et al.* [1975] and *Kyle* [1976].

Extent of Knowledge

Only the Cape Crozier area of Mount Terror has been mapped geologically. There are 20 geochemical analyses from this area and two from the summit of Mount Terra Nova [*Kyle*, 1976], most of which include trace elements. *Cole et al.* [1971] included modal analyses of 11 samples from Cape Crozier. There are four K-Ar age determinations from Cape Crozier, and a single, imprecise date from the summit of Mount Terra Nova [*Armstrong*, 1978]. McGibbon (personal communication, 1987) has collected additional geochemical and isotopic data on lavas from Cape Crozier.

Bibliography

Armstrong, 1978
Cole and Ewart, 1968
Cole et al., 1971
Debenham, 1923
Goldich et al., 1975
Jones and Walker, 1972
Kyle, 1971, 1976
Kyle and Cole, 1974
Prior, 1907
Smith, 1954
Stuckless et al., 1981
Treves, 1967

Copyright American Geophysical Union

[redacted]

[redacted]

[redacted]

[redacted]

[redacted]

Copyright American Geophysical Union

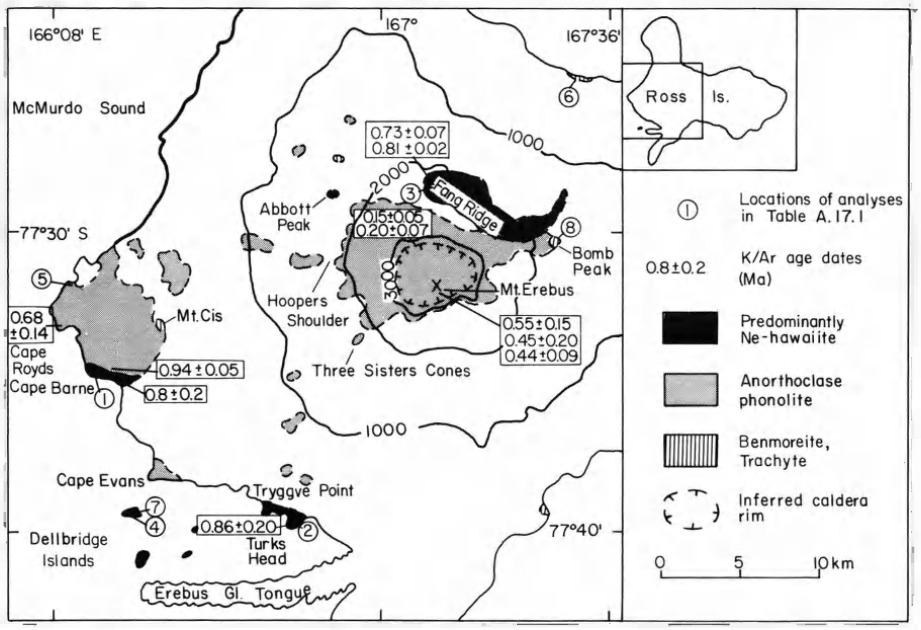

Copyright American Geophysical Union

benmoreite lavas crop out in eroded volcanic cones which form the Dellbridge Islands and sea cliffs on the southwest side of Mount Erebus (Figure A.17.2). The lower parts of these cones generally consist of pillow lavas, pillow breccias, and hyaloclastites. The upper parts consist of lava flows with minor to major amounts of lapilli tuff and laharic deposits.

Fang Ridge is 4 km long and trends NW-SE on the northeast side of Mount Erebus (Figures A.17.1 and A.17.2). It rises to 3159 m and has a near-vertical cliff 100–200 m high on the southwest side and a >45° dip slope of flow tops and scree on the northeast side. The lower part of Fang Ridge consists mainly of massive blocky lapilli tuffs, which are probably lahar deposits. These are overlain by basanite, *ne*-hawaiite, *ne*-mugearite, and *ne*-benmoreite flows. Fang Ridge is probably the eroded remnant of a vent formed on the side of a juvenile Mount Erebus [*Kyle*, 1976].

Small flows and endogenous domes of benmoreite, phonolite, and trachyte form "Mount Cis," Bomb Peak, Abbott Peak, and sea cliffs on the northeast and southeast sides of Mount Erebus (Figure A.17.2).

The slopes of Mount Erebus between 2000 and 3200 m dip 30°–40° and consist of short anorthoclase phonolite flows. The summit region is a plateau with its rim at about 3200 m and sloping about 10°S. The plateau is thought to be a caldera filled by anorthoclase phonolite lavas [*Kyle*, 1976]. The steep-sided active summit cone is located on the south side of the plateau and rises to 3794 m. It is mostly covered by partially decomposed lava bombs and a lag deposit of anorthoclase crystals. An elliptical crater ("Main Crater"), 600 m by 500 m, occurs within the cone, and a smaller inactive crater ("Side Crater") occurs on the south side (Figure A.17.3). The vertical walls of these craters reveal that the summit cone is composed mainly of flows, capped by a pyroclastic breccia.

"Main Crater," about 110 m deep, has a nearly flat floor. The phonolite lava lake and "Active Vent" occur in the northern half of a circular pit called "Inner Crater," which is about 250 m in diameter and 100 m deep and is situated on the north side of "Main Crater."

Petrologic Characteristics

A continuous, strongly undersaturated sodic differentiation lineage occurs on Mount Erebus [*Kyle et al.*, 1989], consisting of basanite, *ne*-hawaiite, *ne*-mugearite, *ne*-benmoreite, and anorthoclase phonolite; it is termed the Erebus lineage (EL) [*Kyle*, 1976] (Table A.17.1; Figures A.17.4–A.17.6). EL lavas are predominantly coarsely porphyritic and contain phenocrysts of olivine, clinopyroxene, opaque oxides, feldspar, apatite, and accessory feldspathoids and pyrrhotite. Clinopyroxene phenocrysts are salites, and they show little variation in chemistry from basanite to anorthoclase phonolite. Feldspar phenocrysts vary continuously from bytownite in basanites to anorthoclase in phonolites. They range in length from 1 to 4 cm in *ne*-hawaiite to *ne*-benmoreite and from 1 to 10 cm in anorthoclase phonolite.

EL lavas range widely in composition from basanite to anorthoclase phonolite (Table A.17.1) and exhibit smooth, continuous trends in all geochemical variation diagrams (Figures A.17.4 and A.17.5). The basanites are moderately evolved (9–130 ppm Cr, 10–63 ppm Ni) and are not primary mantle melts. EL lavas are light rare earth element (REE) enriched (La/Yb = 21.7–30.2). Incompatible element concentrations are high and increase with increasing sample differentiation (Zr ranges from 347 ppm in basanite to 1008 ppm in anorthoclase phonolite).

The geochemistry of the EL indicates that it probably evolved from a basanite parental magma by fractional crystallization of the observed phenocryst phases. Mass balance modeling of major elements [*Moore*, 1986] shows that anorthoclase phonolite is a 23.5% residual liquid of primitive basanite similar to that occurring at Hut Point Peninsula, Ross Island. Sr isotopic ratios in anorthoclase phonolite (0.7032 [see *Stuckless and Ericksen*, 1976]) are identical to primary basanites of Ross Island, indicating that crustal contamination was negligible in the evolution of the EL.

Volumetrically insignificant amounts of less undersaturated benmoreites, phonolites, and trachytes also occur on Mount Erebus (Figure A.17.6). These lavas are generally microporphyritic and have trachytic textures. Olivine and pyroxene microphenocrysts are iron-rich (51–57 and 21–26 at. % Fe, respectively), and kaersutite microphenocrysts occur in some samples. The benmoreites, phonolites, and trachytes form distinct trends from the EL on most geochemical variation diagrams. They are enriched in Fe and have different incompatible element ratios (Zr/Nb is 3.28–4.22 compared to 2.73–3.78 in the EL). These lavas may have evolved from an alkali basalt parental magma at a temperature, pressure, and oxygen fugacity different from those at which the EL lavas evolved. Trachyte from Mount Cis has an elevated Sr isotopic ratio (0.7049 [see *Stuckless and Ericksen*, 1976]), indicating that crustal contamination occurred during its evolution.

Chronologic Data

Eleven K-Ar dates range from 0.94 to 0.15 Ma, indicating that Mount Erebus has formed within the last million years and is the youngest major volcanic center in the Erebus volcanic province. The youngest anorthoclase phonolite flows at Cape Barne and Cape Royds (Figure A.17.2) were dated at 0.94 ± 0.05 Ma [*Armstrong*, 1978] and 0.68 ± 0.14 Ma [*Treves*, 1967], respectively; *ne*-hawaiite flows at Cape Barne and Turks Head (Figure A.17.1) have ages of 0.8 ± 0.2 Ma [*Armstrong*, 1978] and 0.86 ± 0.20 [*Moore and Kyle*, 1987], respectively. These dates indicate that the lower slopes of Mount Erebus formed between 1 and 0.7 Ma.

Ages of 0.81 ± 0.02 Ma were obtained from the lowermost unit and 0.73 ± 0.07 Ma from the uppermost unit at Fang Ridge [*Armstrong*, 1978]. Anorthoclase phonolite from the rim of the summit plateau of Mount Erebus was dated at 0.15 ± 0.05 Ma [*Armstrong*, 1978], suggesting that the summit caldera formed and filled with lavas before 0.02 Ma. Anorthoclase phenocrysts and glass inclusions in them from the summit cone of Mount Erebus have K-Ar ages ranging

Copyright American Geophysical Union

TABLE A.17.1. Representative Chemical Analyses of Volcanic Rocks From Mount Erebus

	1	2	3	4	5	6	7	8
SiO_2	43.32	47.19	49.00	50.77	55.81	55.93	57.24	63.51
TiO_2	3.78	2.72	2.29	1.95	1.07	1.10	0.61	0.43
Al_2O_3	15.38	18.24	18.31	18.91	18.03	19.74	19.07	15.33
FeO*	12.08	9.33	8.81	7.78	7.71	4.59	5.69	6.15
MnO	0.22	0.22	0.22	0.22	0.30	0.18	0.24	0.21
MgO	6.77	3.13	3.02	2.20	1.35	1.23	0.65	0.14
CaO	10.66	7.52	6.16	5.55	3.75	3.20	2.44	1.44
Na_2O	4.63	5.89	7.66	6.90	7.06	7.77	8.06	6.56
K_2O	1.72	2.83	3.42	3.38	3.50	4.33	4.65	5.23
P_2O_5	1.21	1.22	1.08	0.93	0.41	0.44	0.18	0.05
LOI	0.03	0.78	0.42	0.17	-0.22	0.15	-0.17	0.18
Total	99.82	99.05	100.39	98.76	98.75	98.66	98.65	99.23
Ba	485	721	833	909	1109	1064	1221	304
Ce	149.8	195.3	197.5	218.1	228.4	204.2	213.8	325.1
Cr	130	2	6	<2	<2	2	<2	2
Cu	0.38	0.62	0.66	0.83	0.73	1.20	0.94	3.69
Eu	43	56	36	21	10	10	12	<10
Ga	3.63	4.01	3.59	4.11	3.83	4.27	2.99	2.91
Hf	21	22	23	24	25	27	26	33
La	8.49	9.78	11.06	12.57	13.92	18.10	17.04	25.2
Lu	70.0	94.7	98.8	107.9	113.0	103.9	114.0	164.9
Nb	0.40	0.51	0.54	0.59	0.61	0.71	0.65	1.17
Nd	111	163	173	192	193	236	220	258
Ni	67	86	85	95	88	80	75	145
Pb	63	10	10	7	7	7	8	9
Rb	<4	<4	<4	<4	6	<4	8	31
Sc	44	62	71	72	81	96	98	159
Sm	20.30	6.42	5.68	5.09	2.07	2.80	1.05	2.79
Sr	12.45	14.46	12.78	13.89	12.22	12.02	10.27	21.0
Ta	1100	1295	1166	1188	923	990	538	13
Tb	6.57	9.46	10.61	11.30	11.43	13.73	13.2	14.59
Th	1.33	1.64	1.52	1.70	1.44	1.57	1.26	2.87
U	7.2	11.3	11.8	13.9	14.3	17.5	17.0	25.4
V	1.6	3.2	3.4	4.7	4.8	5.2	5.2	7.9
W	291	73	76	37	10	13	<10	<10
Y	37	46	42	47	43	49	41	92
Yb	2.55	3.35	3.44	3.95	3.93	4.74	4.21	7.88
Zn	104	111	99	118	122	99	101	269
Zr	363	482	550	608	634	855	812	1085

All analyses by XRF and instrumental neutron activation; analysts were J.A. Moore and P.R. Kyle. LOI, loss on ignition.

*Total Fe expressed as FeO.

1. Basanite, Cape Barne.
2. *Ne*-hawaiite, Tryggve Point.
3. *Ne*-mugearite, Fang Ridge.
4. *Ne*-benmoreite, north-westernmost of Dellbridge Islands (Inaccessible Island).
5. Benmoreite, northeastern coast of Ross Island.
6. Anorthoclase phonolite, Cape Royds.
7. Phonolite, north-westernmost of Dellbridge Islands (Inaccessible Island).
8. Trachyte, Bomb Peak.

Copyright American Geophysical Union

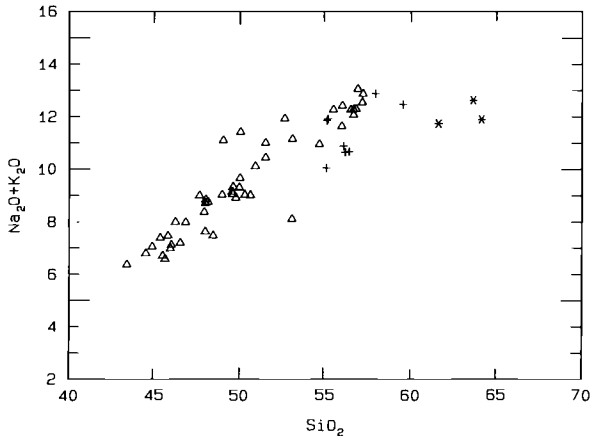

Fig. A.17.4. Alkali versus silica plot for rocks from Mount Erebus and satellitic centers. All are new analyses, recalculated to 100% volatile-free, with total Fe expressed as FeO [*Moore*, 1986]. Old analytical data from the literature are reviewed and summarized by *Kyle* [1976] and *Moore* [1986]; they show no significant differences from those presented above. Erebus lineage (triangles), kaersutite-bearing benmoreites and phonolites (pluses), and trachytes (asterisks).

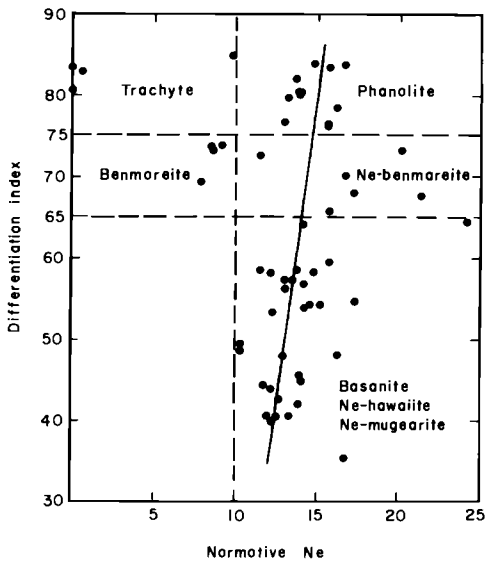

Fig. A.17.6. Division of Mount Erebus lavas into the strongly undersaturated (Ne > 10%) Erebus lineage and weakly undersaturated and oversaturated benmoreites and trachytes (Ne < 10%) of the enriched iron series (EFS) [from *Moore and Kyle*, 1987].

from 0.55 to 0.44 Ma [*Armstrong*, 1978]. These ages are too old, since the phenocrysts come from the active summit vent and indicate a uniformly distributed excess Ar anomaly in the phonolite lava.

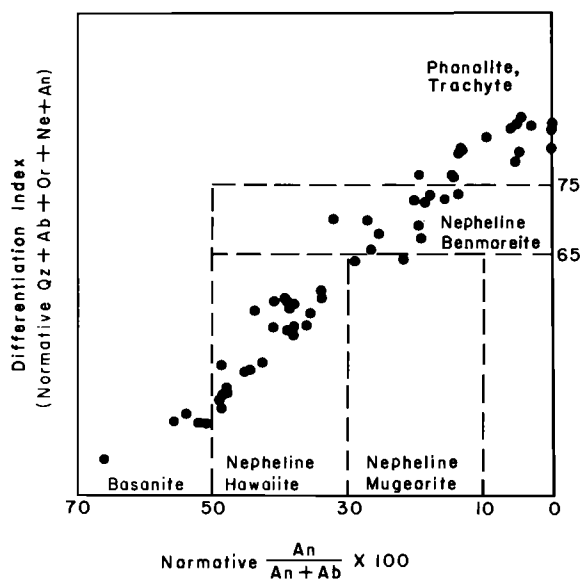

Fig. A.17.5. Plot of differentiation index [*Thornton and Tuttle*, 1960] against normative plagioclase, showing nomenclature of lavas from Mount Erebus and adjacent areas [from *Moore and Kyle*, 1987].

Extent of Knowledge

Outcrop occurs on approximately 10% of Mount Erebus and is easily accessible. The volcanic geology and its stratigraphy of the basanite to *ne*-benmoreite cones along the southwestern coast and at Fang Ridge are well exposed by deep erosion. The internal structure and stratigraphy of Mount Erebus itself is poorly known because of the youthful age of the volcano. Only the uppermost units are exposed in coastal cliffs and the walls of the summit crater.

Mount Erebus is the most studied volcano in Antarctica, having been the subject of research since it was discovered in 1841. The results of early investigations of the field geology, petrography, mineralogy, and geochemistry of the lavas are summarized by *Smith* [1954]. Post-International Geophysical Year (1957) studies include field geology [*Treves*, 1962, 1967; *Luckman*, 1974; *Kyle*, 1976; *Wright et al.*, 1983], mineralogy [*Carmichael*, 1962, 1963, 1967; *Carmichael and MacKenzie*, 1964; *Boudette and Ford*, 1966; *Kyle*, 1977; *Weiblen et al.*, 1981], geochemistry [*Carmichael*, 1964; *Treves*, 1967; *Berlin and Henderson*, 1969; *Luckman*, 1974; *Goldich et al.*, 1975, 1981; *Kyle*, 1976; *Kyle and Rankin*, 1976; *Sun and Hanson*, 1976; *Stuckless et al.*, 1981; *Mason et al.*, 1982; *Irving and Frey*, 1984; *Moore and Kyle*, 1986], K-Ar age dates [*Treves*, 1967; *Armstrong*, 1978], and Sr and Pb isotopes [*Stuckless and Ericksen*, 1976; *Sun and Hanson*, 1975; *Jones et al.*, 1983]. A comprehensive thesis on the geology, mineralogy, and geochemistry of Mount Erebus by *Moore* [1986] summarizes previous work and presents new data.

Copyright American Geophysical Union

More recent studies of Mount Erebus include the volcanic activity [*Kyle,* 1986*a*], seismicity [*Kienle et al.,* 1984, 1986; *Nagata,* 1984; *Dibble et al.,* 1984], gravity [*Nagata,* 1984], deformation of the summit [*Blick et al.,* 1986], and magmatic gases [*Rose et al.,* 1985; *Chuan et al.,* 1986].

Bibliography

Armstrong, 1978
Berlin and Henderson, 1969
Blick et al., 1986
Boudette and Ford, 1966
Carmichael, 1962, 1963, 1964, 1967
Carmichael and MacKenzie, 1964
Chuan et al., 1986
Dibble et al., 1984
Goldich et al., 1975, 1981
Holdsworth and Ugolini, 1965
Irving and Frey, 1984
Jones et al., 1983
Kienle et al., 1984, 1986
Kurasawa, 1977
Kyle , 1976, 1977, 1986*a*
Kyle and Cole, 1974
Kyle and Rankin, 1976
Kyle et al., 1979, 1989
Luckman, 1974
Mason et al., 1982
Moore, 1986
Moore and Kyle, 1985, 1986, 1987
Mountain, 1925
Nagata, 1984
Rose et al., 1985
Smith, 1954
Stuckless and Ericksen, 1976
Stuckless et al., 1981
Sun and Hanson, 1975, 1976
Tazieff, 1978
Treves, 1962, 1967
Ugolini, 1967
Weiblen et al., 1981
Wright et al., 1983

Copyright American Geophysical Union

A.18. Hut Point Peninsula

Type of volcano: Basalt scoria cones, lava flows and associated pyroclastic rocks, phonolite dome and flows.

Location: Ross Island (77°40′–77°50′S, 166°40′–166°50′E).

Height above sea level: 0–431 m.

Evidence of Holocene activity: None.

Author of report: P.R. Kyle.

Date of report: January 1987.

Fig. A.18.1. Geologic sketch map of Hut Point Peninsula [from *Kyle*, 1981*a*].

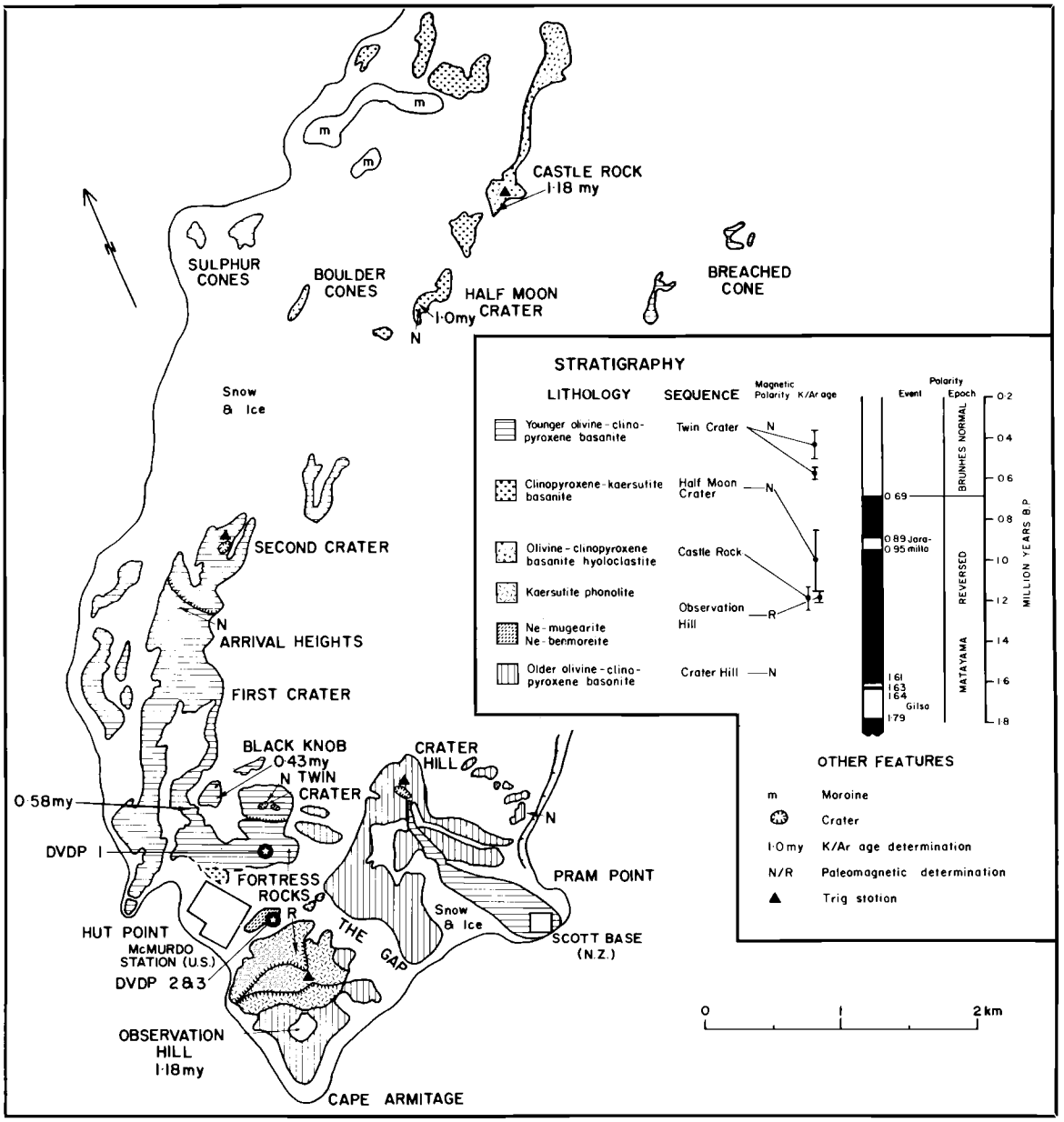

Copyright American Geophysical Union

Form and Structure

Hut Point Peninsula is a 20-km-long, 2- to 4-km-wide en echelon line of volcanic cones that extend in a southwest direction from Mount Erebus (Figures A.III.2 and A.18.1). At the southern end of the peninsula are numerous small, well-exposed basaltic scoria cones with thin flows and associated pyroclastic rocks [*Kyle*, 1981*a*]. Observation Hill (Figure A.18.1) is a 228-m-high endogenous phonolite dome. The Dry Valley Drilling Project (DVDP) drilled three holes at the southern end of Hut Point Peninsula (Figure A.18.2.) [*Kyle*, 1981*a*]. The deepest (DVDP 3)

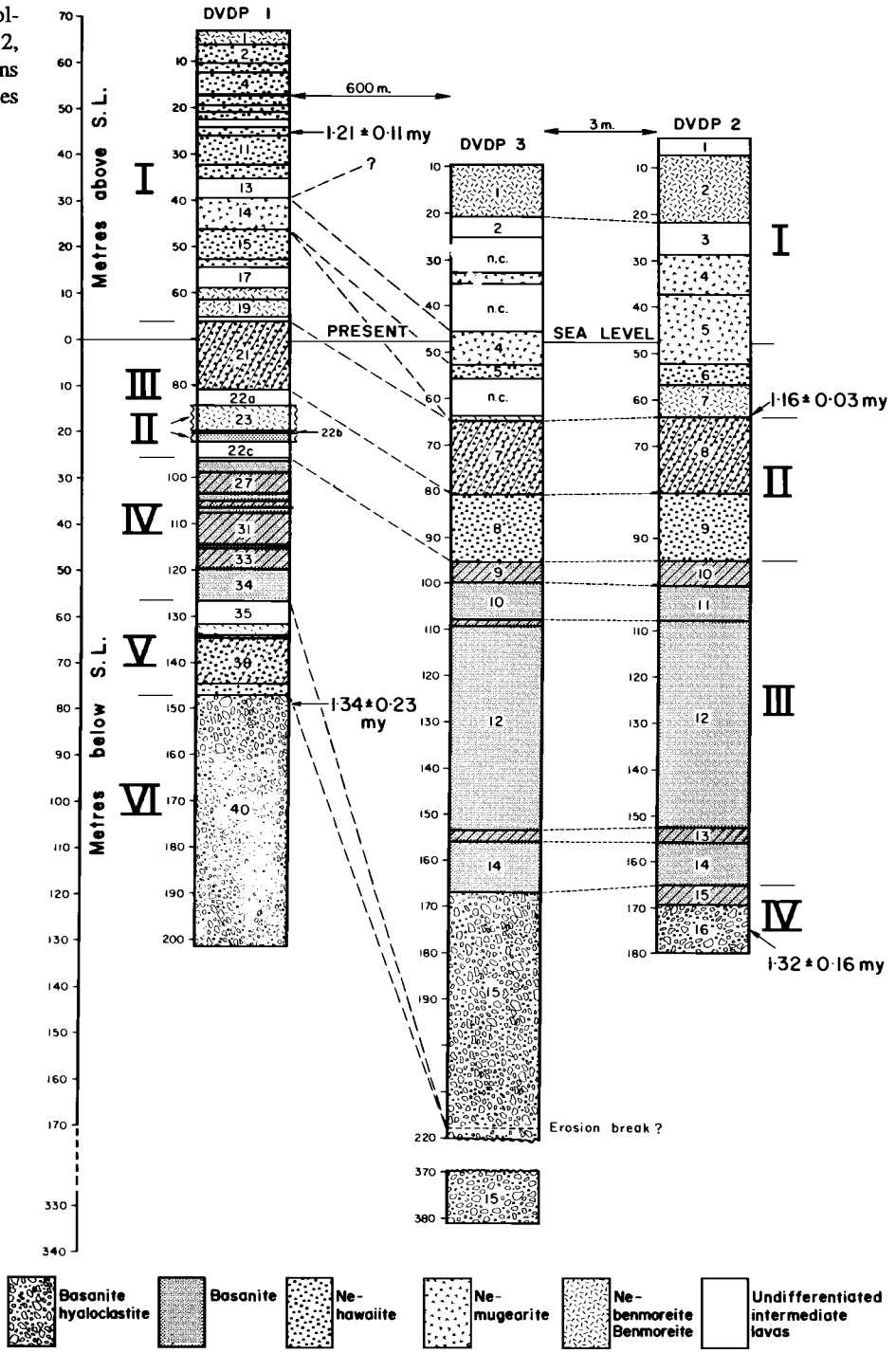

Fig. A.18.2. Geologic columns for DVDP holes 1, 2, and 3. Tentative correlations are shown by dashed lines [from *Kyle*, 1981*a*].

Copyright American Geophysical Union

TABLE A.18.1. Representative Chemical Analyses of Volcanic Rocks From Hut Point Peninsula

	1	2	3	4	5
SiO_2	41.68	42.15	47.27	51.90	54.82
TiO_2	4.06	4.66	2.95	1.85	1.16
Al_2O_3	12.92	15.84	17.61	19.31	20.41
Fe_2O_3	3.06	4.73	3.35	3.01	1.99
FeO	8.48	8.27	6.06	3.96	2.52
MnO	0.18	0.22	0.21	0.20	0.18
MgO	12.13	5.54	3.72	2.07	1.24
CaO	11.32	10.60	7.76	5.43	3.46
Na_2O	3.16	4.51	6.07	7.26	8.50
K_2O	1.48	2.09	3.11	3.70	4.57
H_2O^-	0.84	1.30	0.81	0.60	0.26
LOI	--	0.10	0.40	--	0.49
Total	99.31	100.01	99.32	99.29	99.60
Ba	277	348	545	695	709
Cr	469	31	56	15	8
Cs	0.31	0.45	0.65	1.6	2.0
Cu	52	42	29	15	14
Dy	4.7	7.6	6.3	6.3	5.5
Er	2.5	3.7	3.5	3.2	3.7
Eu	2.7	4.7	3.9	3.4	2.6
Gd	7.0	11	11	8.8	8.3
Hf	5.8	7.5	10	14	20
Ho	1.1	1.5	1.5	1.3	1.4
La	53	91	91	140	150
Nb	80	150	140	190	280
Nd	49	88	78	74	61
Ni	276	25	22	8	8
Pb	8.0	18	13	21	30
Pr	13	24	21	23	20
Rb	30	41	72	97	139
Sm	9.2	15	11	11	9.2
Sn	2.0	2.3	2.3	3.0	3.7
Sr	829	1242	1374	1194	782
Tb	0.94	1.4	1.2	1.2	1.0
Th	4.7	6.5	13	18	26
U	1.2	1.7	3.6	5.0	8.8
V	300	291	208	77	55
Y	33	58	36	41	41
Yb	1.6	2.4	2.8	3.5	4.3
Zn	82	109	111	109	105

All XRF and spark source mass spectrometry analyses from *Kyle* [1981*b*]. Dashes, not determined. LOI, loss on ignition.

1. 2-105.53. Basanite, DVDP hole 2, 105.53 m deep.
2. 1-90.72. Basanite, DVDP 1, 90.72 m.
3. 2-76.38. Phonotephrite, DVDP 2, 76.38 m.
4. 2-61.23. Tephriphonolite, DVDP 2, 61.23 m.
5. 25793. Phonolite, Observation Hill.

Copyright American Geophysical Union

reached 381-m depth and contained a thick sequence of basaltic hyaloclastite underlying the flows (Figure A.18.2).

Petrologic Characteristics

Volcanic rocks from Hut Point Peninsula consist of a well-defined differentiation sequence which ranges from basanite to phonolite (Table A.18.1 and Figure A.18.3) [*Kyle,* 1981*b*; *Stuckless et al.,* 1981]. The intermediate rocks are well represented and consist of *ne*-hawaiite, *ne*-mugearite, and *ne*-benmoreite. *Kyle* [1981*b*] named this suite of lavas the DVDP lava lineage and modeled its evolution by crystal fractionation models. Detailed mineral chemistry is also described by *Kyle* [1981*b*]. Xenoliths are common in the volcanic rocks and are described briefly in a review by *Kyle et al.* [1987].

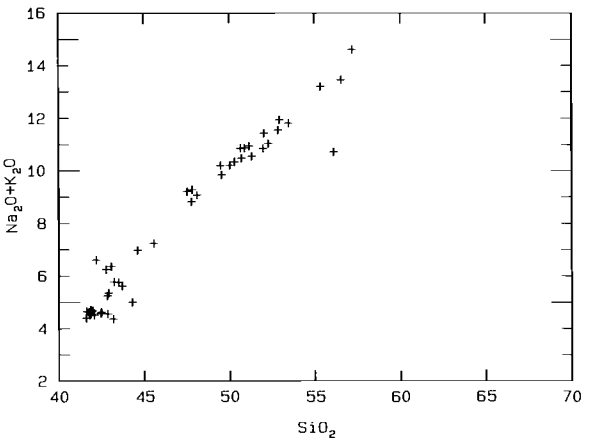

Fig. A.18.3. Alkali versus silica plot for analyzed samples of volcanic rocks from Hut Point Peninsula. All data are from *Kyle* [1981*b*].

Chronologic Data

K-Ar dates range from 0.44 ± 0.1 Ma to 1.34 ± 0.23 Ma for surface lava samples and core samples from DVDP 1 and 2 (see *Kyle* [1981*b*] for summary). Ten additional K-Ar dates are given by *Polyakov et al.* [1976] quoted by *Stuiver and Braziunas* [1985], but as these generally show no agreement with other existing data, they are not considered to be reliable.

Extent of Knowledge

Hut Point Peninsula is one of the best documented areas within the McMurdo Volcanic Group. The DVDP cores give an excellent picture of the subsurface of the area [*Kyle,* 1981*a*]. Geochemical and mineral analyses for DVDP core samples and surface samples are the most detailed in the McMurdo Volcanic Group.

Bibliography

Armstrong, 1978
Cole et al., 1971
Forbes et al., 1974
Goldich et al., 1975
Kyle, 1981*a, b*
Kyle and Rankin, 1976
Kyle and Treves, 1974
Kyle et al., 1979, 1987
Polyakov et al., 1976
Sun and Hanson, 1975
Treves and Kyle, 1973

Copyright American Geophysical Union

A.19. White Island, Black Island, and Brown Peninsula

Type of volcano: Basaltic shield volcanoes and cinder cones; phonolitic flows, plugs, and domes.

Location: Ross Ice Shelf south of McMurdo Sound, southern Victoria Land (78°00′–78°20′S, 165°05′–167°40′E).

Height above sea level: 0–1041 m.

Evidence of Holocene activity: None.

Authors of report: A.C. Wright and P.R. Kyle.

Date of report: June 1986.

Form and Structure

The volcanic complexes of White Island and Black Island protrude through the Ross Ice Shelf to reach elevations of 762 m and 1041 m, respectively (Figure A.19.1). Brown Peninsula is a similar volcanic complex and reaches a height of 816 m. It separates Koettlitz Glacier from the Ross Ice Shelf and is joined to the much larger volcanic edifice of Mount Discovery (2681 m) by a low moraine-covered saddle.

The exposed volcanic rocks in all three areas are subaerial. Unlike White Island, which is largely shrouded by snow and ice, Black Island and Brown Peninsula are essentially ice-free. Despite this, much of the volcanic geology is obscured by moraine and talus deposits (Figure A.19.1).

Brown Peninsula consists of a series of coalescing, north-south aligned, basaltic to silicic volcanic centers [*Kyle et al.*, 1979]. Pyroclastic deposits are present locally but are inadequate as stratigraphic markers [*Cole and Ewart*, 1968]. Vents between Tuff Bluff and Frame Ridge, and at Rainbow Ridge are older, and all but the youngest flow at Rainbow Ridge are considerably modified by glacial erosion [*Cole and Ewart*, 1968]. The youngest vents on Brown Peninsula

Fig. A.19.1. Geologic sketch map of Brown Peninsula, Black Island, and the northern part of White Island, after *Cole and Ewart* [1968], *Cole et al.* [1971], and *Kyle et al.* [1979]. Encircled numbers refer to the location of analyzed samples cited in Table A.19.1; boxed numbers refer to K-Ar ages in millions of years.

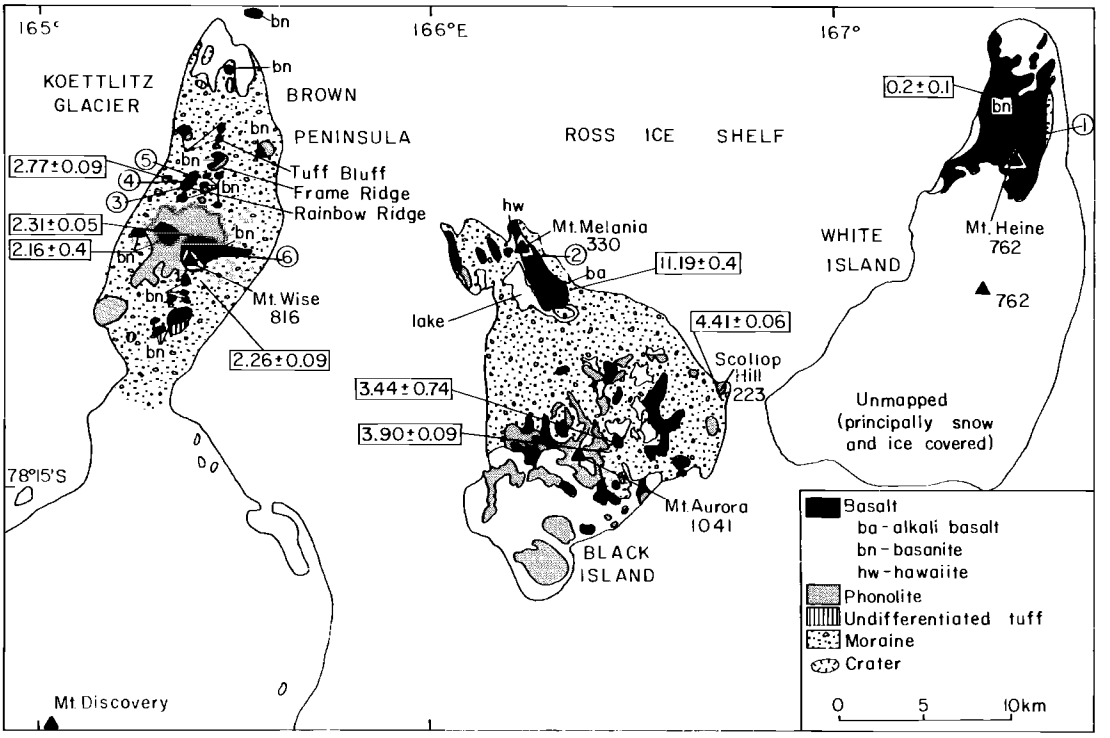

Copyright American Geophysical Union

are near Mount Wise and show no marked glacial erosion.

On Black Island, in the Mount Melania area, basaltic to trachytic lavas were erupted from coalescing domes [*Cole and Ewart,* 1968]. These rocks have been severely modified by glacial erosion, but outcrop patterns suggest a northwest alignment of vents. The main mass of the island is underlain by a series of coalescing basalt cones, which may have been erupted along the eastern margin of an older caldera [*Cole and Ewart,* 1968]. A relatively major volcanic center for the overlying sequence of trachytic flows, plugs, and domes was located in the vicinity of Mount Aurora. Isolated scoria cones, crudely aligned along east-southeast trends, clearly postdate this trachyte sequence. Finally, a second phase of trachyte volcanism erupted local flows. Two trachyte domes, forming the southern part of the island, are probably related to this later phase of trachytic volcanism.

Only the northern, relatively ice-free portion of White Island has been mapped geologically [*Cole et al.,* 1971]. It consists of two overlapping basanitic shields, surmounted by younger basanitic cones aligned in a north-south direction.

On the basis of the morphological similarity of eruptive sequences at Black Island, Brown Peninsula, and Cape Bird (Ross Island), *Cole and Ewart* [1968] erected a fourfold scheme of classification:

Formation	Type Locality
Trachyte Hill Formation	Cape Bird
Nubian Basalt Formation	Black Island
Aurora Trachyte Formation	Black Island
Melania Basalt Formation	Black Island

Cole et al. [1971] extended the use of this classification to other areas, including White Island. However, the use of these formations in areas other than their type localities is misleading and is not recommended [*Kyle et al.,* 1979].

Petrologic Characteristics

The volcanic sequence on Brown Peninsula consists of at least three basaltic (basanite, hawaiite, mugearite) to silicic (benmoreite, phonolite) eruptive cycles [*Kyle et al.,* 1979] (Figure A.19.2). The basanites are porphyritic with seriate phenocrysts of olivine (Fa_{74-40}), opaque oxides, and brown glass. *Ne*-hawaiites are typically vesicular and are characterized by phenocrysts of kaersutite, rare olivine (commonly with kaersutite or clinopyroxene reaction rims), and rare green clinopyroxene, in a groundmass of kaersutite, brown clinopyroxene, plagioclase (An_{60-33}), opaque oxide, and brown glass. The *ne*-benmoreites contain seriate phenocrysts of kaersutite, minor clinopyroxene, and rare oligoclase and olivine, in a pilotaxitic groundmass of oligoclase (An_{20}) and albite, clinopyroxene, and opaque oxides. Both kaersutite and olivine characteristically display opaque oxide reaction rims. *Smith* [1954] described a phonolitic rock from Brown Peninsula as a fine-grained

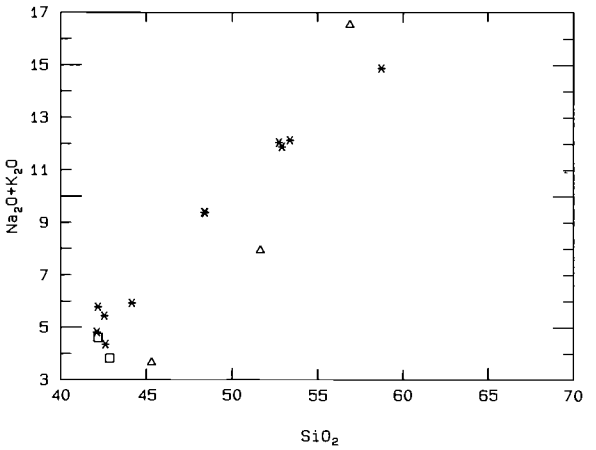

Fig. A.19.2. Alkali versus silica plot for volcanic rocks from White Island (squares), Black Island (triangles), and Brown Island (asterisks). All analyses are recalculated to 100% volatile-free, with total Fe expressed as FeO. Sources: *Goldich et al.* [1975] and *Kyle et al.* [1979].

aggregate of small feldspars with minor interstitial magnetite, and rare aegirine-augite and sphene. Representative analyses are given in Table A.19.1 and are plotted in Figure A.19.2.

The volcanic rocks of Black Island are olivine-augite, plagioclase, and hornblende basalts; trachybasalts; and hornblende and pyroxene trachytes [*Cole and Ewart,* 1968]. Geochemical analyses [*Goldich et al.,* 1975] indicate the presence of alkali basalt (Table A.19.1) and hawaiite in the Mount Melania area and of phonolite near Mount Aurora. From a comparison with the rocks of Brown Peninsula, most of the basalts on Black Island are probably basanites and hawaiites, and the trachytes are probably benmoreitic to phonolitic in composition.

The White Island rocks are all porphyritic clinopyroxene olivine basanites. *Cole et al.* [1971] described them as basalts, but geochemical analyses [*Goldich et al.,* 1975] indicate that samples from both the older and the younger sequences are basanitic in composition. Three $^{87}Sr/^{86}Sr$ ratios from this area average 0.7038 [*Jones and Walker,* 1972].

Chronologic Data

A K-Ar age of 2.77 Ma (Figure A.19.1) on the youngest flow at Rainbow Ridge places a minimum age on the rocks in the Rainbow Ridge, Frame Ridge, and Tuff Bluff area of Brown Peninsula. Three more ages on rocks from the vicinity of Mount Wise constrain the age of the youngest phase of volcanic activity there to 2–2.5 Ma. The northwest part of Black Island is considerably older (11.2 Ma) than the rest of the island, where ages range from 3.9 to 3.4 Ma [*Armstrong,* 1978]. Basalts underlying fossiliferous sediments at Scallop Hill have yielded a K-Ar date of 4.48

Copyright American Geophysical Union

TABLE A.19.1. Representative Chemical Analyses of Volcanic Rocks From White Island, Black Island, and Brown Peninsula

	White Island	Black Island	Brown Peninsula			
	1	2	3	4	5	6
SiO_2	42.7	45.0	42.52	48.46	52.60	58.64
TiO_2	3.27	3.07	3.80	2.56	1.38	0.28
Al_2O_3	12.8	13.3	14.50	18.17	20.02	22.55
Fe_2O_3	3.10	5.30	13.09*	9.53*	6.44*	0.97
FeO	7.96	6.38	--	--	--	0.99
MnO	0.19	0.19	0.21	0.21	0.19	tr
MgO	12.7	9.50	7.98	3.91	2.10	0.16
CaO	12.5	12.5	11.54	7.24	4.46	1.43
Na_2O	2.85	2.61	3.74	6.37	7.77	9.87
K_2O	0.96	1.03	1.69	3.04	4.04	4.98
P_2O_5	0.63	0.54	0.91	0.74	0.44	tr
H_2O	0.17	0.53	--	--	--	0.43
CO_2	--	0.08	--	--	--	--
LOI	--	--	--	0.07	0.56	--
Total	99.83	100.03	99.98	100.29	100.00	100.30
Ag	1.2	0.3	--	--	--	--
Ba	300	240	287	493	638	--
Be	2.4	2.2	--	--	--	--
Ce	<100	<100	--	195	235	--
Co	54	45	--	--	--	--
Cr	870	510	292	70	53	--
Cs	--	--	--	1.2	1.8	--
Cu	56	85	58	28	16	--
Dy	--	--	--	6.1	6.4	--
Er	--	--	--	2.9	3.6	--
Eu	--	--	--	3.4	3.6	--
Gd	--	--	--	8.7	9.0	--
Hf	--	--	--	8.5	10	--
Ho	--	--	--	1.2	1.2	--
La	43	35	--	86	125	--
Nd	--	--	--	65	66	--
Ni	300	150	131	34	18	--
Pb	<1	1.6	--	17	20	--
Pr	--	--	--	18	21	--
Rb	30	36	32	77	110	--
Sm	--	--	--	10.5	10.5	--
Sn	<3.0	5.1	--	--	--	--
Sr	740	640	1062	1063	896	--
Tb	--	--	--	1.2	1.2	--
Th	--	--	--	16	23	--
U	--	--	--	4.4	7.3	--
V	280	300	265	143	59	--
Y	25	23	--	--	--	--
Yb	2.6	2.7	--	3.2	4.2	--
Zn	120	126	102	112	107	--
Zr	240	260	--	--	--	--

Dashes, not determined; tr, trace. LOI, loss on ignition.
*Total Fe expressed as Fe_2O_3.

1. 4267. Basanite, north of Mount Heine, White Island [*Goldich et al.*, 1975].
2. 7367. Alkali basalt, Mount Melania, Black Island [*Goldich et al.*, 1975].
3. 24086. Basanite, Rainbow Ridge, Brown Peninsula [*Kyle et al.*, 1979].
4. 24088. *Ne*-hawaiite, Rainbow Ridge, Brown Peninsula [*Kyle, et al.*, 1979].
5. 24089. *Ne*-benmoreite, Rainbow Ridge, Brown Peninsula [*Kyle et al.*, 1979].
6. Phonolite, Brown Peninsula [*Prior*, 1907].

Copyright American Geophysical Union

Ma (Webb, personal communication, 1981). A single age of 0.2 Ma [*Kyle*, 1981*c*] from White Island indicates that this is the youngest of the three volcanic complexes. There is no evidence to suggest that volcanism on Brown Peninsula, Black Island, or White Island is still active.

Extent of Knowledge

Initial geologic and petrographic investigations of the area were made by *Cole and Ewart* [1968] (Brown Peninsula and Black Island) and *Cole et al.* [1971] (White Island). Vents have not been located, although major craters are indicated on Brown Peninsula and White Island.

A detailed study of the volcanic geology [*Adams,* 1973] and geochemistry [*Adams,* 1973; *Kyle,* 1976] of the Rainbow Ridge area, Brown Peninsula, is summarized by *Kyle et al.* [1979]; they discussed petrologic nomenclature and recommended the restriction of formations defined by *Cole and Ewart* [1968] to their type localities.

There are 11 geochemical analyses of rocks from Brown Peninsula [*Prior,* 1907; *Adams*, 1973; *Goldich et al.,* 1975; *Kyle,* 1976], three from Black Island [*Goldich et al.,* 1975], and two from White Island [*Goldich et al.,* 1975]. Trace-element analyses are available for all but one.

Bibliography

Adams, 1973
Armstrong, 1978
Cole and Ewart, 1968
Cole et al., 1971
Debenham, 1923
Eggers, 1979
Ferrar, 1907
Goldich et al., 1975, 1981
Jones and Walker, 1972
Kyle, 1976, 1981*c*
Kyle and Cole, 1974
Kyle et al., 1979
Prior, 1907
Smith, 1954
Vella, 1969

Copyright American Geophysical Union

[redacted]

[redacted]

[redacted]

[redacted]

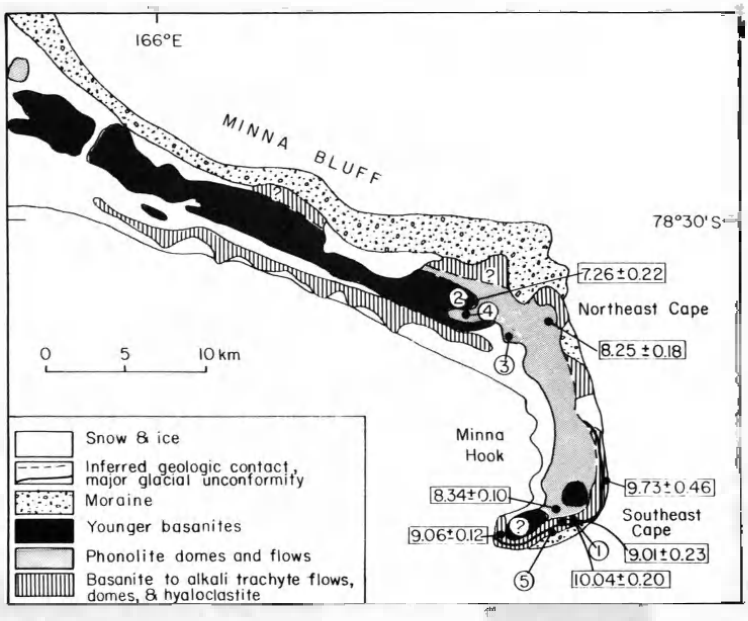

[redacted]

[redacted]

Copyright American Geophysical Union

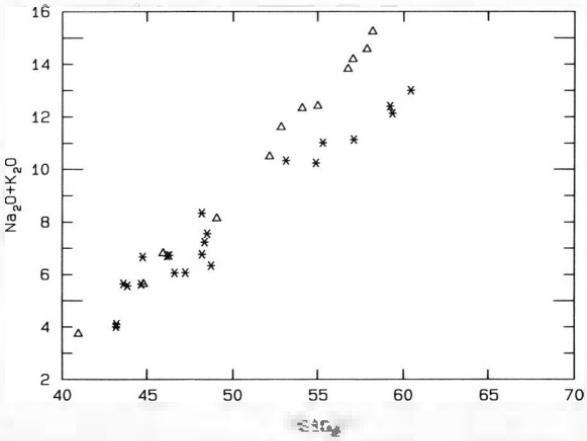

Copyright American Geophysical Union

TABLE A.20.1. Representative Chemical Analyses From Minna Bluff

	1	2	3	4	5
SiO_2	43.13	44.84	52.77	57.52	57.83
TiO_2	3.24	3.31	1.27	0.13	0.46
Al_2O_3	15.27	15.89	19.09	20.36	18.60
Fe_2O_3**	12.13	11.88	7.89	4.96	5.86
MnO	0.20	0.19	0.21	0.22	0.20
MgO	7.54	6.85	2.02	0.22	0.44
CaO	10.44	10.70	4.07	1.49	2.02
Na_2O	3.73	3.98	7.41	8.98	7.26
K_2O	1.75	1.67	4.19	5.51	4.85
P_2O_5	0.97	0.84	0.37	0.06	0.17
LOI	1.57	-0.11	0.18	0.59	1.57
Total	99.97	100.26	100.10	100.04	99.26
As*	2.0	<3.3	2.8	11	1.3
Ba	632	526	559	254	1141
Ba*	571	511	553	287	1160
Ce*	124.5	132	141	192	160
Cr	213	205	20	<10	<10
Cr*	217	190	16	<0.8	<0.3
Cs	0.54	0.64	1.2	1.5	1.0
Cu	46	47	<15	<15	35
Eu*	3.17	3.06	2.00	1.25	1.83
Ga	20	22	24	27	21
Hf*	6.77	7.42	10.4	15.5	13.8
La*	60.7	65.5	78.1	120	92.4
Lu*	0.41	0.38	0.49	0.71	0.48
Nb	99	91	120	180	148
Nd*	53.2	59.4	46.8	56.6	45.8
Ni	95	84	13	<5	<5
Pb	5	5	10	14.0	11
Rb	42	45	118	171	130
Rb*	42	49	110	166	126
Sb	0.1	0.1	0.2	0.4	0.2
Sc	23	22.9	6.1	0.2	0.5
Sm	10.50	10.10	30.30	7.96	6.30
Sr	1088	903	499	95	445
Ta*	5.68	5.62	8.48	12.7	9.9
Tb*	2.68	2.40	3.04	4.36	2.74
Th	4	7	14	27	19
Th*	3.8	6.8	14.6	24.0	18.3
U*	2.0	1.8	4.8	6.4	2.86
V	243	286	79	3	3
Y	34	33	32	43	25
Yb*	1.25	1.21	0.94	1.02	0.74
Zn	84	98	95	131	79
Zr	296	323	538	844	731

All determinations made by XRF analysis unless indicated otherwise; all data from *Wright-Grassham* [1987]. LOI, loss on ignition.

*Determination by instrumental neutron activation analysis.

**Total Fe expressed as Fe_2O_3.

1. AW84797. Tephrite, lava tongue in palagonitized sediment.
2. AW82163. Tephrite, flow capping Minna Bluff.
3. AW82156. Tephriphonolite, dome.
4. AW82165. Phonolite, flow.
5. AW84791. Trachyte, dome.

Copyright American Geophysical Union

A.21. Mount Discovery

Type of volcano: Composite benmoreite-phonolite central volcano overlain by basanite-hawaiite cinder cones and associated lava flows.

Location: Between Koettlitz Glacier and the Ross Ice Shelf, southern Victoria Land (78°12′–78°25′S, 164°40′–165°40′E).

Height above sea level: 2681 m.

Evidence of Holocene activity: None.

Authors of report: A.C. Wright and P.R. Kyle.

Date of report: March 1987.

Form and Structure

Mount Discovery is a weakly dissected central volcano which rises from sea level to 2681 m. The volcano has a summit cone of interbedded benmoreite lava flows, debris flow deposits, and volcanogenic sedimentary rocks, capped by extensive phonolite flows erupted both from the summit and from several domes on the northern side of the mountain (Figures A.21.1–A.21.3). These flows either reach sea level or are covered by younger volcanic rocks and moraine on the northern and eastern flanks of the mountain. Unwelded phonolitic pumice lapilli near the

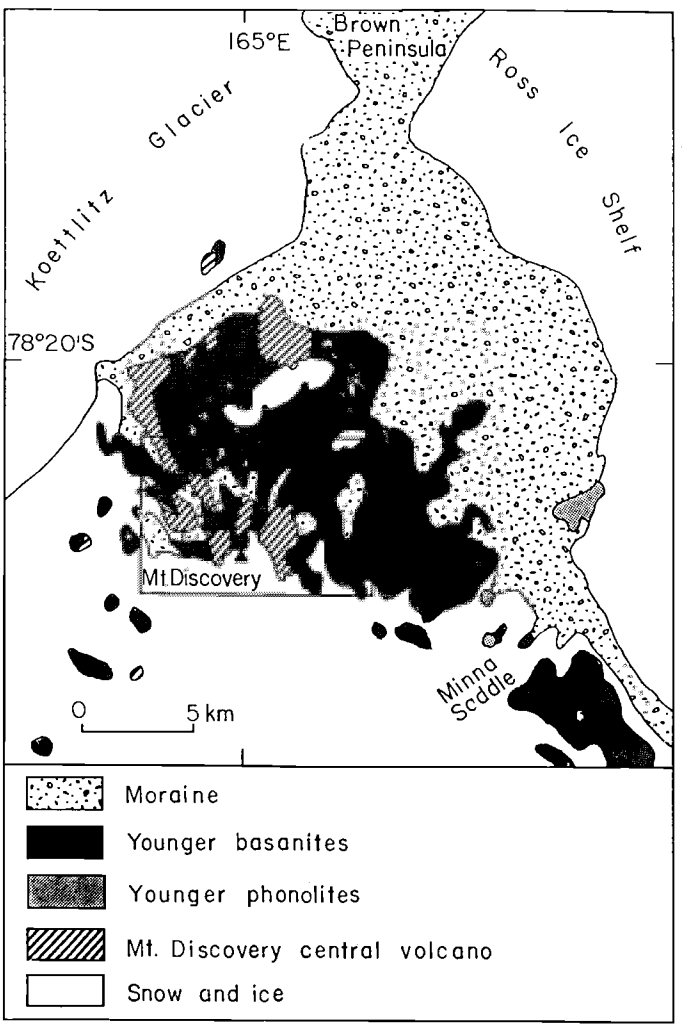

Fig. A.21.1. Geologic sketch map of Mount Discovery; the area outlined is shown in detail in Figure A.21.2.

Copyright American Geophysical Union

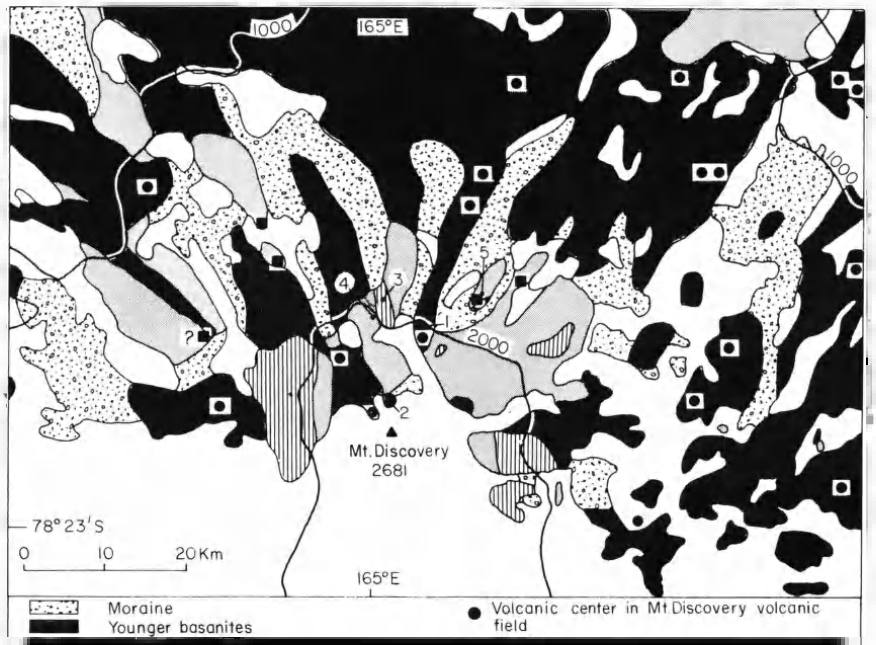

Copyright American Geophysical Union

TABLE A.21.1. Representative Chemical Analyses of Volcanic Rocks From Mount Discovery

	1	2	3	4	5
SiO_2	42.94	48.46	51.46	57.81	58.92
TiO_2	3.96	2.76	1.83	0.94	0.28
Al_2O_3	14.28	17.69	18.92	18.83	19.06
Fe_2O_3**	14.06	10.87	8.07	5.89	4.72
MnO	0.22	0.26	0.23	0.23	0.26
MgO	7.81	3.66	2.25	1.04	0.44
CaO	10.63	7.96	4.83	2.42	0.87
Na_2O	4.18	5.45	7.07	6.99	8.61
K_2O	1.81	2.21	3.68	4.60	5.46
P_2O_5	0.89	1.39	0.92	0.33	0.07
LOI	-0.60	-0.63	0.10	0.65	0.84
Total	100.18	100.08	99.36	99.73	99.53
Ba	517	797	1063	1078	112
Ba*	497	776	972	1102	<160
Ce*	144	223	210	197	260
Cr	181	<10	<10	<10	<10
Cr*	186	1.7	1.1	<0.5	<0.9
Cs*	0.38	0.45	0.83	1.06	1.90
Cu	79	17	19	<15	<15
Eu*	3.55	4.95	4.58	2.63	1.07
Ga	24	22	24	23	29
Hf*	9.37	9.53	12.5	14.4	25.2
La*	68.4	106	100	105	144
Lu*	0.36	0.48	0.53	0.51	0.75
Nb	104	142	197	186	309
Nd*	66.9	98.7	90.4	68.2	75.9
Ni	82	<5	5	<5	<5
Pb	7	7	6	11	16
Rb	42	51	76	103	164
Rb*	38	49	75	102	157
Sb*	--	0.1	0.2	0.2	0.5
Sc*	24.9	6.3	3.6	1.6	0.6
Sm*	12.4	16.7	14.1	9.49	10.7
Sr	1025	1990	1614	536	32
Ta*	6.59	8.53	11.2	11.4	19.0
Tb*	1.38	1.65	1.60	1.06	1.35
Th	7	6	12	19	35
Th*	7.8	9.8	13.6	17.8	30.6
U*	1.8	2.2	4.3	4.4	9.1
V	316	107	41	20	<3
Y	36	42	43	33	51
Yb*	2.61	3.17	3.62	3.23	4.73
Zn	108	110	89	98	135
Zr	409	453	641	737	1282

All determinations made by XRF analysis unless indicated otherwise; all data from *Wright-Grassham* [1987]. Dash, not determined. LOI, loss on ignition.

*Determination by instrumental neutron activation analysis.

**Total Fe expressed as Fe_2O_3.

1. AW84728. Basanite flow at about 2000 m, north side of Mount Discovery.
2. AW84753. Hawaiite flow at about 2400 m, near the summit of Mount Discovery.
3. AW84718. *Ne*-benmoreite flow at about 1900 m, north side of Mount Discovery.
4. AW84719. Trachyte flow at about 2000 m, north side of Mount Discovery.
5. AW84741. Phonolite dome at about 1950 m, north side of Mount Discovery.

Copyright American Geophysical Union

summit are interpreted as remnants of a summit cinder cone. Basanite-hawaiite cinder cones and lava flows of the Mount Discovery volcanic field form an almost continuous mantle to the older rocks below 1800 m.

Kyle and Cole [1974] suggested that Mount Discovery is located at the intersection of the southern extension of the Rennick fault and a northeast trending structure, which in part may be a northern extension of the Hillary fault.

Petrologic Characteristics

Ne-benmoreite, phonolite, and trachyte have been recorded from the central volcano of Mount Discovery [*Goldich et al.*, 1975; *Kyle*, 1976; *Wright-Grassham*, 1987] (Table A.21.1). The younger cinder cones and flows are predominantly basanite, hawaiite, and phonolite.

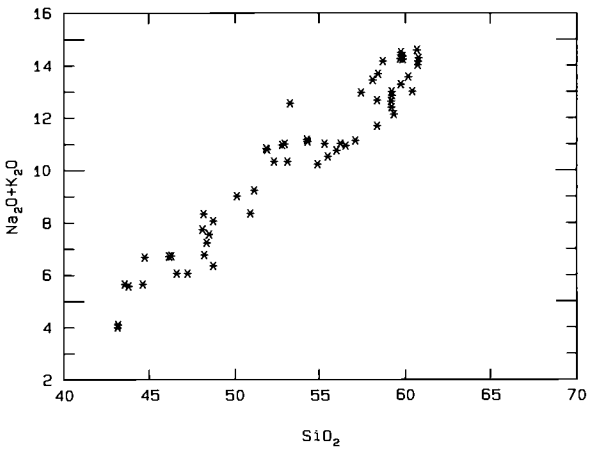

Fig. A.21.4. Alkali versus silica plot for all known analyses of volcanic rocks from Mount Discovery [from *Wright-Grassham*, 1987].

Major-element analyses from the central volcano and the Mount Discovery volcanic field show separate trends (Figure A.21.4). Mild peralkalinity is developed in the most evolved rocks, a result of plagioclase fractionation. *Stuckless and Ericksen* [1976] reported an $^{87}Sr/^{86}Sr$ ratio of 0.7033 for a hawaiite from the Mount Discovery volcanic field, collected near the summit.

Chronologic Data

A feldspar separate from a basalt collected near the summit of Mount Discovery has yielded a K-Ar age of 5.44 Ma [*Armstrong*, 1978]. Seven K-Ar ages indicate that the central volcano at Mount Discovery formed about 5.3 ± 0.1 Ma, whereas later parasitic vents are as young as 1.87 Ma [*Wright-Grassham*, 1987].

Extent of Knowledge

Mount Discovery was first visited in 1958 by a New Zealand survey party, and the geological samples collected were later analyzed by *Kyle* [1976]. *Treves* [1968, 1970] collected samples from near the summit for geochemical analysis [*Goldich et al.*, 1975] and K-Ar dating [*Armstrong*, 1978]. Field investigations of the upper northern slopes were conducted by *Wright et al.* [1984, 1986]. Detailed petrologic and geochemical studies are given by *Wright-Grassham* [1987].

Bibliography

Armstrong, 1978
Goldich et al., 1975
Kyle, 1976
Kyle and Cole, 1974
Kyle et al., 1979
Stuckless and Ericksen, 1976
Treves, 1968, 1970
Wright et al., 1984, 1986
Wright-Grassham, 1987

Copyright American Geophysical Union

A.22. Mount Morning

Type of volcano: Eroded trachytic subvolcanic complex; alkali basalt to trachyandesite domes and flows; hawaiite to phonolite central volcano and parasitic domes; basanitic cinder cones and flows.

Location: 22 km west-southwest of Mount Discovery, southern Victoria Land (78°20′–78°32′S, 163°15′–164°30′E).

Height above sea level: 400–2723 m.

Evidence of Holocene activity: None.

Authors of report: A.C. Wright and P.R. Kyle.

Date of report: January 1987.

Form and Structure

Mount Morning is located 25 km east of the southern end of the Royal Society Range. It has good exposures on its northern slopes (above 1000 m) and on two ridges ("Riviera Ridge" and "Hurricane Ridge") extending from its eastern flanks (Figures A.22.1 and A.22.2).

Volcanic rocks in this area were erupted during two main episodes of activity, in Miocene and Quaternary times. The older Miocene rocks crop out at the lower ends of "Riviera" and "Hurricane" ridges, as isolated windows of deeply eroded subvolcanic complexes. "Gandalf Ridge," at the northern end of "Hurricane Ridge," has Miocene volcanic rocks resting unconformably on Koettlitz Group basement

Fig. A.22.1. Geologic map of Mount Morning.

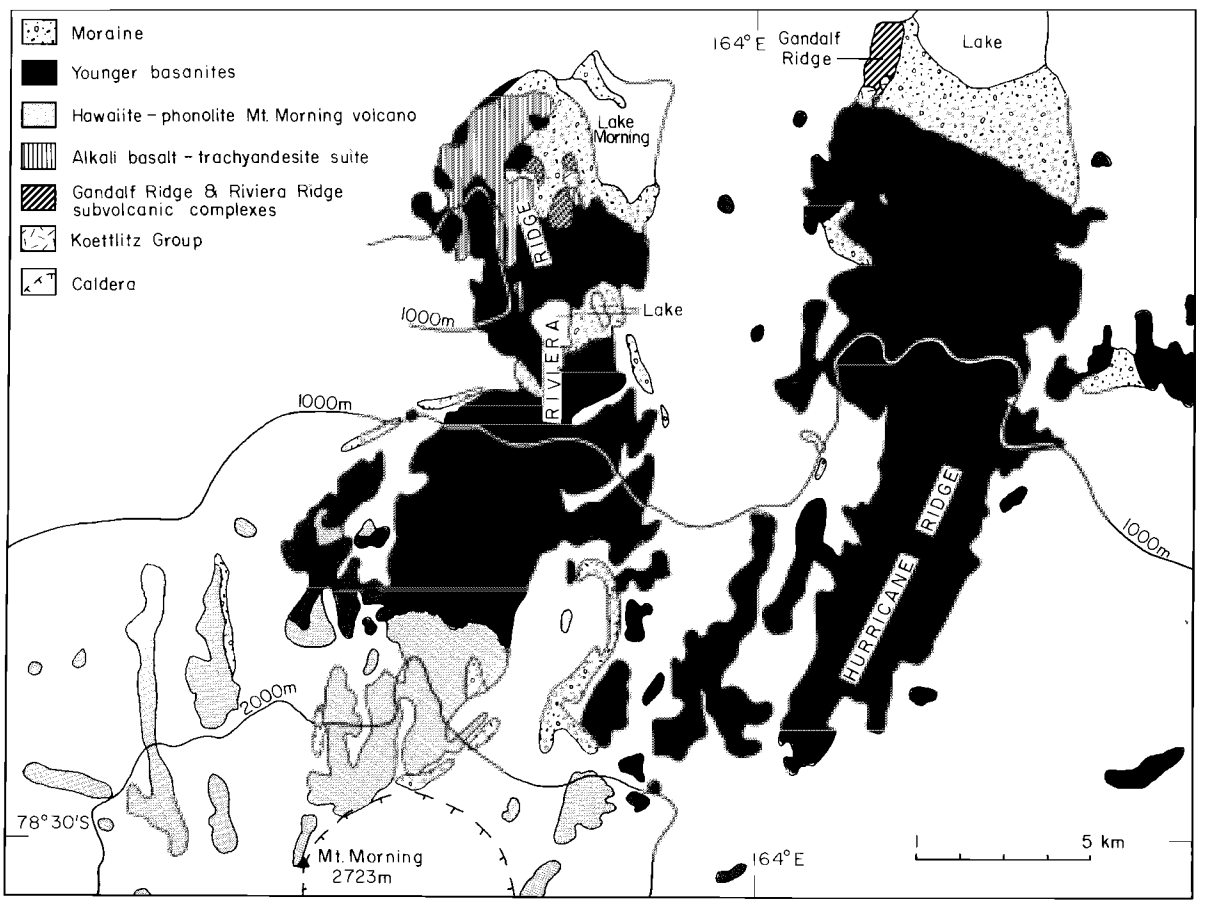

Copyright American Geophysical Union

Copyright American Geophysical Union

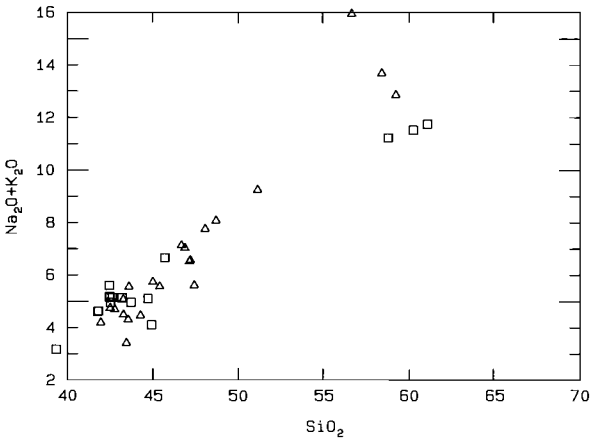

Fig. A.22.3. Alkali versus silica plot for analyzed samples of Quaternary volcanic rocks from Mount Morning (triangles) and younger (<7 Ma) volcanic rocks from Mason Spur (squares). All analyses are recalculated to 100% volatile-free, with total Fe expressed as FeO. Data are from *Wright-Grassham* [1987] and *Muncy* [1979].

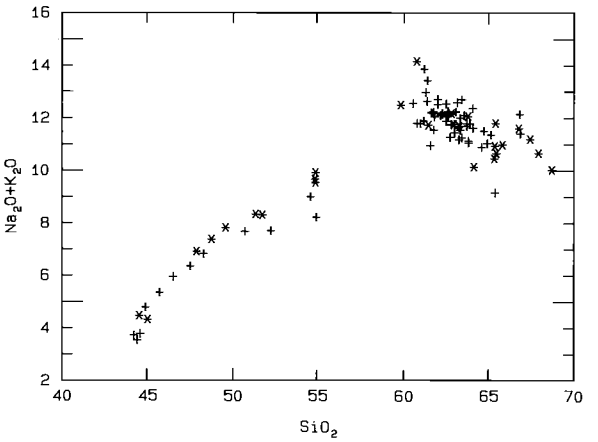

Fig. A.22.4. Alkali versus silica plot for analyzed samples of older (>11 Ma) volcanic rocks from Mount Morning ("Gandalf Ridge" and "Riviera Ridge") (asterisks) and Mason Spur (pluses). All analyses are recalculated to 100% volatile-free, with total Fe expressed as FeO. Data are from *Wright-Grassham* [1987] and *Muncy* [1979].

clinopyroxene, feldspar, opaque oxide, and apatite [*Muncy,* 1979]. The Mount Morning volcanic rocks belong to a basanite-phonolite trend [*Wright-Grassham,* 1987].

Chronologic Data

Whole-rock K-Ar age determinations on trachyandesite flows (18.7 Ma) intruded by dikes (17.6–15.8 Ma) from the "Gandalf Ridge" subvolcanic complex [*Armstrong,* 1978; *Muncy,* 1979] indicate that the volcanism here is the oldest known in the Erebus volcanic province. The subvolcanic complex at Riviera Ridge is a little younger, with *Q*-trachyte flows (15.2 Ma) intruded by dikes 14.6 Ma in age; these are overlain by flows dated at 13.0 to 14.1 Ma [*Wright-Grassham,* 1987]. A parasitic phonolite dome on the northern side of Mount Morning has yielded a K-Ar date of 1.15 Ma [*Armstrong,* 1978]. *Polyakov et al.* [1976] (quoted by *Stuiver and Braziunas* [1985]) gave ages ranging from 1.0 to 2.4 Ma for Mount Morning.

Extent of Knowledge

Muncy [1979] examined "Gandalf Ridge" and part of "Riviera Ridge," and H.L. Muncy and P.R. Kyle made a geological reconnaissance of the Mount Morning area in 1978. A more detailed geological study of the Mount Morning area is described by *Wright-Grassham* [1987].

Bibliography

Armstrong, 1978
Kyle and Cole, 1974
Muncy, 1979
Treves, 1967
Wright-Grassham, 1987

Copyright American Geophysical Union

TABLE A.22.1. Representative Chemical Analyses of Volcanic Rocks From the Mount Morning Area

	1	2	3	4	5	6	7	8	9
SiO_2	42.37	45.26	48.95	50.33	50.89	54.95	57.97	63.53	63.81
TiO_2	3.92	3.74	2.72	2.42	2.27	1.20	0.50	0.56	0.46
Al_2O_3	16.21	18.33	16.70	15.20	18.21	17.74	19.58	12.50	16.28
Fe_2O_3	14.38**	12.17**	11.84**	6.44	8.94**	9.84**	4.70**	7.99	2.81
FeO	--	--	--	5.84	--	--	--	0.80	1.12
MnO	0.20	0.15	0.26	0.23	0.20	0.30	0.21	0.31	0.07
MgO	6.82	4.77	3.81	2.90	2.71	1.64	0.57	0.11	0.44
CaO	12.10	11.28	7.20	6.20	6.40	4.40	2.00	0.45	1.95
Na_2O	3.21	3.38	5.25	4.34	5.89	6.68	8.48	6.37	4.70
K_2O	1.00	0.98	2.15	2.21	3.29	3.01	5.09	4.65	5.68
P_2O_5	0.73	0.54	1.58	1.03	0.70	0.47	0.14	0.08	0.08
LOI	-0.52	0.11	-0.34	2.41	0.32	0.41	0.26	1.90	2.34
Total	100.41	100.71	100.12	99.55	99.82	100.64	99.46	99.25	99.74
Ba	401	415	696	908	894	1291	462	58	825
Cr	86	66	14	--	26	10	--	2	2
Cu	21	<15	<15	9	<15	81	<15	6	8
La*	39.3	--	--	65.6	68.3	99.7	99.8	194.6	73.7
Lu*	0.31	--	--	0.6	0.44	0.63	0.63	1.6	0.5
Ni	44	25	<5	5	12	7	<10	5	5
Pb	4	<3	--	8	12	8	15	2	18
Rb	25	17	44	49	71	59	145	112	160
Sc*	23.7	--	--	14.2	6.42	8.25	0.69	0.7	3.5
Sm*	8.67	--	--	14.1	8.78	17.1	6.92	28.8	9.5
Sr	1117	1268	1591	588	984	1273	287	19	166
Th	3	<3	--	3	10	8	26	20	18
V	379	282	83	--	104	8	10	5	13
Y	29	21	41	50	31	50	34	96	39
Yb*	2.09	--	--	4.7	2.75	4.11	3.92	12.3	2.5
Zn	81	65	81	138	77	82	101	342	59
Zr	214	165	404	373	420	559	822	1626	642

All determinations made by XRF analysis unless indicated otherwise. Dashes, not determined. LOI, loss on ignition.
*Determination by instrumental neutron activation analysis.
**Total Fe expressed as Fe_2O_3.

1. AW86057. Younger basanite, "Hurricane Ridge" [*Wright-Grassham*, 1987].
2. AW86036. Alkali basalt from the alkali basalt - trachyandesite suite, "Riviera Ridge" [*Wright-Grassham*, 1987].
3. AW86012. Younger basanite, "Riviera Ridge" [*Wright-Grassham*, 1987].
4. 77M11. Trachyandesite, "Gandalf Ridge" [*Muncy*, 1979].
5. AW86121. Phonotephrite flow, northern slopes of Mount Morning [*Wright-Grassham*, 1987].
6. AW86025. Trachyandesite dome from the alkali basalt - trachyandesite suite, "Riviera Ridge" [*Wright-Grassham*, 1987].
7. AW86127. Phonolite dome, near the summit of Mount Morning [*Wright-Grassham*, 1987].
8. 77M27. Pantellerite, "Gandalf Ridge" [*Muncy*, 1979].
9. 77M80. *Q*-trachyte, "Riviera Ridge" [*Muncy*, 1979].

Copyright American Geophysical Union

A.23. Mason Spur

Type of volcano: Deeply eroded, basanite to trachytic volcanic complex unconformably overlain by basanitic tuff and cinder cones, lava flows, and a trachyte dome.

Location: 25 km southwest of Mount Discovery, southern Victoria Land (78°32′–78°38′S, 164°07′–164°38′E).

Evidence of Holocene activity: None.

Authors of report: A.C. Wright and P.R. Kyle.

Date of report: October 1987.

Form and Structure

Mason Spur is a 10-km-long ridge separating Eady Ice Piedmont and the Ross Ice Shelf (Figures A.23.1 and A.23.2). Excellent geologic exposures are afforded by 1000-m-high bluffs on the southeastern side of the ridge, and along the ridge crest. The area is largely ice-free, but moraine and colluvium cover is significant.

There are two stratigraphically distinct episodes of volcanism [*Wright-Grassham,* 1987]. The older sequence (Mason volcanic complex) is a predominantly peralkaline trachyte volcanic complex composed of coarse, heterolithic volcanic breccias associated with domes and flows, unconformably overlain by a unit comprising debris flow deposits, massive and bedded tuffs, and cinder and agglutinate deposits. These are unconformably overlain by two separate sequences of lava flows, above which there are basanite to benmoreite flows and minor tuffs. A major north-northeast trending dike swarm at "Birthday Bluffs" was intruded after the eruption of the earlier flow sequence. A second dike swarm is associated with the younger basanite to benmoreite activity and is controlled by northeast trending faults that parallel the face of the bluffs.

The younger volcanic sequence comprises a trachyte dome, well-bedded trachyte tuff-ring deposits, and numerous basanite and tephrite cinder and agglutinate cones with associated lava flows. Several of these lava flows drape over the bluffs, indicating that the Mason Spur scarp formed prior to the eruption of the younger volcanic sequence.

Fig. A.23.1. Geologic sketch map of Mason Spur; encircled numbers refer to the location of samples analyzed in Table A.23.1.

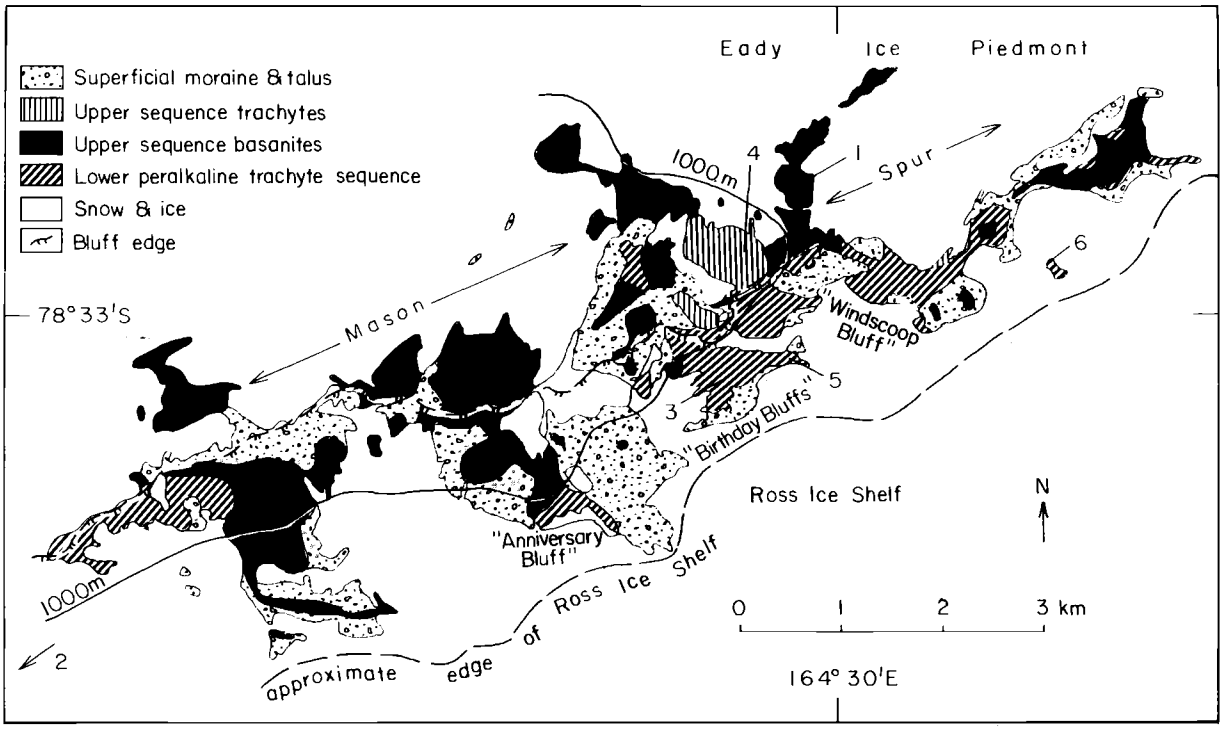

Copyright American Geophysical Union

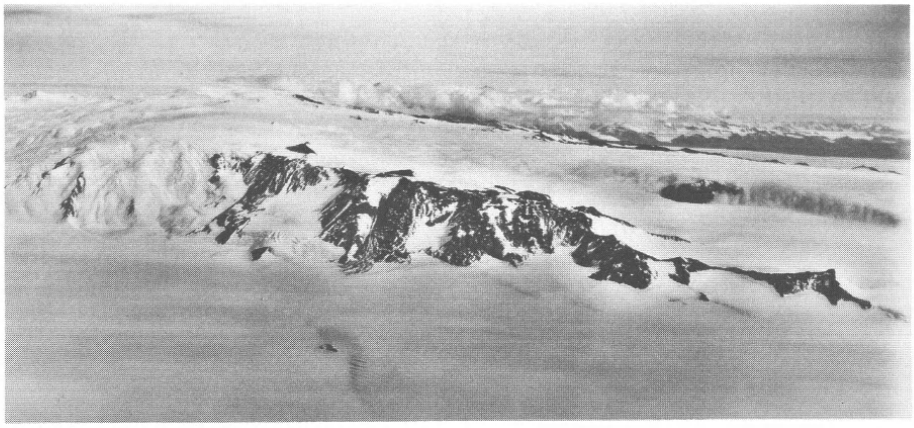

Fig. A.23.2. Oblique aerial view looking northwest of Mason Spur. (U.S. Navy photograph, TMA 476 F33 012.)

TABLE A.23.1. Representative Chemical Analyses of Volcanic Rocks From Mason Spur

	1	2	3	4	5	6
SiO_2	42.14	46.00	53.29	60.02	63.70	66.82
TiO_2	3.63	2.89	1.65	0.47	0.61	0.84
Al_2O_3	13.55	15.60	17.45	17.54	14.66	16.82
Fe_2O_3	13.80*	3.66	7.65	3.20	6.64	2.53
FeO	--	7.85	1.11	3.40	0.40	0.04
MnO	0.21	0.23	0.19	0.22	0.32	0.04
MgO	10.34	6.49	1.36	0.62	0.19	0.17
CaO	11.36	9.49	5.64	2.15	0.49	0.46
Na_2O	3.52	4.61	4.81	6.51	6.41	6.18
K_2O	1.15	2.10	3.19	4.97	4.93	5.97
P_2O_5	1.06	0.84	0.63	0.14	0.05	0.15
LOI	-0.76	-0.65	3.16	0.22	1.49	0.54
Total	100.0	99.11	100.13	99.14	99.89	100.56
Ba	513	934	857	1613	26	38
Cr	363	285	14	<10	<10	<10
Cu	37	27	<15	<15	<15	<15
Ga	15	17	25	26	32	32
Nb	73	109	104	173	184	154
Ni	133	90	<5	6	<5	<5
Pb	3	<3	9	18	11	12
Rb	27	39	73	99	95	73
Sr	1303	1810	1032	294	3	6
Th	<3	<3	8	13	15	10
V	295	191	46	<10	<3	<3
Y	33	32	41	73	81	45
Zn	92	94	112	124	129	78
Zr	208	303	450	813	987	458

All analyses by XRF. Analyst A.C. Wright. Dash, not determined. LOI, loss on ignition.

*Total Fe expressed as Fe_2O_3.

1. AW83538. Olivine basanite, upper sequence, "Surprise Cone."
2. AW83413. Olivine basanite, upper sequence, "TriCones."
3. AW83513. Trachyandesite dike, upper sequence, west end of "Birthday Bluffs."
4. AW83647. Trachyte dome, upper sequence.
5. AW83567. Peralkaline *Q*-trachyte intrusion, lower sequence, "Dad's Nose."
6. AW83411. Peralkaline *Q*-trachyte, lower sequence, "Chalcedony Island."

Copyright American Geophysical Union

Petrologic Characteristics

The Mason volcanic complex is composed primarily of peralkaline trachytes and *Q*-trachytes [*Wright-Grassham,* 1987]. Their modal mineralogy consists of alkali feldspar, pyroxenes of ferroaugite to aegirine composition, and aenigmatite, with accessory arfvedsonite and relict titanomagnetite in some samples. The less common basanite to benmoreite lavas are composed of olivine, clinopyroxene, titanomagnetite, and plagioclase. Relict kaersutite has been found in one benmoreite sample.

The SiO_2 range of the Mason volcanic complex trachytes lies between 58 and 67% (Table A.23.1 and Figure A.22.4). A much wider variation occurs for many trace elements (e.g., 449–1203 ppm for Zr and 1034–1.6 ppm for Sr). The large variation in Sr, coupled with large negative Eu anomalies in some samples, is evidence of significant plagioclase fractionation and would support a model in which increasing peralkalinity was generated by progressive plagioclase fractionation. However, a mass balance model in which the peralkaline trachytes were derived from less evolved rocks in the Mason volcanic complex has not been found. A broad scatter in the values of incompatible element ratios suggests that processes other than fractional crystallization have contributed to the diversity of the rock types present.

Basanite and tephrite lavas from the younger sequence (Figure A.22.3) are composed of olivine, clinopyroxene, titanomagnetite, and plagioclase and are typically more porphyritic than lavas of similar composition from the Mason volcanic complex. Kaersutite is common in the tephrites. Lavas from the trachyte dome contain alkali feldspar, green clinopyroxene, and titanomagnetite and are characterized by fayalitic olivine (Fa_{80}.).

Chronologic Data

Incremental $^{40}Ar/^{39}Ar$ determinations on three samples from the lower Mason volcanic complex exhibit disturbed spectra, with plateau ages of 11.46–12.80 Ma. These ages are 0.6–0.9 m.y. younger than the total gas ages. Lavas from the upper Mason volcanic complex have K-Ar ages of 11.7–12.1 Ma. This activity is followed by a 5- to 6-m.y. period of volcanic quiescence before the onset of the younger activity, as marked by a K-Ar age of 6.1 Ma determined on the trachyte dome. The unweathered geomorphic form of the youngest volcanoes at Mason Spur suggests that they are less than 100,000 years old.

Extent of Knowledge

Geologic mapping and detailed sample collection were undertaken in the 1983–1984 and 1985–1986 field seasons [*Wright et al.,* 1984, 1986]. Incremental $^{40}Ar/^{39}Ar$ determinations were made on three samples and K-Ar age determinations on a further five samples [*Wright-Grassham,* 1987]. Major- and trace-element analyses were determined for 79 samples by XRF and instrumental neutron activation analysis [*Wright-Grassham,* 1987]. Electron microprobe analyses of minerals in four trachyte samples and one benmoreite sample have also been made [*Wright-Grassham,* 1987].

Bibliography

Wright et al., 1984, 1986
Wright-Grassham, 1987

Copyright American Geophysical Union

A.24. Royal Society Range

Type of volcano: Principally cinder cones and lava flows.

Location: Between the Royal Society Range and Koettlitz Glacier, southern Victoria Land (78°04′–78°26′S, 162°35′–164°20′E).

Height above sea level: 0–3000 m.

Evidence of Holocene activity: Tephra layers in glaciers, geomorphic evidence.

Authors of report: A.C. Wright and P.R. Kyle.

Date of report: October 1987.

Fig. A.24.1. Geologic map of McMurdo Volcanic Group rocks exposed in the foothills of the Royal Society Range [after *Blank et al.*, 1963; *Keys et al.*, 1977; *Skinner et al.*, 1976; *Wright*, 1980]. Encircled numbers refer to the location of analyzed samples cited in Table A.24.1; boxed numbers refer to K-Ar ages in millions of years.

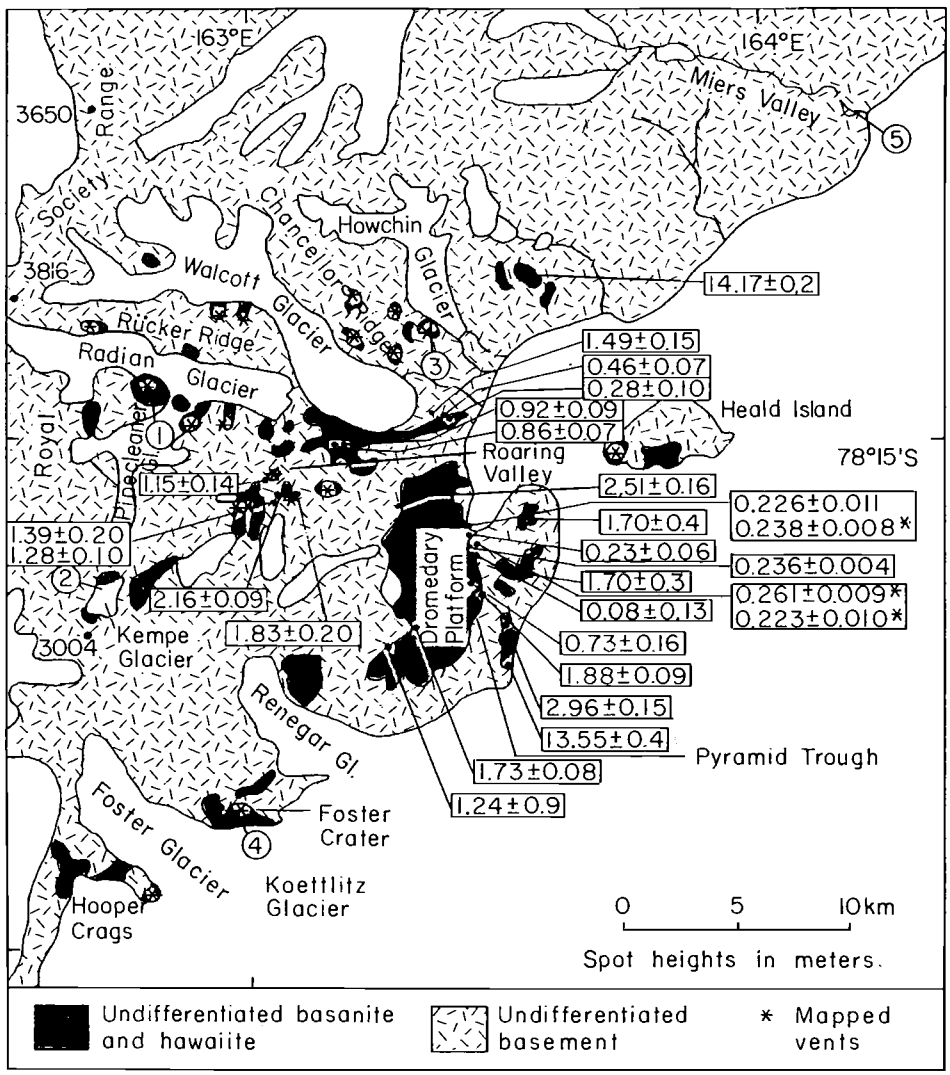

Copyright American Geophysical Union

Form and Structure

The foothills east of the Royal Society Range (0–3000 m high) are dissected by valley glaciers which have fluctuated in height and extent throughout the period of volcanism, causing some modification to the nature and form of certain volcanic deposits. Volcanism was presumably associated with major block faulting along the eastern margin of the Transantarctic Mountains, but apparently the location of individual vents was not controlled by known lineaments.

There are over 50 vents within the area, ranging in size from tiny scoria mounds to larger cones (up to 300 m high) of intercalated scoria, agglutinate, bombs, and lava flows (Figure A.24.1). These larger structures are commonly intruded by dikes, and in some there is evidence of a central plug. The basanite cones forming the Dailey Islands, which lie some 35 km northeast of Roaring Valley, are similar to those found throughout the foothills of the Royal Society Range.

Lava flows within the cinder cones are thin (30–100 cm thick), whereas those that extend beyond their cones are typically 3–10 m thick. Most flows are less than 4 km long, and none exceed 10 km. In Roaring Valley and on Mount Dromedary, successive flows cover areas of 5 and 12 km, respectively, but flows in the valley here have been channeled and ponded by higher ice levels than occur at present. A stream gully east of Walcott Glacier tongue exposes a 30-m sequence of at least five separate flows [*Blank et al.*, 1963].

Subaqueous (presumably subglacial) eruption has produced hyaloclastite at a vent in the Koettlitz Glacier névé [*Skinner et al.*, 1976]. Minor pillow lavas are associated with "Foster Crater" vent, a vent to the east of Pipecleaner Glacier, and vents in the Hooper Crags area [*Skinner et al.*, 1976]. All other reported volcanism was subaerial, although some may have been of supraglacial origin. Many outcrops have been glacially eroded and have lost most or all of the agglutinate and scoriaceous deposits associated with them.

Reports of a kenyte flow [*Blank et al.*, 1963], later reclassified as trachybasalt [*Goldich et al.*, 1975] and *ne*-hawaiite [*Kyle*, 1976], near the mouth of Miers Valley have not been substantiated by the author. However, a debris flow containing trachytic-textured, plagioclase-hawaiite boulders was observed at approximately the same

TABLE A.24.1. Representative Chemical Analyses of Volcanic Rocks From the Foothills of the Royal Society Range

	1	2	3	4	5
SiO_2	42.48	43.15	43.30	43.57	50.00
TiO_2	3.34	3.41	3.42	3.90	2.36
Al_2O_3	12.88	14.57	12.80	14.99	18.70
Fe_2O_3	3.75	13.31*	3.19	13.66*	2.85
FeO	7.87	--	9.33	--	5.85
MnO	0.19	0.19	0.19	0.19	0.20
MgO	10.88	7.82	10.90	8.18	2.58
CaO	11.08	11.72	12.90	10.96	6.73
Na_2O	2.52	3.41	2.62	2.7	6.35
K_2O	1.12	1.24	0.93	1.2	3.43
P_2O_5	--	0.64	0.55	0.63	0.99
H_2O	--	--	0.10	--	0.36
CO_2	--	--	0.03	--	0.03
SrO	--	--	0.09	--	0.15
BaO	--	--	0.03	--	0.07
NiO	0.02	--	--	--	--
Cr_2O_3	0.08	--	--	--	--
LOI	0.94	--	--	0.13	--
Total	97.26	99.46	100.40	100.15	99.90

Dashes, not determined. LOI, loss on ignition.
*Total Fe expressed as Fe_2O_3.

1. Vesicular basanite, vent on east end of ridge between Radian and Pipecleaner glaciers [*McIver and Gevers*, 1970].
2. Basanite tephra layer, Kempe Glacier [*Keys et al.*, 1977].
3. Basanite, "Brandau Vent" [*Goldich et al.*, 1975].
4. Kaersutite basanite, "Foster Crater" [*Kirsch*, 1981].
5. *Ne*-hawaiite, Miers Valley [*Goldich et al.*, 1975].

Copyright American Geophysical Union

location. This deposit is interbedded with sediments, and the volcanic lithologies within the debris flow may not have been derived locally.

Petrologic Characteristics

With the exception of the Miers Valley hawaiite deposits, all McMurdo Volcanic Group rocks in this area are porphyritic basanites with variable relative proportions of olivine and clinopyroxene phenocrysts (some in glomeroporphyritic clots) and minor amounts of phenocrystic plagioclase and opaque minerals. Some lavas contain megacrysts of clinopyroxene, and at "Foster Crater" both phenocrysts and megacrysts of kaersutite are present. Olivine, clinopyroxene, plagioclase, opaque minerals, and glass are the usual groundmass phases.

Ultramafic xenoliths, presumably mantle derived, and crustal-derived xenocrysts and xenoliths occur locally [*Kyle et al.*, 1987]. At "Foster Crater" [*Kirsch*, 1981] and "Brandau Vent" [*McIver and Gevers*, 1970] they are abundant and compositionally varied [*Berg et al.*, 1989; *Gamble et al.*, 1988; *Kalamarides and Berg*, 1989]. At "Foster Crater" some xenoliths represent an ultramafic, metasomatized, cumulate source [*Kirsch*, 1981], whereas others are obviously derived from locally exposed basement rocks.

There are few major-element variations among the 10 analyzed basanites from this area. Typical analyses are given in Table A.24.1, together with the analysis of the *ne*-hawaiite from Miers Valley. Analyses are plotted in Figure A.24.2.

$^{87}Sr/^{86}Sr$ ratios of 0.7033, 0.7032, and 0.7047 [*Jones and Walker*, 1972] have been determined on samples from this area.

Chronologic Data

Of the 24 K-Ar ages shown in Figure A.24.1, only two are older than 2.96 Ma; these may represent a much older period of volcanism, between 13.5 and 14.2 Ma. Most vents are the products of Quaternary activity and cannot be considered extinct. Tephra layers in the ice of Kempe Glacier [*Keys et al.*, 1977], K-Ar ages as young as 0.08 Ma, and well-preserved geomorphic forms all attest to the young age of some centers within this area.

Five unpublished K-Ar ages (Denton, personal communication, 1985) on basalt cones in the Pyramid Trough range from 223 to 261 ka.

Extent of Knowledge

Most of the volcanic outcrops have been mapped from a distance or from air photographs. The distinctive color contrast between volcanic and basement rocks, coupled with generally good exposures, has facilitated this, but the number and size of outcrops have been exaggerated by the inclusion of volcanic moraines and talus. Although many vents are known to occur in the vicinity of Mount Dromedary and north of Howchin Glacier [*Blank et al.*, 1963] and Kempe Glacier [*Keys et al.*, 1977], they remain unlocated on maps.

More detailed descriptions of deposits are limited to Hooper Crags [*Skinner et al.*, 1976], "Foster Crater" [*Wright*, 1979*a*, 1980; *Kirsch*, 1981], Roaring Valley, Heald Island, "Chancellor Ridge," Rücker Ridge [*Wright*, 1979*b*, *c*, 1980], "Brandau Vent" [*McIver and Gevers*, 1970], tephra layers in Kempe Glacier [*Keys et al.*, 1977], and the hawaiite debris flow deposit in Miers Valley [*Wright*, 1978]. *Armstrong* [1978] included magnetic polarity determinations for some of the dated samples.

Bibliography

Armstrong, 1978
Berg, 1989
Berg et al., 1989
Blank et al., 1963
Gamble and Kyle, 1987
Gamble et al., 1988
Goldich et al., 1975
Jones and Walker, 1972
Kalamarides and Berg, 1989
Kalamarides et al., 1987
Keys et al., 1977
Kirsch, 1981
Kyle, 1976
Kyle et al., 1987
McIver and Gevers, 1970
Skinner et al., 1976
Stuckless and Ericksen, 1976
Stuiver et al., 1981
Wright, 1978, 1979*a*, *b*, *c*, 1980
Wright-Grassham, 1987

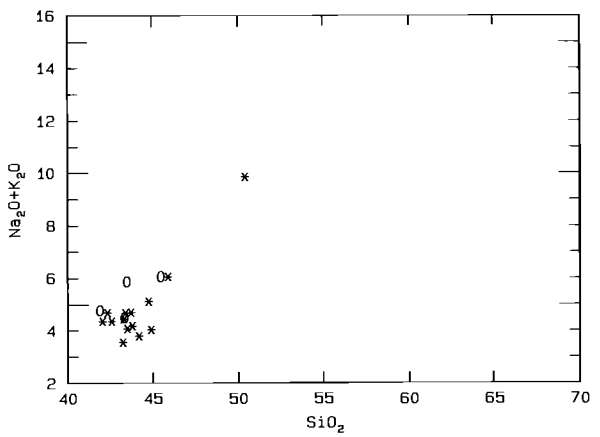

Fig. A.24.2. (opposite) Alkali versus silica plot for samples of volcanic rocks from the Royal Society Range (asterisks) and Taylor Valley (circles).

Copyright American Geophysical Union

A.25. Taylor and Wright Valleys

Type of volcano: Cinder cones and lava flows.

Location: Middle and lower Taylor Valley, and lower Wright Valley, southern Victoria Land (77°28′–77°48′S, 162°07–162°43′E).

Height above sea level: 400–1400 m.

Evidence of Holocene activity: None.

Authors of report: A.C. Wright and P.R. Kyle.

Date of report: November 1985.

Form and Structure

Wright and Taylor valleys are two major, glacially carved valleys, with 1500–2000 m of relief, that extend from the Transantarctic Mountains to McMurdo Sound (Figure A.25.1). McMurdo Volcanic Group rocks are located along the walls and on the floor of the lower, ice-free portions of each valley. Outcrops at lower elevations in Taylor Valley are glaciated [*Haskell et al.*, 1965].

Information from drill holes in eastern Taylor Valley suggests that magmatism was associated with early Pliocene

Fig. A.25.1. Geologic map of McMurdo Volcanic Group rocks exposed in the Taylor Valley area [after *Angino et al.*, 1962; *McCraw*, 1962; *Kurasawa*, 1978; *Porter and Beget*, 1981]. Boxed numbers refer to K-Ar ages in millions of years.

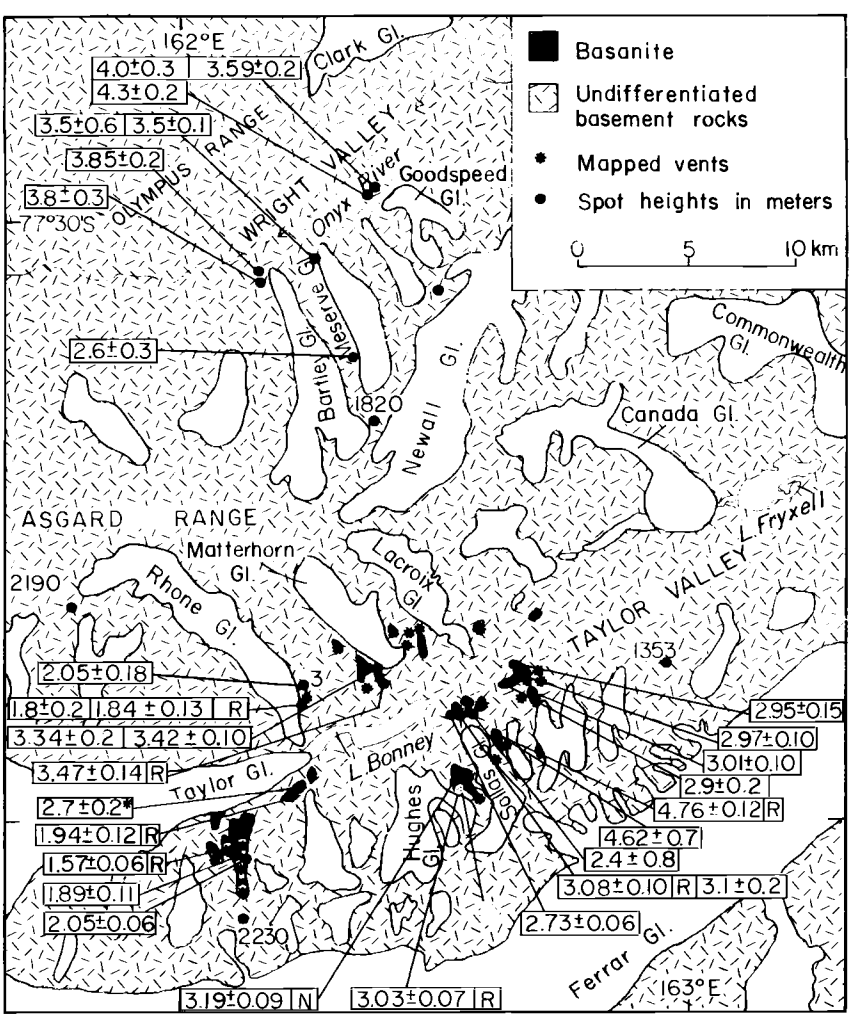

Copyright American Geophysical Union

and Pliocene-Pleistocene uplift along the eastern margin of the Transantarctic Mountains [*Elston and Bressler*, 1981].

There are some 30 scoriaceous mounds up to 60 m high in Taylor Valley; each probably represents an eruptive center [*Haskell et al.*, 1965]. Cones are generally less than 250 m in diameter, and flows are less than 10 m thick [*Pederson et al.*, 1981].

Although Wright Valley is unmapped, there are several basaltic cones along the south wall and floor of the valley, toward its eastern end. There are several reported occurrences of windblown and waterlain ash deposits in both valleys [*Linkletter*, 1971; *Jones et al.*, 1973; *McSaveney*, 1973].

Petrologic Characteristics

The volcanic rocks of Taylor Valley are porphyritic basanites with olivine, clinopyroxene, and labradorite phenocrysts. *Haskell et al.* [1965] noted variations in phenocryst content from rocks with less than 5% labradorite to rocks containing up to 15% euhedral olivine, 8–12% labradorite, and minor clinopyroxene to rocks with up to 20% olivine, 10% clinopyroxene, and rare labradorite. Those rocks rich in mafic phenocrysts commonly contain dolerite inclusions up to 2.5 cm across. The typical holocrystalline groundmass averages 45% labradorite, 35% clinopyroxene, 20% iron oxides, and minor amounts of glass. Major- and trace-element analyses are given in Table A.25.1, and analyses are plotted in Figure A.24.2. $^{87}Sr/^{86}Sr$ ratios fall within a narrow range, with an average of 0.7039 [*Jones and Walker*, 1972].

Chronologic Data

Thirty-one K-Ar age determinations fall within a narrow time span of 4.76–1.57 Ma (Figure A.25.1). Between 4.76 Ma and 2.4 Ma, volcanism occurred throughout the Taylor and Wright valleys volcanic fields. However, after 2.4 Ma the locus of activity contracted to the present position of Taylor Glacier snout. There is no evidence of Holocene activity, and the field is considered extinct.

Extent of Knowledge

No coherent study has been made of the volcanic rocks in this area. Reconnaissance mapping of Taylor Valley recorded their existence on regional geologic maps [*Haskell et al.*, 1965; *Porter and Beget*, 1981]. There are no published maps of the volcanic outcrops in Wright Valley.

Considerable effort has gone into dating these volcanic rocks, mainly by geomorphologists interested in delineating the glacial history of the area [*Armstrong et al.*, 1968; *Denton and Armstrong*, 1968; *Fleck et al.*, 1972; *Armstrong*, 1978]. A few chemical analyses have been made by *Smith* [1954], *Armstrong et al.* [1968], and *Goldich et al.* [1975]. *Armstrong* [1978] determined magnetic polarity on eight samples he had dated. Ground magnetic traverses have been carried out over 11 patches of volcanic rock in the area [*Ervin and Wolf*, 1977; *Pederson et al.*, 1981].

TABLE A.25.1. Representative Chemical Analyses of Volcanic Rocks From Taylor Valley

	1	2	3	4
SiO_2	41.47	42.92	43.1	45.0
TiO_2	5.19	3.77	3.32	2.9
Al_2O_3	14.31	15.34	14.3	14.8
Fe_2O_3	3.96	3.71	4.89	--
FeO	11.48	10.39	8.55	13.0*
MnO	0.22	0.23	0.21	0.22
MgO	7.07	7.25	8.30	7.1
CaO	10.03	10.98	10.0	9.3
Na_2O	3.13	3.15	4.31	4.3
K_2O	1.59	1.30	1.51	1.7
P_2O_5	0.49	tr	0.63	0.65
H_2O	0.93	0.35	0.66	0.8
CO_2	--	0.08	0.02	0.16
ZrO	0.005	0.03	--	--
SrO	0.08	0.06	0.12	--
BaO	0.04	0.057	0.05	--
S	--	0.10	--	--
C	--	0.10	--	--
F	--	0.20	--	--
Total	100.51	100.02	99.97	100.13

Dashes, not determined; tr, trace.
*Total Fe expressed as FeO.

1. Basanite, lava flow from "Black Hill" [*Smith*, 1954].
2. Basanite, "Cheyenne Crater" [*Smith*, 1954].
3. Basanite, small vent on western edge of Sollas Glacier [*Goldich et al.*, 1975].
4. Basanite, average of four samples [*Armstrong et al.*, 1968].

Bibliography

Adams and Christoffel, 1962
Angino et al., 1962
Armstrong, 1978
Armstrong et al., 1968
Denton and Armstrong, 1968
Elston and Bressler, 1981
Ervin and Wolf, 1977
Fleck et al., 1972
Goldich et al., 1975
Haskell et al., 1965
Jones and Walker, 1972
Jones et al., 1973
Kurasawa, 1978
Linkletter, 1971
McCraw, 1962
McSaveney, 1973
Pederson et al., 1981
Porter and Beget, 1981
Prior, 1907
Smith, 1954

Copyright American Geophysical Union

A.IV. Southernmost Ross Embayment

A.26. Sheridan Bluff

Type of volcano: Isolated occurrence of hyaloclastite and lava flows.

Location: 5 km southeast of Mount Saltonstall, upper Scott Glacier, central Transantarctic Mountains (86°58′S, 163°20′W).

Height above sea level: 2270 m.

Evidence of Holocene activity: None.

Authors of report: E. Stump, S.G. Borg, and M.F. Sheridan.

Date of report: January 1986.

Form and Structure

The volcanic sequence at Sheridan Bluff rests unconformably on an irregular, glacially eroded surface of early Paleozoic granodiorite which gains in elevation toward Mount Saltonstall. The volcanic sequence has a maximum thickness of about 200 m, pinching out to the northwest along the rising erosion surface (Figure A.26.1). A basal pillow breccia (10 m thick) passes upward into hyaloclastite breccia composed of a yellow palagonite matrix with angular pillow fragments, many of which still preserve parts of their original glassy, chilled margins. The hyaloclastite has a maximum thickness of 85 m, pinching out to the northwest. The section continues upward with a lava flow, followed by a hyaloclastite unit (5–10 m thick) and nine subaerially erupted lava flows (110 m thick in total). The eruptive vent for these rocks is not exposed.

Petrologic Characteristics

The hyaloclastite breccia consists of vesicular glass fragments, crystal fragments of olivine and minor amounts of clinopyroxene and plagioclase, and accidental lithic fragments (mainly basalt). Parallel-laminated, wavy and cross-stratified bedforms are common in the breccia. Individual bed thickness is one to several centimeters.

The basaltic lavas fall into two distinct groups: one is mildly alkaline (five lavas have 1–5 wt % normative *ne*), and the other is olivine tholeiite (five lavas with normative *hy*). Representative analyses are given in Table A.26.1.

Phenocryst mineralogy of the two groups is very similar, including olivine, plagioclase, and clinopyroxene. Phenocrysts and crystal aggregates form 4–25% in all but two of the lavas, the remainder being fine-grained groundmass. Two lava flows contain about 30–40% ophitic plagioclase in clinopyroxene and 5–8% olivine, the balance being plagioclase laths in an aphanitic groundmass.

Olivine phenocrysts and crystal aggregates (0.1–2 mm in diameter) form 1–9% of the lavas. Olivine cores have a composition of Fo_{80}–Fo_{85} throughout the sequence. Crystal margins are iron enriched, varying from Fo_{70} to Fo_{56}.

Clinopyroxene is colorless in the olivine tholeiites and brown to purplish brown (perhaps titaniferous) in the mildly alkaline group. Crystals are rarely larger than about 0.5 mm. The groundmass contains plagioclase, clinopyroxene, opaque oxides, and very often olivine. The only mineralogical differences between the two groups is the titaniferous(?) augite in the alkaline group and a tendency

Fig. A.26.1. Sketch of the east face of Sheridan Bluff (made from a photograph). PB, pillow breccia; B, breccia; gr, granodiorite. Numbers indicate sample sites.

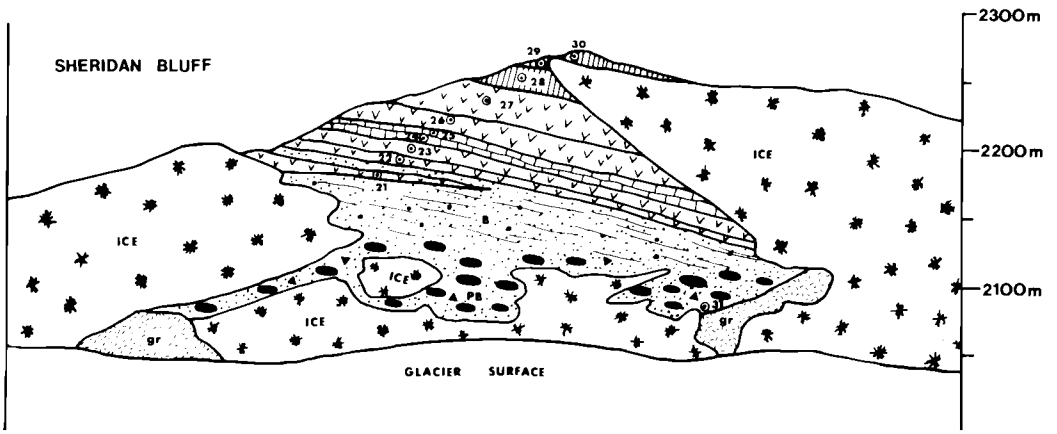

Copyright American Geophysical Union

for the alkaline lavas to contain more plagioclase laths than the olivine tholeiites.

The two groups are clearly distinct in major-element chemistry. Although both groups average 49.50 wt % SiO_2, the alkaline group has 1.77 wt % K_2O (s = 0.13), whereas the tholeiitic group has only 0.67 wt % K_2O (s = 0.11). TiO_2, Al_2O_3, and P_2O_5 are significantly lower, but total iron is significantly higher, in the olivine tholeiites. Thus it appears that there were two distinct magmas erupted at Sheridan Bluff (Sheridan et al., unpublished data, 1986).

TABLE A.26.1. Representative Chemical Analyses of Basalts From Sheridan Bluff

	1	2
SiO_2	49.53	50.31
TiO_2	2.05	1.53
Al_2O_3	16.50	15.44
Fe_2O_3*	10.44	11.98
MnO	0.15	0.16
MgO	6.91	6.73
CaO	9.32	8.72
Na_2O	3.92	3.93
K_2O	1.47	0.81
P_2O_5	0.61	0.22
LOI	1.53	0.64
Total	100.90	99.83

LOI, loss on ignition.
*Total Fe expressed as Fe_2O_3.
1. ANT 24. Mildly alkaline olivine basalt.
2. ANT 27. Olivine tholeiite.

Chronologic Data

The average of three conventional K-Ar whole-rock dates from different lava flows is 18.32 ± 0.35 Ma. Two $^{40}Ar/^{39}Ar$ dates on whole-rock lavas gave concordant age spectra of 19.43 ± 0.65 Ma and 19.75 ± 1.57 Ma, indicating that contamination by excess argon was unlikely [*Stump et al.*, 1980].

Extent of Knowledge

Sheridan Bluff was discovered in 1962–1963 and briefly described by *Doumani and Minshew* [1965]. The locality was reexamined and the section measured in 1978–1979 [*Stump et al.*, 1980].

Bibliography

Doumani and Minshew, 1965
Stump et al., 1980
Treves, 1965

Copyright American Geophysical Union

A.27. Mount Early

Type of volcano: Shield or moberg.
Location: Upper Scott Glacier, central Transantarctic Mountains (87°04′S, 153°46′W).
Height above sea level: 2720 m.
Evidence of Holocene activity: None.
Authors of report: E. Stump, S.G. Borg, and M.F. Sheridan.
Date of report: January 1986.

Form and Structure

Mount Early is the southernmost volcano in the world. It is a deeply dissected shield-shaped cone rising 475 m above the surrounding ice at the margin of the East Antarctic ice sheet. The volcano displays elements of the moberg stratigraphy described from subglacial eruptions in Iceland (Figure A.27.1). The core is a shield-shaped pile of pillow lavas. These are mantled by pillow breccias that grade upward into fine-grained palagonite breccia. The palagonite breccia is massive in its lower portion but becomes bedded higher in the section. The palagonite mantle is a bright yellow in comparison with the black of the pillow basalts, and has been largely stripped off the core, except on the eastern face, where it is preserved to the base of the volcano. Observations from about 200-m distance suggest that the volcano is capped south of the summit by lavas.

Petrologic Characteristics

The magma erupted at Mount Early is a mildly alkaline olivine basalt, with less than 5 wt % normative *ne*.

TABLE A.27.1. Representative Chemical Analyses of a Basalt From Mount Early

	1
SiO_2	50.36
TiO_2	2.25
Al_2O_3	16.68
Fe_2O_3*	10.44
MnO	0.14
MgO	5.56
CaO	8.20
Na_2O	4.40
K_2O	2.03
P_2O_5	0.74
LOI	1.53
Total	100.80

LOI, loss on ignition.
*Total Fe expressed as Fe_2O_3.
1. ANT 34. Mildly alkaline olivine basalt.

Fig. A.27.1. Sketch cross section of Mount Early (made from a photograph). PL, pillow lava; PB, pillow breccia; B, breccia. Numbers indicate sample sites.

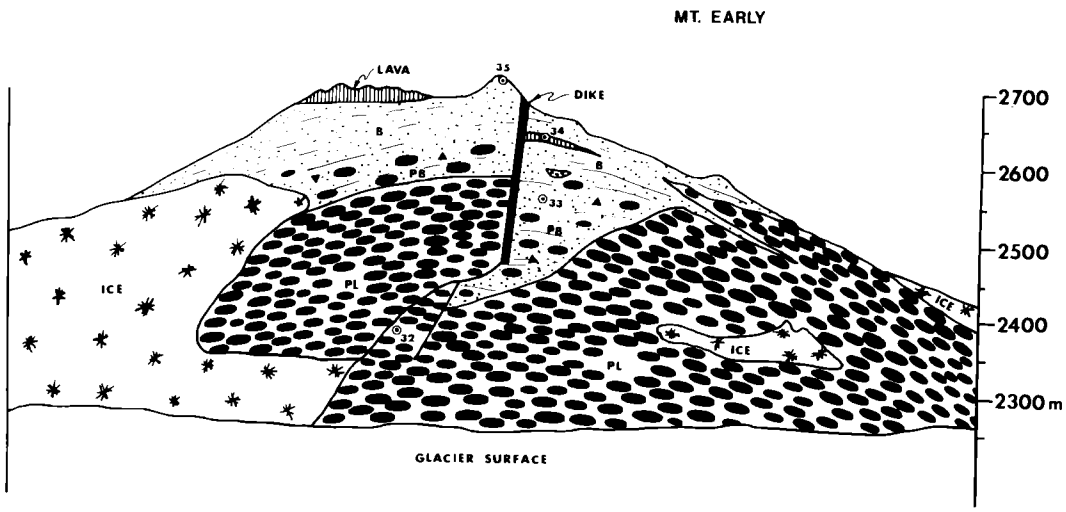

Copyright American Geophysical Union

Phenocrysts of olivine (Fo_{70}–Fo_{85}), purplish-brown clinopyroxene (titanaugite?), and radial clusters of plagioclase form up to 5% of the lava; the groundmass is indeterminate. This magma is similar to the alkaline magma erupted at Sheridan Bluff (Sheridan et al., unpublished data, 1986 (see IVD A.26)). A representative chemical analysis is given in Table A.27.1.

Chronologic Data

An apparent age of 15.86 ± 0.30 Ma has been obtained by conventional K-Ar dating of a whole-rock sample from a lava flow at the core of Mount Early [*Stump et al.*, 1980].

Extent of Knowledge

Mount Early was discovered in December 1934 but was not visited by geologists until 1962–1963 [*Doumani and Minshew*, 1965]. It was reexamined in 1978–1979, when the field party climbed to the summit along the northeastern spine.

Bibliography

Doumani and Minshew, 1965
Stump et al., 1980
Treves, 1965

BIBLIOGRAPHY

Adams, J., Petrology and petrochemistry of an alkaline cone, McMurdo Sound, B.Sc. (Hons.) thesis, Victoria Univ. of Wellington, New Zealand, 1973.

Adams, R.D., and D.A. Christoffel, Total magnetic field surveys between New Zealand and the Ross Sea, *J. Geophys. Res.*, *67*(2), 805-814, 1962.

Adamson, R.G., and R.J. Cavaney, Volcanic debris layers near Mt. Melbourne, northern Victoria Land, Antarctica, *N. Z. J. Geol. Geophys.*, *10*(2), 409-421, 1967.

Angino, E.E., M.D. Turner, and E.J. Zeller, Reconnaissance geology of lower Taylor Valley, Victoria Land, Antarctica, *Geol. Soc. Am. Bull.*, *73*, 1553-1561, 1962.

Armstrong, R.L., K-Ar dating: Late Cenozoic McMurdo Volcanic Group and Dry Valley glacial history, Victoria Land, Antarctica, *N. Z. J. Geol. Geophys.*, *21*(6), 685-698, 1978.

Armstrong, R.L., W. Hamilton, and G.H. Denton, Glaciation in Taylor Valley, Antarctica, older than 2.7 million years, *Science*, *159*, 187-189, 1968.

Barrett, P.J., Oligocene sequence cored at CIROS-1, western McMurdo Sound, *N. Z. Antarct. Rec.*, *7*, 1-7, 1987.

Barrett, P.J., and B.C. McKelvey, Stratigraphy, *Bull. N. Z. Dep. Sci. Ind. Res.*, *237*, 9-51, 1986.

Barrett, P.J., B.C. McKelvey, and B.C. Walker, Sand provenance, *Bull. N. Z. Dep. Sci. Ind. Res.*, *237*, 137-144, 1986.

Barrett, S.I.D., Seismic and video telemetry studies of Mount Erebus, Antarctica, B.Sc. (Hons.) thesis, Victoria Univ. of Wellington, New Zealand, 1987.

Behrendt, J.C., A.K. Cooper, and A. Yuann, Interpretation of marine magnetic gradiometer and multichannel seismic-reflection observations over the western Ross Sea shelf, Antarctica, in *The Antarctic Continental Margin: Geology and Geophysics of the Western Ross Sea, Earth Sci. Ser.*, vol. 5B, edited by A.K. Cooper and F.J. Davey, pp. 155-177, Circum-Pacific Council for Energy and Resources, Houston, Tex., 1987.

Berg, J.H., Geology, petrology, and tectonic implications of crustal xenoliths in Cenozoic volcanic rocks of southern Victoria Land, in *Geological Evolution of Antarctica*, edited by M.R.A. Thomson, J.A. Crame, and J.W. Thomson, Cambridge University Press, New York, in press, 1989.

Berg, J.H., R.J. Moscati, and D.L. Herz, A petrologic geotherm from a continental rift in Antarctica, *Earth Planet. Sci. Lett.*, *93*, 98–108, 1989.

Berkley, J.L., Mars weathering analogs: Secondary mineralization in Antarctic basalts, *Proc. Lunar Planet. Sci.*, *12B*, 1481-1492, 1981.

Berkley, J.L., and M.J. Drake, Weathering on Mars: Antarctic analog studies, *Icarus*, *45*, 231-249, 1981.

Berlin, R., and C.M.B. Henderson, The distribution of Sr and Ba between the alkali feldspar, plagioclase and groundmass phases of porphyritic trachytes and phonolites, *Geochim. Cosmochim. Acta*, *33*, 247-255, 1969.

Blank, H.R., R.A. Cooper, R.H. Wheeler, and I.A.G. Willis, Geology of the Koettlitz-Blue Glacier Region, southern Victoria Land, Antarctica, *Trans. R. Soc. N. Z. Geol.*, *2*(5), 79-99, 1963.

Blick, G.H., P.M. Otway, and B.J. Scott, Volcanic deformation monitoring of Mt. Erebus, Antarctica, *Int. Volc. Congr. N. Z. Abstr.*, 229, 1986.

Copyright American Geophysical Union

Bosum, W., D. Damaske, J.C. Behrendt, and R. Saltus, The aeromagnetic survey of northern Victoria Land and western Ross Sea during GANOVEX IV and a geophysical/geological interpretation, in *Geological Evolution of Antarctica,* edited by M.R.A. Thomson, J.A. Crame, and J.W. Thomson, Cambridge University Press, New York, in press, 1989.

Boudette, E.L., and A.B. Ford, Physical properties of anorthoclase from Antarctica, *Am. Mineral., 51,* 1374-1387, 1966.

Broadie, J.W., A shallow shelf around Franklin Island in the Ross Sea, Antarctica, *N. Z. J. Geol. Geophys., 2,* 108-119, 1959.

Broady, P., D. Given, L. Greenfield, and K. Thompson, The biota and environment of fumaroles on Mt. Melbourne, northern Victoria Land, *Polar Biol., 7,* 97-113, 1987.

Carmichael, I.S.E., Pantelleritic liquids and their phenocrysts, *Min. Mag., 33,* 86-113, 1962.

Carmichael, I.S.E., The crystallization of feldspar in volcanic acid liquids, *Q. J. Geol. Soc. London, 119,* 95-131, 1963.

Carmichael, I.S.E., Natural liquids and the phonolite minimum, *Geol. J., 4,* 55-60, 1964.

Carmichael, I.S.E., The iron-titanium oxides of salic volcanic rocks and their associated ferromagnesian silicates, *Contrib. Mineral Petrol., 14,* 36-64, 1967.

Carmichael, I.S.E., and W.S. MacKenzie, The lattice parameters of high temperature triclinic sodic feldspar, *Min. Mag., 33,* 949-962, 1964.

Chuan, R.L., J. Palais, W.I. Rose, and P.R. Kyle, Fluxes, sizes, morphology and compositions of particles in the Mt. Erebus volcanic plume, December 1983, *J. Atmos. Chem., 4,* 467-477, 1986.

Cole, J.W., and A. Ewart, Contributions to the volcanic geology of the Black Island, Brown Peninsula, and Cape Bird areas, McMurdo Sound, Antarctica, *N. Z. J. Geol. Geophys., 11,* 793-828, 1968.

Cole, J.W., P.R. Kyle, and V.E. Neall, Contributions to the Quaternary geology of Cape Crozier, White Island, and Hut Point Peninsula, McMurdo Sound region, Antarctica, *N. Z. J. Geol. Geophys., 14,* 528-546, 1971.

Coombs, D.S., and J.F.G. Wilkinson, Lineages and fractionation trends in undersaturated volcanic rocks from the East Otago Volcanic Province (New Zealand) and related rocks, *J. Petrol. 10,* 440-501, 1969.

Cooper, A.K., F.J. Davey, and J.C. Behrendt, Seismic stratigraphy and structure of the Victoria Land basin, western Ross Sea, Antarctica, in *The Antarctic Continental Margin: Geology and Geophysics of the Western Ross Sea, Earth Sci. Ser.,* vol. 5B, edited by A.K. Cooper and F.J. Davey, pp. 27-65, Circum-Pacific Council for Energy and Resources, Houston, Tex., 1987.

Cox, A., Paleomagnetic research on volcanic rocks of McMurdo Sound, *Antarct. J. U. S., 1,* 136, 1966.

Crowder, D.F., Geology of a part of North Victoria Land, Antarctica, *U.S. Geol. Surv. Prof. Pap., 600-D,* 95-107, 1968.

Dalrymple, G.B., Critical tables for the conversion of K-Ar ages from old to new constants, *Geology, 7,* 558-560, 1979.

David, T.W.E., and R.E. Priestley, Glaciology, physiography, stratigraphy and tectonic geology of South Victoria Land, *Rep. Br. Antarct. Exped. 1907-09, Geol., 1,* 319 pp., 1914.

David, T.W.E., W.F. Smeeth, and J.W. Schofield, Notes on Antarctic rocks collected by Mr. C.E. Borchgrevinck, *J. Proc. R. Soc. N. S. W.* (for 1895), *29,* 461-492, 1896.

Debenham, F., The physiography of the Ross Archipelago, in *British Antarctic "Terra Nova" Expedition, 1910-1913,* 40 pp., Harrison, London, 1923.

Denton, G.H., and R.L. Armstrong, Glacial geology and chronology of the McMurdo Sound region, *Antarct. J. U.S., 3*(4), 99-101, 1968.

Denton, G.H., and T.J. Hughes (Ed.), *The Last Great Ice Sheets,* John Wiley, New York, 1981.

Denton, G.H., H.W. Borns, Jr., M.G. Grosswald, M. Stuiver, and R.L. Nichols, Glacial history of the Ross Sea, *Antarct. J. U.S., 10*(4), 160-164, 1975.

Dibble, R.R., J. Kienle, P.R. Kyle, and K. Shibuya, Geophysical studies of Erebus volcano, Antarctica, from 1974-1981, *N. Z. J. Geol. Geophys., 27,* 425-455, 1984.

Dibble, R.R., S.I.D. Barrett, K. Kaminuma, S. Miura, J. Kienle, C.A. Rowe, P.R. Kyle, and W.C. McIntosh, Time comparisons between video and seismic signals from explosions in the lava lake of Erebus volcano, *Bull. Disaster Prev. Res. Inst. Kyoto Univ.,* in press, 1989.

Doumani, G.A., and V.H. Minshew, General geology of the Mount Weaver area, Queen Maud Mountains, Antarctica, in *Geology and Paleontology of the Antarctic, Antarct. Res. Ser.,* vol. 6, edited by J.B. Hadley, pp. 127-139, AGU, Washington, D. C., 1965.

Dow, J.A.S., and V.E. Neall, Summary of the geology of the lower Rennick Glacier, in *Antarctic Geology and Geophysics,* edited by R.J. Adie, pp. 339-344, Universitetsforlaget, Oslo, 1972.

Dow, J.A.S., and V.E. Neall, Geology of the lower Rennick Glacier, northern Victoria Land, Antarctica, *N. Z. J. Geol. Geophys., 17,* 659-714, 1974.

Eggers, A.J., Scallop Hill Formation, Brown Peninsula, McMurdo Sound, Antarctica, *N. Z. J. Geol. Geophys., 22*(3), 353-361, 1979.

Elston, D.P., and S.L. Bressler, Magnetic stratigraphy of DVDP drill cores and late Cenozoic history of Taylor Valley, Transantarctic Mountains, Antarctica, in *Dry Valley Drilling Project, Antarct. Res. Ser.,* vol. 33, edited by L.D. McGinnis, pp. 413-425, AGU, Washington, D. C., 1981.

Ervin, C.P., and M.G. Wolf, Ground magnetic studies of volcanic rocks in the Taylor and Wright Valley regions, *Antarct. J. U.S., 12*(4), 105, 1977.

Ferrar, H.T., Report on the field geology of the region explored during the Discovery Antarctic Expedition 1901-4, *Natl. Antarct Exped. 1901-1904, Nat. Hist., 1, Geol.,* 1-100, 1907.

Fitzgerald, P.G., M. Sandiford, P.J. Barrett, and A.J.W. Gleadow, Asymmetric extension associated with uplift

Copyright American Geophysical Union

and subsidence in the Transantarctic Mountains and Ross Embayment, *Earth Planet. Sci. Lett., 81,* 67-78, 1986.

Fleck, R.J., L.M. Jones, and R.E. Behling, K-Ar dates of the McMurdo volcanics and their relation to the glacial history of Wright Valley, *Antarct. J. U.S., 7,* 244-246, 1972.

Forbes, R.B., D.L. Turner, and J.R. Carden, Age of trachyte from Ross Island, Antarctica, *Geology, 2,* 297-298, 1974.

Funaki, M., Paleomagnetism of Hut Point Peninsula volcanic sequence, *Mem. Natl. Inst. Polar Res. Spec. Issue Jpn., 14,* 186-193, 1979.

Funaki, M., Paleomagnetic investigation of McMurdo Volcanics, Antarctica, *Antarct. Rec., 77,* 1-19, 1983.

Funaki, M., Paleomagnetic investigation of McMurdo Sound region, southern Victoria Land, Antarctica, *Mem. Natl. Inst. Polar Res., Ser. C,* no. 16, 81 pp., 1984.

Gair, H.S., The geology from the upper Rennick Glacier to the coast, northern Victoria Land, Antarctica, *N. Z. J. Geol. Geophys., 10,* 309-344, 1967.

Gair, H.S., A. Sturm, S.J. Carryer, and G.W. Grindley, The geology of northern Victoria Land (sheet 13, northern Victoria Land), in *Geologic Maps of Antarctica, Antarct. Map Folio Ser.,* folio 12, plate XII, edited by V.C. Bushnell and C. Craddock, American Geographical Society, New York, 1969.

Gamble, J.A., and P.R. Kyle, The origins of glass and amphibole in spinel-wehrlite xenoliths from Foster Crater, McMurdo Volcanic Group, Antarctica, *J. Petrol., 28*(5), 755-780, 1987.

Gamble, J.A., P.J. Barrett, and C.J. Adams, Basaltic clasts from Unit 8, *Bull. N. Z. Dep. Sci. Ind. Res., 237,* 145-152, 1986.

Gamble, J.A., F. McGibbon, P.R. Kyle, M.A. Menzies, and I. Kirsch, Metasomatized xenoliths from Foster Crater, Antarctica: Implications for lithospheric structure and processes beneath the Transantarctic Mountain front, *J. Petrol. Spec. Lithosphere Issue,* 109-138, 1988.

Gleadow, A.J.W., and P.G. Fitzgerald, Uplift history and structure of the Transantarctic Mountains: New evidence from fission track dating of basement apatites in the Dry Valley area, southern Victoria Land, *Earth Planet. Sci. Lett., 82,* 1-14, 1987.

Goldich, S.S., S.B. Treves, N.H. Suhr, and J.S. Stuckless, Geochemistry of the Cenozoic volcanic rocks of Ross Island and vicinity, Antarctica, *J. Geol., 83,* 415-435, 1975.

Goldich, S.S., J.S. Stuckless, N.H. Suhr, J.B. Bodkin, and R.C. Wamser, Some trace element relationships in the Cenozoic volcanic rocks from Ross Island and vicinity, Antarctica, in *Dry Valley Drilling Project, Antarct. Res. Ser.,* vol. 33, edited by L.D. McGinnis, pp. 215-228, AGU, Washington, D. C., 1981.

Hamilton, W., Geology of northeastern Victoria Land, *Antarct. Proj. Off. U.S. Navy Bull., 6,* 68-69, 1965.

Hamilton, W., Tectonics of Antarctica, *Tectonophysics, 4,* 555-568, 1967*a*.

Hamilton, W., The Hallett Volcanic Province, *Antarct. J. U.S., 2,* 177-178, 1967*b*.

Hamilton, W., The Hallett Volcanic Province, Antarctica, *U.S. Geol. Surv. Prof. Pap., 456C,* 62 pp., 1972.

Harrington, H.J., Nomenclature of rock units in the Ross Sea region, Antarctica, *Nature, 182*(4631), 290-291, 1958.

Harrington, H.J., Narrative of a visit to the newly-discovered Emperor Penguin rookery at Coulman Island, Ross Sea, Antarctica, *Notornis, 8*(5), 127-132, 1959.

Harrington, H.J., B.L. Wood, I.C. McKellar, and G.J. Lensen, Topography and geology of the Cape Hallett District, Victoria Land, Antarctica, *N. Z. Geol. Surv. Bull.* (new ser.), *80,* 100 pp., 1967.

Harwood, D.M., Diatoms, *Bull. N Z. Dep. Sci. Ind. Res., 237,* 69-107, 1986.

Haskell, T.R., J.P. Kennett, W.M. Prebble, G. Smith, and I.A.G. Willis, The geology of the middle and lower Taylor Valley of South Victoria Land, Antarctica, *Trans. R. Soc. N. Z. Geol., 2,* 169-186, 1965.

Holdsworth, G., and F.C. Ugolini, Fumarolic ice towers on Mount Erebus, Ross Island, Antarctic, *J. Glaciol., 5,* 878-879, 1965.

Irving, A.J., and F.A. Frey, Trace element abundances in megacrysts and their host basalts: Constraints on partition coefficients and megacryst genesis, *Geochim. Cosmochim. Acta, 48,* 1201-1221, 1984.

Jensen, H.I., Report on the petrology of the alkaline rocks of Mt. Erebus, Antarctica, *Rep. Br. Antarct. Exped. 1907-1909, Geol., 2,* 93-128, 1916.

Johnston, A.C., Suppression of earthquakes by large continental ice sheets, *Nature, 330,* 467-469, 1987.

Jones, J.G., Intraglacial volcanoes of the Laugarvatn region, south-west Iceland-I, *Q. J. Geol. Soc. London, 124,* 197-211, 1969.

Jones, L.M., and R.L. Walker, Geochemistry of the McMurdo Volcanics, Victoria Land, 1, Strontium isotope composition, *Antarct. J. U.S., 7,* 142-144, 1972.

Jones, L.M., J.A. Whitney, and J.C. Stormer, A volcanic ash deposit, Wright Valley, *Antarct. J. U.S., 8,* 270-272, 1973.

Jones, L.M., G. Faure, K.S. Taylor, and C.E. Corbato, The origin of salts on Mount Erebus and along the coast of Ross Island, Antarctica, *Isot. Geosci., 1,* 57-64, 1983.

Jordan, H., Tectonic observations in the Hallett Volcanic Province, Antarctica, *Geol. Jahrb., Reihe B, 41,* 111-125, 1981.

Kalamarides, R.I., and J.H. Berg, Geochemistry and tectonic implications of lower-crustal granulites included in Cenozoic volcanic rocks of southern Victoria Land, in *Geological Evolution of Antarctica,* edited by M.R.A. Thomson, J.A. Crame, and J.W. Thomson, Cambridge University Press, New York, in press, 1989.

Kalamarides, R.I., J.H. Berg, and R.A. Hank, Lateral isotopic discontinuity in the Lower Crust: An example from Antarctica, *Science, 237,* 1192-1195, 1987.

Keys, J.R., P.W. Anderton, and P.R. Kyle, Tephra and debris layers in the Skelton Névé and Kempe Glacier,

Copyright American Geophysical Union

south Victoria Land, Antarctica, *N. Z. J. Geol. Geophys.*, *20*(5), 971-1002, 1977.

Keys, J.R., W.C. McIntosh, and P.R. Kyle, Volcanic activity of Mount Melbourne, northern Victoria Land, *Antarct. J. U.S.*, *18*(5), 10-11, 1983.

Kienle, J., K. Kaminuma, and R.R. Dibble, Seismicity of Mount Erebus and vicinity, 1983-1984, *Antarct. J. U.S.*, *19*(5), 25-27, 1984.

Kienle, J., C. Rowe, and R. Dibble, Seismicity of Mount Erebus, Antarctica: 1980-1985, *Int. Volc. Congr. N. Z. Abstr.*, 248, 1986.

Kirsch, I.D., Evidence for mantle metasomatism in ultramafic inclusions from Foster Crater, Antarctica, M.S. thesis, Ohio State Univ., Columbus, 1981.

Kreuzer, H., A. Hohndorf, H. Lenz, U. Vetter, F. Tessensohn, B. Muller, H. Jordan, W. Harre, and C. Besang, K/Ar and Rb/Sr dating of igneous rocks from North Victoria Land, Antarctica, *Geol. Jarhb., Reihe B, 41,* 267-273, 1981.

Kurasawa, H., Strontium isotope studies of the Ross Island volcanics, Antarctica, *Mem. Natl. Inst. Polar Res. Spec. Issue Jpn., 4,* 67-73, 1975.

Kurasawa, H., Volcanism and volcanic rocks in Antarctica (in Japanese with English abstract), *Antarct. Rec., 58,* 204-234, 1977.

Kurasawa, H., Geochemistry of Ferrar dolerite dikes and Cenozoic volcanics of the Dry Valley region, *Dry Val. Drilling Proj. Bull., 8,* p. 34-38, 1978.

Kyle, P.R., The geology and geochemistry of Cape Crozier, Ross Island, Antarctica, B.Sc. (Hons.) thesis, Victoria Univ. of Wellington, New Zealand, 1971.

Kyle, P.R., Geology mineralogy, and geochemistry of the Late Cenozoic McMurdo Volcanic Group, Victoria Land, Antarctica, Ph.D. thesis, Victoria Univ. of Wellington, New Zealand, 1976.

Kyle, P.R., Mineralogy and glass chemistry of recent volcanic ejecta from Mt. Erebus, Ross Island, Antarctica, *N. Z. J. Geol. Geophys., 20,* 1123-1146, 1977.

Kyle, P.R., Geologic history of Hut Point Peninsula as inferred from DVDP 1, 2, and 3 drillcores and surface mapping, in *Dry Valley Drilling Project, Antarct. Res. Ser.*, vol. 33, edited by L.D. McGinnis, pp. 427-445, AGU, Washington, D. C., 1981*a*.

Kyle, P.R., Mineralogy and geochemistry of a basanite to phonolite sequence at Hut Point Peninsula, Antarctica, based on core from Dry Valley Drilling Project Drillholes 1, 2 and 3, *J. Petrol., 22,* 451-500, 1981*b*.

Kyle, P.R., Glacial history of the McMurdo Sound area as indicated by the distribution and nature of McMurdo Volcanic Group rocks, in *Dry Valley Drilling Project, Antarct. Res. Ser.*,vol. 33, edited by L.D. McGinnis, pp. 403-412, AGU, Washington, D. C., 1981*c*.

Kyle, P.R., Volcanic geology of The Pleiades, northern Victoria Land, Antarctica, in *Antarctic Geoscience,* edited by C. Craddock, pp. 747-754, University of Wisconsin Press, Madison, 1982.

Kyle, P.R., Volcanic activity of Mt. Erebus, Antarctica: 1972-1984, *Int. Volc. Congr. N. Z., Abstr.*, 250, 1986*a*.

Kyle, P.R., Mineral chemistry of late Cenozoic McMurdo Volcanic Group rocks from The Pleiades, northern Victoria Land, in *Geological Investigations in Northern Victoria Land, Antarct. Res. Ser.*, vol. 46, edited by E. Stump, pp. 305-337, AGU, Washington, D. C., 1986*b*.

Kyle, P.R., and J.W. Cole, Structural control of volcanism in the McMurdo Volcanic Group, Antarctica, *Bull. Volcanol., 38,* 16-25, 1974.

Kyle, P.R., and R. Price, Occurrences of rhonite in the McMurdo Volcanic Group, Antarctica and Otago Volcano, New Zealand, *Am. Mineral., 60,* 722-725, 1975.

Kyle, P.R., and P.C. Rankin, REE geochemistry of late Cenozoic alkaline lavas of the McMurdo Volcanic Group, Antarctica, *Geochim. Cosmochim. Acta, 40,* 1497-1507, 1976.

Kyle, P.R., and S.B. Treves, Geology of DVDP 3, Hut Point Peninsula, Ross Island, Antarctica, *Dry Vall. Drilling Proj. Bull., 3,* 13-48, 1974.

Kyle, P.R., J. Adams, and P.C. Rankin, Geology and petrology of the McMurdo Volcanic Group at Rainbow Ridge, Brown Peninsula, Antarctica, *Geol. Soc. Am. Bull., 90,* 676-688, 1979.

Kyle, P.R., D.H. Elliot, and J.F. Sutter, Jurassic Ferrar Supergroup tholeiites from the Transantarctic Mountains, Antarctica and their relationship to the initial fragmentation of Gondwanaland, in *Gondwana Five,* edited by M.M. Cresswell and P. Vella, pp. 283-287, A.A. Balkema, Rotterdam, 1981.

Kyle, P.R., R.R. Dibble, W.F. Giggenbach, and J. Keys, Volcanic activity associated with the anorthoclase phonolite lava lake, Mount Erebus, Antarctica, in *Antarctic Geoscience,* edited by C. Craddock, pp. 735-745, University of Wisconsin Press, Madison, 1982.

Kyle, P.R., A.C. Wright, and I. Kirsch, Ultramafic xenoliths in the late Cenozoic, McMurdo Volcanic Group, Western Ross Sea embayment, Antarctica, in *Mantle Xenoliths,* eidted by P. Nixon, pp. 287-293, John Wiley, New York, 1987.

Kyle, P.R., J.A. Moore, and M.F. Thirlwall, Petrologic evolution of anorthoclase phonolite lavas at Mount Erebus, Ross Island, Antarctica, *J. Petrol.*, in press, 1989.

Le Bas, M.J., R.W. Le Maitre, A. Streckeisen, and B. Zanettin, A chemical classification of volcanic rocks based on the total alkali-silica diagram, *J. Petrol., 27,* 745-750, 1986.

LeCouteur, P.C., and E.C. Leitch, Preliminary report on the geology of an area southwest of the upper Tucker Glacier, northern Victoria Land, in *Antarctic Geology,* edited by R.J. Adie, pp. 229-236, North-Holland, Amsterdam, 1964.

LeMasurier, W.E., W.C. McIntosh, P.J. Ellerman, and A.C. Wright, USCGS *Glacier* cruise 1, December 1982-January 1983: Reconnaissance of hyaloclastites in the western Ross Sea region, *Antarct. J. U.S.*, *18*(5), 60-61, 1983.

Linkletter, G.O., Weathering and soil formation in the dry

Copyright American Geophysical Union

valleys of Southern Victoria Land, *Antarct. J. U.S.*, *6*(5), 214, 1971.

Luckman, P.C., Products of submarine volcanism in the McMurdo Sound region, Ross Island, Antarctica, B.Sc. thesis, Victoria Univ. of Wellington, New Zealand, 1974.

Lyon, G.L., Stable isotope stratigraphy of ice cores and the age of the last eruption at Mount Melbourne, Antarctica, *N. Z. J. Geol. Geophys.*, *29*(1), 135–138, 1986.

Lyon, G.L., and W.F. Giggenbach, Geothermal activity in Victoria Land, Antarctica, *N. Z. J. Geol. Geophys.*, *17*(3), 511-521, 1974.

Mankinen, E.A., and A. Cox, Paleomagnetic investigation of some volcanic rocks from the McMurdo volcanic province, Antarctica, *J. Geophys. Res.*, *93*, 11,599–11,612, 1988.

Mason, R.A., J.V. Smith, J.B. Dawson, and S.B. Treves, A reconnaissance of trace elements in anorthoclase megacrysts, *Min. Mag.*, *46*, 7-11, 1982.

McCraw, J.D., Volcanic detritus in Taylor Valley, Victoria Land, Antarctica, *N. Z. J. Geol. Geophys.*, *5*(5), 740-745, 1962.

McDougall, I., and A.-U. Rahman, Age of the Gauss-Matayama boundary and of the Kaena and Mammoth events, *Earth Planet. Sci. Lett.*, *14*, 367-380, 1972.

McGibbon, F.M., Geochemistry and petrology of ultramafic xenoliths of the Erebus volcanic province, in *Geological Evolution of Antarctica*, edited by M.R.A. Thomson, J.A. Crame, and J.W. Thomson, Cambridge University Press, New York, in press, 1989.

McGinnis, L.D., D.D. Wilson, W.J. Burdelik, and T.H. Larsen, Crust and upper mantle study of McMurdo Sound, in *Antarctic Earth Science*, edited by R.L. Oliver, P.R. James, and J.B. Jago, pp. 204-208, Cambridge University Press, New York, 1983.

McGinnis, L.D., R.H. Bowen, J.M. Erickson, B.J. Allred, and J.L. Kreamer, East-west Antarctic boundary in McMurdo Sound, *Tectonophysics*, *114*, 341-356, 1985.

McIntosh, W.C., and J.A. Gamble, A subaerial eruptive environment for the Hallett Coast volcanoes, in *Geological Evolution of Antarctica*, edited by M.R.A. Thomson, J.A. Crame, and J.W. Thomson, Cambridge University Press, New York, in press, 1989.

McIver, J.R., and T.W. Gevers, Volcanic vents below the Royal Society Range, Central Victoria Land, Antarctica, *Trans. R. Soc. S. Afr.*, *73*, 65-88, 1970.

McMahon, B.E., and H. Spall, Results of paleomagnetic investigation of selected cores recovered by Dry Valley Drilling Project (abstract), *Dry Vall. Drilling Proj. Bull.*, *4*, 37-38, 1974*a*.

McMahon, B.E., and H. Spall, Paleomagnetic data from unit 13, DVDP hole 2, Ross Island, *Antarct. J. U.S.*, *9*(5), 229-232, 1974*b*.

McSaveney, M.J., New data for a Cenozoic history of Wright Valley, Southern Victoria Land, *Antarct. J. U.S.*, *8*, 266-268, 1973.

Moore, J.A., Mineralogy, geochemistry and petrogenesis of the lavas of Mount Erebus, Antarctica, M.S. thesis, Geosci. Dep., N. Mex. Inst. of Mining and Technol., Socorro, 1986.

Moore, J.A., and P.R. Kyle, Evolution of anorthoclase phonolite, Mount Erebus, Antarctica, *Geol. Soc. Am. Abstr. Programs*, *17*, 668, 1985.

Moore, J.A., and P.R. Kyle, Mantle upwelling and evolution of phonolitic magmas at Ross Island, Antarctica, *Int. Volc. Congr. N. Z. Abstr.*, 188, 1986.

Moore, J.A., and P.R. Kyle, Volcanic geology of Mount Erebus, Ross Island, Antarctica, *Proc. Natl. Inst. Polar Res. Symp. Antarct. Geosci.*, *1*, 48–65, 1987.

Mortimer, G., M. Schmidt-Thomé, and F. Tessensohn, Stratigraphic problems in the upper part of the Bowers Supergroup, north Victoria Land, Antarctica, *Geol. Jahrb., Reihe B*, *60*, 83-103, 1984.

Mountain, E.D., Potash-oligoclase from Mount Erebus, Antarctica and anorthoclase from Mount Kenya, East Africa, *Min. Mag.*, *20*(109), 331-345, 1925.

Mueller, P., Zur Klassifikation der Massengesteine, *Geol. Jahrb., Reihe D*, *9*, 3-19, 1974.

Mueller, P., M. Schmidt-Thomé, H. Kreuzer, and G. Mortimer, Peralkaline magmatism of the Malta Plateau, north Victoria Land, and its geological setting, *Geol. Jahrb., Reihe E*, *38*, in press, 1989.

Muncy, H.L., Geologic history and petrogenesis of alkaline volcanic rocks, Mount Morning, Antarctica, M.S. thesis, Ohio State Univ., Columbus, 1979.

Nagata, T., Geophysical studies of Mt. Erebus, *Antarct. J. U.S.*, *19*(5), 22-24, 1984.

Nathan, S., and F.J. Schulte, Recent thermal and volcanic activity on Mount Melbourne, Northern Victoria Land, Antarctica, *N. Z. J. Geol. Geophys.*, *10*, 422-430, 1967.

Nathan, S., and F.J. Schulte, Geology and petrology of the Campbell-Aviator divide, Northern Victoria Land, Antarctica, 1, Post Paleozoic rocks, *N. Z. J. Geol. Geophys.*, *11*(4), 940-975, 1968.

Noll, M., Geochemistry and petrogenesis of the alkaline lavas and their associated xenoliths, Mount Overlord, Northern Victoria Land, Antarctica, M.S. thesis, N. Mex. Inst. of Mining and Technol., Socorro, 1985.

Pederson, D.R., G.E. Montgomery, L.D. McGinnis, C.P. Ervin, and H.K. Wong, Aeromagnetic survey of Ross Island, McMurdo Sound, and the Dry Valleys, in *Dry Valley Drilling Project, Antarct. Res. Ser.*, vol. 33, edited by L.D. McGinnis, pp. 7-25, AGU, Washington, D. C., 1981.

Polyakov, M.M., A. Krylov, and T.I. Mazina, New data on radiogeochronology of Antarctic Cenozoic vulcanites 160 E-100 W (in Russian), *Inform. Byull. Sov. Antarkt. Eksped.*, *93*, 19-26, 1976.

Porter, S.C., and J.E. Beget, Provenance and depositional environments of late Cenozoic sediments in permafrost cores from lower Taylor Valley, Antarctica, in *Dry Valley Drilling Project, Antarct. Res. Ser.*, vol. 33, edited by L.D. McGinnis, pp. 351-363, AGU, Washington, D. C., 1981.

Priestley, R.E., *Antarctic Adventure, Scott's Northern Party*, 382 pp., T. Fisher, Unwin, London, 1914.

Copyright American Geophysical Union

Priestley, R.E., Physiography (Robertson Bay and Terra Nova Regions), in *British Antarctic "Terra Nova" Expedition, 1910-1913,* 87 pp., Harrison, London, 1923.

Prior, G.T., Petrographical notes on the rock specimens collected in Antarctic regions during the voyage of H.M.S. *Erebus* and *Terror* under Sir James Clark Ross in 1839-43, *Min. Mag., 12,* 69-91, 1899.

Prior, G.T., Report on the rock specimens collected by the *Southern Cross* Antarctic Expedition, in *Report on the Collections of Natural History Made in the Antarctic Regions During the Voyage of the "Southern Cross,"* edited by R.B. Sharpe, pp. 321-332, British Museum, London, 1902.

Prior, G.T., Report on the rock specimens collected during the *Discovery* Antarctic Expedition 1901-1904, *Natl. Antarct. Exped. 1901-1904, Nat. Hist., 1, Geol.,* 101-140, 1907.

Rastall, R.H., and R.E. Priestley, The slate-greywacke formation of Robertson Bay, *Antarct. Terra Nova Exped. 1910, Nat. Hist. Rep. Geol., 1,* 121-129, 1921.

Riddolls, B.W., and G.T. Hancox, The geology of the upper Mariner Glacier region, North Victoria Land, Antarctica, *N. Z. J. Geol. Geophys., 11*(4), 881-899, 1968.

Rose, W.I., R.L. Chuan, and P.R. Kyle, Rate of sulfur dioxide emission from Erebus volcano, Antarctica, December, 1983, *Nature, 316,* 710-712, 1985.

Ross, J.C., *A Voyage of Discovery and Research in the Southern and Antarctic Regions, During the Years 1839-43,* 2 vols., Murray, London, 1847.

Skinner, D.N.B., B.C. Waterhouse, G.M. Brehaut, and K. Sullivan, New Zealand Geological Survey Antarctic Expedition 1975-76, Skelton-Koettlitz glaciers, Rep. *DS58,* Dep. of Sci. Ind. Res., N. Z. Geol. Surv., Wellington, 1976.

Smith, W.C., The volcanic rocks of the Ross Archipelago, *Nat. Hist. Rep. Br. Antarct. Terra Nova Exped. 1910, Geol., 2,* 1-107, 1954.

Smith, W.C., The volcanic rocks of Cape Adare, South Victoria Land, *Nat. Hist. Rep. Br. Antarct. Terra Nova Exped. 1910, Geol., 2,* 109-150, 1959.

Smith, W.C., Volcanic rocks of Cape Adare and erratics from Terra Nova Bay region, *Nat. Hist. Rep. Br. Antarct. Terra Nova Exped. 1910, Geol., 2,* 151-206, 1964.

Steiger, R. H., and E. Jäger, Subcommission on geochemistry: Convention on the use of decay constants in geo- and cosmochemistry, *Earth Planet. Sci. Lett., 36,* 359-362, 1977.

Stuckless, J.S., and R.L. Ericksen, Strontium isotope geochemistry of the volcanic rocks and associated megacrysts and inclusions from Ross Island and vicinity, Antarctica, *Contrib. Mineral. Petrol., 58,* 111-126, 1976.

Stuckless, J.S., A.T. Miesch, S.S. Goldich, and P.W. Weiblen, A *Q*-mode factor for the petrogenesis of the volcanic rocks from Ross Island and vicinity, Antarctica, in *Dry Valley Drilling Project, Antarct. Res. Ser.,* vol. 33, edited by L.D. McGinnis, pp. 257-280, AGU, Washington, D. C., 1981.

Stuiver, M., and T.F. Braziunas, Compilation of isotopic dates from Antarctica, *Radiocarbon, 27*(2A), 117-304, 1985.

Stuiver, M., G.H. Denton, T.J. Hughes, and J.L. Fastook, History of the marine ice sheet in West Antarctica during the last glaciation: A working hypothesis, in *The Last Great Ice Sheets,* edited by G.H. Denton and T.J. Hughes, pp. 319-436, John Wiley, New York, 1981.

Stump, E., M.F. Sheridan, S.G. Borg, and J.F. Sutter, Early Miocene subglacial basalts, the East Antarctic ice sheet and uplift of the Transantarctic Mountains, *Science, 207,* 757-759, 1980.

Stump, E., J.R. Holloway, S.G. Borg, and R.L. Armstrong, Discovery of a Tertiary granite pluton, northern Victoria Land, *Antarct. J. U.S., 18*(5), 17-18, 1983.

Sturm, A., and S.J. Carryer, Geology of the region between the Matusevich and Tucker glaciers, northern Victoria Land, Antarctica, *N. Z. J. Geol. Geophys., 13*(2), 408-435, 1968.

Sun, S.S., and G.N. Hanson, Origin of Ross Island basanitoids and limitations upon the heterogeneity of mantle sources for alkali basalts and nephelinites, *Contrib. Mineral. Petrol., 52,* 77-106, 1975.

Sun, S.S., and G.N. Hanson, Rare earth evidence of differentiation of McMurdo Volcanics, Ross Island, Antarctica, *Contrib. Mineral. Petrol., 54,* 139-155, 1976.

Tazieff, H., About Antarctic hyaloclastites, *Bull. Volcanol., 41,* 1-2, 1978.

Tessensohn, F., and G. Wörner, The Ross Sea rift system (Antarctica)—Structure, evolution and analogues, in *Geological Evolution of Antarctica,* edited by M.R.A. Thomson, J.A. Crame, and J.W. Thomson, Cambridge University Press, New York, in press, 1989.

Thornton, C.P., and O.F. Tuttle, Chemistry of igneous rocks, I, Differentiation index, *Am. J. Sci., 258,* 664-684, 1960.

Treves, S.B., The geology of Cape Evans and Cape Royds, Ross Island, Antarctica, in *Antarctic Research, Geophys. Monogr. Ser.,* vol. 7, edited by H. Wexler et al., pp. 40-46, AGU, Washington, D. C., 1962.

Treves, S.B., Igneous and metamorphic rocks of the Ohio Range Horlick Mountains, Antarctica, in *Geology and Paleontology of the Antarctic, Antarct. Res. Ser.,* vol. 6, edited by J.B. Hadley, pp. 117-125, AGU, Washington, D. C. 1965.

Treves, S.B., Volcanic rocks from the Ross Island, Marguerite Bay, and Mount Weaver areas, Antarctica, Proceedings of the Symposium on Pacific-Antarctic Sciences, Tokyo, 1966, *JARE Sci. Rep., Special Issue 1,* 136-149, Inst. of Polar Res., Tokyo, 1967.

Treves, S.B., Volcanic rocks of the Ross Island area, *Antarct. J. U.S., 3*(4), 108, 1968.

Treves, S.B., Volcanic rocks of the Ross Island area, *Antarct. J. U.S., 5*(4), 103, 1970.

Copyright American Geophysical Union

Treves, S.B., and P.R. Kyle, Review of the geology of Hut Point Peninsula, Ross Island, Antarctica, *Dry Vall. Drilling Proj. Bull.*, *2*, 1-10, 1973.

Turnbull, G., Some paleomagnetic measurements in Antarctica, *Arctic*, *12*, 151-157, 1959.

Ugolini, F.C., Soils of Mount Erebus, Antarctica, *N. Z. J. Geol. Geophys.*, *10*, 431-442, 1967.

Vella, P., Surficial geological sequence, Black Island and Brown Peninsula, McMurdo Sound, Antarctica, *N. Z. J. Geol. Geophys.*, *12*, 761-770, 1969.

Warren, G., Geology of the Terra Nova Bay - McMurdo Sound area, Victoria Land (sheet 14, Terra Nova Bay - McMurdo Sound area), in *Geologic Maps of Antarctica, Antarct. Map Folio Ser.*, folio 12, plate XIII, edited by V.C. Bushnell and C. Craddock, American Geographical Society, New York, 1969.

Waterhouse, B.C., Western Ross Sea - Balleny Islands Expedition: January-March, 1965, Report, Dep. of Sci. Ind. Res., N Z. Geol. Surv., Wellington, 1965.

Weiblen, P.W., W.C. Hunter, J.S. Stuckless, K.J. Schulz, and M.G. Mudrey, Jr., Correlation of clinopyroxene compositions with environment of formation based on data from Ross Island volcanics, Antarctica, in *Dry Valley Drilling Project, Antarct. Res. Ser.*, vol. 33, edited by L.D. McGinnis, pp. 229-246, AGU, Washington, D. C., 1981.

Wilson, A.T., G.H. Hendy, and A.M. Taylor, Peridot on Ross Island, Antarctica, *Aust. Gemmol.*, 124-125, 1974.

Wilson, E.A., *Album (of) Panoramas, National Antarctic Expedition 1901-4*, Royal Society of London, London 1908.

Wörner, G., and L. Viereck, Subglacial to emergent volcanism at Shield Nunatak, Mt. Melbourne Volcanic Field, Antarctica, *Polarforschung*, *57*(1,2), 27-41, 1987.

Wörner, G., and L. Viereck, The Mt. Melbourne volcanic field (Victoria Land, Antarctica), I, Field observations, *Geol. Jahrb.*, in press, 1989.

Wörner, G., H. Niephaus, J. Hertogen, and L. Viereck, The Mt. Melbourne volcanic field (Victoria Land, Antarctica), II, Geochemistry and magmagenesis, *Geol. Jahrb.*, in press, 1989.

Wright, A.C., A reconnaissance study of the McMurdo Volcanics northwest of Koettlitz Glacier, *N. Z. Antarct. Rec.*, *1*(2), 10-15, 1978.

Wright, A.C., McMurdo Volcanics at Foster Crater, Southern Foothills of the Royal Society Range, Central Victoria Land, Antarctica, internal report, 19 pp., N. Z. Geol. Surv., Otara, 1979*a*.

Wright, A.C., McMurdo Volcanics northwest of Koettlitz Glacier, Antarctica, internal report, 41 pp., N. Z. Geol. Surv., Otara, 1979*b*.

Wright, A.C., McMurdo Volcanics on Chancellor Ridge, Southern Foothills of the Royal Society Range, Central Victoria Land, Antarctica, internal report, 22 pp., N. Z. Geol. Surv., Otara, 1979*c*.

Wright, A.C., Landforms of McMurdo Volcanic Group, Southern Foothills of the Royal Society Range, Antarctica, *N. Z. J. Geol. Geophys.*, *23*, 605-613, 1980.

Wright, A.C., W.C. McIntosh, and P. Ellerman, Volcanic geology of Turks Head, Tryggve Point, and Minna Bluff, southern Victoria Land, *Antarct. J. U.S.*, *18*, 35-36, 1983.

Wright, A.C., P.R. Kyle, W.C. McIntosh, and I.Klich, Geological field investigations of volcanic rocks at Mount Discovery and Mason Spur, McMurdo Sound, *Antarct. J. U.S.*, *19*(5), 20-21, 1984.

Wright, A.C., P.R. Kyle, J.A. Moore, and K. Meeker, Geological investigations of volcanic rocks at Mount Discovery, Mount Morning and Mason Spur, McMurdo Sound, *Antarct. J. U.S.*, *21*, 1986.

Wright-Grassham, A.C., Volcanic geology, mineralogy and petrogenesis of the Discovery volcanic subprovince, southern Victoria Land, Antarctica, Ph.D. dissertation, N. Mex. Instit. of Mining and Technol., Socorro, 1987.

Yagi, K., Y. Hariya, and K. Onuma, Stability relation of kaersutite, *J. Fac. Sci. Hokkaido Univ., Ser. IV*, *16*, 331-342, 1975.

Copyright American Geophysical Union

Copyright American Geophysical Union

Summary

W.E. LeMasurier

Frontispiece. Mount Sidley, a Pliocene phonolitic shield volcano, the highest (4181 m) volcano in Antarctica. The back wall of the caldera seen here is about 1200 m high; the caldera floor is about 5 km in diameter.

Introduction

The volcanoes of Marie Byrd Land form a coherent province, distinctively marked by its petrologic characteristics and its spatial and chronologic patterns of volcanic evolution. It lies along a 900-km segment of the Pacific coast of Antarctica (Figure B.I) and is comparable in size to the Cascade volcanic chain of North America. The province is highly alkaline, bimodal, sodic, and dominated by basaltic rocks but includes a broad spectrum of felsic differentiates. The term felsic is used in a general sense in this section to include all trachytes, phonolites, rhyolites, pantellerites, and comendites. There are 18 large central volcanoes and more than 30 small satellitic volcanic centers in the Marie Byrd Land Province. For descriptive purposes, these are grouped into the 16 individual volcano descriptions (IVD's) that follow. Figure B.II is an index map showing the location and map coverage of each IVD; numbers refer to the sequence in which they are presented. At least two of the major volcanoes are probably active, and three are regarded as possibly active, but no eruption has been directly observed.

The continental ice sheet and the polar climate have had significant effects on the nature of rock exposures in this region. The surface of the ice sheet is near sea level on the coast but rises inland to an elevation of about 2000 m. Therefore the bases of volcanic sections are exposed mainly near the coast, and only the upper portions of the inland volcanoes are exposed. Mount Cumming and Mount Hartigan (Figures B.7.1 and B.8.1), for example, appear to be insignificant, but they are about the same elevation as Mount Murphy (Figure B.1.1). Most volcanoes, even those of Miocene age, are morphologically well preserved and the rocks exceptionally fresh, because the ice sheet is not an effective agent of erosion and rates of weathering are slow. However, the lack of erosional dissection conceals the internal structure of most volcanoes and limits the opportunities for stratigraphic sampling.

Marie Byrd Land is among the least accessible and least frequently visited regions in Antarctica, and none

Copyright American Geophysical Union

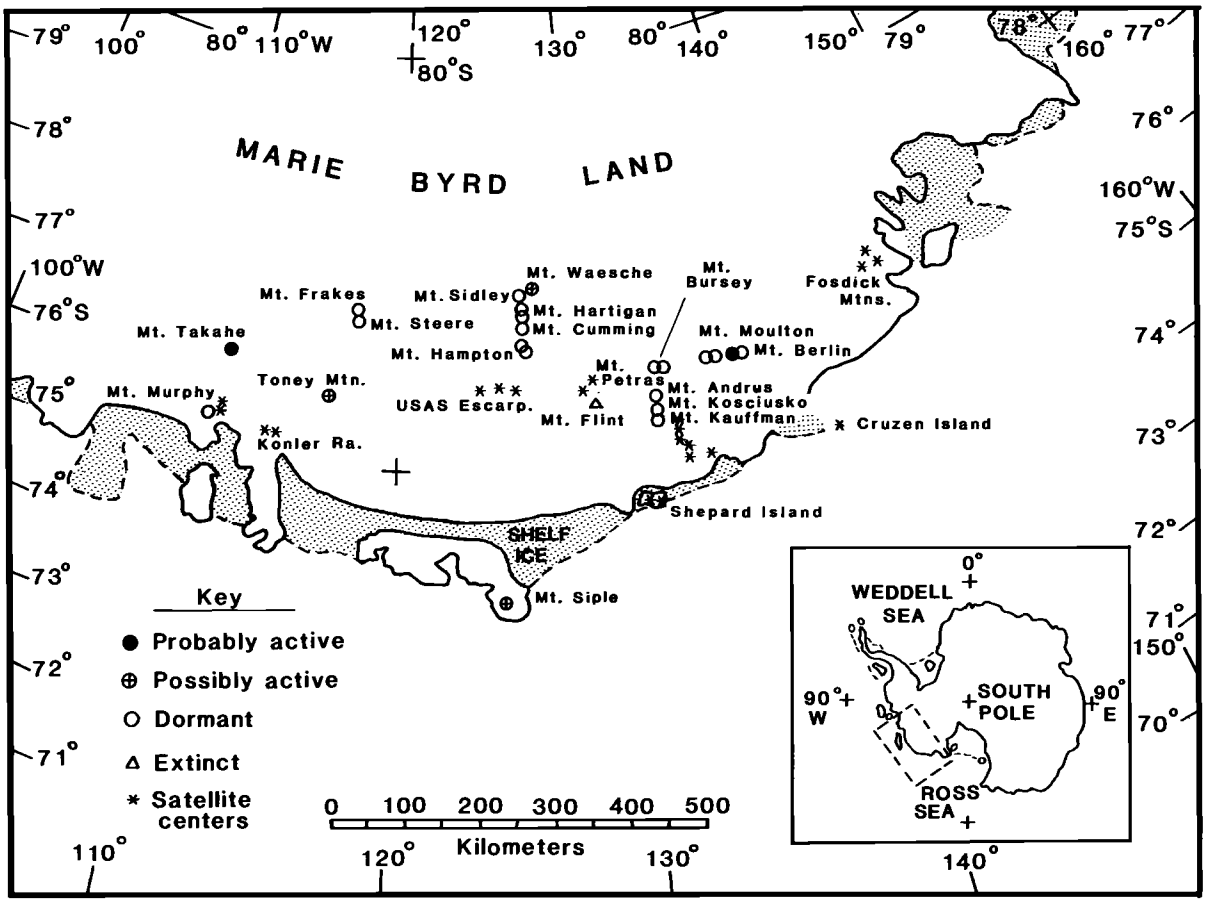

Fig. B.I. Index map of Marie Byrd Land volcanoes showing estimated eruptive potential [from *LeMasurier and Rex,* 1982*b*]. The satellitic volcanic centers symbol represents the generalized locations of more than 30 small, predominantly basaltic, individual eruptive centers described in IVD B.16. All 18 major volcanoes listed in Table B.I are shown here.

of these volcanoes has been subjected to what most volcanologists would think of as a detailed study.

Mount Takahe (see IVD B.2), the most thoroughly studied volcano in the province, was first visited in the 1957–1958 summer season, then again during a helicopter reconnaissance in 1967–1968, and most recently in 1984–1985, when all accessible exposures were visited during a 3-week investigation. Perhaps a total of 25 days have been spent on the outcrop, and about 60 days have been spent close enough to the volcano to observe an eruption directly, if one had occurred. Mount Siple (see IVD B.5), the least studied major volcano, was visited for the first and only time in February 1984, when three localities were sampled during 1 day of good weather. There are perhaps 10 days when an eruption of Mount Siple could have been directly observed. The section on extent of knowledge in each of the following individual volcano descriptions, which refers mainly to the extent of field observation, falls between these two extremes. None of these volcanoes is on a supply route to an Antarctic field station, and no commercial air routes pass near the region. Satellite photographs offer the possibility of detecting an eruption, and these have been used to suggest very recent activity for Mount Siple (see IVD B.5).

The analytical data available as of March 1989 include 136 K-Ar age determinations, 221 major- and minor-element rock analyses, 35 Sr and Nd isotopic analyses, and microprobe analyses of all phases in 55

Copyright American Geophysical Union

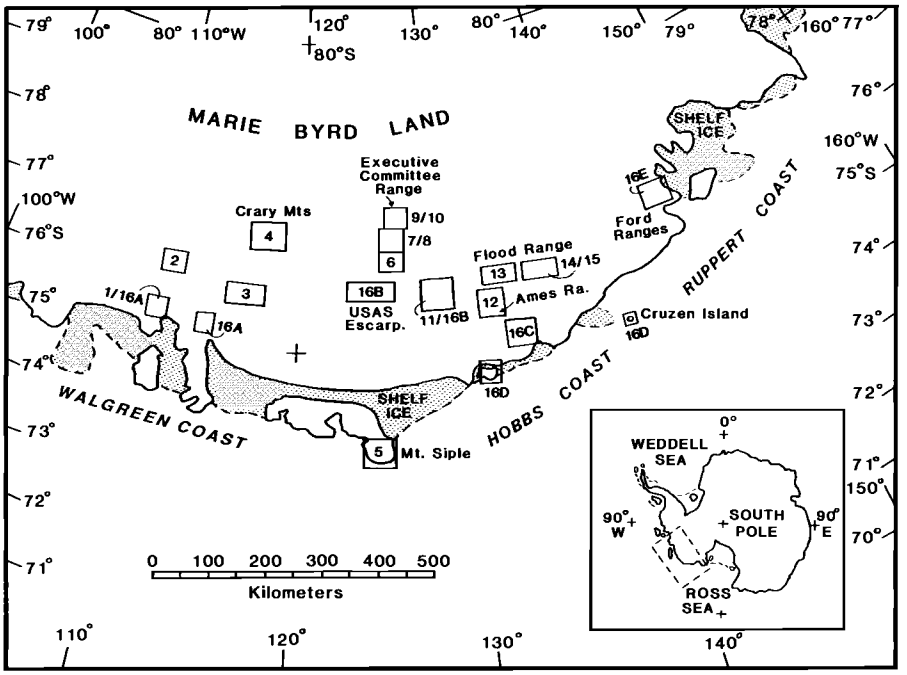

Fig. B.II. Index map of the individual volcano descriptions which follow. IVD's B.1–B.15 include the 18 major volcanoes. The dimensions of each rectangle approximate the coverage of large-scale maps included in each individual volcano description. Satellitic volcanic centers are described in IVD B.16 and illustrated in maps shown in Figures B.16A.1, B.16B.1, B.16B.3, B.16C.1, B.16D.1, and B.16.E.1.

rock samples. Over half of these data became available during the latter stages of preparing this part of the volume. Therefore some summary statements are based on thoroughly analyzed and published data, and others on a cursory examination of data that have not yet been carefully studied.

Physical Characteristics

The relations found at well-exposed major centers suggest that the vertical succession illustrated schematically in Figure B.III represents a common theme of structural development in this province. It has been observed throughout Marie Byrd Land (MBL) (and Ellsworth Land to the east) that the unconformity at the base of the Cenozoic section is a very flat erosion surface. It truncates crystalline rocks with ages ranging from early Paleozoic to as young as 80 Ma and is directly overlain by volcanic rocks with ages that range from late Oligocene to late Pliocene. The rock types that directly overlie the unconformity are basalts, basanites, tephrites, and hawaiites; they occur as flows, Strombolian tephra, and hyaloclastites, the proportions of which vary from one locality to another. Collectively, these have been termed basal successions [*LeMasurier*, 1972*a*]. The maximum exposed thicknesses of these basaltic rocks have been found in the major central volcanoes, underlying felsic and intermediate rocks. This relationship is described in the appropriate individual volcano descriptions (i.e., IVD's B.1, B.3, and B.4) and represented schematically in Figure B.III. In addition to these major occurrences of basaltic rock there are more than 30 widely separated volcanic localities that consist of basaltic cinder cones, tuff cones, and erosional remnants of older (up to 28 Ma) flow and hydroclastic sequences. Many of these are exposed in contact with basement rock and clearly represent small-scale satellitic eruptions rather than the tops of concealed sequences. They are described in IVD B.16 and illustrated in the accompanying maps (see Figures B.16A.1, B.16B.1, B.16B.3, B.16C.1, B.16D.1, and B.16E.1).

Hyaloclastites (in the sense of *Fisher and Schmincke* [1984, p. 233]) are common in the basal parts of volcanic sections throughout MBL (see Figure B.III and IVD's B.1 and B.16). They represent eruptions beneath, or in contact with, glacial ice and have been used to help reconstruct the glacial history of the past 30 m.y. [*LeMasurier*, 1972*a*, *b*; *LeMasurier and Rex*, 1982*a*, 1983]. In more temperate regions these rocks would probably occur

Copyright American Geophysical Union

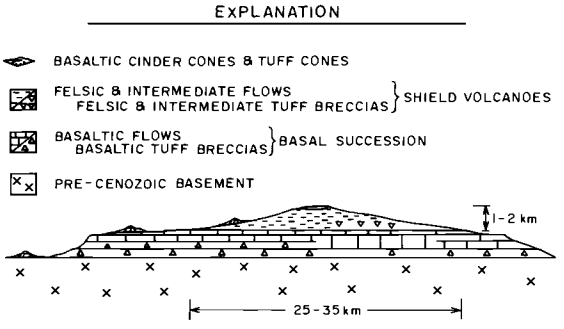

Fig. B.III. Schematic diagram with approximate scale, illustrating structural and stratigraphic relationships of volcanic rocks in Marie Byrd Land. "Basal successions" typically include lava flows, Strombolian bombs and cinders, and palagonitized hydroclastic deposits. Proportions of the latter depend on the position of active vents with respect to contemporaneous ice level. Similar facies are found among the felsic and intermediate rocks of the overlying shield volcanoes, but hydroclastic facies are less common there because of generally higher stratigraphic levels (see Mount Takahe (IVD B.2), Mount Sidley (IVD B.9), and Mount Berlin (IVD B.15) for examples of felsic hydroclastic facies). Complex lateral and vertical hydroclastic to subaerial facies changes are common and are believed to represent ice level fluctuations during eruptive history. Transition from basal succession to shield volcano may be topographically abrupt and represent a long time interval (e.g., Toney Mountain, left side of diagram and IVD B.3), or it may take place within a smooth topographic profile (e.g., Mount Murphy, right side of diagram and IVD B.1). Basaltic cinder cones and tuff cones occur in a variety of structural and stratigraphic positions, as shown, and may be as much as 5–10 m.y. younger than the underlying shield volcano (e.g., IVD's B.1, B.7, B.11, B.12, and B.13).

as flows and Strombolian tephra in shield volcanoes and fissure-fed flow sequences.

Overall, the field relations indicate that volcanism was initially basaltic at nearly all localities and commonly took place in a subglacial or periglacial environment. This activity was then followed by felsic volcanism (the felsic shield volcanoes described below) in a more restricted number of centers. Trachyte rests on basement rock at Kouperov Peak (see IVD B.16C), the only exception observed so far to the relations just described.

The 18 large central volcanoes (Figure B.I, Table B.I) occur as single cones, as closely coalesced doublets, and as linear chains of single and coalesced volcanoes. Each is characterized by two or more of the following features: (1) large size (10- to 50-km base diameter), (2) a caldera 1–10 km in diameter, and (3) predominantly felsic compositions. Ten are more than 3000 m in summit elevation (Table B.I), and Mount Sidley (4181 m) is the highest volcano in Antarctica. They are described in IVD's B.1–B.15. All 18 appear to be shield volcanoes, composed mainly of flow rock (in some cases mainly of felsic flow rock), with constructional slopes of 10°–15°. The 1200-m caldera wall exposures at Mount Sidley (see IVD B.9) and 2000-m cirque wall exposures at Mount Murphy (see IVD B.1) offer the best direct evidence of flow rock predominance in these volcanoes (see also IVD's B.12, B.14, and B.15). Hyaloclastites of felsic and intermediate compositions are found around the bases of Mount Takahe (see IVD B.2) and Mount Berlin (see IVD B.15), and agglutinates are also common; but Plinian and pyroclastic flow deposits have not been found in MBL. Thus the most violent eruptions in the province appear to have been Strombolian and Surtseyan. Parasitic cones of various types (Figure B.III) are commonly of basaltic compositions that are indistinguishable from the rocks at the base of the volcanic sections.

Block faulting of the prevolcanic erosion surface, combined with the rapid rise of ice level inland, makes it difficult to estimate the sizes of volcanoes and the volumes and proportions of rock types. The bases of inland volcanoes could lie anywhere from -3000 m (e.g., Toney Mountain (see IVD B.3)) to just below the +2000-m surface of the ice sheet. The estimated volumes presented in the individual volcano descriptions are for exposed portions of the volcano only. The amount of basalt in the basal successions is especially difficult to estimate, and the seismic data at Toney Mountain (see IVD B.3) suggest that the volume of basalt beneath the ice sheet may be very large. Although the felsic rock in the major volcanoes is abundant and conspicuous, it probably constitutes only one third to one tenth of the total volume of volcanic rock in the province [*LeMasurier and Wade*, 1976].

Chemical Characteristics

Marie Byrd Land volcanoes are distinguished by an abundance of felsic rocks and a great range in their composition. Petrologic lineages are difficult to recognize, because there is no clear correspondence

Copyright American Geophysical Union

TABLE B.I. Major Central Volcanoes of the Marie Byrd Land Volcanic Province

Volcano (IVD)	Analyzed Rock Compositions	Elevation, m	K-Ar Indicated Age Range*
1. Mount Takahe (B.2) (76°15′S, 112°W)	Basanite, hawaiite, mugearite, benmoreite, trachyte	3460	Pleistocene-Holocene (?)*
2. Mount Berlin (B.15) (76°S, 136°W)	Mugearite, peralkaline trachyte	3478	Pliocene-Holocene (?)
3. Toney Mountain (B.3) (75°45′S, 116°W)	Benmoreite, trachyte, comendite	3595	Pleistocene
4. Mount Waesche (B.10) (77°10′S, 127°W)	Hawaiite/mugearite (south caldera), comendite (north caldera)	3292	Pliocene-Holocene (?)
5. Mount Siple (B.5) (73°30′S, 127°W)	Alkali basalt	3110	Pliocene-Holocene (?)
6. Mount Frakes (B.4) (76°48′S, 117°45′W)	Basanite, phonolite	3654	Pliocene-Pleistocene
7. Mount Sidley (B.9) (77°S, 126°W)	Phonolite, phonolitic trachyte	4181	Pliocene
8. Mount Moulton (B.14) (76°00′S, 135°00′W)	Pantellerite	3078	Pliocene
9. Mount Kauffman (B.12) (75°35′S, 132°30′W)	Trachyte	2364	Miocene-Pliocene
10. Mount Bursey (B.13) (76°00′S, 132°30′W)	Mugearite, trachyte	2787	Miocene-Pliocene
11. Mount Hartigan (B.8) (76°50′S, 126°W)	Hawaiite/mugearite (south caldera), alkaline rhyolite (north caldera)	2811	late Miocene
12. Mount Hampton (B.6) (76°25′S, 126 °W)	Phonolite, phonolitic trachyte, basanite (parasitic cones only)	3323	middle Miocene-late Miocene
13. Mount Steere (B.4) (76°44′S, 117°45′W)	Benmoreite, basanite	3558	late Miocene
14. Mount Cumming (B.7) (76°40′S, 126 °W)	Pantellerite, trachyte, basanite (parasitic cone only)	2612	late Miocene
15. Mount Kosciusko (B.12) (75°43′S, 132°13′W)	Pantellerite, pantelleritic trachyte	2909	late Miocene
16. Mount Andrus (B.12) (75°50′S, 132°20′W)	Pantellerite, pantelleritic trachyte, mugearite	2978	middle Miocene-Holocene (?)
17. Mount Murphy (B.1) (75°20′S, 110°45′W)	Alkali basalt, benmoreite, trachyte	2703	late Miocene
18. Mount Flint (B.11) (75°40′S, 129°W)	Trachyte, basanite (parasitic cones only)	2695	early Miocene-middle Miocene

Volcanoes are listed approximately in order of increasing age of the youngest precaldera lavas [*LeMasurier and Rex*, 1982*b*].
*Holocene(?) notation is based on occurrence of samples too young to be dated by K-Ar (0.2 Ma) and/or fumarolic activity.

between the saturation characteristics of closely associated felsic and basaltic rocks. For example, at Mount Murphy (see IVD B.1) *hy*-normative basalts underlie *ne*-normative trachytes, and at Toney Mountain (see IVD B.3) comendites overlie *ne*-hawaiites, contrary to the persistence of saturation characteristics that is commonly the basis for recognizing lineages [*Coombs and Wilkinson*, 1969].

Table B.I summarizes the lithologic characteristics of each major volcano, and Figure B.IV shows the ranges among some chemical parameters that are commonly used to describe alkalinity and tectonic environment. Classification and nomenclature follow the International Union of Geological Sciences (IUGS) system [*Le Bas et al.*, 1986], based on the total alkalis versus silica (TAS) diagram. Figure

Copyright American Geophysical Union

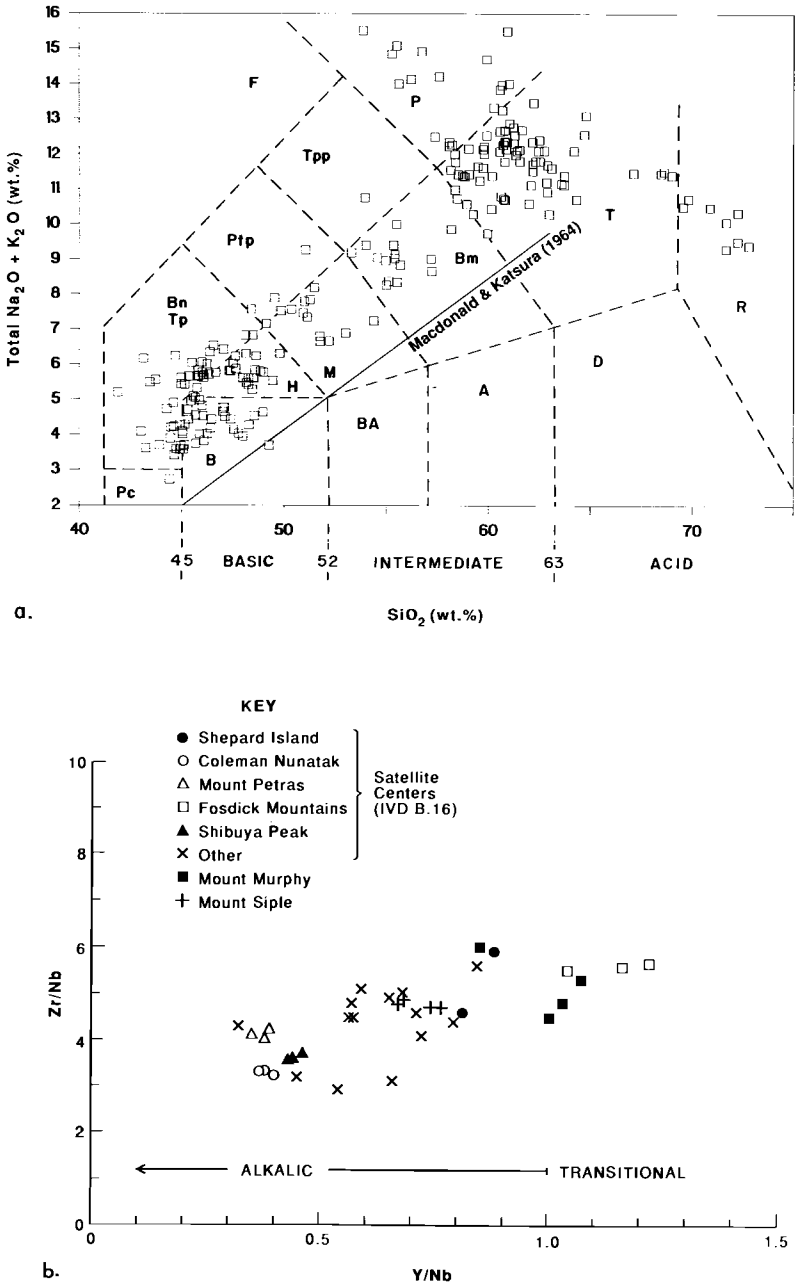

Fig. B.IV. (*a*) Alkali versus silica plot of all (221) MBL samples. IUGS classification [*Le Bas et al.,* 1986] shown by dashed line. Abbreviations: Pc, picrobasalt; Bn, basanite (>10% ol); Tp, tephrite (<10% ol); F, foidites; B, basalt; H, hawaiite; Ptp, phonotephrite; Tpp, tephrophonolite; P, phonolite; M, mugearite; Bm, benmoreite; T, trachyte; BA, basaltic andesite; A, andesite; D, dacite; R, rhyolite, including pantellerite and comendite. *Macdonald and Katsura* [1964] alkali basalt - tholeiite boundary is shown by a solid line. (*b*) Zr/Nb versus Y/Nb plot for MBL basaltic rocks, showing alkalic and within-plate character of this suite [*Pearce and Cann,* 1973]. Y/Nb for tholeiites is >2.0. (*c*) Na_2O versus K_2O plot for all MBL rocks. The (Na_2O - 2 = K_2O) line marks the boundary between sodic and potassic rocks [*Le Bas et al.,* 1986]. (*d*) Agpaitic (peralkalinity) index versus SiO_2 for rocks with SiO_2 values greater than 52%. Peralkaline rocks lie above the dashed line.

Copyright American Geophysical Union

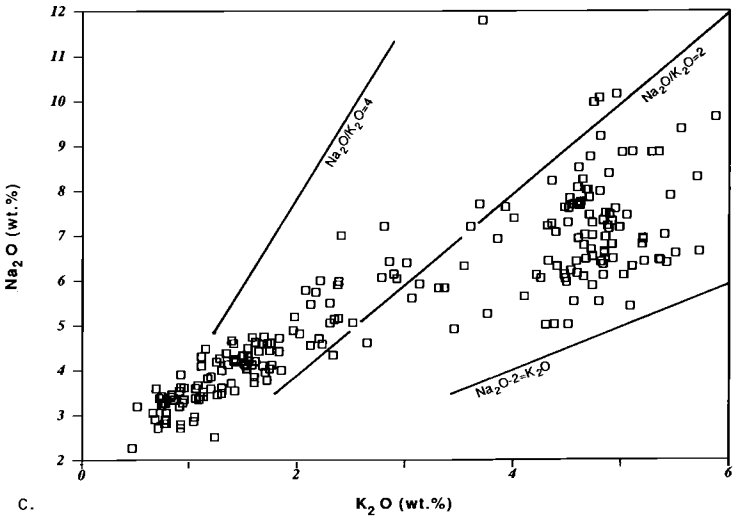

c.

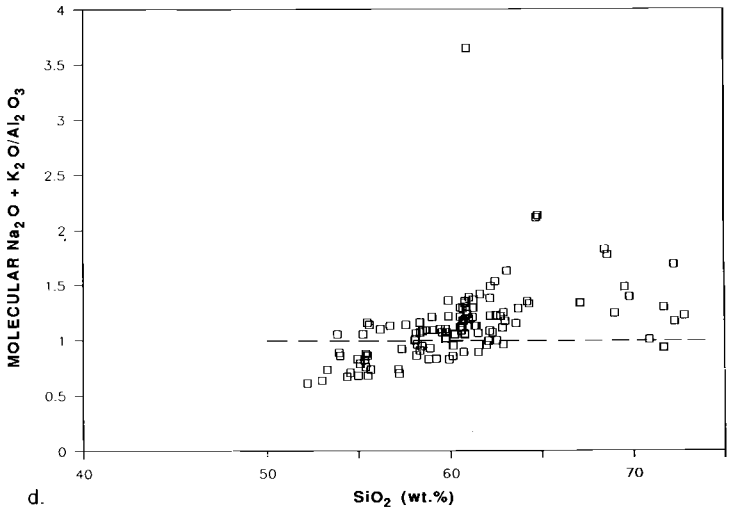

d.

Fig. B.IV. (continued)

B.IV*a* illustrates the alkaline character of the province, the broad compositional range of felsic rocks, and the commonness of basaltic rock types (basalt, basanite, tephrite, hawaiite) and trachyte. The province is strongly bimodal, in the sense that highly evolved rocks (felsic rocks as defined above) and basaltic rocks are much more common than the mugearites and benmoreites that lie between them on the diagram. Intermediate rocks, in the sense of *Le Bas et al.* [1986], include all phonolites and most trachytes and are clearly not less common than acid rocks.

The basalts are predominantly *ne*-normative, the IUGS criterion for alkali basalt, but they range from basanites with about 14% *ne* to the transitional *hy*-normative basalts at Mount Murphy, Mount Siple, and the Fosdick Mountains (see IVD's B.1, B.5, and B.16E). The Y/Nb ratio (Figure B.IV*b*) similarly indicates a wide range in alkalinity [*Pearce and Cann*, 1973]. All MBL rocks are sodic series (Figure B.IV*c*), and a large proportion of the felsic rocks are peralkaline (Figure B.IV*d*).

Other chemical traits presented below illustrate the within-plate character of the province, the close

Copyright American Geophysical Union

similarity to oceanic island geochemistry, and the apparent lack of crustal involvement in the evolution of the felsic rocks.

Basaltic Rocks. Figures B.IV*b* and B.V illustrate the relationship of chemical characteristics to tectonic setting for basaltic rocks. Present-day tectonic boundaries indicate that MBL is a within-plate province associated with continental rifting, and this is reflected in the Ti-Zr-Y relationships as well as the Y/Nb ratios [*Pearce and Cann*, 1973]. However, Figures B.V*b* and B.VI*a* illustrate that these rocks cannot be readily distinguished from oceanic island basalts by chemical or isotopic criteria, which is a commonly observed trait of alkaline rocks [*Schwarzer and Rogers*, 1974; *Pearce et al.*, 1977]. The most nonoceanic trait of the province seems to lie in the

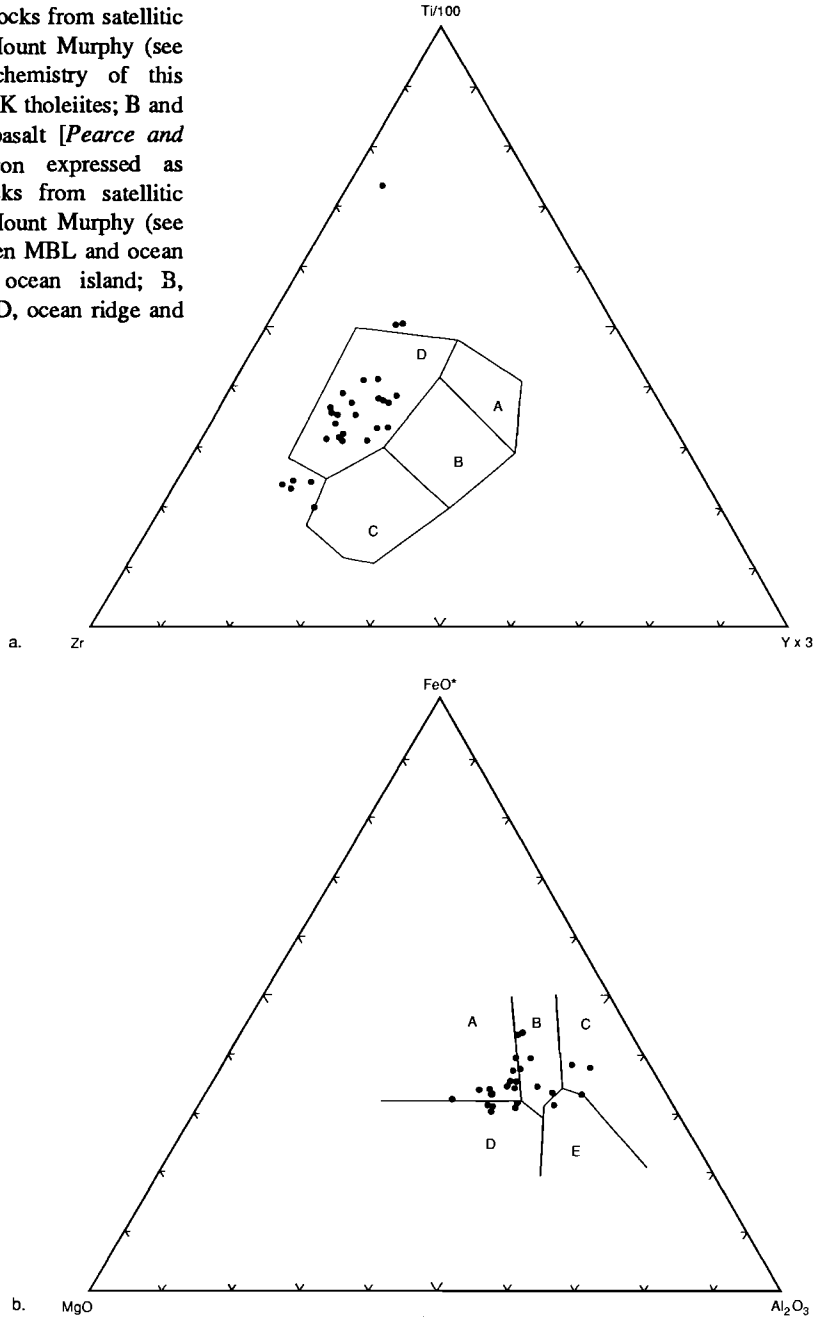

Fig. B.V. (*a*) Ti-Zr-Y plot of basaltic rocks from satellitic volcanic centers (see IVD B.16) and Mount Murphy (see IVD B.1), illustrating within-plate chemistry of this province. Abbreviations: A and B, low-K tholeiites; B and C, calc-alkali basalt; D, within-plate basalt [*Pearce and Cann*, 1973]. (*b*) FeO* (total iron expressed as FeO)-MgO-Al_2O_3 plot of basaltic rocks from satellitic volcanic centers (see IVD B.16) and Mount Murphy (see IVD B.1), illustrating similarities between MBL and ocean island basalts. Abbreviations: A, ocean island; B, continental; C, spreading center island; D, ocean ridge and floor; E, orogenic [*Pearce et al.*, 1977].

Copyright American Geophysical Union

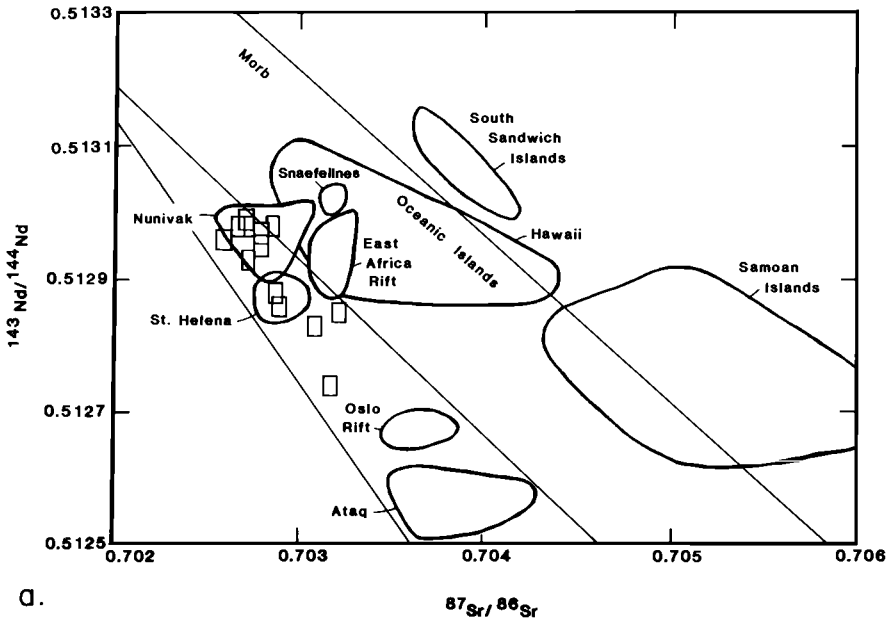

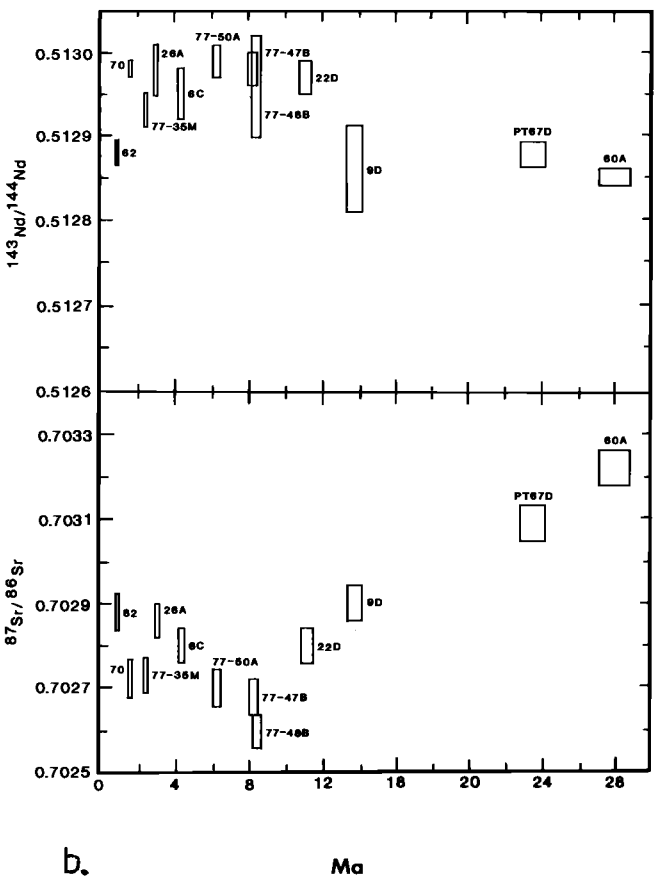

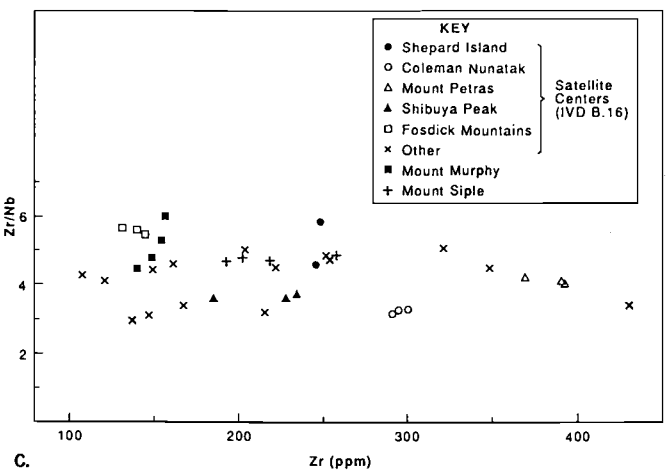

Fig. B.VI. (*a*) $^{143}Nd/^{144}Nd$ versus $^{87}Sr/^{86}Sr$ diagram for basaltic rocks from Marie Byrd Land and other magmatic provinces [*Futa and LeMasurier*, 1983]. (*b*) Temporal variation of $^{87}Sr/^{86}Sr$ and $^{143}Nd/^{144}Nd$ initial ratios of basaltic rocks from Marie Byrd Land [*Futa and LeMasurier*, 1983]. (*c*) Zr/Nb versus Zr plot for basaltic rocks from the satellitic volcanic centers, plus Mount Murphy and Mount Siple.

Copyright American Geophysical Union

abundance and diversity of felsic rocks and in the lack of a persistence of saturation patterns [*Coombs*, 1963].

Some characteristics of the basalt source region have been inferred from Figure B.VI. Isotopic studies indicate generally high $^{143}Nd/^{144}Nd$ and exceptionally low $^{87}Sr/^{86}Sr$ values for the basaltic rocks, which is consistent with their derivation from a depleted mantle source and a lack of crustal contamination [*Futa and LeMasurier*, 1983]. Figure B.VI*b* suggests a change in source characteristics with time, from a more continental or ocean island type of source region toward one that approaches midocean ridge basalt characteristics. This is consistent with the evolving rift environment described in the last section of this summary. The Zr/Nb ratio is believed to be insensitive to degree of partial melting and therefore to be a good indicator of the degree of homogeneity in the source region [*Pearce and Norry*, 1979]. Thus the spread of Zr/Nb values in Figure B.VI*c*, coupled with the clustering of points from individual volcanic centers, suggests significant heterogeneity in the source.

Chemical variation related to fractional crystallization processes is suggested in Figure B.VII. MgO and Ni show a coherent pattern of rapid decrease among basaltic rocks, and the variation of Cr (not shown) is almost identical to that of Ni. Fractionation of olivine and clinopyroxene, both common as phenocrysts, is a likely cause of these patterns. A variable degree of iron enrichment is apparent from

Fig. B.VII. Variation diagrams illustrating the behavior of MgO, FeO_t, and Ni, represented by all analyzed Marie Byrd Land samples. A, $Na_2O + K_2O$; F, total Fe as FeO; M, MgO.

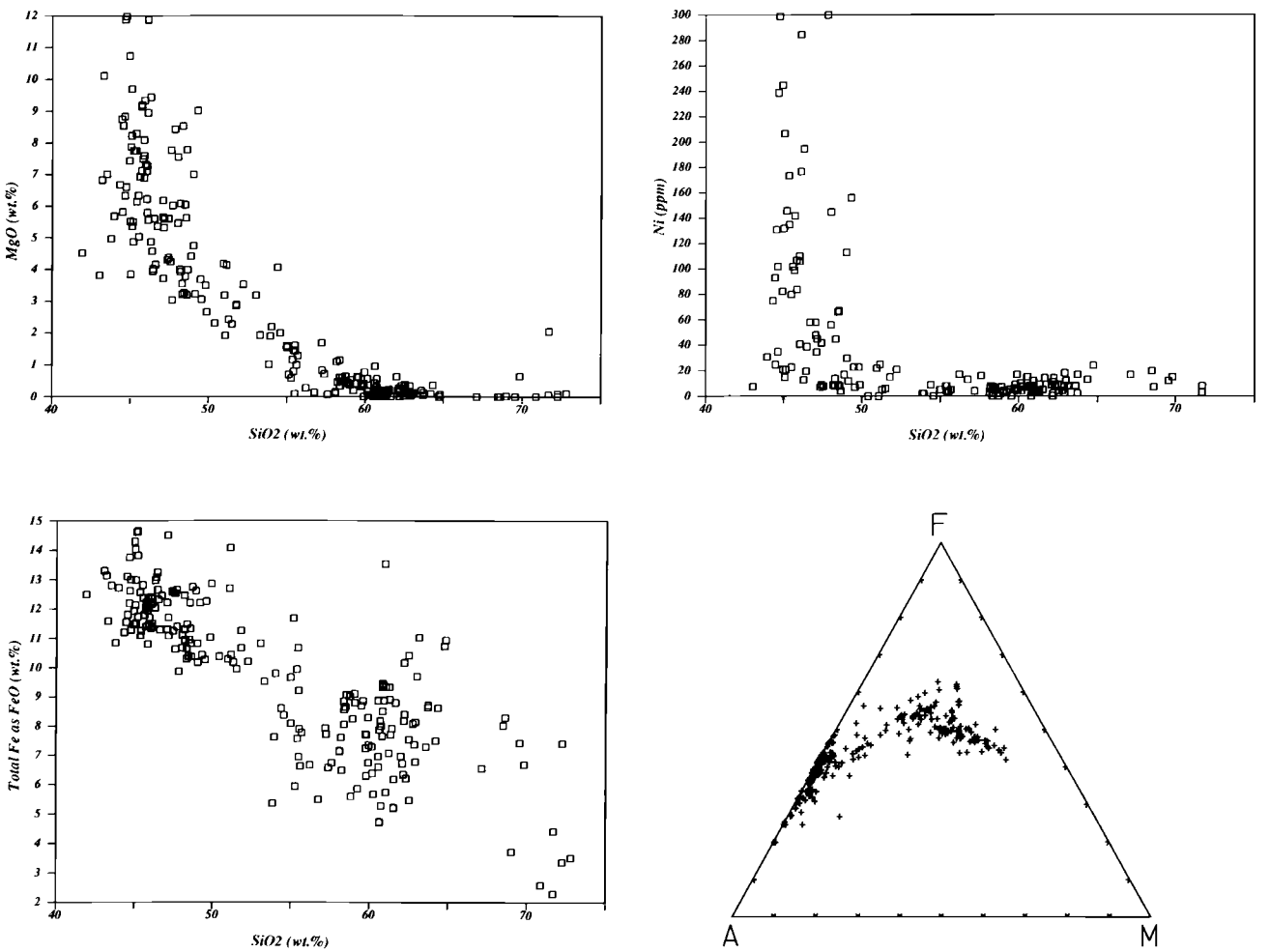

Copyright American Geophysical Union

the AFM diagram and from the variation of FeO. The variability is most pronounced in the felsic rocks, however (see discussion below).

Some examples of mineral compositions are presented in IVD's B.1, B.3, and B.11, for basaltic rocks, and in IVD's B.6 and B.7, for associated ultramafic nodules. The most unusual aspect of these data is the suggestion that reverse zoning in plagioclase phenocrysts and normal zoning in associated mafic phenocrysts are common associations. The diversity of the nodule suite is represented by the spinel lherzolite, websterite, and dunite analyses from adjacent volcanoes in the Executive Committee Range. These nodules are most commonly found in basaltic cinder cones and tuff cones, and spinel lherzolite seems to be the most common type.

Acid and Intermediate Rocks. Rocks with more than 52% SiO_2 [*Le Bas et al.*, 1986] are found, with few exceptions, in the major central volcanoes listed in Table B.I and described in IVD's B.1–B.15. The most evolved rocks include phonolites, trachytes, comendites, pantellerites, and metaluminous rhyolites. Trachyte is the most abundant of these and the most persistent through time, being a major component of the oldest (Mount Flint) and of the youngest (Mount Berlin and Mount Takahe) volcanoes. The available data indicate that each volcano is composed of only a small part of the province-wide compositional spectrum, as implied in Table B.I, and that individual volcanoes differ greatly from one to another, even among closely coalesced doublets [*LeMasurier and Rex*, 1989*a*]. The chemical analyses presented here were selected primarily to represent the range of rock types that have been found at each volcano and only secondarily to represent their proportions.

Compositional data for minerals in acid and intermediate rocks are presented in IVD's B.3, B.6, B.7, B.10, B.14, and B.15. Both reverse zoning and normal zoning are common in the alkali feldspar phenocrysts. Pyroxene phenocrysts range from ferrosalite to Na-hedenbergite to aegirine-augite in composition. Iron-rich olivine phenocrysts are found occasionally in both oversaturated and undersaturated rocks; aenigmatite is a common phenocryst in comendites, pantellerites, and trachytes; amphibole phenocrysts are rare but are most commonly found in rhyolitic rocks. Ti-rich pyroxenes and oxides are common. The typical MBL phenocryst assemblage is completely anhydrous; but the most common exceptions are found among rhyolitic rocks.

The AFM and FeO_t diagrams (Figure B.VII) illustrate variable degrees of iron enrichment. The scale and field distribution of this variability can be seen by contrasting the low-Fe rocks from comenditic volcanoes (IVD's B.3, B.8, and B.10) with the Fe-enriched rocks from pantelleritic and some trachytic volcanoes (e.g., IVD's B.12 and B.13). Compositional bimodality is also evident in these diagrams.

Figure B.VIII shows 35- to 40-fold increases in Rb and Zr over the entire compositional range and also illustrates the high incompatible element abundances that are characteristic of within-plate volcanic suites. In both diagrams, most basaltic samples lie along a straight and coherent trend. The wide scatter among samples of more evolved compositions suggests that multiple processes, or perhaps multiple controls of one process, concentrated these elements in residual liquids.

The Ba, Sr, and rare earth element diagrams (Figures B.VIII and B.IX) provide different perspectives on the possible roles of feldspar fractionation. The sharp drop in Ba around SiO_2 = 60% coincides roughly with the appearance of alkali feldspar phenocrysts around the benmoreite/trachyte boundary and probably represents the onset of alkali feldspar fractionation. Sr shows a much wider range of values than Ba among basaltic rocks but, like Ba, an abrupt drop to low values in all rocks with $SiO_2 > 60\%$. Rare earth element data show pronounced negative Eu anomalies among the felsic rocks, and no anomaly or slightly positive Eu anomalies in the basalt to benmoreite/trachyte range (Figure B.IX) [*LeMasurier et al.*, 1976]. Feldspar fractionation seems therefore to have left a clear imprint on the trace-element chemistry of the felsic rocks. Among basaltic and intermediate rocks, however, the complexity of variation suggests that factors such as source rock heterogeneity and degree of partial melting, state of oxidation, and roles of clinopyroxene and feldspar fractionation need to be evaluated after more detailed study of individual centers before generalizations can be made. The available Sr isotopic data for acid and intermediate rocks (Table B.II) suggest that crustal contamination was not a significant petrogenetic

Copyright American Geophysical Union

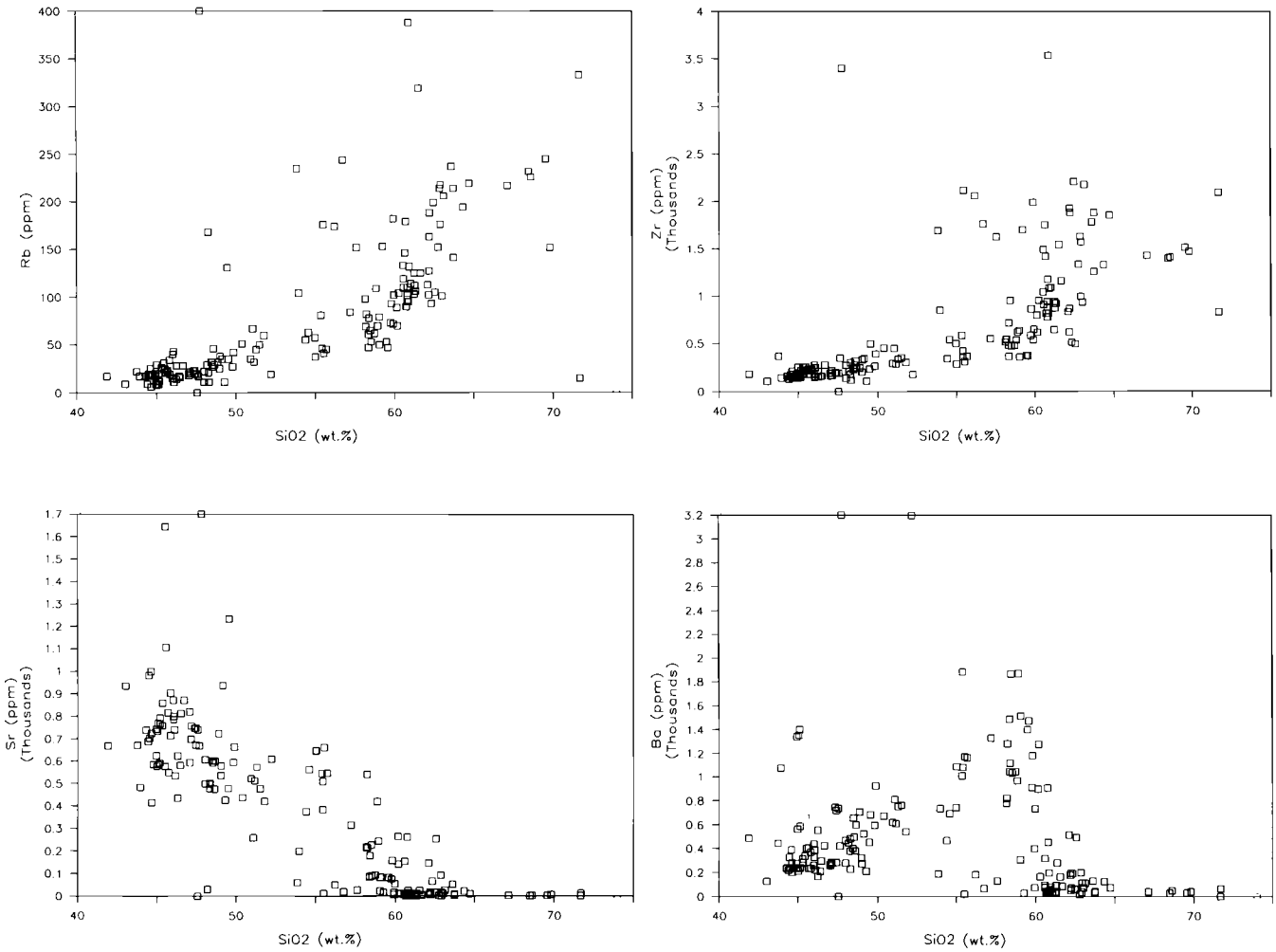

Fig. B.VIII. Variation of selected large ion lithophile (LIL) and high field strength (HFS) elements versus SiO_2, represented by all analyzed Marie Byrd Land samples.

process in this province [*LeMasurier and Wade*, 1976; Futa and LeMasurier, unpublished data, 1989].

Chronologic Characteristics

It was mentioned earlier that there are no dependable criteria for estimating relative ages of MBL volcanoes, because of their relative lack of erosional dissection. This is well illustrated by comparing Mount Hampton (Figures B.6.1 and B.6.2), which formed around 10–12 Ma, with Mount Takahe (Figure B.2.1), which is no older than 0.5 Ma. The deep dissection of Mount Murphy (IVD B.1), which seems anomalous given its apparent age of 8–9 Ma, may be related to its nearness to the coast and greater exposure above the ice sheet, compared with inland volcanoes. In spite of anomalies, volcano elevation in this region is not related to erosional processes, degree of dissection is not clearly related to age, and the chronology of volcanic events at almost any scale can only be reliably determined by K-Ar dating.

The K-Ar data suggest that volcanic eruptions began in this province at about 28–30 Ma and have become increasingly frequent toward the present, with peaks of activity at 8–12 Ma and 0–1 Ma (Figure B.X). Loss of the older record due to erosion is probably less of a factor in this province than almost anywhere else in the world, but concealment of a significant proportion of the older rocks beneath the ice sheet is very likely. The K-Ar data selected for

Copyright American Geophysical Union

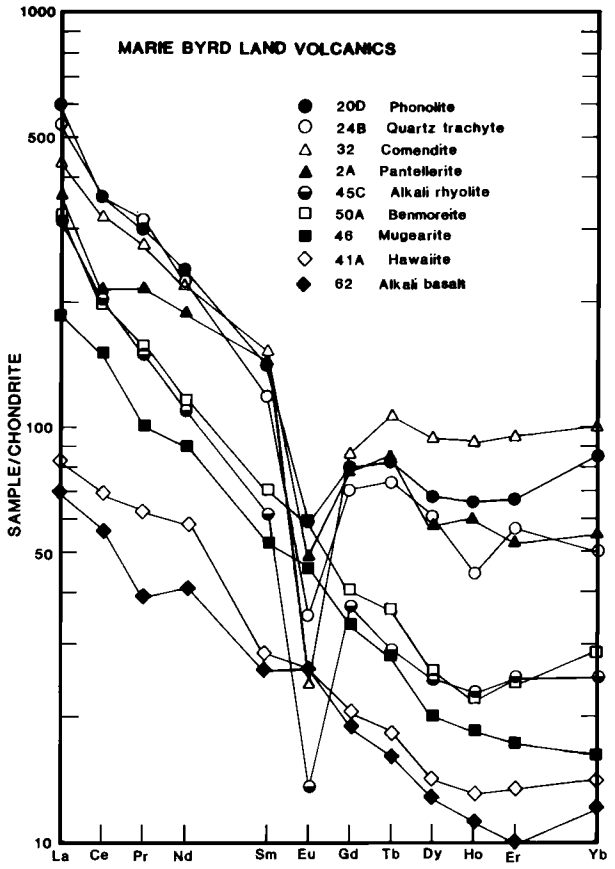

Fig. B.IX. Rare earth element (REE) variation in nine selected samples representing variation in mafic to felsic rocks (data from *LeMasurier et al.* [1976]).

Figure B.X exclude questionable dates and multiple dates of the same volcanic event.

Individual volcanoes appear to have gone through a relatively rapid shield-building phase, followed by caldera formation and then by very infrequent waning activity [*LeMasurier and Rex,* 1982*b*]. Data from the Ames and Flood ranges (IVD's B.12, B.13, and B.15) suggest that shield building may have taken 1–2.5 m.y. Mount Takahe (IVD B.2) is unusual, because it apparently formed entirely within the last 300,000–400,000 years. A late stage of basaltic parasitic cone activity took place on many of the major volcanoes, at times ranging from <0.1 m.y. to 10 m.y. after the youngest precaldera eruptions (for examples, see IVD's B.1, B.2, B.7, B.12, and B.13).

Conspicuous chronologic patterns have been produced by migrations of felsic volcanic activity along the lengths of linear chains, and more subtle patterns have been produced by the apparently sequential uplift of basement blocks and their overlying basaltic sections. These patterns are described below in their tectonic context. In comparing the petrologic character of each volcano with its K-Ar age, no change in the geochemistry of the lavas with time can be recognized.

The potential for future activity of MBL volcanoes is difficult to assess, because there are no observational records and no ^{14}C datable materials available. Ash layers in ice cores south of this province have

TABLE B.II. Strontium Isotopic Composition of Marie Byrd Land Acid and Intermediate Rocks

Sample	Description	$^{87}Sr/^{86}Sr_N$	Rb, ppm	Sr, ppm	Rb/Sr	$^{87}Sr/^{86}Sr$ Initial Ratio
69A	Benmoreite, Crary Mountains	0.7030	113	462	0.245	--
65c	Benmoreite, Mount Takahe	0.7029	101	44	2.29	0.7029
53b	Trachyte, Mount Sidley	0.7064	242	20	12.1	0.7034
20b	Phonolite, Mount Hampton	0.7097	150	10	15.0	0.7047
71A	Phonolite, Mount Frakes	0.7031	142	52	2.7	--

Data are from *LeMasurier and Wade* [1976]. Dashes, not determined.

Copyright American Geophysical Union

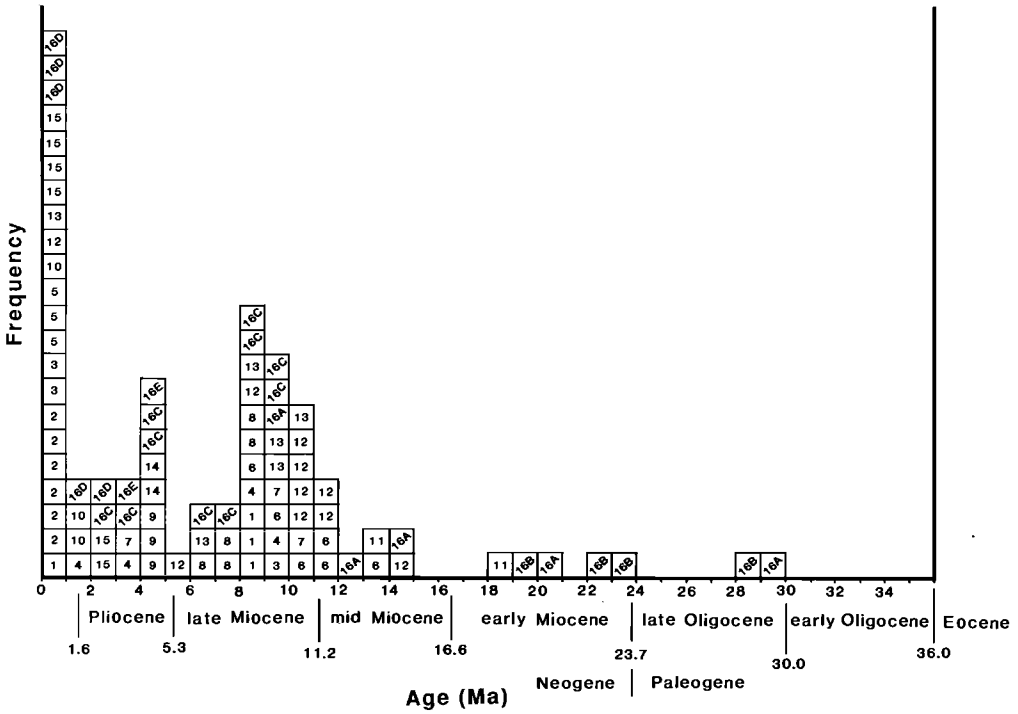

Fig. B.X. Histogram of K-Ar ages for the Marie Byrd Land volcanic province. Numbers within boxes refer to the respective individual volcano descriptions, which include maps showing sample locations. See text for discussion.

been attributed to eruptions of Mount Takahe [*LeMasurier*, 1972*c*; *Kyle et al.*, 1981] and possibly Mount Waesche and Toney Mountain [*LeMasurier*, 1972*c*]. This implies major eruptions within the last 30,000 years and hence a high potential for future eruptions of these volcanoes, if the correlations are accurate. Mount Siple (IVD B.5) has been suspected of recent activity, on the basis of the appearance of a plume(?) in satellite photos, but an overflight of the volcano 3 months after the most recent plume sighting revealed no evidence of an eruption [*Smithsonian Institution*, 1988*a*, *b*].

K-Ar ages <0.2 Ma are thought to be a good indicator of potential activity if the materials dated are precaldera rocks, but the predictive value of very young ages for parasitic cone basalts is less certain [*LeMasurier and Rex*, 1982*b*]. Basaltic activity throughout MBL has been essentially random in its geographic and temporal distribution throughout the past 30 m.y., and the Antarctic plate has not moved with respect to the MBL hotspot [*LeMasurier and Rex*, 1989*a*]. This suggests the possibility that some parasitic cones represent a recurrence of basaltic activity that is unrelated to the evolution of the host shield volcano. This suspicion is strengthened at Mount Murphy (IVD B.1), where Quaternary parasitic cone basalts are *ne*-normative and contain over 200 ppm Ni and the Miocene shield volcano basalts are *hy*-normative and contain less than 20 ppm Ni. In Figure B.I the distinction between volcanoes shown as "probably active" and those shown as "possibly active" is based on the amount of data available, especially the K-Ar ages of precaldera lavas, presence or absence of fumarolic activity, and correlation with ash layers in ice cores.

Tectonic Relationships

Marie Byrd Land lies on the north flank of the West Antarctic rift system, more than 1000 km from the nearest plate boundary (see map inside front cover). The rift system is 600–800 km wide (Figure I (Overview)) and follows a sub–sea level bedrock trough that extends from the Ross Sea across southern MBL toward the Bellingshausen Sea, separating MBL from the volcanic provinces of the western Ross

Copyright American Geophysical Union

Embayment [*LeMasurier*, 1978; *LeMasurier and Rex*, 1989*a*]. There has been episodic, rift-related volcanism and contemporaneous block faulting in MBL from late Oligocene time to the present, although the rift now appears to be aseismic. The effects of this prolonged interaction include a basin and range bedrock topography characterized by deep ice-filled grabens, a complex distribution of hydroclastic deposits that reflects both vertical tectonic displacements and large-scale fluctuations of the polar ice sheet, and both linear and vertical patterns of fault-related volcanism that suggest progressive doming and extension of the lithosphere within a stationary plate. Highlights of these features are outlined below, keyed to the appropriate individual volcano descriptions and published references.

A simple pattern of structurally controlled volcanism is suggested by the north-south and east-west alignments of the Executive Committee Range (IVD's B.6–B.10), Ames and Flood ranges (IVD's B.12–B.15), Crary Mountains (IVD B.4), and Toney Mountain (IVD B.3); by the rectilinear north-south and east-west boundaries of basement nunataks along the Hobbs Coast (Figure B.16C.2); and by the east-west orientation of the Usas Escarpment (IVD B.16.B). However, faults cannot easily be demonstrated by traditional stratigraphic methods in MBL, because the post-Paleozoic rocks are mainly igneous and lack reliable stratigraphic horizons. The early Tertiary erosion surface, the best horizon available, has been displaced to elevations that range between +2700 m (Mount Petras (see IVD B.16)) and -3000 m (Toney Mountain (see IVD B.3)), far exceeding the 50 m or less of erosional relief on the surface [*LeMasurier and Rex*, 1983]. This is the most direct evidence of large-scale faulting that has yet been found.

Figure B.XI shows elevations of the erosion surface at all localities where it is preserved beneath volcanic rocks, and it shows further that the ages of the volcanic rocks increase on successively higher block-faulted remnants of the surface. A 100 m m.y.$^{-1}$ rate of uplift can be calculated from this diagram, if one assumes that the erosion surface formed near sea level and that uplift of each block began at the inception of volcanism. Details of the calculation and an evaluation of the assumptions are given by *LeMasurier and Rex* [1983].

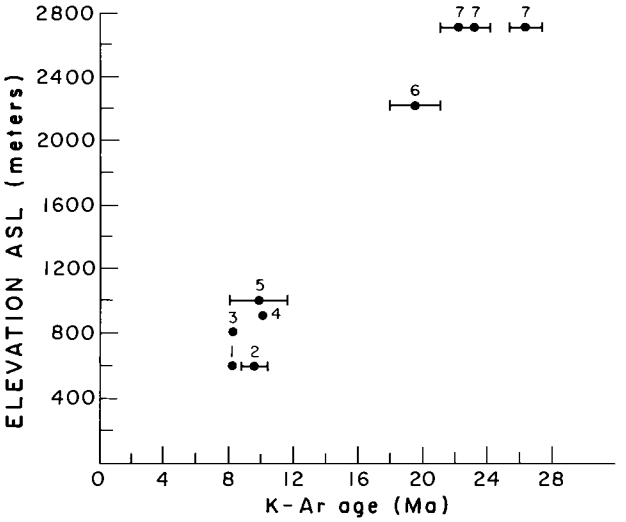

Fig. B.XI. Elevations of prevolcanic erosion surface remnants versus ages of the oldest volcanic rocks resting on the surface (revised from *LeMasurier and Rex* [1983]). Data are from the satellitic volcanic centers (see IVD's B.16A, B.16B, and B.16C). Error bars are shown only where errors are more than twice the size of the plotted circle. Abbreviations: 1, Holmes Bluff (see IVD B.16C); 2, Bowyer Butte (see IVD B.16C); 3, Kouperov Peak (see IVD B.16C); 4, Patton Bluff (see IVD B.16C); 5, Kohler Range (see IVD B.16A); 6, Usas Escarpment (see IVD B.16B); and 7, Mount Petras (see IVD B.16B).

The subglacial bedrock topography of MBL (Figure B.XII) conveys a strong suggestion that the landscape has been modified by basin and range faulting. The numerous narrow topographic basins, extending below -1000 m, are unusually deep for a continental setting, and the commonness of north-south and east-west orientations suggests an element of structural control in their origin. It seems inconsistent to attribute the depth of these basins primarily to glacial erosion, when the ice sheet seems so ineffectual in eroding exposed bedrock and when their geometry does not yield sensible flow patterns. The basins have therefore been interpreted as grabens that formed beneath the ice sheet in late Cenozoic time [*LeMasurier and Rex*, 1982*a*], with glacial ice forming the main component of basin fill and with perhaps a small component of sedimentary fill deposited during infrequent periods of deglaciation. In view of the lack of hard data, no fault symbols are shown. We suggest, however, that Figure B.XII shows a tectonic landscape in which the steep

Copyright American Geophysical Union

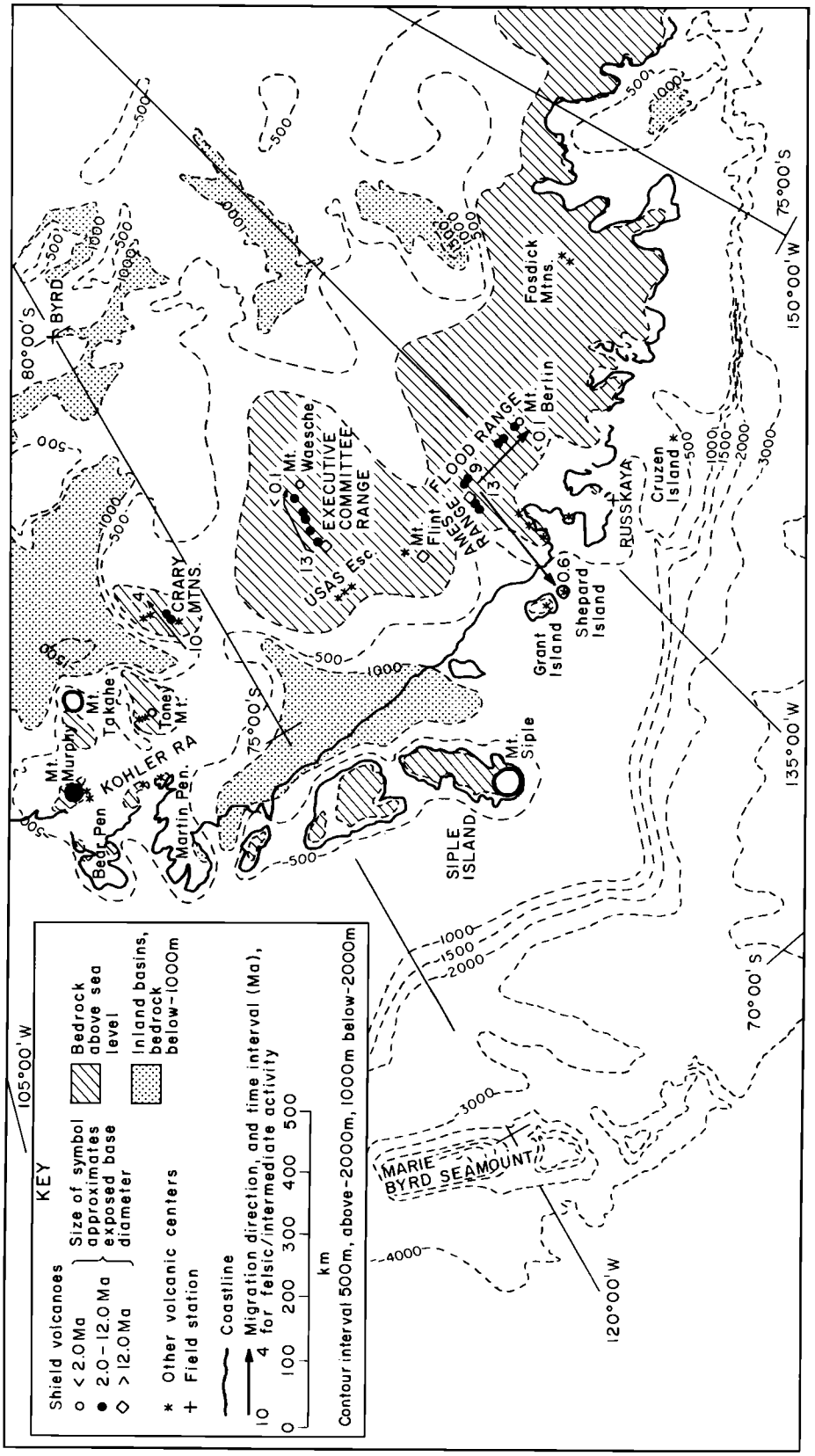

Fig. B.XII. Map of Marie Byrd Land volcanic region, showing contours on the largely subglacial bedrock surface (modified from *Drewry* [1982]) and locations of volcanoes. See text for discussion.

Copyright American Geophysical Union

boundaries between topographic highs and lows are fault scarps, with little or no erosional modification. The major shield volcanoes have been added to this diagram, together with a schematic representation of other volcanic features, to produce a "tectonic map" that is largely free of interpretive symbols. This may be compared with Figure I (Overview), which includes a large amount of interpretive material.

Migrations of volcanic activity along linear ranges are also represented on Figure B.XII. Migrations of activity are common on mobile lithospheric plates, where they are usually interpreted as hot spot tracks, but they seem anomalous on the immobile Antarctic plate. In addition to the contemporaneous migrations of activity in orthogonal and opposing directions, shown in Figure B.XII, the MBL linear ranges show the following characteristics [*LeMasurier and Rex*, 1989*a*]. (1) The migrations involve only the felsic and intermediate rock types in central volcanoes. No migration pattern has been recognized in basaltic rocks, despite the fact that they are the most abundant and widespread rocks in MBL. (2) Major petrologic differences between adjacent volcanoes are common in a single chain (cf. Mount Sidley and Mount Waesche (see IVD's B.9–B.10)), which contrasts markedly with the repetition of evolutionary patterns seen in the well-studied Hawaiian chain. (3) Spacings between calderas tend to be systematic and small (e.g., 6 and 18 km in the Executive Committee Range). Together with characteristic 2 (above), this constrains the size of magma chambers and the possible role of magma-driven fracture propagation mechanisms. (4) In aggregate, the MBL migrations appear to represent a contemporaneous displacement of activity from the center to the perimeter of the province, along north-south and east-west oriented linear ranges, such that the youngest volcanoes are now at the perimeter of the province and the oldest are near its center. This is shown in Figure B.XII by using different symbols for the oldest and youngest volcanoes.

In trying to assess the significance of this pattern the critical points are that plate motion cannot be a relevant factor, that the process responsible for the pattern must be one that affects the evolved rocks but has no influence on basaltic rocks, and that it must accommodate abrupt changes in magma composition from one volcano to the next along each chain. To explain this complex pattern, *LeMasurier and Rex* [1989*a*] have devised a multistage model that involves random rise of basaltic magma from the asthenosphere, entrapment of the largest volume batches within the crust, and systematic release of the differentiated magmas by tectonic reactivation of relict fracture sets. The centrifugal pattern of migration suggests that reactivation has been driven by crustal doming, centered in the Mount Flint–Mount Petras area (IVD's B.11 and B.16B). Although the pattern is complex and difficult to summarize briefly, the main point that is relevant to this province summary is that this linear pattern, like the pattern of age versus elevation, seems most likely to be understood by invoking explanations that are linked to rift evolution on a stationary plate.

In other rift provinces it has been postulated that tectonics and magmatism are driven by a rise of the asthenosphere/lithosphere boundary beneath the rift, accompanied by attenuation and doming of the continental lithosphere [*Eaton*, 1979; *Gass et al.*, 1978]. The isotopic composition of basaltic rocks in Marie Byrd Land is consistent with their derivation from the asthenosphere [*Futa and LeMasurier*, 1983], seismic data suggest attenuation of the crust beneath the axial part of the rift system [*Bentley*, 1973; *Cooper et al.*, 1982], and the elevation of basement rock at Mount Petras is consistent with the doming postulated to explain the migration patterns of post 15-Ma volcanic activity. This mechanism has therefore been adopted as a conceptual framework for rift evolution and magmatism in Marie Byrd Land that can be tested by continuing petrologic studies.

ACKNOWLEDGMENTS

Work in Marie Byrd Land was supported by NSF grants DPP 77-27546 and DPP 80-20836. I am grateful to I.G. Gass for a thorough and very helpful review of this entire section and to P.D. Rowley, J.L. Smellie, and J.W. Thomson for reviews of various parts of the section.

Copyright American Geophysical Union

Copyright American Geophysical Union

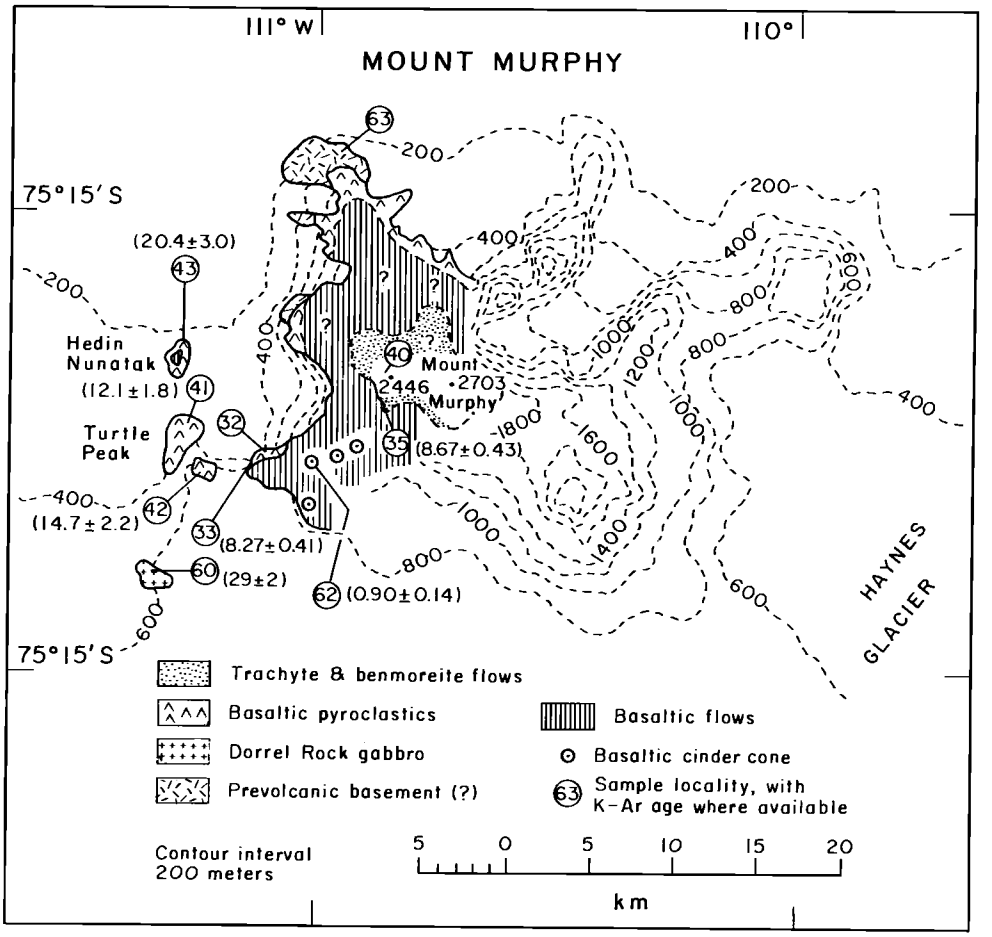

Fig. B.1.2. Geologic sketch map of Mount Murphy and neighboring nunataks. Geology is by W.E. LeMasurier; base map is the Mount Murphy quadrangle (1973), scale 1:250,000 USGS Reconnaissance Series, Antarctica, U.S. Geological Survey.

A pre-Cenozoic age is tentatively assigned to these rocks because the extent of alteration is fairly typical of the Mesozoic volcanic suite in this region. None of the samples are suitable for dating or chemical analysis. If the age inference is correct, then the estimated volume of 580 km^3 should be close to the true volume of Mount Murphy volcano, and the estimated proportion of felsic rocks may also be reasonably accurate.

The lower 200–250 m of the basal succession consists of hyaloclastites and palagonitized Strombolian tephra with subordinate interbedded subaerial flows, all grouped in Figure B.1.2 as basaltic pyroclastics; tillite occurs at the base of one hyaloclastite bed within this part of the section. The next 700 m of section, up to about the 1350-m level, is predominantly subaerial basaltic flow rock with occasional (and inaccessible) interbedded yellow tuffs. Only subaerial flow rock was found above 1350 m. The record suggests that this volcano grew up through an ice sheet, the level of which fluctuated through a range of at least 200–250 m during the eruptive history of the volcano.

Nearly all of the area above 2000 m is part of the main summit area of Mount Murphy proper, and it may represent a small felsic cone built on top of the main basalt shield. If this is true, then the total volume of felsic rock is between 11 and 18 km^3, or between 1.5% and 2.5% of the total volume of the volcano, and is quantitatively appropriate for fractionation from a basalt parent. This is the only volcano in Marie Byrd Land where it has been possible to estimate directly the proportion of felsic rock. The volume of exposed felsic rock is much larger in several of the other major volcanoes (e.g., Mount Berlin, Mount Sidley, Mount Bursey, Toney Mountain, Mount Takahe, and the Ames Range), but the volume of basaltic rock beneath each of them is unknown.

Basaltic cinder cones are common around the southwest ridge of Mount Murphy, much more so than could be

Copyright American Geophysical Union

TABLE B.1.1. Representative Chemical Analyses and CIPW Norms of Volcanic Rocks From Mount Murphy

	1	2	3	4	5	6	7
SiO_2	45.08	45.13	46.19	46.26	55.00	55.52	60.17
TiO_2	4.16	4.20	2.22	2.61	1.41	1.38	0.45
Al_2O_3	13.69	13.62	13.76	13.89	18.02	18.29	17.35
Fe_2O_3	4.43	3.81	2.91	1.72	3.64	5.31	5.67
FeO	10.64	11.24	9.60	10.49	4.82	3.12	1.28
MnO	0.26	0.26	0.15	0.20	0.24	0.21	0.19
MgO	5.36	5.50	11.87	9.44	1.54	1.42	0.17
CaO	10.53	10.35	9.53	9.90	5.50	5.48	1.79
Na_2O	2.91	3.05	3.04	3.26	5.90	5.97	7.38
K_2O	0.68	0.66	0.79	0.77	2.37	2.38	4.00
P_2O_5	0.96	0.95	0.42	0.42	0.52	0.67	0.08
H_2O^+	--	--	0.20	--	--	--	--
H_2O^-	0.39	0.18	--	--	0.29	--	1.08
F	0.05	0.06	0.03	0.03	0.03	0.06	0.03
Total	99.86	99.81	100.62	98.96	99.60	100.07	99.61
Q	--	--	--	--	--	1.17	--
or	4.02	3.90	4.67	4.55	14.01	14.06	23.64
ab	24.62	25.81	19.43	20.73	49.92	50.52	61.04
an	22.29	21.53	21.57	20.99	15.69	16.09	2.40
ne	--	--	3.40	3.71	--	--	0.76
di	19.38	19.40	18.48	20.65	6.79	5.24	0.91
wo	--	--	--	--	--	--	2.20
hy	7.78	4.87	--	--	0.48	1.11	--
ol	4.07	7.57	23.44	19.90	2.91	--	--
mt	4.42	5.52	4.22	2.49	5.28	6.74	3.44
il	7.90	7.98	4.22	4.96	2.68	2.62	0.85
hm	--	--	--	--	--	0.66	3.30
ap	2.22	2.20	1.00	0.97	1.20	1.55	0.19
Ba	1350	1398	222	168	1087	1173	1276
Ce	80	71	56	61	123	115	165
Co	47	50	--	54	10	5	--
Cr	28	25	514	337	4	--	--
Cu	65	66	--	68	12	18	6
Ga	19	21	--	19	24	23	30
La	40	34	24	20	68	61	96
Nb	29	31	26	28	80	74	127
Ni	15	21	285	195	5	4	4
Pb	6	6	--	5	7	7	7
Rb	8	9	11	14	37	41	70
Sr	584	590	533	622	648	661	140
Th	4	2	--	--	5	11	14
U	2	--	1	--	--	--	3
V	386	388	231	252	54	56	14
Y	31	32	22	23	40	38	59
Zn	113	106	--	83	86	72	118
Zr	154	149	156	153	285	310	617

All 1985 (85-) samples analyzed by XRF at University of Nottingham, England; FeO determined by potassium dichromate titration and F by selective ion electrode (SIE). Sample 67-62 analyzed by wet chemistry by H.B. Wiik, Geological Survey of Finland. Dashes, not detected.

1. 85-32G. Basalt, main shield, Mount Murphy.
2. 85-32B. Basalt, main shield, Mount Murphy.
3. 67-62. Basalt, parasitic cone.
4. 85-38. Basalt, parasitic cone.
5. 85-35C. Benmoreite, main shield at 1900-m level.
6. 85-40A. Benmoreite, main shield summit.
7. 85-40B. Trachyte, main shield summit.

Copyright American Geophysical Union

represented in Figure B.1.2. No ultramafic nodules were found.

Petrologic Characteristics

The basal succession basalts are unusual in being *hy*-normative. Samples 32B and 32G (Table B.1.1) are representative of seven analyzed basal succession rocks, five of which are *hy*-normative. Elsewhere in the MBL province, among 105 analyzed basaltic rock samples, only three are *hy*-normative: one of two from Patton Bluff (see individual volcanic description (IVD) B.16C), one of four from the Fosdick Mountains (see IVD B.16E), and one of seven from Mount Siple (see IVD B.5). No felsic or intermediate rocks have yet been found at these latter three localities.

The analyzed felsic and intermediate rocks at Mount Murphy include four benmoreites and two trachytes, all collected from three widely separated and stratigraphically different localities. These are represented by three analyses in Table B.1.1. Most unusual for this province is the fact that no peralkaline rocks were found here. The only other major volcanoes in Marie Byrd Land where peralkaline rocks have not yet been found are Mount Siple (see IVD B.5) and Mount Steere (see IVD B.4), both of which are virtually unexplored. It is also unexpected that one of the trachytes is *ne*-normative. One might have expected *Q*-normative felsic rocks to be associated with *hy*-normative basalts [*Coombs*, 1963].

All of the analyzed parasitic cone basalts are *ne*-normative, which sets them apart from the basal succession basalts. They also have higher Mg numbers and 10 times higher Ni content than the main shield lavas. Sample 62 has the most primitive petrochemical characteristics of any analyzed sample in this province, i.e., Mg# = 0.70, $^{87}Sr/^{86}Sr$ = 0.70288, and $^{143}Nd/^{144}Nd$ = 0.51288 [*Futa and LeMasurier*, 1983]. It also displays the small positive Eu anomaly that is characteristic of basalts and basanites in Marie Byrd Land [*LeMasurier et al.*, 1976]. Mineral compositions for this sample are given in Table B.1.2.

Chronologic Data

K-Ar dating of this volcano is still in progress, but representative dates from completed analyses are given in the geologic map shown in Figure B.1.2. All dates shown are from the main shield volcano lavas except sample 62, which is from a parasitic cone. The data suggest that the shield-building stage, including basal succession and felsic cone lavas, took place during a relatively brief time interval in the late Miocene, at about 8–9 Ma. The one dated parasitic cone lava was apparently erupted in the Pleistocene, following roughly 7.5 m.y. of quiescence. None of the parasitic cones occurs in a posterosional location, where field relations could serve as a check on the validity of the date, and this is the only volcano in the province where the depth of erosion provides an opportunity for this relationship to be seen. However, it seems common in this province for basaltic parasitic cone activity to have taken place sporadically for 5–10 m.y. after the shield-building stage, as, for example, at Mount Andrus (see IVD B.12), Mount Bursey (see IVD B.13), Mount Cumming (see IVD B.7), and the Mount Flint–Reynolds Ridge volcano (see IVD B.11).

The late Miocene ages obtained so far from Mount Murphy suggest that its period of most vigorous activity was contemporaneous with the eruption of basal succession rocks in the Crary Mountains (see IVD B.4), 230 km to the

TABLE B.1.2. Chemical Compositions of Minerals in Basalt 62A, Mount Murphy Volcano

	Olivine			Augite	Plagioclase	Oxide 1	Oxide 2
	P Core	P Rim	G	G	G	G	G
SiO_2	39.35	38.07	37.51	47.80	53.11	0.19	2.05
TiO_2	0.03	0.04	0.06	2.49	0.19	2.25	23.06
Al_2O_3	0.05	0.07	0.05	5.83	28.87	22.25	4.37
Cr_2O_3	0.01	0.03	0.03	0.25	0.01	30.79	2.09
FeO*	17.38	23.84	25.99	8.64	0.80	31.34	65.37
MnO	0.39	0.34	0.35	0.14	0.00	0.19	0.47
MgO	42.72	36.90	35.74	13.43	0.16	11.36	2.08
CaO	0.31	0.40	0.49	21.00	12.36	0.02	0.36
Na_2O	0.00	0.05	0.04	0.48	4.24	0.05	0.13
K_2O	0.00	0.02	0.02	0.04	0.28	0.00	0.01
Total	100.24	99.76	100.28	100.10	100.02	98.44	99.99
Analysis	1	2	18	17	7	21	24

Analyses by Y. Kawachi, University of Otago, New Zealand, by WDS (wavelength dispersive) electron microprobe. G, groundmass. P, phenocryst.

*Total Fe expressed as FeO.

Copyright American Geophysical Union

southwest. The basal succession at nearby Toney Mountain (see IVD B.3) appears to be about 0.5 m.y. older, but the error bars at all three localities overlap each other, and there are not enough dates to define the chronologies clearly. Nevertheless, late Miocene time seems to have been a period of voluminous basalt volcanism in this sector of Marie Byrd Land, coincident with a time of continental glaciation [*LeMasurier et al.*, 1986*b*].

Extent of Knowledge

Mount Murphy was first described from aerial photographs taken in 1947 and is named for Robert Cushman Murphy, who studied the wildlife of South Georgia during the 1912–1913 summer. It was first visited for about 5 hours on January 6, 1968, during a helicopter-supported reconnaissance. Localities 62 and 63 were visited, as well as Dorrel Rock and Turtle Peak. A more thorough study was undertaken in January 1985. During a 4-day period, 11 localities were visited from the base to the summit of the southwest ridge. A total of 19 analyses and four K-Ar dates are available.

Bibliography

Andrews and LeMasurier, 1973
Futa and LeMasurier, 1983
González-Ferrán and González-Bonorino, 1972
González-Ferrán and Vergara, 1972
LeMasurier, 1972*a, b, c*
LeMasurier and Rex, 1982*a,b*
LeMasurier et al., 1976, 1986*b*
McIntosh et al., 1985

Copyright American Geophysical Union

Copyright American Geophysical Union

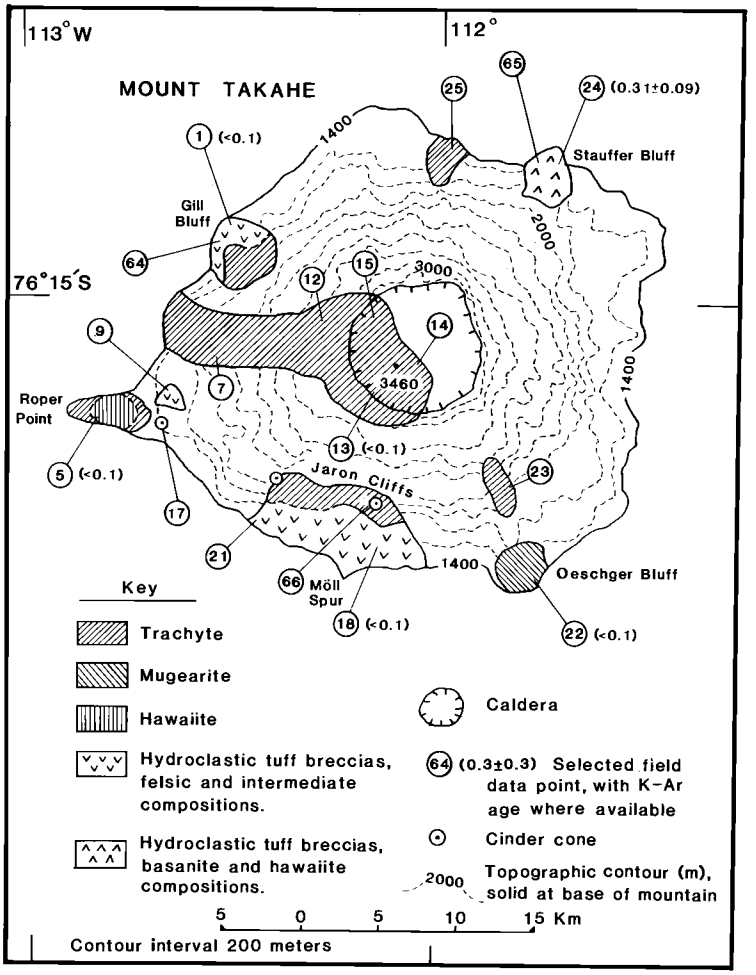

Fig. B.2.2. Geologic sketch map of Mount Takahe. Geology is by W.E. LeMasurier; base map is the Mount Takahe quadrangle (1972), scale 1:250,000 USGS Reconnaissance Series, Antarctica, U.S. Geological Survey. Circled numbers are field locality numbers from 1967 and 1985 expeditions.

Hydroclastic deposits, welded Strombolian spatter, and heterolithic lahar deposits are found locally but seem everywhere to be subordinate to lava. No magmatic pyroclastic rocks have been found. Radial fissure vents have been identified on the volcano flanks, and other fissure vents occur along the west rim of the caldera, where they appear to have been controlled by ring fractures.

The latest stage of activity is represented by cinder cones, on the upper flanks of the volcano (localities 21 and 66), and by tuff cones and tuff-cone/cinder-cone transitional structures on the lower flanks (localities 9, 17, and top of 24). Slightly elevated outcrops in the center of the summit caldera may represent the top of a postcaldera trachyte dome.

Petrologic Characteristics

A total of 42 chemical analyses clearly indicate that the compositional range at Mount Takahe is bimodal and that surface exposures are dominated by peralkaline trachyte (Table B.2.1; Figure B.2.4). Basanite has been found only in late-stage cinder cones and tuff cones, and the hawaiite samples are all from Roper Point and Stauffer Bluff. The latter locality has yielded the oldest K-Ar dates (0.31 Ma) at Mount Takahe. These dates, and analogies with other Marie Byrd Land volcanoes, suggest the possibility that hawaiite

Fig. B.2.3. (opposite) Subaerial to intraglacial facies transition at Gill Bluff. Subhorizontal trachyte flows on the left pass laterally into distally dipping flow foot breccias on the right. The flow foot breccias include isolated, elongated, unfragmented pillows roughly 4 m long, with thick (3–6 cm) glassy margins, interbedded with palagonitized trachytic hyaloclastite characterized by blocky, nonvesicular vitric clasts. The passage (transition) zone here is roughly vertical, suggesting that the transition was controlled by ice walls at the interface between the volcanic pile and the continental ice sheet. Good subglacial drainage of meltwater is implied, in marked contrast to classic flow foot breccias (and table mountains), where a static waterline is represented by a horizontal passage zone [*Jones and Nelson*, 1970]. Vertical relief shown is 300–400 m. Note figures in the lower right for scale.

Copyright American Geophysical Union

Copyright American Geophysical Union

TABLE B.2.1. Representative Chemical Analyses of Volcanic Rocks From Mount Takahe

	1	2	3	4	5	6	7
SiO_2	46.34	48.13	52.20	59.35	59.90	59.94	60.90
TiO_2	2.85	2.00	2.32	1.03	0.86	1.10	0.38
Al_2O_3	17.45	17.15	15.98	14.74	14.74	16.62	6.42
Fe_2O_3	3.46	3.24	2.11	1.65	1.62	2.26	4.25
FeO	9.97	9.55	8.32	7.36	6.84	5.31	9.71
MnO	0.22	0.25	0.25	0.30	0.32	0.26	0.63
MgO	4.59	4.00	3.53	0.60	0.40	0.76	0.03
CaO	8.57	7.57	6.58	2.20	1.63	1.86	0.62
Na_2O	4.37	4.81	4.55	7.27	7.59	5.64	11.80
K_2O	1.34	2.02	2.12	4.73	4.94	4.10	3.70
P_2O_5	0.80	0.57	0.66	0.28	0.16	0.23	0.13
H_2O^+	0.69	0.75	--	--	--	0.79	--
H_2O^-	0.09	0.07	--	--	--	0.18	--
F	--	--	0.05	0.04	0.03	0.05	0.38
CO_2	0.00	0.00	--	--	--	0.00	--
Total	100.74	100.11	99.57	99.46	99.38	99.10	99.81
Ba	766	641	3196	1044	399	1733	81
Ce	125	141	73	178	183	192	1112
Co	28	32	18	7	0	3	6
Cr	6	6	42	0	7	13	0
Cu	26	25	34	6	4	5	11
Ga	21	21	23	28	33	36	48
La	38	65	42	98	96	87	614
Nb	41	53	36	109	121	136	581
Ni	6	0	21	2	4	5	12
Pb	3	7	8	10	11	15	52
Rb	19	33	19	61	72	102	388
Sr	735	560	611	88	17	54	12
Th	3	0	4	10	17	14	97
U	0	0	0	2	3	2	20
V	258	218	163	31	21	30	0
Y	36	46	33	63	66	59	350
Zn	100	141	83	168	171	170	809
Zr	196	259	178	477	536	650	3536

All trace elements and major elements for all 1985 (85-) samples analyzed by XRF at University of Nottingham, England; FeO determined by potassium dichromate titration and F by selective ion electrode (SIE). Major elements for all 1967 (67-) samples determined by wet chemistry by H.B. Wiik, Geological Survey of Finland. Dashes, not determined.

1. 67-65B. Basanite, Stauffer Bluff.
2. 67-67A. Hawaiite, Roper Point.
3. 85-22c. Mugearite, Oeschger Bluff.
4. 85-18c. Trachyte, Möll Spur.
5. 85-13A. Trachyte, obsidian, west rim of caldera (Bucher Rim).
6. 67-65c. Trachyte, Stauffer Bluff.
7. 85-25A. Trachyte(?), Knezevich Rock.

may be more abundant in the interior and stratigraphically lower parts of the volcano than in surface exposures.

The hawaiites and basanites contain normative *ne*, but nepheline is rarely seen in thin section. Modal analyses show an occurrence range of 3–9% for phenocrysts, mainly plagioclase, with lesser amounts of olivine and titanomagnetite. The groundmass includes plagioclase, titanaugite, 2–9% olivine, and opaque minerals (Table B.2.2).

The dominant characteristics of the felsic rocks are peralkalinity and silica saturation. Among the 28 analyzed felsic rocks, all but three are peralkaline, with agpaitic indices ranging up to 3.65. They are almost equally divided

Copyright American Geophysical Union

TABLE B.2.2. Representative CIPW Norms and Modal Analyses of Volcanic Rocks From Mount Takahe

	1	2	3	4	5	6	7
			CIPW Norms				
Q	0.00	0.00	0.00	0.00	0.00	3.39	14.49
C	0.00	0.00	0.00	0.00	0.00	0.08	0.00
or	7.92	11.94	12.53	27.95	29.19	24.54	21.87
ab	26.44	26.92	38.50	44.64	45.86	51.30	12.42
an	24.05	19.24	16.92	0.00	0.00	7.83	0.00
ne	5.70	7.46	0.00	2.63	1.33	0.00	0.00
ac	0.00	0.00	0.00	4.77	4.69	0.00	12.30
ns	0.00	0.00	0.00	1.54	2.46	0.00	17.10
di	10.94	12.14	9.49	7.96	6.20	0.00	1.98
wo	5.53	6.09	0.00	0.00	0.00	0.00	0.00
hy	0.00	0.00	6.39	0.00	0.00	7.72	17.40
ol	12.63	11.78	5.80	7.42	7.26	0.00	0.00
mt	5.02	4.70	3.06	0.00	0.00	2.39	0.00
hm	0.00	0.00	0.00	0.00	0.00	0.00	0.00
il	5.41	3.80	4.41	1.96	1.63	1.55	0.72
ap	1.90	1.35	1.53	0.65	0.37	0.49	0.30
			*Modal Analyses**				
Phenocrysts, %							
Plag	7.0	1.2				--	
Ca-Cpx	--	0.2				--	
Oliv	0.3	0.8				--	
Opaq	0.1	--				--	
Groundmass, %							
Plag	51.4	19.8				--	
Alk fsp	--	--				66.0	
Ca-Cpx	15.0	1.2				--	
Na-Cpx	--	--				7.6	
Amph	--	--				15.1	
Oliv	9.0	5.6				7.2	
Opaq	15.8	--				0.4	
Glass/matr	1.6	71.2				3.7	
% Phenocrysts	7.8	7.6				0	

Dashes, not detected.
*Based on 500 counts. Analyses by W.E. LeMasurier and R.M. Burke.
1. 67-65B. Basanite, Stauffer Bluff.
2. 67-67A. Hawaiite, Roper Point.
3. 85-22c. Mugearite, Oeschger Bluff.
4. 85-18c. Trachyte, Möll Spur.
5. 85-13A. Trachyte, obsidian, west rim of caldera (Bucher Rim).
6. 67-65c. Trachyte, Stauffer Bluff.
7. 85-25A. Trachyte(?), Knezevich Rock.

between *Q*-normative (up to 14.26%) and *ne*-normative (up to 8.97%) varieties. Most samples have less than 5% *Q* or *ne*.

In a volcano dominated by moderately peralkaline, silica-saturated trachytes the one sample in the phonolite field (Figure B.2.4) stands out conspicuously as an example of extreme peralkalinity and also of the ambiguities of the classification scheme. It has an agpaitic index of 3.65, and with 14.49% normative *Q* it clearly does not belong among phonolites (see Table B.2.2, sample 85-25A). The very high concentrations of incompatible elements (Table B.2.1), coupled with extreme iron enrichment, indicate that it is a highly evolved product of fractional crystallization and belongs among pantellerites, yet its SiO_2 content and differentiation index are too low to be included among the

Copyright American Geophysical Union

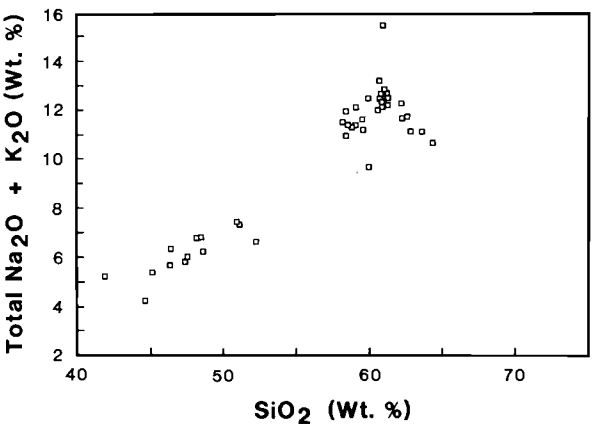

Fig. B.2.4. Alkali versus silica plot of 42 analyzed samples from Mount Takahe.

rhyolites of any common classification scheme. Only one other sample among the 28 felsic analyses could be viewed as transitional between this extreme composition and the bulk of Mount Takahe trachytes. This is also the most extreme example of peralkalinity yet found in Marie Byrd Land. Its occurrence at Mount Takahe, rather than at Mount Andrus (see IVD B.12), where pantellerites are much more common, suggests a somewhat unpredictable aspect to the environment in which pantellerites evolve, as suggested earlier by *Coombs* [1963].

All felsic samples contain alkali feldspar, green soda-iron pyroxenes, brown amphiboles, and opaque minerals. Most contain small amounts of olivine. Phenocrysts occur in amounts less than 5% and may include a large proportion of feldspar or virtually none. Other phenocryst minerals include green pyroxenes, olivines, magnetite(?), and apatite. One cognate inclusion contains 6% sodalite.

Chronologic Data

A late Quaternary age for Mount Takahe was indicated by the K-Ar ages of three samples collected during the 1967–1968 reconnaissance [*LeMasurier,* 1972*a, c*], and this has been confirmed by recently completed results from the 1984–1985 field season. Among 12 new dates the oldest is 0.31 ± 0.09 Ma (Figure B.2.2), and the remainder are all younger than 0.1 Ma (LeMasurier and Rex, unpublished data, 1987). This suggests a remarkably short time interval for the shield-building stage compared with those for other volcanoes in this province (cf. Mount Berlin (see IVD B.15), Mount Andrus (see IVD B.12), and Mount Bursey (see IVD B.13)). These dates also suggest that there was one time period, possibly two, within the past 100,000 years when the ice sheet stood approximately 300 m higher than it does now.

The very young K-Ar ages and the large size of the volcano suggest that Mount Takahe is still active [*LeMasurier and Rex,* 1982*b*]. However, no fumarolic activity, warm ground, or other evidence of recent activity has been observed. *LeMasurier* [1972*c*] and *Kyle et al.* [1981] have suggested that some tephra layers in ice cores from Byrd Station (80°S, 120°W) and Dome C (77°S, 120°E) were derived from eruptions of Mount Takahe, on the basis of the petrographic and chemical characteristics of vitric and crystal clasts in the ash layers and on consideration of atmospheric circulation patterns. If this is true, it would indicate eruptions within the past 30,000 years.

Extent of Knowledge

One locality was visited (Figure B.2.2, locality 17) and described by the 1957–1958 Marie Byrd Land Traverse party [*Anderson,* 1960]. Four additional localities (Figure B.2.2, localities 5, 64, 65, and 66) were visited briefly during a 1967–1968 helicopter reconnaissance [*LeMasurier,* 1972*a, b*]. From December 1984 to January 1985 all accessible exposures were visited during an intensive 3-week period [*McIntosh et al.,* 1985], making it now the most thoroughly studied volcano in the Marie Byrd Land province. Preliminary chemical and K-Ar data from the 1984–1985 season are presented here for the first time.

Mount Takahe was named by members of the 1957–1958 Marie Byrd Land Traverse party, who, in December 1957, were the first people to visit the mountain. The takahe is a nearly extinct flightless bird native to New Zealand, and its name was applied as a nickname to the U.S. Navy LC-47 aircraft that resupplied the traverse party.

Bibliography

Anderson, 1960
González-Ferrán and González-Bonorino, 1972
González-Ferrán and Vergara, 1972
Kyle et al., 1981
LeMasurier, 1972*a, b, c*
LeMasurier and Rex, 1982*a, b*
LeMasurier and Wade, 1976
McIntosh et al., 1985

Copyright American Geophysical Union

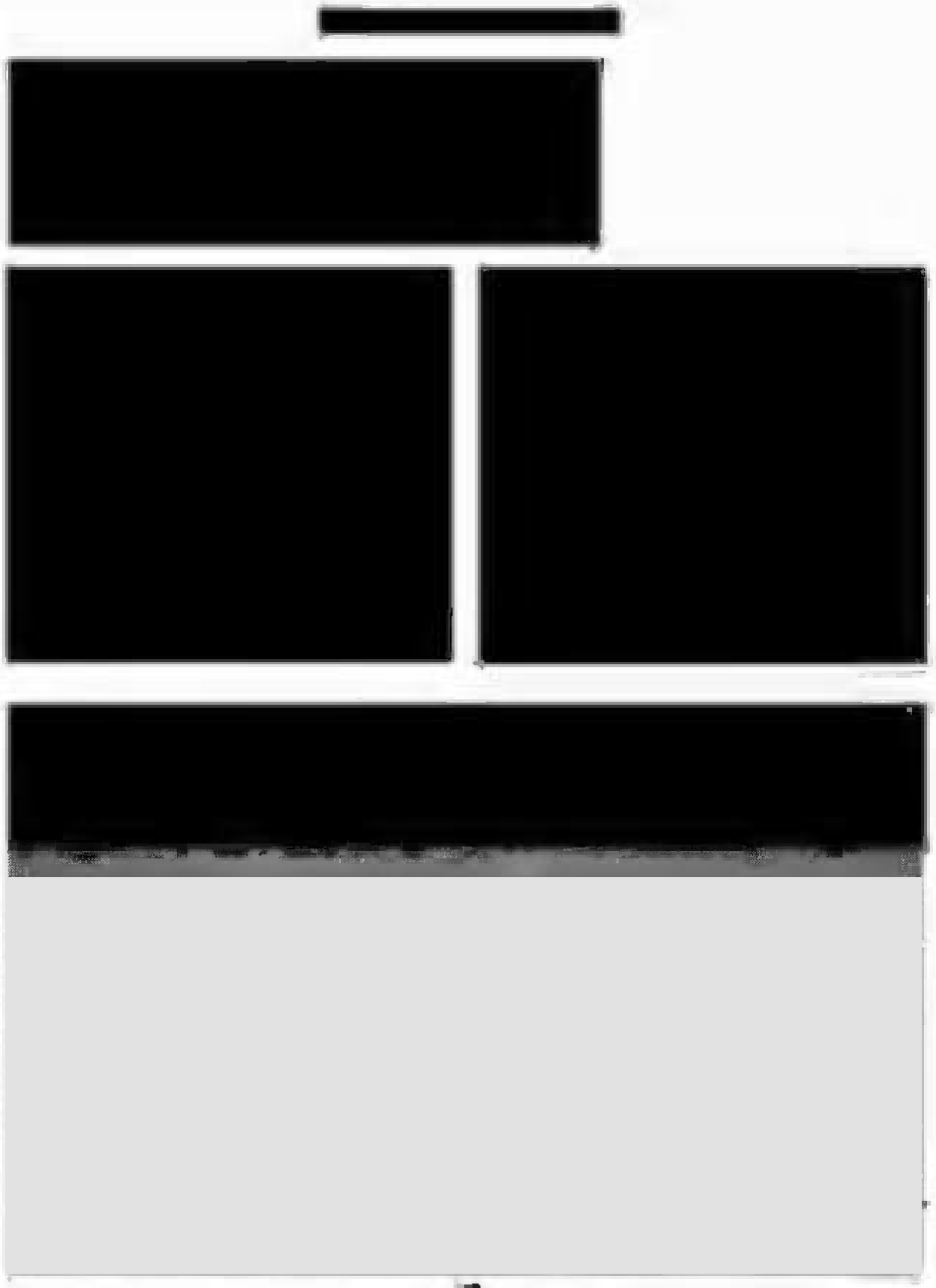

Copyright American Geophysical Union

Copyright American Geophysical Union

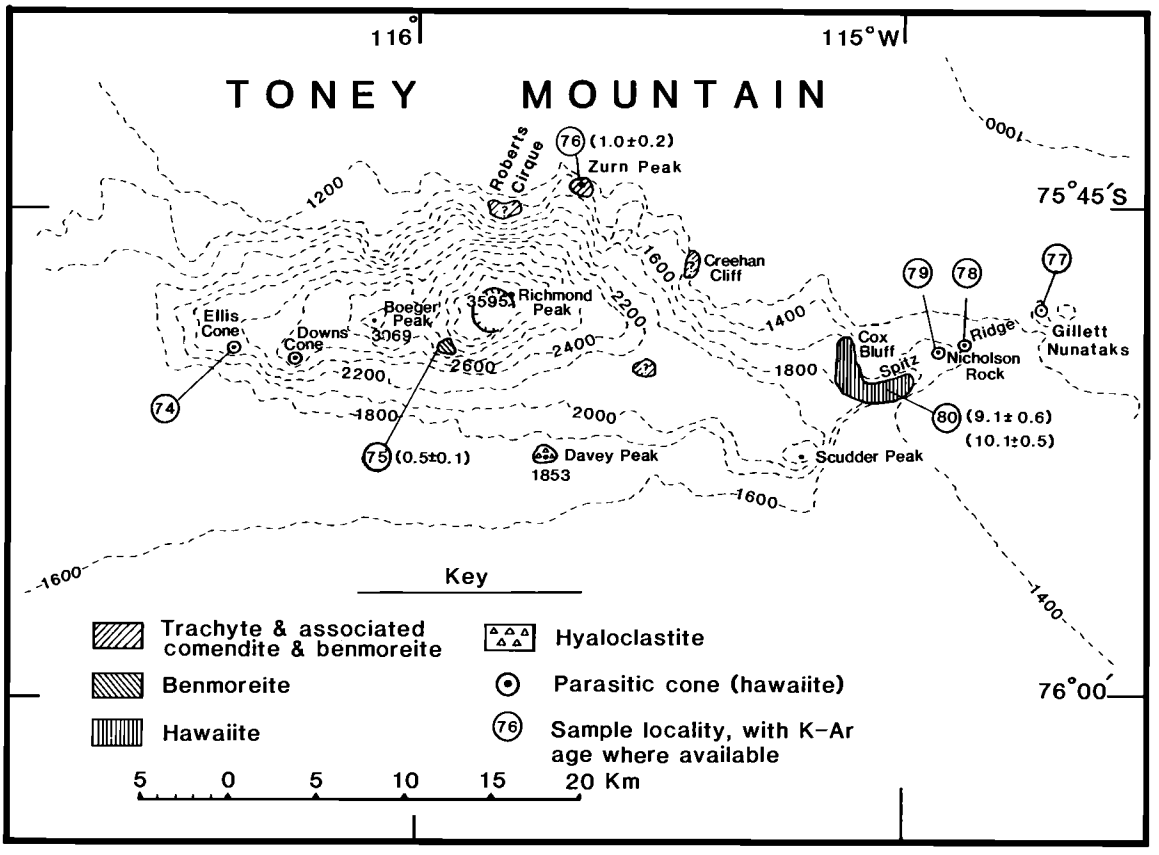

Fig. B.3.3. Reconnaissance geologic map of Toney Mountain. The possibility of fault-controlled boundaries, not shown here for lack of data, is discussed in the text in the section on form and structure. Geology is by W.E. LeMasurier; base map is the Toney Mountain quadrangle (1973), scale 1:250,000 USGS Reconnaissance Series, Antarctica, U.S. Geological Survey. Contour interval is 200 m.

phenocrysts and less so in olivine. The large proportion of phenocrysts, and the predominance of olivine and plagioclase among them, suggest long residence times in a high-level magma chamber. Repeated influxes of new magma may be recorded by the complex resorption phenomena.

The chemical characteristics of the felsic cone are represented by samples from only two localities. These show a range of composition from nonperalkaline benmoreite and trachyte to weakly peralkaline (peralkalinity index of 1.17) comendite (Tables B.3.1 and B.3.2). The benmoreites and trachytes show a range in silica saturation from 1.8% normative *Q* to roughly equal proportions of normative *hy* and *ol*.

None of these samples contains modal quartz. The single comendite sample contains phenocrysts of alkali feldspar and brown amphibole that are set in a matrix of glass. The benmoreites and trachytes are characterized by phenocrysts of alkali feldspar, hortonolitic olivine, and clinopyroxenes that vary from lavender titanaugite to green augite (Tables B.3.3 and B.3.4). Some individual clinopyroxene phenocrysts are zoned from pale lavender cores to pale green rims. Brown amphibole phenocrysts and plagioclase megacrysts are occasionally seen; magnetite and apatite microphenocrysts are common. The groundmass mineral assemblage is the same as the phenocryst assemblage and includes, remarkably, minor amounts of olivine.

Chronologic Data

Three dates on the basal succession at Cox Bluff have yielded K-Ar ages of 9.1–10.1 Ma (Table B.3.5 [*LeMasurier*, 1972*a*, *c*]). The felsic cone has been dated at two localities, which yielded ages of 1.0 Ma at the base and 0.5 Ma on the upper slopes (Table B.3.5 and Figure B.3.3). Samples from the parasitic cones are not suitable for dating, because of fumarolic oxidation and large proportions of tachylitic glass.

There is a possibility that quartz and amphibole clasts in ash bands in the Byrd Station ice core were derived from eruptions of Toney Mountain within the past 30,000 years [*LeMasurier*, 1972*c*].

Copyright American Geophysical Union

TABLE B.3.1. Representative Chemical Analyses of Volcanic Rocks From Toney Mountain

	1	2	3	4
SiO_2	48.46	57.19	60.72	72.26
TiO_2	2.38	1.22	0.76	0.16
Al_2O_3	17.68	17.24	16.91	12.54
Fe_2O_3	1.55	3.78	1.90	1.87
FeO	9.56	4.53	3.56	1.70
MnO	0.19	0.19	0.14	0.07
MgO	6.04	1.69	0.55	0.09
CaO	8.47	4.10	3.13	0.27
Na_2O	3.99	5.25	6.14	6.11
K_2O	1.30	3.76	4.59	4.21
P_2O_5	0.52	0.52	0.20	0.02
H_2O^+	0.49	0.25	0.00	0.42
H_2O^-	0.07	0.01	0.00	0.00
F	0.07	0.10	0.04	0.00
CO_2	0.00	0.00	0.00	0.00
Total	99.79	99.83	98.64	99.72
Ba	399	1328	909	12
Ce	99	173	215	324
Co	35	21	--	0
Cr	133	0	21	6
Cu	44	25	--	4
Ga	20	34	--	44
La	40	83	76	137
Nb	59	94	89	424
Ni	66	4	8	8
Pb	6	7	--	53
Rb	32	84	90	420
Sr	600	314	260	4
Th	8	14	12	65
U	2	5	1	13
V	163	66	15	7
Y	32	79	66	276
Zn	69	109	--	396
Zr	229	550	816	2198

Major elements determined by wet chemistry by H.B. Wiik, Geological Survey of Finland. Trace elements analyzed by XRF at University of Nottingham, England. Dashes, not detected.

1. 80A. Hawaiite, Cox Bluff, Toney Mountain.
2. 75. Benmoreite, Toney Mountain.
3. 76A. Trachyte, Toney Mountain.
4. 76D. Comendite vitrophyre, Toney Mountain.

TABLE B.3.2. CIPW Norms and Modal Analyses of Table B.3.1 Samples

	1	2	3	4
		CIPW Norms		
Q	0.00	1.83	0.61	22.85
or	7.64	22.22	27.14	24.87
ab	29.36	44.40	55.19	41.06
an	26.35	12.38	5.03	0.00
ne	3.76	0.00	0.00	0.00
ac	0.00	0.00	0.00	5.41
ns	0.00	0.00	0.00	1.04
di	9.65	3.75	7.37	1.07
hy	0.00	5.89	1.19	2.65
ol	16.81	0.00	0.00	0.00
mt	1.61	5.48	1.99	0.00
il	3.30	2.32	1.06	0.30
ap	1.08	1.23	0.42	0.05
		*Modal Analyses**		
Phenocrysts, %				
Plag	4.8	17.0	23.2	--
Alk fsp	--	--	--	8.8
Ca-Cpx	5.2	--	--	--
Na-Cpx	--	2.0	--	--
Amph	--	--	--	0.2
Oliv	6.6	2.2	0.6	--
Groundmass, %				
Plag	45.8	58.0	58.4	--
Analc	--	--	0.4	--
Ca-Cpx	11.6	--	--	--
Na-Cpx	--	7.2	10.8	--
Apat	0.4	0.8	0.2	--
Oliv	15.0	3.6	1.0	--
Opaq	10.6	9.2	5.2	--
Glass/matr	--	--	0.2	91.0
% Phenocrysts	17.6	21.2	23.8	9.0

Dashes, not detected.

*Based on 500 counts. Analyses by W.E. LeMasurier and R.M. Burke.

1. 80A. Hawaiite, Cox Bluff, Toney Mountain.
2. 75. Benmoreite, Toney Mountain.
3. 76A. Trachyte, Toney Mountain.
4. 76D. Comendite vitrophyre, Toney Mountain.

Extent of Knowledge

Toney Mountain was first visited in December 1957 by an oversnow traverse party from Byrd Station and again by the 1959–1960 Byrd Station Traverse. A seismic refraction traverse across the west end of the massif in 1959–1960 has provided the only seismic information available for any of the Cenozoic volcanoes in Marie Byrd Land. Toney Mountain was visited again during the 1967–1968 helicopter-supported reconnaissance of Marie Byrd Land. Samples from the numbered localities in the map shown in Figure B.3.3 were all collected at that time. Toney Mountain is named for George R. Toney, scientific leader at Byrd Station in 1957.

Bibliography

Bentley and Clough, 1972
Doumani, 1960
Doumani and Ehlers, 1962
LeMasurier, 1972*a, b, c*
LeMasurier and Rex, 1982*b*, 1983
LeMasurier and Wade, 1976

Copyright American Geophysical Union

TABLE B.3.3. Representative Chemical Compositions of Minerals in Hawaiite (80A) From Toney Mountain

	Olivine			Plagioclase			Ilmenite	Magnetite	Augite		
	P Core	P Rim	G	P Core	P Rim	G	G	G	P Core	P Rim	G
SiO_2	39.83	35.59	35.05	55.65	53.67	54.96	0.26	0.31	47.42	48.53	46.18
TiO_2	0.00	0.04	0.07	0.06	0.15	0.16	51.97	27.13	3.58	2.54	4.00
Al_2O_3	0.05	0.01	0.04	27.54	27.92	27.53	0.07	0.91	4.76	3.68	5.41
Cr_2O_3	0.08	0.03	0.00	0.00	0.00	0.04	0.01	0.01	0.05	0.05	0.02
FeO*	13.42	30.97	40.51	0.34	0.64	0.59	44.01	67.88	9.87	10.12	10.06
MnO	0.19	0.59	0.91	0.04	0.01	0.00	0.77	0.82	0.20	0.22	0.14
MgO	46.25	32.25	23.10	0.06	0.07	0.05	2.47	1.56	11.66	11.99	11.29
CaO	0.31	0.29	0.47	9.90	11.17	11.14	0.06	0.08	22.26	22.01	21.80
Na_2O	0.03	0.00	0.05	5.72	5.26	5.19	0.06	0.05	0.60	0.55	0.67
K_2O	--	0.01	0.03	0.43	0.40	0.37	0.00	0.04	0.01	0.00	0.02
Total	100.16	99.79	100.21	99.74	99.29	100.01	99.67	98.79	100.41	99.68	99.58
Analysis	1	2	21	7	6	13	27	28	23	24	16

Analyses by Y. Kawachi, University of Otago, New Zealand, by WDS electron microprobe. Dash, not detected. G, groundmass. P, phenocryst.

*Total Fe expressed as FeO.

TABLE B.3.4. Representative Chemical Compositions of Minerals in Benmoreite (75) From Toney Mountain

	Feldspar			Olivine		Cpx (Green)	Hbl (Brown)	Oxide
	P Core	P Rim	G	P Core	P Rim	G	G	G
SiO_2	64.25	66.25	65.07	32.17	32.83	51.15	48.38	--
TiO_2	0.24	--	--	--	--	0.45	1.11	23.29
Al_2O_3	22.01	20.17	21.25	--	--	0.93	4.50	1.32
FeO*	--	--	--	51.45	52.51	15.18	18.62	72.77
MnO	--	--	--	1.88	2.03	0.61	0.64	0.96
MgO	--	--	--	14.12	12.98	10.05	12.16	0.22
CaO	2.76	1.20	2.49	0.33	0.17	21.80	9.63	--
Na_2O	7.07	7.21	7.99	--	--	0.29	2.68	--
K_2O	3.55	5.12	3.09	--	--	--	1.05	--
Total	99.88	99.95	99.89	99.95	100.52	100.46	98.77	98.56
Analysis	61	62	12	41	40	18	21	27

Analyses by Y. Kawachi, University of Otago, New Zealand, by WDS electron microprobe. Dashes, not detected. G, groundmass. P, phenocryst.

*Total Fe expressed as FeO.

TABLE B.3.5. K-Ar Dates of Volcanic Rocks From Toney Mountain

Sample	Comments	K, %	$^{40}Ar_R$	Vol. $^{40}Ar_R$, cm^3/g STP $\times 10^5$	Date, Ma
75	Trachyandesite	2.56	6.7	0.0042	0.5 ± 0.1
			10.2	0.0061	
76A	Trachyte, date on feldspars	1.21	3.0	0.0047	1.0 ± 0.2
80B	Basalt	1.26	53.6	0.0482	9.1 ± 0.6
			52.3		
80c	Basalt	1.24	47.5	0.0512	10.1 ± 0.5
			50.9	0.0468	

$^{40}Ar_R$, radiogenic ^{40}Ar. Decay constants used are $\lambda_\beta = 4.962 \times 10^{-10}\ yr^{-1}$, $\lambda_\epsilon = 0.581 \times 10^{-10}\ yr^{-1}$, and $^{40}K = 0.01167$ at. % [*Steiger and Jäger*, 1977]. Analyses by D.C. Rex, University of Leeds, England.

Copyright American Geophysical Union

B.4. CRARY MOUNTAINS

Type of volcano: Two felsic shield volcanoes on a platform of basaltic lava flows and pyroclastic rocks.

Location: Bakutis Coast sector (76°45′S, 117°50′W); includes Mount Frakes, Mount Steere, Mount Rees, and Boyd Ridge volcanoes.

Height: Mount Rees, 2709 m above sea level, 900 m above ice level; Mount Steere, 3558 m above sea level, 1800 m above ice level; Mount Frakes, 3654 m above sea level, 1900 m above ice level; Boyd Ridge, 2375 m above sea level, 800 m above ice level.

Estimated combined volume: 400 km^3.

Evidence of Holocene activity: None.

Authors of report: W.E. LeMasurier, Y. Kawachi, and D.C. Rex.

Dates of report: January 1983, revised August 1987.

Fig. B.4.1. Reconnaissance geologic map of the Crary Mountains. Geology is by W.E. LeMasurier; base map is the Crary Mountains quadrangle (1973), scale 1:250,000 USGS Reconnaissance Series, Antarctica, U.S. Geological Survey.

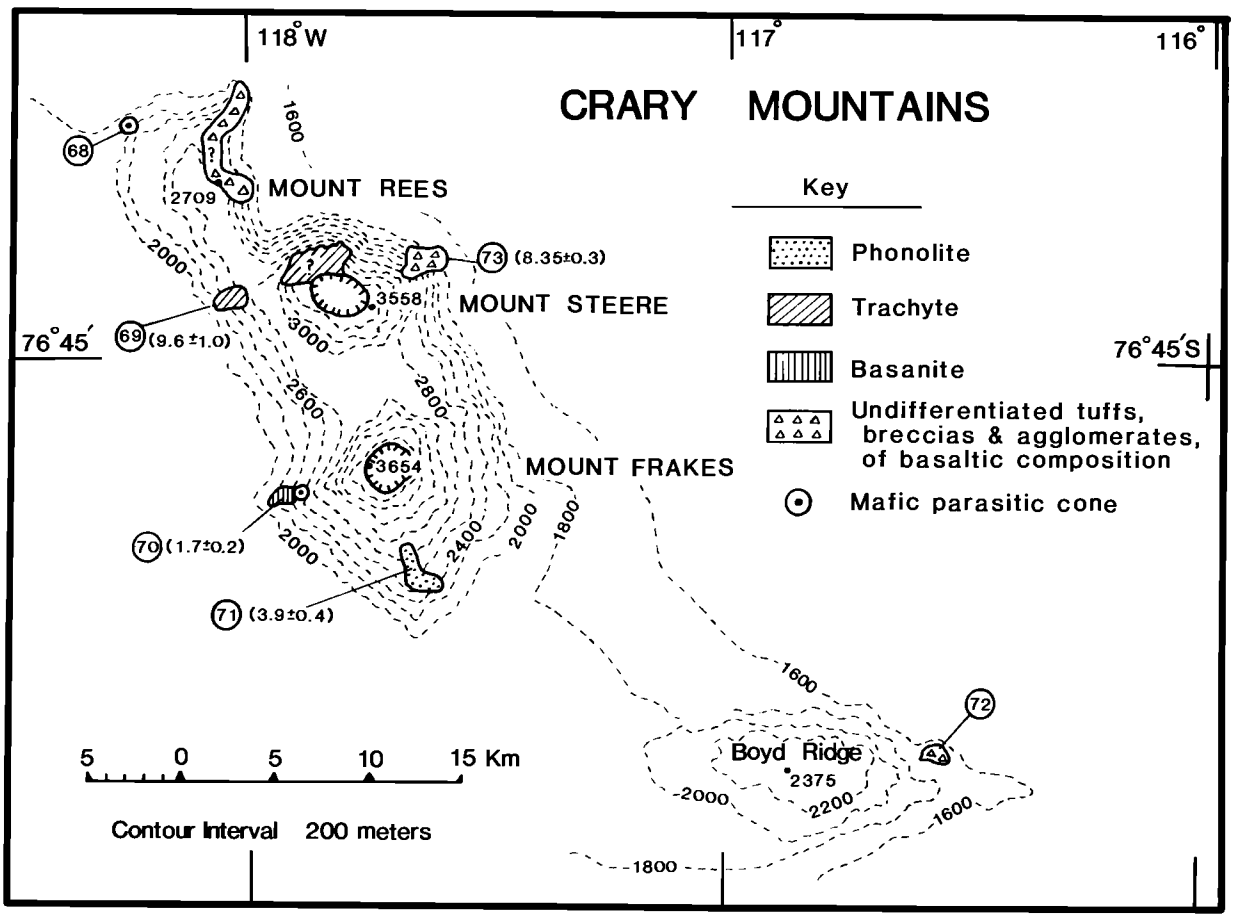

Copyright American Geophysical Union

Copyright American Geophysical Union

TABLE B.4.1. Chemical Analyses of Rocks From the Crary Mountains

	1	2	3	4
SiO_2	44.99	45.82	55.26	58.82
TiO_2	2.00	2.06	0.40	0.41
Al_2O_3	17.67	17.33	20.63	20.09
Fe_2O_3	11.75	2.80	3.31	5.00
FeO	3.46	8.29	2.96	1.11
MnO	0.21	0.20	0.24	0.13
MgO	3.85	8.10	0.57	0.44
CaO	8.43	8.67	1.40	2.64
Na_2O	4.47	4.29	10.06	7.69
K_2O	1.15	1.54	4.79	3.68
P_2O_5	0.23	1.04	0.19	0.18
H_2O^+	2.01	0.30	0.42	0.30
H_2O^-	0.30	0.00	0.00	0.00
F	0.00	0.10	0.16	0.07
CO_2	0.00	0.00	0.00	0.00
Total	100.52	100.54	100.39	100.56
Ba	330	369	400	969
Ce	78	96	248	134
Co	43	37	0	4
Cr	9	319	0	8
Cu	14	63	9	18
Ga	20	19	32	25
La	37	45	138	80
Nb	49	66	320	115
Ni	0	107	0	2
Pb	0	6	14	14
Rb	26	34	145	109
Sr	559	713	68	418
Th	2	1	28	19
U	0	0	7	6
V	295	205	12	13
Y	30	29	86	27
Zn	98	77	154	73
Zr	167	233	919	536

Major elements determined by wet chemistry by H.B. Wiik, Geological Survey of Finland. Trace elements analyzed by XRF at University of Nottingham, England.

1. 73. Basanite, Mount Steere.
2. 70. Basanite, Mount Frakes.
3. 71A. Phonolite, Mount Frakes.
4. 69A. Phonolitic trachyte, Mount Steere.

TABLE B.4.2. CIPW Norms and Modal Analyses of Table B.4.1 Samples

	1	2	3	4
		CIPW Norms		
or	6.80	9.10	28.30	21.74
ab	19.59	18.19	28.34	53.76
an	24.76	23.48	0.00	9.44
ne	9.87	9.80	27.68	6.11
ac	0.00	0.00	4.98	0.00
di	13.17	10.38	4.88	1.93
ol	16.50	20.56	2.13	2.18
mt	2.18	2.18	2.31	2.81
hm	0.00	0.00	0.00	3.06
il	3.80	3.91	0.76	0.78
ap	0.55	2.46	0.45	0.43
		*Modal Analyses**		
Phenocrysts, %				
Plag	0.0	3.4	0.0	0.0
Alk fsp	0.0	0.0	24.2	11.2
Neph	0.0	0.0	2.0	0.0
Cpx (lavender)	0.0	0.4	0.0	0.0
Cpx (green)	0.0	0.0	0.2	0.4
Oliv	0.0	5.8	0.2	0.6
Opaq	0.0	0.0	0.2	1.2
Groundmass, %				
Plag	37.4	32.6	0.0	0.0
Alk fsp	0.0	0.0	11.6	47.0
Cpx	21.2	8.6	0.4	3.2
Oliv	0.0	8.0	0.0	0.0
Opaq	21.4	26.4	0.6	16.4
Glass/matr	3.4	14.8	60.6	10.8
Alter	16.4	0.0	0.0	9.2
% Phenocrysts	tr	9.6	26.8	13.4

tr, trace.

*Based on 500 counts. Analyses by W.E. LeMasurier and R.M. Burke.

1. 73. Basanite. Mount Steere.
2. 70. Basanite, Mount Frakes.
3. 71A. Phonolite, Mount Frakes.
4. 69A. Phonolitic trachyte, Mount Steere.

The single accessible outcrop of felsic rock on the lower western flank of Mount Steere is composed of metaluminous phonolitic trachyte (Table B.4.1). Petrographically, it is composed of alkali feldspar, augite, and olivine phenocrysts set in a turgid matrix of opaque-charged glass. An uncorrected $^{87}Sr/^{86}Sr$ ratio of 0.7030 has been obtained for this sample [*LeMasurier and Wade,* 1976].

The basal succession and parasitic cones are both composed of basanite, judging from only two chemical analyses and five thin sections. These rocks contain close to 10% normative *ne* and are composed, in most cases, of a few percent of fresh olivine phenocrysts and variably resorbed plagioclase and clinopyroxene phenocrysts, all set in a groundmass of plagioclase, olivine, titanaugite, opaque minerals, and glass. Sample 70 (Table B.4.1) has a small positive Eu anomaly [*LeMasurier et al.,* 1976] and an

Copyright American Geophysical Union

TABLE B.4.3. Representative Chemical Compositions of Minerals in Anorthoclase Phonolite From Mount Frakes

	Feldspar			Nepheline	Cpx	Oxide	
	P Core	P Rim	M	M	M	M	Glass
SiO_2	66.51	65.19	67.00	46.79	51.34	--	49.68
TiO_2	0.14	--	--	--	0.16	18.18	--
Al_2O_3	21.03	21.41	20.21	32.55	0.82	1.33	28.71
FeO*	--	--	--	0.51	16.47	74.10	2.64
MnO	--	--	--	--	0.91	1.56	--
MgO	--	--	--	0.17	7.39	0.48	0.30
CaO	1.22	1.82	0.58	0.28	21.86	--	0.72
Na_2O	8.52	8.05	7.60	16.41	0.64	--	15.36
K_2O	3.18	3.17	4.95	3.66	--	--	3.35
Total	100.61	99.64	100.34	100.37	99.59	95.65	100.76
Analysis	12	11	37	30	8	20	4

Analyses by Y. Kawachi, University of Otago, New Zealand, by EDS (energy dispersive) electron microprobe. Dashes, not detected. P, phenocryst. M, microphenocrysts.

*Total Fe expressed as FeO.

TABLE B.4.4. K-Ar Ages of Rocks From the Crary Mountains

Sample	Locality	Comments	K, %	$^{40}Ar_R$	Vol. $^{40}Ar_R$ cm^3/g STP $\times 10^{-5}$	Age, Ma
70a	Mount Frakes	Basalt	1.34	9.4	0.0078	1.7 ± 0.2
				13.9	0.0061	
71A	Mount Frakes	Phonolite, dated on	3.55	48.4	0.0597	3.9 ± 0.4
		nepheline and		45.9	0.0487	
		anorthoclase		50.1	0.0537	
73	Mount Steere	Basalt	0.97	47.0	0.0331	8.35 ± 0.3
				38.0	0.0321	
69A	Mount Steere	Trachyte, dated on	1.62	41.9	0.0658	9.6 ± 1.0
		feldspar		51.4	0.0557	

$^{40}Ar_R$, radiogenic ^{40}Ar. Decay constants used are $\lambda_\beta = 4.962 \times 10^{-10}$ yr^{-1}, $\lambda_\varepsilon = 0.581 \times 10^{-10}$ yr^{-1}, and $^{40}K = 0.01167$ at. % [*Steiger and Jäger*, 1977]. Analyses by D.C. Rex, University of Leeds, England.

initial $^{87}Sr/^{86}Sr$ ratio of 0.70271 [*Futa and LeMasurier*, 1983]. Both of these characteristics are common among basanites in Marie Byrd Land.

Although the data are limited at this volcanic center, the petrologic relationships appear to be similar to those at the much better exposed Mount Hampton (see IVD B.6). In both cases, phonolitic rocks are associated with basanites, and no rocks have been found that are intermediate between these extreme compositions.

Chronologic Data

The K-Ar ages from the basal succession at Mount Steere (sample 73) and from the presumably stratigraphically higher and younger felsic rock (sample 69) are in conflict with the inferred geological relationships, as noted earlier (Figure B.4.1 and Table B.4.4). This probably cannot be resolved satisfactorily until it is possible to collect new material and study the field relations in more detail. The basal succession basanite has been analyzed in two different laboratories and yielded a similar K-Ar age [*LeMasurier and Rex*, 1982*a*]. The data suggest that Mount Steere was active in the interval 8–10 Ma (late Miocene) and is probably therefore substantially older than Mount Frakes. The 3.9-Ma date at Mount Frakes is from a phonolite flow near the base of the mountain, where the oldest lava flows usually crop out, suggesting that shield building was a middle to late Pliocene event. Cinder-cone activity 2 m.y. later (sample 70a) is consistent with the relationship between cinder-cone and shield-building activity observed at many Marie Byrd Land volcanoes.

Copyright American Geophysical Union

Extent of Knowledge

The Crary Mountains were first visited during the 1959–1960 Byrd Station Traverse; the team visited "the few accessible outcrops" on the south, west, and north sides of the range by means of oversnow tracked vehicles [*Doumani,* 1960; *Doumani and Ehlers,* 1962; *Boudette and Ford,* 1966]. A 1-day helicopter reconnaissance was conducted in January 1968. All points visited and sampled during that reconnaissance are numbered in Figure B.4.1; cliff exposures, viewed only in helicopter passes, are queried where shown in the figure. The Crary Mountains are named for Albert P. Crary, deputy chief scientist for the U.S.-IGY Antarctic Program in 1957–1958.

Bibliography

Boudette and Ford, 1966
Doumani, 1960
Doumani and Ehlers, 1962
Futa and LeMasurier, 1983
LeMasurier, 1972*a, b*
LeMasurier and Rex, 1982*a*, 1989*a*
LeMasurier and Wade, 1976
LeMasurier et al., 1976

Copyright American Geophysical Union

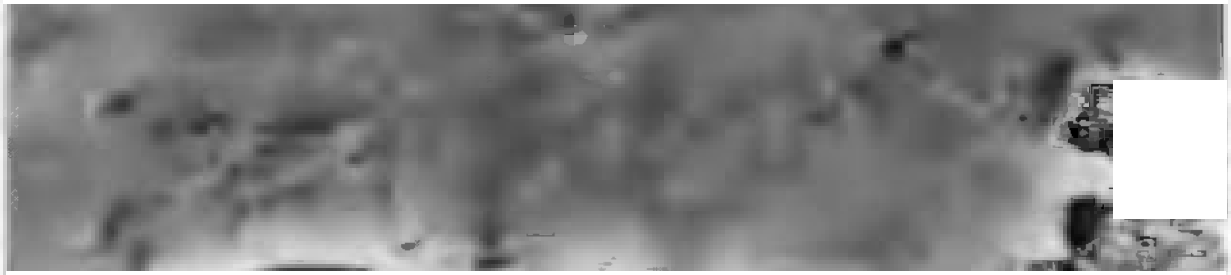

Copyright American Geophysical Union

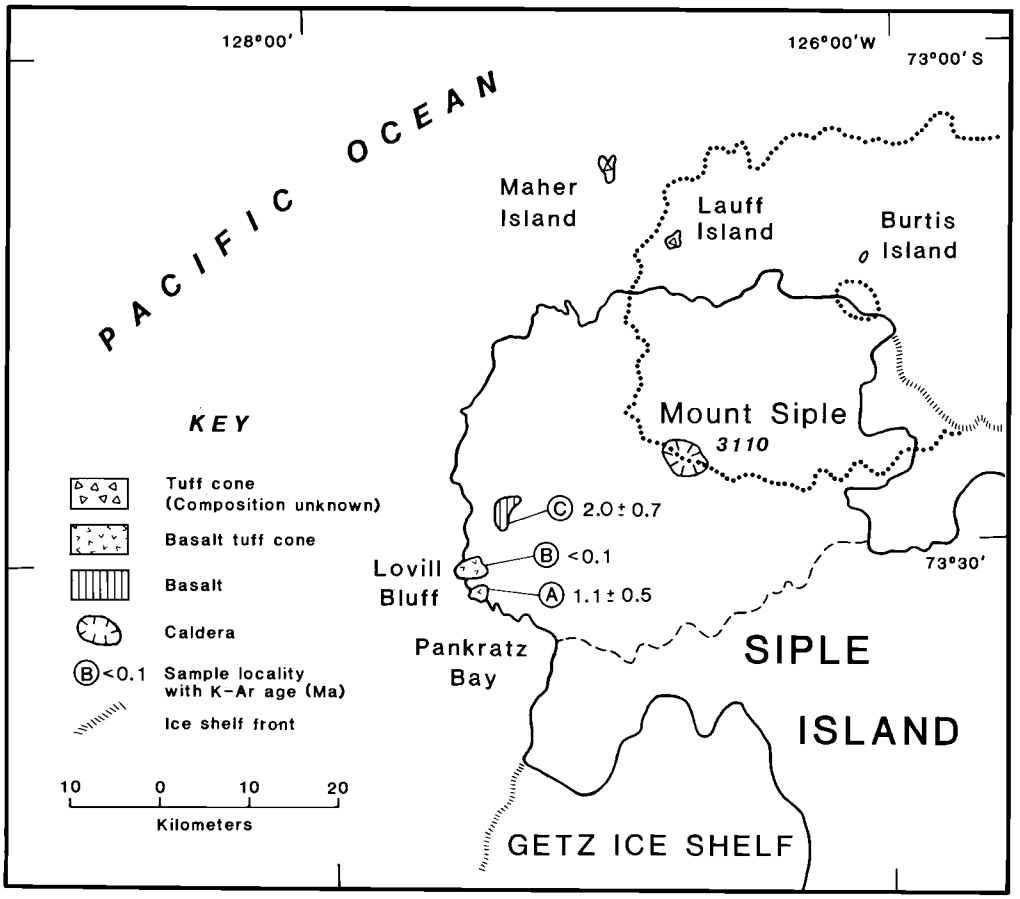

Fig. B.5.2. Geologic sketch map of Mount Siple; the only localities that have been visited are A, B, and C. Maher Island and Lauff Island were observed at close range with binoculars. Geology is by W.E. LeMasurier; K-Ar ages are from LeMasurier and Rex (unpublished data, 1989). Base map is Antarctica Sketch Map Hobbs Coast–Byrd Land (1965), scale 1:500,000, U.S. Geological Survey. Revised geographic coordinates, corrected to 1984 U.S. Geological Survey observations (Kelmelis, unpublished data, 1985), are shown. The position of Mount Siple volcano, as it appears on published maps, is shown by dotted lines. The dashed line represents the inferred contact between volcanic rock and prevolcanic basement, estimated from computer-enhanced satellite imagery (courtesy of B.K. Lucchitta). Note that the corrected coastal profile and the revised positions of Maher, Lauff, and Burtis islands are not shown.

observations of nearby Maher and Lauff islands, indicate that tuff cones are common at sea level and just beyond the shoreline of Mount Siple, presumably as a result of Surtseyan eruptions from satellitic vents.

One hundred and fifty meters above sea level a 30-m thickness of subhorizontal basalt flows was observed at locality C (Figure B.5.2). At sea level on the south side of the tuff cone at locality A, one third of the beach cobbles were found to be composed of coarse-grained basaltic flow rock, apparently derived from a short distance upslope. These observations suggest that the lower portion of the main Mount Siple volcano is a basaltic shield volcano analogous to Mount Murphy (see IVD B.1). Although no localities near the summit have been visited, it is likely that felsic flow rocks make up the summit portion of the volcano, again by analogy with the other major volcanoes in Marie Byrd Land.

Petrologic Characteristics

All of the samples available from Mount Siple are basalt. Analyses of samples that are believed to be from the main shield volcano are listed in Table B.5.1 (see samples W83-6A-2 and W83-5). Sample W83-5 is particularly

Copyright American Geophysical Union

TABLE B.5.1. Chemical Analyses and CIPW Norms of Volcanic Rocks From Mount Siple

	1	2	3	4
SiO_2	45.46	47.03	47.11	48.98
TiO_2	3.21	2.80	2.75	1.77
Al_2O_3	15.15	15.11	15.90	14.74
Fe_2O_3	1.28	2.33	2.03	1.54
FeO	11.67	10.12	9.89	9.43
MnO	0.19	0.19	0.18	0.18
MgO	6.34	6.18	5.32	7.00
CaO	8.42	9.64	9.61	9.03
Na_2O	3.54	3.59	3.48	3.51
K_2O	1.42	1.06	1.30	1.13
P_2O_5	0.71	0.53	0.69	0.91
F	0.09	0.07	0.07	0.06
Total	97.38	98.58	98.27	98.22
or	8.39	6.26	7.68	6.68
ab	23.11	25.83	26.31	29.70
an	21.26	21.99	23.93	21.13
ne	3.71	2.46	1.70	0.00
di	13.13	18.38	15.88	14.54
hy	0.00	0.00	0.00	4.06
ol	18.22	13.73	13.00	14.41
mt	1.78	3.38	2.94	2.23
il	6.10	5.32	5.22	3.36
ap	1.64	1.23	1.60	2.11
Ba	338	256	286	322
Ce	100	71	94	100
Co	54	47	38	41
Cr	102	155	76	277
Cu	45	42	42	43
Ga	22	20	25	21
La	40	25	32	26
Nb	53	41	46	42
Ni	80	58	35	113
Pb	2	6	6	3
Rb	31	20	22	25
Sr	575	593	697	535
Th	0	1	1	7
U	0	0	3	0
V	163	216	180	132
Y	36	31	34	28
Zn	112	105	106	108
Zr	257	192	218	202

All samples analyzed by XRF at University of Nottingham, England; FeO determined by wet chemistry and F by selective ion electrode (SIE).

1. W83-1. Basalt, locality B, Lovill Bluff.
2. W84-119. Basalt, locality A, Lovill Bluff.
3. W83-6A-2. Basalt, locality A, beach cobble.
4. W83-5. Basalt, locality C.

noteworthy because in all of Marie Byrd Land, *hy*-normative basalts have been found only at Mount Siple, at Mount Murphy (see IVD B.1), and at two of the satellite centers (see IVD's B.16C and B.16E). Sample W83-5 is unusually low in TiO_2, especially in comparison with the Mount Murphy rocks, which are unusually high in TiO_2. There is a suggestion in these analyses that the late satellitic cones are more undersaturated than the main shield lavas, similar to the better documented relationship at Mount Murphy.

Chronologic Data

Although data are sparse, the results obtained from the February 1984 expedition suggest that Mount Siple is Pliocene to Quaternary in age. Distal flank exposures have consistently yielded the oldest dates from among the best documented Marie Byrd Land volcanoes (see, for example, IVD's B.2, B.12, B.13, and B.15). This suggests that locality C lavas (2.0 Ma) may be among the oldest at Mount Siple. Furthermore, the results of field and K-Ar studies at Mount Murphy (see IVD B.1) indicate that the coastal shield volcanoes here are more susceptible to erosion than the relatively undissected inland volcanoes. The lack of deep dissection of Mount Siple, when compared to Mount Murphy (8.3 Ma), is therefore consistent with its overall young age.

Mount Siple has been considered possibly active because of the young age of the main shield and the existence of a satellitic cone at Lovill Bluff that is too young to be dated (see Figure B.I). Satellite images suggesting sporadic eruptive activity during 1988 came recently to the author's attention. The best available images are presented in Figure B.5.3. An aerial inspection on December 30, 1988, found no evidence of fresh ash, new craters, or disruption of snowpack [*Smithsonian Institution*, 1988*b*]. Furthermore, monitoring of the satellite data by NASA for SO_2 emissions, for a period of one week after the October 4 plume sighting, failed to find an SO_2 signal above its 4 metric ton limit of detection (Walter, NASA Goddard Space Flight Center, oral communication, 1989).

Extent of Knowledge

Mount Siple was first visited on February 22, 1984 [*LeMasurier*, 1984]. Only three localities were visited (see Figure B.5.2) during a 1-day helicopter reconnaissance. Maher and Lauff islands were observed at close hand from shipboard, and two other rock exposures were photographed by Seaman A.R. Sullivan during a helicopter reconnaissance of ice conditions [*LeMasurier*, 1984]. It is estimated that roughly 80% of the accessible exposures at Mount Siple remain to be visited.

Mount Siple is named after Paul A. Siple (who originally named it Mount Ruth Siple, after his wife). He was a

Copyright American Geophysical Union

Copyright American Geophysical Union

Copyright American Geophysical Union

Copyright American Geophysical Union

TABLE B.6.1. Representative Chemical Analyses of Rocks From Mount Hampton and Whitney Peak Volcanoes

	Whitney Peak			Mount Hampton				
	1	2	3	4	5	6	7	8
SiO_2	55.41	62.08	62.89	44.60	45.75	55.49	55.60	56.21
TiO_2	1.20	0.58	0.45	3.33	1.90	2.22	0.20	0.75
Al_2O_3	15.04	15.66	15.97	13.27	17.11	19.01	17.80	18.43
Fe_2O_3	4.39	3.72	3.22	4.04	1.50	4.97	4.60	4.31
FeO	6.72	3.37	3.88	8.56	10.61	2.47	2.50	2.79
MnO	0.33	0.20	0.19	0.19	0.19	0.21	0.10	0.23
MgO	0.79	0.20	0.11	8.84	7.50	0.08	0.99	0.27
CaO	4.45	2.32	1.24	9.36	9.00	1.23	2.10	1.53
Na_2O	5.83	6.10	6.10	3.60	3.72	10.14	9.20	8.85
K_2O	3.31	5.02	4.83	1.30	1.60	4.95	4.80	5.28
P_2O_5	0.40	0.12	0.07	0.54	0.33	0.06	0.13	0.09
H_2O^+	--	--	1.02	--	0.63	1.50	0.50	--
H_2O^-	0.36	--	0.11	--	0.07	--	--	0.61
F	0.05	0.11	--	0.04	--	0.13	0.20	0.04
CO_2	--	--	--	--	--	--	0.30	--
Total	98.28	99.48	100.08	97.67	99.91	100.31	99.57	99.07
$^{87}Sr/^{86}Sr$ (initial)	--	--	--	--	0.70280	0.7047	--	--
Ba	1885	515	--	388	471	22	265	184
Ce	186	287	--	86	124	398	249	415
Co	--	--	--	--	47	16	5	--
Cr	0	30	--	222	249	0	5	0
Cu	--	--	--	--	49	9	11	--
Ga	--	--	--	--	19	56	36	--
La	62	96	--	34	60	181	129	152
Nb	76	126	--	46	77	388	208	342
Ni	8	9	--	102	123	3	3	17
Pb	--	--	--	--	5	17	13	--
Rb	46	113	--	25	41	176	145	174
Sr	385	147	--	999	765	12	203	51
Th	0	9	--	6	8	31	29	38
U	2	3	--	0	0	7	8	5
V	20	7	--	246	237	3	42	10
Y	55	81	--	27	39	138	82	136
Zn	--	--	--	--	103	291	171	--
Zr	422	834	--	213	317	2116	1466	2058

Major elements determined by wet chemistry by H.B. Wiik, Geological Survey of Finland. Trace elements analyzed by XRF at University of Nottingham, England. Dashes, not determined.

1. 23A. Benmoreite, Whitney Peak.
2. 23CA. Trachyte, Whitney Peak.
3. 24B. *Q*-trachyte, Whitney Peak.
4. 17. Basanite, parasitic cone, Mount Hampton.
5. 22D. Basanite, Mount Hampton.
6. 20b. Phonolite, Mount Hampton.
7. 25. Phonolite, Mount Hampton.
8. 21. Phonolite, Mount Hampton.

Copyright American Geophysical Union

TABLE B.6.2. Representative CIPW Norms and Modal Analyses of Rocks From Mount Hampton and Whitney Peak Volcanoes

	Whitney Peak			Mount Hampton				
	1	2	3	4	5	6	7	8
				CIPW Norms				
Q		3.50	5.29	--	--	--	--	
or	19.56	29.66	28.54	7.68	9.45	29.25	28.36	31.20
ab	48.70	51.62	51.59	19.11	14.90	22.77	28.35	29.43
an	5.10	0.53	1.94	16.21	25.27	--	--	
ne	0.34		--	6.15	8.97	25.71	19.76	19.49
ac			--	--	--	13.70	11.44	8.35
di	12.39	5.83	3.31	21.39	14.16	5.06	5.21	6.07
hy		1.46	2.60	--	--	--	--	
ol	2.21		--	13.66	19.92	1.48	2.12	0.50
mt	6.37	5.39	4.67	5.86	2.18	0.34	0.94	2.06
il	2.28	1.10	0.86	6.33	3.61	0.38	1.42	1.42
ap	0.95	0.28	0.17	1.28	0.78	0.14	0.31	0.21
				*Modal Analyses**				
Phenocrysts, %								
Plag			--	--	0.6	--	--	
Alk fsp			11.6	--	--	tr	8.2	
Cpx (lavender)			--	tr	--	--	--	
Cpx (green)			0.4	--	--	tr	0.2	
Amph			--	--	--	--	1.0	
Oliv			0.4	3.6	5.0	--	1.6	
Opaq			--	--	--	tr	1.0	
Groundmass, %								
Plag			--	22.0	28.4	--	--	
Alk fsp			39.0	--	--	20.0	41.6	
Cpx			22.4	20.0	19.6	29.0	33.6	
Amph			4.0	--	--	17.4	--	
Oliv			--	11.4	5.6	--	--	
Opaq			2.6	26.6	27.8	--	12.8	
Glass/matr			19.6	16.4	13.0	33.6	--	
% Phenocrysts			12.4	3.6	5.6	<1	12.0	

Dashes, not detected; tr, trace.

*Based on 500 counts. Analyses by W.E. LeMasurier and R.M. Burke.

1. 23A. Benmoreite, Whitney Peak.
2. 23CA. Trachyte, Whitney Peak.
3. 24B. *Q*-trachyte, Whitney Peak.
4. 17. Basanite, parasitic cone, Mount Hampton.
5. 22D. Basanite, Mount Hampton.
6. 20b. Phonolite, Mount Hampton.
7. 25. Phonolite, Mount Hampton.
8. 21. Phonolite, Mount Hampton.

Copyright American Geophysical Union

TABLE B.6.3. Representative Chemical Compositions of Minerals in Ultramafic Nodules From Mount Hampton

	Spinel Lherzolite (31b)				Websterite (17c)	
	Olivine	Diopside	Enstatite	Spinel	Bronzite	Augite
SiO_2	40.96	52.50	54.95	0.13	51.26	48.13
TiO_2	0.03	0.53	0.12	0.11	0.30	1.23
Al_2O_3	0.02	6.25	4.24	58.16	5.17	7.56
Cr_2O_3	0.00	0.74	0.24	9.02	0.05	0.08
FeO*	10.16	2.60	5.95	10.50	15.04	8.10
MnO	0.09	0.08	0.07	0.07	0.28	0.18
MgO	48.84	15.62	33.34	20.46	25.68	13.64
CaO	0.08	20.86	0.72	0.00	1.00	20.20
Na_2O	0.02	1.38	0.10	0.01	0.05	0.98
K_2O	0.01	0.04	0.03	0.00	0.01	0.00
NiO	0.42	0.10	0.05	0.39	0.10	0.05
Total	100.64	100.71	99.81	98.86	98.94	100.15
Analysis	3	8	11	1	9	6

All samples analyzed by Y. Kawachi, University of Otago, New Zealand, by WDS electron microprobe.

*Total Fe expressed as FeO.

benmoreite samples, consistent with the overall pattern shown for the Executive Committee Range. Isotopic study of Executive Committee Range rocks indicates initial $^{87}Sr/^{86}Sr$ values of 0.70272–0.70368 for basalts and hawaiites and 0.70268–0.71068 for mugearites, benmoreites, and all felsic rocks (Futa and LeMasurier, unpublished data, 1987). The published initial $^{87}Sr/^{86}Sr$ ratio for basanite sample 22D (Table B.6.1) is 0.70280 [*Futa and LeMasurier,* 1983], and for phonolite sample 20b (Table B.6.1) the value is 0.7047 [*LeMasurier and Wade,* 1976]. Preliminary conclusions from this work are that the basalt magmas were generated from a depleted mantle source area within the asthenosphere and that the mechanisms which produced the felsic magmas involved little or no contamination by the continental lithosphere. Figure B.VI*a* illustrates the unusual isotopic characteristics of the source area.

Chronologic Data

The K-Ar dates shown in Figure B.6.3 are from *LeMasurier and Rex* [1989*a*]. They indicate that Mount Hampton is younger than Whitney Peak, which is consistent with the morphology of the two volcanoes. All the dated Mount Hampton samples are phonolitic except for the parasitic cone basanite at locality 22, which yielded a date of 11.4 Ma. The dates suggest that the main period of activity at Mount Hampton was late Miocene. Large conical snow and ice towers on the caldera rim have been interpreted as dormant fumarolic ice towers [*LeMasurier and Wade,* 1968], suggesting the possibility of Holocene activity at Mount Hampton; such activity is not unprecedented among the Miocene volcanoes in Marie Byrd Land (cf. Mount Andrus). Ice towers are produced in a polar environment by condensation and freezing of vapors around an active fumarolic vent. (See Figure B.15.2 for an example of an active fumarolic ice tower.)

Felsic volcanic activity in the Executive Committee Range began at the Mount Hampton–Whitney Peak volcano and migrated southward in a manner that is characterized by systematic spacings between calderas and by systematic decreases in the ages of felsic rocks from Mount Hampton to Mount Waesche. This phenomenon appears to be related to tectonically induced fracture propagation, as discussed in detail by *LeMasurier and Rex* [1989*a*]. Felsic volcanoes in the Ames and Flood ranges (IVD's B.12–B.15) show similar characteristics.

Extent of Knowledge

Mount Hampton has been visited only once, in December 1967, by a helicopter-supported reconnaissance team that visited 10 localities in 2 days of fieldwork. Earlier descriptions of Mount Hampton were based on 1958–1960 U.S. Navy aerial photographs and an October 1959 aerial reconnaissance [*Doumani,* 1964].

The Executive Committee Range was discovered during a December 15, 1940, reconnaissance flight by the U.S. Antarctic Service Expedition and named for the executive committee of the expedition. Mount Hampton is named for Ruth Hampton, Department of the Interior, who was a member of the committee.

Copyright American Geophysical Union

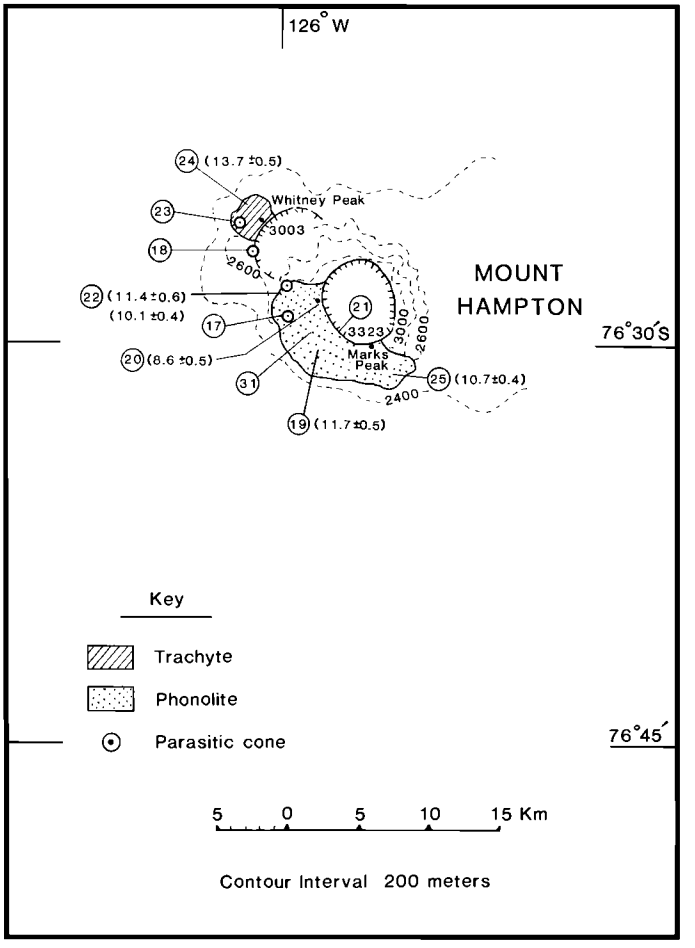

Fig. B.6.3. Geologic sketch map of Mount Hampton. Geology is by W.E. LeMasurier; K-Ar dates are from *LeMasurier and Rex* [1989*a*]. Base map is the Mount Hampton quadrangle (1960), scale 1:250,000 USGS Reconnaissance Series, Antarctica, U.S. Geological Survey.

Bibliography

Doumani, 1964
Futa and LeMasurier, 1983
González-Ferrán and González-Bonorino, 1972
González-Ferrán and Vergara, 1972
LeMasurier, 1972*a, b*
LeMasurier and Rex 1982*a, b*, 1989*a, b*
LeMasurier and Wade, 1968, 1976
LeMasurier et al., 1976

Copyright American Geophysical Union

Copyright American Geophysical Union

Form and Structure

Mount Cumming occurs as an isolated single caldera rim that barely projects above the level of the ice sheet in the central Executive Committee Range (Figure B.7.1). The 3.5-km diameter of the caldera and its elevation above sea level are comparable with the Ames Range and Mount Bursey cones, but Mount Cumming is much less exposed because of the high level of the continental ice sheet around the Executive Committee Range. All of the exposures at Mount Cumming are lava flows, which suggest that the volcano is a trachytic shield, at least in its summit region.

Petrologic Characteristics

The caldera rim exposures at Mount Cumming are composed of pantelleritic trachytes (Tables B.7.1 and B.7.2), with agpaitic indices between 1.05 and 1.35 and normative *Q* values between 2.3 and 7.5. Mount Cumming is the only occurrence of pantelleritic rocks in the Executive Committee Range. The major difference between these oversaturated rocks and the comenditic rocks found farther south, at Mount Hartigan (see IVD B.8) and Mount Waesche (see IVD B.10), is that total iron and the sum of normative femic minerals are considerably higher in the pantelleritic rocks than in the comendites. Complete rare earth element (REE) data have been obtained for one trachyte sample. It displays the expected negative Eu anomaly and an unusually high enrichment in light REE [*LeMasurier et al.*, 1976].

Petrographically, the trachytes contain a few phenocrysts of alkali feldspar, augite, equant opaque minerals (titanomagnetite?), and occasional iron-rich olivine, in a matrix of alkali feldspar, augite, equant opaque minerals, glass, and possibly a minor amount of aenigmatite.

The parasitic cone on the west flank of the volcano (Figure B.7.2, locality 26) is composed of olivine-phyric basanite with abundant inclusions of mafic and ultramafic nodules, including spinel lherzolite, websterite, chromite-bearing dunite (Table B.7.3), and troctolite. A sample of the basanite and one included lherzolite nodule have each been analyzed for Rb/Sr and Sm/Nd isotopic compositions and for REE. The REE pattern of the basanite is, like the mafic lavas elsewhere in the Marie Byrd Land province, similar to that of primary alkali basalts and nephelinites from oceanic islands, and its initial $^{87}Sr/^{86}Sr$ ratio is 0.70286 [*Futa and LeMasurier*, 1983]. The lherzolite has extremely low REE abundances, and in both isotopic systems it departs significantly in composition from its host lava and from all other analyzed basaltic rocks in the province (highest in $^{87}Sr/^{86}Sr$ and lowest in $^{143}Nd/^{144}Nd$); its initial $^{87}Sr/^{86}Sr$ ratio is 0.70317. The only other nodule-bearing localities in the Executive Committee Range are the basanite parasitic cones on Mount Hampton.

TABLE B.7.1. Chemical Analyses of Volcanic Rocks From Mount Cumming

	1	2	3	4
SiO_2	46.07	60.80	62.90	64.20
TiO_2	2.48	0.58	0.55	0.50
Al_2O_3	14.22	14.40	13.17	12.60
Fe_2O_3	1.50	4.40	1.50	6.90
FeO	10.15	5.50	6.85	1.30
MnO	0.16	0.17	0.24	0.06
MgO	8.95	0.22	0.02	0.09
CaO	9.11	2.60	1.61	1.30
Na_2O	4.11	6.30	6.78	6.90
K_2O	1.58	4.40	4.91	5.20
P_2O_5	0.56	0.09	0.05	0.02
H_2O^+	0.74	0.50	--	0.05
H_2O^-	--	--	0.48	--
F	0.09	0.08	0.16	0.23
Total	99.72	100.04	98.74	99.35
Ba	389	3354	113	80
Ce	109	133	506	311
Co	45	6	--	--
Cr	370	--	8	--
Cu	69	5	--	6
Ga	21	25	--	34
La	39	77	184	146
Nb	68	103	228	187
Ni	177	--	18	2
Pb	6	12	--	67
Rb	43	63	218	181
Sr	739	161	15	10
Th	6	10	39	28
U	4	3	3	5
V	230	18	4	14
Y	29	59	145	114
Zn	98	144	--	246
Zr	247	516	1568	1177

Major elements determined by wet chemistry by H.B. Wiik (sample 26A), Geological Survey of Finland, and by Skyline Laboratory, Denver, Colorado (samples 27A, 28, and 29). Trace elements analyzed by XRF at University of Nottingham, England. Dashes, not detected.

1. 26A. Basanite, Mount Cumming.
2. 28. Pantelleritic trachyte, Mount Cumming.
3. 29. Pantelleritic trachyte, Mount Cumming.
4. 27A. Pantelleritic trachyte, Mount Cumming.

Chronologic Data

The K-Ar data shown in Figure B.7.2 suggest that shield-building activity at Mount Cumming took place at 10

Copyright American Geophysical Union

TABLE B.7.2. CIPW Norms and Modal Analyses of Volcanic Rocks From Mount Cumming

	1	2	3	4	5
		CIPW Norms			
Q	--	2.26	5.52	7.47	
or	9.34	26.00	29.01	30.72	
ab	15.62	49.56	40.40	35.85	
an	15.69	--	0	--	
ne	10.37	--	--	--	
ac	--	3.28	4.34	19.83	
ns	--	--	2.78	--	
di	20.51	10.34	6.83	3.57	
wo	0.54	--	--	0.23	
hy	--	1.87	8.54	--	
ol	18.55	--	--	--	
mt	2.18	4.74	--	0.07	
il	4.71	1.10	1.05	0.95	
ap	1.33	0.21	0.11	0.05	
fr	--	0.16	0	0.47	
		*Modal Analyses**			
Phenocrysts, %					
Plag		--		--	0.4
Alk fsp		4.8		0.8	--
Cpx		tr		tr	--
Oliv		tr		--	3.8
Opaq		tr		--	--
Groundmass, %					
Plag		--		--	24.6
Alk fsp		45.6		58.2	--
Cpx		29.4		11.0	7.2
Amph		tr		3.8	--
Oliv		--		--	12.6
Opaq & Acc		4.6		1.6	14.2
Glass/matr		15.6		24.6	36.8
% Phenocrysts		4.8		0.8	4.2

Dashes, not detected; tr, trace.
*Based on 500 counts. Analyses by W.E. LeMasurier and R.M. Burke.
1. 26A. Basanite, Mount Cumming.
2. 28. Pantelleritic trachyte, Mount Cumming.
3. 29. Pantelleritic trachyte, Mount Cumming.
4. 27A. Pantelleritic trachyte, Mount Cumming.
5. 26B. Basanite, Mount Cumming.

Ma and was followed by a 7-m.y. period of dormancy prior to the formation of the basanite parasitic cone. This is consistent with the pattern of basaltic activity found in other volcanoes of this region, for example, Ames Range, Mount Bursey, and Mount Hampton.

Extent of Knowledge

Mount Cumming has been visited only once, on December 5, 1967, by a helicopter-supported reconnaissance team that visited five localities in 1 day of fieldwork.

Copyright American Geophysical Union

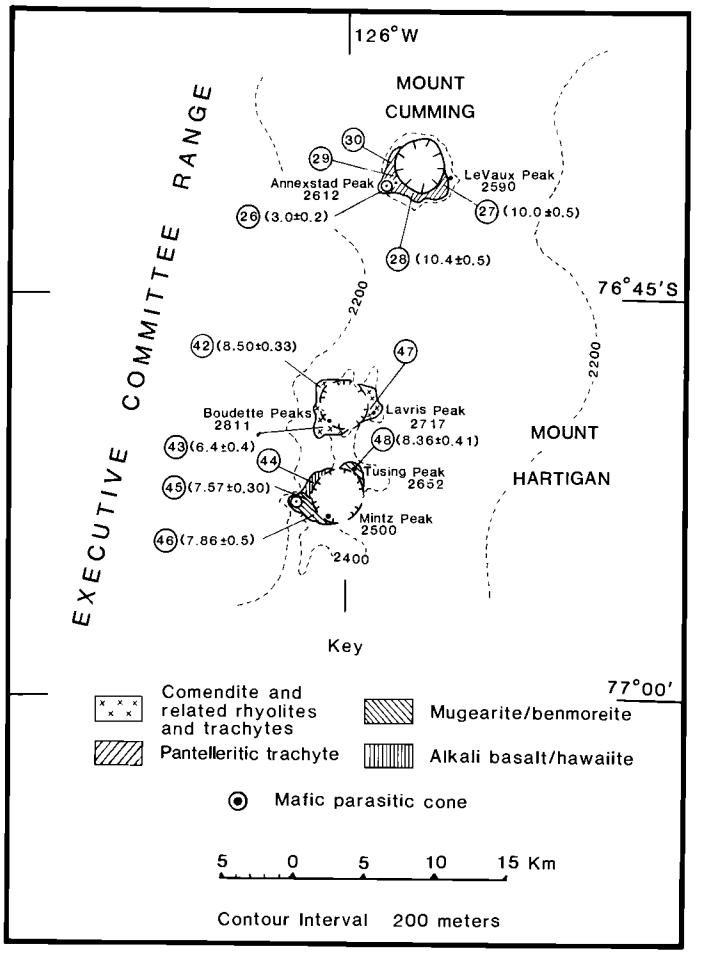

Fig. B.7.2. Geologic sketch map of Mount Cumming and Mount Hartigan. Geology is by W.E. LeMasurier; K-Ar dates are from *LeMasurier and Rex* [1989*a*]. Base map is the Mount Hampton quadrangle (1960), scale 1:250,000 USGS Reconnaissance Series, Antarctica, U.S. Geological Survey.

TABLE B.7.3. Representative Chemical Compositions of Minerals in Dunite 26A From Mount Cumming

	Olivine	Chromite	Pentlandite(?)
SiO_2	40.05	0.05	1.87
TiO_2	0.02	3.05	0.07
Al_2O_3	0.25	20.27	0.59
Cr_2O_3	0.03	37.53	1.50
FeO*	11.99	25.16	53.87
MnO	0.16	0.11	0.00
MgO	47.16	13.43	0.17
CaO	0.16	0.01	0.00
Na_2O	0.02	0.01	0.04
K_2O	0.00	0.00	0.00
NiO	0.38	0.29	19.64
Total	100.22	99.92	77.75
Analysis	4	7	11-3

All samples analyzed by Y. Kawachi, University of Otago, New Zealand, by WDS electron microprobe.

*Total Fe expressed as FeO.

Earlier descriptions of Mount Cumming were based on 1958–1960 U.S. Navy aerial photographs and an October 1959 aerial reconnaissance [*Doumani*, 1964].

Mount Cumming is named for Hugh S. Cumming, Jr., State Department member of the executive committee of the U.S. Antarctic Service Expedition (1939–1941).

Bibliography

Doumani, 1964
Futa and LeMasurier, 1983
González-Ferrán and González-Bonorino, 1972
González-Ferrán and Vergara, 1972
LeMasurier and Rex, 1989*a, b*
LeMasurier and Wade, 1976
LeMasurier et al., 1976

Copyright American Geophysical Union

Copyright American Geophysical Union

TABLE B.8.1. Representative Chemical Analyses of Volcanic Rocks From Mount Hartigan

	Southern Peak					Northern Peak		
	1	2	3	4	5	6	7	8
SiO_2	48.59	50.37	51.75	51.76	53.00	61.98	69.00	71.68
TiO_2	2.49	1.37	2.56	2.57	2.30	0.53	0.25	0.09
Al_2O_3	19.61	21.01	16.13	15.52	15.90	15.51	12.80	13.85
Fe_2O_3	3.84	6.69	5.35	4.12	3.80	5.02	4.10	1.61
FeO	6.92	4.36	6.45	6.97	7.40	2.45	0.04	0.86
MnO	0.18	0.21	0.21	0.19	0.11	0.23	0.02	0.03
MgO	3.20	2.31	2.85	2.90	3.20	0.62	0.02	0.07
CaO	8.40	5.62	7.12	7.33	7.10	2.51	0.52	0.20
Na_2O	3.99	5.06	4.58	4.33	4.70	5.87	6.30	5.00
K_2O	1.85	2.51	2.23	2.33	2.20	4.73	5.10	4.30
P_2O_5	0.32	0.48	0.60	0.63	0.50	0.08	0.00	0.05
H_2O^+	0.35	0.20	0.15	0.00	0.00	0.34	0.50	1.59
H_2O^-	0.03	0.05	0.07	0.00	0.00	0.18	0.00	0.96
F	0.08	0.10	0.00	0.07	0.11	0.00	0.24	0.18
CO_2	0.00	0.00	0.00	0.00	0.00	0.00	0.60	0.00
Total	99.85	100.34	100.05	98.72	100.43	99.72	100.19	100.40
Ba	381	673	2249	541	495	84	31	0
Ce	98	153	150	149	82	170	301	105
Co	25	18	3	--	28	7	0	16
Cr	40	15	0	29	21	0	0	0
Cu	56	19	8	--	48	4	0	3
Ga	28	26	27	--	25	32	37	38
La	51	63	88	15	8	68	104	51
Nb	61	78	102	61	53	148	195	213
Ni	8	0	0	15	8	0	0	3
Pb	10	13	16	--	7	157	38	34
Rb	46	51	106	60	45	205	216	333
Sr	475	437	177	421	450	10	8	3
Th	8	10	13	7	2	30	35	39
U	2	5	2	--	0	6	7	12
V	216	108	13	180	195	3	5	0
Y	39	50	70	46	35	63	81	127
Zn	88	137	149	--	90	146	202	159
Zr	319	455	634	304	248	576	1118	830

Major elements determined by wet chemistry by H.B. Wiik (samples 44A, 45B, and 47), Geological Survey of Finland, and by Skyline Laboratory, Denver, Colorado (48, 45C, 46B, 42A, and 43A). Trace elements analyzed by XRF at University of Nottingham, England. Dashes, not determined.

1. 45B. Hawaiite, southern peak, Mount Hartigan.
2. 44A. Mugearite, southern peak, Mount Hartigan.
3. 48. Mugearite, southern peak, Mount Hartigan.
4. 45C. Mugearite, southern peak, Mount Hartigan.
5. 46B. *Hy*-mugearite, southern peak, Mount Hartigan.
6. 42A. Trachyte, northern peak, Mount Hartigan.
7. 43A. Comendite, northern peak, Mount Hartigan.
8. 47. Rhyolite, northern peak, Mount Hartigan.

Copyright American Geophysical Union

TABLE B.8.2. Representative CIPW Norms and Modal Analyses of Volcanic Rocks From Mount Hartigan

	Southern Peak					Northern Peak		
	1	2	3	4	5	6	7	8
				CIPW Norms				
Q	--	--	0.29	0.40	--	5.80	17.1	25.67
C	--	0.90	--	--	--	--	--	0.73
or	10.93	14.82	13.18	13.77	13.07	27.95	30.10	25.41
ab	30.53	40.16	38.74	36.64	39.77	49.65	37.70	42.29
an	30.14	24.74	16.87	16.03	15.89	2.01	--	0.67
ne	1.74	1.44	--	--	--	--	--	--
ac	--	--	--	--	--	--	12.00	--
ns	--	--	--	--	--	--	0.50	--
di	7.73	--	11.76	13.32	13.31	3.33	--	--
wo	--	--	--	--	--	2.36	--	--
hy	--	--	4.98	6.20	4.63	--	--	0.33
ol	7.26	4.50	--	--	2.67	--	--	--
mt	5.57	9.70	7.76	5.97	5.51	7.11	--	2.33
hm	--	--	--	--	--	0.12	--	--
il	4.73	2.60	4.86	4.88	4.37	1.01	0.13	0.17
ap	0.74	1.11	1.42	1.46	1.16	0.19	--	0.12
fr	--	--	--	--	--	--	0.34	--
cc	--	--	--	--	--	--	0.30	--
				*Modal Analyses**				
Phenocrysts, %								
Plag	--	1.6			--		--	
Alk fsp	--	--			--		7.4	
Cpx	--	--			--		0.2	
Oliv	--	1.2			--		--	
Opaq	--	1.2			--		0.2	
Groundmass, %								
Qtz	--	--			--		2.8	
Plag	69.4	46.2			--		--	
Alk fsp	--	--			74.0		45.2	
Cpx	11.2	19.0			10.6		16.0	
Biot	--	3.4			--		--	
Apat	3.0	0.4			0.6		--	
Oliv	7.4	6.6			6.0		--	
Opaq	12.0	20.2			6.0		8.4	
Glass/matr	--	0.6			3.4		19.8	
% Phenocrysts	--	4.0			--		7.8	

Dashes, not present (norms), not detected (modes).
*Based on 500 counts. Analyses by W.E. LeMasurier and R.M. Burke.
1. 45B. Hawaiite, southern peak, Mount Hartigan.
2. 44A. Mugearite, southern peak, Mount Hartigan.
3. 48. Mugearite, southern peak, Mount Hartigan.
4. 45C. Mugearite, southern peak, Mount Hartigan.
5. 46B. *Hy*-mugearite, southern peak, Mount Hartigan.
6. 42A. Trachyte, northern peak, Mount Hartigan.
7. 43A. Comendite, northern peak, Mount Hartigan.
8. 47. Rhyolite, northern peak, Mount Hartigan.

Copyright American Geophysical Union

and similar to the preparasitic cone shield lavas at Mount Waesche (southern volcano) in chemistry and mineralogy. The more differentiated rocks appear to become less undersaturated with increasing differentiation, rather than more undersaturated, as is the case at Mount Waesche. Three of the four analyzed Mount Hartigan mugearites are *hy*-normative. All rocks of the southern volcano are composed of plagioclase, titanaugite, olivine, and opaque minerals. Titanaugite zoned to green iron-rich rims is found mainly in the mugearites. Minor amounts of biotite (<5%) occur in some of these lavas, mainly in the groundmass. Biotite is uncommon in Marie Byrd Land lavas, and Mount Hartigan is one of its major occurrences. Apatite is unusually abundant (up to 3%; see Table B.8.2) and commonly occurs as phenocrysts clustered with opaque titanomagnetite(?) microphenocrysts. Many of the southern volcano rocks have an unusually coarse grained (2–4 mm) equigranular texture, suggesting that they represent the interiors of thick ponded flows. The less common porphyro-aphanitic rocks contain phenocrysts of plagioclase and olivine, with lesser amounts of titanaugite, opaque minerals, and apatite totaling between 3% and 20% of the rock.

Rare earth element data have been obtained on three samples, a comendite, a metaluminous trachyte, and a mugearite. The comendite shows a large negative Eu anomaly, and the mugearite a small positive one, as is typical for the Executive Committee Range suite [*LeMasurier et al.,* 1976]. The trachyte is unusual in displaying a small positive Eu anomaly which, together with its very high Ba concentration (1600 ppm), suggests that feldspar fractionation was not a significant factor in its petrogenesis. The mugearite (sample 48) and a metaluminous rhyolite (sample 45C) are represented in Figure B.IX.

An initial $^{87}Sr/^{86}Sr$ ratio of 0.7033 has been obtained on one hawaiite (Table B.8.1, sample 45B), and a mugearite (sample 44A) yielded an initial ratio of 0.7036 [*LeMasurier and Wade,* 1976].

Chronological Data

Neither the morphology of the two Mount Hartigan volcanoes nor the K-Ar dates give a reliable indication that one is older than the other (see Figure B.7.2). They appear to have developed contemporaneously between 6.0 and 8.1 Ma. Mount Hartigan activity seems to be clearly older than the activity of Mount Sidley, to the south, and younger than the main period of activity at Mount Cumming, to the north.

Extent of Knowledge

Mount Hartigan has been visited once, on December 10, 1967, by a helicopter-supported reconnaissance team that visited seven localities in 1 day of fieldwork. Earlier descriptions of Mount Hartigan were based on 1958–1960 U.S. Navy aerial photographs and an October 1959 aerial reconnaissance [*Doumani,* 1964].

Mount Hartigan is named for Rear Admiral Charles C. Hartigan, U.S. Navy, Navy Department member of the executive committee of the U.S. Antarctic Service Expedition (1939–1941).

Bibliography

Doumani, 1964
González-Ferrán and González-Bonorino, 1972
LeMasurier and Rex, 1989*a, b*
LeMasurier and Wade, 1976

Copyright American Geophysical Union

Copyright American Geophysical Union

Copyright American Geophysical Union

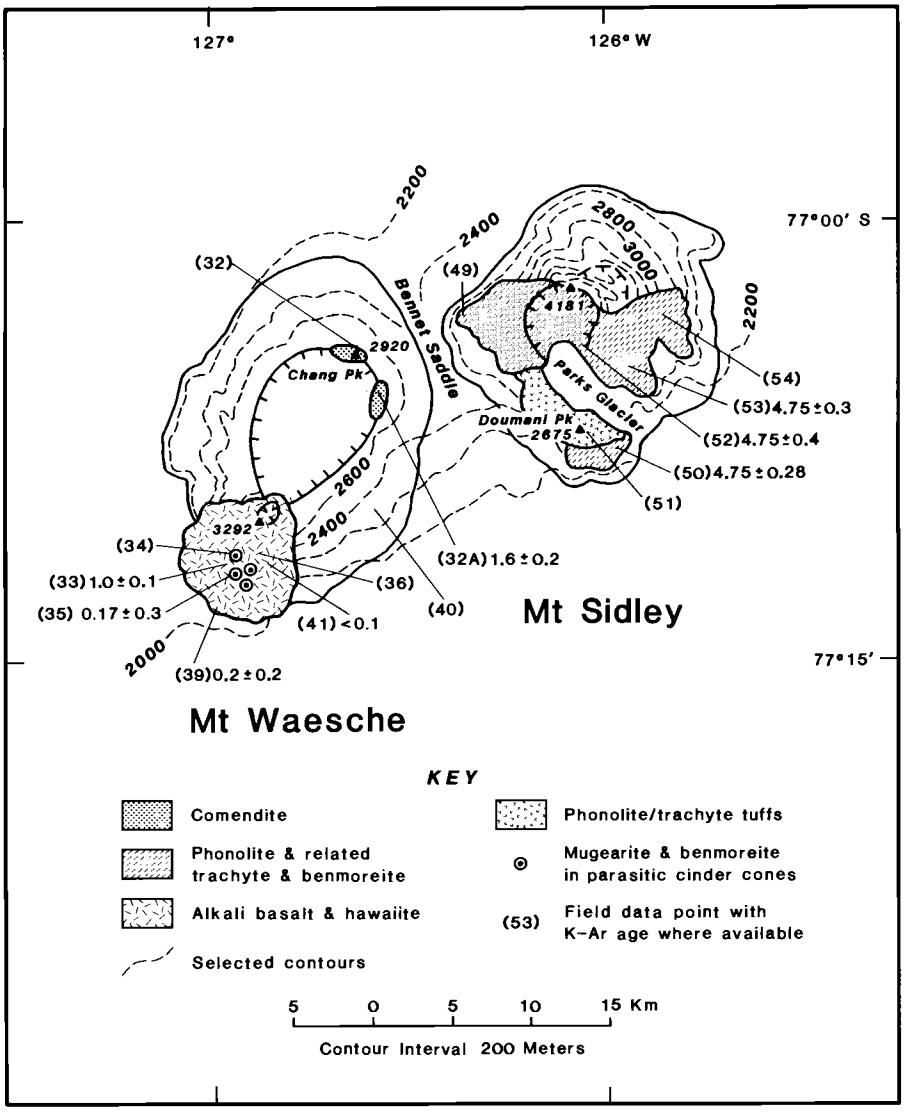

Fig. B.9.3. Geologic sketch map of Mount Sidley and Mount Waesche volcanoes. Geology is by W.E. LeMasurier; K-Ar dates are from *LeMasurier and Rex* [1989*a*]. Base map is the Mount Sidley quadrangle (1960), scale 1:250,000 USGS Reconnaissance Series, Antarctica, U.S. Geological Survey.

described from the Crary Mountains [*Boudette and Ford,* 1966], and it is also a common rock type at Mount Hampton, at the northern end of the ECR.

Green aegirine-augite occurs in the groundmass and as sparse microphenocrysts in all the trachytes and phonolites (LeMasurier and Kawachi, unpublished microprobe data, 1987). A paler-colored augite, transitional to pale lavender titanaugite, is found in the benmoreites. Phenocrysts of fayalite and nearly opaque aenigmatite are found in most Mount Sidley lavas in small amounts (<1%). One phonolite with abundant nepheline microphenocrysts was observed. The olivine andesites of *Doumani and Ehlers* [1962] and the soda andesites and trachyandesites of *González-Ferrán and González-Bonorino* [1972] are probably benmoreites, according to the terminology used here. The occurrence of basalt in this volcano, noted in some preliminary reports, has not been verified by analytical data.

Chronologic Data

A 4.7 ± 0.4 Ma date has been obtained from a sample at the base of the stratigraphic section exposed in the caldera wall. The other two dates are from the highest pretuff stratigraphic levels accessible on the volcano. They suggest

Copyright American Geophysical Union

Copyright American Geophysical Union

TABLE B.9.1. Chemical Analyses and CIPW Norms of Volcanic Rocks From Mount Sidley

	1	2	3	4	5
SiO_2	53.85	53.94	55.34	56.74	61.51
TiO_2	0.47	1.00	0.90	0.28	0.38
Al_2O_3	21.06	17.54	16.79	18.95	16.03
Fe_2O_3	4.44	6.06	1.50	4.31	4.26
FeO	1.38	2.16	8.59	1.63	2.34
MnO	0.19	0.24	0.25	0.18	0.14
MgO	1.01	1.91	1.15	0.13	0.22
CaO	1.51	2.65	4.02	1.18	1.45
Na_2O	9.64	6.91	6.39	9.37	6.93
K_2O	5.87	3.85	3.01	5.55	5.20
P_2O_5	0.18	0.66	0.59	0.06	0.06
H_2O^+	0.91	3.47	0.00	0.00	1.73
H_2O^-	0.19	0.27	0.32	0.84	0.00
F	0.10	0.08	0.06	0.14	0.24
CO_2	0.00	0.00	0.00	0.00	0.00
Total	100.70	100.66	99.74	99.36	100.25
or	34.68	22.75	17.78	32.79	30.72
ab	18.69	45.71	46.72	26.14	53.35
an	0.00	5.48	8.25	0.00	0.00
ne	30.85	6.90	3.97	21.90	0.08
ac	5.20	0.00	0.00	11.20	4.51
di	4.92	2.61	6.80	4.78	4.37
ol	0.17	2.49	9.77	0.25	0.00
mt	3.71	4.85	2.18	0.64	3.92
hm	0.09	2.72	0.00	0.00	0.00
il	0.89	1.90	1.71	0.53	0.72
ap	0.43	1.56	1.40	0.14	0.14
Ba	189	735	1011	68	166
Ce	244	209	237	362	333
Co	12	7	--	--	4
Cr	0	0	27	6	9
Cu	14	9	--	--	15
Ga	35	35	--	--	36
La	131	97	99	152	152
Nb	377	235	119	337	289
Ni	2	2	8	13	5
Pb	19	9	--	--	33
Rb	235	104	81	244	319
Sr	61	199	544	20	25
Th	45	17	10	51	55
U	12	4	3	5	15
V	0	30	14	8	5
Y	81	78	38	105	113
Zn	129	155	--	--	165
Zr	1686	850	587	1760	1541

Major elements analyzed by wet chemistry by H.B. Wiik, Geological Survey of Finland. Trace elements analyzed by XRF at University of Nottingham, England. Dashes, not determined.

1. 49A. Peralkaline phonolite, Mount Sidley.
2. 52A. Tephrophonolite, Mount Sidley.
3. 50A. Benmoreite, Mount Sidley.
4. 54A. Phonolite, Mount Sidley.
5. 53b. Trachyte, Mount Sidley.

Copyright American Geophysical Union

B.10. MOUNT WAESCHE

Type of volcano: Two coalesced shield volcanoes.

Location: Southern end of the Executive Committee Range (77°10′S, 126°50′W).

Height: Mount Waesche, 3292 m above sea level, 1200 m above ice level; Chang Peak, 2920 m above sea level, 700 m above ice level.

Estimated combined exposed volume: 160 km^3.

Evidence of Holocene activity: A possible source of ash layers in the Byrd Station ice core.

Authors of report: W.E. LeMasurier and Y. Kawachi.

Dates of report: March 1983, revised July 1987.

Form and Structure

Mount Waesche is a closely coalesced doublet in which the higher, more conspicuous volcano, referred to here as Mount Waesche volcano, appears to have developed on the caldera rim of an older volcano, the Chang Peak volcano (see Figures B.9.1 and B.9.3). The exposed portions of both volcanoes are composed entirely of flow rock, except for a large dike, perhaps 500 m long, of vertically stratified hydroclastic tuff at locality 40 (see Figures B.9.2 and B.9.3). The two volcanoes are clearly separable from one another on the basis of morphology and by the marked differences in composition noted below. The parasitic cones are actually smaller than indicated in the map shown in Figure B.9.3 and more numerous; several are aligned along radial fissure vents.

Petrologic Characteristics

Chang Peak. This volcano has only two exposures, both on the caldera rim and both offering only a limited range of sampling. Chang Peak itself (Figure B.9.3) is composed of aphyric comendite pumice (Table B.10.1), and the second locality (32A) is composed of comenditic vitrophyre, with phenocrysts of quartz, alkali feldspar, ilmenite, and aenigmatite (Tables B.10.2 and B.10.3). Peralkaline rocks of this type, with a low percentage of normative femics and with aenigmatite as the predominant mafic phenocryst species, have been found only here and at Mount Hartigan northern caldera (see IVD B.8) and Toney Mountain (see IVD B.3).

Chemically, the pumice and the vitrophyre at Chang Peak volcano are very similar to one another, suggesting that the 30% phenocrysts in the vitrophyre do not represent crystal sorting or accumulation. Figure B.IX shows the rare earth element (REE) pattern for the pumice (sample 32), with its characteristically large negative Eu anomaly. The Zr and Rb values for these two samples are among the highest in the Marie Byrd Land province (cf. Figure B.VIII).

Mount Waesche. This volcano offers excellent exposures over its entire south facing flank. The preparasitic cone shield lavas are a petrographically uniform association of plagioclase-phyric *ne*-hawaiites (Table B.10.2). Plagioclase phenocrysts (21–33% of the rock) and olivine and titanaugite phenocrysts (1–4% each) are set in an intersertal matrix of plagioclase, titanaugite, olivine, opaque minerals, and tachylite. The bulk chemical compositions of these rocks are very similar to one another, in spite of large variations in phenocryst proportions, and they are also similar in composition to some phaneritic cognate (gabbroic) inclusions (Table B.10.1), suggesting that the porphyritic rocks are not crystal cumulates. Excellent examples of pyroxene fractionation trends are found among the gabbroic inclusions. Table B.10.4 presents an example of normal zoning, from a lavender titanaugite core to a green aegirine-hedenbergite rim. Also noteworthy in this sample is the reverse zoning of feldspar. This unusual characteristic of reverse zoning in feldspar and normal zoning of ferromagnesian minerals can also be seen in the phenocryst assemblage of hawaiites of Toney Mountain (see IVD B.3). Its significance has not been determined.

Figure B.IX shows the REE pattern that has been obtained for one of the shield lavas (sample 41A), with its characteristic small positive Eu anomaly [*LeMasurier et al.*, 1976]. The initial $^{87}Sr/^{86}Sr$ ratio of this sample is 0.7029 [*LeMasurier and Wade*, 1976].

The parasitic cones on Mount Waesche are composed of black vesicular lavas, cinders, bombs, and blocks with compositions ranging from *ne*-mugearite to *ne*-benmoreite. The phenocryst and groundmass mineralogy of these rocks is very similar to that of the shield hawaiites and basanites, except that in the benmoreites the pyroxenes are zoned to green soda-rich rims. Texturally, most cinder-cone lavas contain less than 5% phenocrysts, and the benmoreites have a trachytic groundmass. All of the analyzed parasitic cone lavas contain nearly twice as much normative *ne* as the analyzed shield lavas, suggesting a trend toward progressive undersaturation during fractional crystallization.

Copyright American Geophysical Union

TABLE B.10.1. Representative Chemical Analyses of Volcanic Rocks From Mount Waesche and Chang Peak

	Mount Waesche Shield Volcano				Mount Waesche Parasitic Cone		Chang Peak	
	1	2	3	4	5	6	7	8
SiO_2	48.17	48.28	48.28	49.46	51.27	54.00	71.69	72.80
TiO_2	2.18	2.21	1.87	1.82	1.83	1.75	0.25	0.18
Al_2O_3	18.58	17.65	19.14	18.48	17.02	16.40	10.79	10.62
Fe_2O_3	5.25	3.18	7.04	4.82	2.97	3.10	2.02	2.38
FeO	6.22	7.79	3.97	5.94	7.51	7.00	2.60	1.38
MnO	0.21	0.19	0.15	0.16	0.23	0.13	0.10	0.06
MgO	3.93	3.55	3.22	3.69	2.42	2.20	2.04	0.11
CaO	9.62	9.70	9.58	9.39	6.70	5.50	0.77	0.22
Na_2O	4.12	4.18	4.30	4.26	5.78	7.00	5.51	5.01
K_2O	1.36	1.43	1.11	1.28	2.07	2.40	4.56	4.38
P_2O_5	0.62	0.63	0.48	0.44	0.67	0.50	0.02	0.00
H_2O^+	0.12	0.00	1.11	0.64	0.00	0.00	0.24	0.00
H_2O^-	0.08	0.00	0.00	0.33	0.00	0.00	0.00	0.00
F	0.11	0.08	0.05	0.07	0.12	0.18	0.32	0.00
CO_2	0.00	0.00	0.00	0.00	0.00	0.00	0.00	0.00
Total	100.57	98.87	100.30	100.45	98.58	100.16	100.59	99.52
Ba	446	482	378	452	752	616	64	22
Ce	96	174	79	96	147	148	473	291
Co	38	--	34	--	--	11	3	0
Cr	24	7	25	64	25	0	9	0
Cu	53	--	68	--	--	24	7	0
Ga	21	--	23	--	--	25	37	35
La	54	93	39	36	57	71	214	142
Nb	71	11	38	46	97	106	286	219
Ni	9	8	14	23	5	3	8	3
Pb	7	--	5	--	--	5	57	53
Rb	29	168	21	131	45	47	315	341
Sr	630	477	497	478	574	405	13	10
Th	4	26	3	2	5	8	55	51
U	3	2	0	1	3	3	13	11
V	197	38	215	165	57	74	4	5
Y	33	9	29	33	48	51	217	170
Zn	85	--	67	--	--	105	358	273
Zr	212	304	179	234	338	434	2086	1557

Major elements determined by wet chemistry by H.B. Wiik, Geological Survey of Finland. Trace elements analyzed by XRF, and F by selective ion electrode (SIE), at University of Nottingham, England. Dashes, not determined.

1. 33C. Hawaiite, shield lava, Mount Waesche.
2. 34A. Hawaiite, shield lava, Mount Waesche.
3. 41BA. Hawaiite, cognate inclusion, Mount Waesche.
4. 41A. Hawaiite, shield lava, Mount Waesche.
5. 34BA. *Ne*-mugearite, parasitic cone lava, Mount Waesche.
6. 35A. Benmoreite, parasitic cone lava, Mount Waesche.
7. 32A. Comendite vitrophyre, Chang Peak.
8. 32. Comendite glass, Chang Peak.

Copyright American Geophysical Union

TABLE B.10.2. CIPW Norms and Modal Analyses of Table B.10.1 Samples

	Mount Waesche Shield Volcano				Mount Waesche Parasitic Cone		Chang Peak	
	1	2	3	4	5	6	7	8
				CIPW Norms				
Q	--	--	--	--	--	--	23.48	29.72
or	8.07	8.45	6.56	7.56	12.23	14.18	26.94	25.88
ab	30.49	28.74	34.28	33.73	38.06	42.34	30.11	30.24
an	28.19	25.18	29.65	27.52	14.38	6.25	--	--
ne	2.37	3.59	1.14	1.26	5.88	9.15	--	--
ac	--	--	--	--	--	--	5.84	6.88
ns	--	--	--	--	--	--	2.30	1.01
di	12.44	15.55	11.48	13.07	12.13	14.88	3.04	0.96
hy	--	--	--	--	--	--	8.13	2.12
ol	5.53	7.01	1.89	5.13	6.45	4.21	--	--
mt	7.61	4.61	7.86	6.99	4.31	4.50	--	--
hm	--	--	1.62	--	--	--	--	--
il	4.14	4.20	3.55	3.46	3.48	3.32	0.48	0.34
ap	1.44	1.46	1.11	1.02	1.55	1.18	0.05	--
				*Modal Analyses**				
Phenocrysts, %								
Qz	--	--	--	--		--	14.4	
Plag	21.0	24.0	--	33.0		1.2	--	
Alk fsp	--	--	--	--		--	12.8	
Ca-Cpx	1.0	1.0	--	2.0		tr	--	
Na-Cpx	--	--	--	--			tr	
Aenig	--	--	--	--			3.0	
Oliv	0.8	0.6	--	4.8		--	--	
Opaq	--	0.6	--	--		--	tr	
Groundmass, %								
Plag	29.8	23.6	58.2	15.0		41.0	--	
Ca-Cpx	18.4	25.4	14.4	16.6		16.2	--	
Oliv	5.0	4.4	6.2	3.6		4.0	--	
Opaq	21.4	17.8	3.2	17.4		23.6	--	
Glass/matr	2.6	2.6	--	6.4		13.8	69.8	
Alter	--	--	18.0	1.2		--	--	
% Phenocrysts	22.8	26.2	--	39.8		1.2	30.2	

Dashes, not detected; tr, trace.
*Based on 500 counts. Analyses by W.E. LeMasurier and R.M. Burke.
1. 33C. Hawaiite, shield lava, Mount Waesche.
2. 34A. Hawaiite, shield lava, Mount Waesche.
3. 41BA. Hawaiite, cognate inclusion, Mount Waesche.
4. 41A. Hawaiite, shield lava, Mount Waesche.
5. 34BA. *Ne*-mugearite, parasitic cone lava, Mount Waesche.
6. 35A. Benmoreite, parasitic cone lava, Mount Waesche.
7. 32A. Comendite vitrophyre, Chang Peak.
8. 32. Comendite glass, Chang Peak.

Chronologic Data

Five K-Ar dates have been obtained from the Mount Waesche and Chang Peak volcanoes [*LeMasurier and Rex*, 1989*a*]. They suggest that the Chang Peak precaldera lavas were erupted at approximately 1.6 Ma and that the Mount Waesche shield volcano formed at roughly 1.0 Ma, which is consistent with their morphological relationships. The youngest lavas on Mount Waesche are too young to be dated by K-Ar methods (i.e., <0.1 Ma). The occurrence of

Copyright American Geophysical Union

TABLE B.10.3. Representative Chemical Compositions of Phases in Comendite Vitrophyre (32A), Chang Peak

	Feldspar				
	Core	Rim	Aenigmatite	Ilmenite	Glass
SiO_2	67.68	66.91	40.87	--	72.32
TiO_2	--	--	8.39	51.04	--
Al_2O_3	18.35	18.15	0.41	--	9.00
FeO*	0.29	0.60	41.11	46.50	5.32
MnO	--	--	0.72	1.39	--
CaO	--	--	0.35	--	--
Na_2O	6.56	5.73	7.11	--	4.58
K_2O	6.88	7.98	--	--	4.57
Cl	--	--	--	--	0.24
Total	99.77	99.38	98.95	98.93	96.04
Analysis	5	6	11	9	12

Dashes, not detected. Analyses by Y. Kawachi, University of Otago, New Zealand, by WDS electron microprobe.
*Total Fe expressed as FeO.

TABLE B.10.4. Representative Chemical Compositions of Minerals in Plutonic Cognate Inclusion (41bb), Mount Waesche

	Alkali Feldspar		Aegirine-augite					
	Core	Rim	Core	Rim	Olivine	Aenigmatite	Oxide	Sodalite
SiO_2	65.72	63.49	49.13	50.09	30.48	40.67	0.06	38.81
TiO_2	0.09	0.09	1.96	0.07	0.04	8.96	31.34	0.01
Al_2O_3	20.57	21.93	2.13	0.28	0.01	0.95	0.62	31.14
Cr_2O_3	--	--	0.02	0.01	--	--	0.01	0.01
FeO*	0.07	0.13	15.37	24.70	59.84	39.81	67.23	0.52
MnO	--	--	0.24	0.34	1.85	0.78	0.82	0.03
MgO	--	0.01	9.23	1.98	6.42	0.96	0.51	0.01
CaO	1.05	3.27	21.56	16.44	1.39	0.81	--	0.02
Na_2O	8.05	8.23	0.55	4.21	--	7.02	0.44	25.64
K_2O	4.72	1.79	--	--	--	0.01	--	0.01
Total	100.28	98.94	100.20	98.12	100.05	99.97	100.64	96.18
Analysis	1	4	3	15	7	57	6	34

Analyses by Y. Kawachi, University of Otago, New Zealand, by WDS electron microprobe. Dashes, not detected.
*Total Fe expressed as FeO.

Ti-augite clasts in some of the ash layers in the Byrd Station ice core suggests that they may have been derived from Mount Waesche, which implies eruptions within the past 30,000 years [*LeMasurier*, 1972*c*].

Extent of Knowledge

Mount Waesche has been visited once, in December 1967, by a helicopter-supported reconnaissance team that visited nine localities in 2 days of fieldwork. Earlier descriptions of Mount Waesche were based on 1958–1960 U.S. Navy aerial photographs and an October 1959 aerial reconnaissance [*Doumani*, 1964].

Mount Waesche is named for Vice Admiral Russell R. Waesche, U.S. Coast Guard, who was a member of the executive committee of the U.S. Antarctic Service Expedition (1939–1941).

Bibliography

Doumani, 1964
González-Ferrán and González-Bonorino, 1972
González-Ferrán and Vergara, 1972
LeMasurier, 1972*c*
LeMasurier and Rex, 1982*a*, *b*, 1989*a*, *b*
LeMasurier and Wade, 1976
LeMasurier et al., 1976

Copyright American Geophysical Union

Copyright American Geophysical Union

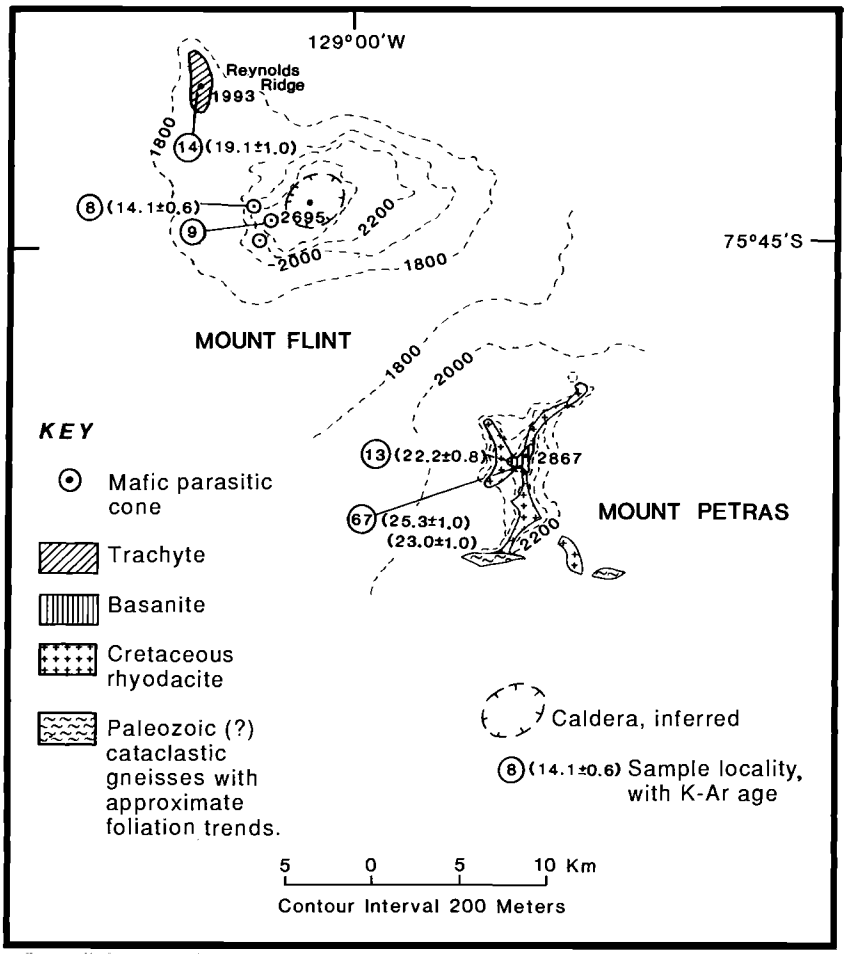

Fig. B.11.2. Geologic sketch map of the Mount Flint–Reynolds Ridge volcano and neighboring Mount Petras (see IVD B.16B). Geology is by W.E. LeMasurier; K-Ar dates are from Table B.11.4. Base map is the McCuddin Mountains quadrangle (1973), scale 1:250,000 USGS Reconnaissance Series, Antarctica, U.S. Geological Survey.

been observed. One cinder cone contains an abundance of ultramafic nodules; most of these are apparently two-pyroxene pyroxenites (websterites) with small amounts of thoroughly blackened olivine. Some of the nodules contain abundant kaersutite (LeMasurier and Kawachi, unpublished microprobe data, 1985). Basanite sample 9D (Table B.11.1) has yielded an initial $^{87}Sr/^{86}Sr$ ratio of 0.70290 [*Futa and LeMasurier*, 1983].

Chronologic Data

The trachyte at Reynolds Ridge is the oldest trachyte flow rock that has been found in Marie Byrd Land and appears to represent the initiation of centralized felsic volcanic activity in Marie Byrd Land (Table B.11.4). The available dates and chemical data suggest that this volcano evolved through a trachytic shield-building phase, followed by a waning stage of basaltic parasitic cone activity: a history that was to be repeated by most of the younger volcanoes in the province. Activity at Mount Flint appears to have ended about the time when the Mount Andrus (IVD B.12) and Whitney Peak–Mount Hampton (IVD B.6) centers were in their early stages of development.

Extent of Knowledge

Mount Flint and Reynolds Ridge have been visited once, in November 1967, by a helicopter-supported reconnaissance team that visited three localities in a half day of field work. The potential for more detailed future work at this volcano is small, because of limited outcrops, except that the nodule locality (see Figure B.11.2) is well worth more intensive examination. Mount Flint and Reynolds Ridge are named for Robert B. Flint, Jr., a U.S. atmospheric geophysicist, and Warren Reynolds, U.S. Department of State.

Copyright American Geophysical Union

TABLE B.11.1. Chemical Analyses of Volcanic Rocks From the Mount Flint–Reynolds Ridge Volcano

	1	2	3
SiO_2	46.02	48.42	59.78
TiO_2	2.56	1.74	0.54
Al_2O_3	16.45	18.95	16.25
Fe_2O_3	4.61	8.01	4.56
FeO	7.19	3.18	3.60
MnO	0.18	0.18	0.26
MgO	7.27	3.26	0.31
CaO	9.14	7.33	1.49
Na_2O	4.03	5.46	7.31
K_2O	1.74	2.12	4.91
P_2O_5	0.71	0.11	0.07
H_2O^+	0.20	0.77	1.00
H_2O^-	0.00	0.16	0.12
F	0.10	0.00	0.00
CO_2	0.00	0.00	0.00
Total	100.20	99.69	100.20
Ba	437	697	1750
Ce	104	144	153
Co	46	22	12
Cr	234	6	0
Cu	67	30	12
Ga	21	18	21
La	47	70	81
Nb	72	87	81
Ni	106	0	2
Pb	7	8	5
Rb	40	48	52
Sr	786	1160	894
Th	9	9	2
U	2	0	0
V	261	193	119
Y	31	35	45
Zn	93	79	123
Zr	277	366	377

Major elements determined by wet chemistry by H.B. Wiik, Geological Survey of Finland. Trace elements analyzed by XRF, and F by selective ion electrode (SIE), at University of Nottingham, England.

1. 9D. Basanite, Mount Flint summit.
2. 8A. Tephrite, Mount Flint summit.
3. 14E. Trachyte, Reynolds Ridge.

TABLE B.11.2. CIPW Norms and Modal Analyses of Volcanic Rocks From the Mount Flint–Reynolds Ridge Volcano

	1	2	3	4
		CIPW Norms		
or	10.28	12.53	29.01	
ab	20.40	29.42	48.39	
an	21.66	20.94	--	
ne	7.42	9.09	4.26	
ac	--	--	4.94	
di	15.23	11.45	6.02	
ol	11.71	1.97	1.13	
mt	6.68	5.79	4.15	
hm	--	4.01	--	
il	4.86	3.30	1.03	
ap	1.64	0.25	0.17	
		*Modal Analyses**		
Phenocrysts, %				
Plag	2.8	4.0	5.0	--
Alk fsp	--	--	--	2.4
Ca-Cpx	--	--	1.8	--
Na-Cpx	--	--	--	0.2
Amph	--	0.4	--	--
Apat	--	--	0.6	--
Oliv	5.0	2.6	1.2	--
Opaq	--	0.6	1.0	--
Groundmass, %				
Plag	38.2	43.2	30.6	--
Alk fsp	--	--	--	35.0
Anal	--	--	1.0	--
Ca-Cpx	15.8	16.2	28.4	--
Na-Cpx	--	--	--	33.0
Amph	--	--	--	15.6
Oliv	9.2	16.8	14.8	--
Opaq	24.8	16.2	14.8	--
Glass/matr	4.2	--	7.2	13.8
Alter	--	--	6.8	--
% Phenocrysts	7.8	7.6	9.6	2.6

Dashes, not detected.

*Based on 500 counts. Analyses by W.E. LeMasurier and R.M. Burke.

1. 9D. Basanite, Mount Flint.
2. 8A. Tephrite, Mount Flint.
3. 14E. Trachyte, Reynolds Ridge.
4. 14A. Felsite, Reynolds Ridge.

Copyright American Geophysical Union

TABLE B.11.3. Representative Chemical Compositions of Minerals in Tephrite 8A, Mount Flint–Reynolds Ridge Volcano

	Plagioclase			Olivine			Oxide	
	P Core	P Rim	G	P Core	P Rim	G	P	G
SiO_2	59.47	53.38	53.88	32.99	34.25	35.44	0.18	0.23
TiO_2	0.02	0.08	0.11	0.03	0.04	0.09	23.83	9.38
Al_2O_3	26.08	28.09	28.24	0.01	--	0.08	2.19	2.53
Cr_2O_3	--	0.05	0.07	0.01	--	0.01	0.04	0.01
FeO*	0.21	0.67	0.72	49.48	42.73	34.35	66.04	81.57
MnO	0.01	0.03	0.04	0.67	1.79	1.02	0.52	0.50
MgO	0.01	0.01	0.01	16.17	20.23	27.79	2.02	1.84
CaO	7.78	11.57	10.94	0.32	0.39	0.52	0.03	0.07
Na_2O	6.28	4.61	5.17	0.04	0.03	0.59	0.13	0.01
K_2O	0.60	0.37	0.39	0.02	0.02	0.03	--	0.02
Total	100.46	98.86	99.56	99.73	99.87	99.38	94.98	96.17
Analysis	5	6	4	25	28	9	34	39

Analyses by Y. Kawachi, University of Otago, New Zealand, by WDS electron microprobe. Dashes, not detected. G, groundmass. P, phenocryst.
*Total Fe expressed as FeO.

TABLE B.11.4. K-Ar Dates of Volcanic Rocks From the Mount Flint–Reynolds Ridge Volcano

Sample	Locality	Comments	K, %	$^{40}Ar_R$	Vol. $^{40}Ar_R$, cm^3/g STP $\times 10^{-5}$	Age, Ma
8A	Mount Flint	Tephrite	1.66	47.8	0.0947	14.1 ± 0.6
		(whole rock)		65.2	0.0882	
14E	Reynolds Ridge	Trachyte (feldspar)	3.52	56.6	0.2634	19.1 ± 1.0

$^{40}Ar_R$, radiogenic ^{40}Ar. Decay constants used are $\lambda_\beta = 4.962 \times 10^{-10}\ yr^{-1}$, $\lambda_\varepsilon = 0.581 \times 10^{-10}\ yr^{-1}$, and $^{40}K = 0.01167$ at. % K. Analyses by D.C. Rex, University of Leeds, England.

Bibliography

Futa and LeMasurier, 1983
González-Ferrán and González-Bonorino, 1972
González-Ferrán and Vergara, 1972
LeMasurier and Rex, 1989*a, b*

Copyright American Geophysical Union

Copyright American Geophysical Union

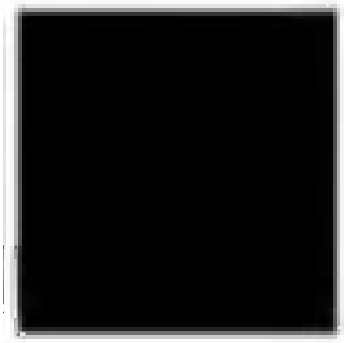

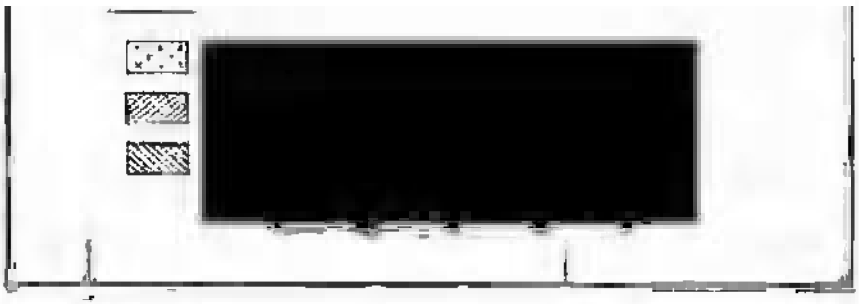

Copyright American Geophysical Union

the few outcrops north of Rosenberg Glacier and south of Gardiner Ridge appear to be related to Mount Kosciusko. They are composed of flow rock, with Strombolian cinders and bombs occurring as an additional constituent in the parasitic cones. Such rocks, and the approximately 14° constructional slopes, suggest that Mount Kosciusko is a trachytic shield volcano.

The geology of Mount Kauffman volcano is known from one good exposure on its northwest flank and from an inaccessible cliff exposure on its southeast side. The cliff is interpreted as a caldera or explosion crater wall, because flows dip away from it to the west, to the northwest, and to the north. The accessible exposure is entirely flow rock, but the cliff appears to be composed of interbedded flows, black cinders, and yellow, palagonitized fragmental (hydroclastic?) deposits which lie stratigraphically beneath the accessible flows. The structure of the entire volcano may be transitional from a tuff cone to a small trachytic shield volcano.

Petrologic Characteristics

Mount Andrus is one of the better exposed volcanoes in Marie Byrd Land. A total of 16 chemical analyses have been published [*González-Ferrán and Vergara,* 1972; *LeMasurier and Wade,* 1976; *LeMasurier and Rex,* 1989*a*], and five representative analyses are presented in Table B.12.1. These represent Mount Andrus as predominantly a pantellerite volcano, with subordinate amounts of mugearite occurring as interbedded flows and parasitic cones. The Mount Andrus pantellerites are the most peralkaline lavas in all of the combined Ames and Flood ranges. They are glass-rich rocks with a sparse phenocryst assemblage (<5%) of alkali feldspar, aegirine-augite, and occasional Fe-rich olivine, set in a matrix of alkali feldspar, aegirine-augite, aenigmatite, and glass.

The mugearites are sometimes highly porphyritic, with up to approximately 25% of phenocrystic plagioclase, olivine, titanaugite, aegirine-augite, anorthoclase, and opaque minerals in varying stages of resorption and reaction, all in a single sample. Regardless of phenocryst proportions, the groundmass is made up of plagioclase, pale lavender augite, olivine, and opaque minerals. The sample most representative of liquid composition (see Table B.12.1, sample 67B4) contains normative *hy* and *ol* (Table B.12.2); others contain up to 5% normative *ne*, among samples with fewer than 1% phenocrysts.

Mount Kosciusko and Mount Kauffman are represented by analyses from only three localities. Both volcanoes appear to be composed of trachytes that are less peralkaline, less silica saturated, and richer in Ba than those at Mount Andrus. Some of the trachytes are *ne*-normative (up to 8.9% *ne*), in contrast to the Mount Andrus felsic rocks, all of which are *Q*-normative. Petrographically, the Mount Kosciusko and Mount Kauffman trachytes are similar to the Mount Andrus pantellerites except that they contain little or no groundmass aenigmatite, and one of the phonolitic trachytes contains nepheline microphenocrysts.

Chronologic Data

Mount Andrus is one of the oldest trachytic shield volcanoes in Marie Byrd Land, being contemporaneous only with Mount Hampton (see IVD B.6) and younger than the Mount Flint–Reynolds Ridge volcano (see IVD B.11). The K-Ar age data (Figure B.12.3) suggest that there were preliminary eruptions at about 14 Ma but that the main shield-building phase took place between 10 and 11.5 Ma. The Mount Kosciusko cone may have formed contemporaneously with, or slightly later than, Mount Andrus. The two dates from the same locality on Mount Kauffman suggest that it formed 3.5 m.y. later than the Mount Andrus and Mount Kosciusko volcanoes. Data from the parasitic cone at Mount Andrus suggest that following the main shield-building phase, these volcanoes remain potentially active for as much as 10 m.y., at least for small-scale eruptions [*LeMasurier and Rex,* 1982*a*]. Other volcanoes where parasitic cone activity followed the termination of shield-building eruptions by 5–10 m.y. include Mount Bursey (see IVD B.13), Mount Cumming (see IVD B.7), Mount Murphy (see IVD B.1), and Mount Flint (see IVD B.11).

The overall pattern of K-Ar ages of felsic rocks in the Ames Range suggests a northward migration of felsic shield-building activity, a continuation of which may be represented by Quaternary felsic activity at Shepard and Grant islands (see IVD B.16D), 140 km north of Mount Kauffman [*LeMasurier and Rex,* 1989*a*].

Extent of Knowledge

The Ames Range was discovered by the U.S. Antarctic Service Expedition (1939–1941) during aerial reconnaissance flights. It was not visited on the ground, however, until November 1967, when four localities were sampled by a helicopter-supported reconnaissance team. Ten additional localities were studied and sampled in December 1977, during a second helicopter-supported field season that focused its activities on the western half of the volcanic province. No systematic stratigraphic sampling has been done.

The Ames Range was named in 1939–1941 by Rear Admiral Richard E. Byrd for his father-in-law, Joseph Ames. The individual volcanic peaks are named for Lieutenant Carl H. Andrus, U.S. Navy; Captain Henry M. Kosciusko, U.S. Navy; and Commander S.K. Kauffman, U.S. Navy, all of whom were prominent in U.S. Navy support of the U.S. Antarctic Research Program during the mid-1960s.

Copyright American Geophysical Union

TABLE B.12.1. Representative Chemical Analyses of Volcanic Rocks From the Ames Range

	Mount Andrus					Mount Kosciusko	Mount Kauffman
	1	2	3	4	5	6	7
SiO_2	51.00	62.50	62.74	64.72	68.61	59.78	61.00
TiO_2	2.00	0.65	0.56	0.68	0.50	0.30	0.27
Al_2O_3	15.10	14.20	14.32	8.62	9.33	16.78	16.60
Fe_2O_3	8.00	6.60	2.89	3.18	2.79	6.19	4.60
FeO	5.50	1.60	5.48	7.87	5.79	0.72	1.60
MnO	0.18	0.06	0.24	0.34	0.21	0.21	0.04
MgO	3.20	0.25	0.14	0	0	0.34	0.18
CaO	5.30	1.40	1.19	0.59	0.42	1.91	1.40
Na_2O	5.50	7.00	7.60	8.21	7.20	7.14	8.30
K_2O	2.30	5.40	4.51	4.35	4.31	4.88	5.70
P_2O_5	1.40	0.04	0.07	0.05	0.01	0.10	0.02
H_2O^+	0	0.50	0.58	0	0	0	0.50
H_2O^-	0	0	0	0	0	0.77	0
F	0.15	0.52	0.14	0.09	0.18	0.06	0.07
CO_2	0	0	0	0	0	0	0
Total	99.63	100.72	100.46	98.70	99.35	99.18	100.28
Ba	641	63	20	73	48	1181	153
Ce	207	145	345	660	412	240	209
Co	18	4	0	--	0	--	0
Cr	0	0	6	6	4	0	0
Cu	16	10	3	--	1	--	6
Ga	22	31	47	--	38	--	31
La	91	84	132	225	192	98	110
Nb	96	98	223	305	251	128	167
Ni	0	0	4	24	7	9	0
Pb	4	12	18	--	32	--	9
Rb	34	86	152	219	226	93	100
Sr	1133	20	3	10	3	157	12
Th	2	10	26	35	34	15	16
U	3	3	7	7	10	2	3
V	87	17	13	8	12	7	7
Y	50	45	125	211	147	71	64
Zn	124	106	295	--	348	--	131
Zr	452	1517	334	1853	408	864	921

All samples analyzed by XRF at University of Nottingham, England; FeO determined by wet chemistry and F by selective ion electrode (SIE). Major elements for sample 3B determined by wet chemistry by H.B. Wiik, Geological Survey of Finland. Dashes, not determined.

1. 67B4. Mugearite, southwest tip of Mount Andrus.
2. 67B6. Pantelleritic trachyte, Mount Andrus.
3. 3B. Pantelleritic trachyte, south side of Mount Andrus.
4. AR41C. Pantellerite glass, north side of Mount Andrus.
5. AR44D2. Pantellerite, Mount Andrus.
6. AR40B. Phonolitic trachyte, Mount Kosciusko.
7. 67B8. Phonolite, Mount Kauffman.

Copyright American Geophysical Union

TABLE B.12.2. CIPW Norms and Modal Analyses of Volcanic Rocks From the Ames Range

	Mount Andrus				Mount Kosciusko		Mount Kauffman
	1	2	3	4	5	6	7
			CIPW Norms				
Q	0	3.60	1.31	18.08	23.16	0	0
or	13.59	31.91	26.65	25.71	25.47	28.84	33.68
ab	46.52	42.97	48.54	20.12	24.00	53.58	33.68
an	9.73	0	0	0	0	0	0
ne	0	0	0	0	0	3.02	8.90
ac	0	14.30	8.36	9.20	8.07	1.12	13.31
ns	0	0	1.45	9.06	6.46	0	0.34
di	5.31	2.36	4.83	2.32	1.80	1.83	5.49
wo	0	0	0	0	0	2.70	0
hy	4.52	0.06	7.38	12.73	9.24	0	0
ol	1.05	0	0	0	0	0	0.13
mt	11.60	2.40	0	0	0	2.14	0
hm	0	0	0	0	0	4.33	0
il	3.80	1.24	1.06	1.29	0.95	0.57	0.51
ap	3.32	0.11	0.17	0.11	0.02	0.23	0.05
fr	0.18	1.06	0	0	0	0	0.14
			*Modal Analyses**				
Phenocrysts, %							
Plag	0	1.4	0				0
Alk fsp	0	0	1.0				0.6
Na-Cpx	0	tr	0				0.2
Aenig	0	0	0				0.2
Groundmass, %							
Plag	41.2	42.4	0				0
Alk fsp	0	0	13.2				45.6
Ca-Cpx	1.6	22.4	12.2				27.0
Amph	1.0	0	0				0
Apat	0.2	0	0				0
Oliv	0.4	0	0				0
Opaq	39.2	17.6	0				6.0
Glass/matr	16.4	9.2	70.6				19.8
Alter	0	0	3.0				0.6
% Phenocrysts	0	1.4	1.0				1.0

tr, trace.

*Based on 500 counts. Analyses by W.E. LeMasurier and R.M. Burke.

1. 67B4. Mugearite, southwest tip of Mount Andrus.
2. 67B6. Pantelleritic trachyte, Mount Andrus.
3. 3B. Pantelleritic trachyte, south side of Mount Andrus.
4. AR41C. Pantelleritic glass, north side of Mount Andrus.
5. AR44D2. Pantellerite, Mount Andrus.
6. AR40B. Phonolitic trachyte, Mount Kosciusko.
7. 67B8. Phonolitic, Mount Kauffman.

Bibliography

González-Ferrán and González-Bonorino, 1972
González-Ferrán and Vergara, 1972
LeMasurier and Rex, 1982*a, b*, 1983, 1989*a, b*
LeMasurier and Wade, 1976

Copyright American Geophysical Union

B.13. MOUNT BURSEY

Type of volcano: Trachytic shield volcano.
Location: Flood Range (76°00′S, 133°00′W).
Height: 2787 m above sea level, 1000 m above ice level.
Estimated volume: 290 km^3.
Evidence of Holocene activity: None.
Author of report: W.E. LeMasurier.
Dates of report: April 1983, revised July 1987.

Fig. B.13.1. Geologic sketch map of the Mount Bursey volcanoes. Geology is by W.E. LeMasurier; K-Ar dates are from *LeMasurier and Rex* [1989*a*]. Base map is from the Mount Kosciusko (1973) and Mount Berlin (1973) quadrangles, scale 1:250,000 USGS Reconnaissance Series, Antarctica, U.S. Geological Survey.

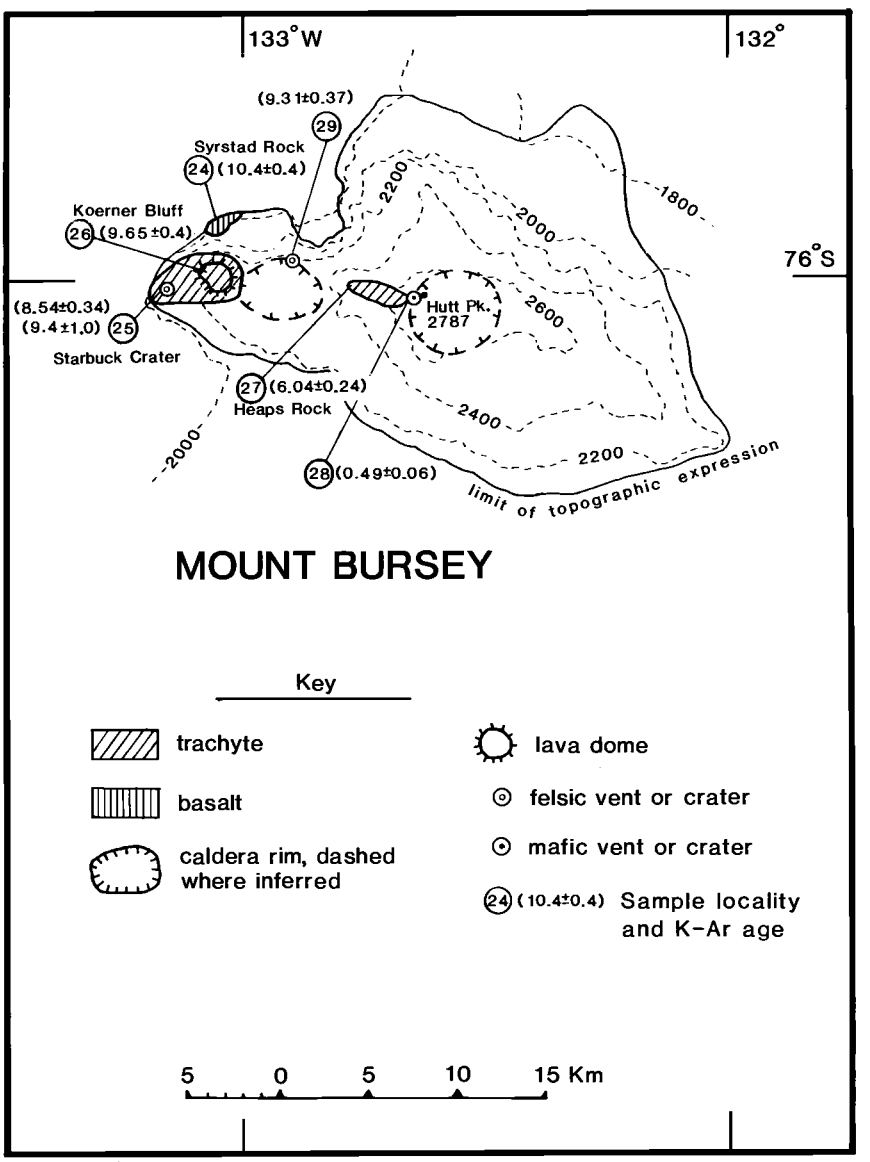

Copyright American Geophysical Union

Copyright American Geophysical Union

TABLE B.13.1. Representative Chemical Analyses and CIPW Norms of Volcanic Rocks From Mount Bursey

	Hutt Peak Volcano			Koerner Bluff Volcano			
	1	2	3	4	5	6	7
SiO_2	45.51	60.56	62.17	58.91	60.64	61.40	63.10
TiO_2	4.43	0.58	0.66	0.67	0.10	0.44	0.76
Al_2O_3	14.90	16.32	11.87	16.08	17.89	14.90	10.23
Fe_2O_3	2.24	3.47	7.32	4.62	4.31	6.80	6.00
FeO	10.36	3.48	3.58	4.10	0.84	1.80	5.63
MnO	0.18	0.18	0.29	0.25	0.20	0.06	0.34
MgO	5.03	0.42	0.17	0.42	0.00	0.14	0.10
CaO	8.40	1.63	1.16	2.72	0.88	2.20	1.00
Na_2O	4.66	8.06	6.92	6.11	8.86	6.60	7.26
K_2O	1.39	4.59	4.60	4.47	5.10	5.50	4.35
P_2O_5	1.57	0.12	0.07	0.25	0.01	0.04	0.07
H_2O^+	0.00	0.00	0.00	0.00	0.59	0.00	0.17
H_2O^-	0.00	0.25	0.89	0.58	0.59	0.00	0.17
F	0.08	0.07	0.11	0.04	0.00	0.13	0.14
Total	98.75	99.74	99.81	99.20	99.42	100.22	99.14
Q	0.00	0.00	5.57	0.97	0.00	1.94	10.82
or	8.21	27.13	27.18	26.42	30.14	32.50	25.71
ab	28.84	46.29	35.45	51.70	43.51	46.01	28.40
an	15.64	0.00	0.00	3.25	0.00	0.00	0.00
ne	5.74	6.55	0.00	0.00	10.90	0.00	0.00
ac	0.00	8.64	20.36	0.00	9.99	8.64	17.36
ns	0.00	0.00	0.00	0.00	0.00	0.00	3.10
di	12.97	6.34	4.67	7.38	1.96	0.75	4.00
wo	0.00	0.00	0.00	0.00	0.88	3.64	0.00
hy	0.00	0.00	3.75	0.33	0.00	0.00	7.85
ol	11.97	2.37	0.00	0.00	0.00	0.00	0.00
mt	3.25	0.70	0.41	6.70	1.24	4.74	0.00
il	8.41	1.10	1.25	1.27	0.19	0.84	1.44
ap	3.64	0.28	0.15	0.58	0.02	0.11	0.16
fr	0.00	0.00	0.00	0.00	0.00	0.26	0.00
Ba	654	319	54	1870	38	469	112
Ce	144	196	526	204	318	207	601
Co	35	9	3	--	3	9	0
Cr	25	6	13	0	9	5	6
Cu	36	4	8	--	5	6	8
Ga	20	35	47	0	39	32	42
La	55	98	248	83	178	101	268
Nb	60	170	333	104	231	127	394
Ni	23	7	11	7	8	0	8
Pb	5	12	25	--	18	21	35
Rb	25	110	163	70	146	94	206
Sr	1644	153	17	244	12	23	26
Th	3	23	34	13	30	7	44
U	0	6	3	2	9	4	13
V	271	19	13	12	0	14	15
Y	31	71	172	57	91	79	191
Zn	129	158	404	--	231	185	452
Zr	220	909	1925	622	1751	766	2178

All samples analyzed by XRF at University of Nottingham, England; FeO determined by wet chemistry and F by selective ion electrode (SIE). Dashes, not determined.

1. BU28A. Basanite, Hutt Peak summit.
2. BU28B. Phonolitic trachyte, Hutt Peak summit.
3. BU27B. *Q*-trachyte, Heaps Rock.
4. BU29B. Trachyte, northwest flank of Mount Bursey.
5. BU26A. Phonolite, Koerner Bluff.
6. 67A7. Trachyte, Starbuck Crater.
7. BU25B. *Q*-trachyte, Starbuck Crater.

Copyright American Geophysical Union

The Hutt Peak parasitic cone appears to postdate caldera formation and to be controlled by ring fractures. The evolution of the entire volcanic complex apparently conforms to a general pattern observed elsewhere in Marie Byrd Land in which an initial basaltic stage of volcanism was followed by construction of trachyte shield volcanoes, which in turn, after a period of quiescence of up to 10 m.y., was followed by postcaldera mafic parasitic cone activity (cf. IVD's B.1, B.7, B.11, and B.12). The locus of shield-building activity at Mount Bursey appears to have migrated from west to east, just the opposite of the overall westward direction of migration in the Flood Range [*LeMasurier and Rex,* 1989*a*].

Extent of Knowledge

Koerner Bluff and Starbuck Crater were first visited in November 1967 by a helicopter-supported reconnaissance team. All of the six localities identified in Figure B.13.1 were visited and sampled, again by helicopter, during 1 day of fieldwork in December 1977. Exposures at Mount Bursey are limited, even by Marie Byrd Land standards, and there is not a great deal of potential for more detailed future work at this volcano.

The Flood Range was discovered by the 1934 Byrd Antarctic Expedition from distant sightings and named by Rear Admiral Richard E. Byrd for his uncle, Senator Henry D. Flood (Virginia). Mount Bursey is named for Jacob Bursey, a member of the 1928–1930 Byrd Antarctic Expedition and dog driver with the U.S. Antarctic Service sledging party which visited the west end of the Flood Range (Mount Berlin) in 1940.

Bibliography

González-Ferrán and González-Bonorino, 1972
González-Ferrán and Vergara, 1972
LeMasurier and Rex, 1982*a*, 1983, 1989*a*, *b*

Copyright American Geophysical Union

Copyright American Geophysical Union

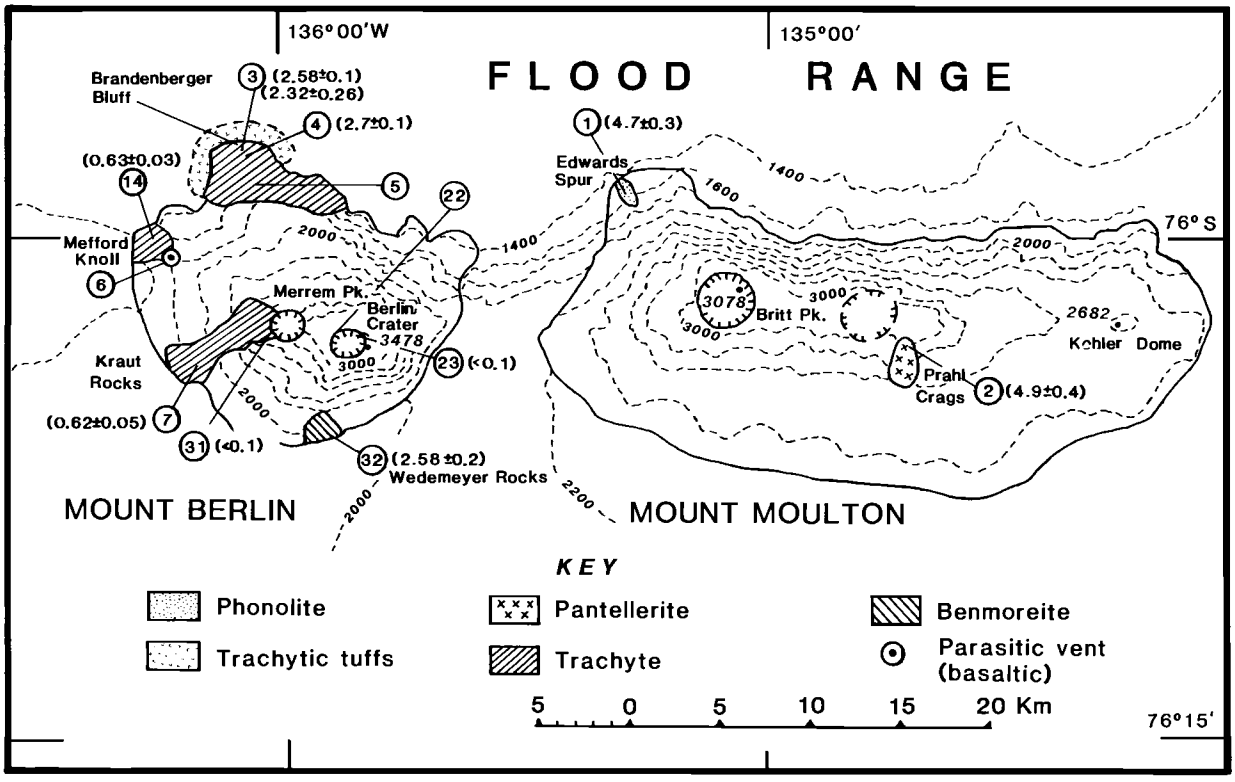

Fig. B.14.2. Geologic sketch map of the Mount Moulton and Mount Berlin volcanoes. Geology is by W.E. LeMasurier; K-Ar dates (in parentheses) are from *LeMasurier and Rex* [1989*a*]. Base map is from Mount Kosciusko (1973) and Mount Berlin (1973) quadrangles, scale 1:250,000 USGS Reconnaissance Series, Antarctica, U.S. Geological Survey.

and B.14.3). The glass is richer in SiO_2 and total iron, poorer in Na_2O, and less peralkaline than the whole rock. It is unlikely that any of these characteristics are related to hydration or devitrification [*Noble,* 1967; *Macdonald and Bailey,* 1973], because the rock is virtually anhydrous (Table B.14.1) and the glass appears to be completely isotropic. Figure B.IX shows the rare earth element pattern for sample 2A, with the large negative Eu anomaly characteristic of felsic rocks in this province [*LeMasurier et al.,* 1976]. The initial $^{87}Sr/^{86}Sr$ ratio of this sample is 0.70493 (Futa and LeMasurier, unpublished data, 1987).

Chronologic Data

Samples from both localities on Mount Moulton have yielded essentially the same K-Ar age (4.7 Ma and 4.9 Ma). Mount Moulton appears to be older than Mount Berlin (see IVD B.15), to the west, and younger than Mount Bursey (see IVD B.13), at the east end of the Flood Range (Figure B.II). The locus of felsic activity therefore appears to have migrated systematically westward in the Flood Range. over the past 8 m.y., at a rate of about 1 cm yr^{-1} [*LeMasurier and Rex,* 1989*b*].

Extent of Knowledge

The two outcrops at Mount Moulton were first visited in November 1967 and were revisited in December 1977. Unfortunately, there is little potential for more detailed geologic work at these two volcanoes. Mount Moulton is named for Richard S. Moulton, chief dog driver with the 1939–1941 U.S. Antarctic Service Expedition, which visited the west end of Flood Range in December 1940.

Bibliography

González-Ferrán and González-Bonorino, 1972
LeMasurier and Rex, 1983, 1989*a, b*
LeMasurier and Wade, 1976
LeMasurier et al., 1976

Copyright American Geophysical Union

TABLE B.14.1. Chemical Analyses of Volcanic Rocks From Mount Moulton

	1	2
SiO_2	60.54	69.80
TiO_2	0.26	0.37
Al_2O_3	15.45	10.87
Fe_2O_3	5.24	4.03
FeO	2.25	3.08
MnO	0.23	0.22
MgO	0.00	0.65
CaO	0.92	0.29
Na_2O	8.84	6.20
K_2O	5.00	4.53
P_2O_5	0.03	0.03
H_2O^+	0.00	0.10
H_2O^-	0.47	0.00
F	0.02	0.00
Total	99.25	100.17
Ba	78	40
Ce	404	330
Co	--	0
Cr	8	16
Cu	--	37
Ga	--	45
La	139	141
Nb	237	213
Ni	15	15
Pb	--	25
Rb	119	152
Sr	8	7
Th	24	26
U	4	7
V	2	5
Y	115	130
Zn	--	305
Zr	1491	1468

Major elements determined by wet chemistry by H.B. Wiik, Geological Survey of Finland. Trace elements analyzed by XRF at University of Nottingham, England. Dashes, not determined.

1. 1A. Phonolitic trachyte, Edwards Spur (West volcano).
2. 2A. Pantellerite, Prahl Crags (East volcano).

TABLE B.14.2. CIPW Norms and Modal Analyses of Volcanic Rocks From Mount Moulton

	1	2
	CIPW Norms	
Q	0.00	20.62
or	29.55	26.76
ab	40.69	30.69
ne	5.93	0.00
ac	15.16	11.66
ns	1.39	1.98
di	3.90	1.07
hy	0.00	6.52
ol	1.59	0.00
il	0.49	0.70
ap	0.07	0.07
fr	0.09	0.00
	*Modal Analyses**	
Phenocrysts, %		
Qtz	--	6.4
Alk fsp	0.2	15.0
Na-Cpx	--	0.2
Amph	--	2.2
Aenig	--	tr
Oliv	--	tr
Groundmass, %		
Alk fsp	27.0	--
Na-Cpx	40.0	--
Amph	13.0	--
Opaq	2.0	--
Glass/matr	17.8	76.2
Alter	--	9.0
% Phenocrysts	0.2	23.8

Dashes, not detected; tr, trace.

*Based on 500 counts. Analyses by W.E. LeMasurier and R.M. Burke.

1. 1A. Phonolite, West volcano.
2. 2A. Pantellerite, East volcano.

Copyright American Geophysical Union

TABLE B.14.3. Representative Chemical Compositions of Minerals and Glass in Pantellerite Vitrophyre (2A) From Mount Moulton

	Anorthoclase	Na-Hedenbergite	Aenigmatite	Fayalite	Glass
SiO_2	67.73	49.33	41.65	30.36	71.91
TiO_2	0.02	0.28	8.46	0.05	0.26
Al_2O_3	17.82	0.08	0.13	0.00	7.27
Cr_2O_3	0.03	0.00	0.00	0.01	0.03
FeO*	0.88	29.29	41.17	65.10	8.24
MnO	0.01	1.07	1.02	3.73	0.35
MgO	0.00	0.39	0.16	0.67	0.00
CaO	0.02	15.94	0.17	0.62	0.29
Na_2O	6.50	2.60	7.48	0.05	5.76
K_2O	6.93	0.01	0.00	0.00	4.40
NiO	0.02	0.05	0.00	0.00	0.04
Total	99.95	99.01	100.25	100.59	98.55
Analysis	6	2	4	1B	13

All samples analyzed by Y. Kawachi, University of Otago, New Zealand, by WDS electron microprobe.

*Total Fe expressed as FeO.

Copyright American Geophysical Union

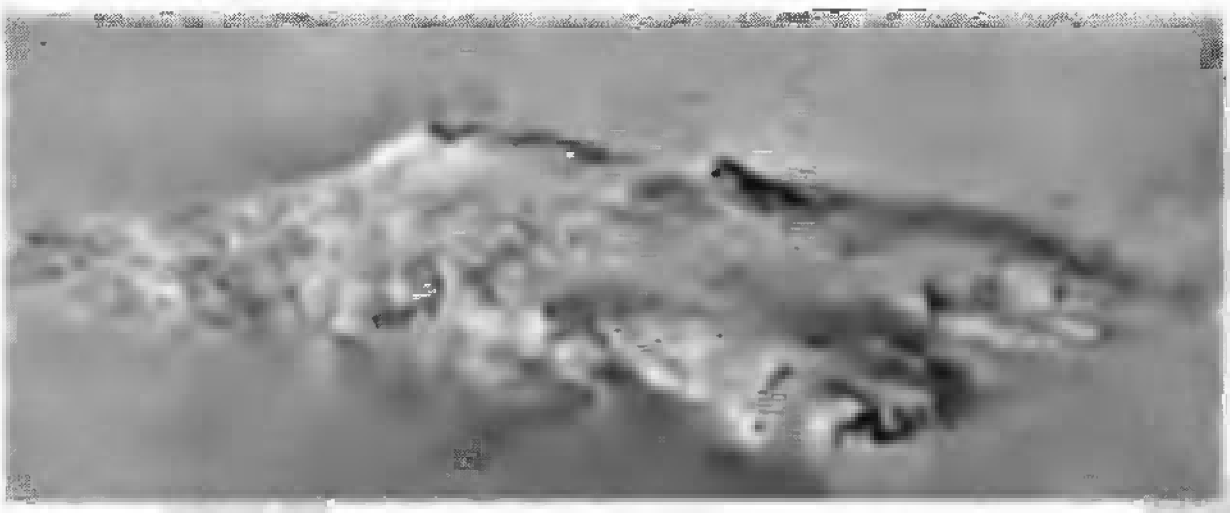

Copyright American Geophysical Union

TABLE B.15.1. Representative Chemical Analyses of Volcanic Rocks From Mount Berlin

	1	2	3	4	5	6	7	8
SiO_2	44.99	54.55	57.23	58.09	60.71	60.81	61.63	62.21
TiO_2	2.81	1.78	1.33	0.31	0.50	0.57	0.51	0.52
Al_2O_3	14.24	18.59	17.94	17.63	14.97	14.80	12.88	13.11
Fe_2O_3	2.82	0.45	4.26	3.46	5.94	4.12	6.92	2.59
FeO	9.60	7.96	3.89	4.01	2.66	4.80	2.57	6.07
MnO	0.19	0.21	0.26	0.23	0.21	0.28	0.28	0.27
MgO	7.88	2.01	0.82	0.15	0.30	0.10	0.00	0.00
CaO	9.16	4.72	3.78	2.13	1.30	1.42	1.09	1.09
Na_2O	3.84	5.92	5.60	7.82	7.66	7.49	8.00	8.75
K_2O	1.60	3.13	3.06	4.52	4.61	4.85	4.69	4.71
P_2O_5	0.78	0.86	0.52	0.11	0.04	0.05	0.05	0.05
H_2O^+	0.00	0.10	0.48	0.00	1.11	0.00	0.00	0.00
H_2O^-	0.00	0.03	0.00	0.48	0.00	0.20	0.24	0.00
F	0.07	0.13	0.00	0.00	0.00	0.00	0.11	0.08
Total	98.98	100.44	99.17	98.93	100.01	99.49	98.97	99.45
Ba	561	693	731	1435	189	200	87	72
Ce	110	175	172	173	203	294	365	546
Co	42	25	10	0	0	4	--	--
Cr	219	0	4	5	7	3	9	9
Cu	56	12	8	4	2	5	--	--
Ga	18	30	29	26	41	40	--	--
La	55	73	82	92	96	137	126	188
Nb	63	105	116	146	198	218	194	270
Ni	132	0	0	0	0	8	14	14
Pb	6	9	13	9	14	15	--	--
Rb	29	63	13	64	115	15	125	--
Sr	733	562	535	112	10	12	5	6
Th	4	11	10	10	15	19	27	43
U	3	1	10	3	5	19	4	43
V	232	73	55	8	17	13	4	6
Y	32	58	58	59	77	94	111	150
Zn	101	164	138	139	243	264	--	--
Zr	256	541	630	734	1172	1174	1160	1878

All samples analyzed by XRF at University of Nottingham, England, and University of Otago, New Zealand; FeO determined by wet chemistry and F by selective ion electrode (SIE). Dashes, not determined.

1. BN14D. Porphyritic basanite, Mefford Knoll.
2. 67A35. Porphyritic benmoreite, Wedemeyer Rocks.
3. BN31D. Porphyritic benmoreite, Merrem Peak.
4. BN4C. Phonolite, Brandenberger Bluff.
5. BN23C. Trachyte, summit of Mount Berlin.
6. BN31A. Trachyte, Merrem Peak.
7. BN22B. Pantelleritic trachyte, summit of Mount Berlin.
8. BN31E. Pantelleritic trachyte, Merrem Peak.

parently consists of two coalesced trachytic shield volcanoes resting on a base that is at least partly hydroclastic.

Petrologic Characteristics

Table B.15.1 presents eight analyses from among 15 that are available from 10 localities (see Figure B.14.2). These suggest that there are no major petrologic differences between the Berlin Crater and Merrem Peak cones and that the predominant rock type at each is peralkaline trachyte. Subordinate rock types include phonolite, benmoreite, and basanite. The phonolites are petrographically indistinguishable from the trachytes, and chemical gradations between the two are common. Pantelleritic trachytes have also been found, but only around the summit calderas of Merrem Peak and Berlin Crater.

Copyright American Geophysical Union

TABLE B.15.2. CIPW Norms and Modal Analyses of Volcanic Rocks From Mount Berlin

	1	2	3	4	5	6	7	8
				CIPW Norms				
Q	0.00	0.00	4.34	0.00	0.00	0.00	2.02	3.16
or	9.46	18.49	18.08	26.71	27.24	28.66	27.71	27.83
ab	17.77	42.71	47.39	46.11	48.50	44.83	40.13	41.20
an	16.89	14.92	14.78	0.00	0.00	0.00	0.00	0.00
ne	7.97	3.99	0.00	10.59	1.53	2.33	0.00	0.00
ac	0.00	0.00	0.00	0.58	11.87	11.92	20.02	7.49
ns	0.00	0.00	0.00	0.00	0.00	0.17	1.12	5.66
di	19.05	2.45	0.48	8.67	5.34	5.96	4.53	4.53
hy	0.00	0.00	3.72	0.00	0.00	0.00	1.99	8.38
ol	15.53	11.61	0.00	0.30	0.70	4.23	0.00	0.00
mt	4.09	0.65	6.16	4.75	2.64	0.00	0.00	0.00
il	5.34	3.38	2.53	0.59	0.95	1.08	0.97	0.99
ap	1.81	2.04	1.20	0.25	0.09	0.12	0.12	0.11
				*Modal Analyses**				
Phenocrysts, %								
Alk fsp		19.2						
Ol		1.2						
Opaq		0.8						
Groundmass, %								
Alk fsp		26.4						
Anal		0.2						
Na-Cpx		17.6						
Ne		1.0						
Amph		1.0						
Oliv		8.2						
Apat		1.0						
Opaq		14.0						
Glass/matr		9.4						
% Phenocrysts		21.2						

*Based on 500 counts. Analyses by W.E. LeMasurier and R.M. Burke.

1. BN14D. Porphyritic basanite, Mefford Knoll.
2. 67A35. Porphyritic benmoreite, Wedemeyer Rocks.
3. BN31D. Porphyritic benmoreite, Merrem Peak.
4. BN4C. Phonolite, Brandenberger Bluff.
5. BN23C. Trachyte, summit of Mount Berlin.
6. BN31A. Trachyte, Merrem Peak.
7. BN22B. Pantelleritic trachyte, summit of Mount Berlin.
8. BN31E. Pantelleritic trachyte, Merrem Peak.

Petrographically, the trachytes and phonolites usually contain less than 5% phenocrysts. Alkali feldspar is normally the dominant phenocryst phase, accompanied by lesser amounts of green Na-hedenbergite, opaque minerals clustered with apatite, and occasionally fayalite, set in a pilotaxitic matrix (Tables B.15.2 and B.15.3). Aenigmatite was not observed as a phenocryst but is common in the groundmass. Cognate xenoliths of Na-hedenbergite syenite are common at several localities; those associated with phonolitic flows contain fayalite.

Oversaturated trachytes show an abrupt drop in Ba and Sr and an equally abrupt increase in Rb and Zr. These effects are seen in only a few of the undersaturated trachytes and phonolites, however (see Table B.15.1), and therefore the influence of anorthoclase crystallization on trachyte compositions is not yet clear.

Benmoreites at Mount Berlin occur as distinctive coarsely porphyritic rocks with a superficial resemblance to anorthoclase phonolite (kenyte). In most cases they consist of roughly 20% anorthoclase phenocrysts, about 1 cm in

Copyright American Geophysical Union

Copyright American Geophysical Union

ne-normative. Mount Berlin and Mount Waesche (see IVD B.10) are the only volcanoes in Marie Byrd Land where evidence suggesting a secular change in lava composition has been found.

Mount Berlin represents the westernmost progression of volcanic activity in the Flood Range. Felsic activity appears to have migrated systematically westward from Mount Bursey to Mount Moulton to Mount Berlin, a distance of about 80 km over the past 8 m.y. [*LeMasurier and Rex,* 1989*a*].

Extent of Knowledge

Mount Berlin was first visited in December 1940, as part of the U.S. Antarctic Service Expedition (USAS), but no geologic work was done. It was subsequently visited by helicopter-supported reconnaissance teams in November 1967 and again, more comprehensively, in November and December 1977. Mount Berlin is well exposed (by Marie Byrd Land standards), and most exposures have been visited, but none have been studied and sampled in systematic detail. There is considerable potential for more detailed study, especially of the hydroclastic deposits at Brandenberger Bluff.

Mount Berlin is named for Leonard M. Berlin, leader of the USAS party that visited the mountain in 1940.

Bibliography

González-Ferrán and González-Bonorino, 1972
González-Ferrán and Vergara, 1972
LeMasurier and Rex, 1982*b*, 1983, 1989*a, b*
LeMasurier and Wade, 1968

Copyright American Geophysical Union

B.16. SATELLITIC VOLCANIC CENTERS

The satellitic volcanic centers include cinder cones, tuff cones, tuyas or table mountains, and composite Strombolian-phreatomagmatic structures, together with erosional remnants of uncertain structure and scale, all of which lie beyond the major central volcanic cones. They encompass more than 30 small individual eruptive centers, some of which are monogenetic and others recurrently active over as much as 5–10 m.y. They are mainly basaltic in composition (i.e., basanite, tephrite, basalt, or mafic hawaiite) with exceptions found at Dorrel Rock, Kouperov Peak, Shepard Island, and Grant Island, and all are less than 1 km^3 in exposed volume. Some are contemporaneous with the activity of nearby large felsic cones and could represent consanguineous satellitic activity, as, for example, the relationship of the Hobbs Coast satellitic centers to the major volcanoes of the Ames and Flood ranges. In many other cases they are not chronologically or geographically related to any felsic cones and seem to represent decentralized, almost continuous mafic volcanic activity that has characterized the province for the past 25–30 m.y. [*LeMasurier and Rex,* 1989*a*].

The basaltic rocks in all of these centers are alkaline, and nearly all contain normative *ne* (up to 13.4%). Beyond these gross similarities, however, there are frequently distinctive chemical differences from one center to another, even among those centers that are close geographic neighbors and are roughly contemporaneous in their activity. The Miocene-Pliocene centers on the Hobbs Coast (see IVD B.16C) are a good example. Detailed Sm/Nd and Rb/Sr isotopic studies have been done on basalt samples from the Walgreen Coast (see IVD B.16A), Mount Petras (see IVD B.16B), and the Hobbs Coast (see IVD B.16C) centers [*Futa and LeMasurier,* 1983].

Phenocryst assemblages include examples of olivine alone, olivine + augite, and olivine + augite + plagioclase. Pyroxene and plagioclase phenocrysts commonly show evidence of multiple cycles of growth and resorption. The groundmass of these rocks is uniformly characterized by plagioclase, olivine, titaniferous augite, and opaque minerals.

The satellitic volcanic centers are arbitrarily grouped below into five chronologic-geographic units to facilitate description and comparison. To avoid repetition, their petrologic characteristics will be described separately in only a few cases.

Copyright American Geophysical Union

B.16A. MIOCENE AND OLDER CENTERS, WALGREEN COAST

Type of volcano: Subvolcanic pluton (Dorrel Rock), remnants of shield volcanoes or table mountain (Turtle Peak and Hedin Nunatak), isolated flows (Kohler Range).

Location: On the coast of the Amundsen Sea, easternmost Marie Byrd Land; Mount Murphy–Kohler Range region.

Height above sea level: 300–800 m (see Figure B.16A.1).

Evidence of Holocene activity: None.

Author of report: W.E. LeMasurier.

Date of report: August 1986.

Form and Structure, Petrologic Characteristics, and Chronologic Data

Dorrel Rock. Dorrel Rock is the only intrusive rock in Marie Byrd Land related to the Cenozoic volcanic suite, with the exception of the cognate xenoliths found in some lava flows. It is an isolated nunatak composed entirely of equigranular alkaline gabbro (Table B.16A.1), with a pronounced north-south oriented feldspar flow structure. East-west cross joints are occupied by dikes of mugearite and aegirine-augite syenite (Table B.16A.1). Published dates for the gabbro (53. 1 ± 4.2, 44 ± 2, 42 ± 2 Ma) and the syenite (28 ± 2 Ma) contradict the cogenetic relationship between these two rock types that is implied by the field relations [*LeMasurier*, 1972*a*; *LeMasurier and Rex*, 1982*a*]. The 28-Ma date for the syenite, shown in Figure B.16A.1, is believed to be the most credible of the dates, partly because there was contemporaneous and near-contemporaneous volcanic activity to the west (see IVD B.16B) and also because the strongly zoned feldspars in the gabbro suggest the possibility of argon retention and therefore an anomalously old date [*LeMasurier and Rex*, 1982*a*]. The major significance of Dorrel Rock is that it appears to represent the inception of Cenozoic alkaline magmatism in this province, either in the Eocene or, more likely, in the late Oligocene. It is also of interest that syenitic (trachytic) magma was produced at that time. There is a patchy record suggesting fairly continuous basaltic volcanism in this province from 28 Ma to very recent time, but trachytic and other felsic eruptive activity apparently did not begin until the formation of the Mount Flint–Reynolds Ridge volcano (see IVD B.11), roughly 10 m.y. after the Dorrel Rock magma consolidated [*LeMasurier and Rex*, 1982*a*, 1989*a*]. A sample of Dorrel Rock gabbro (60A) has yielded an initial $^{87}Sr/^{86}Sr$ ratio of 0.70322 [*Futa and LeMasurier*, 1983].

Turtle Peak and Hedin Nunatak. These two large and entirely volcanic nunataks lie 5 km west of the base of Mount Murphy (Figure B.16A.1). They are both flat topped, very steep sided, and somewhat elongate north-south, with a vertical relief of 250–300 m. Each consists of stratigraphically complex assemblages of subhorizontally bedded hydroclastic deposits, subaerial flows, and Strombolian tephra, of basaltic composition. Hyaloclastites predominate at the base of Turtle Peak and are interbedded with subaerial flows in the upper half of the section. They appear to become more vesicular toward the top of the peak. At Hedin Nunatak, palagonitized and unpalagonitized Strombolian tephras are abundant at the base of the section, interbedded with pillow lavas (or pahoehoe toes?) in some places, and overlain by a summit section of subaerial lava flows. Both nunataks, but Turtle Peak especially, seem to represent the emergence of a volcanic pile from a subglacial (Turtle Peak) or periglacial (Hedin Nunatak) environment to one that was completely subaerial.

Field relationships and gross compositional similarities suggest the possibility that both nunataks may be outliers of the Mount Murphy basal succession and, thus, that all three belong to the same shield volcano complex. The K-Ar data are not extensive here, but available dates suggest that Mount Murphy formed in the late Miocene, Turtle Peak in the middle Miocene, and Hedin Nunatak in the early Miocene (Figure B.16A.1). Furthermore, the *hy*-normative Mount Murphy basalts seem distinctively different from the *ne*-normative basalts and basanites at Turtle Peak and Hedin Nunatak. The former contain 5–8% normative *hy*, as compared to 2.5–5.5% normative *ne* and more than 10% normative *ol* in the latter (Table B.1.1 and Table B.16A.2). Note also the unusually high TiO_2 and extraordinarily high Ba values of the Mount Murphy "main shield" basalts. At this time, therefore, the analytical and field data together seem to indicate that Turtle Peak and Hedin Nunatak are erosional remnants of small shield volcanoes or table mountains that are independent of each other and perhaps 4–12 m.y. older than the Mount Murphy shield volcano.

Kohler Range. Two small patches of volcanic rock have been observed in the Kohler Range, resting on the early Tertiary erosion surface at elevations of about 800 m. The yellow tuff reported west of Morrison Bluff (Wade, personal communication, 1968) was observed at close range from the air but was never visited. The thin veneer of lava near Leister Peak (Figure B.16A.1) has been visited and

Copyright American Geophysical Union

TABLE B.16A.1. Representative Chemical Analyses of Volcanic Rocks From the Walgreen Coast Satellitic Centers

	Dorrel Rock			Turtle Peak		Hedin Nunatak		Kohler Range
	1	2	3	4	5	6	7	8
SiO_2	43.03	53.28	61.52	46.03	46.47	44.91	44.92	45.03
TiO_2	6.05	1.21	0.28	3.15	3.15	2.95	2.45	2.00
Al_2O_3	17.57	18.07	18.45	15.63	15.66	14.84	13.40	16.00
Fe_2O_3	6.07	3.51	2.70	2.35	2.41	4.11	2.83	3.82
FeO	7.84	6.37	2.77	10.30	10.15	8.23	8.93	9.55
MnO	0.16	0.19	0.12	0.23	0.22	0.19	0.18	0.19
MgO	3.82	1.93	0.19	5.80	5.60	7.45	10.74	8.23
CaO	10.80	4.90	1.50	10.22	10.27	11.11	10.74	9.33
Na_2O	3.37	5.83	6.45	3.61	3.53	3.34	2.81	3.26
K_2O	0.72	3.36	5.35	0.92	0.91	0.95	0.77	0.76
P_2O_5	0.11	0.33	0.04	0.78	0.81	0.76	0.45	0.04
H_2O^+	0.37	1.39	0.46	0.00	0.00	0.00	0.00	1.50
H_2O^-	0.08	0.16	0.01	0.16	0.00	0.00	0.88	0.15
F	0.02	0.00	0.00	0.05	0.04	0.06	0.02	0.00
CO_2	0.65	0.00	0.00	0.00	0.00	0.00	0.00	0.10
Total	100.66	100.53	99.84	99.69	99.62	99.71	99.90	100.38
Ba	125	246	346	328	294	275	236	372
Ce	6	229	197	69	77	68	58	67
Co	22	0	4	41	39	41	65	48
Cr	21	0	0	65	61	174	636	271
Cu	27	3	0	59	58	9	80	79
Ga	23	38	26	21	20	20	18	18
La	8	108	76	42	26	34	29	38
Nb	5	172	126	34	35	40	36	47
Ni	8	0	0	41	39	83	245	151
Pb	3	11	10	6	11	6	4	0
Rb	9	88	114	15	16	20	17	13
Sr	934	44	68	799	813	741	624	627
Th	5	9	8	2	5	7	2	1
U	0	6	2	0	2	0	2	1
V	387	23	12	284	289	306	265	220
Y	8	90	41	27	25	28	22	31
Zn	44	211	72	94	92	79	90	86
Zr	108	861	430	149	161	185	161	147

Major elements for samples 60A, 60C, 60D, and 84 determined by wet chemistry by H.B. Wiik, Geological Survey of Finland. All other data determined at University of Nottingham, England; FeO determined by wet chemistry, F by selective ion electrode (SIE), and other elements by XRF.

1. 60A. Gabbro, Dorrel Rock.
2. 60C Mugearite dike, Dorrel Rock.
3. 60D Syenite dike, Dorrel Rock.
4. 41F Basalt, Turtle Peak.
5. 41D Basalt, Turtle Peak.
6. 43C Basanite, Hedin Nunatak.
7. 43D Basanite, Hedin Nunatak.
8. 84. Basalt, Leister Peak, Kohler Range.

Copyright American Geophysical Union

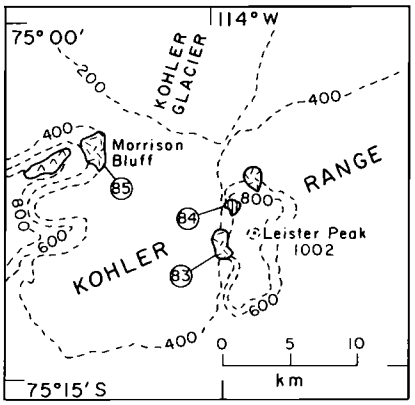

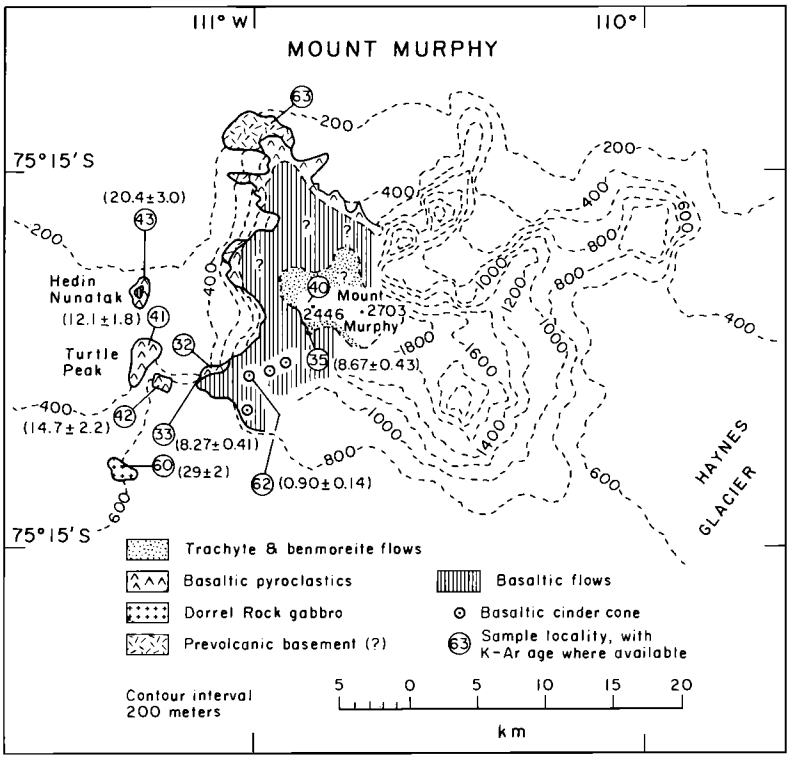

Fig. B.16A.1. Geologic sketch maps of the Walgreen Coast satellitic centers and of Mount Murphy. Geology is by W.E. LeMasurier; K-Ar ages are from *LeMasurier and Rex* [1982*a*, 1983]. Base maps are the Mount Murphy and Toney Mountain quadrangles (1973), scale 1:250,000 USGS Reconnaissance Series, Antarctica, U.S. Geological Survey.

sampled. It appears to be contemporaneous with the basal succession lavas at Toney Mountain (see IVD B.3) but chemically more like the lavas at Turtle Peak and Hedin Nunatak than those at Toney Mountain.

Extent of Knowledge

Dorrel Rock and the Leister Peak (Kohler Range) locality have each been visited once, in January 1968. Turtle Peak was visited briefly during the same reconnaissance. In January 1985, Hedin Nunatak was visited for the first time and Turtle Peak revisited during 1 day of fieldwork on the outlying nunataks near Mount Murphy. Sixteen chemical analyses and 12 K-Ar dates were available at the time of writing.

Bibliography

Futa and LeMasurier, 1983
LeMasurier, 1972*a*
LeMasurier and Rex, 1982*a*, 1983, 1989*a*
LeMasurier and Wade, 1976

Copyright American Geophysical Union

TABLE B.16A.2. CIPW Norms and Modal Analyses of Volcanic Rocks From the Walgreen Coast Satellitic Centers

	Dorrel Rock			Turtle Peak		Hedin Nunatak		Kohler Range
	1	2	3	4	5	6	7	8
				CIPW Norms				
or	4.26	19.85	31.61	5.44	5.38	5.61	4.55	4.49
ab	22.81	38.11	54.31	24.16	25.89	19.44	16.40	20.21
an	30.69	13.22	5.60	23.73	24.20	22.70	21.68	26.78
ne	3.09	6.07	0.13	3.46	2.16	4.78	4.00	4.00
ac	0.00	0.00	0.00	0.00	0.00	0.00	0.00	0.00
di	17.26	7.49	1.37	18.00	17.66	22.08	23.05	15.63
wo	0.00	0.00	0.00	0.00	0.00	0.00	0.00	0.00
ol	1.06	6.10	1.81	13.04	12.55	10.91	18.75	17.67
mt	8.26	5.09	3.92	3.41	3.49	5.96	4.10	5.54
hm	0.38	0.00	0.00	0.00	0.00	0.00	0.00	0.00
il	11.49	2.30	0.53	5.98	5.98	5.60	4.65	3.80
ap	0.24	0.78	0.10	1.81	1.88	1.76	1.04	0.09
fr	0.00	0.00	0.00	1.68	1.72	1.60	0.97	0.00
cc	1.48	0.00	0.00	0.00	0.00	0.00	0.00	0.23
				*Modal Analyses**				
Phenocrysts, %								
Plag	0.0	0.0	0.0	0.4				
Alk fsp	0.0	0.0	43.0	0.0				
Ca-Cpx	0.0	0.0	0.0	1.2				
Na-Cpx	0.0	0.0	0.8	0.0				
Oliv	0.0	0.0	0.0	4.6				
Opaq	0.0	0.0	0.4	0.0				
Groundmass, %								
Plag	52.3	0.0	0.0	36.6				
Alk fsp	0.0	52.0	40.4	0.0				
Cpx	36.5	4.4	5.4	25.2				
Ne	0.0	1.2	0.0	0.0				
Amph	0.7	15.4	7.4	0.0				
Aenig	1.2	23.4	0.0	0.0				
Oliv	0.0	0.0	0.0	12.4				
Opaq	8.2	4.8	2.2	17.0				
Glass/matr	0.0	0.0	0.0	2.6				
Alter	1.1	0.0	0.0	0.0				
% Phenocrysts	0.0	0.0	44.2	6.2				

*Based on 500 counts. Analyses by W.E. LeMasurier and R.M. Burke.

1. 60A. Gabbro, Dorrel Rock.
2. 60C. Mugearite dike, Dorrel Rock.
3. 60D. Syenite dike, Dorrel rock.
4. 41F. Basalt, Turtle Peak.
5. 41D. Basalt, Turtle Peak.
6. 43C. Basanite, Hedin Nunatak.
7. 43D. Basanite, Hedin Nunatak.
8. 84. Basalt, Leister Peak, Kohler Range.

Copyright American Geophysical Union

B.16B. MIOCENE-OLIGOCENE CENTERS, MOUNT PETRAS, AND THE USAS ESCARPMENT

Type of volcano: Unknown; possible remnants of table mountains and/or tuff cones.
Location: ~200–250 km inland from the Amundsen Sea coast (76°S, 124°–129°W).
Height above sea level: Mount Petras, 2700–2900 m; Usas Escarpment, 2200 m.
Evidence of Holocene activity: None.
Author of report: W.E. LeMasurier.
Date of report: August 1986.

Form and Structure, Petrologic Characteristics, and Chronologic Data

Four diverse localities are here grouped together because they appear to lie along an east-west structural trend that includes all of the oldest volcanic localities in the province (Figures B.I, B.II, and B.X). The distance from Mount Petras to Mount Aldaz is 120 km.

Mount Petras. The Mount Petras massif is a sharply angular mountain (Figures B.16B.1 and B.16B.2) composed mainly of a late Mesozoic volcanic complex, truncated at the 2700-m level by an early Tertiary erosion surface, and surmounted by an ~200-m section of subhorizontally stratified basaltic hyaloclastites [*LeMasurier et al.*, 1981]. The crude bedding, weakly vesicular clasts, and lack of accretionary lapilli or other significant subaerial component,

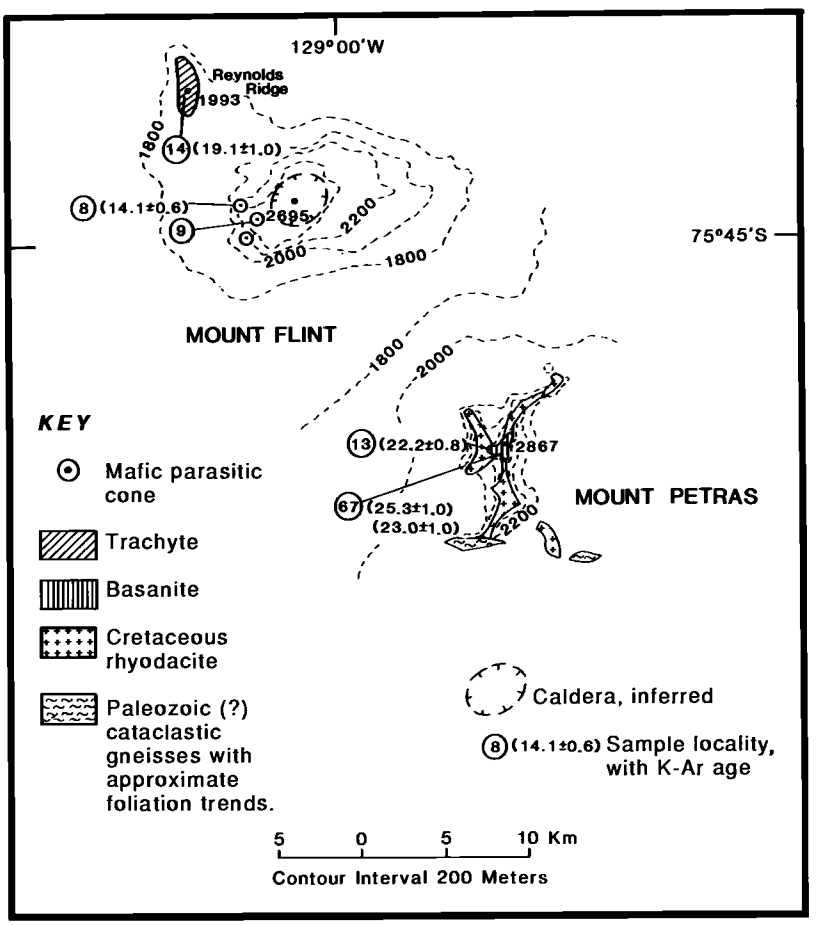

Fig. B.16B.1. Geologic sketch map of Mount Petras and Mount Flint. Geology is by W.E. LeMasurier; K-Ar dates are from *LeMasurier and Rex* [1982*a*, 1983]. Base map is the McCuddin Mountains quadrangle (1973), scale 1:250,000 USGS Reconnaissance Series, Antarctica, U.S. Geological Survey.

Copyright American Geophysical Union

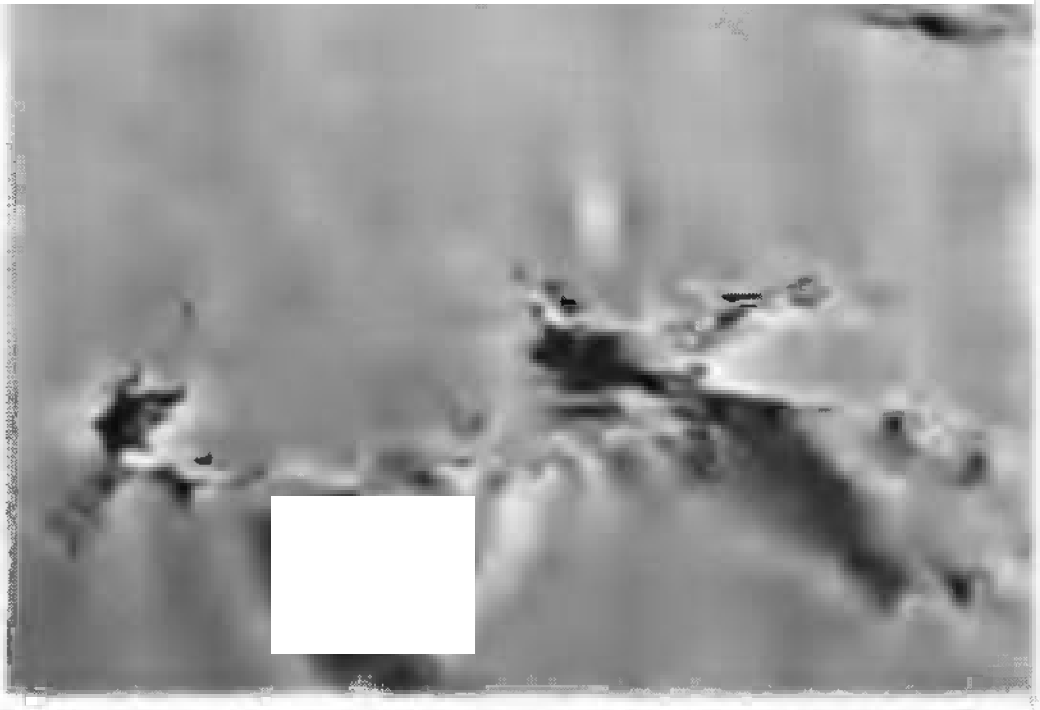

Copyright American Geophysical Union

TABLE B.16B.1. Representative Chemical Analyses of Volcanic Rocks From Mount Petras and the Usas Escarpment

	Mount Petras		Usas Escarpment	
	1	2	3	4
SiO_2	45.36	48.16	45.31	47.63
TiO_2	2.35	2.56	2.69	2.00
Al_2O_3	18.39	15.86	15.34	17.98
Fe_2O_3	2.50	2.35	4.49	4.98
FeO	9.00	9.18	8.53	8.17
MnO	0.17	0.21	0.16	0.19
MgO	6.14	6.08	7.76	3.04
CaO	8.14	8.20	7.90	6.70
Na_2O	3.95	4.59	3.45	4.62
K_2O	1.70	1.72	1.26	1.61
P_2O_5	0.06	0.79	0.67	0.44
H_2O^+	1.91	0.00	2.52	2.07
H_2O^-	0.37	0.00	0.00	0.34
F	0.00	0.00	0.06	0.03
CO_2	0.00	0.00	0.20	0.30
Total	100.04	99.71	100.34	100.10
Ba	494	492	313	421
Ce	147	160	84	120
Co	34	34	47	27
Cr	198	163	268	6
Cu	45	47	41	25
Ga	21	19	17	24
La	64	67	8	105
Nb	89	95	53	78
Ni	87	78	174	0
Pb	7	5	6	4
Rb	36	42	24	17
Sr	742	752	757	669
Th	8	9	4	10
U	0	2	0	3
V	235	223	231	107
Y	35	36	30	44
Zn	102	105	93	103
Zr	370	383	254	349

Major elements determined by wet chemistry by H.B. Wiik, Geological Survey of Finland (13B, 56B, and 58B), and by XRF at University of Otago, New Zealand (PT67D). All trace elements determined by XRF at University of Nottingham, England; F determined by selective ion electrode (SIE).

1. 13B. Basanite, Mount Petras.
2. PT67D. Hawaiite, Mount Petras.
3. 56B. Basalt, Mount Aldaz, Usas Escarpment.
4. 58B. Hawaiite, Usas Escarpment.

TABLE B.16B.2. CIPW Norms and Modal Analyses of Volcanic Rocks From Mount Petras and the Usas Escarpment

	Mount Petras		Usas Escarpment	
	1	2	3	4
CIPW Norms				
or	10.05	10.16	7.45	9.51
ab	17.94	26.66	27.30	36.37
an	27.43	17.59	22.65	23.57
ne	8.39	6.60	1.02	1.47
ac	0.00	0.00	0.00	0.00
ns	0.00	0.00	0.00	0.00
di	10.28	14.68	9.79	4.06
wo	0.00	0.00	0.00	0.00
hy	0.00	0.00	0.00	0.00
ol	15.45	13.91	16.17	9.95
mt	3.62	3.41	6.51	7.22
hm	0.00	0.00	0.00	0.00
il	4.46	4.86	5.11	3.80
ap	0.13	1.83	1.55	1.02
fr	0.00	0.00	0.00	0.00
cc	0.00	0.00	0.43	0.68
*Modal Analyses**				
Phenocrysts, %				
Plag	0.2		--	3.2
Oliv	1.0		2.0	4.0
Opaq	0.0		--	1.4
Groundmass, %				
Plag	36.0		35.4	43.0
Cpx	31.2		0.0	5.0
Oliv	12.2		16.8	7.6
Opaq	19.4		9.8	19.2
Glass/matr	0.0		35.2	16.6
Alter	0.0		0.8	0.0
% Phenocrysts	1.2		2.0	8.6

Dashes, not detected.

*Based on 500 counts. Analyses by W.E. LeMasurier and R.M. Burke.

1. 13B. Basanite, Mount Petras.
2. PT67D. Hawaiite, Mount Petras.
3. 56B. Basalt, Usas Escarpment.
4. 58B. Hawaiite, Usas Escarpment.

a basaltic cinder cone. Lherzolite nodules were found in the basal flow and in the cinder cone lavas. The age of the basal flow, and elevation of the contact, fit the uplift curve shown in Figure B.XI, suggesting a close relationship between volcanism and fault displacement along the escarpment, as noted above for Mount Petras.

At locality 58, basalt flow rock and palagonitized hyaloclastite tuff breccias have yielded the oldest K-Ar age

Copyright American Geophysical Union

Copyright American Geophysical Union

of any volcanic rock in Marie Byrd Land (28.2 ± 1.2 Ma). At the east end of the exposure the deposit is horizontally stratified, matrix-poor tuff and includes a large proportion of flow rock. This grades westward into steeply north dipping, matrix-rich tuff breccias, with highly vesicular sideromelane clasts. This relationship may represent a transition from subaerial flows to subglacial flow foot breccia, or an intercalation of flows and hydroclastic tuff cone deposits. The vertical relief on the exposure is not adequate to define the structure unambiguously.

The exposure at locality 59, east of Mount Galla, is a small outcrop that appears to be mainly Strombolian tephra. No material suitable for dating or chemical analysis was found.

Extent of Knowledge

Mount Petras and the Usas Escarpment were discovered during the U.S. Antarctic Service Expedition, 1939–1941, after which the escarpment is named. Mount Petras is named for Theodore A. Petras, pilot of the airplane that made the discovery flight. The first visit to Mount Petras and the Usas Escarpment (then the "Un-named" escarpment) was made during the 1959–1960 Executive Committee Range oversnow traverse [*Doumani*, 1960; *Doumani and Ehlers*, 1962]. A more extensive visit was made by the helicopter-supported 1967–1968 Marie Byrd Land survey, and Mount Petras was visited again by a helicopter-supported party in 1977–1978. Only five K-Ar dates and five chemical analyses of Cenozoic rocks are available.

Bibliography

Doumani, 1960
Doumani and Ehlers, 1962
Futa and LeMasurier, 1983
González-Ferrán and González-Bonorino, 1972
LeMasurier, 1972*a*
LeMasurier and Rex, 1982*a*, 1983, 1989*a*
LeMasurier and Wade, 1976
LeMasurier et al., 1979, 1981
McIntosh, 1981

Copyright American Geophysical Union

B.16C. MIOCENE-PLIOCENE CENTERS, HOBBS COAST

Type of volcano: Isolated flows (Patton Bluff, Kouperov Peak, Holmes Bluff, and Bowyer Butte), composite cinder cone - tuff cone (Cousins Rock), table mountain(?) remnant (Coleman Nunatak and Shibuya Peak).

Location: Hobbs Coast sector of the Amundsen Sea (75°S, 133°–135°W).

Height above sea level: 400–1000 m.

Evidence of Holocene activity: None.

Author of report: W.E. LeMasurier.

Date of report: August 1986.

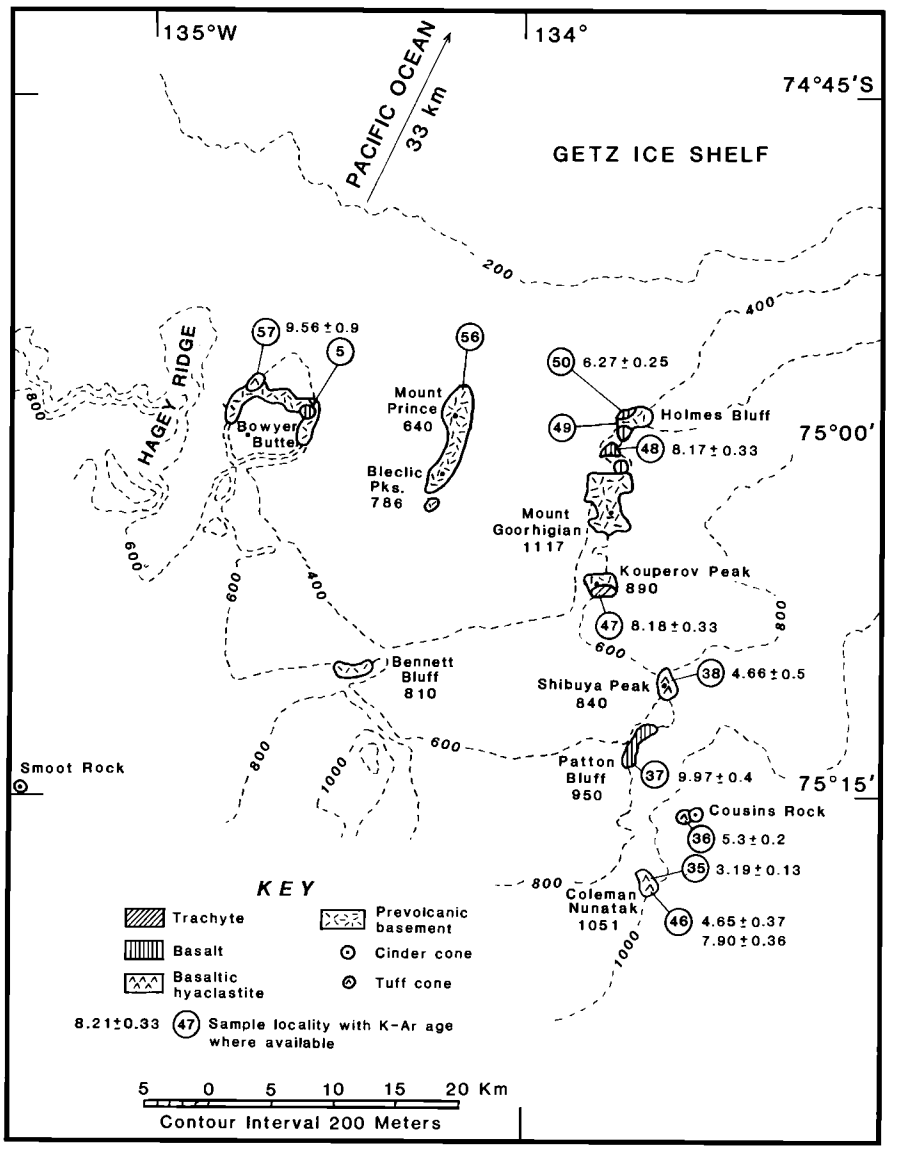

Fig. B.16C.1. Geologic sketch map of Miocene-Pliocene volcanic rocks on the Hobbs Coast. Geology is by W.E. LeMasurier; K-Ar dates are from *LeMasurier and Rex* [1983]. Base maps are the Mount Kosciusko (1973) and Grant Island (1970) quadrangles, scale 1:250,000 USGS Reconnaissance Series, Antarctica, U.S. Geological Survey.

Copyright American Geophysical Union

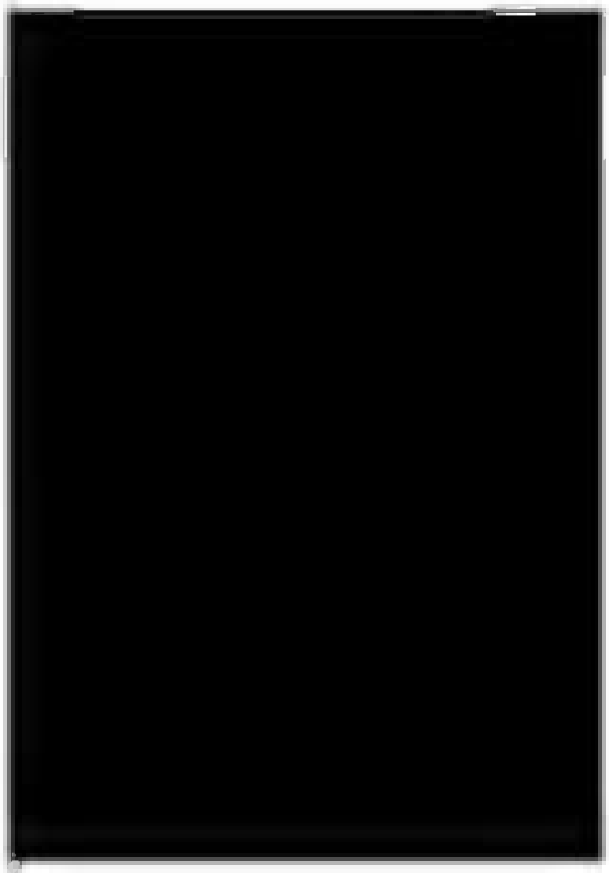

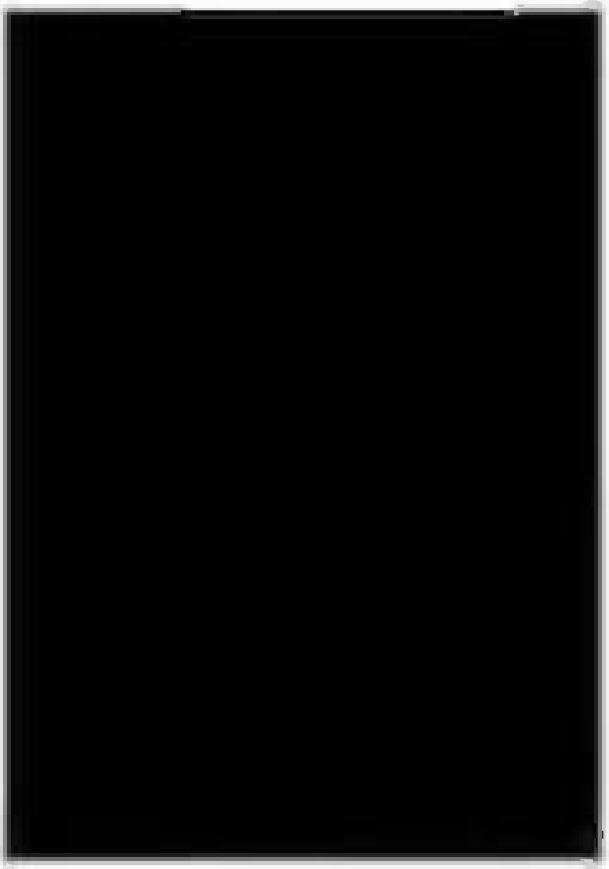

Copyright American Geophysical Union

TABLE B.16C.1. Representative Chemical Analyses and CIPW Norms of Miocene-Pliocene Volcanic Rocks From the Hobbs Coast

	Coleman Nunatak		Patton Bluff	Shibuya Peak		Kouperov Peak		Holmes Bluff		Bowyer Butte
	1	2	3	4	5	6	7	8	9	10
SiO_2	43.16	43.47	45.68	45.33	45.67	46.08	58.21	45.81	48.56	43.27
TiO_2	3.76	3.84	2.61	2.73	2.79	2.74	0.54	2.43	2.19	1.82
Al_2O_3	15.21	14.66	14.77	16.46	14.86	16.93	18.33	15.72	15.65	16.19
Fe_2O_3	5.37	3.63	3.48	1.59	3.72	4.30	3.29	5.37	3.27	5.66
FeO	8.31	9.54	8.27	9.67	8.71	7.53	3.54	7.27	7.89	6.51
MnO	0.27	0.12	0.08	0.17	0.18	0.22	0.17	0.21	0.10	0.15
MgO	6.83	7.01	9.15	8.30	7.12	5.56	0.45	7.60	7.79	10.12
CaO	9.78	9.89	9.16	10.13	9.45	9.10	2.16	9.35	9.52	9.85
Na_2O	4.43	3.77	2.51	3.37	3.85	4.21	7.68	4.14	3.41	2.71
K_2O	1.72	1.24	1.06	1.20	1.41	4.59	4.59	1.13	0.92	0.92
P_2O_5	0.87	0.79	0.56	0.45	0.78	0.76	0.14	0.84	0.44	0.04
H_2O^+	0.00	0.00	0.00	0.00	0.00	0.00	0.00	0.00	0.00	1.97
H_2O^-	0.00	0.57	1.01	0.07	0.71	0.73	0.20	0.61	0.84	0.60
F	0.00	0.00	0.00	0.08	0.05	0.00	0.01	0.00	0.00	0.00
CO_2	0.00	0.00	0.00	0.00	0.00	0.00	0.00	0.00	0.00	0.00
Total	99.74	99.00	98.61	100.38	99.10	99.57	99.30	100.86	100.79	99.81
or	10.28	10.16	7.33	7.09	8.33	8.33	27.13	8.92	6.68	5.44
ab	13.09	13.69	21.24	15.42	21.67	25.01	46.47	21.26	28.25	15.29
an	16.48	18.00	25.37	26.24	19.10	23.13	1.95	19.85	24.06	29.30
ne	13.21	9.86	0.00	7.10	5.91	5.75	10.03	7.46	0.33	4.14
di	21.07	20.95	13.17	17.15	18.35	13.56	6.69	16.80	16.37	15.30
hy	0.00	0.00	4.93	0.00	0.00	0.00	0.00	0.00	0.00	0.00
ol	8.65	11.39	14.17	17.87	12.66	9.66	0.68	11.61	14.35	16.03
mt	7.79	5.26	5.05	2.31	5.39	6.23	4.77	7.79	4.74	8.21
il	7.14	7.29	4.96	5.18	5.30	5.20	1.03	4.61	4.16	3.46
ap	2.02	1.83	1.30	1.04	1.81	1.76	0.32	1.95	1.02	0.08
Ba	559	553	282	281	405	370	1281	493	254	321
Ce	133	140	73	67	105	83	147	121	50	65
Co	45	43	52	58	39	43	5	37	43	56
Cr	102	103	329	290	211	82	0	220	285	391
Cu	43	44	63	73	66	47	15	57	63	69
Ga	18	19	19	20	18	20	24	17	20	17
La	69	69	35	37	51	39	79	56	31	37
Nb	91	91	49	52	63	51	146	67	41	48
Ni	67	64	192	135	99	51	8	113	154	241
Pb	4	6	5	6	8	3	8	3	0	0
Rb	37	37	24	26	23	26	82	28	15	20
Sr	1031	1038	639	859	816	767	214	961	550	633
Th	5	3	1	1	1	0	12	3	0	2
U	4	0	0	2	0	0	0	5	0	2
V	313	309	237	258	235	232	11	227	224	252
Y	35	34	28	3	29	33	44	30	28	26
Zn	91	83	83	85	98	90	112	84	82	77
Zr	296	301	222	186	234	252	547	215	203	137

Major elements determined by wet chemistry by H.B. Wiik, Geological Survey of Finland (6C and 5), and by XRF at University of Nottingham, England (77-47D), and University of Otago, New Zealand (77-35M, 46B, 37A, 47B, 50A, and 48B). All trace elements determined by XRF at University of Nottingham; F determined by selective ion electrode (SIE) and FeO determined by wet chemistry at University of Nottingham for all samples except 6C and 5.

1. 77-35M. Tephrite, Coleman Nunatak.
2. 77-46B. Basanite, Coleman Nunatak.
3. 77-37A. *Hy*-basalt, Patton Bluff.
4. 6C. Basalt, Shibuya Peak.
5. 77-38A. Hawaiite, Shibuya Peak.
6. 77-47B. Tephrite, Kouperov Peak.
7. 77-47D. Phonolite, Kouperov Peak.
8. 77-50A. Hawaiite, Holmes Bluff.
9. 77-48B. Basalt, Holmes Bluff.
10. 5. Basalt, Bowyer Butte.

Copyright American Geophysical Union

samples range between 0.70258 and 0.70280, all among the lowest obtained for Marie Byrd Land rocks.

Chronologic Data

The K-Ar dates from the Hobbs Coast nunataks have played a key role in estimating rates of uplift, documenting glacial history, helping illustrate the petrologic independence of each basalt locality, and helping estimate magma production rates. The age of the base of the section at each nunatak appears to increase with increasing elevation, and this relationship (see Figure B.XI), when extended to include Mount Petras, Mount Aldaz, and the Kohler Range, forms a basis for estimating rates of uplift in the whole province [*LeMasurier and Rex,* 1983]. There appears to be a pattern, implicit in this interpretation of Figure B.XI, in which the inception of volcanic activity is followed by uplift of horsts and subsidence of grabens in the area affected by volcanism.

There is no apparent geographic pattern to the activity in these small centers [*LeMasurier and Rex,* 1989*a*]. The differences in age from one center to another reinforce the inference, derived from petrochemical differences, that each eruptive center represents a separate event of magma generation from sources that were grossly similar but not interconnected.

The hyaloclastites at Bowyer Butte and Shibuya Peak have yielded K-Ar dates of 9.56 and 4.66 Ma, respectively. These are suggestive of continental glaciation in middle Miocene and early Pliocene time, because the flatness of the unconformity, and the apparently postvolcanic age of uplift, point to an environment of low relief near sea level at the time the hyaloclastites were formed [*LeMasurier and Rex,* 1982*a*].

The ~150-m thickness of hyaloclastite at Coleman Nunatak has been sampled and dated at several levels from the bottom to the top of the section. A representative sample of dates is shown in Figure B.16C.1. The dates show good correlation with stratigraphic position, and it appears therefore that the section has accumulated as a result of multiple, small-scale eruptions over a period of at least 5 m.y. This stands out as an example of a very low magma production rate, in marked contrast to the major volcanic centers such as Mount Murphy (see IVD B.1) or Mount Takahe (see IVD B.2), where large shield volcanoes apparently formed in <1 m.y.

Extent of Knowledge

This group of nunataks was discovered during a reconnaissance flight by the U.S. Antarctic Service Expedition (1939–1941) and first visited in November 1967 by the helicopter-supported Marie Byrd Land Survey. More detailed investigations were carried out during the November–December 1977 season, again by helicopter-supported geologic field parties. This report is based on a total of 23 K-Ar dates, 15 chemical analyses, and 5 Rb/Sr and Sm/Nd isotopic analyses. Most of these nunataks are named for meteorologists and atmospheric physicists who were involved with scientific projects at Byrd Station (80°S, 120°W) in 1961 and 1962.

Bibliography

Futa and LeMasurier, 1983
LeMasurier, 1972*a*
LeMasurier and Rex, 1982*a*, 1983, 1989*a*, *b*
LeMasurier et al., 1979
McIntosh, 1981

Copyright American Geophysical Union

B.16D. PLIOCENE-PLEISTOCENE HOBBS COAST VOLCANOES

Type of volcano: Tuff cone(s) (Mathewson Point), composite Strombolian-phreatomagmatic cone (Mount Obiglio), lava dome(?) (Mount Colburn), table mountain (Cruzen Island).

Locations: Hobbs and Ruppert coasts (~74°30′S, 131°–133° and ~140°W).

Height above sea level: 247–510 m.

Evidence of Holocene activity: None.

Author of report: W.E. LeMasurier.

Date of report: August 1986.

Form and Structure, Petrologic Characteristics, and Chronologic Data

Shepard Island and Grant Island. This volcanic center is characterized by the apparently contemporaneous eruption of a highly diverse suite of lavas and hyaloclastites from numerous small vents in Pleistocene time (Figure B.16D.1). Small volume and highly differentiated products are the hallmarks of this locality. The structure and form of individual eruptive centers are not well preserved. The Mathewson Point hyaloclastites are fine-grained, evenly laminated deposits with large-scale cross-bedding, beds rich in accretionary lapilli, and numerous examples of soft-sediment deformation, all of which indicate that this is a tuff cone or tuff-cone complex that has been truncated on the seaward side. The original constructional geometry of the deposit is not clear.

Mount Obiglio (Grant Island) is an isolated small cone composed of palagonitized Strombolian tephra. It evidently represents a transition between Strombolian and Surtseyan eruptive behavior.

At Mount Petinos an ~500-m thickness of crystal-rich, highly vesicular, subhorizontally stratified hyaloclastite tuff and tuff breccia is exposed in a vertical sea cliff. The age and composition of this deposit suggest that it is not part of the nearby Mathewson Point eruptive center. It can only be interpreted in broad terms as either a shallow subaquatic deposit or a phreatomagmatic tuff-cone deposit.

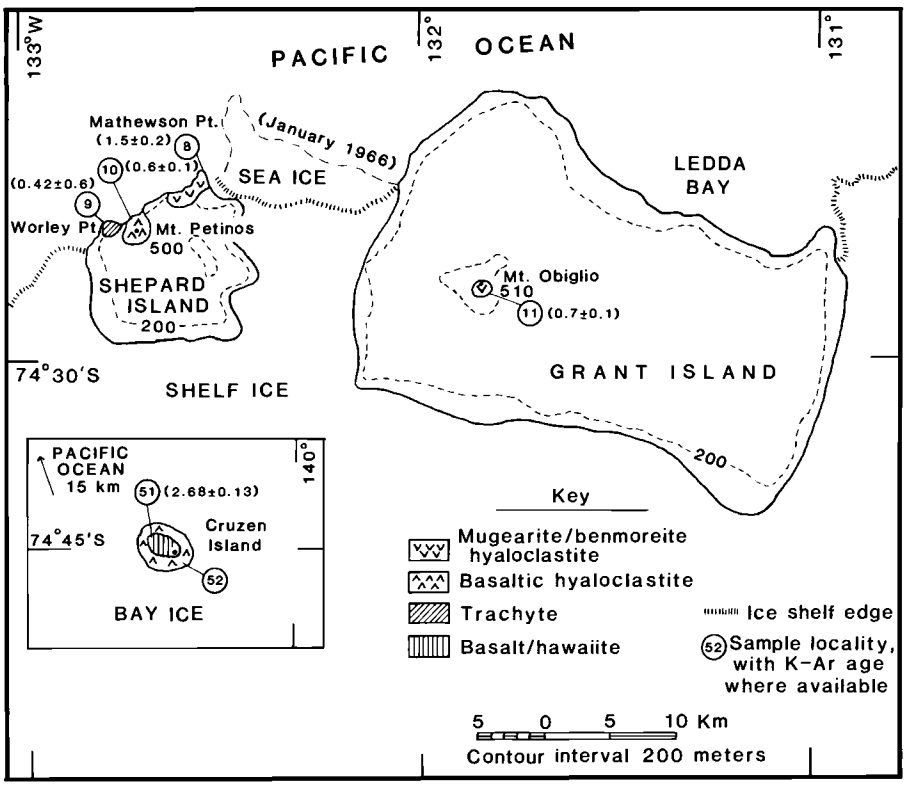

Fig. B.16D.1. Geologic sketch map of Pliocene-Pleistocene Hobbs Coast volcanoes. Geology is by W.E. LeMasurier; K-Ar dates are from *LeMasurier and Rex* [1983]. Base maps are the Grant Island and Cape Burks quadrangles (1970), scale 1:250,000 USGS Reconnaissance Series, Antarctica, U.S. Geological Survey.

Copyright American Geophysical Union

TABLE B.16D.1. Representative Chemical Analyses and CIPW Norms of Volcanic Rocks From Shepard, Grant, and Cruzen Islands

	Shepard Island			Grant Island	Cruzen Island
	1	2	3	4	5
SiO_2	47.06	48.86	62.31	55.11	48.30
TiO_2	2.84	3.33	0.49	0.72	2.15
Al_2O_3	14.93	14.14	15.32	15.04	13.88
Fe_2O_3	4.23	3.23	1.87	5.00	2.43
FeO	10.71	9.72	4.53	7.19	9.29
MnO	0.32	0.18	0.17	0.40	0.15
MgO	3.73	4.42	0.34	0.69	8.54
CaO	7.77	8.38	1.80	4.09	8.92
Na_2O	4.74	4.19	6.38	4.92	3.59
K_2O	1.69	1.61	5.42	3.45	0.69
P_2O_5	1.88	0.79	0.42	0.25	0.35
H_2O^+	0.00	0.00	0.00	0.00	0.00
H_2O^-	0.00	0.00	0.34	1.99	0.00
F	0.00	0.08	0.04	0.00	0.03
CO_2	0.00	0.00	0.00	0.00	0.00
Total	99.89	98.83	99.43	98.85	98.37
Q	0.00	0.00	0.35	2.41	0.00
or	9.99	9.51	32.03	20.39	4.08
ab	34.48	34.00	48.63	41.63	30.38
an	14.47	15.02	0.00	8.76	19.72
ne	3.05	0.79	0.00	0.00	0.00
ac	0.00	0.00	4.72	0.00	0.00
di	9.85	17.64	5.43	8.59	18.05
hy	0.00	0.00	5.63	5.89	0.02
ol	12.19	9.05	0.00	0.00	17.62
mt	6.13	4.68	0.35	7.25	3.52
il	5.39	6.32	0.93	1.37	4.08
ap	4.36	1.83	0.97	0.58	0.81
Ba	645	706	192	3922	229
Ce	157	104	180	202	43
Co	41	--	--	0	45
Cr	11	25	5	0	293
Cu	33	--	--	11	63
Ga	22	--	--	28	21
La	58	44	68	102	23
Nb	54	42	78	118	29
Ni	7	17	8	0	45
Pb	0	--	--	8	3
Rb	23	32	93	45	11
Sr	794	723	65	477	500
Th	2	5	2	5	2
U	2	1	2	5	0
V	208	203	7	25	208
Y	44	37	1	72	21
Zn	152	--	--	194	108
Zr	246	248	513	641	120

Major elements determined by XRF at University of Nottingham, England (SI10D, SI9D, and CI51C), and University of Otago, New Zealand (SI8D and GI11C). For all samples, trace elements determined by XRF, F by selective ion electrode (SIE), and FeO by wet chemistry, all at University of Nottingham. Dashes, not determined.

1. SI8D. Basanite, Mathewson Point, Shepard Island.
2. SI10D. Hawaiite, Mount Petinos, Shepard Island.
3. SI9D. Trachyte, Worley Point, Shepard Island.
4. GI11C. Benmoreite, Mount Obiglio, Grant Island.
5. CI51C. Basalt, Cruzen Island.

Copyright American Geophysical Union

The Worley Point trachyte is a platy flow rock that was originally mistaken by the first reconnaissance party for a well-indurated sandstone [*Klimov*, 1967], and it is represented on geologic maps of that era as the Shepard Island quartzite [*Craddock*, 1970, 1972; *Wade*, 1969; *Wade and Wilbanks*, 1972]. A subsequent visit established that the rock is trachyte and that the original error was probably related to the fact that the entire exposure occurs in a penguin rookery and is covered with penguin guano [*LeMasurier et al.*, 1980].

The wide range in composition of the rocks at Shepard Island and Grant Island (see Table B.16D.1) can only be matched elsewhere in Marie Byrd Land in the large shield volcanoes. It seems quite possible that this locality represents the initial stage in the development of a felsic shield volcano, by analogy with Mount Berlin, for example (see IVD B.15), where the two large late Pleistocene trachyte cones were apparently preceded by two earlier and less voluminous cycles of activity dated at 0.6 Ma and 2.5 Ma. The Shepard Island–Grant Island center can also be viewed as a renewal of felsic activity along the Ames Range line, representing the continued northward migration of felsic volcanism that began at Mount Andrus (see IVD B.12) in the mid-Miocene [*LeMasurier and Rex*, 1989*a*]. The analyses presented in Table B.16D.1 suggest that magmatic evolution here is characterized by compositions that vary from slightly undersaturated to slightly oversaturated, becoming peralkaline in the latter (trachytic) stages of evolution. In these gross compositional characteristics this volcanic center is comparable to Mount Berlin (see IVD B.15), Mount Bursey (see IVD B.13), and Mount Takahe (see IVD B.2).

The very young K-Ar ages of felsic and intermediate rocks at Shepard and Grant islands suggest that this volcanic center has a moderately high potential for future activity [*LeMasurier and Rex*, 1982*b*].

Cruzen Island. Cruzen Island is located 240 km west of Shepard Island and 70 km north of the closest coastal exposures. It is the best example of an Icelandic table mountain type of volcano in this province, with a flat top and vertical sides roughly 200 m high. The lower 50–75 m of section is composed of basaltic hyaloclastite and is overlain by horizontal subaerial basalt flows extending to the summit. Lherzolite nodules are abundant in the hyaloclastite at locality 52 (Figure B.16D.1). One analysis, representing the only accessible flow rock on the island, is presented in Table B.16D.1.

A single K-Ar date (2.68 ± 0.13 Ma) suggests a late Pliocene age for the activity at Cruzen Island, roughly contemporaneous with the most recent activity at Coleman Nunatak (see IVD B.16C) and the earliest activity at Mount Berlin (see IVD B.15).

Cruzen Island is included here with Shepard Island and Grant Island only as part of a group of near coastal volcanic islands of Pliocene-Pleistocene age; no implied relationship is intended. The extent of knowledge does not merit a separate entry, and it could equally well have been included in IVD B16C or IVD B.16E.

Extent of Knowledge

Shepard Island and Grant Island were visited during 1966–1967 and 1977–1978 austral summers by helicopter-supported geologic field parties. A total of five K-Ar dates and four chemical analyses were available during the preparation of this report. Cruzen Island was visited during 1 day of fieldwork in December 1977.

Bibliography

Craddock, 1970, 1972
Klimov, 1967
LeMasurier and Rex, 1982*b*, 1983, 1989*a*, *b*
LeMasurier et al., 1980
McIntosh, 1981
Wade, 1969
Wade and Wilbanks, 1972

Copyright American Geophysical Union

B.16E. FOSDICK MOUNTAINS

Type of volcano: Multiple (maximum of 15) scoria cones, tuff cones, and composite Strombolian-phreatomagmatic cones.

Location: Predominantly on the flanks of the Fosdick Mountains (76°30′S, 145°W), Ford Ranges, possibly related to flanking faults.

Height above sea level: 400–1125 m.

Evidence of Holocene activity: None.

Authors of report: W.E. LeMasurier and F.A. Wade.[1]

Date of report: August 1986.

[1]Deceased October 1978.

General Description

The Fosdick Mountains and Vulcan Nunatak (Figure B.16E.1) were first visited by P. Siple and by F.A. Wade in 1934 as part of the second expedition led by Rear Admiral R.E. Byrd. *Fenner* [1938] subsequently described volcanic rocks collected by Siple, including the ultramafic nodules characteristic of at least three of these volcanoes. The area was revisited by Wade and by L.A. Warner in 1940 (U.S. Antarctic Service Expedition under Rear Admiral R.E. Byrd) and by Wade and J.R. Wilbanks in 1966–1967. Volcanic rocks were described briefly by *Warner* [1945] and mapped by *Wade et al.* [1977]. The area is notable mainly for the relative abundance of mantle xenoliths and

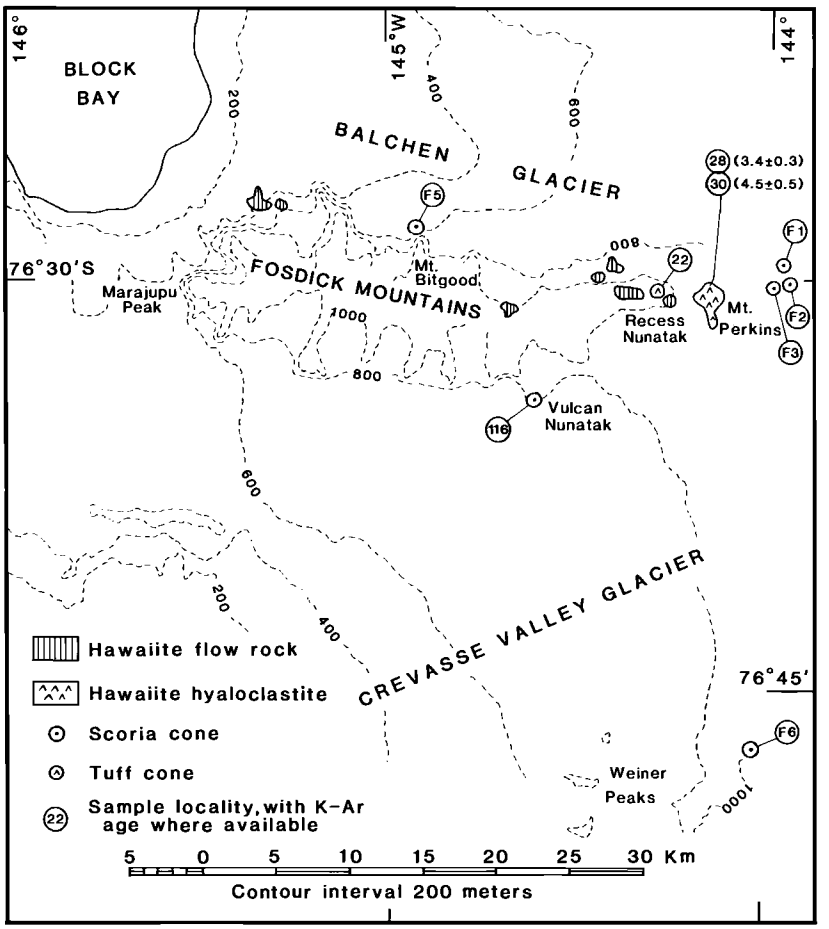

Fig. B.16E.1. Geologic sketch map of the Fosdick Mountains (modified from *Wade et al.* [1977]). K-Ar ages are from *LeMasurier and Rex* [1982*a*].

Copyright American Geophysical Union

TABLE B.16E.1. Chemical Analyses and CIPW Norms of Volcanic Rocks From the Fosdick Mountains

	1	2	3	4
SiO_2	47.55	47.80	47.99	49.27
TiO_2	2.32	2.15	2.27	1.92
Al_2O_3	13.28	13.32	13.61	13.82
Fe_2O_3	3.11	1.94	3.33	1.02
FeO	7.83	8.13	7.68	9.52
MnO	0.16	0.17	0.16	0.15
MgO	7.77	8.43	7.56	9.03
CaO	10.23	9.83	9.91	9.12
Na_2O	3.41	3.26	3.22	3.19
K_2O	0.74	0.78	0.74	0.52
P_2O_5	0.37	0.35	0.35	0.26
H_2O^+	0.00	0.00	0.00	0.00
H_2O^-	1.83	1.46	1.34	0.50
F	0.02	0.02	0.02	0.02
CO_2	0.00	0.00	0.00	0.00
Total	98.62	97.64	98.18	98.34
or	4.37	4.61	4.37	3.07
ab	27.82	27.59	27.25	26.99
an	18.75	19.41	20.50	21.86
ne	0.56	0.00	0.00	0.00
di	23.86	21.90	21.26	17.65
hy	0.00	0.42	5.73	8.81
ol	11.64	14.53	7.76	13.70
mt	4.51	2.81	4.83	1.48
il	4.41	4.08	4.31	3.65
ap	0.86	0.81	0.81	0.60
fr	0.80	0.76	0.76	0.55
Ba	266	294	278	211
Ce	28	32	43	25
Cr	233	262	248	355
La	21	22	23	16
Nb	26	23	25	12
Ni	140	162	145	156
Rb	11	13	11	11
Sr	515	482	498	425
Th	5	9	0	0
U	4	0	0	2
V	202	184	193	166
Y	27	8	29	24
Zr	144	131	140	110

All samples analyzed by XRF at University of Nottingham, England; FeO determined by wet chemistry and F by selective ion electrode (SIE).

1. 66D-27 Basalt, Mount Perkins.
2. 66D-28. Basalt, Mount Perkins.
3. 66D-30. Basalt, Mount Perkins.
4. 66D-91. Basalt, locality F5.

for the *hy*-normative basalt occurrences (Table B.16E.1). The only dates considered to be reliable indicate a Pliocene age for the activity at Mount Perkins [*LeMasurier and Rex*, 1982*a*], roughly contemporaneous with the activity at Shibuya Peak (see IVD B.16C), Coleman Nunatak (see IVD B.16C), and Mount Moulton (see IVD B.14).

Bibliography

Fenner, 1938
LeMasurier and Rex, 1982*a*
Wade and Wilbanks, 1972
Wade et al., 1977
Warner, 1945

Copyright American Geophysical Union

BIBLIOGRAPHY

Anderson, V.H., The petrography of some rocks from Marie Byrd Land, Antarctica, USNC-IGY Antarctic Glaciological Data: Field Work 1958 and 1959, *Rep. 825-2*, part VIII, 27pp., Ohio State Univ., Columbus, 1960.

Andrews, J.T., and W.E. LeMasurier, Rates of Quaternary glacial erosion and corrie formation, Marie Byrd Land, Antarctica, *Geology, 1*, 75–80, 1973.

Bentley, C.R., Crustal structure of Antarctica, *Tectonophysics, 20*, 229–240, 1973.

Bentley, C.R., and F.K. Chang, Geophysical exploration in Marie Byrd Land, Antarctica, in *Antarctic Snow and Ice Studies II, Antarct. Res. Ser.*, vol. 16, pp. 1–38, edited by A.P. Crary, AGU, Washington, D. C., 1971.

Bentley, C.R., and J.W. Clough, Antarctic subglacial structure from seismic refraction measurements, in *Antarctic Geology and Geophysics*, edited by R.J. Adie, pp. 683–691, Universitetsforlaget, Oslo, 1972.

Bentley, C.R., A.P. Crary, N.A. Ostenso, and E.C. Thiel, Structure of West Antarctica, *Science, 131*, 131–136, 1960.

Boudette, E.L., and A.B. Ford, Physical properties of anorthoclase from Antarctica, *Am. Mineral., 51*(9–10), 1374–1387, 1966.

Coombs, D.S., Trends and affinities of basaltic magmas and pyroxenes as illustrated on the diopside-olivine-silica diagram, *Spec. Pap. Mineral. Soc. Am., 1*, 227–250, 1963.

Coombs, D.S., and J.F.G. Wilkinson, Lineages and fractionation trends in saturated volcanic rocks from the East Otago volcanic province (New Zealand) and related rocks, *J. Petrol., 10*, 440–501, 1969.

Cooper, R.A., C.A. Landis, W.E. LeMasurier, and I.G. Speden, Geologic history and regional patterns in New Zealand and West Antarctica—Their paleotectonic and paleogeographic significance, in *Antarctic Geoscience*, edited by C. Craddock, pp. 43–53, University of Wisconsin Press, Madison, 1982.

Craddock, C., Geologic map of Antarctica, scale 1: 10,000,000, in *Geologic Maps of Antarctica, Antarct. Map Folio Ser.*, folio 12, plate 20, edited by V.C. Bushnell and C. Craddock, American Geographical Society, New York, 1970.

Craddock, C., Geologic map of Antarctica, scale 1: 5,000,000, American Geographical Society, New York, 1972.

Dort, W., Jr., Late Cenozoic volcanism in Antarctica, in *Antarctic Geology and Geophysics*, edited by R.J. Adie, pp. 645–652, Universitetsforlaget, Oslo, 1972.

Doumani, G.A., Geological observations in West Antarctica during recent oversnow traverses, *IGY Bull. Nat. Acad. Sci., 41*, 6–10, 1960.

Doumani, G.A., Volcanoes of the Executive Committee Range, Byrd Land, in *Antarctic Geology*, edited by R.J. Adie, pp. 666–675, North-Holland, Amsterdam, 1964.

Doumani, G.A., and E.G. Ehlers, Petrography of rocks from mountains in Marie Byrd Land, West Antarctica, *Geol. Soc. Am. Bull., 73*(7), 877–882, 1962.

Drewry, D.J. (Ed.), Antarctica: Glaciological and geophysical folio, Scott Polar Res. Inst., Cambridge, England, 1982.

Eaton, G.P., A plate tectonic model for late Cenozoic crustal spreading in the western United States, in *Rio Grande Rift: Tectonics and Magmatism*, edited by R.E. Riecker, pp. 7–32, AGU, Washington, D. C., 1979.

Ellerman, P.J., Depositional environments and post-depositional alteration of Cenozoic hyaloclastites in Antarctica, Ph.D. dissertation, Univ. of Colorado, Boulder, 1989.

Fenner, C.N., Olivine fourchites from Raymond Fosdick Mountains, Antarctica, *Geol. Soc. Am. Bull., 49*, 367–400, 1938.

Fisher, R.V., and H.-U. Schmincke, *Pyroclastic Rocks*, Springer-Verlag, New York, 1984.

Futa, K., and W.E. LeMasurier, Nd and Sr isotopic studies on Cenozoic mafic lavas from West Antarctica: Another source for continental alkali basalts, *Contrib. Mineral. Petrol., 83*, 38–44, 1983.

Gass, I.G., D.S. Chapman, H.N. Pollack, and R.S. Thorpe, Geological and geophysical parameters of mid-plate volcanism, *Phil. Trans. R. Soc. London, Ser. A, 288*, 581–597, 1978.

González-Ferrán, O., Cadeñas volcanicas de la Tierra Maria Byrd, Antarctica Occidental, *Bol. Inst. Antart. Chil.*, no. 4, 19–24, 1969.

González-Ferrán, O., and F. González-Bonorino, The volcanic ranges of Marie Byrd Land between long. 100° and 140°W, in *Antarctic Geology and Geophysics*, edited by R.J. Adie, pp. 261–276, Universitetsforlaget, Oslo, 1972.

González-Ferrán, O., and M. Vergara, Post-Miocene volcanic petrographic provinces of West Antarctica and their relation to the southern Andes of South America, in *Antarctic Geology and Geophysics.*, edited by R.J. Adie, pp. 187–195, Universitetsforlaget, Oslo, 1972.

Grindley, G.W., and P.J. Oliver, Palaeomagnetism of Cretaceous volcanic rocks from Marie Byrd Land, Antarctica, in *Antarctic Earth Science*, edited by R.L. Oliver, P.R. James and J.B. Jago, pp. 573–578, Cambridge University Press, New York, 1983.

Halpern, M., Sr 87/86 ratios of ultramafic nodules and host basalt from the McMurdo area and Ford Ranges, Antarctica, *Antarct. J. U.S., 4*, 206–207, 1969.

Halpern, M., Rubidium-strontium dates and Sr^{87}/Sr^{86} initial

Copyright American Geophysical Union

ratios of rocks from Antarctica and South America: A progress report, *Antarct. J. U.S.*, *5*, 160–161, 1970.

Halpern, M., Rb-Sr total-rock and mineral ages from the Marguerite Bay area, Kohler range and Fosdick Mountains, in *Antarctic Geology and Geophysics*, edited by R.J. Adie, pp. 197–204, Universitetsforlaget, Oslo, 1972.

Hamilton, W., and E.L. Boudette, Quaternary alkaline basalt-trachyte province, Marie Byrd Land and South Victoria Land, Antarctica, *Proc. Int. Symp. Volcanol. Jpn.*, pp. 18–19, 1962.

Irvine, T.N., and W.R.A. Baragar, A guide to the chemical classification of the common volcanic rocks, *Can. J. Earth Sci.*, *8*, 523–548, 1971.

Jones, J.G., and P.H.H. Nelson, The flow of basalt lava from air into water—its structural expression and stratigraphic significance, *Geol. Mag.*, *107*, 13–19, 1970.

Klimov, L.V., Some results of geological observations in Marie Byrd Land, 1966–67, *Sov. Antarct. Exped. Inform. Bull.*, Engl. Transl., *66*, 18–25, 1967.

Kyle, P.R., P.A. Jezek, E. Mosley-Thompson, and L.G. Thompson, Tephra layers in the Byrd Station ice core and the Dome C ice core, Antarctica and their climatic importance, *J. Volcanol. Geotherm. Res.*, *11*, 29–39, 1981.

Le Bas, J.J., R.W. Le Maitre, A. Streckeisen, and B. Zanettin, A chemical classification of volcanic rocks based on the total alkali-silica diagram, *J. Petrol.*, *27*, 745–750, 1986.

Le Maitre, R.W., A proposal by the IUGS Subcommission on the Systematics of Igneous rocks for a chemical classification of volcanic rocks based on the total alkali silica (TAS) diagram, *Aust. J. Earth Sci.*, *31*, 243–255, 1984.

LeMasurier, W.E., Volcanic record of Cenozoic glacial history of Marie Byrd Land, in *Antarctic Geology and Geophysics*, edited by R.J. Adie, pp. 251–260, Universitetsforlaget, Oslo, 1972*a*.

LeMasurier, W.E., Volcanic record of Antarctic glacial history: Implications with regard to Cenozoic sea levels, in *Polar Geomorphology, Spec. Publ. 4*, compiled by R.J. Price and D.E. Sugden, pp. 59–74, Institute of British Geographers, London, 1972*b*.

LeMasurier, W.E., Marie Byrd Land Quaternary volcanism: Byrd ice core correlations and possible climatic influences, *Antarct. J. U.S.*, *7*, 139–414, 1972*c*.

LeMasurier, W.E., The Cenozoic West Antarctic rift system and its associated volcanic and structural features, *Geol. Soc. Am. Abstr. Programs*, *10*, 443, 1978.

LeMasurier, W.E., Relationship between pillow lavas, hyaloclastites, and the crystal content of glass in the subaquatic volcanoes of West Antarctica, paper presented at the Symposium on Arc Volcanism, IAVCEI, Tokyo-Hakone, Japan, 1981.

LeMasurier, W.E., Mt. Siple volcano, Marie Byrd Land, *Antarct. J. U.S.*, *19*, 33–35, 1984.

LeMasurier, W.E., and D.C. Rex, Volcanic record of Cenozoic glacial history in Marie Byrd Land and western Ellsworth Land: Revised chronology and evaluation of tectonic factors, in *Antarctic Geoscience*, edited by C. Craddock, pp. 725–734, University of Wisconsin Press, Madison, 1982*a*.

LeMasurier, W.E., and D.C. Rex, Eruptive potential of volcanoes in Marie Byrd Land, West Antarctica, *Antarct. J. U.S.*, *17*, 34–36, 1982*b*.

LeMasurier, W.E., and D.C. Rex, Rates of uplift and scale of ice level instabilities recorded by volcanic rocks in Marie Byrd Land, West Antarctica, in *Antarctic Earth Sciences*, edited by R.L. Oliver, P.R. James, and J.B. Jago, pp. 663–670, Cambridge University Press, New York, 1983.

LeMasurier, W.E., and D.C. Rex, Evolution of linear volcanic ranges in Marie Byrd Land, West Antarctica, *J. Geophys. Res.*, *94*, 7223–7236, 1989*a*.

LeMasurier, W.E., and D.C. Rex, Tectonic significance of linear volcanic ranges in Marie Byrd Land in late Cenozoic time, in *Geological Evolution of Antarctica*, edited by M.R.A. Thomson, J.A. Crame, and J.W. Thomson, Cambridge University Press, New York, in press, 1989*b*.

LeMasurier, W.E., and F.A. Wade, Fumarolic activity in Marie Byrd Land, *Science*, *162*, 352, 1968.

LeMasurier, W.E., and F.A. Wade, Volcanic history in Marie Byrd Land: Implications with regard to southern hemisphere tectonic reconstructions, in *Proceedings of the International Symposium on Andean and Antarctic Volcanology Problems*, edited by O. González-Ferrán, pp. 398–424, IAVCEI, Rome, 1976.

LeMasurier, W.E., P.R. Kyle, and P.C. Rankin, Rare-earth element geochemistry of volcanic rocks from the Executive Committee Range, Marie Byrd Land, *Antarct. J. U.S.*, *11*(4), 263–267, 1976.

LeMasurier, W.E., O. Melander, G.W. Grindley, and W.C. McIntosh, Tillite, glacial striae, and hyaloclastite associations on the Hobbs Coast, Marie Byrd Land, *Antarct. J. U.S.*, *14*, 48–50, 1979.

LeMasurier, W.E., G.W. Grindley, and D.C. Rex, The unsuccessful search for the Shepard Island Quartzite in Marie Byrd Land, *Antarct. J. U.S.*, *15*, 20–21, 1980.

LeMasurier, W.E., W.C. McIntosh, and D.C. Rex, Mid-Tertiary glacial history recorded at Mt. Petras, Marie Byrd Land, *Antarct. J. U.S.*, *16*, 19–21, 1981.

LeMasurier, W.E., W.C. McIntosh, and P.J. Ellerman, Pyroclastic facies in Marie Byrd Land volcanoes (abstract), paper presented at International Volcanological Congress, IAVCEI, Hamilton, New Zealand, 1986*a*.

LeMasurier, W.E., W.C. McIntosh, and D.C. Rex, Miocene glacial history recorded at Mount Murphy volcano in eastern Marie Byrd Land, *Antarct. J. U.S.*, *21*, 52–54, 1986*b*.

Macdonald, R., and D.K. Bailey, The chemistry of the peralkaline oversaturated obsidians, *U.S. Geol. Surv. Prof. Pap. 440-N-1*, 37 pp., 1973.

Copyright American Geophysical Union

Macdonald, G.A., and T. Katsura, Chemical composition of Hawaiian lavas, *J. Petrol.*, *5*, 82–133, 1964.

McIntosh, W.C., Rock magnetism and paleomagnetism of Antarctic hyaloclastites, M.S. thesis, 145 pp., Univ. of Colorado, Boulder, 1981.

McIntosh, W.C., and W.E. LeMasurier, Rock magnetism and opaque mineralogy of hyaloclastites from Marie Byrd Land and Ross Island, *Antarct. J. U.S.*, *16*, 25–27, 1981.

McIntosh, W.C., W.E. LeMasurier, P.J. Ellerman, and N.W. Dunbar, A re-interpretation of glacio-volcanic interaction at Mt. Takahe and Mt. Murphy, Marie Byrd Land, Antarctica, *Antarct. J. U.S.*, *20*, 57–59, 1985.

Noble, D.C., Sodium, potassium and ferrous iron contents of some secondarily hydrated natural silicic glasses, *Am. Mineral.*, *52*, 280–286, 1967.

Pearce, J.A., and J.P. Cann, Tectonic setting of basic volcanic rocks determined using trace element analyses, *Earth Planet. Sci. Lett.*, *19*, 290–300, 1973.

Pearce, J.A., and M.J. Norry, Petrogenetic implications of Ti, Zr, Y, and Nb variations in volcanic rocks, *Contrib. Mineral. Petrol.*, *69*, 33–47, 1979.

Pearce, J.A., B.E. Gorman, and T.C. Birkett, The relationship between major element chemistry and tectonic environment of basic and intermediate volcanic rocks, *Earth Planet. Sci. Lett.*, *36*, 121–132, 1977.

Schwarzer, J.S., and J.J.W. Rogers, A worldwide comparison of alkali olivine basalts and their differentiation trends, *Earth Planet. Sci. Lett.*, *23*, 286–296, 1974.

Seward, D., P.R. Kyle, and W.E. LeMasurier, Fission track ages of Marie Byrd Land volcanic rocks, *Antarct. J. U.S.*, *15*, 19, 1980.

Smithsonian Institution, Mt. Siple, Marie Byrd Land, Antarctica, *SEAN Bull.*, *13*(9), 6, 1988*a*.

Smithsonian Institution, Mt. Siple, Marie Byrd Land, Antarctica, *SEAN Bull.*, *13*(12), 20, 1988*b*.

Smithsonian Institution/SEAN, *Global Volcanism 1975–1985*, Prentice-Hall, Englewood Cliffs, N.J., 1989.

Steiger, R.H., and E. Jäger, Subcommission on geochemistry: Convention on the use of decay constants in geo- and cosmochemistry, *Earth Planet. Sci. Lett.*, *36*, 359–362, 1977.

Stock, J., and P. Molnar, Revised history of early Tertiary plate motion in the south-west Pacific, *Nature*, *325*, 495–499, 1987.

Wade, F.A., Geology of Marie Byrd Land, in *Geologic Maps of Antarctica, Antarctic Map Folio Ser.*, folio 12, plate 17, edited by V.C. Bushnell and C. Craddock, American Geographical Society, New York, 1969.

Wade, F.A., and J.R. Wilbanks, Geology of Marie Byrd and Ellsworth lands, in *Antarctic Geology and Geophysics*, edited by R.J. Adie, pp. 207–214, Universitetsforlaget, Oslo, 1972.

Wade, F.A., C.A. Cathey, and J.B. Oldham, Reconnaissance Peninsula quadrangle, Marie Byrd Land, Antarctica, scale 1:250,000, *Antarct. Geol. Map A-7*, U.S. Geol. Surv., Reston, Va., 1977.

Warner, L.A., Structure and petrography of the southern Edsel Ford Ranges, Antarctica, *Proc. Am. Phil. Soc.*, *89*(1), 78–122, 1945.

Copyright American Geophysical Union

Copyright American Geophysical Union

Summary

P.D. Rowley, J.W. Thomson, J.L. Smellie, T.S. Laudon, K.E. La Prade, and W.E. LeMasurier

Frontispiece. Basaltic lava flow near Mount Pinafore, Elgar Uplands, showing well-developed colonnade and entablature columnar jointing. The flow is about 60m thick. (Photograph by M.J. Hole.)

Introduction

The upper Cenozoic volcanic rocks exposed in Alexander Island, Palmer Land, and Ellsworth Land are referred to informally here as the Bellingshausen volcanic province, although they are a geographical group rather than a volcanic entity. The province extends for 1600 km along the Pacific coast of West Antarctica (Figure C.I) and contains some of the least accessible and most poorly known areas in Antarctica. Cenozoic volcanic rocks are widely scattered in the province, and most of the exposures are small, isolated, and badly eroded, suggesting that they are pre-Quaternary; original volcanic landforms are preserved in few places. Study of many of the volcanic fields has been only at a reconnaissance level, some of it many years ago. Thus the locations of most volcanic centers are unknown, and they are probably largely under ice. Few volcanoes are named except for those in the Hudson Mountains. Sizable volcanic fields occur only in the Hudson Mountains, in the Jones Mountains, and at several places on Alexander Island (Table C.I). Some of the more interesting fields in the province have received the least amount of study: for example, no fieldwork has been undertaken in the Hudson Mountains since the 1960s, and the volcanic rocks from there have received only a cursory field and laboratory investigation.

Cenozoic volcanic rocks have not been found in Palmer Land [*British Antarctic Survey,* 1982]. However, *Singleton* [1980] noted a small intrusive mass of fresh alkaline basalt [*Smellie*, 1987] in the Seward Mountains (72°31′S, 66°04′W), although its precise age is unknown.

Individual volcano descriptions (IVD's) are listed from north to south. The region is incompletely surveyed, and detailed elevation data for snow surfaces and rock exposures are sparse. Nonetheless, most Cenozoic volcanic rocks in the province occur at elevations of less than 1250 m above sea level.

Copyright American Geophysical Union

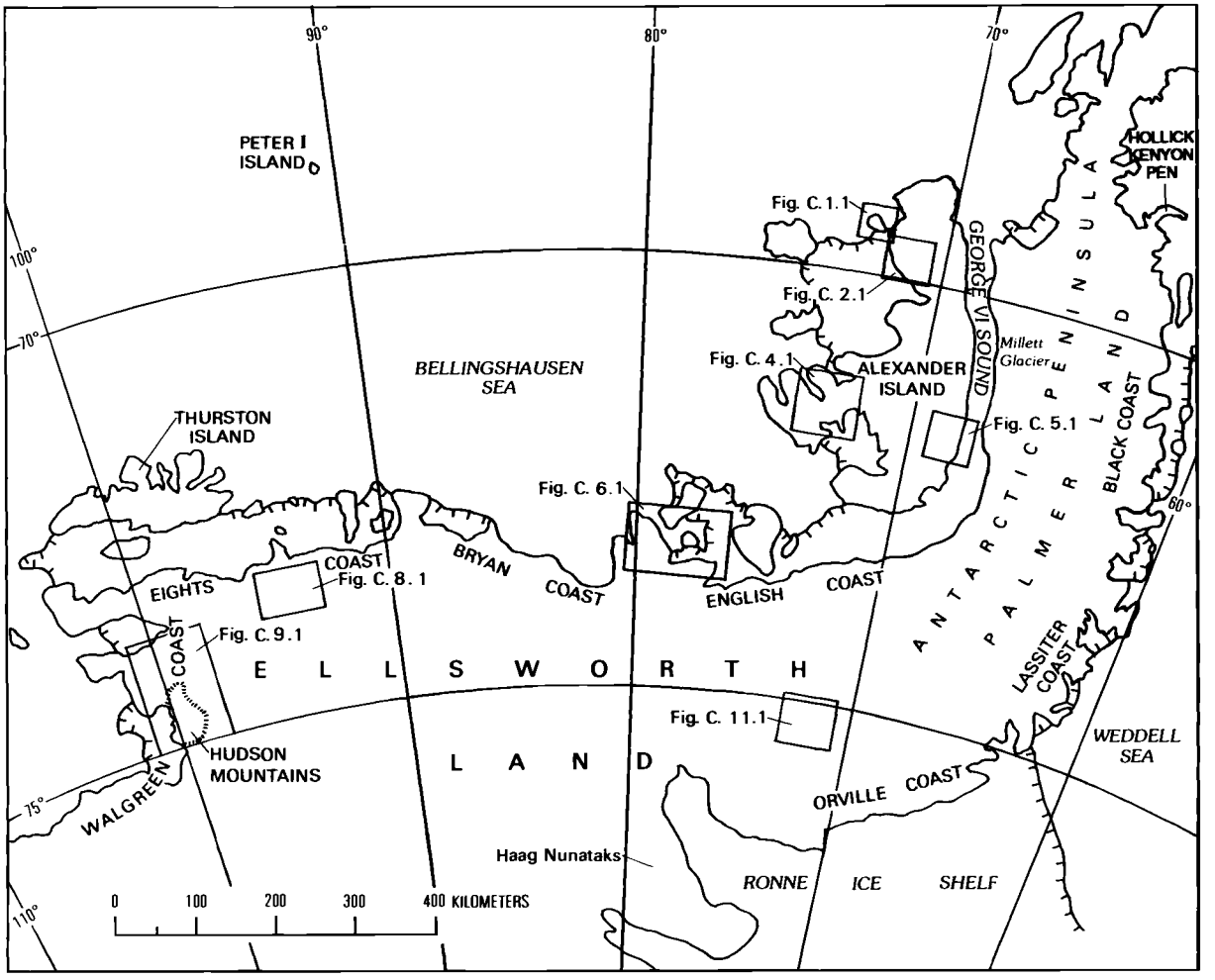

Fig. C.I. Index map of the Bellingshausen volcanic province showing geographic features mentioned in the text. Locations of figures given in the IVD's are outlined. Hachured lines mark the edges of ice shelves. The location for IVD C.3 is included in Figure C.2.1, that for IVD C.7 in Figure C.6.1, and that for IVD C.10 in Figure C.11.1.

Tectonic Setting

Although few contacts with older rocks are exposed, most Cenozoic volcanic rocks of this province are believed to rest with angular unconformity on calc-alkaline plutonic and volcanic rocks, which represent a magmatic arc that evolved from at least the late Paleozoic to Late Cretaceous [*Williams et al.*, 1972; *Dalziel*, 1982; *Pankhurst*, 1982; *Rowley and Williams*, 1982; *Thomson et al.*, 1983; *British Antarctic Survey*, 1985*a*; *Storey et al.*, 1987; *Rowley et al.*, 1989]. Associated sedimentary deposits of fore-arc basins and mélange wedges occur on the Pacific side of the magmatic arc (in Alexander Island and western Antarctic Peninsula) and of back-arc basins on the Atlantic side (in eastern Antarctic Peninsula and eastern Ellsworth Land). Subduction terminated first during the Cretaceous in the western part of the arc (in Marie Byrd Land and this province) and progressively later in northern parts (Graham Land) [*Herron and Tucholke*, 1976; *Barker*, 1982].

West Antarctica consists of at least four structural blocks of continental lithosphere (Figure C.II) and

Copyright American Geophysical Union

TABLE C.I. Summary of Occurrences of Cenozoic Basaltic Rocks of the Bellingshausen Volcanic Province

IVD	Name	Type	Height Above Sea Level, m	Deposit	Composition	Date, Ma
C.1	Rothschild Island (69°36′S, 72°33′W)	Small volcanic field	0–400	Palagonite tuff, lava flows, dikes	Tephrite, basanite	late Miocene or early Pliocene 5.4 ± 0.7
C.2	Mount Pinafore–Debussy Heights (69°46′S, 70°52′W; 69°53′S, 71°23′W)	Volcanic field	1000–1500, 800	Palagonite tuff, lava flows	Basanite, tephrite, hawaiite	late Miocene to early Pliocene 7.7 ± 0.6 to 3.9 ± 0.4
C.3	Hornpipe Heights (69°52′S, 70°35′W)	Small volcanic field	800	Agglutinate, lava flows, subaerial tuff	Basanite	Pliocene 2.5 ± 0.8
C.4	Beethoven Peninsula (71°44′S, 73°41′W)	Volcanic field	250–1050	Palagonite tuff, lava flows, volcanic breccia	Hawaiite, basalt, potassic trachybasalt	Pliocene to Pleistocene (?) 2.5 to <1 (?)
C.5	SE Alexander Island (~71°36′S, 68°30′W)	Dikes	100–250	Dikes	Potassic trachybasalt, phonotephrite	Miocene 15 ± 1
C.6	Rydberg Peninsula (73°19′S, 78°53′W)	Volcanic field	400	Lava flows	Hawaiite	late Cenozoic
C.7	Snow Nunataks (73°35′S, 77°06′W)	Volcanic field	0–600	Palagonite tuff, lava flows, dikes	Hawaiite, basalt	late Cenozoic
C.8	Jones Mountains (73°32′S, 94°00′W)	Volcanic field	750–1500	Palagonite tuff, lava flows, dikes	Basalt, tephrite	Miocene
C.9	Hudson Mountains (74°25′S, 99°30′W)	Volcanic field with stratovolcanoes, parasitic cones	200–750	Palagonite tuff, lava flows, volcanic breccia	Basalt, hawaiite	late Miocene to Pliocene 8.5 ± 1.0 to 3.7 ± 0.2
C.10	Henry Nunataks (75°08′S, 72°36′W)	Small volcanic field	1200–1450	Lava flows, dike	Potassic trachybasalt	late Cenozoic
C.11	Merrick Mountains (75°06′S, 72°04′W)	Small volcanic field	1250	Lava flows, flow breccia	Basanite	late Miocene(?) 6(?)

probably other smaller ice-covered crustal blocks, all of which differ from each other in lithology and/or structural trends [*Behrendt*, 1964*a*, *b*; *Schopf*, 1969; *Bentley and Clough*, 1972; *Dalziel and Elliot*, 1982; *Bentley*, 1983; *Grunow et al.*, 1987]. These four major crustal blocks are Antarctic Peninsula–eastern Ellsworth Land, Ellsworth Mountains–Whitmore Mountains plus Haag Nunataks area, western Ellsworth Land (Thurston Island), and Marie Byrd Land. The continental area covered in this section consists of the western Ellsworth Land block and the southern Antarctic Peninsula block. These blocks probably resulted from fragmentation during the breakup of Gondwanaland. After breakup, the blocks migrated only short distances, after which they collided and had similar postcollisional (Jurassic(?) to Cenozoic) geologic histories [*Rowley*, 1983; *Schmidt and Rowley*, 1986; *Rowley et al.*, 1989; *Storey*, 1989].

The Cenozoic volcanic rocks in this province, however, are related to a younger, entirely different tectonic setting from that of the crustal blocks, namely, extension [*Storey and Garrett*, 1985] that affected the area regardless of which older crustal block it belonged to and apparently uncontrolled by

Copyright American Geophysical Union

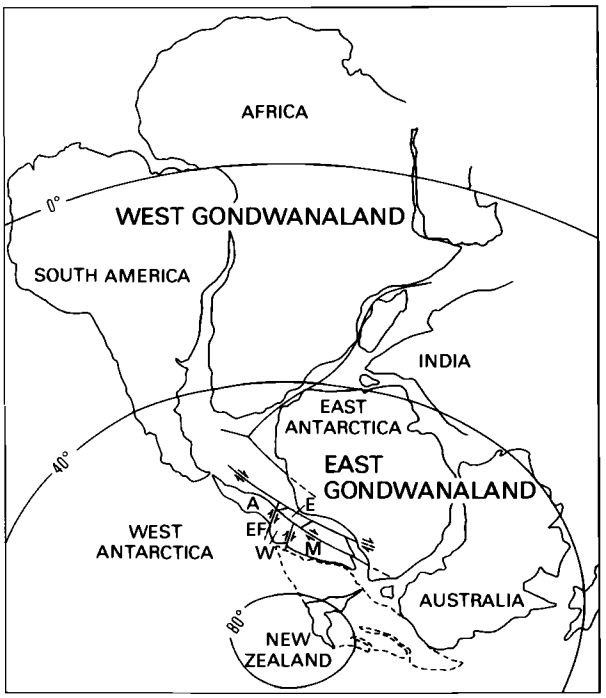

Fig. C.II. Reconstruction of Gondwanaland during Middle Jurassic continental rifting but before Late Jurassic seafloor spreading between West and East Gondwanaland [after *Rowley et al.*, 1989]. A, Antarctic Peninsula–eastern Ellsworth Land block; E, Ellsworth Mountains–Whitmore Mountains–Haag Nunataks block; W, western Ellsworth Land block; M, Marie Byrd Land block; EF, Ellsworth fault [see *Kellogg and Rowley*, 1989].

the former faults that separated the blocks. Such extensional block faulting is similar to that inferred in Marie Byrd Land [*LeMasurier*, 1972*a*, *b*; *LeMasurier and Wade*, 1976; *LeMasurier and Rex*, 1982, 1983; *Bentley*, 1983] and other parts of the Antarctic Peninsula [*Smellie*, 1987; *Smellie et al.*, 1988]. A comparable relationship between extension and bimodal alkaline volcanism is well known in the Basin and Range province of western North America and in many other parts of the world.

Normal faults are abundant on Alexander Island (Figure C.I), where they strike north [*British Antarctic Survey*, 1981; *Burn*, 1984], and in southeastern Rothschild Island, where they strike northeast [*Care*, 1980]. George VI Sound, a narrow north trending ice-filled waterway between Alexander Island and Palmer Land, is a classic linear graben, representing a zone of intra-arc extension during the Tertiary [*Crabtree et al.*, 1985; *Storey and Garrett*, 1985]; most faults in the adjacent land areas also strike north [*British Antarctic Survey*, 1982]. In parts of eastern Ellsworth Land, sparse seismic reflection and gravity studies [*Behrendt*, 1964*b*, *c*] and radio-echo soundings [*Doake et al.*, 1983] have delineated rough sub-ice topography, including valleys nearly 2000 m below sea level; such topography suggests that Cenozoic block faulting took place at least in some places [*Laudon*, 1972, 1982]. In western Ellsworth Land the general easterly trend of Thurston Island and the Jones Mountains suggests control by block faults of this same strike [*Drake*, 1962; *Craddock et al.*, 1964]; geophysical studies [*Bentley*, 1962] confirm that the Jones Mountains consist of an east trending bedrock highland. *Lopatin and Polyakov* [1974] suggested that the locations of the volcanoes in the Hudson Mountains are controlled by north and east striking fractures.

Physical Characteristics

The Bellingshausen volcanic province contains deeply eroded and/or poorly studied upper Cenozoic basaltic rocks at 11 localities (Figure C.I and Table C.I), most of which represent small to moderate-sized volcanic fields formed during extensional tectonism. Several volcanic fields occur on and near Alexander Island (see IVD's C.1–C.5). None of these appear to contain primary landforms. The rock types consist mostly of hyaloclastite tuff and locally interbedded pillow lava flows. Such rocks formed under or against ice or under water [see *Fisher and Schmincke*, 1984]. Tillite occurs locally in the hyaloclastite succession, which in some places lies above a glacially polished surface developed on older rocks. The hyaloclastite and pillow lava sequence is overlain in some places by scoriaceous basalt flows that were mostly deposited subaerially; at Hornpipe Heights (see IVD C.3), agglutinate, including aerodynamically molded bombs, makes up the subaerial part of the section. Dikes mapped in southeastern Alexander Island (see IVD C.5) are all that remain of a presumed former volcanic field.

Several small volcanic fields occur in eastern Ellsworth Land. Only subaerial basaltic lava flows are exposed at Rydberg Peninsula (see IVD C.6) and Henry Nunataks (see IVD C.10). Mount Combs (on Rydberg Peninsula), although entirely ice covered,

Copyright American Geophysical Union

may be the only primary volcanic landform in eastern Ellsworth Land. Snow Nunataks (see IVD C.7), forming a short east trending chain of eroded volcanic outcrops, consist largely of hyaloclastite, interbedded pillow lava flows, and local dikes, apparently overlain at Mount McCann by a succession of subaerial basaltic flows. The small exposures in the Merrick Mountains (see IVD C.11) also seem to contain both lower hyaloclastite and upper subaerial lava flows.

Two moderate-sized volcanic fields occur in western Ellsworth Land. The one in the Jones Mountains (see IVD C.8) rests on a glacially striated unconformity locally overlain by a tillite. As elsewhere in the province, the volcanic sequence consists of hyaloclastite and related lava flows overlain by subaerial flows; all the rocks are intruded by basaltic dikes. Primary volcanic landforms were not seen. Lack of primary landforms contrasts with the volcanic field in the Hudson Mountains (see IVD C.9), the largest and best exposed in the province, where some craters and small parasitic cones have survived erosion. Most of this volcanic field, however, is thought to consist of three badly eroded large stratovolcanoes: Teeters Nunatak, Mount Moses, and Mount Manthe volcanoes. The sequence in the Hudson Mountains consists largely of subglacial and subaqueous hyaloclastite tuff and interbedded basaltic lava flows overlain by subaerial lava flows that locally compose the parasitic cones. A sequence of subglacial or subaqueous pillow lava flows underlies these hyaloclastites and flows.

The general stratigraphy in all these localities is similar to sequences in Marie Byrd Land that have been better studied [*LeMasurier*, 1972*a*, *b*; *LeMasurier and Wade*, 1976; *LeMasurier and Rex*, 1982] (see also the section on Marie Byrd Land in this volume). Thus the hyaloclastite and local pillow lava flow sequence, as well as the lower pillow lava sequence in the Hudson Mountains, bear many similarities to the hydroclastic sections in Marie Byrd Land and reflect similar subglacial and periglacial environments of eruption (cf. IVD's B.1, B.2, and B.16).

Petrology

Neogene-Recent volcanism of the Bellingshausen volcanic province is entirely in a within-plate setting, with the eruption of predominantly basaltic rocks containing the high total alkali and incompatible element abundances, low range of silica contents (42–51 wt %), and interelement ratios (e.g., high Nb/Zr, Ti/Y, Zr/Y, low Ba/La, La/Nb) characteristic of non-orogenic, alkaline magmas from oceanic and continental settings (Figures C.III and C.IV) [*Smellie*, 1987; *Hole*, 1988; *Hole et al.*, 1989]. Sr and Nd iso-

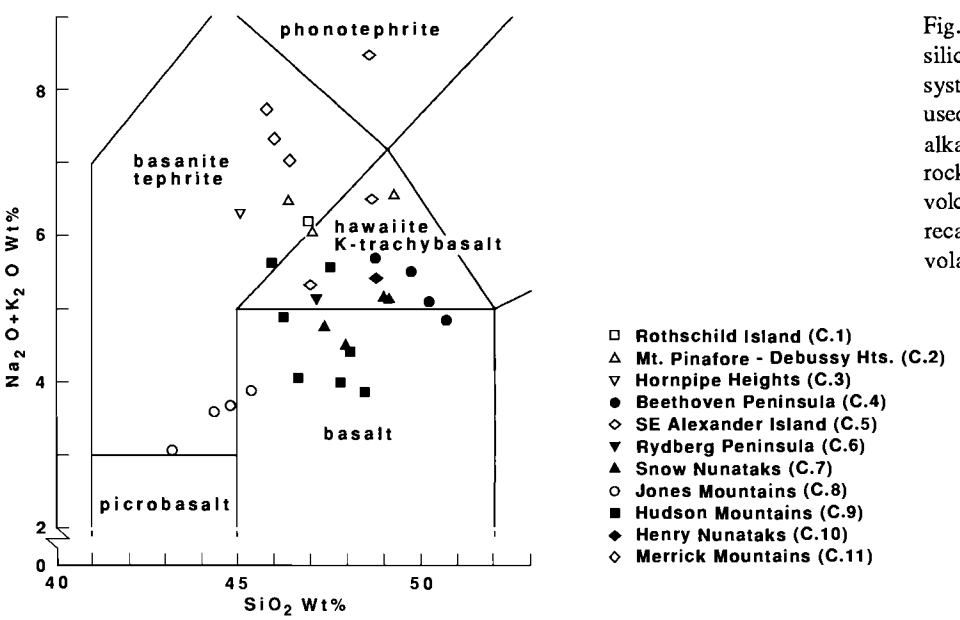

Fig. C.III. Total alkali versus silica diagram illustrating the system of rock nomenclature used, and the inflated total alkali contents of the volcanic rocks in the Bellingshausen volcanic province. All analyses recalculated to 100% on a volatile-free basis.

Copyright American Geophysical Union

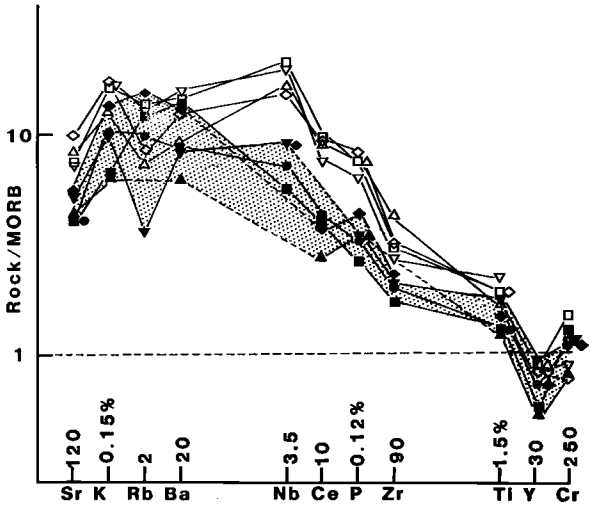

Fig. C.IV. Spidergrams of MORB-normalized incompatible element abundances for selected mafic rocks from the principal volcanic outcrop areas. Basanite and tephrite (open symbols) show greater enrichment in most incompatible elements, and patterns peak at Nb, whereas the basalt-hawaiite-potassic trachybasalt spidergrams (solid symbols) peak at K or Ba. The basalt-hawaiite-potassic trachybasalt spidergram envelope (excluding camptonite) is shaded, to emphasize differences with the basanite, tephrite, and camptonite. Symbols as in Figure C.III; normalizing values are from *Pearce* [1983].

topic compositions are available only for Alexander Island samples, which exhibit a restricted range of both $^{87}Sr/^{86}Sr$ (0.70275–0.70342) and $^{143}Nd/^{144}Nd$ (0.51286–0.51296) ratios consistent with a mantle origin [*Hole*, 1988; *Hole et al.*, 1989]. Using the classification of *Le Bas et al.* [1986], the outcrops mainly comprise a sodic series of (alkaline) basalt, hawaiite, basanite, and tephrite. Rocks with potassic compositions are much rarer and were encountered only at Hudson Mountains and Beethoven Peninsula (potassic trachybasalt) and southeastern Alexander Island (camptonite dikes corresponding to potassic trachybasalt and phonotephrite). The camptonites are also distinguished by inflated Sr contents (1136-1357 ppm), very high K/Rb ratios (1198-1760), and very low Rb/Sr ratios (0.11-0.14), and they are compositionally and petrographically unique in this province.

Lava flow sequences in the individual outcrops are compositionally restricted, and two broad natural divisions can be distinguished: Basanite and tephrite are restricted to northern Alexander Island (Elgar Uplands, Rothschild Island), Merrick Mountains, and Jones Mountains, whereas basalt, hawaiite and potassic trachybasalt form the outcrops at Beethoven Peninsula, southeastern Alexander Island, Snow Nunataks, Rydberg Peninsula, Henry Nunataks, and Hudson Mountains. Basanite is highly undersaturated, with *ne* >10% (ranging up to 17.83%; norms calculated with Fe_2O_3/FeO = 0.15), whereas basalt, tephrite, hawaiite, and potassic trachybasalt are typically less undersaturated (*ne* < 10%) and include slightly saturated compositions (up to 6.33% *hy*) at Beethoven Peninsula and Hudson Mountains. In addition, basanite, tephrite, and camptonite are generally more enriched in the incompatible elements (especially Nb, Zr, P, Ce, Sr (see Figure C.IV)) and are more potassic, with Na_2O/K_2O ratios of 0.95–2.73 (mean: 1.89), compared with 1.87–4.10 (mean: 2.88) in basalt, hawaiite, and potassic trachybasalt (excluding camptonite). Spidergrams normalized to mid-ocean ridge basalt (MORB) are convex upward and peak at Nb in basanite and tephrite and at K or Ba in basalt, hawaiite, and potassic trachybasalt (Figure C.IV). Because only major oxide data are currently available for samples from Jones Mountains, their petrologic affinities are still uncertain.

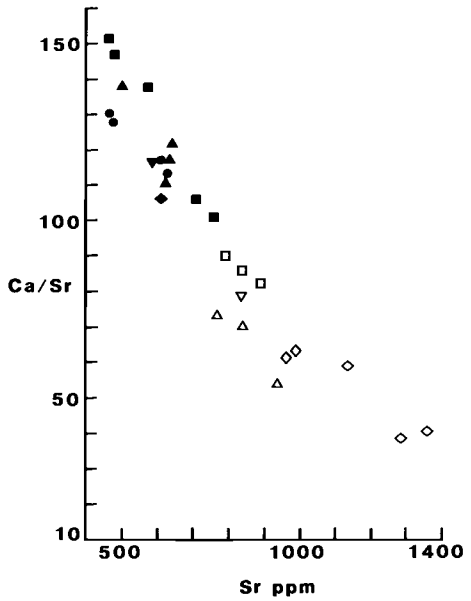

Fig. C.V. Ca/Sr versus Sr plot, showing the pronounced negative covariation for all samples, attributed to fractional crystallization of clinopyroxene. Symbols as in Figure C.III.

Copyright American Geophysical Union

Many of the basanite and tephrite samples have the high Ni and Mg numbers (123–339 ppm and 67–72, respectively; Mg number = ($Mg/Mg + Fe^{2+}$) molecular proportion) of very primitive liquids. They have evidently undergone little or no fractionation during ascent from the mantle, a conclusion supported by the presence of locally abundant ultramafic nodules. By contrast, even the least evolved basalt, hawaiite, and potassic trachybasalt have significantly lower Ni and Mg numbers (<191 ppm and <63, respectively), and they do not contain ultramafic nodules. Within any local sequence, Cr, Ni, and MgO contents decrease as ($FeO + Fe_2O_3$)/($FeO + Fe_2O_3 + MgO$) ratios increase, attesting to strong compositional control by crystal fractionation of olivine and clinopyroxene. Although clinopyroxene is a relatively uncommon phenocryst phase [*Smellie*, 1987], its influence on magma compositions is confirmed by the observed strong decrease of Ca/Sr ratios with increasing Sr (Figure C.V). Conversely, despite the presence of plagioclase phenocrysts in some lavas in most outcrops, any effects of plagioclase extraction have not been detected so far.

Nb/Y versus Nb variations (Figure C.VI) define a positive slope, the steepness of which cannot be explained solely by fractional crystallization of the observed phenocryst phases. This suggests that variations in the degree of partial melting were more important in defining the overall trend, since Nb abundances and Nb/Y ratios will both increase as the extent of partial melting decreases [*Hole*, 1988]. All the samples analyzed have low but relatively constant Y contents (Figures C.IV and C.VII), and they are enriched in light rare earth elements, with chondrite-normalized La/Y ratios increasing from 4.47–12.06 (mean: 6.57) in basalt, hawaiite, and potassic trachybasalt (excluding camptonite) to 8.94–15.58 (mean: 12.07) in basanite, tephrite, and camptonite. These relationships are consistent with the generation of the magmas by variable partial melting of a garnet-bearing mantle source, with the relative degree of melting increasing from basanite, tephrite, and camptonite to basalt, hawaiite, and potassic trachybasalt (excluding camptonite) [cf. *Smellie*, 1987; *Hole*, 1988]. However, unlike other outcrops, significant Y variation occurs in lava flows from the Hudson Mountains and possibly Beethoven Peninsula, and a crude positive covariation exists with

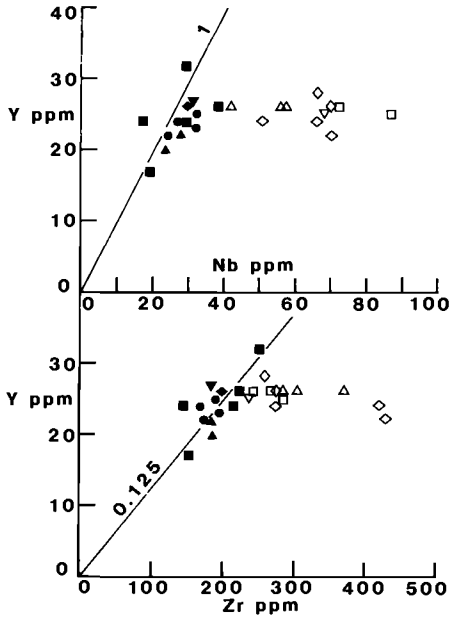

Fig. C.VII. Plots of Y versus Nb and Y versus Zr. Y contents are nearly constant in samples from most outcrops, attributed to partial melting of a garnet-bearing mantle source. The more variable Y abundances in samples from the Hudson Mountains and Beethoven Peninsula (see additional data for Beethoven Peninsula given by *Hole* [1988]) suggest that garnet was not residual in the mantle source for these rocks. Symbols as in Figure C.III.

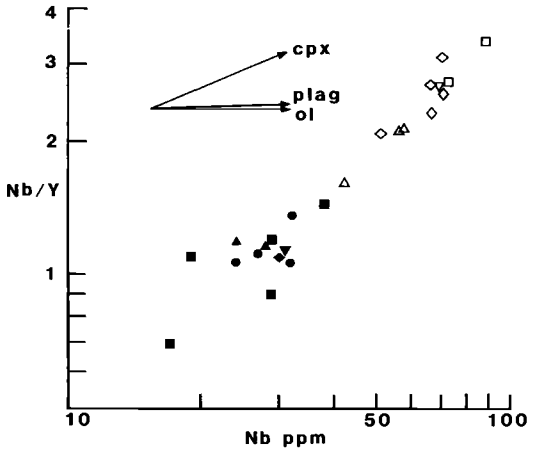

Fig. C.VI. Nb/Y versus Nb variations plot. Fractional crystallization vectors for 50% crystallization of olivine (ol), plagioclase (plag), and clinopyroxene (cpx) are also shown and demonstrate that the much steeper slope for outcrops in this province cannot be explained solely by crystallization of these three phases. A relationship by variable partial melting is a more likely explanation for the overall trend shown. Symbols as in Figure C.III.

Copyright American Geophysical Union

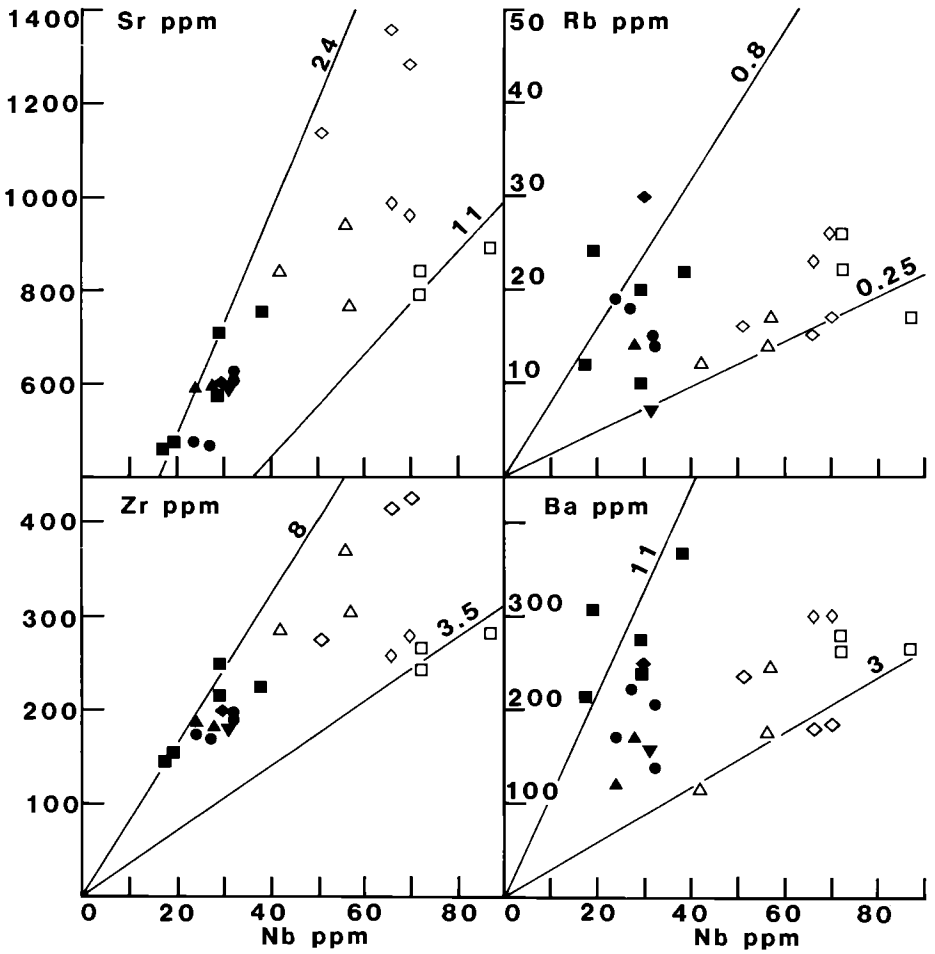

Fig. C.VIII. Binary trace-element plots. The wide variation in interelement ratios may be due to compositional variation in the mantle sources or to differences in partition coefficients for these elements at very low degrees of melting. Symbols as in Figure C.III.

Zr and Nb (Figure C.VII), suggesting the possibility that garnet may not have been residual during the formation of these magmas.

Multiple positive correlations can generally be distinguished on binary incompatible element diagrams (Figure C.VIII), demonstrating the wide variation in incompatible element ratios throughout this province. The variations in Alexander Island samples were interpreted by *Hole* [1988] to be a result of slight but significant differences in mineral:melt partition coefficients at very low degrees of melting and/or melting of a compositionally heterogeneous mantle source. *Hole* [1988] also identified a group of samples from one locality on Beethoven Peninsula (IVD C.4) that contain more radiogenic Sr and less radiogenic Nd ($^{87}Sr/^{86}Sr$ = 0.70342; $^{143}Nd/^{144}Nd$ = 0.51286) than other Alexander Island basalt. The same samples are also distinguished by higher Rb/Nb, Ba/Nb (Figure C.IX), Th/Ta, and K/Nb ratios, and the combination of correlated trace-element and isotopic characteristics was interpreted as an effect inherited from melting a mantle source containing a minor but geochemically significant subduction zone component [*Hole*, 1988]. Although isotopic data are absent for outcrops other than Alexander Island in this province, the similarity in Rb/Nb, Ba/Nb, and K/Nb ratios between samples from Beethoven Peninsula, Hudson Mountains, and Henry Nunataks (Figure C.IX) suggests that a similar explanation may be possible for the origin of the samples from all three areas.

Copyright American Geophysical Union

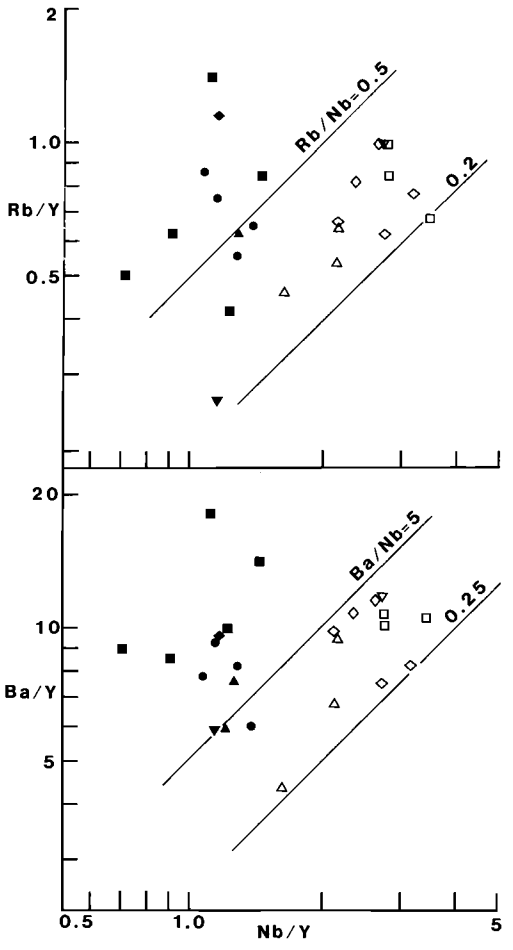

Fig. C.IX. Rb/Y versus Nb/Y and Ba/Y versus Nb/Y plots, showing the inflated Ba/Nb and Rb/Nb ratios of samples from the Hudson Mountains, Henry Nunataks, and Beethoven Peninsula, attributed to a possible "subduction zone enrichment" of their mantle source [*Hole,* 1988]. Symbols as in Figure C.III.

Chronology

Nearly all the Cenozoic volcanic rocks of this province are moderately to deeply dissected. Except for inconclusive reports of steam from Table Nunatak, situated off the eastern end of Hollick-Kenyon Peninsula, extreme northeastern Palmer Land [*Smellie et al.,* 1988], and in the Hudson Mountains, and for a suggestion that a rich algal flora in a freshwater pool at Gluck Peak, Beethoven Peninsula, may be due to high heat flow (Hole, unpublished data, 1986), all volcanoes appear to be extinct. Most are thought to be of late Tertiary age, based on their general physiographic appearance (Table C.I). A limited number of whole-rock K-Ar ages and a fission-track age are given in the IVD's. Most isotopic ages, however, were determined long ago and include discrepant ages and those with large error bars. (Where necessary, isotopic ages have been corrected using current decay constants [*Steiger and Jäger,* 1977].) Some of these were determined on glass samples, which generally give spurious values, rather than on holocrystalline basalt. These data, nonetheless, suggest that most volcanic rocks in the province are younger than about 10 m.y., those on Alexander Island (except for the camptonite dikes) ranging from 8 to <1 m.y.

No province-wide geographic trend to the ages can be discerned from available data. On a local scale, some centers in some volcanic fields show linear and rectangular patterns, suggestive of control by intersecting orthogonal joints.

Acknowledgments

We are indebted to the late F.A. Wade for his assistance in helping us understand the geology of Ellsworth Land and to P.L. Williams for his assistance in the study of the southern Antarctic Peninsula. We are grateful for previously unpublished data and photographs that were supplied to us by T.W. Bastien, R.W. Burn, R. Hutchison, K.S. Kellogg, C.E. King, P.R. Kyle, A.B. Moyes, P.M. Otway, R.G.B. Renner, W.A. Schaefer, B.C. Storey, and M.R.A. Thomson. We thank Dorothy Vitaliano for translating the article by *Lopatin et al.* [1974], and M.A. Kuntz, F. Barker, D.H. Elliot, I.G. Gass, and J. Whitford-Stark for technical reviews.

Copyright American Geophysical Union

C.1. ROTHSCHILD ISLAND

Type of volcano: Not known. Deposits consist of three small eroded masses of palagonite tuff and lapillistone, of olivine-phyric basaltic dikes, and of minor lava flows.

Location: Southeastern Rothschild Island (69°36′S, 72°33′W), off the northwestern coast of Alexander Island.

Height above sea level: 0-400 m.

Evidence of Holocene activity: None.

Authors of report: J.W. Thomson, P.D. Rowley, and M.J. Hole.

Date of report: October 1987.

Form and Structure

The volcanic rocks on Rothschild Island form three small outcrops with an exposed thickness of ~100 m [*Care,* 1980] (Figure C.1.1); no contacts with other rock formations have been observed. The volcanic rocks consist mostly of cross-bedded palagonite tuff and lapillistone (locally containing clasts of hyalobasalt), and minor olivine-phyric basaltic lava flows. Black scoriaceous hyalobasalt scree caps one outcrop [*Care,* 1980]. *Care* [1980] considered all the volcaniclastic rocks to be hyaloclastites, but the term was used loosely, and the deposits may be either hyalotuffs

Fig. C.1.1. Geologic sketch map of Rothschild Island [after *British Antarctic Survey,* 1981]. Rock exposure is outlined; pattern of rock unit is shown for the exposure and the snow and ice cover near it. Because topographic control has not been determined in the area, form lines (dashed lines) are used instead of contours.

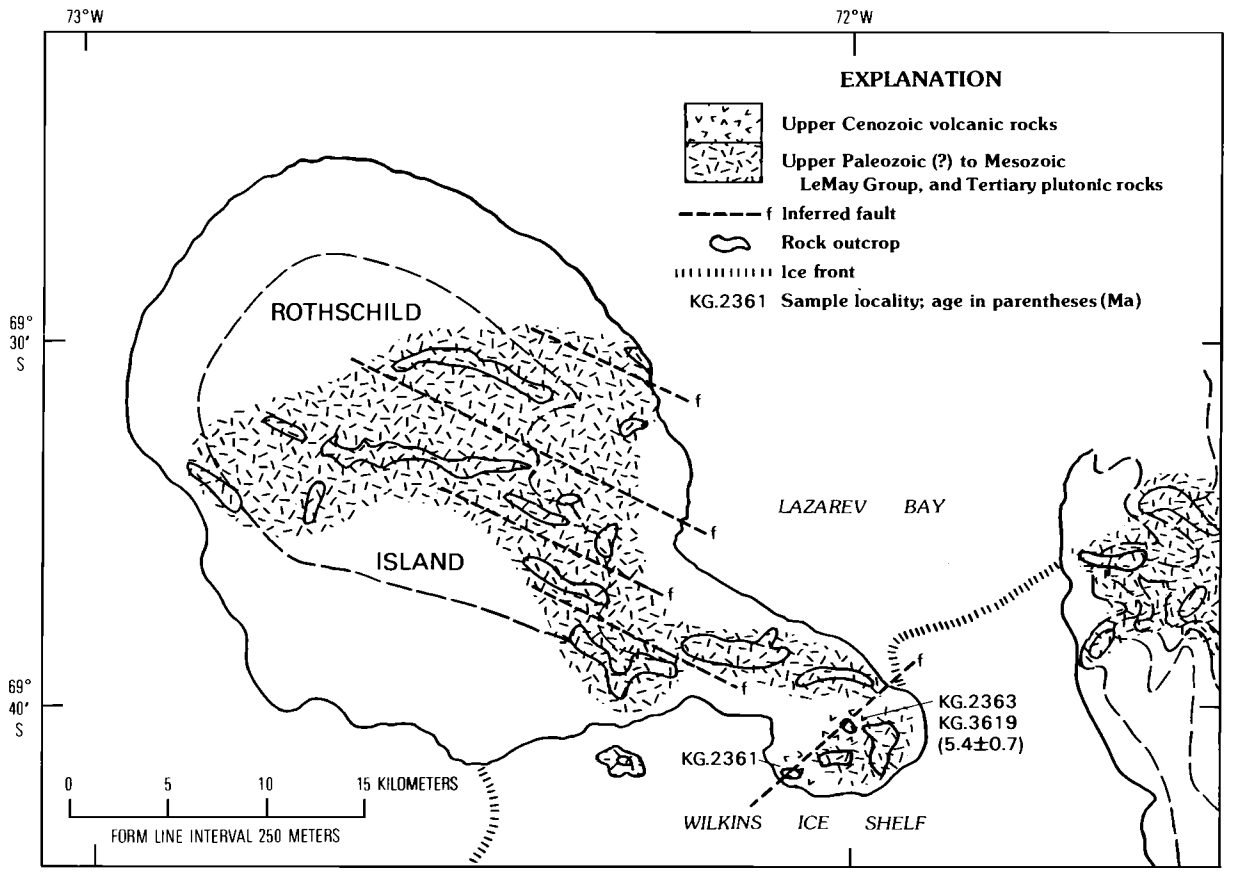

Copyright American Geophysical Union

TABLE C.1.1. Chemical Analysis and CIPW Norms of a Lava Flow From Rothschild Island

	1
SiO_2	46.90
TiO_2	2.65
Al_2O_3	14.42
Fe_2O_3	1.15
FeO	8.41
MnO	0.15
MgO	9.19
CaO	10.03
Na_2O	3.88
K_2O	2.21
P_2O_5	0.85
LOI	-0.3
Total	99.86
or	13.29
ab	17.36
an	14.62
ne	7.83
di	23.22
ol	15.04
mt	1.77
il	5.06
ap	1.80
Ba	263
Ce	91.74
Cr	360
Eu	2.55
Hf	6.26
La	53.94
Lu	0.29
Nb	72
Nd	41.25
Ni	201
Rb	26
Sm	8.25
Sr	837
Ta	4.64
Tb	0.91
Th	6.03
Y	26
Yb	1.98
Zr	267

Major oxides and trace elements analyzed by XRF; rare earth elements and Hf, Ta, and Th analyzed by instrumental neutron activation analysis. FeO and Fe_2O_3 calculated from Fe_t using constant Fe_2O_3/FeO ratios of 0.15 for norm calculation [see *Hole*, 1988]. LOI, loss on ignition.

1. KG3619.1. Tephrite, southeastern Rothschild Island [*Hole*, 1988, Table 1].

or even reworked deposits [*Smellie et al.*, 1988]. Two consanguineous vesicular olivine-phyric basaltic dikes intrude the volcanic rocks. No primary volcanic landforms were noted.

Petrologic Characteristics

The palagonite tuff consists of vitric-rich deposits of sideromelane shards, vesicular hyalobasalt clasts, sparse tachylite clasts, and crystals of olivine, pyroxene, spinel, and plagioclase. The hyalobasalt clasts contain phenocrysts of titanaugite, enstatite, and olivine in a hyalopilitic groundmass of plagioclase and Fe-Ti oxides. Chemically, the lava flows are *ne*-normative basanite and tephrite (Table C.1.1). The basalt dikes are hypocrystalline and contain phenocrysts of forsteritic olivine, labradorite, titaniferous augite (some of which show sieve textures and may be xenocrystal in origin), and, locally, enstatite in a groundmass containing olivine, clinopyroxene, plagioclase, and Fe-Ti oxides. A modal analysis of a hypocrystalline dike [*Care*, 1980, Table III] shows olivine (11%), clinopyroxene (8%), orthopyroxene (2%), and plagioclase (1%). The dikes locally contain lherzolite xenoliths.

Chronologic Data

A K-Ar date of 5.4 ± 0.7 Ma has been obtained from a tephrite flow [*Smellie et al.*, 1988].

Extent of Knowledge

The high parts of Rothschild Island were first sighted by Bellingshausen in 1821. The island was visited for the first time in January 1976 by a British Antarctic Survey (BAS) aircraft to establish a topographic station. During the following austral summer (1976–1977) the island was explored, and outcrops of the volcanic rocks were studied by B.W. Care as part of a BAS reconnaissance geologic mapping project on Alexander Island [*Care*, 1980]. The outcrops were revisited briefly in 1985–1986 by M.J. Hole during a BAS study of upper Cenozoic alkaline volcanic rocks in the Antarctic Peninsula region.

Bibliography

Care, 1980
Hole, 1988
Smellie et al., 1988

Copyright American Geophysical Union

C.2. MOUNT PINAFORE–DEBUSSY HEIGHTS

Type of volcano: Not known. Deposits consist of widely scattered small outcrops of basaltic lava flows and associated palagonite tuff and breccia.

Location: Mount Pinafore (southern Elgar Uplands, 69°46′–69°49′S, 70°45′–70°55′W) and Debussy Heights (69°53′S, 71°15′W), northern Alexander Island.

Height above sea level: Elgar Uplands, ~1000–1500 m; Debussy Heights, ~800 m.

Evidence of Holocene activity: None.

Authors of report: M.J. Hole and J.W. Thomson.

Date of report: October 1987.

Form and Structure

Upper Cenozoic volcanic rocks occur as widely scattered exposures in the Mount Pinafore area and at Debussy Heights (Figure C.2.1). Southeast of the summit of Mount Pinafore a 60-m-thick columnar-jointed lava flow overlies 15 m of well-laminated, fine-grained, buff-colored tuff and matrix-supported yellow lapillistone containing poorly developed cross-bedding. The top of a boulder bed (>1 m thick) which is visible at the base of the exposure contains subrounded to rounded, glacially striated cobbles and boulders of lower Tertiary calc-alkaline andesite and upper Paleozoic(?) to Mesozoic LeMay Group (LMG) mudstone and siltstone [*Burn,* 1984] set in a buff-colored

Fig. C.2.1. Geologic sketch map of the Elgar Uplands–Hornpipe Heights–Debussy Heights area [after *British Antarctic Survey,* 1981]. Rock exposure is outlined; pattern of rock unit is shown beyond the limit of the exposure; form lines are dashed.

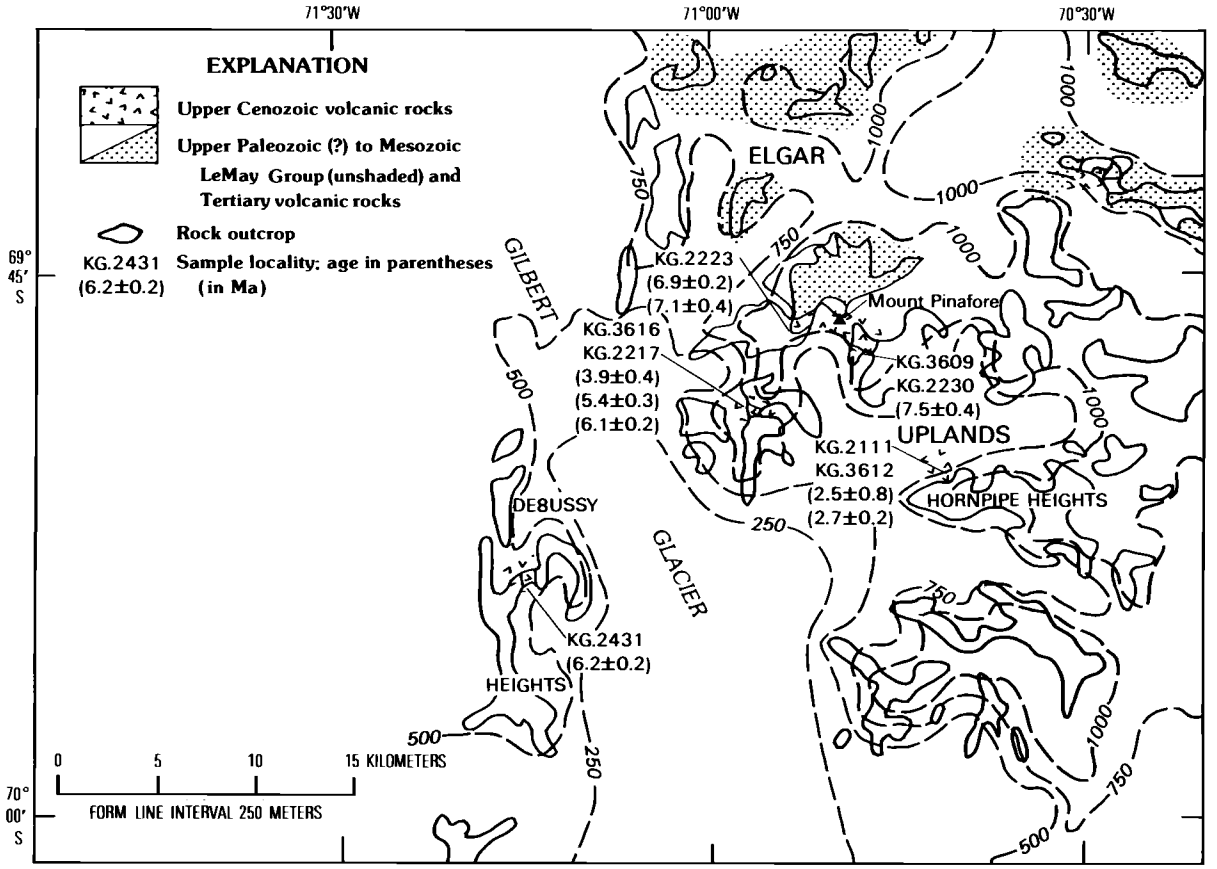

Copyright American Geophysical Union

Copyright American Geophysical Union

Pinafore area and the occurrence of palagonitized volcaniclastic rocks at all exposures suggest that they were erupted in a subaqueous or subglacial environment [*Burn and Thomson*, 1981].

At Debussy Heights a 6-m lava flow of glassy basaltic rock is truncated by nonvesicular palagonite breccia containing some sedimentary clasts. Pods of vesicular palagonite breccia and brecciated and palagonitized nonvesicular basaltic rocks also crop out in association with friable buff-colored palagonite breccia (Burn, BAS unpublished field notes, 1976).

Petrologic Characteristics

Olivine is the dominant phenocryst in the lava flows, and the groundmass is typically hyalopilitic; spinel lherzolite nodules are abundant within all flows. The predominant rock type is silica-undersaturated (5–11% normative *ne*) basanite and tephrite with minor hawaiite (Table C.2.1). These rocks are considerably more evolved than those found at Hornpipe Heights (see IVD C.3), having lower MgO (<9%) and Ni (<140 ppm) abundances and higher $(FeO + Fe_2O_3)/(FeO + Fe_2O_3 + MgO)$ ratios (0.60–0.65). Their low CaO/Al_2O_3 ratios compared with the basanite at Hornpipe Heights also suggest that clinopyroxene crystallization occurred during their genesis. All rocks are enriched in light rare earth elements (La_n/Yb_n = 10–13), with relatively consistent Yb abundances (2.1–2.5 ppm). Relative degrees of incompatible element enrichment suggest that the rocks of Mount Pinafore and its associated outcrops were derived by small but higher degrees of partial melting of a garnet lherzolite source than the basanite of Hornpipe Heights [*Hole*, 1988]. Microprobe analyses of a megacryst and of minerals from an ultramafic nodule are given in Table C.2.2.

TABLE C.2.2. Microprobe Analyses of a Megacryst and of Minerals From Nodules in an Olivine Basalt Lava Flow From Mount Pinafore

	1	2	3	4
SiO_2	38.3	40.3	52.5	54.9
TiO_2	6.0	--	0.08	0.04
Al_2O_3	14.3	--	4.44 (3.33)	4.00 (3.44)
Cr_2O_3	0.0	--	0.95 (0.53)	0.56 (0.40)
FeO	14.6	9.05	2.18	5.76
MnO	0.17	0.13	0.08	0.14
NiO	--	0.31	--	--
MgO	9.3	49.2	16.3	33.2
CaO	9.8	0.07	22.3	0.62
Na_2O	2.89	--	0.74 (0.62)	0.06
K_2O	1.10	--	--	--
Total	96.46	99.06	99.57	99.22

Analyses by R. Hutchinson, Department of Geology, British Museum (Natural History), London. Dashes, not determined.

1. KG.2230.5. Kaersutite megacryst.
2. KG.2230.5. Olivine ($Fo_{90.5}$) from ultramafic nodule.
3. KG.2230.5. Chrome diopside from nodule (values in parentheses from nodule rim).
4. KG.2230.5. Enstatite ($En_{90.9}$) from ultramafic nodule (values in parentheses from nodule rim).

Chronologic Data

Six K-Ar whole-rock dates for basaltic lava flows from the Mount Pinafore area and one from Debussy Heights [*Smellie et al.*, 1988] are summarized below. In each case the lithology is basanite-tephrite.

Location	Sample	Date, Ma
Mount Pinafore area	KG.2217.13	6.0 ± 0.2
		6.2 ± 0.3
Mount Pinafore area	KG.2217.14	5.4 ± 0.3
Mount Pinafore area	KG.2217.16	3.9 ± 0.4
Mount Pinafore	KG.2223.3	7.1 ± 0.4
Mount Pinafore	KG.2223.4	6.9 ± 0.2
Mount Pinafore	KG.2230.1	7.7 ± 0.6
		7.6 ± 0.6
		7.3 ± 0.4
Debussy Heights	KG.2431.5	6.0 ± 0.2
		6.3 ± 0.2

Extent of Knowledge

The Elgar Uplands and Debussy Heights were visited for the first time by R.W. Burn in 1975–1977, during British Antarctic Survey (BAS) reconnaissance geologic mapping on Alexander Island [*Burn and Thomson*, 1981; *British Antarctic Survey*, 1981]. A BAS party revisited the Mount Pinafore area in 1985–1986 to make a detailed study of the volcanic exposures [*Hole et al.*, 1989].

Bibliography

Burn, 1984
Burn and Thomson, 1981
Hole, 1988
Hole et al., 1989
Smellie et al., 1988

Copyright American Geophysical Union

Copyright American Geophysical Union

TABLE C.3.1. Representative Chemical Analysis and CIPW Norms of a Lava Flow From Hompipe Heights, Alexander Island

	1
SiO_2	45.07
TiO_2	3.26
Al_2O_3	14.49
Fe_2O_3	1.37
FeO	9.19
MnO	0.15
MgO	10.36
CaO	9.30
Na_2O	3.89
K_2O	2.44
P_2O_5	0.75
LOI	-0.4
Total	99.87
or	14.38
ab	6.35
an	14.83
ne	14.34
di	21.57
ol	18.73
mt	1.98
il	6.17
ap	1.63
Ba	298
Ce	72.35
Cr	223
Eu	2.36
Hf	5.47
La	40.01
Lu	0.25
Nb	68
Nd	35.82
Ni	195
Rb	25
Sm	5.64
Sr	838
Ta	4.62
Tb	0.97
Th	4.30
Y	25
Yb	1.74
Zr	238

Major oxides and trace elements analyzed by XRF; rare earth elements and Hf, Ta, and Th analyzed by instrumental neutron activation analysis. FeO and Fe_2O_3 calculated from Fe_t using constant Fe_2O_3/FeO ratios of 0.15 for norm calculation [see *Hole*, 1988]. LOI, loss on ignition.

1. KG.3612.5. Basanite, Hompipe Heights [*Hole*, 1988, Table 1].

Chemical analyses show all rocks to be basanite (Table C.3.1). All analyzed samples are strongly silica undersaturated (11–15% normative *ne*) and have high contents of MgO (as much as 12%) and low (FeO + Fe_2O_3)/(FeO + Fe_2O_3 + MgO) ratios (<0.45). All are enriched in light rare earth elements (LREE) (La_n/Yb_n = 13–18) but with relatively constant Yb (1.7–2.0 ppm) and Y (20–25 ppm) abundances. The apparent compatibility of heavy rare earth elements and Y but incompatibility of the LREE (Nb, Ta, etc.) suggest that all samples were derived by small but variable degrees of partial melting of a garnet lherzolite, leaving a garnet-rich residuum [*Hole*, 1988]. However, decreasing Ni abundances with increasing (FeO + Fe_2O_3)/(FeO + Fe_2O_3 + MgO) ratio in the sequence suggest that limited fractional crystallization of olivine may have taken place [*Hole*, 1988].

Chronologic Data

Two basanite lava flows have K-Ar dates of 2.5 ± 0.8 and 2.7 ± 0.2 Ma [*Smellie et al.*, 1988, Table 2]. The subaerial nature of this sequence suggests that no major ice sheet was at this topographic level during the early Pliocene.

Extent of Knowledge

The exposures at Hompipe Heights were visited briefly by R.W. Burn in 1976–1977, during a British Antarctic Survey reconnaissance geologic mapping project on Alexander Island. They were revisited and studied in detail by M.J. Hole in 1985–1986 [*Smellie et al.*, 1988; *Hole et al.*, 1989].

Bibliography

Hole, 1988
Hole et al., 1989
Smellie et al., 1988

Copyright American Geophysical Union

C.4. BEETHOVEN PENINSULA

Type of volcano: Isolated exposures, mostly apparently subglacial tindar deposits of palagonite tuff and lava flows.

Location: Southwestern Alexander Island (71°25′–71°42′S, 72°40′–74°10′W).

Height above sea level: 250–1050 m.

Evidence of Holocene activity: Presence of a freshwater pool with rich algal flora at Gluck Peak may be due to high heat flow.

Author of report: M.J. Hole.

Date of report: October 1987.

Fig. C.4.1. Geologic sketch map of Beethoven Peninsula [after *British Antarctic Survey,* 1981]. Rock exposure is outlined; pattern of rock unit is shown beyond the limit of the exposure; form lines are dashed.

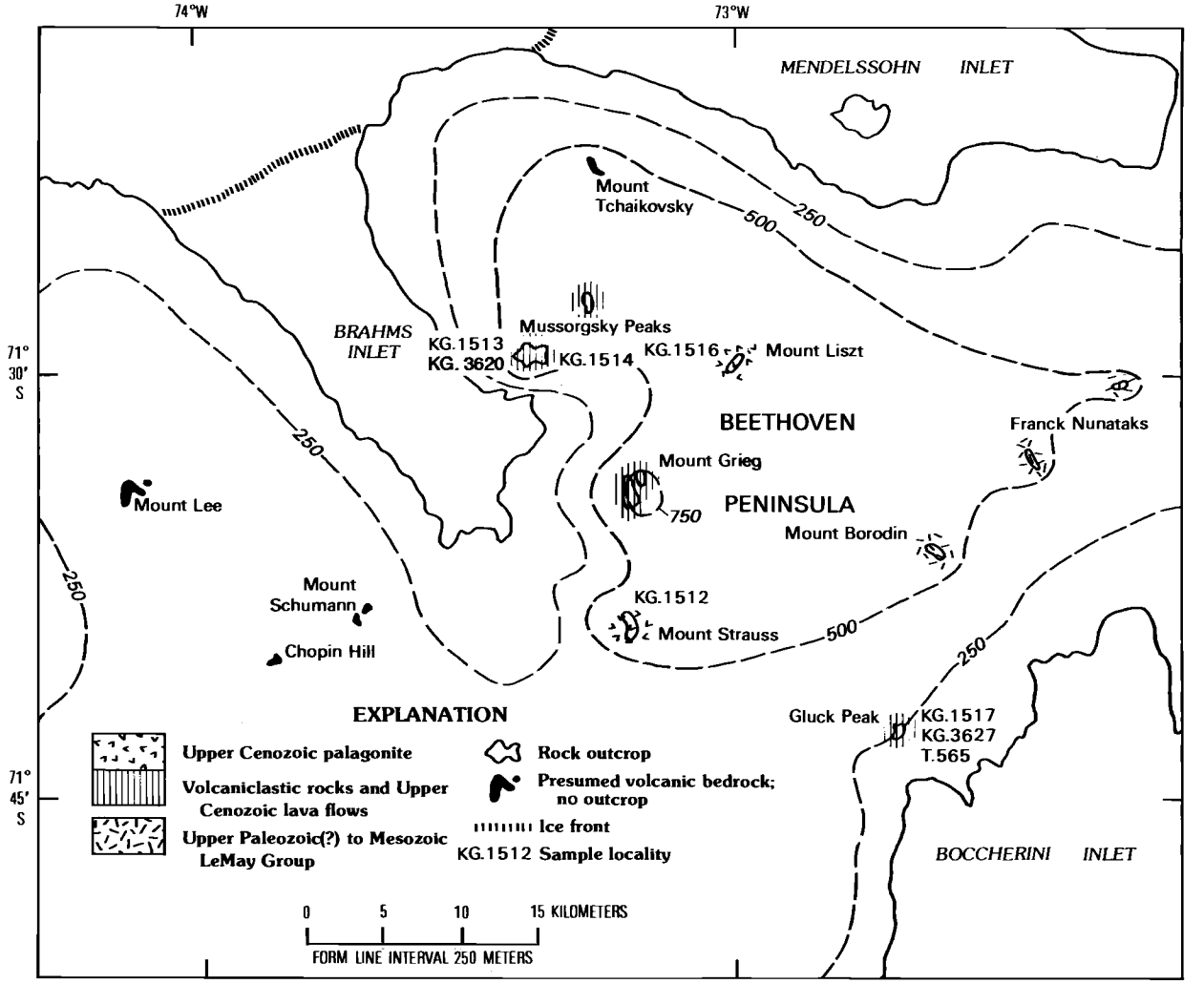

Copyright American Geophysical Union

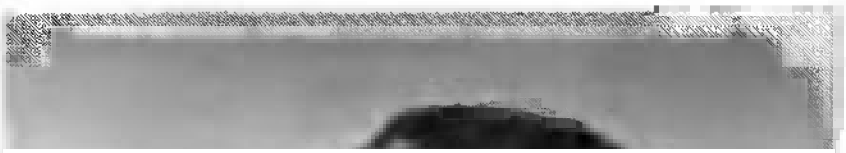

Copyright American Geophysical Union

sequence [*Smellie et al.*, 1988; *Hole et al.*, 1989]. A similar basaltic pillow lava and palagonitized volcaniclastic sequence occurs at Gluck Peak (Figure C.4.1), although all exposed basaltic rocks there are highly vesicular, whereas the Mussorgsky Peaks basaltic rocks are all nonvesicular. Preliminary comparisons with subglacial volcanic sequences in Iceland [*Jones*, 1970] indicate that Mussorgsky Peaks may represent a subglacial tindar sequence deposited in a confined glacial meltwater basin.

Petrologic Characteristics

All basaltic rocks from Mussorgsky Peaks have olivine as the sole phenocryst, but at Gluck Peak, pillow basalt contains both plagioclase and olivine phenocrysts. Major oxide and trace-element analyses show that most lava flows are basalt and hawaiite, which are *hy*-normative (<7%) at Mussorgsky Peaks and slightly *ne*-normative (<7%) at Gluck Peak [*Hole et al.*, 1989] (Table C.4.1). All samples from Beethoven Peninsula are enriched in light rare earth elements (La_n/Yb_n = 7–9) and do not exhibit any Eu anomalies. Like the basaltic rocks of northern Alexander Island, the rocks of Beethoven Peninsula were probably derived by partial melting of a garnet lherzolite [*Hole*, 1988]. However, they represent higher degrees of partial melting than those of the other samples from Alexander Island [*Smellie*, 1987; *Hole et al.*, 1989]. The Gluck Peak hawaiite is more evolved ($(FeO + Fe_2O_3)/(FeO + Fe_2O_3 + MgO)$ = 0.65, MgO < 6%) than the basalt at Mussorgsky Peaks $(FeO + Fe_2O_3)/(FeO + Fe_2O_3 + MgO)$ = 0.5–0.55, MgO = 7.5–8.5%), the lower Ni contents of the basalt presumably reflecting limited fractional crystallization of olivine. Representative modal analyses of the lava flows are given in Table C.4.2.

TABLE C.4.1. Representative Chemical Analyses and CIPW Norms of Lava Flows From Beethoven Peninsula, Alexander Island

	1	2	3	4
SiO_2	48.66	49.70	50.23	50.67
TiO_2	2.39	2.21	1.96	1.86
Al_2O_3	17.14	16.71	15.38	15.16
Fe_2O_3	1.28	1.23	0.68	1.24
FeO	8.48	8.23	9.01	8.29
MnO	0.17	0.13	0.16	0.14
MgO	5.46	5.26	8.09	7.94
CaO	9.96	9.89	8.53	8.56
Na_2O	4.01	3.82	3.54	3.31
K_2O	1.71	1.71	1.57	1.53
P_2O_5	0.44	0.50	0.35	0.38
LOI	--	0.14	--	-0.3
Total	99.70	99.53	100.50	99.08

TABLE C.4.1. (continued)

	1	2	3	4
or	10.14	10.17	9.32	9.13
ab	22.02	26.18	28.51	28.27
an	23.79	23.54	21.55	22.19
ne	6.51	3.44	0.87	--
di	19.03	18.79	15.43	14.97
hy	--	--	--	6.06
ol	11.13	10.77	18.82	13.16
mt	1.86	1.79	0.99	1.81
il	4.55	4.22	3.74	3.57
ap	0.96	1.10	0.77	0.84
Ba	205	138	222	172
Ce	--	41.01	--	40.73
Cr	102	107	275	294
Eu	--	2.08	--	1.61
Hf	--	4.03	--	4.24
La	27	22.90	22	23.90
Lu	--	0.30	--	0.26
Nb	32	32	27	24
Nd	--	28.66	--	19.77
Ni	29	25	75	108
Rb	14	15	18	19
Sm	--	5.87	--	4.99
Sr	604	621	463	475
Ta	--	2.23	--	1.53
Tb	--	0.98	--	0.76
Th	--	3.12	3	3.22
V	250	--	184	--
Y	25	23	24	22
Yb	--	2.19	--	1.74
Zr	190	196	167	173

Major oxides and trace elements analyzed by XRF; rare earth elements and Hf, Ta, and Th analyzed by instrumental neutron activation analysis. For samples 1 and 3, FeO and Fe_2O_3 determined by wet chemistry; for samples 2 and 4, FeO and Fe_2O_3 calculated from Fe_t using constant Fe_2O_3/FeO ratios of 0.15 for norm calculation [see *Hole*, 1988]. Dashes, not determined or below level of detection (elements), not present (norms). LOI, loss on ignition.

1. T.565.1. Hawaiite, Gluck Peak (collected by R.G.B. Renner; analyst, A.B. Moyes).
2. KG.3627.8. Hawaiite pillow lava, Gluck Peak [*Hole*, 1988, Table 1].
3. KG.1513.2. Potassic trachybasalt, Mussorgsky Peaks (collected by C.M. Bell; analyst, A.B. Moyes).
4. KG.3620.7. Basalt pillow lava, Mussorgsky Peaks [*Hole*, 1988, Table 1].

Copyright American Geophysical Union

TABLE C.4.2. Modal Analyses of Lava Flows From Beethoven Peninsula

Mineral	1	2	3	4	5	6	7
Plagioclase	16.4	27.4	28.7	19.2	33.5	26.8	31.8
Clinopyroxene	0	0	39.2	0	36.8	45.4	0
Olivine	15.6	8.3	19.0	10.2	18.8	18.0	12.9
Fe-Ti oxides	0	0	13.1	0	10.2	9.8	0
Glass and palagonite	0	0	0	58.2	0	0	0
Matrix	68.0	64.3	0	12.4	0.7	0	55.3

All analyses from *Bell* [1973, Table 1].

1. KG.1513.1. Hypocrystalline basalt, west Mussorgsky Peaks.
2. KG.1513.2. Hypocrystalline basalt, west Mussorgsky Peaks.
3. KG.1513.3. Holocrystalline basalt, west Mussorgsky Peaks.
4. KG.1513.6. Vitrophyric basalt, west Mussorgsky Peaks.
5. KG.1514.1. Holocrystalline basalt, east Mussorgsky Peaks.
6. KG.1517.1. Holocrystalline basalt, Gluck Peak.
7. KG.1517.3. Holocrystalline basalt, Gluck Peak.

Chronologic Data

Preliminary K-Ar data from a pillow at Mussorgsky Peaks indicate a Pliocene age (2.5 Ma), whereas preliminary K-Ar data from a pillow at Gluck Peak indicate an age of less than 1 Ma (Hole, unpublished data, 1987).

Extent of Knowledge

Beethoven Peninsula was visited for the first time in 1970 by C.M. Bell, as part of a British Antarctic Survey reconnaissance geologic mapping project on Alexander Island [*Bell,* 1973]. The area was revisited briefly in 1975–1976 by R.G.B. Renner during the establishment of a geoceiver station at Gluck Peak [*Renner,* 1982]. The exposures at Mussorgsky Peaks and Gluck Peak were examined in detail in 1985–1986 by M.J. Hole [*Smellie et al.,* 1988; *Hole et al.,* 1989].

Bibliography

Bell, 1973
Hole, 1988
Hole et al., 1989
Renner, 1982
Renner et al., 1982
Smellie et al., 1988

Copyright American Geophysical Union

C.5. SOUTHEASTERN ALEXANDER ISLAND

Type of volcano: Not known. Exposures consist of camptonite dikes.

Location: Several places in southeastern Alexander Island (71°28′–71°45′S, 68°30′W).

Height above sea level: ~100–250 m.

Evidence of Holocene activity: None.

Authors of report: P.D. Rowley and J.L. Smellie.

Date of report: October 1988.

Form and Structure

Several subvertical dikes of camptonite, as much as 2 m wide, cut Lower Cretaceous sedimentary rocks of the Fossil Bluff Group in southeastern Alexander Island [*Horne and Thomson*, 1967] (Figure C.5.1). The dikes may have been feeders for volcanic centers of alkaline volcanic rocks that have been removed completely by erosion.

Petrologic Characteristics

Three dikes have been chemically analyzed (Table C.5.1). Two are potassic trachybasalt and one is phonotephrite; together they form a potassic series (in the sense of *Le Bas et al.* [1986]) with the lowest Na_2O/K_2O ratios (0.95–1.35) in this province. All the analyzed rocks are evolved, with low Mg numbers (58–48) and low Cr and

Fig. C.5.1. Geologic sketch map of southeastern Alexander Island, showing the locations of camptonite dikes [after *British Antarctic Survey*, 1981]. Rock exposure is outlined; pattern of rock unit is shown beyond the limit of the exposure; form lines are dashed.

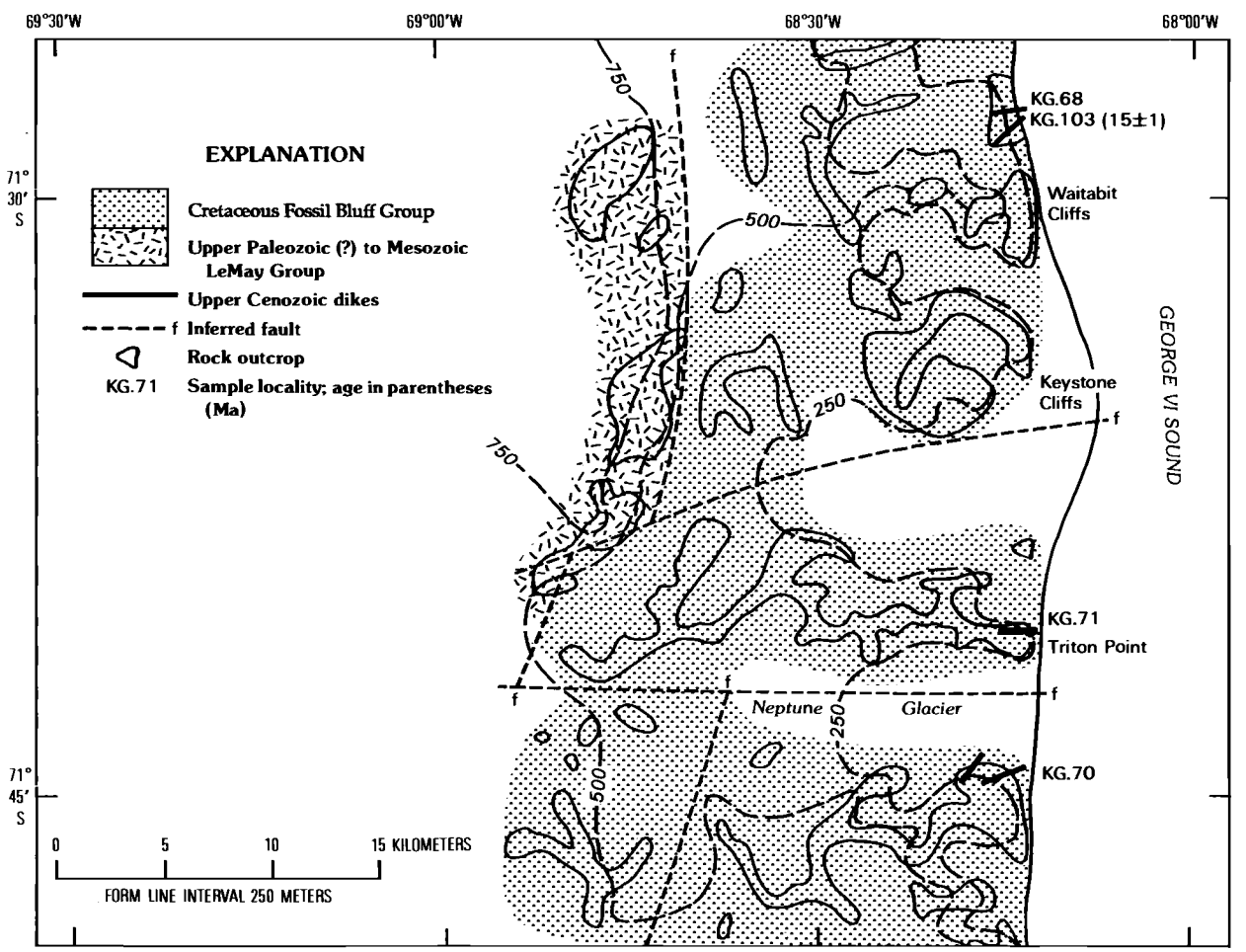

Copyright American Geophysical Union

TABLE C.5.1. Chemical Analyses and CIPW Norms of Camptonite Dikes From Northern Waitabit Cliffs, Southeastern Alexander Island

	1	2	3
SiO_2	45.30	46.40	46.53
TiO_2	2.62	2.26	2.22
Al_2O_3	15.73	16.33	16.33
Fe_2O_3	4.27	3.73	3.53
FeO	5.88	5.89	6.59
MnO	0.16	0.14	0.17
MgO	6.70	4.22	4.89
CaO	9.10	6.73	7.44
Na_2O	2.84	4.64	3.03
K_2O	2.31	3.44	3.18
P_2O_5	0.89	1.09	1.04
LOI	3.60	4.54	4.38
Total	100.04	100.06	100.07
or	13.65	20.33	18.79
ab	21.74	22.15	24.94
an	23.35	13.57	21.56
ne	1.24	9.27	0.38
di	12.67	10.22	6.91
ol	9.92	7.11	10.62
mt	6.19	5.41	5.12
il	4.98	4.29	4.22
ap	2.11	2.58	2.46
Ba	236	184	180
Ce	88	98	109
Cr	191	56	56
Ga	19	24	22
La	32	54	54
Nb	51	70	66
Ni	98	42	41
Pb	9	8	8
Rb	16	17	15
Sr	1136	1282	1357
Th	0	4	2
Y	24	22	24
Zn	74	102	91
Zr	274	427	416

All samples analyzed by XRF; Fe^{2+}/Fe^{3+} ratios determined by wet chemistry (Smellie, unpublished data, 1985). LOI, loss on ignition.

1. KG.68.12. Potassic trachybasalt (collected by R.R. Horne; analyst, J.L. Smellie).
2. KG.103.225. Phonotephrite (collected by M.R.A. Thomson; analyst, J.L. Smellie).
3. KG.103.224. Potassic trachybasalt (collected by M.R.A. Thomson; analyst, J.L. Smellie).

Ni contents. They are distinguished by extraordinarily high Sr contents (1136–1357 ppm) and K/Rb ratios (1191–1760), coupled with very low Rb contents (15-17 ppm) and Rb/Sr ratios (0.011–0.014). The petrogenesis of the camptonite dikes is enigmatic at present and is under investigation.

Most of the camptonite dikes consist of phenocrysts of titanaugite, hornblende, labradorite, olivine, biotite, and Fe-Ti oxides in an altered groundmass of titanomagnetite, apatite, chlorite, zeolite, and, possibly, analcite (Table C.5.2). Two of the dikes examined contain phenocrysts of kaersutite and biotite that are 80 times larger than the other phenocrysts in these rocks [*Horne and Thomson,* 1967].

Chronologic Data

Rex [1970] determined a K-Ar whole-rock date of 15 ± 1 Ma for one of the dikes.

Extent of Knowledge

The dikes were studied in 1963 and 1964 by R.R. Horne and M.R.A. Thomson during British Antarctic Survey reconnaissance mapping projects in southern Alexander Island [*Horne and Thomson,* 1967].

Bibliography

Horne and Thomson, 1967
Rex, 1970

Copyright American Geophysical Union

TABLE C.5.2. Modal Analyses of Camptonite Dikes From Alexander Island

Mineral	1	2	3	4	5	6
Plagioclase	18.8	17.0	18.0	14.6	21.5	31.4
Titaniferous pyroxene	11.0	17.0	14.5	13.0	16.4	24.5
Titaniferous amphibole	17.1	8.0	8.9	21.9	12.0	5.8
Olivine	2.0	0	7.1	12.4	10.3	10.2
Fe-Ti oxides	9.6	7.9	7.4	10.8	8.5	6.9
Chlorite	4.8	0	1.8	3.3	10.2	0
Zeolite	0.5	0.8	0.4	3.2	2.8	0
Calcite	4.3	2.3	1.2	0.3	1.5	6.6
Matrix	31.9	47.0	40.7	20.5	16.8	14.6

Analyses from *Horne and Thomson* [1967, Table II].

1. KG.103.225. Edge of southern camptonite dike, northern Waitabit Cliffs.
2. KG.103.224. Amygdaloidal zone of southern camptonite dike, northern Waitabit Cliffs.
3. KG.68.21. Center of southern camptonite dike, northern Waitabit Cliffs.
4. KG.68.12. Edge of northern olivine-bearing camptonite dike, northern Waitabit Cliffs.
5. KG.68.11. Center of northern olivine-bearing camptonite dike, northern Waitabit Cliffs.
6. KG.70.1. Center of olivine-bearing camptonite dike, cliff on south side of Neptune Glacier at its junction with George VI Sound.

Copyright American Geophysical Union

C.6. RYDBERG PENINSULA

Type of volcano: Small cones(?) and eroded deposits of palagonite tuff and olivine-phyric basaltic lava flows.

Location: Southeastern Rydberg Peninsula (73°19′S, 78°53′W), English Coast, eastern Ellsworth Land.

Height above sea level: ~400 m.

Evidence of Holocene activity: None.

Authors of report: P.D. Rowley and J.W. Thomson.

Date of report: July 1986.

Form and Structure

The only published reference to the geology of Rydberg Peninsula is the brief mention by *Renner et al.* [1982] of subaerially deposited olivine-phyric basaltic lava flows at one small outcrop (Figure C.6.1). They noted that these volcanic rocks resemble samples from Beethoven Peninsula, Alexander Island. No primary volcanic landforms were observed (Renner, BAS unpublished field notes, 1976), but Mount Combs, located about 15 km to the southwest, has the shape of a small cone (about 3.5 km in diameter) that rises at least several hundred meters above the ice surface (U.S. Navy oblique aerial photograph, TMA 1734, F31, no. 239); the same photograph shows no rock exposures on

Fig. C.6.1. Geologic sketch map of the Rydberg Peninsula area and Snow Nunataks, based on U.S. Geological Survey 1:500,000 sketch map of Bryan Coast–Ellsworth Land. The single rock exposure visited on Rydberg Peninsula is indicated by sample locality T.561. The base of Mount Combs is shown by a dashed line. Rock exposure is outlined; pattern of the rock unit is shown beyond the limit of the exposure.

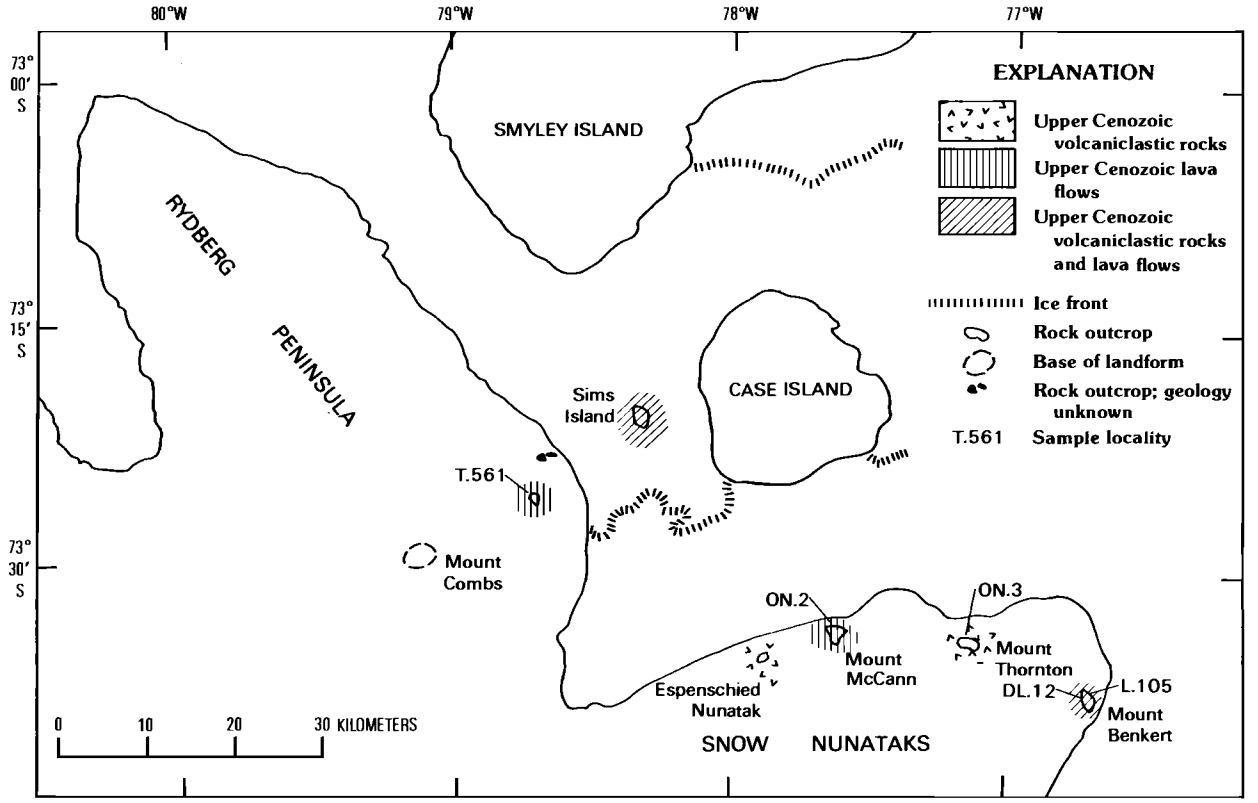

Copyright American Geophysical Union

Copyright American Geophysical Union

TABLE C.6.1. Chemical Analysis and CIPW Norm of a Lava Flow From Rydberg Peninsula

	1
SiO_2	47.08
TiO_2	2.55
Al_2O_3	15.76
Fe_2O_3	1.63
FeO	9.20
MnO	0.18
MgO	7.80
CaO	9.61
Na_2O	3.70
K_2O	1.43
P_2O_5	0.40
Total	99.34
or	8.51
ab	19.51
an	22.32
ne	6.50
di	18.97
ol	16.05
mt	2.38
il	4.88
ap	0.88
Ba	159
Cr	285
La	19
Nb	31
Ni	97
Rb	7
Sr	588
V	233
Y	27
Zr	181

Sample analyzed by XRF. FeO and Fe_2O_3 determined by wet chemistry.

1. T.561.1. Hawaiite (collected by R.G.B. Renner; analyst, A.B. Moyes).

Bibliography

Renner et al., 1982
Rowley et al., 1985, 1989

Copyright American Geophysical Union

Copyright American Geophysical Union

Copyright American Geophysical Union

TABLE C.7.1. Representative Chemical Analyses and CIPW Norms of Basaltic Rocks From Snow Nunataks

	1	2	3	4
SiO_2	44.00	46.30	48.20	48.70
TiO_2	2.30	1.84	2.36	2.09
Al_2O_3	15.70	15.60	16.30	16.10
Fe_2O_3	3.90	2.75	3.10	2.73
FeO	6.12	8.05	7.02	7.71
MnO	0.15	0.16	0.15	0.16
MgO	4.92	7.77	5.58	6.72
CaO	10.20	9.36	10.20	9.63
Na_2O	3.66	3.46	3.67	3.73
K_2O	1.13	0.90	1.44	1.38
P_2O_5	0.53	0.40	0.49	0.47
H_2O^+	3.45	1.79	0.74	0.60
H_2O^-	3.53	1.23	0.66	0.30
Total	99.59	99.61	99.91	100.32
or	7.21	5.51	8.64	8.20
ab	23.46	25.34	26.27	26.57
an	24.92	25.24	24.11	23.25
ne	5.41	2.69	2.85	2.80
di	21.20	16.52	19.68	17.86
ol	5.88	16.05	8.25	12.31
mt	5.95	4.13	4.56	3.98
il	4.72	3.62	4.55	3.99
ap	1.25	0.90	1.09	1.03
Ba	170	120	120	170
Ce	39	27	32	32
Cr	92	210	140	190
Eu	2	<2	2	2
La	24	18	21	21
Nb	--	22	24	28
Nd	26	22	26	24
Ni	36	160	44	110
Rb	<10	10	<10	14
Sr	640	475	590	590
Ta	<40	<40	<40	<40
Th	<4	<4	<4	<4
Ti	1.3%	1.0%	1.3%	1.2%
V	210	180	220	200
Y	20	20	20	22
Yb	2	2	3	2
Zr	--	152	188	180

Major oxides analyzed by XRF; trace elements analyzed by inductively coupled plasma semiquantitative spectrographic analysis (analysts, P.H. Briggs, J.G. Crock, C. Gent, K. Kennedy and J. Kent, U.S. Geological Survey). Dashes, not determined.

1. DL.12A. Margin of basalt dike cutting lava flow/tuff sequence, eastern Mount Benkert (collected by D.J. Lidke).
2. L.105D. Basalt lava flow, eastern Mount Benkert (collected by T.S. Laudon).
3. ON.3B. Hawaiite lava flow, Mount Thornton (collected by J.M. O'Neill).
4. ON.2C. Hawaiite pillow lava flow, Mount McCann (collected by J.M. O'Neill).

Copyright American Geophysical Union

C.8. JONES MOUNTAINS

Type of volcano: Not known. Eroded masses of basaltic palagonite tuff and breccia and basaltic lava flows and dikes.

Location: Jones Mountains (73°30′–73°40′S, 94°10′–95°10′W), western Ellsworth Land.

Height above sea level: 750–1500 m.

Evidence of Holocene activity: None.

Author of report: P.D. Rowley.

Date of report: July 1986.

Form and Structure

No primary volcanic landforms remain in the Jones Mountains (Figure C.8.1), but basaltic tuff and breccia, interbedded with thin basaltic lava flows, are widely exposed [*Craddock et al.*, 1964; *Rutford et al.*, 1968, 1972; *Lopatin et al.*, 1974]. This sequence, as much as 500 m thick, is locally intruded by basaltic dikes and plugs. Tuff and lava flows low in the section are considered to represent hyaloclastite eruptions, whereas flows higher in the sequence apparently represent subaerial deposition [*Rutford et al.*, 1972]. The volcanic rocks rest on a glacially striated unconformity, having a relief of about 50 m and an elevation of about 750 m, developed on a basement complex of intrusive and volcanic rocks of probable Mesozoic age [*Craddock et al.*, 1964] (Figure C.8.2). Tillite and glacial erratics, either underlying or included within the volcanic sequence, locally rest on the unconformity.

Petrologic Characteristics

Basaltic lava flows in the Jones Mountains contain phenocrysts in a narrow compositional range, consisting of olivine (Fo_{78-83}, optically determined), labradorite (An_{52-72}),

Fig. C.8.1. Geologic sketch map of the Jones Mountains, from *Craddock et al.* [1964], *Craddock* [1972], and U.S. Geological Survey 1:500,000 scale sketch map of Thurston Island–Jones Mountains. Rock exposure is outlined; pattern of the rock unit is shown beyond the limit of the exposure. Numbers give surveyed elevations, in meters, of the points shown.

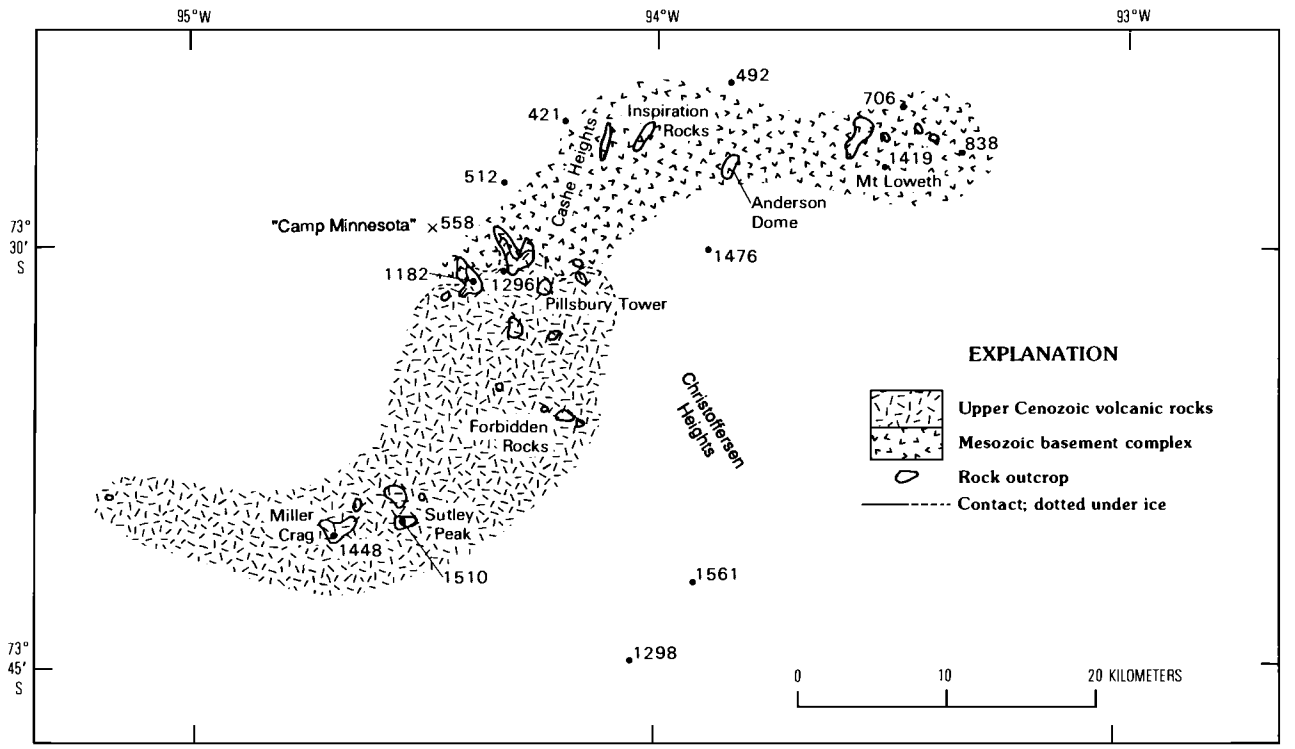

Copyright American Geophysical Union

Copyright American Geophysical Union

TABLE C.8.1. Representative Chemical Analyses and CIPW Norms of Lava Flows From the Jones Mountains

	1	2	3	4
SiO_2	41.84	43.48	44.07	44.39
TiO_2	1.85	2.10	2.04	2.08
Al_2O_3	12.93	13.09	13.96	14.49
Fe_2O_3	1.79	2.24	1.33	2.62
FeO	13.19	12.60	13.03	12.73
MnO	0.22	0.25	0.21	0.25
MgO	12.02	11.43	10.79	8.49
CaO	10.04	9.23	8.97	8.75
Na_2O	2.13	2.50	2.58	2.80
K_2O	0.78	1.03	1.05	1.03
H_2O^+	1.86	1.29	0.39	1.20
H_2O^-	0.45	0.22	0.10	0.36
CO_2	0.44	0.36	1.10	0.44
Total	99.54	99.82	99.62	99.63
or	4.79	6.24	6.42	6.27
ab	7.77	12.52	17.60	19.76
an	24.33	22.01	24.23	24.65
ne	5.94	4.97	2.70	2.52
di	20.04	18.46	11.98	14.16
ol	30.78	28.38	31.05	24.65
mt	2.70	3.33	2.00	3.91
il	3.65	4.09	4.01	4.07

All analyses by wet chemical methods.

1. 61-126. Tephrite, Jones Mountains [*Craddock et al.*, 1964, Table 1].
2. 61-1-4. Tephrite, Jones Mountains [*Craddock et al.*, 1964, Table 1].
3. 61-225-4. Tephrite, Jones Mountains [*Craddock et al.*, 1964, Table 1].
4. 61-12-44. Basalt, Jones Mountains [*Craddock et al.*, 1964, Table 1].

reconnaissance in 1960–1961 [*Craddock et al.*, 1964], 1963–1964 [*Rutford et al.*, 1968, 1972], and 1968–1969 [*Craddock et al.*, 1969]. A joint U.S. Antarctic Research Program and British Antarctic Survey group of geologists revisited the area in 1984–1985 [*British Antarctic Survey*, 1985*b*; *Dalziel and Pankhurst*, 1985].

Bibliography

British Antarctic Survey, 1985*b*
Craddock et al., 1964, 1969
Dalziel and Pankhurst, 1985
Lopatin et al., 1974
Rutford et al., 1968, 1972, 1973

Copyright American Geophysical Union

C.9. HUDSON MOUNTAINS

Type of volcano: Small, only slightly eroded parasitic cones, apparently resting on three larger, more eroded stratovolcanoes; stratovolcanoes consist of palagonite tuff and olivine-phyric basaltic lava flows.

Location: Hudson Mountains and nearby nunataks to the north (73°45′–74°55′S, 98°20′–100°30′W), western Ellsworth Land.

Height above sea level: 200–750 m.

Evidence of Holocene activity: *Lopatin and Polyakov* [1974] reported the possible presence of steam near one of the volcanoes but did not say which one. Satellite data suggested an eruption at Webber Nunatak in 1985 (Kyle, personal communication, 1985).

Authors of report: P.D. Rowley, T.S. Laudon, K.E. La Prade, and W.E. LeMasurier.

Date of report: November 1986.

Form and Structure

The Hudson Mountains and several scattered nunataks just to the north (Figure C.9.1) represent three major eroded volcanoes whose centers underlie Teeters Nunatak, Mount Moses, and Mount Manthe (Figure C.9.2) [*Wade and La Prade,* 1969; *LeMasurier,* 1972*a, b*; *Lopatin and Polyakov,* 1974; *LeMasurier and Wade,* 1976; *LeMasurier and Rex,* 1982; King and Schaefer, unpublished field notes, 1968]. These are named the Teeters Nunatak volcano, Mount Moses volcano, and Mount Manthe volcano (Figure C.9.3). Small parasitic cones, only slightly modified by erosion, apparently rest on the larger volcanoes (Laudon and Bastien, unpublished data, 1968). Similar small cones may underlie Wold Nunatak and, based on its subdued domal shape, Shepherd Dome. Other small cones (at Maish Nunatak, an unnamed nunatak northeast of Mount Moses, and Webber Nunatak) contain shallow but well-defined craters. The nunataks in the Hudson Mountains appear to fall along easterly and northerly trends, suggesting control of eruptive centers by orthogonal fractures. *Lopatin and Polyakov* [1974] suggested that the easterly controlling fractures were faults, although joints would seem to be more likely.

Most volcanoes consist of subaerially deposited basaltic lava flows, but some consist of subglacial or subaqueous hyaloclastite tuff and basaltic lava flows. The stratigraphy of the Hudson Mountains consists of (1) a lower sequence, at least 60 m thick and well exposed at Mount Nickens, of subhorizontal pillow lava flows of plagioclase–olivine–phyric basalt interbedded with sparse vesicular lava flows and hyaloclastite tuff; (2) a middle sequence, ~350–400 m thick, of subhorizontal to steeply dipping, thin-bedded, yellowish-gray hyaloclastite tuff and subordinate basaltic breccia and lava flows; and (3) an upper sequence, as much as 60 m thick, of subhorizontal basaltic lava flows (some of them of pahoehoe type) and minor volcanic bombs, exposed at Maish Nunatak, Mount Moses, and Mount Manthe [*Lopatin and Polyakov,* 1974]. This stratigraphic subdivision is followed in constructing the geologic map of the Hudson Mountains (Figure C.9.1).

The hyaloclastite tuff contains clasts of basaltic rocks and minor prevolcanic granite and gneiss. The tuff is associated with pillow lava flows and consists mostly of sideromelane shards rather than blocky, sparsely vesicular to nonvesicular clasts of both tachylite and sideromelane that characterize the hyaloclastite from Marie Byrd Land [*LeMasurier and Rex,* 1982].

The lower and middle sequences of the Hudson Mountains are broadly similar to the hydroclastic rocks of Marie Byrd Land, which formed in contact with glacial ice [*LeMasurier,* 1972*a, b; LeMasurier and Wade,* 1976; *LeMasurier and Rex,* 1982]. The hyaloclastite tuffs and pillow lavas in the Hudson Mountains probably represent an intraglacial or periglacial eruptive environment also, but no tillites have been found intercalated in these deposits (cf. IVD's B.1, B.16C, C.2, and C.8). Central vents for these tuffs, rather than decentralized fissure vents, probably exist in the Hudson Mountains. Inman Nunatak, where numerous dikes cut the tuff, may be such a center. The upper sequence of the Hudson Mountains could have been deposited under shallow water [*Lopatin and Polyakov,* 1974], but it is more likely that most of it was deposited subaerially. This sequence probably makes up the upper part of the larger, eroded Teeters Nunatak, Mount Moses, and Mount Manthe volcanoes (Figure C.9.2). Prevolcanic basement is not exposed in the Hudson Mountains.

Petrologic Characteristics

Chemical analyses (Table C.9.1) of the volcanic rocks from the Hudson Mountains fall in the fields of basalt, hawaiite, and tephrite (see Figure C.III). They range from mostly silica undersaturated to silica saturated. They are not as alkaline as those in Marie Byrd Land. Despite a relatively narrow range in SiO_2 between the various

Copyright American Geophysical Union

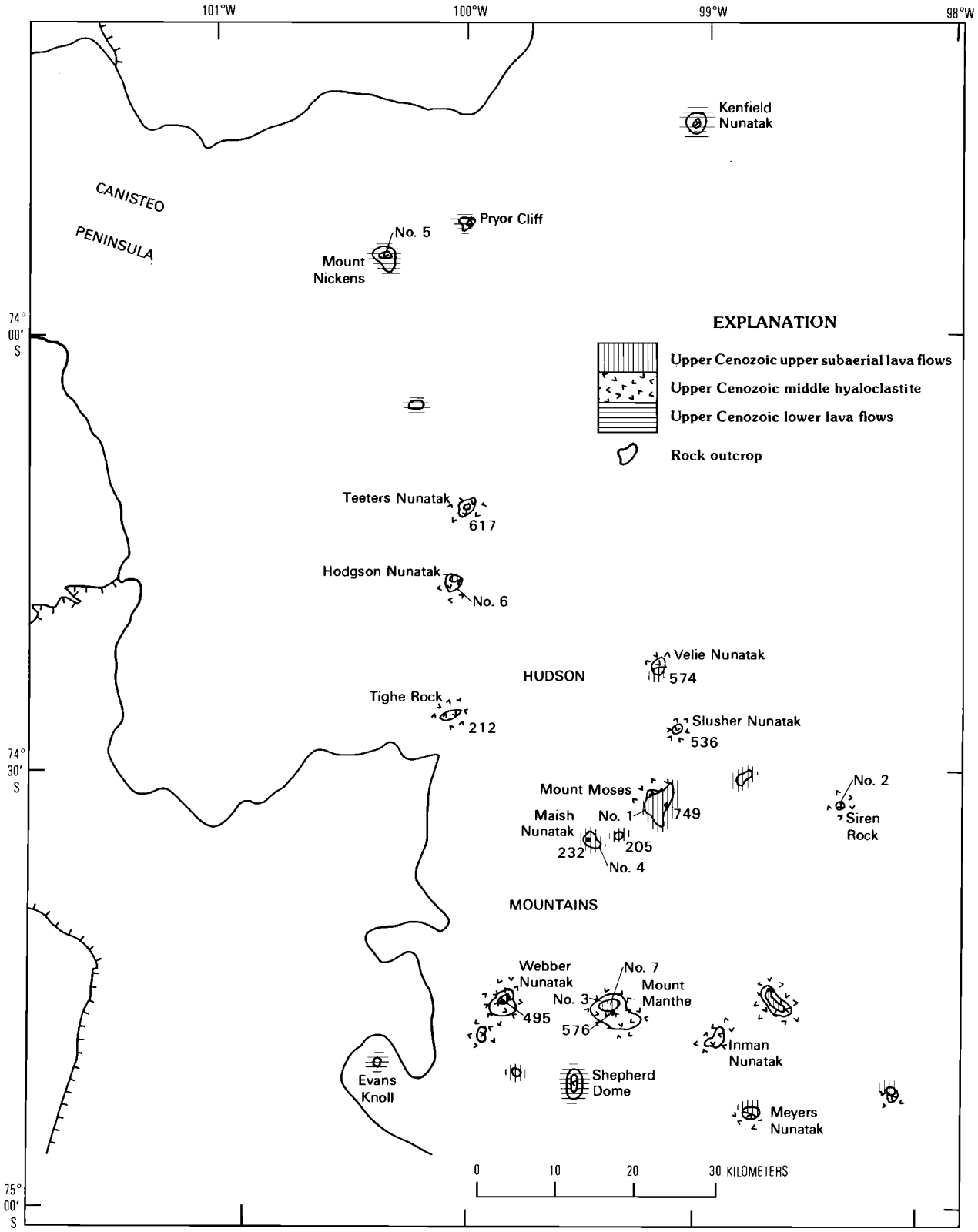

Fig. C.9.1. Geologic map of the Hudson Mountains and adjacent nunataks [after *Lopatin and Polyakov,* 1974; also La Prade and Laudon, unpublished data, 1983]. Hachured lines mark the edges of ice shelves. Numbers 1–7 indicate locations of chemically analyzed samples; other numbers show surveyed elevations, in meters, of the points shown. Base map and elevations are from U.S. Geological Survey 1:500,000 scale sketch map of Thurston Island–Jones Mountains.

Copyright American Geophysical Union

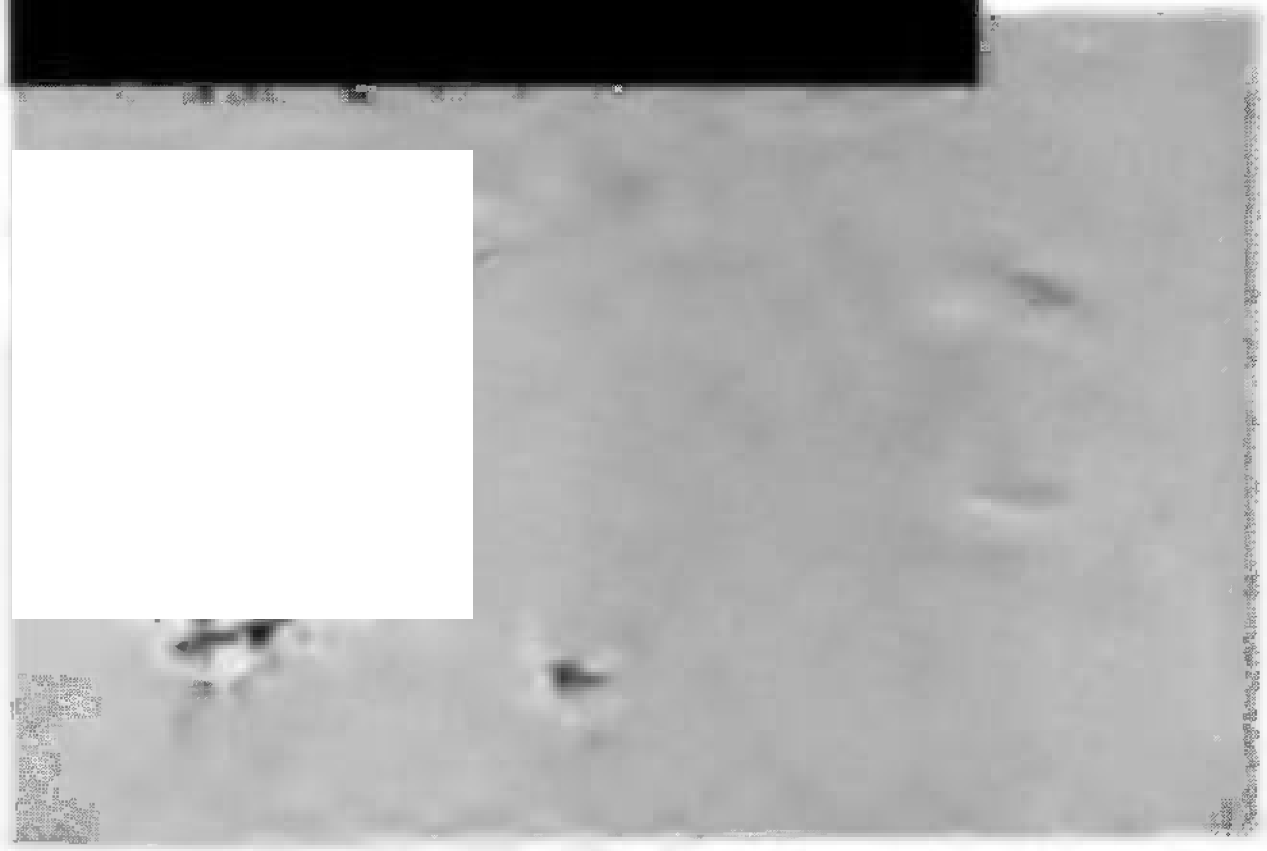

Copyright American Geophysical Union

TABLE C.9.1. Representative Chemical Analyses and CIPW Norms of Volcanic Rocks From the Hudson Mountains

	1	2	3	4	5	6	7
SiO_2	45.79	46.17	46.55	47.36	47.73	47.96	48.43
TiO_2	2.74	2.71	1.89	2.52	1.92	2.12	2.18
Al_2O_3	16.27	15.78	13.40	15.83	14.40	15.36	15.56
Fe_2O_3	1.86	2.23	1.00	2.18	1.38	5.78	1.72
FeO	9.14	9.38	10.43	8.42	9.72	6.64	9.71
MnO	0.17	0.17	0.16	0.16	0.15	0.15	0.15
MgO	5.55	5.89	9.43	5.23	8.30	7.50	8.20
CaO	10.74	11.17	9.57	10.43	9.87	9.40	9.87
Na_2O	4.16	3.76	3.11	4.06	3.24	3.47	3.0
K_2O	1.43	1.14	0.97	1.45	0.79	1.02	0.87
P_2O_5	0.57	0.43	0.31	0.54	0.31	0.38	0.34
H_2O^+	--	--	--	--	--	--	0.45
H_2O^-	--	--	--	--	--	--	--
F	0.04	0.04	0.03	0.02	0.01	--	--
LOI	--	--	0.51	0.37	0.33	0.63	0.52
Total	98.46	98.87	97.36	98.57	98.15	100.41	100.55
or	8.59	6.82	5.92	8.73	4.77	6.05	5.14
ab	15.75	17.60	21.02	21.87	25.43	27.75	25.38
an	21.84	23.08	20.39	21.07	22.92	23.43	26.41
ne	10.84	7.90	3.34	7.11	1.41	0.95	--
di	23.72	24.96	21.85	23.28	20.64	17.15	16.75
hy	--	--	--	--	--	--	1.80
ol	9.96	10.21	21.58	8.65	18.36	14.53	17.14
mt	2.74	3.27	1.50	3.22	2.05	5.27	2.49
il	5.29	5.21	3.71	4.87	3.73	4.04	4.14
ap	1.27	0.95	0.70	1.20	0.69	0.83	0.74
Ba	368	239	307	275	214	--	--
Ce	79	53	39	71	33	--	--
Cr	104	115	309	109	294	--	--
La	31	23	15	27	15	--	--
Nb	38	29	19	29	17	--	--
Ni	37	48	191	35	157	--	--
Rb	22	10	24	20	12	--	--
Sr	755	575	477	706	463	--	--
Th	6	--	4	--	--	--	--
U	--	3	2	1	1	--	--
V	259	269	196	231	229	--	--
Y	26	24	17	32	24	--	--
Zr	225	215	151	250	144	--	--

Samples 1–5 analyzed by XRF at University of Nottingham, England; FeO determined by wet chemistry, and F by selective ion electrode. Dashes, not determined or below level of detection (elements) or not present (norms). LOI, loss on ignition.

1. 24-1-A. Tephrite pillow lava flow, upper sequence, Mount Moses.
2. 32-4-A. Basalt lava flow, middle palagonite tuff sequence, Siren Rock.
3. 42-4-A. Basalt clast, middle palagonite tuff sequence, Mount Manthe.
4. 20-2-B. Glassy rind of hawaiite lava flow, parasitic cone of the upper sequence, Maish Nunatak.
5. 9-1-C. Glassy rind of a basalt pillow, lower pillow lava sequence, Mount Nickens.
6. 159a. Basalt clast in hyaloclastite, Hodgson Nunatak [*Lopatin and Polyakov,* 1974, Table 2]. Analyzed by wet chemical methods.
7. 208b. Basalt lava flow, upper part, Mount Manthe [*Lopatin and Polyakov,* 1974, Table 2]. Analyzed by wet chemical methods.

Copyright American Geophysical Union

TABLE C.9.2. Modal Analyses of Basaltic Rocks From Mount Manthe, Hudson Mountains

Minerals	1	2	3	4
Olivine	14.3	14.6	13.4	12.2
Plagioclase*	40.5	37.4	40.6	46.6
Augite	--	40.6	33.8	--
Fe-Ti oxides	--	7.6	12.2	--
Cryptocrystalline matrix	45.2	--	--	41.2

Dashes, not present.
*Includes interstitial feldspar.
1, 2. H1, H2. Clasts from hyaloclastite sequence (Bastien, unpublished data, 1968).
3, 4. H4, H5. Lava flows overlying hyaloclastite sequence (Bastien, unpublished data, 1968).

analyzed rocks, they have a wide scatter in values of oxides and elements. The range in alkalis, especially Na_2O, is broad, although a trend is narrowly confined in a Na_2O versus K_2O plot.

Lava flows, and lava clasts in the tuffs, are weakly alkaline, plagioclase–olivine–phyric basaltic rocks, consisting of olivine, labradorite-bytownite, and minor clinopyroxene phenocrysts in a holocrystalline, hypohyalline, or holohyalline vesicular groundmass containing plagioclase (An_{53-80}), clinopyroxene (salite-augite), olivine (Fo_{76-85}), Fe-Ti oxides, and secondary minerals [*Lopatin and Polyakov,* 1974]. Hyaloclastite tuff contains the same minerals. Four previously unpublished modal analyses of samples from Mount Manthe are given in Table C.9.2.

Chronologic Data

The fact that cones are only slightly eroded suggests that the rocks are late Tertiary or Quaternary. *Lopatin and Polyakov* [1974] hypothesized that volcanism migrated from north to south with time and that the youngest volcanoes may be showing fumarolic activity at the present time. *Laudon* [1982] and *LeMasurier and Rex* [1982] reported six generally concordant K-Ar whole-rock dates from Mount Manthe. These are 4.9 ± 1.6 Ma for a basalt lava flow in the middle of a 200-m-thick hyaloclastite tuff sequence; 8.5 ± 1.0 Ma for a basalt clast 50 m below the top of the hyaloclastite sequence; 5.0 ± 0.3, 4.6 ± 0.2, and 4.9 ± 0.3 Ma for basalt clasts collected from oldest to youngest rocks near the top of the hyaloclastite sequence; and 5.6 ± 1.9 Ma for the overlying subaerial basalt flows. *LeMasurier and Rex* [1982] published a K-Ar whole-rock date of 3.7 ± 0.2 Ma for a basalt flow within the hyaloclastite tuff sequence at Velie Nunatak. *Lopatin and Polyakov* [1974, Figure 1] reported K-Ar whole-rock dates of 7.3 Ma for a sample from Mount Nickens, 12.3 Ma for a sample from Hodgson Nunatak, and 32.8 Ma for a sample from Mount Manthe; neither analytical data nor error bars for the ages were published, so all of them are suspect. A K-Ar whole-rock age of 21 ± 4 Ma reported by *Rutford et al.* [1968] for a flow near the base of the hyaloclastite sequence of Mount Manthe volcano is considerably older than most other isotopic ages. These data suggest that the major period of activity in the Hudson Mountains was in late Miocene and Pliocene time, but no linear migration pattern is discernible from these data.

Extent of Knowledge

The Hudson Mountains were discovered on February 25, 1940, by members of the U.S. Antarctic Service Expedition on a flight from the U.S.S. *Bear* [*Hawthorne,* 1945]. Mount Manthe was visited briefly on February 11, 1961, by a U.S. Navy aircraft and geologically studied by A.B. Ford, J.M. Aaron, and T.S. Laudon; a few chemical analyses and isotopic ages of rocks collected during this trip were published by *Laudon* [1982]. All of the Hudson Mountains were mapped in reconnaissance in 1968 by a team led by K.E. La Prade. The results of this work were only briefly noted by *Wade and La Prade* [1969] and *Wade and Wilbanks* [1972], but B.G. Lopatin, also a member of the 1968 field party, wrote a more detailed report [*Lopatin and Polyakov,* 1974]. *LeMasurier and Rex* [1982] briefly described the chronology and petrographic characteristics of Hudson Mountains samples provided by Wade. Five previously unpublished chemical analyses of these samples are presented here.

Bibliography

Laudon, 1982
LeMasurier, 1972*a, b*
LeMasurier and Rex, 1982
LeMasurier and Wade, 1976
Lopatin and Polyakov, 1974
Rutford et al., 1968
Wade and La Prade, 1969
Wade and Wilbanks, 1972

Copyright American Geophysical Union

C.10. HENRY NUNATAKS

Type of volcano: Not known. Deposits consist of a southeasterly dipping sequence of lava flows.

Location: Central part of Henry Nunataks (75°08′S, 72°36′W), north of Behrendt Mountains, eastern Ellsworth Land.

Height above sea level: ~1200–1450 m.

Evidence of Holocene activity: None.

Authors of report: J.W. Thomson and K.S. Kellogg.

Date of report: July 1986.

Form and Structure

Henry Nunataks (see Figure C.11.1) consist predominantly of Mesozoic volcanic rocks, mostly porphyritic dacitic lava flows of the Mount Poster Formation [*Rowley et al.*, 1982]. Only the central nunatak in the group is known to have a cap of younger vesicular olivine-phyric basaltic lava flows (Kellogg, unpublished field notes, 1985), but on the basis of distant observation of landforms, it is possible that part of the western end of the easternmost nunatak is also capped by young basaltic rocks. The younger volcanic sequence on the central nunatak forms a 100(?)-m-thick sequence of gray aphanitic basaltic lava flows; the individual vesicular flows have rubbly scoriaceous basal and upper parts. Only one aphanitic basalt dike was observed, cutting the flows in the middle part of the sequence.

Petrologic Characteristics

Only one thin section of a lava flow is available. The rock is vesicular, with glomeroporphyritic olivine phenocrysts and less common plagioclase microphenocrysts embedded in a hyalopilitic groundmass of plagioclase microlites, granular clinopyroxene, olivine, and skeletal crystals of Fe-Ti oxides. Olivine is partly altered to iddingsite. A single chemical analysis of a dike sample (Table C.10.1.) indicates that the rock is potassic trachybasalt.

Chronologic Data

None.

Extent of Knowledge

Henry Nunataks were visited for the first time in January 1985, as part of the 1984–1985 U.S. Geological Survey reconnaissance geologic mapping project in eastern Ellsworth Land [*Rowley et al.*, 1985, 1989]. Only brief observations were possible during an hourlong stopover at the nunataks (Kellogg, unpublished field notes, 1985).

Bibliography

Rowley et al., 1985, 1989

Copyright American Geophysical Union

TABLE C.10.1. Chemical Analysis and CIPW Norms of a Dike From Henry Nunataks

	1
SiO_2	47.90
TiO_2	2.11
Al_2O_3	15.50
Fe_2O_3	3.81
FeO	6.11
MnO	0.15
MgO	7.85
CaO	8.98
Na_2O	3.48
K_2O	1.86
P_2O_5	0.50
H_2O^+	0.87
H_2O^-	0.47
Total	99.59
or	11.19
ab	24.87
an	21.56
ne	2.77
di	16.60
ol	12.49
mt	5.33
il	4.08
ap	1.11
Ba	250
Ce	37
Cr	270
Eu	2
La	24
Nb	30
Nd	25
Ni	170
Rb	30
Sr	590
Ta	<40
Th	4
Ti	1.2%
V	200
Y	26
Yb	3
Zr	200

Major oxides analyzed by XRF; trace elements analyzed by inductively coupled plasma semiquantitative spectrographic analysis.

1. Ke. 241c. Potassic trachybasalt dike cutting vesicular basaltic lava flows, central nunatak of Henry Nunataks (collected by K.S. Kellogg; analysts, P.H. Briggs, J.G. Crock, C. Gent, K. Kennedy, and J. Kent, U.S. Geological Survey).

Copyright American Geophysical Union

C.11. MERRICK MOUNTAINS

Type of volcano: Not known. Deposits consist of eroded, frost-shattered flow breccia and lava flows.

Location: Southwestern Merrick Mountains (75°08′S, 72°12′W).

Height above sea level: ~1250 m (Otway, unpublished data, 1966).

Evidence of Holocene activity: None.

Authors of report: P.D. Rowley, W.R. Vennum, and J.L. Smellie.

Date of report: October 1988.

Fig. C.11.1. Geologic map of the Merrick Mountains and Henry Nunataks, including the small nunataks of basanite (localities Ke.241 and EE.604), after *Laudon et al.* [1970], *Vennum and Laudon* [1988], and U.S. Geological Survey 1:500,000 scale sketch map of Ellsworth Land (east part)–Palmer Land (south part). Dashed line shows probable plutonic contact. Rock exposure is outlined; pattern of the rock unit is shown beyond the limit of the exposure.

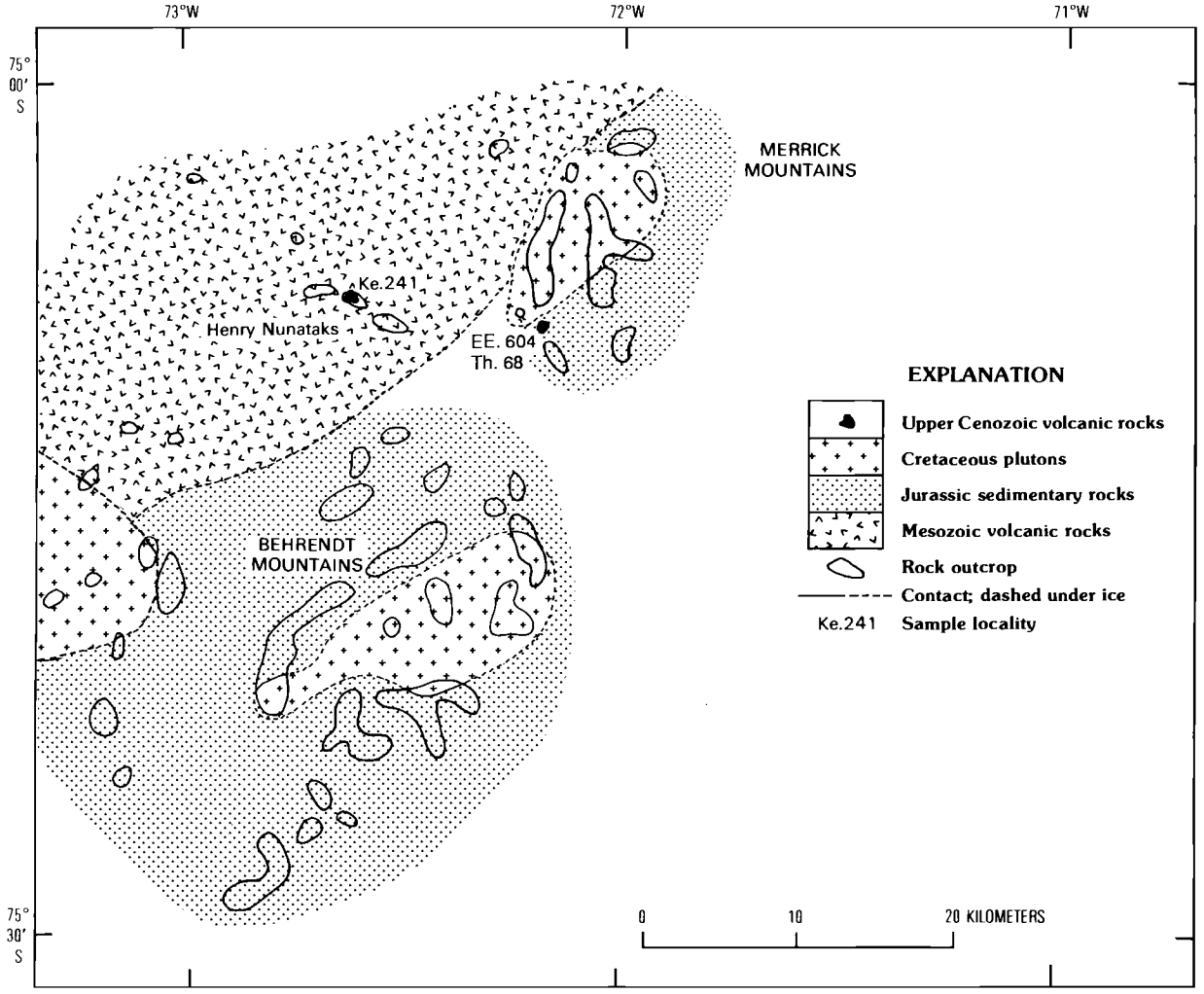

Copyright American Geophysical Union

Form and Structure

The Cenozoic volcanic rocks in the southwestern Merrick Mountains consist of a 10- to 12-m-thick sequence of frost-shattered basanite flow breccia overlain by less voluminous vesicular to scoriaceous lava flows, all exposed in a small (100 × 50 m) nunatak less than 30 m high [*Laudon et al.*, 1970; *Laudon*, 1972, 1982; *Rowley et al.*, 1983; *Vennum and Laudon*, 1988] (Figure C.11.1). Clasts in the flow breccia are as much as 5 cm long and are set in a palagonitized matrix of glassy ash and lapilli. The rocks probably are hyaloclastites that erupted partly or entirely under ice.

Petrologic Characteristics

The rocks are basanite that contain fresh olivine microphenocrysts averaging 0.3–0.5 mm long (maximum 0.75 mm long), set in a hyalopilitic groundmass of plagioclase (as much as An_{55}) laths, granular Fe-Ti oxides, light brown glass, and minor olivine (Fo_{85-95}) [*Vennum and Laudon*, 1988]. The matrix of the flow breccia is a vesicular vitrophyre with petrology similar to that of the flow rocks. The chemical analyses (Table C.11.1) of three samples show that the principal lithology is basanite high in alkalis and normative *ne* (see Figure C.III). Despite high Mg number (61–70), the contents of MgO, Cr, and Ni are low, and the lavas are relatively evolved. Unusually, Cr contents are less than those of Ni. The analyzed samples are most similar in composition to basanite and tephrite in the Mount Pinafore area of Alexander Island.

Chronologic Data

Halpern [1971] reported a K-Ar whole-rock date of 6 Ma for a sample collected in the area. The true age of this rock, however, is tentative inasmuch as Halpern never published any analytical data for the sample or included errors for the age.

Extent of Knowledge

The exposures were discovered during a University of Wisconsin mapping project in 1965–1966 [*Laudon et al.*, 1970]; at that time, rocks were collected for chemical analyses and K-Ar dating [*Halpern*, 1971]. The geology of the nunatak was studied again during the 1977–1978 field season [*Rowley et al.*, 1983].

Bibliography

Halpern, 1971
Laudon, 1972, 1982
Laudon et al., 1970
Rowley et al., 1983
Vennum and Laudon, 1988

Copyright American Geophysical Union

TABLE C.11.1. Chemical Analyses and CIPW Norms of Lava Flows From the Merrick Mountains

	1	2	3
SiO_2	44.64	44.90	45.23
TiO_2	2.24	2.24	2.57
Al_2O_3	15.11	14.38	14.66
Fe_2O_3	2.84	4.21	1.20
FeO	7.49	6.18	9.25
MnO	0.15	0.17	0.15
MgO	8.13	8.21	8.09
CaO	8.13	8.54	8.18
Na_2O	4.24	4.58	4.88
K_2O	2.54	2.59	2.79
P_2O_5	0.79	0.92	0.77
H_2O^+	2.24	--	--
H_2O^-	1.30	--	--
LOI	--	2.45	1.30
Total	99.84	100.06	100.11
or	15.59	15.78	16.84
ab	12.85	13.50	8.35
an	15.26	11.36	10.09
ne	13.22	14.33	18.33
di	17.54	20.76	21.39
ol	15.06	11.33	16.38
mt	4.28	6.30	1.77
il	4.42	4.38	4.99
ap	1.79	2.25	1.86
Ba	300	301	298
Ce	76	86	84
Cr	170	123	73
Dy	5.4	--	--
Er	2.9	--	--
Eu	2.35	--	--
Ga	--	19	20
Gd	7.3	--	--
La	41	52	46
Lu	0.3	--	--
Nb	50	66	70
Ni	160	123	105
Pb	--	9	7
Rb	30	23	26
Sr	850	984	959
Sm	7.2	--	--
Ta	<40	--	--
Tb	1.1	--	--
Th	<4	1	4
Ti	1.1%	--	--
V	180	--	--
Y	25	28	26
Yb	2.3	--	--
Zn	--	93	101
Zr	250	257	277

For sample 1, major elements analyzed by wet chemical methods, and trace elements analyzed by inductively coupled plasma semiquantitative spectrographic analysis (analysts, J.C. Crock, K. Kennedy, P.H. Biggs, and B. King, U.S. Geological Survey). Samples 2 and 3 analyzed by XRF; Fe^{2+}/Fe^{3+} ratios determined by wet chemistry. Dashes, not determined or below level of detection. LOI, loss on ignition.

1. EE.604. Basanite, southwestern Merrick Mountains [*Laudon,* 1972, Table 3].
2. Th.68.2. Basanite (collected by M.R.A. Thomson; analyst, J.L. Smellie).
3. Th.68.1. Basanite [*Smellie,* 1987]. (Sample number given erroneously as Th.67.1 by *Smellie* [1987].)

Copyright American Geophysical Union

BIBLIOGRAPHY

Barker, P.F., The Cenozoic subduction history of the Pacific margin of the Antarctic Peninsula: Ridge crest–trench interactions, *J. Geol. Soc. London, 139,* 787–801, 1982.

Behrendt, J.C., Crustal geology of Ellsworth Land and the southern Antarctic Peninsula from gravity and magnetic anomalies, *J. Geophys. Res., 69,* 2047–2063, 1964*a*.

Behrendt, J.C., Distribution of narrow-width magnetic anomalies in Antarctica, *Science, 144,* 993–995, 1964*b*.

Behrendt, J.C., Antarctic Peninsula Traverse geophysical results relating to glaciological and geological studies, *Res. Rep. Ser. 64-1,* 112 pp., University of Wisconsin Geophysical Polar Research Center, Madison, 1964*c*.

Bell, C.M., The geology of Beethoven Peninsula, south-western Alexander Island, *Br. Antarct. Surv. Bull.,* no. 32, 75–83, 1973.

Bentley, C.R., Glacial and subglacial geography of Antarctica, in *Antarctic Research, Geophys. Monogr. Ser.,* vol. 7, edited by H. Wexler, M.J. Rubin, and J.E. Caskey, Jr., pp. 11–25, AGU, Washington, D. C.,1962.

Bentley, C.R., Crustal structure of Antarctica from geophysical evidence—A review, in *Antarctic Earth Science,* edited by R.L. Oliver, P.R. James, and J.B. Jago, pp. 491–497, Cambridge University Press, New York, 1983.

Bentley, C.R., and J.W. Clough, Antarctic subglacial structure from seismic refraction measurements, in *Antarctic Geology and Geophysics,* edited by R.J. Adie, pp. 683–691, Universitetsforlaget, Oslo, 1972.

British Antarctic Survey, British Antarctic Territory geological map, Sheet 4, Alexander Island, scale 1:500,000, *BAS 500G Ser.,* Cambridge, 1981.

British Antarctic Survey, British Antarctic Territory geological map, Sheet 5, Northern Palmer Land, scale 1:500,000, *BAS 500G Ser.,* Cambridge, 1982.

British Antarctic Survey, Tectonic map of the Scotia arc, scale 1:3,000,000, *BAS Misc. 3,* Cambridge, 1985*a*.

British Antarctic Survey, Annual report, 1984–85, 114 pp., Cambridge, 1985*b*.

Burn, R.W., The geology of the LeMay Group, Alexander Island, *Br. Antarct. Surv. Sci. Rep.,* no. 109, 65 pp., 1984.

Burn, R.W., and M.R.A. Thomson, Late Cenozoic tillites associated with intraglacial volcanic rocks, lesser Antarctica, in *Earth's Pre-Pleistocene Glacial Record,* edited by M.J. Hambrey and W.B. Harland, pp. 199–203, Cambridge University Press, New York, 1981.

Care, B.W., The geology of Rothschild Island, north-west Alexander Island, *Br. Antarct. Surv. Bull.,* no. 50, 87–112, 1980.

Crabtree, R.D., B.C. Storey, and C.S.M. Doake, The structural evolution of George VI Sound, Antarctic Peninsula, *Tectonophysics, 114,* 431–442, 1985.

Craddock, C. (Compiler), Geologic Map of Antarctica, American Geographical Society, New York, 1972.

Craddock, C., T.W. Bastien, and R.H. Rutford, Geology of the Jones Mountains area, in *Antarctic Geology,* edited by R.J. Adie, pp. 171–187, North-Holland, Amsterdam, 1964.

Craddock, C., C.M. White, and R.H. Rutford, The geology of the Eights Coast, *Antarct. J. U.S.. 4*(4), 93–94. 1969.

Dalziel, I.W.D., The early (pre-Middle Jurassic) history of the Scotia arc region—A review and progress report, in *Antarctic Geoscience,* edited by C. Craddock, pp. 111–126, University of Wisconsin Press, Madison, 1982.

Dalziel, I.W.D., and D.H. Elliot, West Antarctica—Problem child of Gondwanaland, *Tectonics, 1*(1), 3–19, 1982.

Dalziel, I.W.D., and R.J. Pankhurst, Tectonics of West Antarctica and its relation to East Antarctica: USARP-BAS geology/geophysics project (1984–1985), *Antarct. J. U.S., 20*(5), 40–41, 1985.

Doake, C.S.M., R.D. Crabtree, and I.W.D. Dalziel, Subglacial morphology between Ellsworth Mountains and Antarctic Peninsula—New data and tectonic significance, in *Antarctic Earth Science,* edited by R.L. Oliver, P.R. James, and J.B. Jago, pp. 270–273, Cambridge University Press, New York, 1983.

Drake, A.A., Jr., Preliminary geologic report on the 1961 U.S. expedition to the Bellingshausen Sea, Antarctica, *Science, 135*(3504), 671–672, 1962.

Fisher, R.V., and H.-U. Schmincke, *Pyroclastic Rocks,* Springer-Verlag, New York, 472 pp., 1984.

Grunow, A.M., D.V. Kent, and I.W.D. Dalziel, Mesozoic evolution of West Antarctica, and the Weddell Sea basin—New paleomagnetic constraints, *Earth Planet. Sci. Lett., 86,* 16–26, 1987.

Halpern, M., Evidence for Gondwanaland from a review of West Antarctic radiometric ages, in *Research in the Antarctic,* edited by L.O. Quam, pp. 717–730, AAAS, Washington, D.C., 1971.

Hawthorne, R., Exploratory flights of Admiral Byrd (1940), *Proc. Am. Philos. Soc., 89*(1), 398a–398e, 1945.

Herron, E.M., and B.E. Tucholke, Sea-floor magnetic patterns and basement structure in the southeastern Pacific, *Initial Rep. Deep Sea Drill. Proj., 35,* 263–278, 1976.

Hole, M.J., Post-subduction alkaline volcanism along the Antarctic Peninsula, *J. Geol. Soc. London, 145,* 985–998, 1988.

Hole, M.J., J.L. Smellie, and G.F. Marriner, Geochemistry and tectonic setting of Cenozoic alkaline basalts from Alexander Island, Antarctic Peninsula, in *Geological Evolution of Antarctica,* edited by M.R.A. Thomson, J.A. Crame, and J.W. Thomson, Cambridge University Press, New York, in press, 1989.

Horne, R.R., and M.R.A. Thomson, Post-Aptian camptonite dykes in south-east Alexander Island, *Br. Antarct. Surv. Bull.,* no. 14, 15–24, 1967.

Copyright American Geophysical Union

Jones, J.G., Intraglacial volcanoes of the Laugarvatn region, southwest Iceland, II, *J. Geol. 78*(2), 127–140, 1970.

Kellogg, K.S., and P.D. Rowley, Tectonic evolution of southeastern Antarctic Peninsula, in *Geological Evolution of Antarctica,* edited by M.R.A. Thomson, J.A. Crame, and J.W. Thomson, Cambridge University Press, New York, in press, 1989.

Laudon, T.S., Stratigraphy of eastern Ellsworth Land, in *Antarctic Geology and Geophysics,* edited by R.J. Adie, pp. 215–223, Universitetsforlaget, Oslo, 1972.

Laudon, T.S., Geochemistry of Mesozoic and Cenozoic igneous rocks, eastern Ellsworth Land, in *Antarctic Geoscience,* edited by C. Craddock, pp. 775–785, University of Wisconsin Press, Madison, 1982.

Laudon, T.S., L.L. Lackey, P.G. Quilty, and P.M. Otway, Geology of eastern Ellsworth Land, in *Geologic Maps of Antarctica, Antarct. Map Folio Ser.,* folio 12, plate 3, edited by V.C. Bushnell and C. Craddock, American Geographical Society, New York, 1970.

Le Bas, M.J., R.W. Le Maitre, A. Streckeisen, and B. Zanettin, A chemical classification of volcanic rocks based on the total alkali-silica diagram, *J. Petrol., 27*(3), 745–750, 1986.

LeMasurier, W.E., Volcanic record of Cenozoic glacial history in Marie Byrd Land, in *Antarctic Geology and Geophysics,* edited by R.J. Adie, pp. 251–259, Universitetsforlaget, Oslo, 1972*a*.

LeMasurier, W.E., Volcanic record of Antarctic glacial history—Implications with regard to Cenozoic ice levels, in *Polar Geomorphology, Spec. Publ. 4,* edited by R.J. Price and D.E. Sugden, pp. 59–74, Institute of British Geographers, London, 1972*b*.

LeMasurier, W.E., and D.C. Rex, Volcanic record of Cenozoic glacial history in Marie Byrd Land and western Ellsworth Land—Revised chronology and evaluation of tectonic factors, in *Antarctic Geoscience,* edited by C. Craddock, pp. 725–734, University of Wisconsin Press, Madison, 1982.

LeMasurier, W.E., and D.C. Rex, Rates of uplift and the scale of ice level instabilities recorded by volcanic rocks in Marie Byrd Land, West Antarctica, in *Antarctic Earth Science,* edited by R.L. Oliver, P.R. James, and J.B. Jago, pp. 663–670, Cambridge University Press, New York, 1983.

LeMasurier, W.E., and F.A. Wade, Volcanic history in Marie Byrd Land—Implications with regard to southern hemisphere tectonic reconstructions, in *Proceedings of the International Symposium on Andean and Antarctic Volcanology Problems,* edited by O. González-Ferrán, pp. 398–424, I.A.V.C.E.I., Rome, 1976.

Lopatin, B.G., and M.M. Polyakov, Geology of the volcanic Hudson Mountains (Walgreen Coast, West Antarctica) (in Russian), *Antarkt. Dokl. Komissii, 13,* 36–51, 1974.

Lopatin, B.G., A.Ya. Krylov, and O.A. Alinpyshev, Major tectonomagmatic stages in the development of Marie Byrd Land and Eights Coast (West Antarctica) determined radiometrically (in Russian), *Antarkt. Dokl. Komissii, 13,* 52–60, 1974.

O'Neill, J.M., and J.W. Thomson, Tertiary mafic volcanic and volcaniclastic rocks of the English Coast, Antarctica, *Antarct. J. U.S., 20*(5), 36–38, 1985.

Pankhurst, R.J., Rb-Sr geochronology of Graham Land, Antarctica, *J. Geol. Soc. London, 139*(6), 701–711, 1982.

Pearce, J.A., Role of the sub-continental lithosphere in magma genesis at active continental margins, in *Continental Basalts and Mantle Xenoliths,* edited by C.J. Hawkesworth and M.J. Norry, pp. 230–249, Shiva, Nantwich, England, 1983.

Renner, R.G.B., An improved gravity base-station network over the Antarctic Peninsula, *Br. Antarct. Surv. Bull.,* no. 51, 145–149, 1982.

Renner, R.G.B., B.J. Dikstra, and J.L. Martin, Aeromagnetic surveys over the Antarctic Peninsula, in *Antarctic Geoscience,* edited by C. Craddock, pp. 363–370, University of Wisconsin Press, Madison, 1982.

Rex, D.C., Age of a camptonite dyke from south-east Alexander Island, *Br. Antarct. Surv. Bull.,* no. 23, 103, 1970.

Rowley, P.D., Developments in Antarctic geology during the past half century, in *Revolution in the Earth Sciences—Advances in the Past Half-Century,* edited by S.J. Boardman, pp. 112–135, Kendall/Hunt, Dubuque, Iowa, 1983.

Rowley, P.D., and P.L. Williams, Geology of the northern Lassiter Coast and southern Black Coast, Antarctic Peninsula, in *Antarctic Geoscience,* edited by C. Craddock, pp. 339–348, University of Wisconsin Press, Madison, 1982.

Rowley, P.D., D.L. Schmidt, and P.L. Williams, Mount Poster Formation, southern Antarctic Peninsula and eastern Ellsworth Land, *Antarct. J. U.S., 17,* 38–39, 1982.

Rowley, P.D., W.R. Vennum, K.S. Kellogg, T.S. Laudon, P.E. Carrara, J.M. Boyles, and M.R.A. Thomson, Geology and plate tectonic setting of the Orville Coast and eastern Ellsworth Land, Antarctica, in *Antarctic Earth Science,* edited by R.L. Oliver, P.R. James, and J.B. Jago, pp. 245–250, Cambridge University Press, New York, 1983.

Rowley, P.D., K.S. Kellogg, and W.R. Vennum, Geologic studies in the English Coast, eastern Ellsworth Land, Antarctica, *Antarct. J. U.S., 20*(5), 34–36, 1985.

Rowley, P.D., K.S. Kellogg, W.R. Vennum, T.S. Laudon, J.W. Thomson, J.M. O'Neill, and D.J. Lidke, Tectonic setting of the English Coast, eastern Ellsworth Land, Antarctica, in *Geological Evolution of Antarctica,* edited by M.R.A. Thomson, J.A. Crame, and J.W. Thomson, Cambridge University Press, New York. in press, 1989.

Rutford, R.H., C. Craddock, and T.W. Bastien, Late Tertiary glaciation and sea-level changes in Antarctica, *Palaeogeogr. Palaeoclimatol. Palaeoecol., 5*(1), 15–39, 1968.

Copyright American Geophysical Union

Rutford, R.H., C. Craddock, C.M. White, and R.L. Armstrong, Tertiary glaciation in the Jones Mountains, in *Antarctic Geology and Geophysics,* edited by R.J. Adie, pp. 239–243, Universitetsforlaget, Oslo, 1972.

Rutford, R.H., W.E. LeMasurier, K.E. La Prade, T.S. Laudon, and J.D. Boellstorff, A summary of the terrestrial record of Antarctic glacial history in Ellsworth Land and Marie Byrd Land, West Antarctica (abstract), *Abstr. Congr. Int. Union Quat. Res. 9th,* 309, 1973.

Schmidt, D.L., and P.D. Rowley, Continental rifting and transform faulting along the Jurassic Transantarctic rift, Antarctica, *Tectonics, 5*(2), 279–291, 1986.

Schopf, J.M., Ellsworth Mountains—Position in West Antarctica due to sea-floor spreading, *Science, 164,* 63–66, 1969.

Singleton, D.G., Geology of Seward Mountains, western Palmer Land, *Br. Antarct. Surv. Bull.,* no. 49, 81–89, 1980.

Smellie, J.L., Geochemistry and tectonic setting of alkaline volcanic rocks in the Antarctic Peninsula—A review, *J. Volcanol. Geotherm. Res., 32* (1–3), 269–285, 1987.

Smellie, J.L., R.J. Pankhurst, M.J. Hole, and J.W. Thomson, Age, distribution and eruptive conditions of late Cenozoic alkaline volcanism in the Antarctic Peninsula and eastern Ellsworth Land—Review, *Br. Antarct. Surv. Bull.,* no. 80, 21–49, 1988.

Steiger, R.H., and E. Jäger, Subcommission on geochronology—Convention on the use of decay constants in geo- and cosmochronology, *Earth Planet. Sci. Lett., 36,* 359–362, 1977.

Storey, B.C., The crustal blocks of West Antarctica within Gondwanaland; reconstruction and break-up model, in *Geological Evolution of Antarctica,* edited by M.R.A. Thomson, J.A. Crame, and J.W. Thomson, Cambridge University Press, New York, in press, 1989.

Storey, B.C., and S.W. Garrett, Crustal growth of the Antarctic Peninsula by accretion, magmatism and extension, *Geol. Mag., 122,* 5–14, 1985.

Storey, B.C., M.R.A. Thomson, and A.W. Meneilly, The Gondwanian orogeny within the Antarctic Peninsula: A discussion, in *Gondwana Six: Structure, Tectonics, and Geophysics, Geophys. Monogr. Ser.,* vol. 40, edited by G.D. McKenzie, pp. 191–198, AGU, Washington, D.C., 1987.

Thomson, M.R.A., R.J. Pankhurst, and P.D. Clarkson, The Antarctic Peninsula—A late Mesozoic-Cenozoic arc (review), in *Antarctic Earth Science,* edited by R.L. Oliver, P.R. James, and J.B. Jago, pp. 289–294, Cambridge University Press, New York, 1983.

Vennum, W.R., and T.S. Laudon, Igneous petrology of the Merrick Mountains, eastern Ellsworth Land, Antarctica, *U.S. Geol. Surv. Prof. Pap., 1351,* 21–34, 1988.

Wade, F.A., and K.E. La Prade, Geology of the King Peninsula, Canisteo Peninsula, and Hudson Mountains areas, Ellsworth Land, Antarctica, *Antarct. J. U.S., 4*(4), 92–93, 1969.

Wade, F.A., and J.R. Wilbanks, Geology of Marie Byrd and Ellsworth lands, in *Antarctic Geology and Geophysics,* edited by R.J. Adie, pp. 207–214, Universitetsforlaget, Oslo, 1972.

Williams, P.L., D.L. Schmidt, C.C. Plummer, and L.E. Brown, Geology of the Lassiter Coast area, Antarctic Peninsula—Preliminary report, in *Antarctic Geology and Geophysics,* edited by R.J. Adie, pp. 143–148, Universitetsforlaget, Oslo, 1972.

Copyright American Geophysical Union

Copyright American Geophysical Union

Summary

J. L. Smellie

Frontispiece. Phreatomagmatic eruption on Deception Island (1967 land center), showing dense, ash-charged column and development of base surge. (Photograph by I.M. Willey.)

Introduction

Graham Land contains numerous outcrops of upper Cenozoic volcanic rocks, mostly restricted to northern and eastern areas (Figure D.I). The region is unique in Antarctica in containing major changes in tectonic environment, which occurred over a short period during the Neogene-Recent, within a geographically limited area (Figure D.II). These changes resulted in the concurrent eruption of compositionally contrasting magma types (e.g., volcanic arc (calc-alkaline) and within-plate (alkaline)). "Transitional" magmas showing a variety of arc, ocean ridge, and within-plate compositional characteristics were erupted during the formation of a small ensialic marginal basin in Bransfield Strait. The arc volcanism described in this province is possibly restricted to the Neogene period, but it may also overlap in part with the earliest within-plate volcanism; marginal-basin volcanism occurred concurrently with the latest stages of the within-plate volcanism (Table D.I).

The outcrops are assigned a Neogene-Recent age principally on the basis of isotopic ages and preservation of original volcanic landforms. Lithologic freshness is also a useful, though nondiagnostic, criterion, since some of the associated volcanic arc rocks have undergone hydrothermal and low-grade burial metamorphic alteration. Individual volcanoes are often poorly defined, principally because of the reconnaissance or cursory nature of the studies. Except for Deception Island [*Baker et al.*, 1975], there have been no integrated modern volcanologic-petrologic studies, as demonstrated by the paucity of published information. For the purposes of the individual volcano descriptions (IVD's), therefore, the outcrops have been grouped geographically.

Tectonic Setting

A long magmatic record of Pacific Ocean crust subduction is preserved in Graham Land, extending from at least 200 Ma [*Pankhurst*, 1982*a*]. The arc is founded principally on a basement formed of low-grade metasedimentary sequences of an upper

Copyright American Geophysical Union

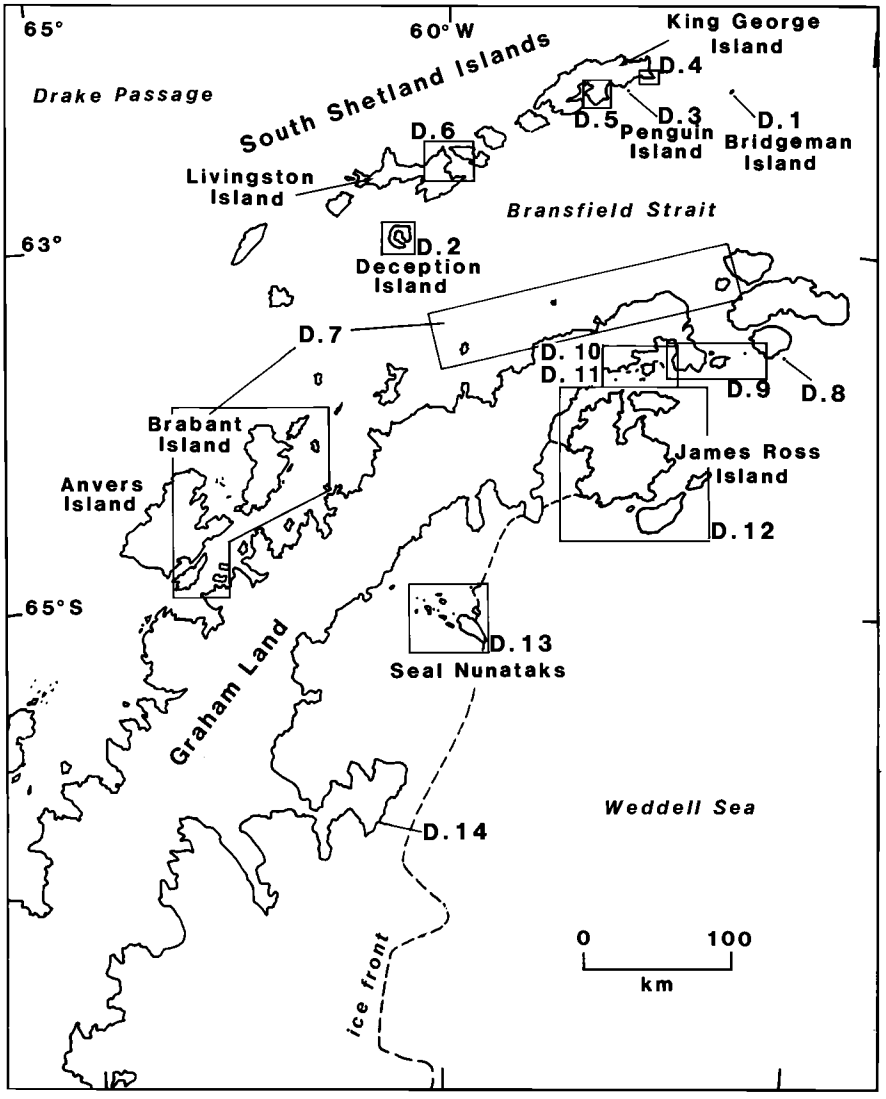

Fig. D.I. Sketch map of Graham Land and the South Shetland Islands, showing the locations of the volcanic outcrops (identified by individual volcano description numbers).

Paleozoic–lower Mesozoic accretionary prism. In addition, lower Paleozoic, high-grade orthogneisses and paragneisses are patchily preserved in eastern and probably southern Graham Land, representing the leading edge of a former continental landmass [e.g., *Dalziel and Elliot*, 1973; *Smellie*, 1981; *Dalziel*, 1982; *Pankhurst*, 1982*a*, 1983; *Moyes and Hamer*, 1983; *Storey and Garrett*, 1985; *Garrett and Storey*, 1987].

From early Tertiary times, arc magmatism ceased progressively from south to north as offset sections of a spreading center collided with the peninsula trench and the Pacific and Antarctic plates became coupled [*Herron and Tucholke*, 1976; *Barker*, 1982; *Saunders et al.*, 1982]. The spreading center is preserved only in Drake Passage (Figure D.II). It became inactive at about 4 Ma [*Barker*, 1976, 1982] and calc-alkaline volcanism has also ceased [*Pankhurst and Smellie*, 1983; *Smellie et al.*, 1984]. The arc volcanism may have been episodic, as is demonstrated within the South Shetland Islands (for which there are the most complete data) by crude age maxima at 130–110, 90–70, 60–40, and 30–20 Ma, and sparse younger ac-

Copyright American Geophysical Union

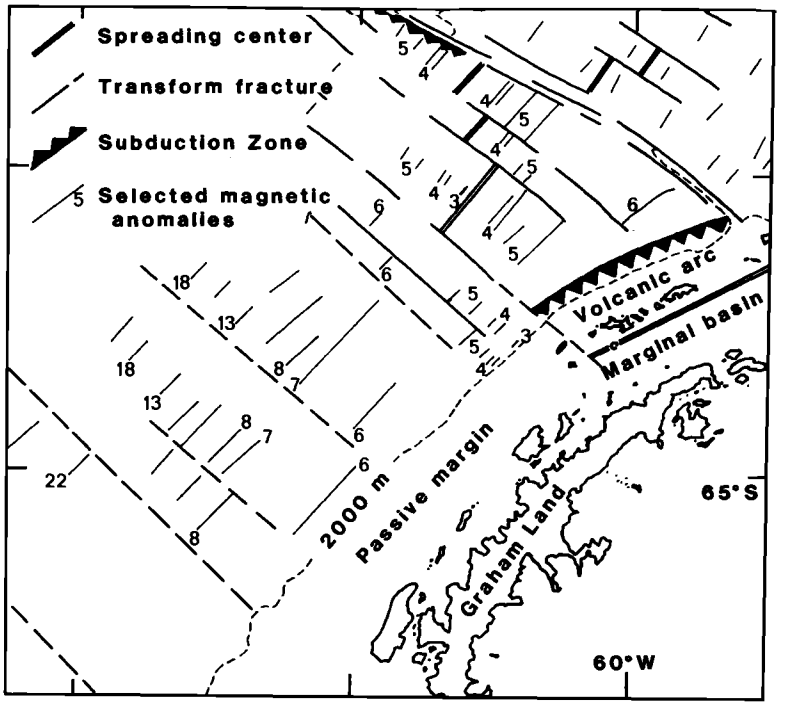

Fig. D.II. Present tectonic setting of Graham Land and the South Shetland Islands, showing magnetic anomaly identifications and simplified principal tectonic features (based on work by *Barker* [1982]).

TABLE D.I. Tectonic Setting and Magma Series: Neogene–Recent Volcanic Rocks, Graham Land Region

	Suprasubduction Zone		Within-Plate Extension
	Arc	Back-Arc	
Fractionating phases	basalts: ol-pl-cpx andesites: pl-cpx-opx-opq--ap±amph	basalts: ol-cpx; pl-ol-cpx andesites: pl-cpx-ol±opx dacites/rhyodacites: pl-opx--cpx-ol-opq	alkali basalts: ol-cpx hawaiites/mugearites: pl-ol-cpx
Remarks	Highly porphyritic	Basaltic rocks sparsely porphyritic or aphyric, becoming moderately porphyritic (≤20% phenocrysts by volume) in the acidic members; pigeonite in the groundmass	Sparsely to moderately porphyritic; clinopyroxene seldom seen as a phenocryst phase but exerted a strong effect on geochemistry; groundmass olivine; spinel-lherzolite nodules occur at Seal Nunataks and in James Ross Island Volcanic Group
Age of volcanism	Neogene	<1 Ma	≤ 7 Ma
Outcrops (IVD)	D.4, D.5, D.7	D.1–D.3, D.6	D.7, D.8–D.14
References	*Smellie et al.* [1984]	*Baker et al.* [1975] *Weaver et al.* [1979]	*Nelson* [1975] *Smellie* [1987]

Abbreviations: pl, plagioclase; ol, olivine; cpx, clinopyroxene; opx, orthopyroxene; opq, opaque oxide; ap, apatite; amph, amphibole; IVD, individual volcano description.

Copyright American Geophysical Union

tivity [*Pankhurst and Smellie*, 1983; *Birkenmajer et al.*, 1986].

An asymmetrical graben, about 450 km long and containing about 32 km of quasi-oceanic crust, separates the South Shetland Islands from northern Graham Land. It has been interpreted as a marginal basin situated behind the South Shetland Islands volcanic arc [*Ashcroft*, 1972; *Davey*, 1972; *Tarney et al.*, 1977; *Weaver et al.*, 1979] (also P.J. Roach, quoted by *Garrett and Storey* [1987]) (Figure D.II). The recent eruptions on Deception Island [e.g., *Baker et al.*, 1975] suggest that volcanism related to spreading is still taking place.

During the late Cenozoic period, alkaline basaltic magmas were also erupted from numerous widely scattered centers situated along the fault-bounded flanks of Graham Land. The volcanism appears to be unrelated to subduction, and there is a consensus that it is a within-plate phenomenon related to regional extension [e.g., *Barker*, 1976; *Baker et al.*, 1977; *Pankhurst*, 1982*b*; *Saunders*, 1982; *Saunders and Tarney*, 1982; *Smellie et al.*, 1984; *Smellie*, 1987].

Fig. D.III. Histograms of whole-rock K-Ar ages determined for volcanic rocks in Graham Land and the South Shetland Islands. Sources are published data using a variety of isotopic constants, none of which is sensitive to correction to current conventional values.

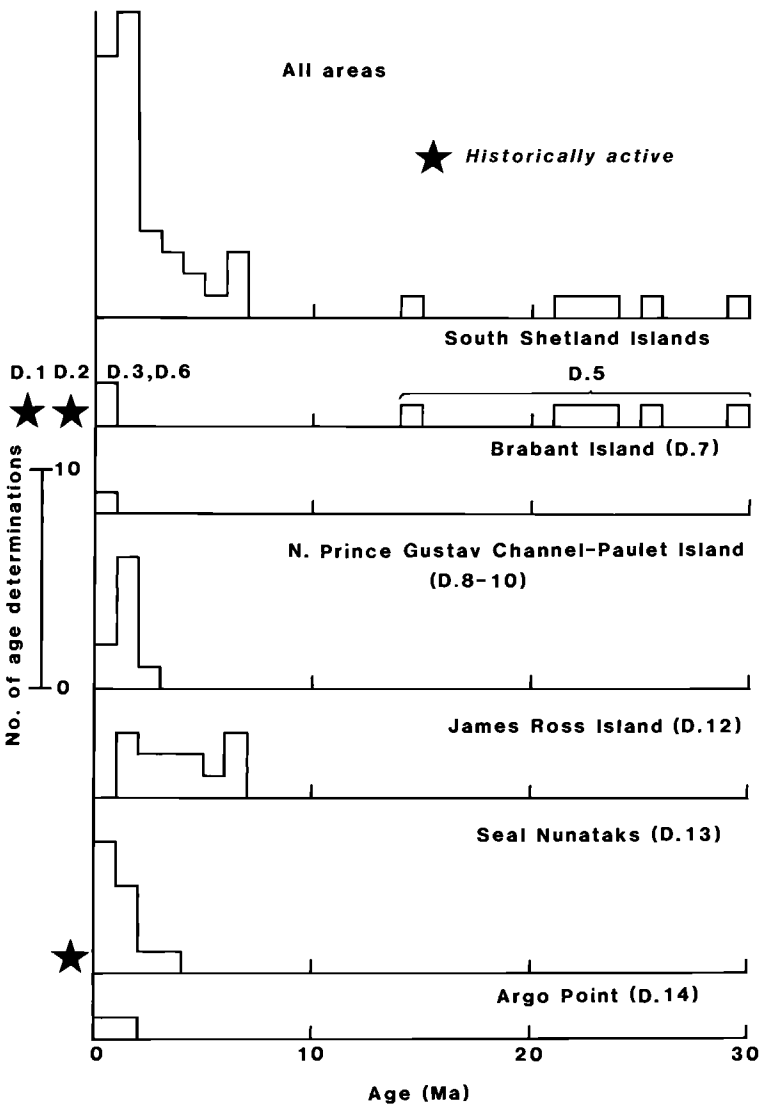

Copyright American Geophysical Union

Chronology

Dikes and lavas of the volcanic arc on southeastern King George Island have yielded mainly early Miocene K-Ar ages (14–29 Ma [*Birkenmajer et al.*, 1986]; Figure D.III). There are no published radiometric ages available for equivalent volcanic arc outcrops on Anvers and Brabant islands and islands in southeastern Bransfield Strait. However, subduction at the South Shetland trench continued until 4 Ma at least [*Barker*, 1982], suggesting that calc-alkaline volcanism could have continued on King George Island until Pliocene times.

Alkaline volcanism has a history extending back to late Miocene times (~7 Ma) at least (Figure D.III). The oldest rocks dated so far come from the James Ross Island group, and volcanic activity reached a peak in the Quaternary. Marginal-basin volcanism has occurred historically on Deception and Bridgeman islands [*Roobol*, 1973, 1979; *Hydrographic Department*, 1974]. All the exposed rocks on Deception Island are normally magnetized and may have formed during the past 700,000 years [*Valencio et al.*, 1979].

Volcanology

Each of the present outcrops was probably constructed in several cone-building episodes from discrete central and flank vents (summarized in Table D.II). The resulting deposits mainly form a proximal association of volcanic lithofacies dominated by lavas, autoclastic breccias, and lahar-like units. Air fall beds are locally important and range from cindery, monomict Strombolian types, often reddened by high-temperature oxidation, to multicolored, polymict Vulcanian units (lithic tuff breccias, agglomerates, and lapillistones). Cross-stratified yellow tuffs are prominent in the Melville Peak volcano, King George Island [*Birkenmajer*, 1982*a*], and their description resembles sand wave beds formed by surges during hydroclastic eruptions [cf. *Fisher and Schmincke*, 1984]; a less well stratified but otherwise superficially similar hydroclastic deposit also occurs at Claude Point, Brabant Island (J.W. Thomson and R.C.R. Willan, personal communications, 1986). Intraformational unconformities are common but mainly of little time-stratigraphic significance. Outcrops on King George and Brabant islands are also associated with locally thick (up to 200 m) volcaniclastic sequences of fluvial, marine, and glacial origin; either these formed during periods of volcanic quiescence or they are synvolcanic and represent a distal ring-plain association of lithologies.

Most of the outcrops are probably the degraded remnants of stratocones, but shield volcanoes are represented by Deception Island, the James Ross Island Volcanic Group (JRIVG), and possibly Seal Nunataks. Deception Island has a submerged basal diameter of about 30 km and a large flooded caldera 9–11 km across. In its original form, it was probably a large composite central volcano with several parasitic cones, which together comprise the precaldera series of yellow palagonite tuffs, agglomerates, and less common lava flows [*Baker et al.*, 1975]. A large volume of pyroclastic rocks was erupted immediately prior to caldera collapse. All postcaldera activity has been confined to small-volume eruptions within the 2-km-wide caldera fault zone. Eruptions at the rim usually resulted in quiet effusions of lava, an exception being the 1969 subglacial pyroclastic fissure eruption of likely sub-Plinian magmatic type (data of *Baker et al.* [1975]). Pyroclastic tuff cones and maars predominate at sea level and were formed by Surtseyan to phreato-Plinian activity (e.g., 1967 and 1970 eruptions).

James Ross Island is the largest center of alkaline volcanism in the Graham Land region. It is a composite shield volcano with a basal diameter of at least 60 km, flanked to the north and northeast by smaller, "satellite" shield volcanoes. Each center is built up of alternating flat-lying pahoehoe lavas and steeply dipping hyaloclastite flow foot breccias, interpreted as sequences of superimposed hyaloclastite deltas formed by lava streams entering seawater [*Jones and Nelson*, 1970; *Nelson*, 1975]. There are also numerous outcrops of highly vesiculated, palagonitized hyalotuffs (in the sense of *Honnorez and Kirst* [1975]) interpreted as tuff-cone or tuff-ring deposits [*Nelson*, 1975]. Subaqueous eruption has been postulated [*Nelson*, 1975] (see also *Baker et al.* [1973]), but the recent discoveries of tillite deposits [*British Antarctic Survey*, 1983; Sykes, BAS unpublished report, 1986] suggest the additional possibility of subglacial eruptions (see also *Smellie et al.* [1988]).

Copyright American Geophysical Union

TABLE D.II. Statistics of Volcanoes in Graham Land and the South Shetland Islands

IVD	Volcano	Volcano Type	Age	Basal Diameter	Summit Elevation Above Volcano Base	Remarks
D.1	Bridgeman Island	Stratovolcano remnant	Recent	15–25 km (submerged)	~1700 m	Historic fumarolic activity
D.2	Deception Island	Polygenetic shield volcano with large flooded caldera	<700,000 years	30 km (submerged)	~1200 m	Erupted 1967, 1969, 1970; numerous postcaldera tuff cones and fissure vents
D.3	Penguin Island	Small stratocone built on lava platform	<1000 years?	1 km	150 m	Dimensions refer to stratocone
D.4	Melville Peak	Eroded stratocone	<20 Ma	3 km (estimated original extent)	549 m	
D.5	Kraków Peninsula,* King George Island	Stratovolcano remnant(s)	Mainly Neogene?	Original dimensions unknown; outcrops occur within an area of about 30 km^2		Possibly two stratocones
D.6	Mount Plymouth Edinburgh Hill Inott Point Sharp Peak	Several small, highly eroded tuff-cone remnants	≤1 Ma	Original tuff cones probably 1–2 km in basal diameter; summit elevations unknown		Incompletely studied; presence of additional vents likely
D.7	Anvers Island, Brabant Island, and southern Bransfield Strait*	Probably several stratocones	Neogene to Recent?	Unknown	Unknown	Incompletely studied; number, location, type, and size of original centers unknown
D.8	Paulet Island	Small composite stratocone built on lava platform	~0.3 Ma	1.6 km	~150 m	Dimensions refer to stratocone
D.9	Tabarin Peninsula	Shield volcano	~1 Ma	20-40 km	730 m	Bisected by major fault; only half of the volcano is preserved
	Rosamel Island	Tuff-cone remnant	Unknown (≤1 Ma?)	>3 km (submerged)	Unknown; summit is 433 m above sea level	
D.11	Cain Nunatak Abel Nunatak	Tuff-cone remnants	Unknown (≤1 Ma?)	Original tuff cones probably ≤1.5 km in basal diameter; summit elevations unknown		Incompletely studied (Abel Nunatak not visited)
D.10, D.12	Mount Haddington	Shield volcano	≤7 Ma	35–60 km	~1470 m	Multiple tuya structure formed of superimposed lava-hyaloclastite sequences
	Terrapin Hill Bibby Point San Fernando Hill	Tuff-cone remnants	≤7 Ma	Original tuff cones may have been ≥5 km in basal diameter; summit elevations ~400–550 m		Poorly known

Copyright American Geophysical Union

TABLE D.II. (continued)

IVD	Volcano	Volcano Type	Age	Basal Diameter	Summit Elevation Above Volcano Base	Remarks
	Northern James Ross Island and Prince Gustav Channel*	Two or more shield volcanoes; probably some minor centers	≤7 Ma	Unknown	Unknown	Incompletely studied
D.13	Seal Nunataks*	Either several small stratocones or one or more dissected shield volcanoes	≤4 Ma	Unknown	Unknown	Poorly studied
D.14	Argo Point	Small scoria cone built on lava platform	≤1.4 Ma	300 m	<100 m	Dimensions refer to scoria cone

Individual volcano description (IVD) numbers correspond to those used in the text and figures.
*Area of volcanic outcrops within which no individual volcanic centers have been identified clearly.

Petrology

Neogene-Recent volcanism in the Graham Land region occurred within three tectonic settings (arc, back-arc, within-plate), and this is reflected in the petrology of the lavas erupted (Table D.I).

Subduction Zone Related Magmatism

Arc magmatism. Volcanic rocks on Brabant and Anvers islands consist of basalts and andesites [*González-Ferrán and Katsui*, 1970; *Alarcón et al.*, 1976], and the only published analysis is of a *hy*-normative, high-alumina basalt of calc-alkaline affinities. However, preliminary geochemical studies on Brabant Island basalts by M. Ringe [see *Furse*, 1986, p. 60] suggest conflicting affinities; some samples have chemical characteristics comparable with magmas of the South Shetland Islands (calc-alkaline), whereas others resemble basalts of the JRIVG (alkaline). The disparity may be reconciled by the changing tectonic setting of the area, which was undergoing active subduction until about 4 Ma [*Barker*, 1982] but has recently been described as a "spreading back-arc basin" (M. Ringe [see *Furse*, 1986]), although total crustal failure has probably not occurred [*Garrett and Storey*, 1987].

Neogene-Recent volcanism on southeastern King George Island forms a basalt-andesite association with high lithophile element contents, low Ti/Zr ratios, negligible Fe-enrichment in an AFM diagram and moderate light rare earth element (LREE) enrichment, characteristic of a calc-alkaline series [*Smellie et al.*, 1984] (Figure D.IV). Features of island arc tholeiites are also evident and include high Ni and Cr contents; moderate Fe*/Mg, K/Rb, and Na_2O/K_2O ratios; and low Rb/Sr. They are regarded as a low-K, high-alumina calc-alkaline suite (with tholeiitic affinities) formed on the thin leading edge of a continental margin because of subduction at the South Shetland trench.

Back-arc magmatism. Volcanism associated with the formation of a very young ensialic marginal basin is restricted to the South Shetland Islands and Bransfield Strait. The lavas are difficult to characterize geochemically, and they display features reminiscent of ocean ridge, island arc, and even within-plate magmas.

Deception Island contains a basalt-dacite series, whereas only basalts and basaltic andesites occur on Bridgeman Island [*Weaver et al.*, 1979]. *Baker et al.* [1975] identified a silica gap between 63% and 66% SiO_2, and this is still evident in the more complete data set of *Weaver et al.* [1979]. On a normative tetrahedron the basalts are olivine tholeiites and quartz tholeiites, with a low-pressure differentiation trend toward *Q*-normative compositions (Figure D.V). However, in the Deception Island lavas, the content of

Copyright American Geophysical Union

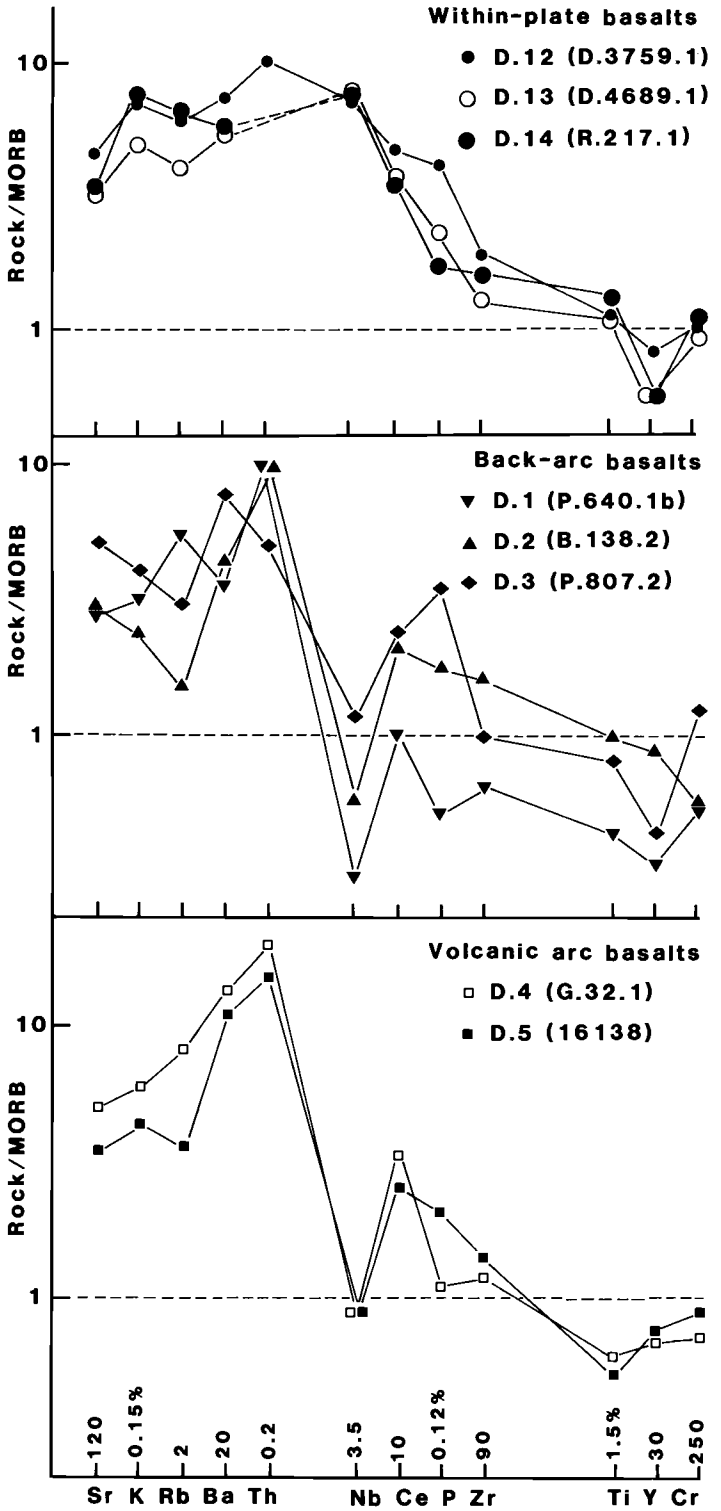

Fig. D.IV. Spidergrams of MORB-normalized incompatible element abundances for selected arc (D.4 and D.5), back-arc (D.1-D.3), and within-plate (D.12-D.14) volcanic rocks from Graham Land and the South Shetland Islands (all basalts except D.1 (basaltic andesite)). Normalizing values are those of *Pearce* [1983].

Copyright American Geophysical Union

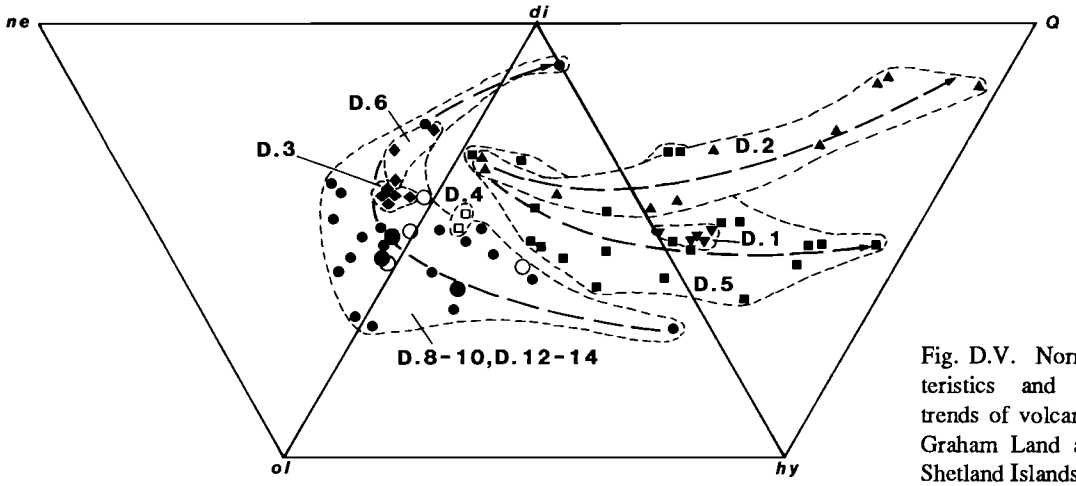

Fig. D.V. Normative characteristics and differentiation trends of volcanic rocks from Graham Land and the South Shetland Islands.

total alkalis approaches that of some alkaline series, although peralkalinity is not achieved. Using the classification of *Le Bas et al.* [1986], mugearites are predominant, followed by trachytes and benmoreites (Figure D.VI). This is principally an effect of the extraordinarily high Na_2O contents (even the basalts generally have >4% Na_2O); the K_2O contents are relatively low, comparable with some calc-alkaline series of island arcs. All the lavas have high Na/K ratios, those in Deception Island basalts being matched only by those in mid-ocean ridge basalt (MORB). Samples from neither island exhibit the pronounced Fe-enrichment trends characteristic of MORB or island arc tholeiites. In general terms, the concentrations of

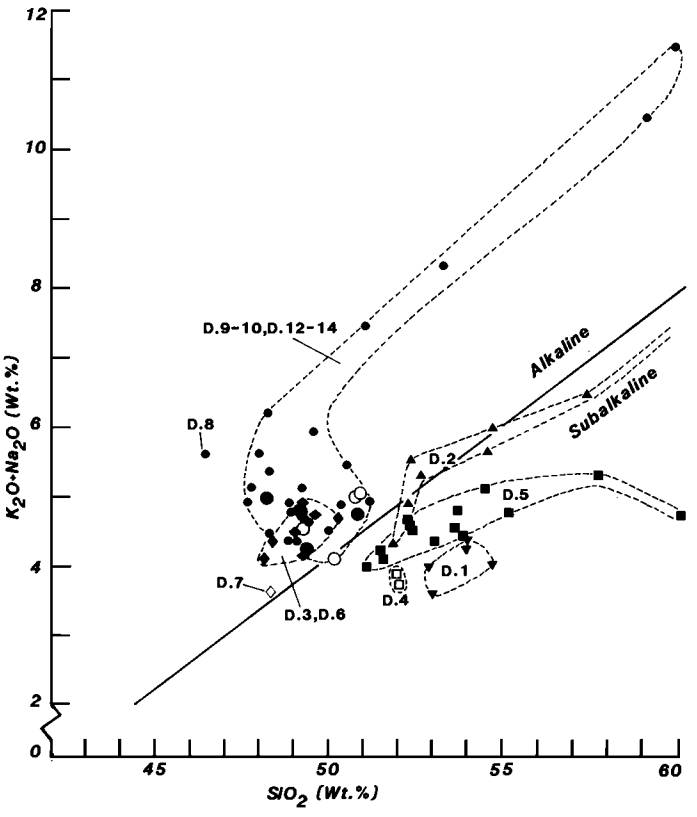

Fig. D.VI. Total alkalis versus silica plot for volcanic rocks from Graham Land and the South Shetland Islands.

Copyright American Geophysical Union

K, Rb, and Ba are at the lower ends of the ranges observed in calc-alkaline suites, overlapping with those for island arc tholeiites and even MORB, although Ba is significantly higher than in most ridge basalts. Chondrite-normalized rare earth element patterns are relatively flat (Ce_N/Yb_N ratios of 1.8–2.2 (basalts)) and closely resemble those of some marginal-basin basalts [e.g., *Saunders et al.*, 1979]. The $^{87}Sr/^{86}Sr$ ratios range from 0.7030 to 0.7036 [*Halpern*, 1970; *Weaver et al.*, 1979]. The most primitive Bridgeman Island lavas may have been generated by 10–20% partial melting of spinel peridotite, whereas only 5% melting of a similar mantle source could have produced the primitive Deception Island lavas [*Weaver et al.*, 1979].

The very young (<1 Ma; see Table D.I) postsubduction basalt lavas on Penguin, Greenwich, and Livingston islands were erupted onto the normal-faulted South Shetland Islands microplate on the northwest flank of Bransfield Strait. They show some compositional characteristics of alkaline rocks, including groundmass olivine, up to 6.3% normative *ne*, and high total alkalis (Figures D.V. and D.VI). Moreover, it is theoretically possible to derive the least evolved lavas by low degrees of partial melting (possibly ≤3%) comparable with alkaline magmas from other provinces [*Weaver et al.*, 1979; *Smellie*, 1987]. However, some lavas contain groundmass pigeonite, and as a group, the lavas are depleted in high field strength elements (HFSE) relative to large ion lithophile elements, and they have low absolute HFSE abundances, low $(Ce/Y)_N$ ratios, and high Na/K and Ti/Zr ratios comparable with island arc tholeiites and some MORB. Penguin Island basalts also have high $^{87}Sr/^{86}Sr$ ratios (~0.7039), attributed to a mantle source contaminated with radiogenic Sr derived from subducted lithosphere [*Weaver et al.*, 1979].

Within-Plate Magmatism

The numerous alkaline volcanic outcrops comprise a sodic series of (alkali) basalt, hawaiite, mugearite, and trachyte (using the classification of *Le Bas et al.* [1986] [cf. *Smellie*, 1987]). However, most of the analyzed rocks are *ne*- and *hy*-normative basalts and hawaiites, and only the JRIVG contains the full range of compositions; trachytes occur only as segregation veins in JRIVG intrusions [*Nelson*, 1975]. Small spinel-lherzolite nodules occur in sparse numbers at two localities in the JRIVG and Seal Nunataks.

In general terms, the lavas contain high total alkali and incompatible element abundances (Figures D.IV and D.VI) and have high Nb/Zr and low Ba/La and La/Nb ratios characteristic of nonorogenic alkaline magmas [*Smellie*, 1987]. The lavas also define a trend from slightly *hy*-normative to *ne*-normative compositions, possibly as a result of moderate- to high-pressure cotectics (Figure D.V) [cf. *Thompson*, 1982]. Basic rocks from the JRIVG and Seal Nunataks have low $^{87}Sr/^{86}Sr$ ratios (0.7028–0.7035) which are typical of within-plate basalts but are generally lower than for the Mesozoic–early Tertiary volcanic arcs of the region [*Pankhurst*, 1982*b*; *Hamer*, 1983; *Smellie et al.*, 1984]. All the magmas are believed to have been generated by small degrees of partial melting (generally <3% and possibly <1%) of a garnet-bearing mantle source [*Weaver et al.*, 1979; *Pankhurst*, 1982*b*; *Smellie*, 1987].

Copyright American Geophysical Union

D.1. BRIDGEMAN ISLAND

Type of volcano: Stratovolcano remnant.

Location: Bransfield Strait (62°03′S, 56°45′W).

Height above sea level: 0–240 m.

Evidence of Holocene activity: Numerous records of fumarolic activity between 1821 and 1880.

Author of report: J.L. Smellie.

Date of report: June 1986.

Form and Structure

Bridgeman Island, measuring 900 m by 600 m and up to 240 m high, is a remnant of a much larger volcanic edifice, eroded and now largely submerged (Figures D.1.1 and D.1.2 and Table D.II). The outcrop can be divided into an upper series of thick (25–30 m) lavas and interbedded pyroclastic rocks mantling an older series of thinner (1–7 m) lavas and pyroclastic rocks. The older series includes, at the north end of the island, structureless agglomerates which probably occupy the neck of a small scoria cone. The younger volcanic rocks were deposited on a very irregular surface with marked unconformity. Coarse pyroclastic rocks infilled surface irregularities to some extent before the extrusion of the younger lavas. An andesite dike intrudes the older neck agglomerate on its west side.

Petrologic Characteristics

The lavas and pyroclastic rocks are entirely formed of high-alumina basaltic andesite generated during the initial stages of back-arc spreading. They display several unusual

Fig. D.1.1. Geologic sketch map of Bridgeman Island (based on work by *González-Ferrán and Katsui* [1970]).

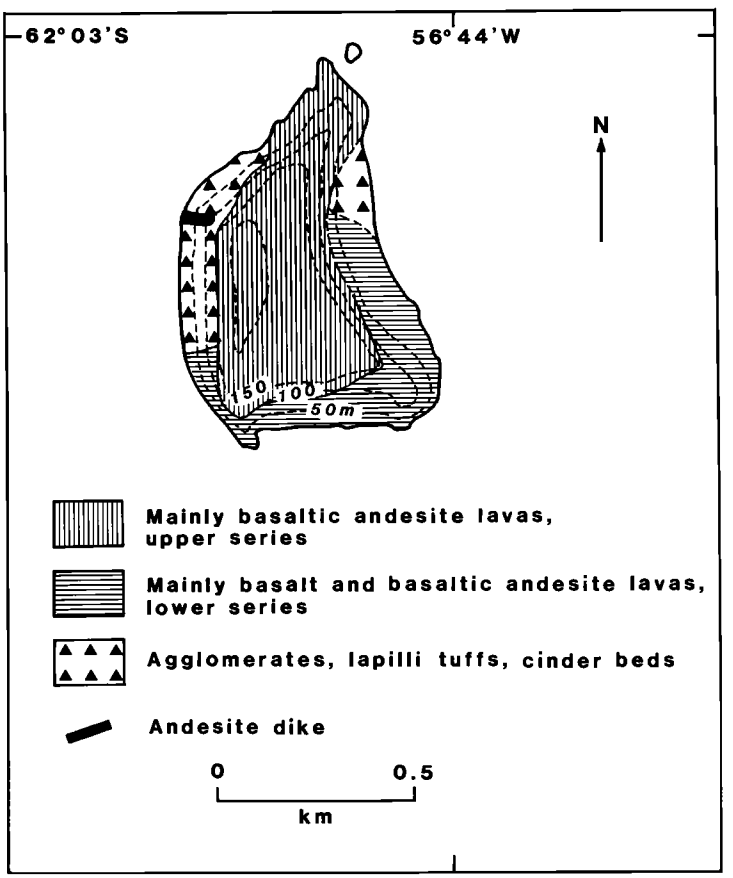

Copyright American Geophysical Union

TABLE D.1.1. Representative Chemical Analyses and CIPW Norms of Volcanic Rocks From Bridgeman Island

	1	2	3	4	5
SiO_2	52.88	53.04	53.96	54.06	54.72
TiO_2	0.64	0.58	0.64	0.75	0.60
Al_2O_3	17.68	18.26	18.17	19.04	18.83
Fe_2O_3*	7.43	7.39	7.38	7.51	6.87
MnO	0.13	0.13	0.13	0.13	0.13
MgO	6.14	5.94	5.10	4.39	5.04
CaO	10.30	10.37	9.50	9.33	9.85
Na_2O	3.54	3.11	3.61	3.86	3.49
K_2O	0.47	0.53	0.67	0.57	0.57
P_2O_5	0.06	0.06	0.07	0.06	0.07
Total	99.27	99.41	99.23	99.70	100.17
Q	0.2	2.1	2.5	2.4	3.7
or	2.8	3.2	4.0	3.4	3.4
ab	30.3	26.6	30.9	32.9	29.6
an	31.3	34.7	31.8	33.2	34.1
di	16.3	13.8	12.7	10.8	11.8
hy	15.3	16.0	14.3	13.3	13.9
mt	2.3	2.3	2.3	2.3	2.1
il	1.2	1.1	1.2	1.4	1.1
ap	0.1	0.1	0.2	0.1	0.2
Ba	70	86	101	84	80
Ce	10	8	8	9	8
Cr	130	87	59	40	67
Ga	19	19	20	22	21
La	2	4	3	2	3
Nb	1	1	1	1	1
Ni	40	28	30	20	22
Pb	5	5	6	7	4
Rb	11	12	18	14	11
Sr	332	311	283	346	319
Th	2	1	4	1	1
Y	10	11	13	11	9
Zn	62	62	67	65	64
Zr	58	69	86	76	76

All samples analyzed by XRF [from *Weaver et al.*, 1979].
*Total Fe expressed as Fe_2O_3.
1. P. 640.1b. Basaltic andesite.
2. P. 642.4. Basaltic andesite.
3. P.646.1. Basaltic andesite.
4. P.640.3a. Basaltic andesite.
5. P.642.2c. Basaltic andesite.

Copyright American Geophysical Union

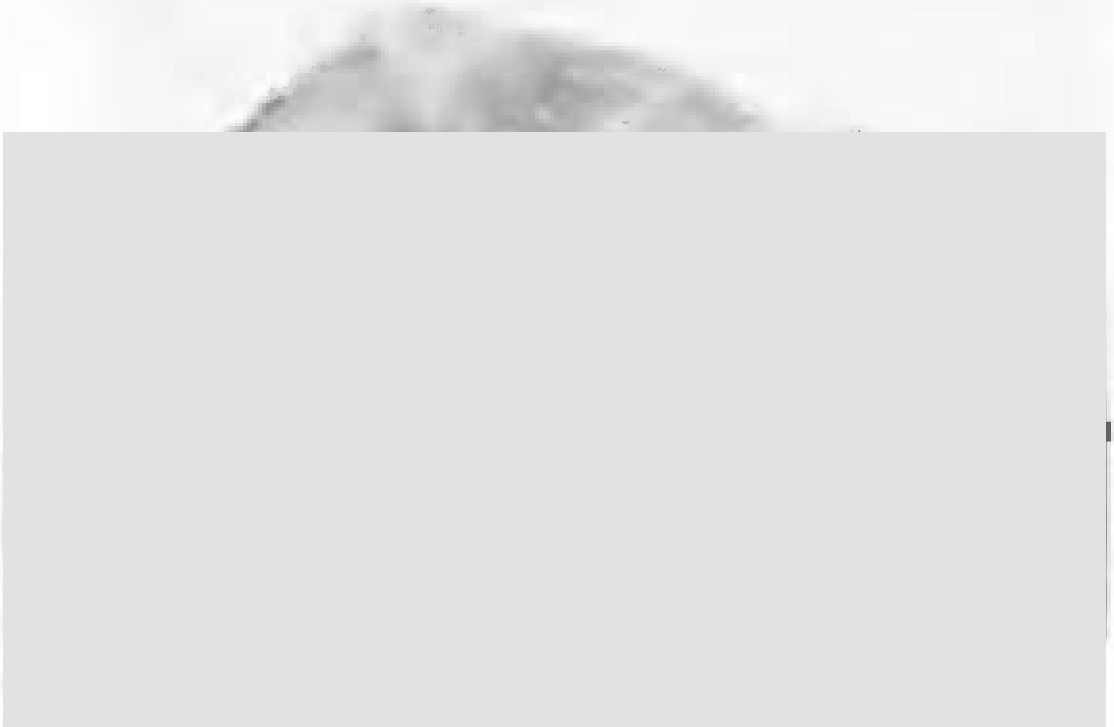

Copyright American Geophysical Union

D.2. DECEPTION ISLAND

Type of volcano: Island caldera.

Location: Bransfield Strait, at the southwestern end of the South Shetland Islands (63°00′S, 60°40′W).

Height above sea level: 0–542 m (Mount Pond).

Evidence of Holocene activity: Eruptions in 1967, 1969, and 1970. Probable eruptions in 1842 and during the period 1912–1917.

Author of report: P.E. Baker.

Dates of report: 1985 (updated by J.L. Smellie, June 1986).

Form and Structure

Deception Island is a horseshoe-shaped island 14 km north-south and 13 km east-west, with permanent glaciers along the Mount Pond ridge in the east and also in the south along the Mount Kirkwood ridge (Figure D.2.1). An almost complete ring of hills encircles the sunken interior of Port Foster (Figure D.2.2), which has a maximum depth of about 190 m below sea level. Access from the open sea into Port Foster is through Neptunes Bellows, a narrow channel cut through the caldera wall. The early Deception Island volcano was built of yellow palagonite tuffs and agglomerates with interspersed lava flows and red scoria horizons. Poorly understood deposits, mainly preserved at two localities, may have formed from pyroclastic flows which were possibly associated with caldera collapse;

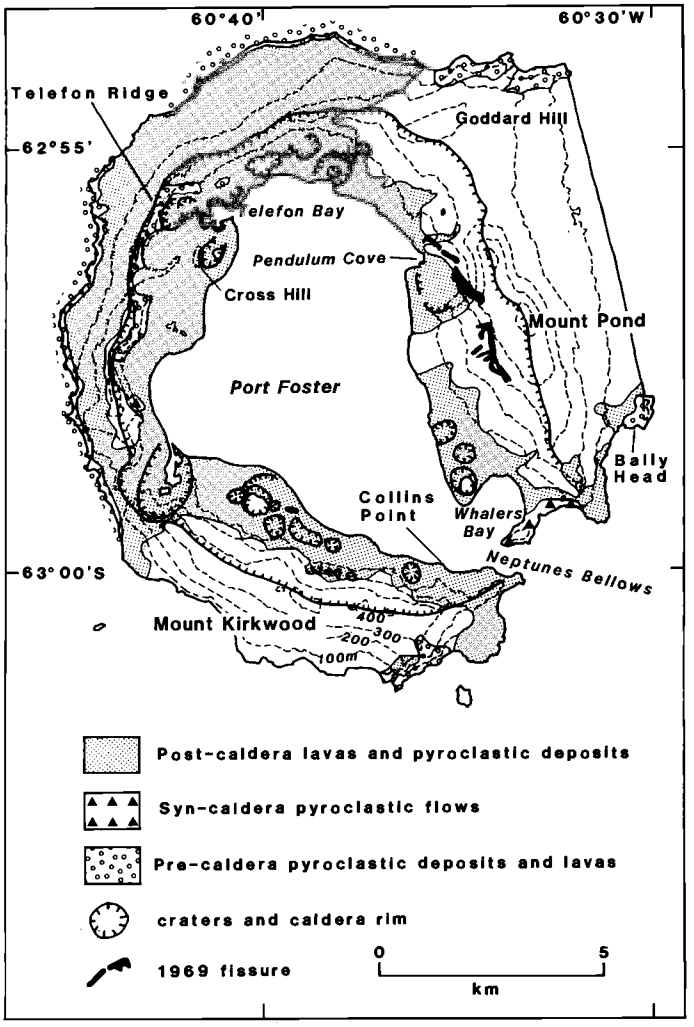

Fig. D.2.1. Geologic sketch map of Deception Island (simplified after *Baker et al.* [1975]).

Copyright American Geophysical Union

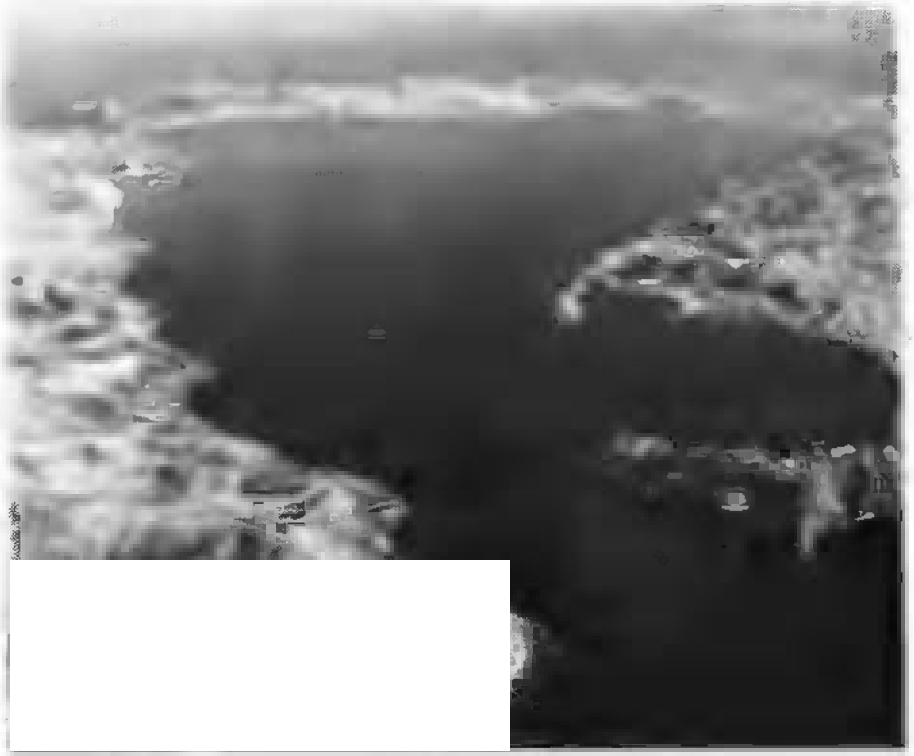

Copyright American Geophysical Union

TABLE D.2.1. Representative Chemical Analyses and CIPW Norms of Volcanic Rocks From Deception Island

	1	2	3	4	5
SiO_2	51.7	51.7	52.46	53.2	54.2
TiO_2	1.65	2.34	2.44	1.81	2.34
Al_2O_3	17.3	15.6	15.12	17.1	15.3
Fe_2O_3*	1.95	2.04	12.16*	2.08	4.20
FeO	6.72	8.87	--	7.05	6.39
MnO	0.15	0.19	0.21	0.17	0.18
MgO	5.96	4.86	4.08	5.25	3.86
CaO	10.2	8.75	8.37	9.32	7.12
Na_2O	4.06	3.74	5.09	3.41	4.27
K_2O	0.44	0.51	0.48	0.51	0.77
P_2O_5	0.24	0.37	0.33	0.29	0.37
H_2O	0.21	0.12	--	0.04	0.08
Total	100.58	99.09	100.74	100.23	99.08
Q	--	1.60	1.9	3.67	6.53
or	2.60	3.01	2.8	3.01	4.55
ab	34.35	31.64	43.0	28.85	36.97
an	27.69	24.28	17.0	29.85	19.86
di	17.34	13.79	17.7	11.83	10.56
hy	4.37	16.38	3.6	15.85	9.24
ol	7.50	--	--	--	--
mt	2.83	2.96	3.8	3.02	6.09
il	3.13	4.44	4.6	3.44	4.44
ap	0.57	0.87	0.8	0.68	0.87
Ba	100	125	89	175	160
Ce	--	--	31	--	--
Co	18	28	--	40	40
Cr	--	--	20	--	40
Ga	--	--	24	--	--
La	--	--	12	--	--
Li	12	13	--	--	16
Nb	--	--	6	--	--
Ni	--	--	9	--	15
Pb	--	--	5	--	--
Rb	5	7	5.6	6	8
Sr	415	350	357	360	365
Th	--	--	1	--	--
V	165	240	--	140	270
Y	26	30	28	27	37
Zn	--	--	87	--	--
Zr	150	195	214	165	225

All samples analyzed by XRF; Fe^{2+}/Fe^{3+} ratios in samples 1, 2, 4–7, 9, and 10 determined by wet chemistry. Dashes, not determined (elements) or not present (norms).

*Total Fe expressed as Fe_2O_3.

1. B.432.1. Almost aphyric basalt, Neptunes Bellows [*Baker et al.*, 1975].
2. B.403.1. Almost aphyric basalt, Baily Head (Rancho Point) [*Baker et al.*, 1975].
3. B.119.1. Basalt (mugearite) [*Weaver et al.*, 1979].
4. B.416.1. Almost aphyric basalt, Mount Kirkwood [*Baker et al.*, 1975].
5. B.311.1. Scoriaceous basaltic andesite (hawaiite), Telefon Ridge [*Baker et al.*, 1975].

Copyright American Geophysical Union

TABLE D.2.1. (continued)

	6	7	8	9	10	11
SiO_2	58.0	61.0	61.91	62.6	67.5	70.10
TiO_2	1.91	1.26	1.26	1.14	0.72	0.50
Al_2O_3	15.9	15.7	15.32	15.6	14.8	14.31
Fe_2O_3*	2.38	1.19	7.25*	0.31	1.39	4.32*
FeO	6.00	5.50	--	6.15	3.16	--
MnO	0.18	0.17	0.21	0.17	0.15	0.13
MgO	2.72	1.71	1.35	1.45	0.70	0.90
CaO	5.73	4.11	3.57	3.59	1.98	3.46
Na_2O	5.46	6.23	6.70	6.66	6.96	4.88
K_2O	0.98	1.23	1.21	1.44	1.80	0.65
P_2O_5	0.37	0.42	0.41	0.37	0.16	0.08
H_2O	0.37	0.18	--	0.29	0.27	--
Total	100.00	98.70	99.19	99.77	99.59	99.33
Q	6.56	7.56	8.8	6.73	14.67	29.6
or	5.85	7.27	7.2	8.51	10.64	3.9
ab	46.20	52.71	57.4	56.35	58.89	41.7
an	15.96	11.25	8.3	8.43	3.83	15.4
di	8.12	5.58	6.0	5.95	4.14	1.2
hy	8.97	8.63	6.0	10.04	3.38	5.4
ol	--	--	--	--	--	--
mt	3.45	1.73	2.8	0.45	2.02	1.7
il	3.62	2.47	2.4	2.17	1.37	1.0
ap	0.90	1.04	1.0	0.87	0.40	0.2
Ba	--	250	199	340	340	68
Ce	--	--	61	--	--	22
Co	--	30	--	9	5	--
Cr	--	25	9	--	--	20
Ga	--	--	24	--	--	6
La	--	--	25	--	--	10
Li	--	30	--	44	48	--
Nb	--	--	13	--	--	3
Ni	--	10	3	--	--	6
Pb	--	--	12	--	--	9
Rb	13	17	20	21	29	14
Sr	320	270	255	240	135	117
Th	--	--	4	--	--	2
V	--	55	--	40	--	--
Y	40	46	66	50	57	36
Zn	--	--	123	--	--	101
Zr	305	370	457	410	535	178

6. B.707.1. Andesitic (benmoreite) bomb, 1967 land center, Telefon Bay [*Baker et al.*, 1975].
7. B.276.1. Andesitic (benmoreite) bomb, 1967 island, Telefon Bay [*Baker et al.*, 1975].
8. B.184.1. Andesite (benmoreite) [*Weaver et al.*, 1979].
9. B.431.1. Dacite (trachyte), Collins Point [*Baker et al.*, 1975].
10. B.429.2. Porphyritic dacite (trachyte), Cross Hill (Laguna Hill) [*Baker et al.*, 1975].
11. B.317.1. Aphyric rhyodacite (silica-rich dacite) [*Weaver et al.*, 1979].

Copyright American Geophysical Union

Copyright American Geophysical Union

Smellie, 1983; *Smellie,* 1983], Deception Island has almost certainly developed entirely within the Quaternary; this, however, has not been substantiated by radiometric dates. *Wilkes* [1845] reported that in 1842 "The whole south side of Deception Island appeared as if on fire." This event is believed to have occurred at the series of craters below Mount Kirkwood. *Orheim* [1972*a*] suggested that there were a series of pyroclastic eruptions during the period 1912–1917, based on the measurement of seasonal windblown dust layers in the ice. In December 1967, activity from three new craters produced a small island in Telefon Bay, and at the same time there was an eruption from a crater near the shore on the north-northeast side of Port Foster (frontispiece). In February 1969 a series of fissures opened in the ice on the west facing slopes of Mount Pond, and pyroclastic emissions occurred from a number of craters along the fracture. Meltwater produced in this activity flooded down into Port Foster, and ice-block lahars developed in places. The Chilean scientific station at Pendulum Cove was totally destroyed, and the British station at Whalers Bay was severely damaged. In August 1970 there was further activity along the northern edge of Telefon Bay, and a chain of new craters developed between Cross (Laguna) Hill and Goddard (Bynon) Hill (Figure D.2.4). A new strip of land was produced, and the 1967 "island" was incorporated within it.

An eruption on July 23, 1987, has been attributed to Deception Island [*Newhall and Dzurisin,* 1988, p. 1015], but there was no sign of a new vent on the island in December 1987, and areas of heated ground monitored in February–March 1987 showed no evidence for a thermal perturbation when reexamined in December 1987. The satellite imagery showing the July 23 "event" is also consistent with interpretation as a cloud effect. Moreover, the locus of the cloud or plume is situated about 220 km east-northeast of Deception Island, and it is therefore unlikely that an eruption occurred on Deception Island during 1987 (Smellie, unpublished data, 1988) (note added in proof, May 1989).

Extent of Knowledge

Deception Island has been extensively investigated (see bibliography).

Bibliography

Adie, 1957
Baker, 1969*a, b*, 1972
Baker and McReath, 1971*a, b*
Baker et al., 1969, 1975, 1977
Brecher, 1975
Brecher et al., 1976
Casertano, 1964
Clapperton, 1969
Corte and Somoza, 1957
Elderfield, 1972*a, b*
Faure et al., 1971
González-Ferrán and Katsui, 1970
González-Ferrán et al., 1971*a, b*
Gourdon, 1914
Hawkes, 1961*b*
Holtedahl, 1929
Kendal, 1831
Lorca, 1976
Newhall and Dzurisin, 1988
Olsacher, 1956
Orheim, 1972*a, b*
Roobol, 1973, 1979, 1982
Sandoval and Silva, 1975
Shultz, 1972*a*, 1976
Tarney et al., 1977
Tyrrell, 1945
Valenzuela et al., 1968, 1970
Viramonte et al., 1976
Weaver et al., 1979
Wilkes, 1845

Copyright American Geophysical Union

D.3. PENGUIN ISLAND

Type of volcano: Small stratovolcano.

Location: Penguin Island (62°06′S, 57°56′W) and southwest extremity of Turret Point, King George Island (62°05′S, 57°57′W).

Height above sea level: 0–180 m.

Evidence of Holocene activity: Marr (see *Tyrell* [1945]) reported residual heat in the principal cone, but there are no historical records of fumarolic or other volcanic activity; *González-Ferrán and Katsui* [1970] and *Birkenmajer* [1982*c*] attributed at least some of the reports of volcanic activity on nearby Bridgeman Island to Penguin Island because a fresh volcanic cone is only preserved on the latter.

Author of report: J.L. Smellie.

Date of report: June 1986.

Form and Structure

Penguin Island measures approximately 1.4 km by 1.7 km, rising to 180 m at Deacon Peak, which is the summit of a prominent, very well preserved basalt scoria cone built of reddish pyroclastic rocks alternating with thin black scoriaceous lavas (Figure D.3.1). The cone has a summit crater about 350 m across and 75 m deep, within which is a small central cone composed of red-brown and black scoriaceous basalt lava (Figure D.3.2). Also within the main crater is a small plug of gray basalt, and a few radial dikes are exposed in the western scalloped face of the

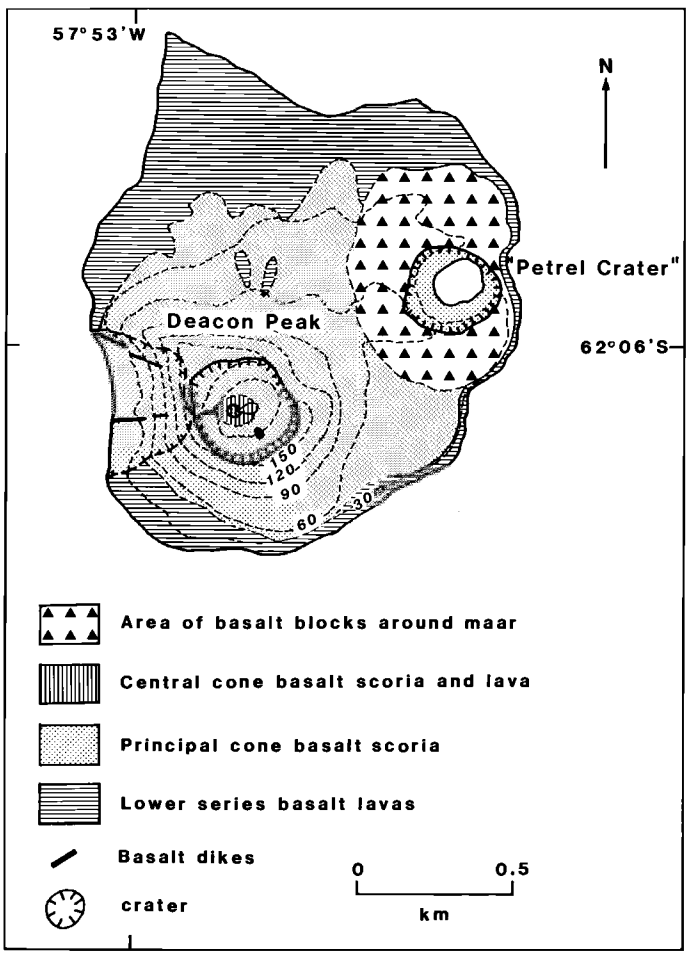

Fig. D.3.1. Geologic sketch map of Penguin Island (based on work by *González-Ferrán and Katsui* [1970]).

Copyright American Geophysical Union

Copyright American Geophysical Union

TABLE D.3.1. Representative Chemical Analyses and CIPW Norms of Volcanic Rocks From Penguin Island

	1	2	3	4	5
SiO_2	49.02	49.25	49.28	49.30	49.57
TiO_2	1.08	1.22	1.26	1.22	1.19
Al_2O_3	15.81	15.34	17.23	16.58	16.64
Fe_2O_3*	9.95	10.39	9.81	9.62	9.54
MnO	0.18	0.18	0.18	0.18	0.17
MgO	8.95	8.84	6.78	7.74	7.79
CaO	10.08	10.46	9.71	10.03	10.15
Na_2O	3.95	3.70	4.30	4.13	4.18
K_2O	0.48	0.47	0.60	0.58	0.60
P_2O_5	0.28	0.26	0.30	0.32	0.42
Total	99.78	100.11	99.45	99.70	100.25
or	2.9	2.8	3.6	3.5	3.6
ab	27.2	27.4	30.0	28.6	28.7
an	24.2	24.0	26.2	25.2	24.9
ne	3.5	2.2	3.7	3.6	3.7
di	19.8	21.5	16.9	18.7	18.6
ol	16.5	15.8	13.3	14.3	14.2
mt	3.1	3.2	3.1	3.0	3.0
il	2.1	2.3	2.4	2.3	2.3
ap	0.7	0.6	0.7	0.8	1.0
Ba	148	132	173	146	157
Ce	20	19	23	22	24
Cr	494	447	192	307	306
Ga	21	22	26	25	29
La	10	7	12	9	10
Nb	2	4	4	4	4
Ni	159	137	78	107	107
Pb	7	6	10	7	6
Rb	5	6	7	5	6
Sr	534	536	657	612	615
Th	1	1	1	1	1
Y	12	10	10	11	13
Zn	69	78	77	73	76
Zr	80	80	92	85	89

All samples analyzed by XRF [from *Weaver et al.*, 1979].
*Total Fe expressed as Fe_2O_3.
1. P.721.3. Alkali basalt.
2. P.802.1. Alkali basalt.
3. P.810.4. Alkali basalt/hawaiite.
4. P.808.1. Alkali basalt.
5. P.807.2. Alkali basalt.

Bibliography

Birkenmajer, 1980, 1982*c*
Ferguson, 1921
González-Ferrán and Katsui, 1970
Hawkes. 1961*a*
Smellie, 1987
Tyrrell, 1945
Weaver et al., 1979

Copyright American Geophysical Union

D.4. MELVILLE PEAK, KING GEORGE ISLAND

Type of volcano: Eroded stratocone.
Location: Melville Peak, King George Island (62°01′S, 57°40′W).
Height above sea level: 0–549 m.
Evidence of Holocene activity: None.
Author of report: J.L. Smellie.
Date of report: June 1986.

Form and Structure

The base of the stratocone rests unconformably on a sequence of fossiliferous (?lower Miocene) tuffaceous glaciomarine strata cut by andesite and basalt dikes (Figure D.4.1); the dikes are unrelated to the Melville Peak volcano and belong to an earlier phase of volcanicity. Two phases of stratocone formation have been recognized. The early, principal phase comprises interbedded basalt lavas and pyroclastic rocks, in beds 5–20 m thick, intruded by a central plug, and a basalt dike. Quaquaversal bedding orientations indicate an original edifice centered on Melville Peak with a diameter of about 3 km. The second phase consists of basaltic agglomerate and lava filling a minor parasitic vent on the east side of Melville Peak, which it intrudes and partially caps.

Petrologic Characteristics

Agglomerates of the first phase are yellow, cross-stratified, well-cemented rocks which contain gray, black, and red basalt lapilli and blocks and country rock fragments set in a yellowish matrix. They can be traced laterally into finer agglomerates, then yellow tuffaceous sandstones, and they alternate with stratified, gray lapilli tuffs. The lavas, plug, and dike are gray and black, with well-developed

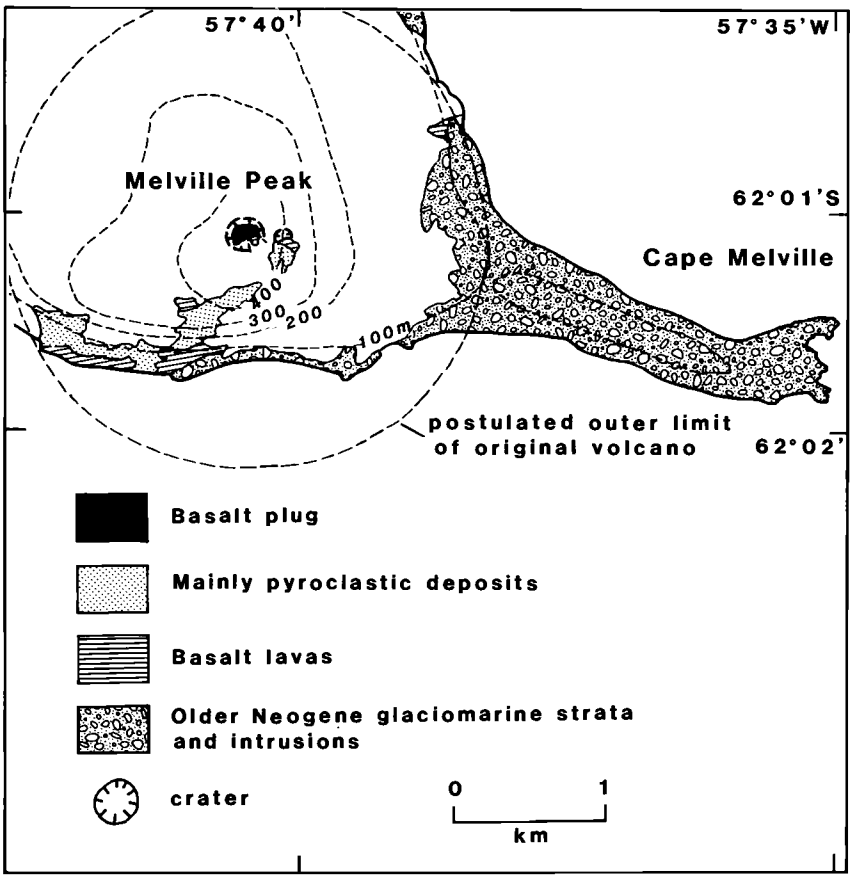

Fig. D.4.1. Geologic sketch map of the Melville Peak area, King George Island (based on work by *Birkenmajer* [1982*a*]).

Copyright American Geophysical Union

TABLE D.4.1. Chemical Analyses and CIPW Norms of Two Lavas From Melville Peak

	1	2
SiO_2	52.00	52.03
TiO_2	0.91	0.88
Al_2O_3	17.14	16.85
Fe_2O_3	1.59	1.43
FeO	5.68	5.71
MnO	0.12	0.14
MgO	7.10	7.30
CaO	10.75	11.22
Na_2O	3.00	2.87
K_2O	0.91	0.89
P_2O_5	0.12	0.13
LOI	0.16	0.00
Total	100.14	100.10
or	5.43	5.31
ab	25.54	24.40
an	30.79	30.61
di	17.79	19.77
hy	13.34	12.99
ol	2.74	2.83
mt	2.32	2.09
il	1.74	1.68
ap	0.30	0.30
Ba	222	269
Ce	22	33
Cr	115	172
Ga	18	17
La	17	16
Nb	2	3
Ni	41	37
Pb	9	8
Rb	16	16
Sr	566	599
Th	3	4
Y	21	20
Zn	56	47
Zr	104	103

Both samples analyzed by XRF; Fe^{2+}/Fe^{3+} ratios determined by wet chemistry. LOI, loss on ignition.

1. G.31.1. Basalt lava (collected by D.J. Jardine; analyst, J.L. Smellie).
2. G.32.1. Basalt lava or plug (collected by D.J. Jardine; analyst, J.L. Smellie).

columnar jointing and prominent phenocrysts of diopsidic augite and olivine. Agglomerate of the second phase is red and is dominated by volcanic bombs. It is intruded by red and brown scoriaceous basalt lava. Only two samples have been analyzed (Smellie, unpublished data, 1986) (Table D.4.1). They are both relatively primitive high-alumina, calc-alkaline basalts very similar to upper Cenozoic basalts from Kraków Peninsula (see IVD D.5).

Chronologic Data

None, but a maximum age is provided by two andesite dikes cutting the glaciomarine sequence at Cape Melville. These are believed to be older than and unrelated to the Melville Peak volcano and have yielded K-Ar dates of about 20 Ma, and an underlying (?) lava (interpreted by *Smellie et al.* [1984] as a boss coeval with the andesite dikes) gave a poorly constrained date of about 17 Ma [*Birkenmajer et al.*, 1985].

Extent of Knowledge

Melville Peak was probably sighted frequently during the numerous sealing expeditions which visited the South Shetland Islands between 1820 and 1822; it was certainly seen by Captain Sherratt and the crew of the *Lady Trowbridge,* who were wrecked off Cape Melville in 1820 and subsequently rescued [*Roberts*, 1957]. Jardine briefly visited Melville Peak in 1949. His observations simply note "little bare rock, most of which . . . is inaccessible," and he collected a single basalt specimen (Jardine, British Antarctic Survey unpublished report, 1950; see also *Hawkes* [1961*a*]). Although *Barton* [1965] mapped the plug at Melville Peak during a visit to Cape Melville in 1960, he does not seem to have examined the peak at close quarters, whereas detailed examination of the exposures was carried out by Birkenmajer during a helicopter-supported visit in 1981 [*Birkenmajer,* 1982*a*].

Bibliography

Barton, 1965
Birkenmajer, 1982*a*, 1984
Birkenmajer et al., 1985
Hawkes, 1961*a*
Roberts, 1957
Smellie et al., 1984

Copyright American Geophysical Union

D.5. KRAKÓW PENINSULA, KING GEORGE ISLAND

Type of volcano: Probably several eroded stratocones.

Location: Numerous localities around the southern and eastern periphery of Kraków Peninsula (62°08′S, 58°15′W), King George Island; also Ternyck Needle (62°05′S, 58°16′W).

Height above sea level: 0 to ~250 m.

Evidence of Holocene activity: None.

Author of report: J.L. Smellie.

Date of report: June 1986.

Form and Structure

Two broad rock groups can be distinguished (Figure D.5.1). A number of formations, separated by angular unconformities, form most of the coastal exposures in the center and west. They consist of gray porphyritic lavas interbedded with agglomerates, lapillistones, tuffs, and lahar-like deposits variably colored red, yellow, green, brown, and black and containing clasts up to 2.5 m across. Most of the lavas are massive, but a few show well-developed columnar jointing. Toward the center of the sequence are distinctly stratified lapilli tuffs and breccias full of vesicular bombs, with interbedded agglomerate and tuffaceous sandstone arranged in cross-stratified, wedge-shaped units; these strata are up to 215 m thick in the west but thin rapidly eastward, and they are interpreted as a fossil cinder cone. The sequence is capped locally by indurated dark green tillites, which infill fossil valleys up to 100 m deep.

The second rock group is best developed in the eastern outcrops where the basal strata mainly comprise a thick (65 m) sequence of fossiliferous (upper Oligocene?) ground-moraine and glaciomarine tillites, and glaciofluvial (esker?) deposits. The glacigenic beds depositionally overlie massive hyaloclastite at Low Head, and the entire sequence rests unconformably on a strongly weathered surface cut across Eocene andesite lavas interbedded with coaly plant-bearing shales (Figure D.5.2). The tillites are

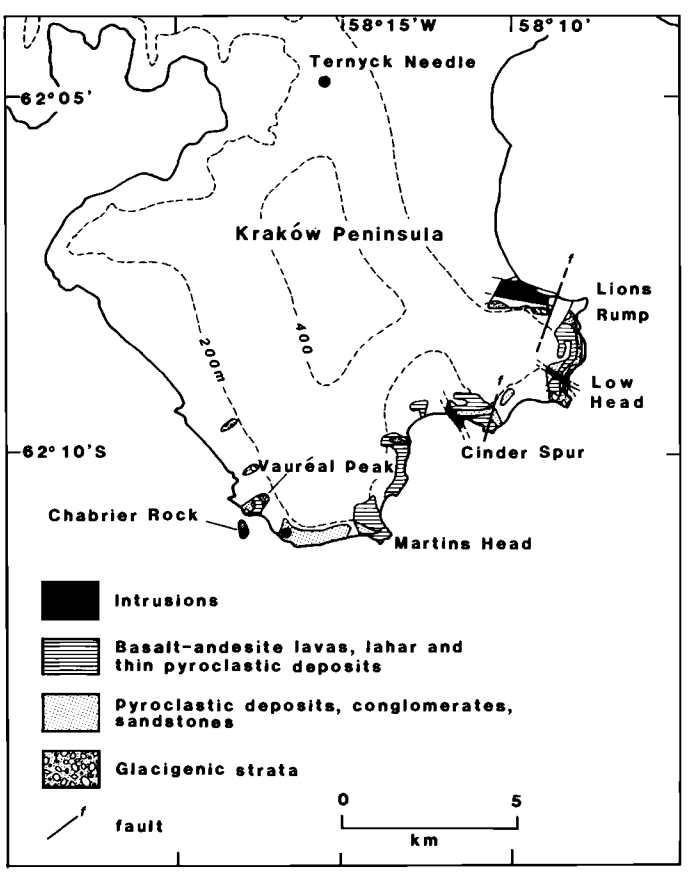

Fig. D.5.1. Geologic sketch map of Kraków Peninsula, King George Island (based on work by *Birkenmajer* [1982*b*] and *Smellie et al.* [1984]).

Copyright American Geophysical Union

Copyright American Geophysical Union

TABLE D.5.1. Representative Chemical Analyses and CIPW Norms of Volcanic Rocks From Kraków Peninsula, King George Island

	Cinder Spur				Martins Head			Ternyck Needle
	1	2	3	4	5	6	7	8
SiO_2	50.51	52.07	54.12	58.88	51.52	52.02	57.18	55.40
TiO_2	0.79	0.73	0.85	0.52	0.75	0.91	0.59	0.70
Al_2O_3	18.35	18.19	18.02	16.85	17.70	18.51	18.24	18.70
Fe_2O_3	1.85	1.68	1.58	1.77	2.00	1.82	1.71	2.15
FeO	6.16	5.61	5.27	4.43	6.65	6.06	4.28	5.39
MnO	0.18	0.19	0.16	0.24	0.19	0.18	0.17	0.13
MgO	5.20	5.76	5.38	3.97	5.18	5.62	4.20	4.90
CaO	10.63	9.42	7.84	6.15	9.53	9.45	7.06	8.92
Na_2O	3.45	3.54	3.70	3.90	3.71	3.82	4.36	3.82
K_2O	0.71	0.77	1.02	0.75	0.80	0.82	0.94	1.44
P_2O_5	0.18	0.20	0.14	0.33	0.22	0.19	0.26	0.14
Total	98.01	98.16	98.08	97.79	98.25	99.40	98.99	101.69
Q	--	--	2.78	12.99	--	--	6.21	1.36
or	4.28	4.63	6.14	4.53	4.81	4.87	5.61	8.37
ab	29.76	30.49	31.89	33.71	31.93	32.49	37.23	31.80
an	33.13	32.03	30.10	26.83	29.78	31.10	27.68	29.15
di	16.04	11.69	7.19	1.92	13.97	12.20	5.04	11.17
hy	5.93	15.74	17.56	15.56	10.37	8.70	13.95	13.43
ol	6.14	0.99	--	--	4.20	5.77	--	--
mt	2.74	2.48	2.33	2.62	2.95	2.65	2.50	3.07
cm	--	0.02	--	--	--	--	--	--
il	1.53	1.41	1.64	1.01	1.45	1.74	1.13	1.31
ap	0.43	0.48	0.34	0.80	0.53	0.45	0.62	0.33
Ba	214	232	325	312	234	232	408	258
Ce	20	16	19	31	25	21	31	27
Cr	35	80	28	10	43	33	20	60
Ga	25	24	26	25	24	23	25	26
La	9	7	8	14	12	11	13	12
Nb	1	--	--	3	3	--	1	3
Ni	26	48	16	3	25	18	9	19
Pb	8	8	6	10	9	5	7	--
Rb	11	13	11	14	14	12	16	30
Sr	449	439	640	473	467	480	535	650
Th	2	4	3	--	2	3	--	--
Y	23	21	15	27	20	20	14	14
Zr	100	118	113	165	114	106	140	114

Analyses 3, 5, 7, and 8 from *Smellie et al.* [1984]; other samples analyzed by A.D. Saunders and S.D. Weaver. All samples analyzed by XRF; Fe^{2+}/Fe^{3+} ratios assumed (0.3 in samples 1–3, 5, and 6; 0.4 in samples 4, 7, and 8). Dashes, not present (norms) or not detected (elements).

1–4. Basalt (1), basaltic andesite (2,3), and andesite (4) lavas.

5–7. Basaltic andesite (5,6) and andesite (7) lavas.

8. G.13.1. Basaltic andesite plug.

Copyright American Geophysical Union

Extent of Knowledge

The first geological observations were made by Marr in 1937 [see *Tyrrell,* 1945]. Although purporting to refer to Martins Head, it is clear from the sketches and description that he was referring to the coastline backing Lions Rump. Coastal exposures between Lions Rump and Cinder Spur were visited by Jardine from sea ice in 1949, and the Lions Rump exposures by Hobbs in 1959 (Jardine, British Antarctic Survey (BAS) unpublished report, 1950; see also *Hawkes* [1961*a*]) (Hobbs, BAS unpublished field notes, 1959). Traveling overland, Barton visited the area between Vauréal Peak and Lions Rump in 1960 [*Barton,* 1965]. The area was visited again and mapped during six days in 1975 by a BAS party together with S.D. Weaver and A.D. Saunders of the University of Birmingham, England [*Smellie et al.,* 1984]. The most detailed geological studies so far have been undertaken by several Polish geologists between 1978 and 1981 [see *Birkenmajer,* 1982*b*].

Bibliography

Barton, 1965
Birkenmajer, 1982*b*
Birkenmajer et al., 1986
Hawkes, 1961*a*
Smellie et al., 1984
Tyrrell, 1945

Copyright American Geophysical Union

D.6. NORTHERN LIVINGSTON AND GREENWICH ISLANDS

Type of volcano: Several small, highly eroded tuff-cone remnants and plugs.

Location: Livingston Island: Edinburgh Hill (62°33′S, 60°01′W), Inott Point (62°31′S, 60°00′W), unnamed nunatak 1.6 km north of Sharp Peak (62°31′S, 60°04′W), Gleaner Heights (62°34′S, 60°54′W). Greenwich Island: Mount Plymouth (62°28′S, 59°49′W).

Height above sea level: 0–530 m.

Evidence of Holocene activity: None.

Author of report: J.L. Smellie.

Date of report: June 1986.

Form and Structure

Very little is known of these outcrops (Figure D.6.1). Edinburgh Hill and Mount Plymouth are prominent basalt plugs with well-developed columnar jointing (Figure D.6.2). That at Mount Plymouth intrudes thin-bedded glassy volcanic breccias, whereas Edinburgh Hill occurs in isolation; the early report of 15 m of tuff forming a cap to the latter has not been confirmed, and the columnar structure described closely resembles colonnade and entablature jointing which, together with the presence of reddish "flow lenses," is also suggestive of a flow remnant. Inott Point and the unnamed nunatak near Sharp Peak are formed of nonstratified, yellow-brown glassy volcanic breccia. A single fresh, amygdaloidal basalt lava flow forms the unnamed outcrop at Gleaner Heights.

Petrologic Characteristics

The plugs and lava are formed of fresh, gray olivine basalt with conspicuous glomeroporphyritic phenocrysts of unaltered olivine and diopsidic augite; the augite

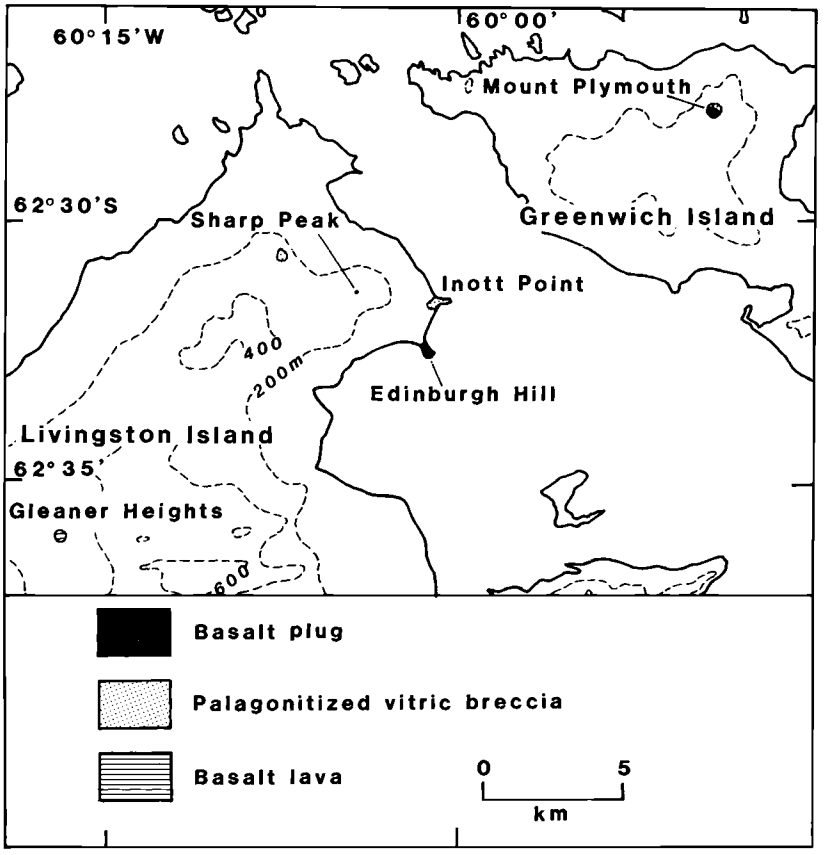

Fig. D.6.1. Geologic sketch map of northern Livingston and Greenwich islands (based on work by *Hobbs* [1968] and *Smellie et al.* [1984]).

Copyright American Geophysical Union

Copyright American Geophysical Union

TABLE D.6.1. Representative Chemical Analyses and CIPW Norms of Volcanic Rocks From Northern Livingston and Greenwich Islands

	1	2	3
SiO_2	48.2	48.4	50.3
TiO_2	1.31	1.26	1.08
Al_2O_3	15.50	17.10	18.10
Fe_2O_3	2.81	2.74	2.55
FeO	7.02	6.84	6.38
MnO	0.16	0.16	0.15
MgO	10.2	8.2	5.0
CaO	10.79	11.45	11.27
Na_2O	3.62	3.96	4.15
K_2O	0.49	0.42	0.56
P_2O_5	0.19	0.18	0.17
Total	100.29	100.71	99.71
or	2.88	2.46	3.32
ab	21.74	21.66	29.70
an	24.45	27.41	29.17
ne	4.71	6.26	2.98
di	22.21	22.49	21.19
ol	16.71	12.87	7.46
mt	4.05	3.94	3.71
cm	0.16	0.10	0.02
il	2.47	2.37	2.06
ap	0.45	0.42	0.40
Ba	143	124	175
Ce	20	14	8
Cr	700	470	110
Ga	19	21	24
La	14	12	9
Nb	4	3	3
Ni	367	206	35
Rb	--	4	7
Sr	477	470	590
Y	12	14	16
Zn	68	66	76
Zr	77	58	50

All samples analyzed by XRF [from *Smellie et al.*, 1984]; Fe^{2+}/Fe^{3+} ratios taken as 0.4. Dash, not determined.

1. P.55.1. Alkali basalt, Mount Plymouth, Greenwich Island.
2. P.54.1. Alkali basalt, Mount Plymouth, Greenwich Island.
3. P.51.1. Alkali basalt, Gleaner Heights, Livingston Island.

Copyright American Geophysical Union

D.7. Brabant Island, Anvers Island, and Islands in Southern Bransfield Strait

Type of volcano: Essentially unknown; probably several stratovolcanoes.

Location: Principally Brabant Island (64°17′S, 62°20′W) and northern Anvers Island (64°35′S, 63°30′W); also several isolated occurrences in southern Bransfield Strait (Liège, Davis, Harry, Tower, and Casy islands and Lafarge Rocks).

Height above sea level: 0–2000 m.

Evidence of Holocene activity: None.

Author of report: J.L. Smellie.

Date of report: June 1986.

Form and Structure

Very little information exists for these outcrops (Figure D.7.1).

Anvers Island. About 1200 m of vertical outcrop occur on northern Anvers Island, but the sequence is virtually inaccessible (Figure D.7.2). It is formed by basaltic lithic tuffs and lavas of olivine basalt and hypersthene-augite-andesite. The rocks are essentially flat-lying except where they abut older plutonic intrusions, where the beds sweep up to rest unconformably at a high angle (30°–70°).

Brabant Island. Up to 300 m of subhorizontal, often columnar-jointed olivine basalts and andesites of the Bahía Bouquet Formation drape and rest unconformably in depressions eroded in (?) upper Tertiary terrestrial volcaniclastic sedimentary rocks. The upper part of the succession exposed at Claude Point (Figure D.7.3) contains a 10- to 40-m-thick sequence of yellowish palagonitized vitric tuffs with dispersed black lava fragments. Similar rocks at Cape Cockburn reach a thickness of 330 m. The lavas were probably erupted from a variety of centers: a (?) vent agglomerate occurs at Metchnikoff Point, and

Fig. D.7.1. Sketch map of the area around eastern Anvers Island and Brabant Island, and isolated outcrops on islands in southeastern Bransfield Strait (inset: T, Tower Island; A, Astrolabe Island; LC, Lafarge Rocks and Casy Island; B, Bransfield Island).

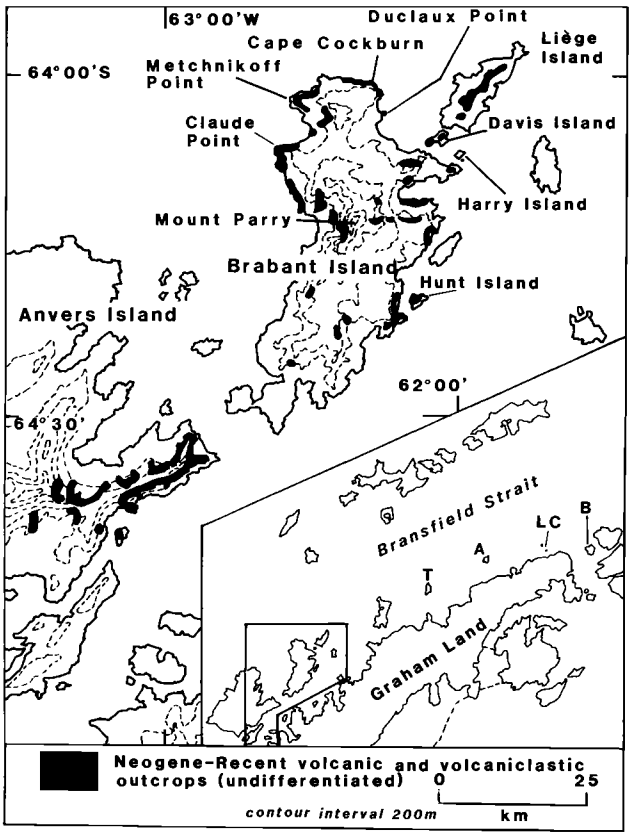

Copyright American Geophysical Union

Copyright American Geophysical Union

columnar-jointed necks have been mapped at Duclaux Point, southwestern Davis Island, and postulated at Mount Parry and the less prominent peak situated about 10 km south-southeast of Mount Parry; not all of these were confirmed during a recent study by Ringe [see *Furse*, 1986].

Island archipelago northeast of Brabant Island. Palagonite tuffs crop out on Davis Island, but the majority of the young volcanic outcrops are formed of horizontal or gently dipping, fresh olivine basalts or andesites, often columnar-jointed; not all of these outcrops have been visited, and none are dated. Numerous porphyritic olivine basalt dikes of uncertain age intruded plutonic and older volcanic rocks on Astrolabe Island.

Submarine shelf north-northwest of Anvers Island. An isolated submarine volcano was discovered in 1988 near the shelf edge, about 110 km north-northwest of Anvers Island (Larter, unpublished data, British Antarctic Survey, 1988). It has a basal diameter of 15 km and rises to a maximum height of about 200 m on the northern side of a possible summit crater. Dredged samples are of fresh olivine basalt (note added in proof, May 1989).

Petrologic Characteristics

The lavas, plugs, and dikes are mainly formed of fresh, dark gray olivine basalt with conspicuous phenocrysts of calcic plagioclase and olivine set in an intersertal to trachytic-textured groundmass of plagioclase, augite, and olivine; some lavas on Brabant Island contain exceptional amounts of magnetite (up to 30% by volume), and hematite is well developed locally. Unaltered brown volcanic glass and zeolite-filled amygdales are also present. The palagonite tuffs comprise basaltic clasts with microlites and euhedral phenocrysts of labradorite (An_{62}), clinopyroxene, and olivine in a glassy matrix; the glass is rimmed with palagonite. A fragment of granodiorite was found in coarse tuffs on Anvers Island. A preliminary geochemical study by Ringe [see *Furse*, 1986] suggested that calc-alkaline basalts and alkaline basalts are both present on Brabant Island, but there is only one published analysis (Table D.7.1).

TABLE D.7.1. Chemical Analysis and CIPW Norm of a Volcanic Rock From Brabant Island

	1
SiO_2	48.25
TiO_2	1.65
Al_2O_3	17.04
Fe_2O_3	2.66
FeO	7.71
MnO	0.18
MgO	7.22
CaO	10.55
Na_2O	3.34
K_2O	0.39
P_2O_5	0.37
Total	99.36
or	2.30
ab	28.26
an	30.37
wo	8.27
en	5.65
fs	2.97
ol	13.73
mt	3.86
il	3.13
ap	0.81

Sample probably analyzed by wet chemistry.
1. OG.344. Olivine basalt, east coast of Brabant Island (Hunt (Pampa) Island?) [*González-Ferrán and Katsui*, 1970].

Chronologic Data

A K-Ar date of less than 1 Ma has been obtained by Ringe [see *Furse*, 1986] from northern Brabant Island, but no details are published yet.

Extent of Knowledge

Numerous sealing and scientific expeditions passed through Bransfield and Gerlache straits, but geological observations are few (summarized by *Hooper* [1962] and *Furse* [1986]). Of historical interest, Roald Amundsen spent his first stay ashore in Antarctica on Brabant Island in 1898; this was also the first recorded instance that tents and sledges were used in Antarctica [*Furse*, 1986]. Geological observations have been made by numerous British and Chilean scientists working in the region between 1955 and 1986 [*Hooper*, 1962; Aitkenhead and Nelson, British Antarctic Survey (BAS) unpublished report, 1962; *Bell*, 1984, BAS unpublished field notes, 1969; Rowe, BAS unpublished report and field notes, 1969; Skinner, BAS unpublished report and field notes, 1969; *González-Ferrán and Katsui*, 1970; *Alarcón et al.*, 1976; Hamer, BAS unpublished field notes, 1979; *British Antarctic Survey*, 1986].

Bibliography

Alarcón et al., 1976
Alfaro and Collao, 1983, 1985
Bell, 1984
British Antarctic Survey, 1986
González-Ferrán and Katsui, 1970
Hooper, 1962
Ringe (see Furse, 1986)

Copyright American Geophysical Union

Copyright American Geophysical Union

TABLE D.8.1. Chemical Analysis and CIPW Norms of a Volcanic Rock From Paulet Island

	1
SiO_2	46.41
TiO_2	2.60
Al_2O_3	16.33
Fe_2O_3	2.18
FeO	7.83
MnO	0.16
MgO	8.11
CaO	9.60
Na_2O	4.30
K_2O	1.34
P_2O_5	0.83
H_2O^+	0.09
H_2O^-	0.13
Total	99.91
or	7.9
ab	19.6
an	21.3
ne	9.1
di	16.9
ol	14.9
mt	3.2
il	4.9
ap	2.0
Ba	205
Ce	108.9
Dy	7.90
Er	4.40
Eu	3.39
Gd	9.51
La	53.8
Lu	0.51
Nd	49.6
Rb	16
Sm	9.10
Sr	1000
Yb	3.68

Major oxides probably determined by wet chemistry; Rb and Sr determined by XRF; Ba and rare earth elements determined by isotope dilution.

1. 27788. Alkali basalt (hawaiite), north end of Paulet Island [*Baker et al.*, 1977; *Pankhurst*, 1982*b*].

clinopyroxene (?titanaugite), and microphenocrysts of plagioclase and opaque oxides.

Chronologic Data

Baker et al. [1977] reported a K-Ar whole-rock date of 0.3 ± 0.1 Ma for an alkali basalt from northern Paulet Island.

Extent of Knowledge

Adie (British Antarctic Survey (BAS) unpublished report, 1948) and Croft (BAS unpublished report, 1947) landed and made geological observations on the northwest coast of Paulet Island where, in 1903, Captain C.A. Larsen and a party from the *Antarctic* spent 9 months overwintering after their ship was crushed and sank in Antarctic Sound [*Nordenskjöld and Andersson*, 1905]. Subsequently, a brief landing was made by *Díaz and Teruggi* [1956], but few details were published. The only detailed study so far was carried out in 1972 by *Baker et al.* [1973].

Bibliography

Baker et al., 1973, 1977
Díaz and Teruggi, 1956
Nordenskjöld and Andersson, 1905
Pankhurst, 1982*b*

Copyright American Geophysical Union

D.9. SOUTHERN TABARIN PENINSULA AND ISLANDS IN ANTARCTIC SOUND

Type of volcano: Essentially unknown. The extensive plateau basalts may have been erupted from fissures or from several small centers on Tabarin Peninsula and Jonassen and Andersson islands. However, the distribution of the outcrops and lithologies and the geophysical interpretation of magnetic anomalies strongly suggest the presence of a single, large shield volcano, possibly centered around Buttress Hill. Rosamel Island resembles a tuff-cone relict.

Location: Southern Tabarin Peninsula (63°36′S, 57°00′W), Jonassen Island (63°32′S, 56°41′W), Andersson Island (63°35′S, 56°35′W), southern Dundee Island (63°29′S, 55°58′W), and Rosamel Island (63°34′S, 56°17′W).

Height above sea level: 0–730 m.

Evidence of Holocene activity: None.

Author of report: J.L Smellie.

Date of report: June 1986.

Form and Structure

Rosamel Island is a degraded tuff-cone remnant composed entirely of northwest dipping palagonite tuffs, with dark volcanic bombs and scoria, erupted from a crater now partially preserved on the southeast flank of the island (Figure D.9.1). No other original volcanic landforms are preserved, and the location(s) of the eruptive center(s) are uncertain. The outcrops on Tabarin Peninsula and Jonassen, Andersson, and Dundee islands consist of steeply dipping (10°–41°) palagonitized tuffs and tuff breccias overlain by flat-bedded lavas (Figure D.9.2). The maximum thickness is developed at Brown Bluff, where a single sequence 730 m thick is exposed, although neither the base nor the top is seen. A mesa-like topography is evident and is caused by the resistant flat-bedded lava cap. The lavas are thin (0.3–1.0 m) and massive, usually separated by about 0.3 m of scoriaceous or ropy-textured, red-stained fragments. They form sequences about 30–35 m thick, sometimes associated with a similar thickness of blocky or aa lavas.

Fig. D.9.1. Geologic sketch map of southern Tabarin Peninsula and Antarctic Sound (based on work by *Nelson* [1975]).

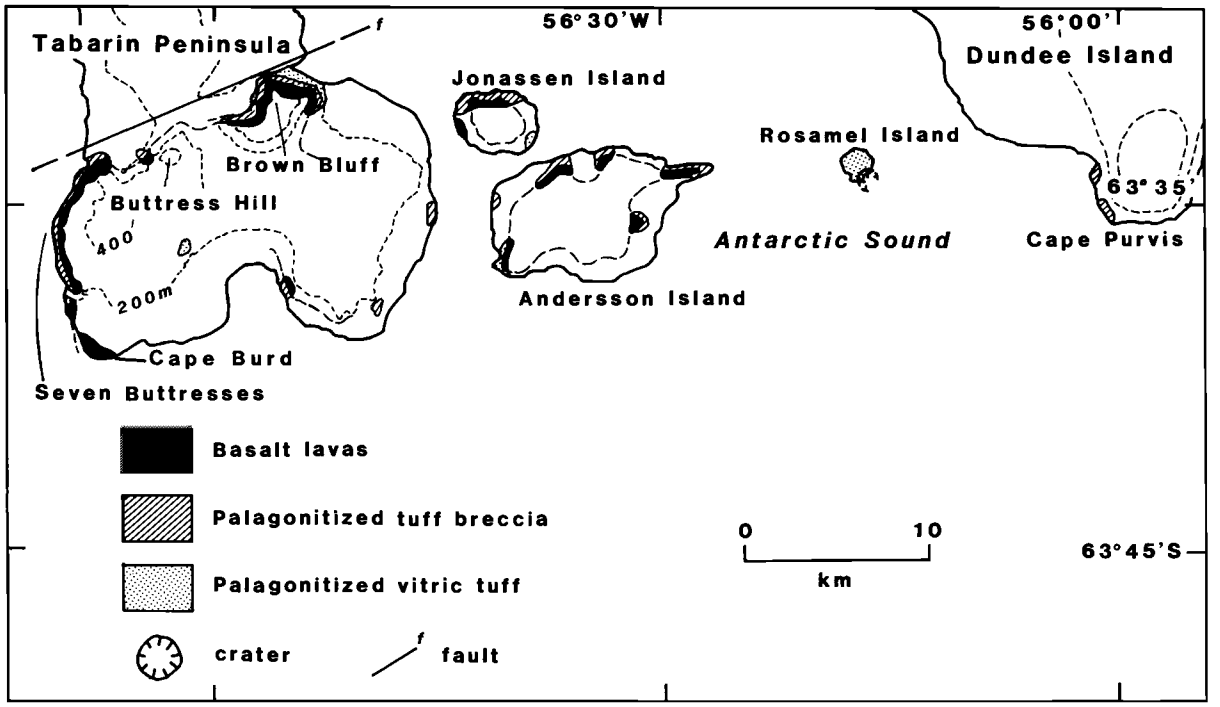

Copyright American Geophysical Union

Copyright American Geophysical Union

Extent of Knowledge

The Swedish South Polar Expedition obtained sketchy geological details of Jonassen, Andersson, and Rosamel islands [*Nordenskjöld and Andersson,* 1905; *Andersson,* 1906]. Unpublished British Antarctic Survey (BAS) reports by W.N. Croft and R.J. Adie described binocular observations of eastern Tabarin Peninsula and the islands in Antarctic Sound, but no landings were made. However, Croft (BAS unpublished report, 1947) subsequently traveled overland and visited and described some of the outcrops in Tabarin Peninsula. In 1961, P.H.H. Nelson spent a day at Brown Bluff and another day between Seven Buttresses and Cape Burd; he also made binocular observations of Jonassen, Andersson, and Rosamel islands during a helicopter survey in which he landed briefly on eastern Andersson Island [*Nelson,* 1975]. Additional details of these localities were included in a report by *Baker et al.* [1973]. The most recent work was by R.D. Hamer (BAS unpublished field notes, 1978), who examined the westernmost extremity of Brown Bluff.

Bibliography

Andersson, 1906
Ashley, 1962
Baker et al., 1973, 1976, 1977
Nelson, 1975
Nordenskjöld and Andersson, 1905
Pankhurst, 1982*b*
Rex, 1976

Copyright American Geophysical Union

D.10. ISLANDS IN NORTHERN PRINCE GUSTAV CHANNEL

Type of volcano: Largely unknown. Several small eruptive centers have been postulated on Egg, Corry, Eagle, and Beak islands based on radial-dipping bedding relations, which are best developed on Egg Island. Alternatively, the outcrops may be part of one or more larger shield volcano(es).

Location: Northern Prince Gustav Channel, including Red Island (63°44′S, 57°52′W), Egg Island (63°41′S, 57°42′W), Tail Island (63°40′S, 57°37′W), Eagle Island (63°40′S, 57°29′W), Vortex Island (63°44′S, 55°38′W), Corry Island (63°43′S, 57°32′W), and Beak Island (63°37′S, 57°18′W).

Height above sea level: 0–558 m.

Evidence of Holocene activity: None.

Author of report: J.L. Smellie.

Date of report: June 1986.

Form and Structure

The islands contain three lithologically distinct volcanic sequences closely similar to those which crop out in Tabarin Peninsula and on James Ross Island (Figure D.10.1). The sequences comprise variably palagonitized, steeply dipping (25°–30°) vitric tuffs and vitric tuff breccias overlain by flat-lying basalt lavas. The complete succession is best seen on Red, Egg, and Corry islands, whereas only partial sequences occur on Tail and Vortex islands. A minimum thickness of about 1200 m can be estimated for the James Ross Island Volcanic Group in this area, based on subaerial outcrops and their postulated submarine extension in Duse Bay. The yellow vitric tuffs are massive to thin bedded, in places showing superb multiple sets of climbing ripples and convolute laminations (Tail and Red islands). They pass up gradationally into coarsely stratified vitric tuff breccias which are, in turn, unconformably succeeded by olivine basalt lavas. The lava sequences are 61 m thick on Beak Island, but they may exceed 90 m in a submarine outcrop northwest of Beak Island. Red scoriaceous subaerial deposits cap the yellow breccias on Egg Island and are interbedded with thin flows of basaltic lava on the summit of Red Island. By contrast with James Ross and Vega

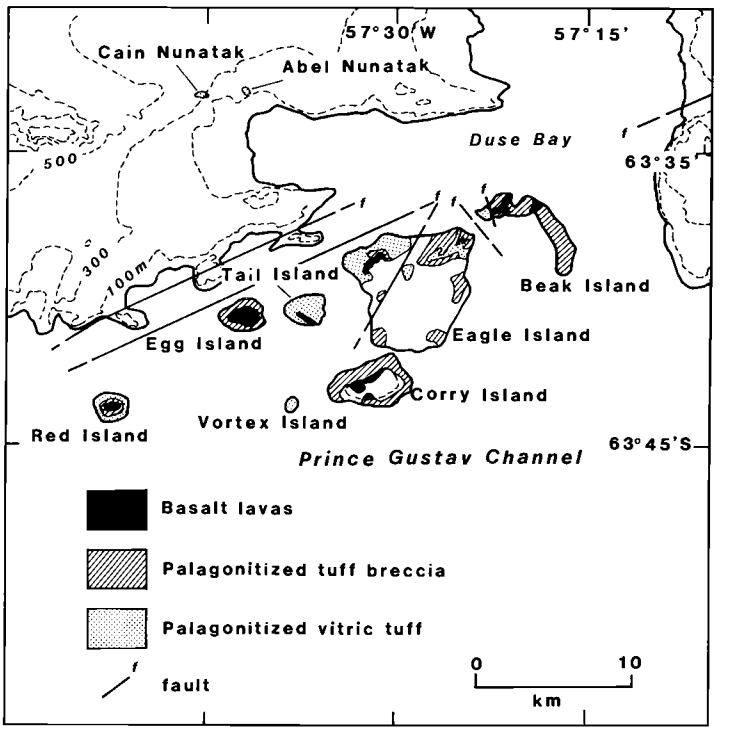

Fig. D.10.1. Geologic sketch map of Cain and Abel nunataks and islands in northern Prince Gustav Channel (based on work by *Nelson* [1975]).

Copyright American Geophysical Union

islands, in which dikes are notably scarce, the islands in northern Prince Gustav Channel contain numerous basalt dikes, with a principal trend parallel to the channel, although also striking at high angles to this. Tail Island is encircled by an annular ring-dike system identified geophysically, with a position roughly coincident with the present island outline.

Petrologic Characteristics

No thin sections of the tuff breccias are available, and only one lava has been sectioned. The lava, from Tail Island, is a fresh rock containing numerous, sometimes glomeroporphyritic anhedral phenocrysts of plagioclase, olivine, and rare clinopyroxene. The very fine grained groundmass is holocrystalline, formed of decussate plagioclase laths, granular opaque oxide, and (?)olivine or possibly clinopyroxene. (?)Analcite occurs in fine trails through the groundmass. The tuffs are variably palagonitized, vitric-rich rocks formed of cuspate to blocky shards, highly vesicular pumice and tachylite, phenocrysts of olivine, plagioclase, and minor clinopyroxene, and rare accessory fragments of fine holocrystalline lavas and titanaugite-bearing hypabyssal rocks. There is generally a fringing cement of zeolite (probably chabazite and rarer spherulitic thomsonite), which also infills vesicles, often accompanied by minor calcite. The lavas are alkaline (hawaiites), resembling those on James Ross Island, but there are few published analyses (Table D.10.1).

TABLE D.10.1. Chemical Analyses and CIPW Norms of Volcanic Rocks From Islands in Prince Gustav Channel

	1	2
SiO_2	47.94	48.28
TiO_2	1.71	2.57
Al_2O_3	16.53	15.37
Fe_2O_3	4.50	2.39
FeO	4.90	8.15
MnO	0.18	0.18
MgO	6.84	7.26
CaO	7.93	9.75
Na_2O	4.21	3.97
K_2O	1.55	1.42
P_2O_5	0.47	0.50
H_2O^+	2.00	0.00
H_2O^-	1.10	0.05
Total	99.86	99.89
or	9.2	8.4
ab	30.6	23.8
an	21.6	19.9
ne	2.7	5.3
di	11.6	20.4
ol	10.2	12.5
mt	6.5	3.5
il	3.3	4.9
ap	1.1	1.2
Rb	--	19
Sr	--	590

Samples probably analyzed by wet chemistry; Rb and Sr determined by XRF. Dashes, not determined.

1. 27839. Hawaiite, Egg Island [*Baker et al.*, 1976].
2. 27812. Hawaiite, Red Island [*Baker et al.*, 1977; *Pankhurst*, 1982*b*].

Chronologic Data

K-Ar dates for samples from Beak Island [*Rex*, 1976], Eagle Island [*Rex*, 1976], southern Tail Island [*Rex*, 1972], and Red Island [*Baker et al.*, 1977] are listed below.

Locality	Lithology	Date, Ma
Beak Island	olivine basalt	1.7 ± 0.2
		2.0 ± 0.2
Eagle Island	olivine basalt	2.0 ± 0.2
		1.7 ± 0.2
Southern Tail Island	basalt	2.7 ± 0.5
Red Island	alkali basalt	1.6 ± 0.2

Extent of Knowledge

Prince Gustav Channel was discovered in 1902 by the Swedish South Polar Expedition during a circumnavigation of James Ross Island [*Nordenskjöld and Andersson*, 1905]. Although the channel was used frequently by field parties sledging to and from the British base at Hope Bay, the first geological studies carried out were those of *Nelson* [1975], traveling over sea ice in the winters of 1960 and 1961. Some of the islands were examined in 1972 by a scientific party using helicopter support [*Baker et al.*, 1973].

Bibliography

Allen, 1966
Ashley, 1962
Baker et al., 1973, 1976, 1977
González-Ferrán, 1983*b*
Nelson, 1975
Nordenskjöld and Andersson, 1905
Pankhurst, 1982*b*
Rex, 1972, 1976

Copyright American Geophysical Union

D.11. CAIN AND ABEL NUNATAKS, TRINITY PENINSULA

Type of volcano: Highly degraded tuff cone(s).

Location: Cain Nunatak (63°33′S, 57°45′W) and Abel Nunatak (63°33′S, 57°41′W), southeastern Trinity Peninsula, Graham Land.

Height above sea level: ~100–400 m.

Evidence of Holocene activity: None.

Author of report: J.L. Smellie.

Date of report: June 1986.

Form and Structure

The two outcrops form isolated nunataks overlooking Prince Gustav Channel (Figure D.10.1); only Cain Nunatak has been visited. A total thickness of about 274 m of palagonite tuffs and olivine basalt breccias is exposed, of which the upper part of the sequence shows conspicuous bedding dipping at low angles to the north-northwest and northeast. A prominent magnetic anomaly is centered on Cain Nunatak and has been attributed to the presence at depth of a reversely magnetized volcanic plug [*Allen,* 1966].

Petrologic Characteristics

The exposed rocks are virtually unaltered vitric lapilli tuffs, mainly formed of pale yellow to brown, highly vesicular glass with a few to many plagioclase microlites and small laths and scattered euhedral-subhedral phenocrysts of olivine, rare calcic plagioclase, and (in one specimen) large, subrounded clinopyroxenes. Some tachylite fragments are also present. Minor rim alteration of glass to greenish-brown (?)smectite has occurred, and a few vesicles contain partial to complete infills of a platy, low-birefringent zeolite.

Chronologic Data

None.

Extent of Knowledge

Abel Nunatak is inaccessible overland due to extensive crevassing and has never been visited. Cain Nunatak was examined on October 16, 1960, by *Aitkenhead* [1975] (see also *Nelson* [1975]).

Bibliography

Aitkenhead, 1975
Allen, 1966
Nelson, 1975

Copyright American Geophysical Union

D.12. JAMES ROSS ISLAND

Type of volcano: A composite shield volcano built of several lava/palagonite breccia sequences interspersed with tuff cones and other pyroclastic products.

Location: James Ross Island (64°09′S, 57°45′W); also on Vega Island (63°50′S, 57°22′W), Carlson Island (63°53′S, 58°16′W), Persson Island (64°12′S, 58°24′W), Lockyer Island (64°27′S, 57°37′W), and Cockburn Island (64°12′S, 56°51′W).

Height above sea level: 0 to ~1470 m.

Evidence of Holocene activity: None.

Author of report: J.W. Thomson.

Dates of report: July 1983 (updated by J.L. Smellie, June 1986).

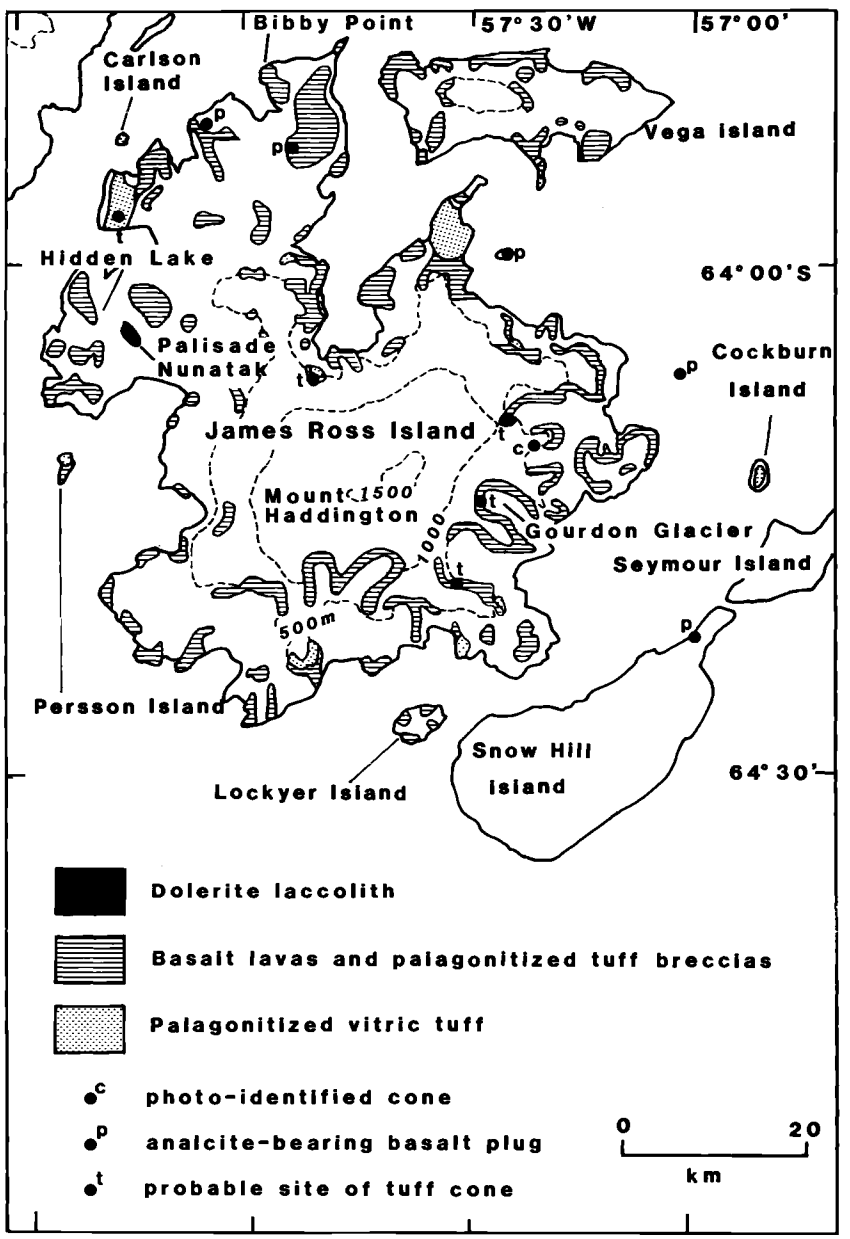

Fig. D.12.1. Geologic sketch map of James Ross Island and environs (based on work by *Nelson* [1975]).

Copyright American Geophysical Union

Form and Structure

James Ross Island represents the largest area of latest Miocene-Pliocene volcanic rocks preserved at the northern tip of the Antarctic Peninsula (Figure D.12.1). Numerous composite lava/palagonite-breccia volcanoes and some tuff cones occur on the island, and there are a few discoidal volcanoes, possibly resulting from subglacial eruptions; evidence for subglacial eruptions is supported by the recent discoveries of marine tillites at the base of the volcanic rocks in several places [*British Antarctic Survey,* 1983; Sykes, British Antarctic Survey unpublished report, 1986]. The total thickness of the volcanic pile is probably about 1500 m. Five phases of volcanism have been recognized, but only two phases are represented in the smaller off-lying islands. Several volcanic centers for the first four phases were mapped during the initial geological survey; in addition a small (?)cinder cone near the plateau edge northeast of Mount Haddington was observed on air photographs taken in January 1980. The volcanic rocks of James Ross Island are commonly exposed in vertical or near-vertical cliffs which rise above gentler slopes formed on the underlying Cretaceous sediments (Figure D.12.2). Each volcanic unit consists of both lavas and breccias; up to four alternations between lavas and breccias have been seen in cliff sections on the east side of the island. The lavas are of the subaerial pahoehoe type and have a characteristic well-defined subhorizontal stratification. Sequences of 25 or more flows were recorded for the phase I lavas, each flow varying from 3 to 6 m in thickness. The texture of the lavas varies from porphyritic to trachytic to uniformly aphantic. Pillow lavas are associated with subaqueous tuffs at several localities. The palagonite breccias (flow foot breccias) locally form partial cones and have an average dip of 35°; the average thickness of these breccias exposed in any unit is ~150 m. Four volcanic plugs have been recognized on James Ross Island; all are circular in outcrop and form pronounced knolls or crags. There are minor swarms of vesicular dikes on the west coast of the island, and a small laccolith crops out at Palisade Nunatak.

Petrologic Characteristics

The James Ross Island volcanic rocks are composed entirely of basalts (*ne* and *hy* normative), hawaiites, mugearites, and trachytes. The palagonite breccias consist of numerous complete and fragmented pillows of olivine basalt set in a coarse-grained tuffaceous matrix; the tuff cones are composed of a mixture of coarse-grained and fine-grained palagonitized vesicular fragments and shards. Analcite-bearing olivine dolerite forms the volcanic plugs and the laccolith; alkaline pegmatitic segregations produced during the final stages of crystallization of the laccolith contain more iron-rich olivine (Fo_{65-54}; optically determined) than in the main intrusion (Fo_{70-55}), discrete crystals of aegirine-augite and rare basaltic hornblende. Vesicular olivine basalt and olivine dolerite dikes are relatively insignificant. Extrusive rocks and dikes contain chabazite, phillipsite, analcite, and natrolite; in the plugs and laccolith, analcite is associated with thomsonite, chabazite, natrolite, and rare gismondite. The intensity of zeolitization of the volcanic rocks increases with the degree of palagonitization. See Table D.12.1 for representative chemical analyses and CIPW norms.

Fig. D.12.2. A 200-m-high cliff section on northern Vega Island, showing steeply dipping vitric tuff breccias (hyaloclastites) overlain unconformably by a thin sequence of flat-lying basalt lavas. The tuff breccias and lavas are cogenetic and formed within a prograding volcanic delta (tuya). (Photograph taken from HMS *Endurance,* 1986.)

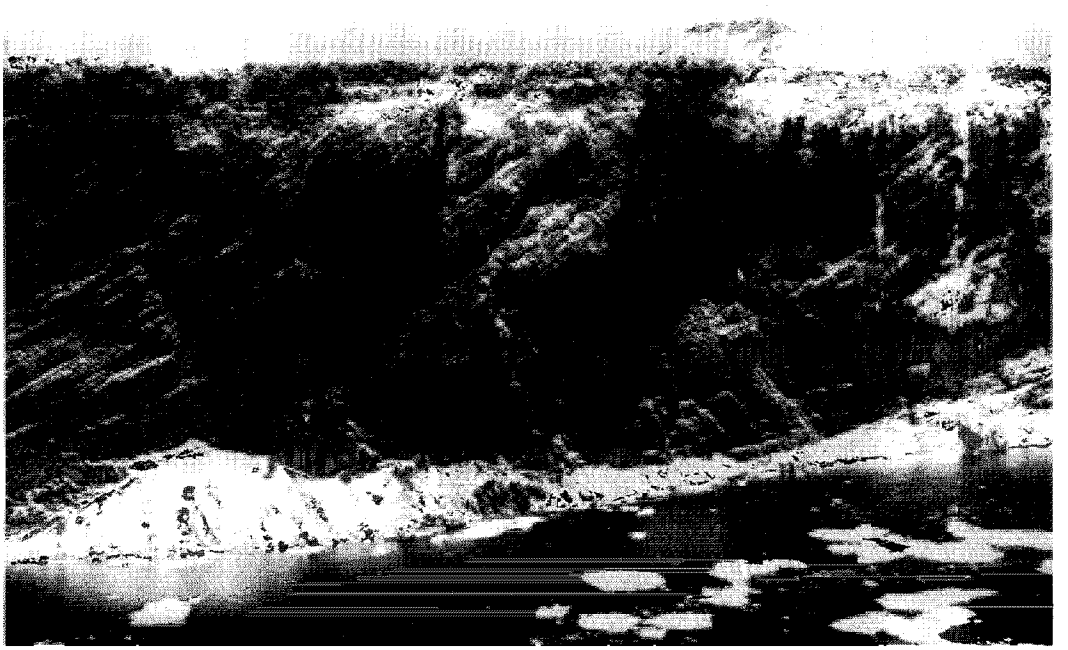

Copyright American Geophysical Union

TABLE D.12.1. Representative Chemical Analyses and CIPW Norms of Volcanic Rocks From James Ross Island

	1	2	3	4	5
SiO_2	48.1	48.2	51.0	57.06	58.58
TiO_2	1.72	2.38	3.37	1.19	0.76
Al_2O_3	15.95	17.62	14.51	18.19	19.23
Fe_2O_3	0.38	1.71	7.88	2.75	2.26
FeO	10.00	8.04	3.92	2.50	2.04
MnO	0.15	0.16	0.17	0.09	0.06
MgO	8.88	4.90	3.09	1.30	0.75
CaO	8.26	8.58	6.74	2.91	2.52
Na_2O	3.37	4.37	4.85	5.69	6.36
K_2O	1.08	1.85	2.65	4.46	4.91
P_2O_5	0.50	0.70	0.92	0.28	0.08
H_2O^+	--	--	--	3.10	2.16
H_2O^-	--	--	--	0.10	0.13
CO_2	--	--	--	0.12	0.13
LOI	0.81	0.37	0.32	--	--
Total	99.20	98.88	99.42	99.74	99.97
or	6.5	11.1	15.8	27.24	29.69
ab	27.3	26.5	41.4	49.78	49.36
an	25.6	23.4	10.1	11.37	9.67
ne	0.9	6.0	--	--	3.07
di	10.4	12.5	13.7	0.77	1.38
hy	--	--	1.4	2.97	--
ol	24.2	11.8	0.1	0.39	1.44
mt	0.6	2.5	3.5	4.13	3.36
il	3.3	4.6	6.5	2.34	1.49
hm	--	--	5.6	--	--
ap	1.2	1.7	2.2	0.67	0.20
cc	--	--	--	0.27	0.30
Ba	146	208	284	--	--
Ce	47	59	92	--	--
Cr	260	34	20	--	--
La	17	30	45	--	--
Nb	25	44	58	--	--
Ni	167	20	18	--	--
Pb	5	8	9	--	--
Rb	12	20	39	--	--
Sr	545	826	392	--	--
Th	2	4	4	--	--
Y	25	29	49	--	--
Zr	177	232	341	--	--

Samples 1–3 analyzed by XRF; samples 4–5 and Fe^{2+}/Fe^{3+} ratios in all samples analyzed by wet chemistry. Dashes, not determined (elements) or not present (norms). LOI, loss on ignition.

1. D.3759.1. Alkali basalt, Bibby Point [*Smellie*, 1987].
2. D.4053.9. Hawaiite, Gourdon Glacier, south side [*Smellie*, 1987].
3. D.4085.7. Mugearite, east of Hidden Lake [*Smellie*, 1987].
4. D.4088.5. Late-stage felsitic vein (trachyte), Palisade Nunatak [*Nelson*, 1975].
5. D.4088.4. Alkali segregation (trachyte), Palisade Nunatak [*Nelson*, 1975].

Copyright American Geophysical Union

TABLE D.12.2. Chronologic Data for James Ross Island

Locality	Lithology	Date, Ma	Reference
James Ross Island	Olivine dolerite laccolith	6.5 ± 0.3 5.4 ± 0.3	1
	Phase II olivine basalt lavas	4.6 ± 0.4 2.0 ± 0.5 1.4 ± 0.3 1.4 ± 0.2	1
	Phase II-IV olivine basalt lavas	4.6 ± 0.4 3.5 ± 0.5 3.3 ± 0.8 2.2 ± 0.5	1
James Ross Island	Olivine basalt fragment in palagonite tuff	2.1 ± 1.0	1
	Pillow lava fragment in palagonite breccia	7 ± 1	2
	Olivine basalt block in palagonite breccia	5 ± 1	2
Seymour Island	Basaltic dike	6.8 ± 0.5	3
Persson Island	Dolerite sill intruding Cretaceous sedimentary rocks	5.4 ± 0.7 4.5 ± 0.5	4

References are (1) *Rex* [1976], (2) *Malagnino et al.* [1978], (3) *Massabie and Morelli* [1977], and (4) *Smellie et al.* [1988].

Chronologic Data

Information for several localities is given in Table D.12.2.

Extent of Knowledge

Most of the available information is based on two oversnow traverses between August and September 1960 and August and November 1961 by P.H.H. Nelson. Because much of the volcanic rock is exposed in sheer cliffs, binoculars were used extensively to examine the units and to locate their contacts. Field mapping was at a scale of 1:50,000, and it led to the early recognition of flow foot breccias formed within volcanic deltas (tuyas) during successive eruptive episodes [*Nelson,* 1975]. James Ross Island is a classic locality for the study of multiple superimposed tuya sequences. Observations on the tillites were made on two days in January 1983 and during a prolonged paleostratigraphic studies field season in 1985–1986 [*British Antarctic Survey,* 1986].

Bibliography

British Antarctic Survey, 1983, 1986
González-Ferrán, 1983*b*
Jones and Nelson, 1970
Malagnino et al., 1978
Massabie and Morelli, 1977
Nelson, 1975
Rex, 1976
Smellie, 1987
Smellie et al., 1988

Copyright American Geophysical Union

D.13. SEAL NUNATAKS

Type of volcano: Uncertain owing to conflicting reports. The nunataks have been described as a series of small volcanic stratocones representing, perhaps, 14 eruptive centers [*González-Ferrán,* 1983*a*]. Alternatively, they may be remnants of one or more larger, strongly dissected shield volcanoes analogous to those in the James Ross Island Volcanic Group [*del Valle et al.,* 1983].

Location: Seal Nunataks, eastern Graham Land (65°00′S, 60°13′W).

Height above sea level: 0–350 m.

Evidence of Holocene activity: *Larsen* [1894] observed Christensen Nunatak on December 11, 1893, and described it as "in full activity." After landing, he recorded much melt and numerous volcanic bombs, which were attributed to the volcanic activity. However, there is no mention of any eruption column, steam effusions, or explosive detonations, and he and his first officer evidently felt no qualms about walking extensively over the nunatak, all of which suggest that the record must be regarded with caution. *Larsen* [1894] also described volcanic activity on Lindenberg Island on the same day, but this time he recorded "funnel-like holes, from which a very black and thick smoke issued from time to time, covering the top itself." This (and the "activity" attributed to Christensen Nunatak?) may record conspicuous steam emissions from fumaroles or possibly hydroclastic eruptions, although both outcrops are now considerably degraded and preserve no cratered landforms. Abundant black and red tephra covering ice around Murdoch Nunatak were observed by González-Ferrán in January 1982 and he ascribed these to relatively recent eruptions on the southeast flank of the nunatak. Fumaroles were recorded at Dallmann and Murdoch nunataks on January 27, 1982. However, during investigations by M.J. Hole in January 1988 (British Antarctic Survey data, 1988), no fresh volcanic cones were observed and, away from the nunataks, tephra occur only in ice-cored moraines, suggesting an origin by glacial, not pyroclastic, distribution. Moreover, fumaroles were not evident at any localities, although water vapor produced by radiant heating of ice-cored moraine was observed on several of the nunataks in this group (note added in proof, May 1989).

Author of report: J.L. Smellie.

Date of report: June 1986.

Form and Structure

Some of the nunataks are said to preserve original volcanic landforms (cone structure: Lindenberg Island and Dallmann, Donald, Bruce, Bull, and Murdoch nunataks [González-Ferrán, 1983*a*]), whereas others are considerably more degraded (Larsen, Evensen, Arctowski, Hertha, Castor, Oceana, and Christensen nunataks) (Figures D.13.1 and D.13.2).

The nunataks may have an internal structure comprising at least two repeated sequences of vitric tuffs and breccias overlain by olivine basalt flows. The volcaniclastic deposits are mainly hydroclastic tuffs, which form alternating, subhorizontal yellowish-brown to red beds (some with fusiform bombs relating to subaerial activity) in the upper parts of nunataks, and underlying breccias formed of lapilli, slabs, and blocks of lava encased in brown palagonitized glass. The lavas principally occur as large unstable accumulations of loose scoriaceous to ropy fragments. Highly vesicular, northwest trending basalt dikes are prominent in most nunataks. They form two sets trending roughly northwest and east-northeast, suggestive of a reticulate fracture system formed by regional extension and rifting. Alternatively, the arcuate dike outcrop pattern is also suggestive of ring dikes or cone sheets related to cauldron subsidence of a large volcanic edifice.

Petrologic Characteristics

There are no published petrographic descriptions of these rocks. In hand specimen, the lavas are highly vesicular basalts with numerous olivine phenocrysts. Some of the tuffs, dikes, and lavas contain abundant ultramafic nodules (spinel lherzolites) and xenoliths of fused (?)Upper Cretaceous white sandstone and pelite. Geochemically, the lavas are *ne*- and *hy*-normative basalts and hawaiites of alkaline affinity closely comparable with the James Ross Island Volcanic Group. (See Table D.13.1 for representative chemical analyses and CIPW norms.)

Copyright American Geophysical Union

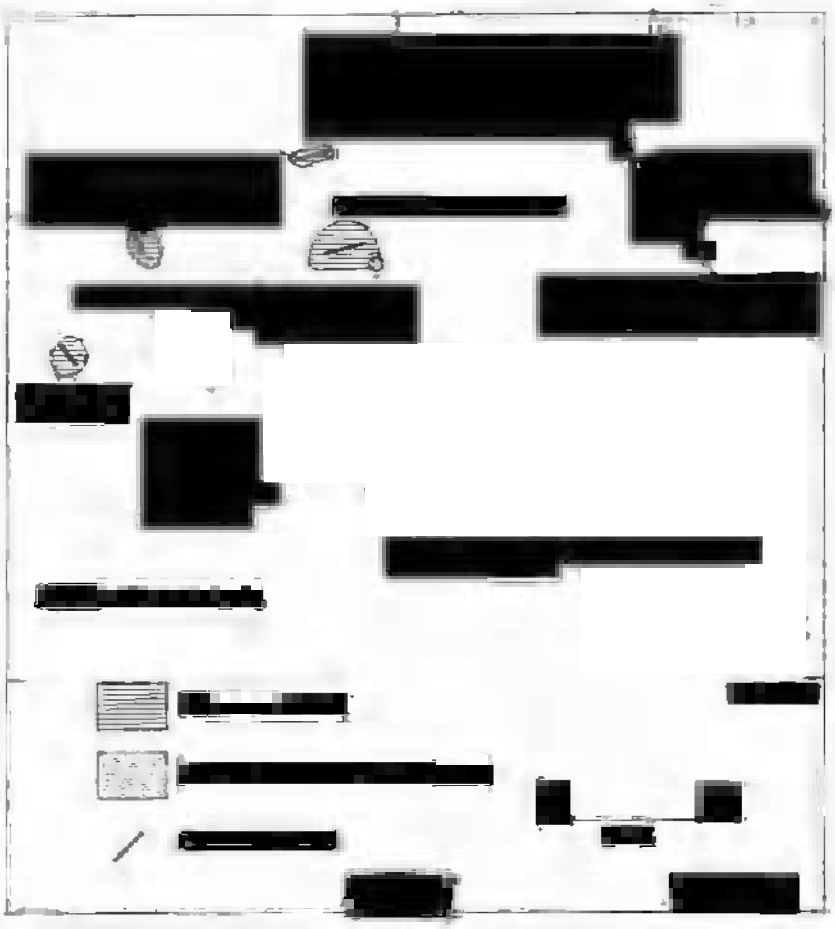

Copyright American Geophysical Union

TABLE D.13.1. Representative Chemical Analyses and CIPW Norms of Volcanic Rocks From Seal Nunataks

	1	2	3	4
SiO_2	47.80	49.20	49.36	50.85
TiO_2	2.73	1.98	1.96	2.32
Al_2O_3	15.13	14.89	14.24	14.93
Fe_2O_3	2.97	11.61*	1.98	11.44*
FeO	8.77	--	9.38	--
MnO	0.14	0.15	0.15	0.20
MgO	7.64	9.19	9.61	5.90
CaO	8.46	8.39	8.25	8.47
Na_2O	3.65	3.65	3.37	3.58
K_2O	1.35	1.11	0.87	1.19
P_2O_5	0.47	0.21	0.25	0.27
H_2O^+	0.58	--	0.35	--
H_2O^-	0.17	--	0.06	--
Total	99.86	100.38	99.82	99.15
or	8.0	6.6	5.1	7.0
ab	28.1	28.5	28.5	30.3
an	20.9	21.0	21.2	21.1
ne	1.5	1.3	--	--
di	14.6	15.6	14.7	15.6
hy	--	--	5.0	12.0
ol	15.5	19.6	17.7	4.4
mt	4.3	2.6	2.9	2.6
il	5.2	3.8	3.7	4.4
ap	1.1	0.5	0.6	0.6
Ba	114	115	--	132
Ce	49.3	35	--	40
Cr	--	276	--	87
Dy	6.04	--	--	--
Er	2.73	--	--	--
Eu	2.76	--	--	--
Gd	7.66	--	--	--
La	24.9	15	--	20
Lu	0.20	--	--	--
Nb	--	26	--	25
Nd	30.2	16	--	20
Ni	--	167	--	83
Rb	8	13	11	14
Sm	6.70	--	--	--
Sr	585	410	375	487
Y	--	17	--	21
Yb	1.90	--	--	--
Zr	--	145	--	149

Samples 1 and 3: major oxides probably determined by wet chemistry; Rb and Sr analyzed by XRF; Ba and rare earth elements determined by isotope dilution. Samples 2 and 4 analyzed by XRF. Dashes, not determined (elements) or not present (norms).

*Total Fe expressed as Fe_2O_3.

1. D.4105.1. Hawaiite, Åkerlundh Nunatak [*Baker et al.*, 1977; *Pankhurst*, 1982*b*].
2. D.4689.1. Alkali basalt, Bull Nunatak [*Saunders*, 1982].
3. D.4114.1. Hawaiite (basalt), Larsen Nunatak [*Baker et al.*, 1977; *Pankhurst*, 1982*b*].
4. D.4691.1 Basalt, Bruce Nunatak [*Saunders*, 1982].

TABLE D.13.2. Chronologic Data for Seal Nunataks

Nunatak	Lithology	Date, Ma	Reference
Åkerlundh	basalt	<1	1,2
Larsen	olivine basalt	<1	1,2
Oceana	basalt	3.0 ± 0.5	1,2
Arctowski	dike	1.4 ± 0.3	3
Evensen	dike	1.4 ± 0.3	3
Evensen	lava	4.0 ± 1	3
Oceana	dike	2.8 ± 0.5	3
Bruce	dike	1.5 ± 0.5	3
Åkerlundh	dike	0.7 ± 0.3	3
Larsen	dike	1.5 ± 0.5	3
Gray	lava	<0.2	3
Donald	lava	<0.2	3
Christensen	?	0.7 ± 0.3	3,4

References are (1) *Rex* [1972], (2) *Rex* [1976], (3) *del Valle et al.* [1983], and (4) *González-Ferrán* [1983*a*].

Chronologic Data

Numerous K-Ar whole-rock dates are available and are summarized in Table D.13.2.

Extent of Knowledge

Following their discovery by C.A. Larsen in 1893 [*Larsen*, 1894], Seal Nunataks were visited in 1902 by the Swedish South Polar Expedition, but only the barest geological details were recorded [*Nordenskjöld and Andersson*, 1905]. Thereafter, numerous British field parties visited the nunataks, but most of the observations were limited, and little information has been published [Stoneley, British Antarctic Survey (BAS) unpublished report, 1952; *Adie* 1953; Standring, BAS unpublished reports, 1953, 1954; Nelson, BAS unpublished report, 1961; *Fleet*, 1968]. *Pankhurst* [1982*b*] and *Saunders* [1982] published some elemental and isotopic data using samples collected by those earlier expeditions. The most recent geological studies are those of *del Valle et al.* [1983] and *González-Ferrán* [1983*a*].

Bibliography

Adie, 1953
Baker et al., 1977
del Valle et al., 1983
Fleet, 1968
González-Ferrán, 1983*a*, *b*
Larsen, 1894
Nordenskjöld and Andersson, 1905
Pankhurst, 1982*b*
Rex, 1972, 1976
Saunders, 1982
Smellie, 1987

Copyright American Geophysical Union

D.14. ARGO POINT

Type of volcano: Small stratocone.

Location: Jason Peninsula, Graham Land (66°15′S, 60°55′W).

Height above sea level: ~360 m (cone is ~175 m above ice shelf; ice shelf surface is ~185 m above sea level in this area).

Evidence of Holocene activity: None.

Author of report: J.W. Thomson.

Date of report: June 1986.

Form and Structure

The summit of Argo Point is a small scoria cone, approximately 300 m in diameter, which has been breached on its northern side (Figure D.14.1). The flanks of the cone are dotted with numerous basaltic bombs and blocks. Basalt lavas and scoria make up the cliffs beneath the scoria cone; these cliffs are undergoing severe ice erosion, and a moraine extends northeastward from Argo Point for over 1 km. No fumarolic activity was observed during the 1977–1978 visit.

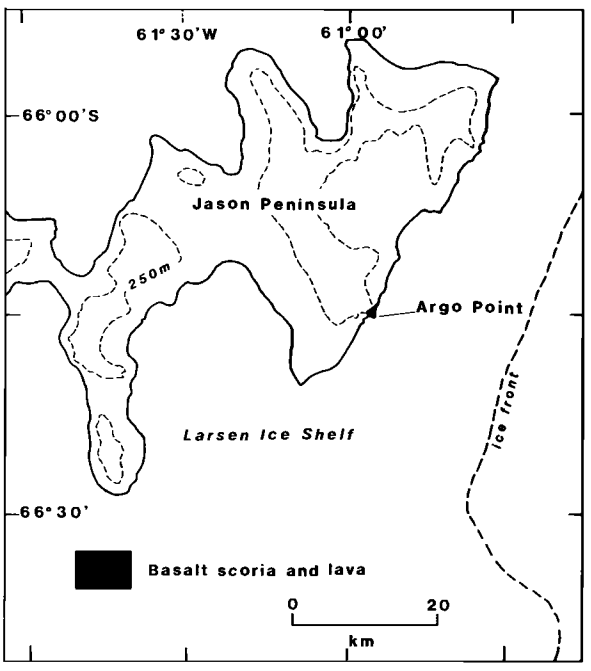

Fig. D.14.1. Sketch map showing the location of Argo Point.

Petrologic Characteristics

Samples collected from Argo Point are fresh, black olivine–microphyric basalt and basaltic scoria, generally highly vesicular and frequently glass coated. Ropy flow textures are common. Partially absorbed felsic xenoliths (1–1.5 cm in diameter) are rare. The lavas are *ne*- and *hy*-normative basalts and hawaiites closely similar to those of the James Ross Island Volcanic Group and at Seal Nunataks (Table D.14.1).

Chronologic Data

K-Ar dates of 0.9 ± 0.1 and 1.4 ± 0.3 Ma have been determined on two samples [*Smellie et al.*, 1988]. The basalt samples were collected from the moraine mentioned earlier (see section on form and structure).

Extent of Knowledge

The top 75 m of the cone is accessible and well exposed but composed only of scoria; a central crater-like depression in the scoria cone is snow filled. The lower flanks of the cone are buried in ice, but its roots are exposed in the ice cliffs and in the moraine. The area was studied by A.D. Saunders for one afternoon during the 1977–1978 season.

Bibliography

Saunders, 1982
Smellie, 1987
Smellie et al., 1988

Copyright American Geophysical Union

TABLE D.14.1. Representative Chemical Analyses and CIPW Norms of Volcanic Rocks From Argo Point

	1	2	3	4
SiO_2	49.25	50.18	50.89	50.95
TiO_2	1.66	1.72	1.69	1.83
Al_2O_3	14.78	14.35	14.68	14.92
Fe_2O_3*	12.32	12.20	11.54	11.54
MnO	0.16	0.16	0.15	0.15
MgO	8.75	8.20	7.55	6.75
CaO	8.34	8.65	8.45	9.13
Na_2O	3.83	3.50	4.25	4.24
K_2O	0.74	0.61	0.79	0.83
P_2O_5	0.27	0.23	0.31	0.30
LOI	--	--	--	+0.27
Total	100.10	99.80	100.30	100.37
or	4.4	3.6	4.7	4.9
ab	31.4	29.6	35.6	34.3
an	21.0	21.6	18.6	19.2
ne	0.6	--	0.2	0.9
di	15.2	16.1	17.3	19.7
hy	--	9.9	--	--
ol	20.1	11.4	16.4	13.9
mt	2.8	2.7	2.6	2.6
il	3.2	3.3	3.2	3.5
ap	0.6	0.5	0.7	0.7
Ba	108	106	133	130
Ce	37	32	37	36.6
Cr	238	245	233	214
Eu	--	--	--	1.73
Hf	--	--	--	3.04
La	19	15	19	19.2
Lu	--	--	--	0.22
Nb	27	21	30	33
Nd	17	15	18	21.0
Ni	197	136	133	75
Rb	8	8	9	8
Sm	--	--	--	4.80
Sr	397	357	438	448
Ta	--	--	--	2.16
Tb	--	--	--	0.77
Th	--	--	--	2.90
Y	17	18	17	21
Yb	--	--	--	1.55
Zr	117	91	119	126

All samples analyzed by XRF [*Saunders,* 1982]; rare earth elements in sample 4 determined by instrumental neutron activation analysis (analyst, A.D. Saunders). Rare earth element data for sample 4 from Saunders (unpublished data, 1986). Dashes, not determined (elements) or not present (norms).

*Total Fe expressed as Fe_2O_3.

1. R.217.1. Fresh, intersertal alkali basalt.
2. R.217.4. Hyalopilitic to variolitic basalt.
3. R.217.9. Olivine basalt (hawaiite).
4. R.217.2. Fresh, intersertal alkali basalt (hawaiite).

Copyright American Geophysical Union

Copyright American Geophysical Union

BIBLIOGRAPHY

Adie, R.J., The rocks of Graham Land, Ph.D. thesis, 259 pp., University of Cambridge, Cambridge, England, 1953.

Adie, R.J., Geological investigations in the Falkland Islands Dependencies before 1940, *Polar Rec., 8,* 502–513, 1957.

Aitkenhead, N., The geology of the Duse Bay—Larsen Inlet area, north-east Graham Land (with particular reference to the Trinity Peninsula Series), *Br. Antarct. Surv. Sci. Rep.,* no. 51, 62 pp., 1975.

Alarcón, B., J. Ambrus, L. Olcay, and C. Vieira, Geología del Estrecho de Gerlache entre los paralelos 64° y 65° lat. sur, Antártica Chilena, *Ser. Cient. Inst. Antart. Chil., 4,* 7–51, 1976.

Alfaro, G., and S. Collao, Exploracion minera en las islas Anvers y Brabante, península Antártica: Resultados preliminares, *Ser. Cient. Inst. Antart. Chil.,* no. 30, 39–47, 1983.

Alfaro, G., and S. Collao, Geología y ocurrencias de minerales de mena en el sector costero de las islas Anvers y Brabante, península Antártica, *Ser. Cient. Inst. Antart. Chil.,* no. 32, 9–38, 1985.

Allen, A., A magnetic survey of north-east Trinity Peninsula, Graham Land, II, Mount Bransfield and Duse Bay to Victory Glacier, *Br. Antarct. Surv. Sci. Rep.,* no. 49, 32 pp., 1966.

Andersson, J.G., On the geology of Graham Land, *Bull. Geol. Inst. Univ. Upsala, 7,* 19–71, 1906.

Ashcroft, W.A., Crustal structure of the South Shetland Islands and Bransfield Strait, *Br. Antarct. Surv. Sci. Rep.,* no. 66, 43 pp., 1972.

Ashley, J., A magnetic survey of north-east Trinity Peninsula, Graham Land, I, Tabarin Peninsula and Duse Bay, *Falkland Isl. Depend. Surv. Sci. Rep.,* no. 35, 35 pp., 1962.

Baker, P.E., A volcano erupts beneath the Antarctic ice, *Geogr. Mag., 42,* 115–126, 1969*a*.

Baker, P.E., Investigations of the 1967 and 1969 volcanic eruptions on Deception Island, South Shetland Islands, *Polar Rec., 14,* 823–826, 1969*b*.

Baker, P.E., Recent volcanism and magmatic variation in the Scotia arc, in *Antarctic Geology and Geophysics,* edited by R.J. Adie, pp. 57–60, Universitetsforlaget, Oslo, 1972.

Baker, P.E., Volcanism and plate tectonics in the Antarctic Peninsula and Scotia arc, in *Proceedings of the International Symposium on Andean and Antarctic Volcanology Problems,* edited by O. González-Ferrán, pp. 347–356, I.A.V.C.E.I., Rome, 1976.

Baker, P.E., and I. McReath, 1970 volcanic eruption at Deception Island, *Nature Phys. Sci., 231,* 5–9, 1971*a*.

Baker, P.E., and I. McReath, Geological investigations on Deception Island, *Antarct. J. U.S., 6,* 85–86, 1971*b*.

Baker, P.E., T.G. Davies, and M.J. Roobol, Volcanic activity at Deception Island in 1967 and 1969, *Nature, 224,* 553–560, 1969.

Baker, P.E., O. González-Ferrán, and M. Vergara, Paulet Island and the James Ross Island Volcanic Group, *Br. Antarct. Surv. Bull.,* no. 32, 89–95, 1973.

Baker, P.E., I. McReath, M.R. Harvey, M.J. Roobol, and T.G. Davies, The geology of the South Shetland Islands, V, Volcanic evolution of Deception Island, *Br. Antarct. Surv. Sci. Rep.,* no. 78, 81 pp., 1975.

Baker, P.E., O. González-Ferrán, and M. Vergara, Geology and geochemistry of Paulet Island and the James Ross Island Volcanic Group, in *Proceedings of the International Symposium on Andean and Antarctic Volcanology Problems,* edited by O. González-Ferrán, pp. 39–47, I.A.V.C.E.I., Rome, 1976.

Baker, P.E., F. Buckley, and D.C. Rex, Cenozoic volcanism in the Antarctic, *Philos. Trans. R. Soc. London, Ser. B., 279,* 131–142, 1977.

Barker, P.F., The tectonic framework of Cenozoic volcanism in the Scotia Sea region—A review, in *Proceedings of the International Symposium on Andean and Antarctic Volcanology Problems,* edited by O. González-Ferrán, pp. 330–346, I.A.V.C.E.I., Rome, 1976.

Barker, P.F., The Cenozoic subduction history of the Pacific margin of the Antarctic Peninsula: Ridge crest-trench interactions, *J. Geol. Soc. London, 139,* 787–801, 1982.

Barth, T.F.W., and P. Holmsen, Rocks from the Antarctandes and the Southern Antilles: Being a description of rock samples collected by Olaf Holtedahl 1927-1928, and a discussion of their mode of origin, *Sci. Results Norw. Antarct. Exped.,* no. 18, 64 pp., 1939.

Barton, C.M., The geology of the South Shetland Islands, III, The stratigraphy of King George Island, *Br. Antarct. Surv. Sci. Rep.,* no. 44, 33 pp., 1965.

Bell, C.M., The geology of islands in southern Bransfield Strait, Antarctic Peninsula, *Br. Antarct. Surv. Bull.,* no. 63, 41–55, 1984.

Biernat, G., K. Birkenmajer, and E. Popiel-Barczyk, Tertiary brachiopods from the Moby Dick Group of King George Island (South Shetland Islands, Antarctica), *Stud. Geol. Pol., 81,* 109–141, 1985.

Birkenmajer, K., Age of the Penguin Island volcano, South Shetland Islands (West Antarctica), by the lichenometric method, *Bull. Acad. Pol. Sci. Ser. Sci. Terre, 27,* 69–76, 1980.

Birkenmajer, K., Structural evolution of the Melville Peak volcano, King George Island (South Shetland Islands, West Antarctica), *Bull. Acad. Pol. Sci. Ser. Sci. Terre, 29,* 341–351, 1982*a*.

Birkenmajer, K., Pliocene tillite-bearing succession of King George Island (South Shetland Islands, Antarctica), *Stud. Geol. Pol., 74,* 7–72, 1982*b*.

Birkenmajer, K., The Penguin Island volcano, South Shet-

Copyright American Geophysical Union

land Islands (Antarctica): Its structure and succession, *Stud. Geol. Pol., 74,* 155–173, 1982*c*.

Birkenmajer, K., Geology of the Cape Melville area, King George Island (South Shetland Islands, Antarctica): Pre-Pliocene glaciomarine deposits and their substratum, *Stud. Geol. Pol., 79,* 7–36, 1984.

Birkenmajer, K., A. Gaździcki, and R. Wrona, Cretaceous and Tertiary fossils in glacio-marine strata at Cape Melville, Antarctica, *Nature, 303,* 56–59, 1983.

Birkenmajer, K., A. Gaździcki, H. Kreuzer, and P. Müller, K-Ar dating of the Melville Glaciation (Early Miocene) in West Antarctica, *Bull. Acad. Pol. Sci. Ser. Sci. Terre, 33,* 15–23, 1985.

Birkenmajer, K., M.C. Delitala, W. Narebski, M. Nicoletti, and C. Petrucciani, Geochronology of Tertiary island-arc volcanics and glacigenic deposits, King George Island, South Shetland Islands (West Antarctica), *Bull. Acad. Pol. Sci. Ser. Sci. Terre, 34,* 257–273, 1986.

Brecher, H.H., Photogrammetric maps of a volcanic eruption area, Deception Island, Antarctica, *Rep. 52,* 10 pp., Inst. of Polar Stud., Ohio State Univ., Columbus, 1975.

Brecher, H.H., M. Nakagawa, and T. Hughes, Volcanic eruptions and the stability of glaciation on Deception Island, Antarctica, in *Proceedings of the International Symposium on Andean and Antarctic Volcanology Problems,* edited by O. González-Ferrán, pp. 59–77, I.A.V.C.E.I., Rome, 1976.

British Antarctic Survey, British Antarctic Territory geological map, sheet 2, Northern Graham Land and South Shetland Islands, scale 1:500,000, *BAS 500G Ser.,* Cambridge, 1979.

British Antarctic Survey, British Antarctic Territory geological map, sheet 3, Southern Graham Land, scale 1:500,000, *BAS 500G Ser.,* Cambridge, 1981.

British Antarctic Survey, Annual Report, 1982-83, 63 pp., Cambridge, 1983.

British Antarctic Survey, Annual Report, 1985-86, 108 pp., Cambridge, 1986.

Casertano, L., Volcanic activity at Deception Island, in *Antarctic Geology,* edited by R.J. Adie, pp. 33–47, North-Holland, Amsterdam, 1964.

Clapperton, C.M., The volcanic eruption at Deception Island, December 1967, *Br. Antarct. Surv. Bull.,* no. 22, 83–90, 1969.

Cordini, I.R., Contribución al conocimiento del sector Antártico Argentino, *Inst. Antart. Argent. Publ.,* no. 1, 277 pp., 1955.

Corte, A.E., and A.L. Somoza, Algunas observaciones geológicas y criopedológicas en la Antartida, II, Observaciones criopedológicas y glaciológicas en las Islas Decepción, Media Luna y Melchior, *Inst. Antart. Argent. Publ.,* no. 4, 65–131, 1957.

Dalziel, I.W.D., The early (pre-Middle Jurassic) history of the Scotia arc region: A review and progress report, in *Antarctic Geoscience,* edited by C. Craddock, pp. 111–126, University of Wisconsin Press, Madison, 1982.

Dalziel, I.W.D., and D.H. Elliot, The Scotia arc and Antarctic margin, in *The Ocean Basins and Margins,* vol. 1, *The South Atlantic,* edited by A.E.M. Nairn and F.G. Stehli, pp. 171–246, Plenum, New York, 1973.

Davey, F.J., Marine gravity measurements in Bransfield Strait and adjacent areas, in *Antarctic Geology and Geophysics,* edited by R.J. Adie, pp. 39–45, Universitetsforlaget, Oslo, 1972.

del Valle, R.A., N.H. Fourcade, and F.A. Medina, Interpretacion preliminar de las edades K/Ar y de los analisis quimicos de las rocas volcánicas y de los diques de los nunataks Foca, Antártida, *Contrib. Inst. Antart. Argent.,* no. 287, 13 pp., 1983.

Díaz, H., and M.E. Teruggi, Contribución a la geología de la Antártida occidental, II, Descripción geológica y petrográfica de algunas localidades de la Antártida occidental, *Inst. Antart. Argent. Publ.,* no. 2, 79–152, 1956.

Díaz, M.T., Significado paleomagnético de los nunataks Foca, *Contrib. Inst. Antart. Argent.,* no. 295, 11 pp., 1983.

Dudziak, J., Cretaceous calcareous nannoplankton from glaciomarine deposits of the Cape Melville area, King George Island (South Shetland Islands, Antarctica), *Stud. Geol. Pol., 79,* 37–51, 1983.

Elderfield, H., Effects of volcanism on water chemistry, Deception Island, Antarctica, *Mar. Geol., 13,* 1–16, 1972*a*.

Elderfield, H., Iron, manganese and silicon in waters of Deception Island, *Br. Antarct. Surv. Bull.,* no. 30, 103–104, 1972*b*.

Everett, K.R., Deception Island eruption, *Antarct. J. U.S., 4,* 87, 1969.

Faure, G., C.H. Shultz, and R.H. Carwile, Isotope composition of strontium in volcanic rocks from Deception Island, *Antarct. J. U.S., 6,* 197–198, 1971.

Ferguson, D., Geological observations in the South Shetland Islands, the Palmer Archipelago, and Graham Land, Antarctica, *Trans. R. Soc. Edinburgh, 53,* 29–55, 1921.

Fisher, R.V., and H.-U. Schmincke, *Pyroclastic Rocks,* 472 pp., Springer-Verlag, New York, 1984.

Fleet, M., The geology of the Oscar II Coast, Graham Land, *Br. Antarct. Surv. Sci. Rep.,* no. 59, 46 pp., 1968.

Fourcade, N.H., Volcanic evolution at Deception Island: Studies during 1970-71, *Antarct. J. U.S., 6,* 86, 1971.

Furse, C., *Antarctic Year: Brabant Island Expedition,* 223 pp., Croom Helm, Beckenham, Kent, England, 1986.

Garrett, S.W., and B.C. Storey, Lithospheric extension on the Antarctic Peninsula during Cenozoic subduction, in *Continental Extensional Tectonics, Spec. Publ. 28,* edited by M.P. Coward, J.F. Dewey, and P.L. Hancock, pp. 419–431, Geological Society of London, 1987.

Gaździcki, A., and R. Wrona, Late Cretaceous and Tertiary fossils from glaciomarine sediments of Melville Peninsula, King George Island (West Antarctica) (in Polish), *Przegl. Geol., 8,* 399–404, 1982.

González-Ferrán, O., The Seal Nunataks: An active vol-

Copyright American Geophysical Union

canic group on the Larsen Ice Shelf, West Antarctica, in *Antarctic Earth Science,* edited by R.L. Oliver, P.R. James, and J.B. Jago, pp. 334–337, Cambridge University Press, New York, 1983*a*.

González-Ferrán, O., The Larsen Rift: An active extension fracture in West Antarctica, in *Antarctic Earth Science,* edited by R.L. Oliver, P.R. James, and J.B. Jago, pp. 344–346, Cambridge University Press, New York, 1983*b*.

González-Ferrán, O., Volcanic and tectonic evolution of the northern Antarctic Peninsula-Late Cenozoic to Recent, *Tectonophysics, 114,* 389–409, 1985.

González-Ferrán, O., and Y. Katsui, Estudio integral del volcanism cenozoico superior de las Islas Shetland del sur, Antártica, *Ser. Cient. Inst. Antart. Chil., 1,* 123–174, 1970.

González-Ferrán, O., F. Munizaga, and H. Moreno, Sintesis de la evolución volcánica de Isla Decepción y la erupción de 1970, *Ser. Cient. Inst. Antart. Chil., 2,* 1–14, 1971*a*.

González-Ferrán, O., F. Munizaga, and H. Moreno, 1970 eruption at Deception Island: Distribution and chemical features of ejected materials, *Antarct. J. U.S., 6,* 87–89, 1971*b*.

Gourdon, E., Sur la constitution minéralogique des Shetland du Sud (île Déception), *C. R. Acad. Sci. Paris, 158,* 583–586, 1914.

Halpern, M., Rubidium-strontium dates and Sr^{87}/Sr^{86} initial ratios of rocks from Antarctica and South America: A progress report, *Antarct. J. U.S., 5,* 159–161, 1970.

Hamer, R.D., Petrogenetic aspects of the Jurassic-Early Cretaceous volcanism, northernmost Antarctic Peninsula, in *Antarctic Earth Science,* edited by R.L. Oliver, P.R. James, and J.B. Jago, pp. 338–342, Cambridge University Press, New York, 1983.

Hawkes, D.D., The geology of the South Shetland Islands, I, The petrology of King George Island, *Falkland Isl. Depend. Surv. Sci. Rep.,* no. 26, 28 pp., 1961*a*.

Hawkes, D.D., The geology of the South Shetland Islands, II, The geology and petrology of Deception Island, *Falkland Isl. Depend. Surv. Sci. Rep.,* no. 27, 43 pp., 1961*b*.

Herron, E.M., and B.E. Tucholke, Sea-floor magnetic patterns and basement structure in the southeastern Pacific, *Initial Rep. Deep Sea Drill. Proj., 35,* 263–278, 1976.

Hobbs, G.J., The geology of the South Shetland Islands, IV, The geology of Livingston Island, *Br. Antarct. Surv. Sci. Rep.,* no. 47, 34 pp., 1968.

Holtedahl, O., On the geology and physiography of some Antarctic and sub-Antarctic islands, *Sci. Results Norw. Antarct. Exped.,* no. 3, 172 pp., 1929.

Honnorez, J., and P. Kirst, Submarine basaltic volcanism: Morphometric parameters for discriminating hyaloclastites from hyalotuffs, *Bull. Volcanol., 39,* 1–25, 1975.

Hooper, P.R., The petrology of Anvers Island and adjacent islands, *Falkland Isl. Depend. Surv. Sci. Rep.,* no. 34, 69 pp., 1962.

Hydrographic Department, *The Antarctic Pilot,* 4th ed., The Admiralty, London, 1974.

Jones, J.G., and P.H.H. Nelson, The flow of basalt lava from air into water—Its structural expression and stratigraphic significance, *Geol. Mag., 107,* 13–19, 1970.

Kendal, E.N., An account of the Island of Deception, one of the New Shetland Isles, *J. R. Geogr. Soc. Lond., 1,* 62–66, 1831.

Lander, J.F., Regional earthquakes recorded at Byrd and South Pole stations, *Antarct. J. U.S., 4,* 212–213, 1969.

Larsen, C.A., The voyage of the *Jason* to the Antarctic regions, *Geogr. J., 4,* 333–344, 1894.

Le Bas, M.J., R.W. Le Maitre, A. Streckeisen, and B. Zanettin, A chemical classification of volcanic rocks based on the total alkali-silica diagram, *J. Petrol., 27,* 745-750, 1986.

Le Maitre, R.W., A proposal by the IUGS Subcommission on the Systematics of Igneous Rocks for a chemical classification of volcanic rocks based on the total alkali silica (TAS) diagram, *Aust. J. Earth Sci., 31,* 243–255, 1984.

Lorca, E., Deception Island: Seismic activity prior to the eruption of 1967, in *Proceedings of the International Symposium on Andean and Antarctic Volcanology Problems,* edited by O. González-Ferrán, pp. 632–645, I.A.V.C.E.I., Rome, 1976.

Malagnino, E.C., E.B. Olivero, C.A. Rinaldi, and J.P. Spikermann, Aspectos geológicos del borde occidental de la Isla James Ross, Antártida, *Actas Congr. Geol. Argent. VII Neuquén, I,* 489–503, 1978.

Massabie, A.C., and J.R. Morelli, Buchitas de la Isla Vicecomodoro Marambio, Sector Antártico Argentino, *Asoc. Geol. Argent. Rev., 32,* 44–51, 1977.

Moyes, A.B., and R.D. Hamer, Contrasting origins and implications of garnet in rocks of the Antarctic Peninsula, in *Antarctic Earth Science,* edited by R.L. Oliver, P.R. James, and J.B. Jago, pp. 358–362, Cambridge University Press, New York, 1983.

Nelson, P.H.H., The James Ross Island Volcanic Group of north-east Graham Land, *Br. Antarct. Surv. Sci. Rep.,* no. 54, 62 pp., 1975.

Newhall, C.G., and D. Dzurisin, Historical unrest at large calderas of the world, *U.S. Geol. Surv. Bull., 1855,* 1108 pp., 1988.

Nordenskjöld, O., Petrographische Untersuchungen aus dem westantarktischen Gebiete, *Bull. Geol. Inst. Univ. Upsala, 6,* 234–246, 1905.

Nordenskjöld, O., and J.G. Andersson, *Antarctica,* 608 pp., Hurst and Blackett, London, 1905.

Olsacher, J., Contribución a la geología de la Antártida Occidental, I, Contribución al conocimiento geológico de la Isla Decepción, *Inst. Antart. Argent. Publ.,* no. 2, 1–76, 1956.

Orheim, O., Glaciological investigations on Deception Island, *Antarct. J. U.S., 5,* 95–97, 1970.

Orheim, O., Volcanic activity on Deception Island, South

Copyright American Geophysical Union

Shetland Islands, in *Antarctic Geology and Geophysics,* edited by R.J. Adie, pp. 117–120, Universitetsforlaget, Oslo, 1972*a*.

Orheim, O., A 200-year record of glacier mass balance at Deception Island, southwest Atlantic Ocean, and its bearing on models of global climatic change, *Rep. 42,* 118 pp., Inst. of Polar Stud., Ohio State Univ., 1972*b*.

Pankhurst, R.J., Rb-Sr geochronology of Graham Land, Antarctica, *J. Geol. Soc. London, 139,* 701–711, 1982*a*.

Pankhurst, R.J., Sr-isotope and trace element geochemistry of Cenozoic volcanic rocks from the Scotia arc and the northern Antarctic Peninsula, in *Antarctic Geoscience,* edited by C. Craddock, pp. 229–234, University of Wisconsin Press, Madison, 1982*b*.

Pankhurst, R.J., Rb-Sr constraints on the ages of basement rocks of the Antarctic Peninsula, in *Antarctic Earth Science,* edited by R.L. Oliver, P.R. James, and J.B. Jago, pp. 367–371, Cambridge University Press, New York, 1983.

Pankhurst, R.J., and J.L. Smellie, K-Ar geochronology of the South Shetland Islands, Lesser Antarctica: Apparent lateral migration of Jurassic to Quaternary island arc volcanism, *Earth Planet. Sci. Lett., 66,* 214–222, 1983.

Pearce, J.A., Role of the sub-continental lithosphere in magma genesis at active continental margins, in *Continental Basalts and Mantle Xenoliths,* edited by C.J. Hawkesworth and M.J. Norry, pp. 230–249, Shiva, Nantwich, Cheshire, England, 1983.

Prior, G.T., Petrographical notes on the rock-specimens collected in Antarctic regions during the voyage of HMS *Erebus* and *Terror* under Sir James Clark Ross, in 1839-43, *Mineral. Mag., 12,* 69–91, 1899.

Rex, D.C., K-Ar age determinations on volcanic and associated rocks from the Antarctic Peninsula and Dronning Maud Land, in *Antarctic Geology and Geophysics,* edited by R.J. Adie, pp. 133–136, Universitetsforlaget, Oslo, 1972.

Rex, D.C., Geochronology in relation to the stratigraphy of the Antarctic Peninsula, *Br. Antarct. Surv. Bull.,* no. 43, 49–58, 1976.

Roberts, B., Chronological list of Antarctic expeditions, *Polar Rec., 9,* 97–134, 1957.

Roobol, M.J., Historic volcanic activity at Deception Island, *Br. Antarct. Surv. Bull.,* no. 32, 23–30, 1973.

Roobol, M.J., A model for the eruptive mechanism of Deception Island from 1820 to 1970, *Br. Antarct. Surv. Bull.,* no. 49, 137–156, 1979.

Roobol, M.J., The volcanic hazard at Deception Island, South Shetland Islands, *Br. Antarct. Surv. Bull.,* no. 51, 237–245, 1982.

Sandoval, N.S., and J.M. Silva, Descripción de las condiciones oceanográficas de la Bahía Foster, Isla Decepción, Enero de 1972, *Ser. Cient. Inst. Antart. Chil., 3,* 80–86, 1975.

Saunders, A.D., Petrology and geochemistry of alkali-basalts from Jason Peninsula, Oscar II Coast, Graham Land, *Br. Antarct. Surv. Bull.,* no. 55, 1–9, 1982.

Saunders, A.D., and J. Tarney, Igneous activity in the southern Andes and northern Antarctic Peninsula: A review, *J. Geol. Soc. London, 139,* 691–700, 1982.

Saunders, A.D., J. Tarney, C.R. Stern, and I.W.D. Dalziel, Geochemistry of Mesozoic marginal basin floor igneous rocks from southern Chile, *Geol. Soc. Am. Bull., 90,* 237–258, 1979.

Saunders, A.D., S.D. Weaver, and J. Tarney, The pattern of Antarctic Peninsula plutonism, in *Antarctic Geoscience,* edited by C. Craddock, pp. 305–314, University of Wisconsin Press, Madison, 1982.

Shultz, C.H., Petrology of the Deception Island volcano, Antarctica, *Antarct. J. U.S., 5,* 97–98, 1970.

Shultz, C.H., Petrologic and volcanologic investigation of Deception Island, *Antarct. J. U.S., 6,* 83–84, 1971.

Shultz, C.H., Eruption at Deception Island, Antarctica, August 1970, *Geol. Soc. Am. Bull., 83,* 2837–2842, 1972*a*.

Shultz, C.H., Petrology of Deception Island volcano, *Antarct. J. U.S., 7,* 152–153, 1972*b*.

Shultz, C.H., Petrology and petrochemistry of Deception Island, Antarctica, in *Proceedings of the International Symposium on Andean and Antarctic Volcanology Problems,* edited by O. González-Ferrán, pp. 498–517, I.A.V.C.E.I., Rome, 1976.

Slaucitajs, L., El conocimiento geomagnético de la Antártida Sudamericana, *Inst. Antart. Argent. Publ.,* no. 3, 114 pp., 1957.

Smellie, J.L., A complete arc-trench system recognized in Gondwana sequences of the Antarctic Peninsula region, *Geol. Mag., 118,* 139–159, 1981.

Smellie, J.L., A geochemical overview of subduction-related igneous activity in the South Shetland Islands, Lesser Antarctica, in *Antarctic Earth Science,* edited by R.L. Oliver, P.R. James and J.B. Jago, pp. 352–356, Cambridge University Press, New York, 1983.

Smellie, J.L., Geochemistry and tectonic setting of alkaline volcanic rocks in the Antarctic Peninsula: A review, *J. Volcanol. Geotherm. Res., 32,* 269–285, 1987.

Smellie, J.L., R.J. Pankhurst, M.R.A. Thomson, and R.E.S. Davies, The geology of the South Shetland Islands, VI, Stratigraphy, geochemistry and evolution, *Br. Antarct. Surv. Sci. Rep.,* no. 87, 85 pp., 1984.

Smellie, J.L., R.J. Pankhurst, M.J. Hole, and J.W. Thomson, Age, distribution and eruptive conditions of Late Cenozoic alkaline volcanism in the Antarctic Peninsula and eastern Ellsworth Land: Review, *Br. Antarct. Surv. Bull.,* no. 80, 21–49, 1988.

Storey, B.C., and S.W. Garrett, Crustal growth of the Antarctic Peninsula by accretion, magmatism and extension, *Geol. Mag., 122,* 5–14, 1985.

Tarney, J., A.D. Saunders, and S.D. Weaver, Geochemistry of volcanic rocks from the island arcs and marginal basins of the Scotia arc region, in *Island Arcs, Deep Sea Trenches and Back-Arc Basins, Maurice Ewing Ser.,* vol. 1, edited by M. Talwani and W.C. Pitman III, pp. 367–377, AGU, Washington, D.C., 1977.

Copyright American Geophysical Union

Tarney, J., S.D. Weaver, A.D. Saunders, R.J. Pankhurst, and P.F. Barker, Volcanic evolution of the northern Antarctic Peninsula and the Scotia arc, in *Andesites: Orogenic Andesites and Related Rocks,* edited by R.S. Thorpe, pp. 371–400, John Wiley, New York, 1982.

Thomas, H.H., On the Innes Wilson collection of rocks and minerals from the South Shetland Islands and Trinity Island, *Trans. R. Soc. Edinburgh, 53,* 81–89, 1921.

Thompson, R.N., Magmatism of the British Tertiary Volcanic Province, *Scott. J. Geol., 18,* 49–107, 1982.

Tyrrell, G.W., A contribution to the petrography of the South Shetland Islands, the Palmer Archipelago, and the Danco Land Coast, Graham Land, Antarctica, *Trans. R. Soc. Edinburgh, 53,* 57–79, 1921.

Tyrrell, G.W., Report on rocks from West Antarctica and the Scotia arc, *Discovery Rep., 23,* 37–102, 1945.

Valencio, D.A., and N.H. Fourcade, Estudio paleomagnético y petrográfico de algunas formaciones Cenozoicas de las Islas Shetland del Sur, *Contrib. Inst. Antart. Argent.,* no. 125, 25 pp., 1969.

Valencio, D.A., J.E. Mendía, and J.F. Vilas, Palaeomagnetism and K-Ar age of Mesozoic and Cenozoic igneous rocks from Antarctica, *Earth Planet. Sci. Lett., 45,* 61–68, 1979.

Valenzuela, E., L. Chávez, and F. Munizaga, Informe preliminar sobre la erupción de Isla Decepción ocurrida en diciembre de 1967, *Bol. Inst. Antart. Chil., 3,* 5–16, 1968.

Valenzuela, E., L. Chávez, and F. Munizaga, Actividad volcánica en Isla Decepción, Antártica, 1967, *Ser. Cient. Inst. Antart. Chil., 1,* 25–39, 1970.

Viramonte, J.G., R.J. Sureda, G.E. Bossi, N.H. Fourcade, and R.H. Omarini, Geochemical and mineralogical study of the high temperature fumaroles from Deception Island, South Shetland, Antarctica, in *Proceedings of the International Symposium on Andean and Antarctic Volcanology Problems,* edited by O. González-Ferrán, pp. 543–561, I.A.V.C.E.I., Rome, 1976.

Weaver, S.D., A.D. Saunders, R.J. Pankhurst, and J. Tarney, A geochemical study of magmatism associated with the initial stages of back-arc spreading: The Quaternary volcanics of Bransfield Strait, from South Shetland Islands, *Contrib. Mineral. Petrol., 68,* 151–169, 1979.

Weaver, S.D., A.D. Saunders, and J. Tarney, Magmatic evolution of the northern Antarctic Peninsula, in *Gondwana Five,* edited by M.M. Cresswell and P. Vella, pp. 251–257, A.A. Balkema, Rotterdam, 1981.

Weaver, S.D., A.D. Saunders, and J. Tarney, Mesozoic-Cenozoic volcanism in the South Shetland Islands and the Antarctic Peninsula: Geochemical nature and plate tectonic significance, in *Antarctic Geoscience,* edited by C. Craddock, pp. 263–273, University of Wisconsin Press, Madison, 1982.

Webster, W.H.B., *Narrative of a Voyage to the Southern Atlantic Ocean, in 1828–30, in H.M. sloop "Chanticleer", under the Command of Capt. Henry Foster,* 2 vols., Richard Bentley, London, 1834.

Wilkes, C., *American Exploring Expedition: Narrative of the United States Exploring Expedition during the years 1838–1842,* vols. I–V, with an atlas, Lea and Blanchard, Philadelphia, Pa., 1845.

Williams, P.L., Volcanic eruption on Deception Island, *Antarct. J. U.S., 4,* 210–211, 1969.

Copyright American Geophysical Union

E. South Sandwich Islands

Copyright American Geophysical Union

Summary

P.E. Baker

Frontispiece. The cone on Bellingshausen Island, looking north from basaltic andesite lava flows. (Photograph by P.E. Baker.)

Introduction

The South Sandwich Islands (56°18′–59°28′S, 26°14′–28°11′W) constitute a young and relatively small island arc extending over a distance of about 350 km along the eastern margin of the Scotia Sea. The term Scotia arc (or Scotia Ridge) is applied to the entire loop of islands and submarine ridges enclosing the Scotia Sea [*Dalziel and Elliot,* 1973] and comprises both continental fragments and remnants of older intraoceanic island arcs [*Barker et al.,* 1982]. The Scotia Sea has developed by successive episodes of back-arc extension over the past 30 m.y. [*Barker et al.,* 1984]. The most recent is that of the Scotia Sea Rise or South Sandwich spreading center which forms the western boundary of the small South Sandwich plate. The South Sandwich Islands are built on oceanic crust created at the back-arc spreading center over the past 8 m.y. [*Barker and Hill,* 1981]. The South Sandwich plate advances eastward at 70 mm yr^{-1} [*Barker et al.,* 1984], as oceanic lithosphere of the South American plate is consumed at the trench: the Benioff zone extends to a depth of 180 km [*Forsyth,* 1975]. Extensive ridge-transform offsets between the South Sandwich Islands and the South Atlantic triple junction (Figure E.I) mean that younger lithosphere is being subducted beneath the southern part of the island arc [*Forsyth,* 1975]. Changes in the characteristics of the lithosphere may account for some of the north-south variation in seismicity but do not appear to exercise any obvious influence on the geochemistry of the volcanic rocks.

There are 11 main islands in the group, together with a number of islets and isolated rocks (Figure E.I and Table E.I). About 10 km to the east of the islands lies the axis of the South Sandwich Trench, where relatively few soundings have been made but depths of over 8000 m have been recorded. The island arc has a simple structure with 10 of the 11 main islands lying on a single axis. Leskov Island is anomalously situated about 56 km to the west of the main axis of the arc, though it does not appear to be part of a separate parallel ridge but rises from a submarine bank linked to Zavodovski Island. The depth of water between the

Copyright American Geophysical Union

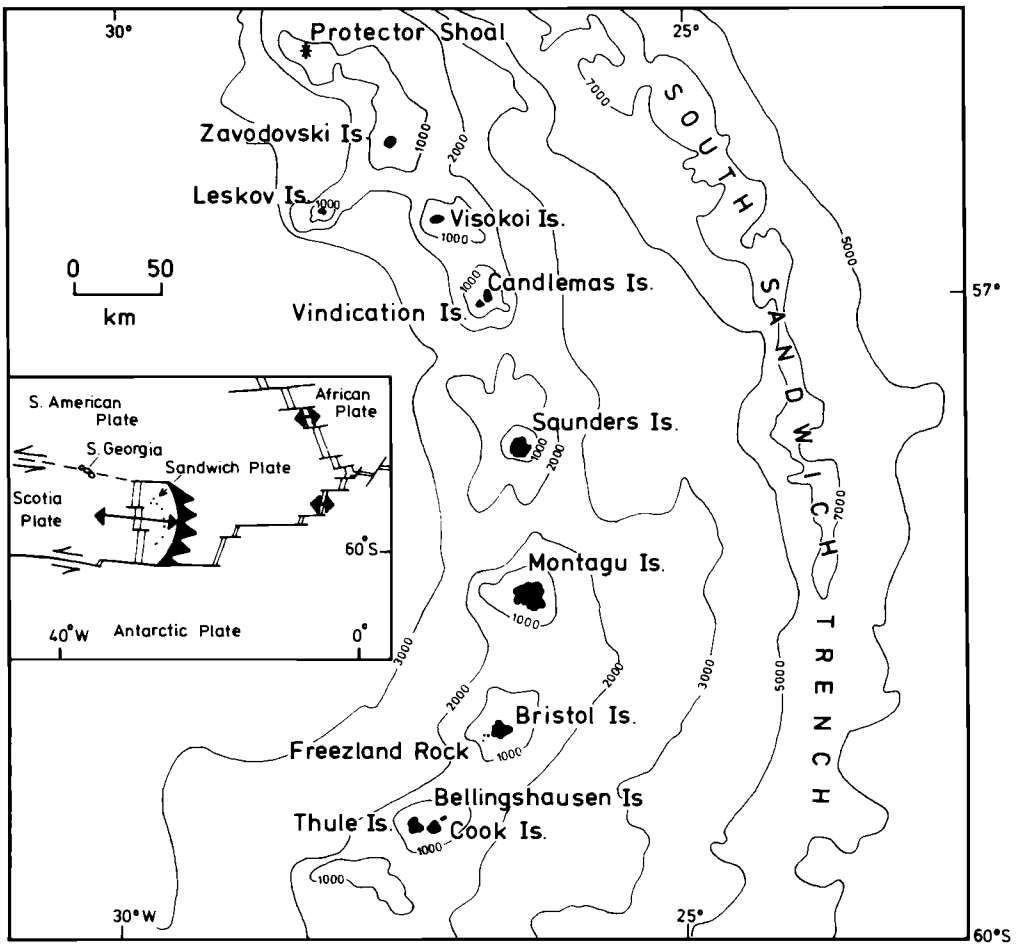

Fig. E.I. Sketch map of the South Sandwich Islands, showing the relative positions of the islands in the group. Inset shows plate boundaries and motions [after *Barker and Hill,* 1981].

islands averages about 2300 m, with a maximum of 2800 m occurring between Saunders and Montagu islands. In contrast, only very shallow water (24 m) separates Candlemas and Vindication islands. Relatively shallow water also divides the three islands of Southern Thule, namely Bellingshausen, Cook, and Thule islands. In 1962 a submarine eruption occurred about 56 km northwest of Zavodovski Island [*Gass et al.,* 1963], and a seamount was subsequently identified and referred to as Protector Shoal. The latter is a broad, gently sloping cone that reaches to within 27 m of the surface and was the source of a substantial volume of rhyolitic pumice.

The South Sandwich Islands are uninhabited and lie well away from commercial shipping and air routes; the nearest permanent habitation is on South Georgia, some 250 km west-northwest of Zavodovski Island. In the nineteenth century, sealers were the main visitors, and in the early part of the twentieth century, whaling fleets were sometimes in the vicinity. The main scientific expeditions were those of RRS *Discovery* in 1930 and HMS *Protector* in 1964. On average it seems unlikely that the South Sandwich Islands have been observed for more than a few days each year. The frequency of visits has probably not changed significantly since the last century.

Morphology

Stratovolcanoes are the dominant landform of the South Sandwich Islands, ranging from the small youthful cone of Bellingshausen Island to the large ice-covered volcano of Mount Michael on Saunders Island, which reaches nearly 1000 m above sea level

Copyright American Geophysical Union

TABLE E.I. Principal Volcanoes of the South Sandwich Islands

IVD	Volcano	Analyzed Rock Composition	Age: Historic Eruptions
E.1	Leskov Island (56°40′S, 28°08′W)	Andesite	0.5 Ma
E.2	Mount Curry, Zavodovski Island (56°18′S, 27°34′W)	Basalt	Holocene 1830
E.3	Protector Shoal (Seamount) (55°55′S, 28°05′W)	Rhyodacite	Holocene 1962
E.4	Mount Hodson, Visokoi Island (56°42′S, 27°09′W)	Basalt, basaltic andesite, andesite	Holocene 1830, 1930
E.5	Vindication Island (57°06′S, 26°46′W)	Basalt, basaltic andesite	Holocene?
E.6	Candlemas Island, Mount Andromeda and Lucifer Hill (57°05′S, 26°43′W)	Basalt, andesite, dacite	Holocene
E.7	Mount Michael, Saunders Island (57°47′S, 26°27′W)	Basalt, basaltic andesite	Holocene
E.8	Montagu Island (58°25′S, 26°20′W)	Basalt, basaltic andesite	1 Ma
E.9	Bristol Island, Mount Darnley (59°02′S, 26°35′W)	Basalt; andesite on Freezland Rock	1935, 1956 3 Ma (Freezland Rock)
E.10	Bellingshausen Island (59°26′S, 27°05′W)	Basaltic andesite	Holocene
E.11	Cook Island (59°28′S, 27°12′W)	Basalt, andesite, dacite	Holocene?
E.12	Thule Island (59°27′S, 27°22′W)	Basalt, andesite, dacite	Holocene

and has a subaerial diameter of about 5 km. Larger islands such as Montagu and Bristol islands are compound structures built mainly of coalescing stratovolcanoes. Others, such as Vindication Island, are severely eroded and represent remnants of former stratovolcanoes. Smaller parasitic pyroclastic cones are common, for example, in the region of Ashen Hills in southeastern Saunders Island (see individual volcano description (IVD) E.7), on the higher part of Montagu Island (see IVD E.8), and on the eastern flanks of Mount Hodson, Visokoi Island (see IVD E.4). The northern part of Candlemas Island (see IVD E.6) is a complex of pyroclastic cones from which several lava flows have been emitted. The most extensive basaltic lava fields form Blackstone Plain in the northern part of Saunders Island, as well as the conspicuous promontory extending out to Hewison Point on Thule Island (see IVD E.12). A possible caldera structure has been tentatively identified in Douglas Strait, between Cook and Thule islands.

There is a striking variation in permanent ice cover from one island to another. Ice may be melted locally as a consequence of volcanic activity (e.g., in the vicinity of active or recent craters high on Bristol or Thule islands), but the dominant control on the thickness and extent of the ice seems to be the size of the islands. The larger islands (e.g., Montagu and Bristol) are mainly ice covered, whereas the smaller islands (such as Leskov and Vindication) are mostly ice-free. However, the islands with the greatest areas of ice also tend to be the highest, so the optimum for ice accumulation is an extensive highland area to provide the necessary catchment for snowfall. Topographic factors exercise the main influence on ice cover, and the effect of heat flux is evidently very restricted.

Copyright American Geophysical Union

Petrology and Geochemistry

Basalt is the dominant rock type of the South Sandwich Islands, making up at least 70% of the total volume. On average, about 60% of this total volume is represented by lava and 40% by tephra. On most islands, basalts and basaltic andesites are the only rock types to be found, but notable exceptions are Candlemas Island, where dacites and andesites make up the young northern area, and Cook Island, where differentiated rocks of similar composition have been found at Reef Point. Leskov Island is unusual in being composed exclusively of porphyritic andesites. Protector Shoal is unique in that it has erupted the only known example of rhyolite in the entire island arc (Table E.3.1). Although the islands have seldom been visited, historic volcanic and/or fumarolic activity has been observed on 8 of the 11 islands. Those lacking any evidence of historic or very recent activity are Vindication, Montagu, and Cook islands.

The lavas of the South Sandwich Islands are all *Q*-normative and may be regarded as belonging to the island arc tholeiite series as defined by *Jakeš and Gill* [1970], although they are in part transitional toward calc-alkaline types. Low-pressure phenocryst assemblages dominated by plagioclase are common, but olivine-clinopyroxene-phyric lavas and dikes (that have been referred to as oceanites) occur near Allen Point on Montagu Island. The common occurrence of aphyric lavas, particularly the andesites and dacites of Candlemas and Cook islands, is in marked contrast to the strongly porphyritic nature of such rocks in most calc-alkaline arcs and cordillera regions. The tholeiitic nature of the arc as a whole is evident from the iron enrichment trend [*Baker*, 1968] (Figure E.II), and the island arc tholeiite characteristics are apparent from the low concentrations of incompatible elements and the chondrite-normalized rare earth element (REE) patterns, which are often, but not invariably, light REE depleted [*Hawkesworth et al.*, 1977].

In general, alkalis are low in the South Sandwich Islands lavas in comparison with rocks of other island arcs. However, for individual islands there are differences in both the range and the rate of increase of total alkalis with SiO_2 (Figure E.III). Saunders, Visokoi, Montagu, and Vindication islands, in the center of the island chain, all have a relatively limited range of rock types but despite this a fairly sharp rate of increase of total alkalis against SiO_2. The southernmost islands (Cook, Thule, and Bellingshausen islands) have a higher proportion of more differentiated rocks which show a more moderate increase of alkalis with silica than the previous group does. Candlemas Island is alone in having both a wide range of rock types but decidedly low total alkalis throughout. Although there are few data from Zavodovski Island, it appears that if taken together with Protector Shoal, the trend at the northern end of the chain would be

Fig. E.II. F (Fe_2O_3 + FeO), M (MgO), A (Na_2O + K_2O) variation diagram for lavas of the South Sandwich Islands. Individual islands are designated as follows: Z, Zavodovski Island; P, Protector Shoal; W, Visokoi Island; L, Leskov Island; V, Vindication Island; C, Candlemas Island; S, Saunders Island; R, Bristol Island and Freezland Rock; B, Bellingshausen Island; K, Cook Island; T, Thule Island; and M, Montagu Island.

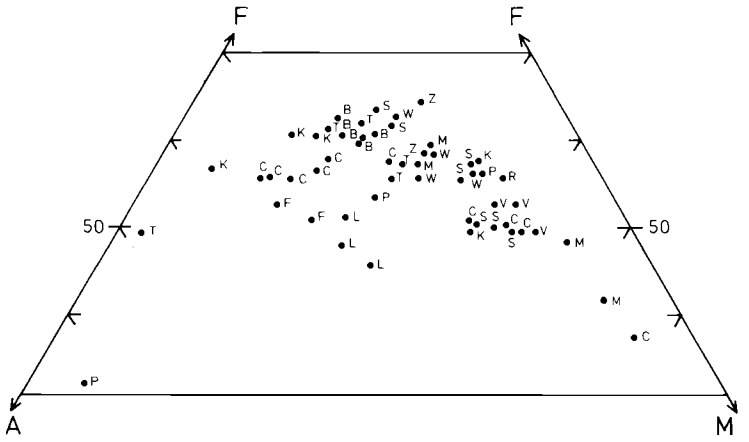

Copyright American Geophysical Union

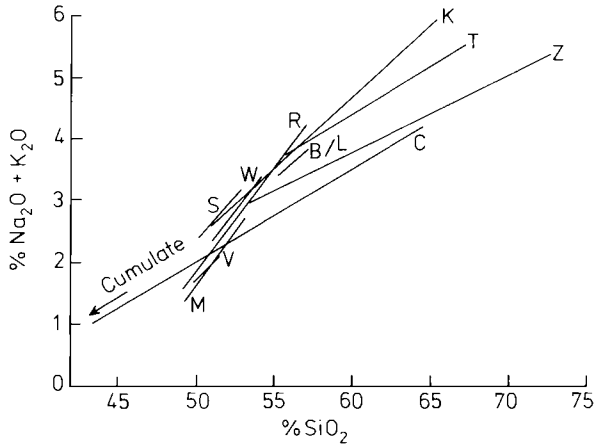

Fig. E.III. Summary alkalis versus silica plot showing trends for individual islands of the South Sandwich Islands group. See Figure E.II for key to island names.

somewhat similar to that of Candlemas Island but slightly more alkali enriched. The South Sandwich Islands are thought to represent an island arc in an early stage of evolution, with partial melting taking place at relatively shallow levels above the subducting slab. Leskov Island, which lies west of the main arcuate axis, is composed of andesites with a more calc-alkaline affinity, perhaps reflecting derivation of magmas from greater depth. The South Sandwich lavas have $^{87}Sr/^{86}Sr$ ratios averaging about 0.7038-0.7039 and $^{143}Nd/^{144}Nd$ ratios of about 0.5130-0.5131 [*Hawkesworth et al.*, 1977]. Low-pressure fractionation of plagioclase, clinopyroxene, and olivine is thought to be responsible for much of the observed petrographic and geochemical variation.

Chronology

The entire structure of the South Sandwich Islands arc can probably be regarded as younger than 5 Ma, the oldest rocks exposed on the islands being about 3 Ma. An andesite from Freezland Rock, off Bristol Island, gave a K-Ar age of 3.1 ± 0.1 Ma [*Baker et al.*, 1977]. Three other ages quoted in the same publication are significantly younger, ranging from 1.0 ± 0.3 Ma for a basalt from Horsburgh Point, Montagu Island, to 0.3 ± 0.1 Ma for a basalt from Sulphur Point, Visokoi Island. There is no indication of any systematic progression of volcanism along the arc, since youthful volcanic cones, such as Bellingshausen Island and northern Candlemas Island, are interspersed with older volcanic centers such as Vindication and Cook islands. The large islands (Montagu, Bristol, and Saunders islands) occur in the central part of the arc and apparently include the oldest lavas. The two volcanoes that have probably been the most persistently active in modern times, Zavodovski and Bellingshausen islands, occur at opposite extremes of the island arc. The anomalously situated Leskov Island does not appear to be significantly different in age from islands on the main arcuate axis; active fumaroles occur on Leskov Island, and a K-Ar date from one of the andesites gave an age of 0.5 ± 0.1 Ma [*Baker et al.*, 1977].

Acknowledgments

Ian Gass and Tom Simkin reviewed this section, and their constructive comments are much appreciated. Grateful thanks also to Wes LeMasurier and Janet Thomson for many editorial improvements and for help with drafting maps.

Copyright American Geophysical Union

E.1. LESKOV ISLAND

Type of volcano: Remnant of a small volcanic cone, mainly lava preserved.

Location: Traversay Islands, northern end of the South Sandwich Islands chain. Leskov Island (56°40′S, 28°08′W) lies in an anomalous position some 56 km west of the main axis of the South Sandwich Islands.

Height above sea level: 190 m.

Evidence of Holocene activity: Fumarolic activity was recorded along the eastern margin of the summit ridge in 1964 and probably also in 1911 [*Filchner,* 1923].

Author of report: P.E. Baker.

Date of report: 1986.

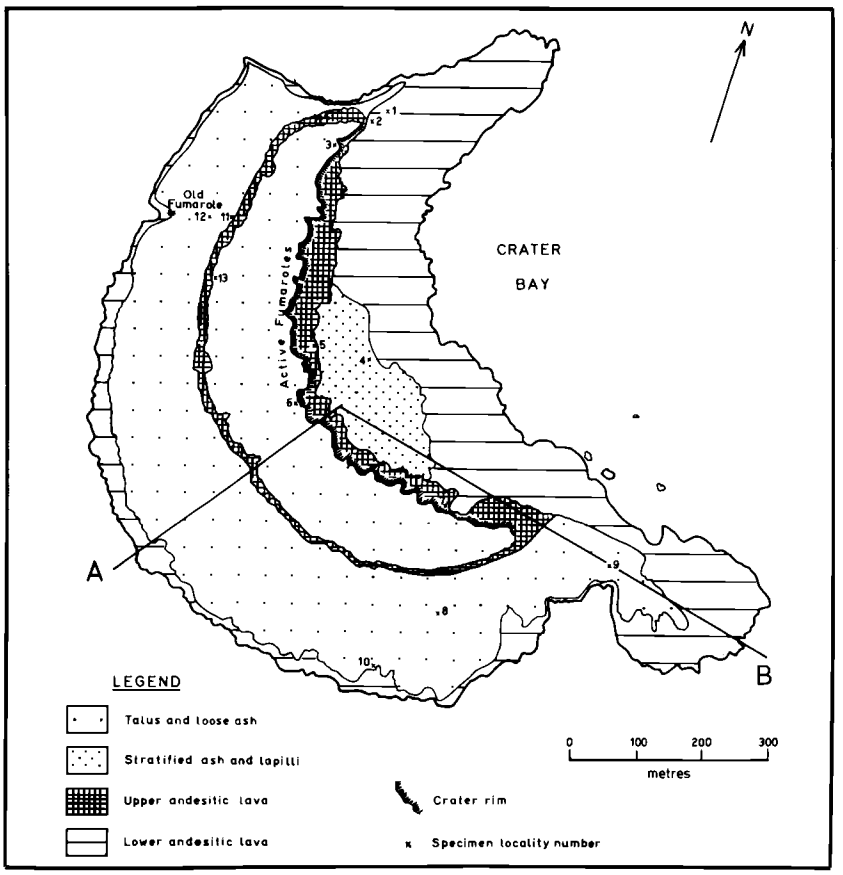

a

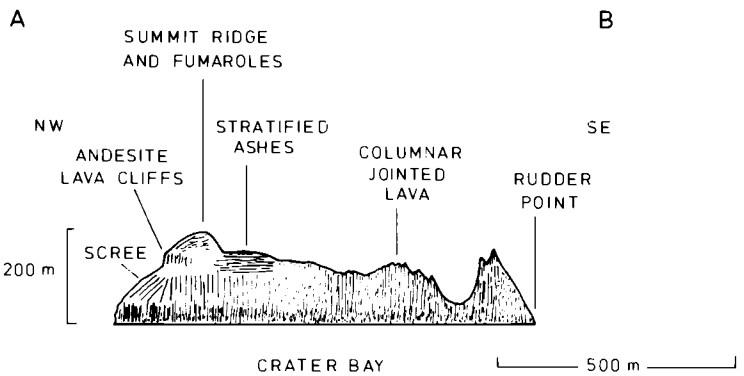

b

Fig. E.1.1. (*a*) Geologic sketch map of Leskov Island, showing the 1964 sample localities. (*b*) Diagrammatic cross section through Leskov Island.

Copyright American Geophysical Union

Form and Structure

The island measures about 900 m by 460 m and has a crescentic shape, with the deep embayment of Crater Bay on its eastern side (Figure E.1.1*a*). It is bounded almost everywhere by steep cliffs which are about 120 m high on the eastern side and 60 m high on the western side of the island. In contrast to the precipitous topography around Crater Bay, the western and southern parts of Leskov Island have a two-tier structure: above the sea cliffs an inclined scree slope extends up to a second line of cliffs at about 120 m above sea level (the scree presumably conceals a former wave-cut terrace or strand line). The island is the surviving part of a small stratovolcano or volcanic cone, and Crater Bay almost certainly represents the site of the main eruptive center. The bulk of the island is composed of thick lavas emplaced as viscous flows or perhaps domes, but a succession of pyroclastic deposits (~9 m thick) which occurs on a platform below the summit ridge (Figure E.1.1*b*) may have been deposited inside the main crater from a small vent on its floor.

Petrologic Characteristics

The lavas are strongly porphyritic or vitrophyric two-pyroxene andesites (Table E.1.1). The most common phenocrysts are plagioclase, followed by hypersthene, augite, and magnetite; olivine, basaltic hornblende, and quartz are uncommon. Loose blocks of gabbro or norite occur in the scree. Chemically, the lavas are calc-alkaline andesites with about 58% SiO_2 and moderate K_2O (~0.8%). Their rather orthodox calc-alkaline characteristics make them quite distinct from the lavas of the other South Sandwich Islands.

Chronologic Data

A K-Ar age determination on a sample of pyroxene-andesite lava gave an age of 0.5 ± 1 Ma [*Baker et al.*, 1977]. Although there was a tentative report of volcanic activity on Leskov Island in 1911 [*Filchner*, 1923], this was probably confined to steam emission from fumaroles along the summit ridge.

Extent of Knowledge

Leskov Island was first sighted by a Russian expedition in 1819 and was observed briefly on a number of subsequent occasions. There is no record of any landings prior to 1961, when the island was visited by boat from RRS *Shackleton*; a further visit was made in 1964 by helicopter from HMS *Protector* [*Holdgate and Baker*, 1979]. A traverse has been made along most of the summit ridge of the island, and samples have been taken from the upper cliff line; most of the main sea cliffs are inaccessible. All the evidence points to a fairly uniform andesite composition for this small island. Sample points from the 1964 reconnaissance are shown in Figure E.1.1*a*.

TABLE E.1.1. Chemical Analysis and CIPW Norm of an Andesite From Leskov Island

	1
SiO_2	59.40
TiO_2	0.77
Al_2O_3	16.97
Fe_2O_3*	7.51
MnO	0.15
MgO	3.57
CaO	7.44
Na_2O	2.98
K_2O	1.09
P_2O_5	0.19
LOI	0.15
Total	100.22
Q	14.26
or	6.44
ab	25.21
an	29.71
di	4.93
hy	15.64
mt	1.29
il	1.46
ap	0.45
Ba	247
Ce	18
Co	26
Cr	37
Cu	53
La	4
Nb	2
Ni	10
Pb	10
Rb	34
Sr	212
Th	1
U	2
V	156
Y	26
Zn	57
Zr	96

All analyses presented in this section (unless otherwise indicated) are new determinations by X ray fluorescence spectrometry at the Department of Geology, University of Nottingham, England. Major oxides are expressed as weight percent, and trace elements as parts per million. For the purposes of norm calculation, Fe_2O_3 is taken as 0.15 FeO. LOI, loss on ignition.

*Total Fe expressed as Fe_2O_3.

1. SSL.5.1. Andesite, summit ridge.

Bibliography

Baker, 1978
Filchner, 1923
Holdgate and Baker, 1979

Copyright American Geophysical Union

E.2. MOUNT CURRY, ZAVODOVSKI ISLAND

Type of volcano: Stratovolcano.

Location: Zavodovski Island (56°18′S, 27°34′W) is the northernmost island in the South Sandwich Islands.

Height above sea level: 551 m.

Evidence of Holocene activity: Intensive fumarolic activity in the summit crater has been reported on numerous occasions since Bellingshausen discovered the island in 1819. A pall of sulfurous vapor was reported in 1964. Fresh lava was reported in 1830 [*Fanning,* 1834], and eruptions of basaltic cinders have occurred probably since that date.

Author of report: P.E. Baker.

Date of report: 1986.

Form and Structure

Zavodovski Island is roughly square in outline (Figure E.2.1), measuring 5.5 km NE-SW by 4.9 km NW-SE. It is composed of a single volcanic cone, Mount Curry, the summit of which lies west of the center of the island. The volcano is flanked by low-lying and gently sloping lava flows on all but its western side, where marine erosion has cut more deeply into the volcanic structure. Two parasitic cones occur on the eastern side of the volcano where the steepest slopes of Mount Curry give way to the lower-lying lava platform. Two fissures, the site of fumarolic activity, extend from the

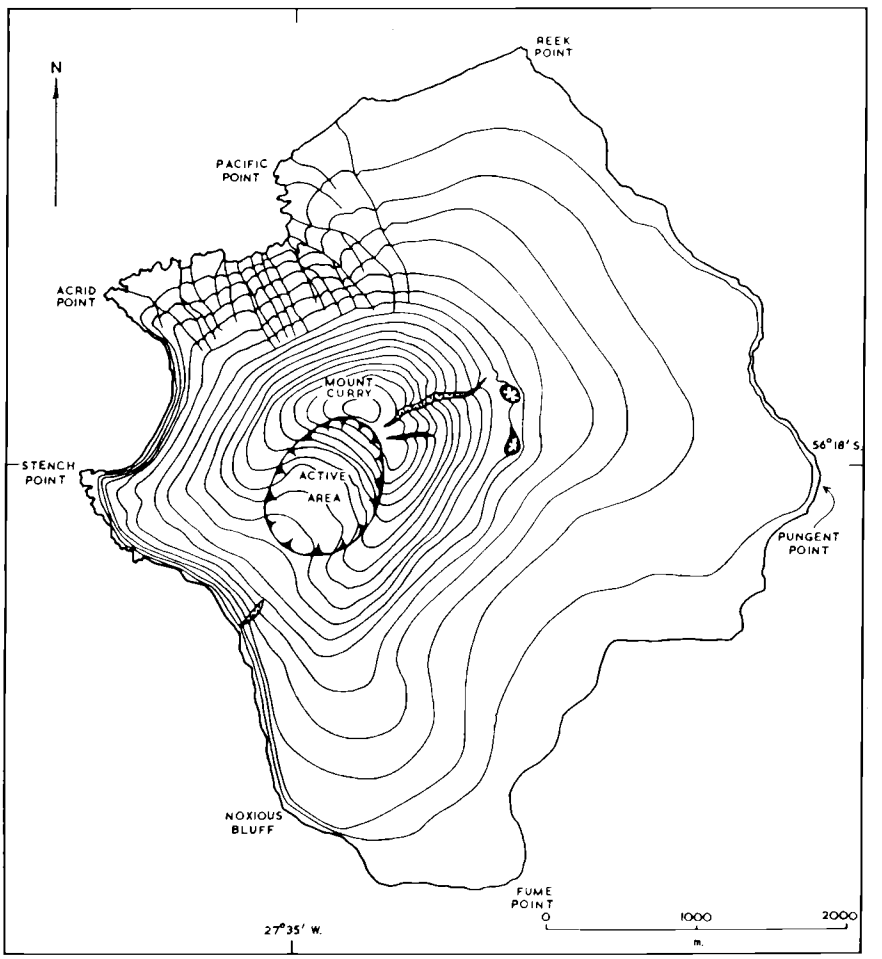

Fig. E.2.1. Sketch map of Zavodovski Island [from *Holdgate and Baker,* 1979]. Here and in subsequent maps in this section, relief is portrayed by means of form lines which should not be interpreted as fixed-interval contours.

Copyright American Geophysical Union

TABLE E.2.1. Representative Chemical Analyses and CIPW Norms of Volcanic Rocks From Zavodovski Island

	1	2
SiO_2	50.88	52.62
TiO_2	0.59	0.87
Al_2O_3	16.22	15.55
Fe_2O_3*	10.47	12.31
MnO	0.18	0.22
MgO	7.95	6.22
CaO	12.23	10.37
Na_2O	1.53	1.47
K_2O	0.12	0.15
P_2O_5	0.03	0.05
LOI	0.00	0.00
Total	100.20	99.83
Q	2.43	8.39
or	0.71	0.89
ab	12.95	12.44
an	37.04	35.39
di	19.16	13.02
hy	24.00	24.73
mt	1.81	2.12
il	1.12	1.65
ap	0.07	0.12
Ba	68	93
Ce	<5	<5
Co	39	45
Cr	160	78
Cu	112	117
La	5	4
Nb	2	2
Ni	39	22
Pb	<2	7
Rb	3	4
Sr	123	128
Th	<1	<1
U	<1	<1
V	269	364
Y	14	18
Zn	66	82
Zr	33	42

For further details regarding the XRF analyses, see Table E.1.1 footnote.

*Total Fe expressed as Fe_2O_3.

1. SSZ.83.1. Basalt, Zavodovski Island (collected by P.H.H. Nelson, 1961; XRF analysis made at University of Nottingham).
2. SSZ.5.5. Basalt, Zavodovski Island (collected by P. Kennett, 1961; XRF analysis made at University of Nottingham).

crater rim toward the two secondary centers. A shallow submarine shelf on the east side of Zavodovski Island is apparently part of the same volcanic edifice. A section through the cone at Stench Point, on the western side of the island, shows a sequence of lava flows interbedded with pyroclastic rocks, many of which are redistributed. More recent pyroclast fall deposits blanket the older relief. Tephra probably make up about 50% of the volume of Zavodovski Island.

The general succession of events appears to have been (1) construction of the main cone, composed of lava flows, agglomerates, and ashfalls; (2) emission of basaltic lava flows, probably from fissures on the eastern flank of the cone; and (3) more recent pyroclast falls, dominantly basaltic cinders.

Petrologic Characteristics

The lava flows are porphyritic or vitrophyric basalts with phenocrysts of plagioclase, olivine, and clinopyroxene. Subcalcic augite has been recognized in the groundmass of one of the samples. A basalt from the east coast of the island is distinguished by relatively high total iron, a high Fe/Mg ratio, and low K_2O (0.20%). The glassy matrix separated from one of the porphyritic basalts is also iron enriched. Representative chemical analyses are shown in Table E.2.1.

Chronologic Data

No radiometric dates are available, but it seems likely that Zavodovski Island may have formed entirely within the last few tens of thousands of years.

Extent of Knowledge

More landings have probably been made on Zavodovski Island than on any other island in the group. The first was by Bellingshausen's party in 1819, and since then landings may have averaged about one every 5 years, though many are likely to have been unrecorded. Whenever visits have been recorded, reference has been made to activity in the form of smoke or gaseous emissions [*Holdgate and Baker,* 1979]. In spite of this, no detailed survey has yet been made, though samples have been collected from the cliffs and scree slopes on the eastern half of the island, and basaltic cinders have been dredged from offshore.

Bibliography

Fanning, 1834
Holdgate and Baker, 1979
Kemp and Nelson, 1931

Copyright American Geophysical Union

E.3. PROTECTOR SHOAL

Type of volcano: Seamount.

Location: Northern end of the South Sandwich Islands, 56 km northwest of Zavodovski Island (55°55′S, 28°05′W).

Depth below sea level: 27 m.

Evidence of Holocene activity: An earthquake on March 5, 1962, and an extensive pumice raft encountered on March 14, 1962, were conclusively shown to have been associated with an eruption of this submarine volcano [*Gass et al.*, 1963].

Author of report: P.E. Baker.

Date of report: 1988.

Form and Structure

Protector Shoal is an asymmetric seamount with a gentle gradient to the north (10° in its lower part) and steeper, more irregular slopes to the south. At least two parasitic cones developed on the main structure [*Holdgate and Baker*, 1979, pp. 68–69].

Petrologic Characteristics

Analyses show the pumice to be of rhyolite or rhyodacite composition, with andesitic inclusions (Table E.3.1) [*Gass et al.*, 1963, p. 327]. The pumice is 80% colorless glass (refractive index, 1.496 ± 0.002) containing crystals of plagioclase (An_{55-56}), hypersthene (En_{55}), and magnetite.

Chronologic Data

The only recorded eruption is that of March 1962, and the only samples available are of the pumice (plus inclusions) believed to have been emitted at that time.

Extent of Knowledge

This is confined to the account of the eruption given by *Gass et al.* [1963] and bathymetric surveys made by HMS *Protector* in 1963 and 1964 [*Holdgate and Baker*, 1979, pp. 7 and 68–69].

TABLE E.3.1. Chemical Analysis and CIPW Norm of Pumice From Protector Shoal

	1		1
SiO_2	67.21	Ba	105
TiO_2	0.40	Ce	<5
Al_2O_3	14.15	Co	4
Fe_2O_3*	4.11	Cr	11
MnO	0.10	Cu	24
MgO	0.99	La	<2
CaO	4.44	Nb	2
Na_2O	5.22	Ni	5
K_2O	0.54	Pb	4
P_2O_5	0.08	Rb	11
LOI	2.96	Sr	106
Total	100.20	Th	<1
		U	<1
Q	23.40	V	26
or	3.19	Y	31
ab	44.17	Zn	50
an	13.59	Zr	92
di	6.71		
hy	4.17		
mt	0.71		
il	0.76		
ap	0.19		

*Total Fe expressed as Fe_2O_3.

1. SSP.1.1. Rhyodacite pumice, 1962 eruption [*Gass et al.*, 1963].

Bibliography

Gass et al., 1963
Holdgate, 1963
Holdgate and Baker, 1979

Copyright American Geophysical Union

E.4. MOUNT HODSON, VISOKOI ISLAND

Type of volcano: Stratovolcano.

Location: Northern part of the South Sandwich Islands (56°42′S, 27°09′W).

Height above sea level: 1005 m.

Evidence of Holocene activity: In 1830, Captain J. Brown [*Fanning,* 1834] referred to Visokoi Island as "a burning mountain with smoke issuing from it in several places," and a plume from Mount Hodson was also observed in 1930 [*Kemp and Nelson,* 1931]. No activity has been reported since then, but a warm patch of ground was noted above Finger Point, in the north of the island, in 1964.

Author of report: P.E. Baker.

Date of report: 1986.

Fig. E.4.1. (*a*) Sketch map of Visokoi Island showing the 1964 sample localities [after *Baker,* 1978; *Holdgate and Baker,* 1979]. Stippled areas depict rock outcrop; the remainder is ice- or snow-covered ground. Regarding form lines, see Figure E.2.1 caption. (*b*) Sketch of Visokoi Island from the south.

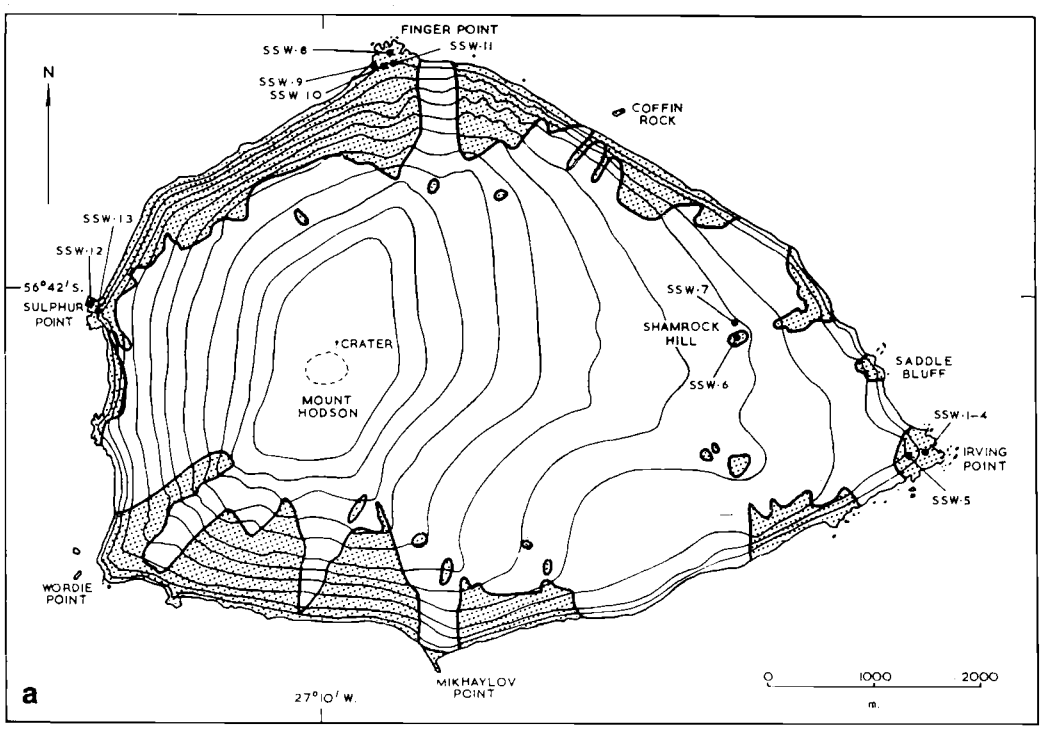

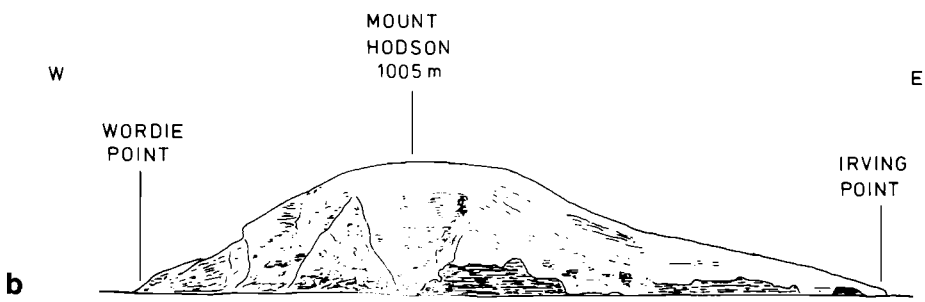

Copyright American Geophysical Union

Form and Structure

Visokoi Island is oval (Figure E.4.1*a*), measuring about 8 km by 6 km, and is composed essentially of a single stratovolcano, Mount Hodson, the summit of which lies west of the center of the island (Figure E.4.1*b*). The slopes of the cone are steep to the north, west, and south but comparatively gentle in the east, toward Irving Point. There are a number of basaltic scoria cones on the lower flanks of the main volcano, the most conspicuous of which is Shamrock Hill. The island is composed of basaltic lava flows and pyroclastic rocks, including thick columnar-jointed lavas at Wordie Point and low-lying lava platforms, for example, at Finger Point. The summit region of Mount Hodson is a smooth ice- and snow-covered platform [*Holdgate and Baker,* 1979], but there was an earlier suggestion of a small crater there [*Kemp and Nelson,* 1931]. The parasitic cones on the eastern slopes are composed of red and black scoria of basaltic andesite composition. *Holdgate and Baker* [1979] summarized the geology of Visokoi Island as follows: "Visokoi is a single stratovolcano constructed mainly of basic lavas and pyroclastics injected by dykes. It has been subjected to intense marine erosion, particularly on its western side, and in very recent times a number of secondary centres, built largely of basaltic scoria and cinders, have been constructed on the lower flanks of the main volcano." Visokoi Island is one of the most heavily ice-covered islands in the province, and its eastern slopes are strongly crevassed.

TABLE E.4.1. Representative Chemical Analyses and CIPW Norms of Volcanic Rocks From Visokoi Island

	1	2	3
SiO_2	51.12	52.61	53.51
TiO_2	0.89	0.97	1.38
Al_2O_3	17.83	16.24	14.73
Fe_2O_3*	10.34	10.83	14.01
MnO	0.19	0.19	0.21
MgO	5.47	5.42	4.11
CaO	11.67	10.49	8.77
Na_2O	2.22	2.43	2.73
K_2O	0.39	0.49	0.57
P_2O_5	0.08	0.09	0.13
LOI	0.00	0.00	0.00
Total	100.20	99.76	100.15
Q	2.17	4.37	6.63
or	2.31	2.90	3.37
ab	18.78	20.56	23.10
an	37.54	31.96	26.26
di	16.38	16.13	13.81
hy	18.45	18.97	20.41
mt	1.78	1.87	2.42
il	1.69	1.84	2.62
ap	0.19	0.21	0.31
Ba	127	149	197
Ce	22	7	12
Co	28	37	40
Cr	75	68	45
Cu	142	139	208
La	4	<2	8
Nb	2	<1	<1
Ni	20	19	11
Pb	5	7	4
Rb	11	11	14
Sr	157	149	131
Th	3	<1	<1
U	2	2	<1
V	280	283	380
Y	21	25	30
Zn	69	85	108
Zr	59	71	90

All analyses were made by XRF. For further details, see Table E.1.1 footnote.

*Total Fe expressed as Fe_2O_3.

1. SSW.10.2. Basalt, Finger Point.
2. SSW.5.1. Basalt, Irving Point.
3. SSW.7.1. Basaltic andesite, Shamrock Hill.

Petrologic Characteristics

The exposed volcanic rocks are exclusively basalts or basaltic andesites. Although many are highly porphyritic, they include sparsely porphyritic and aphyric types. Phenocrysts are plagioclase, clinopyroxene, olivine, magnetite, and less commonly hypersthene. Cristobalite is readily distinguishable in the groundmass of some samples. Chemically, the lavas show pronounced iron enrichment, but their K_2O contents are rather higher than those of lavas from other islands (Table E.4.1).

Chronologic Data

No radiometric ages are available, but the morphology of the island indicates an age of less than 1 Ma, extending virtually to the present time.

Extent of Knowledge

Eighty percent of the island is covered by ice and snow, and rock exposures are confined to the coast, apart from a few of the parasitic centers and isolated outcrops inland. It is estimated that about 40% of the volume of the island is formed by tephra, which crop out in cliff sections but have not been observed as layers within the ice. Most of the existing rock collection comes from the lower eastern part of the island and from the platform at Finger Point and from Sulphur Point. Under favorable conditions, but still with difficulty, landings could probably be effected in a few other places, but it seems unlikely that this would add significantly to existing knowledge.

Bibliography

Baker, 1978
Fanning, 1834
Holdgate and Baker, 1979
Kemp and Nelson, 1931

Copyright American Geophysical Union

E.5. VINDICATION ISLAND

Type of volcano: Remnant of a stratovolcano.
Location: 57°06′S, 26°46′W, 4.5 km west of Candlemas Island.
Height above sea level: 442 m.
Evidence of Holocene activity: None.
Author of report: P.E. Baker.
Date of report: 1986.

Fig. E.5.1. Sketch map of Vindication Island, showing the 1964 sample localities [after *Baker*, 1978; *Holdgate and Baker*, 1979]. Stippled areas depict rock outcrop; the remainder is ice- or snow-covered ground. Regarding form lines, see Figure E.2.1 caption.

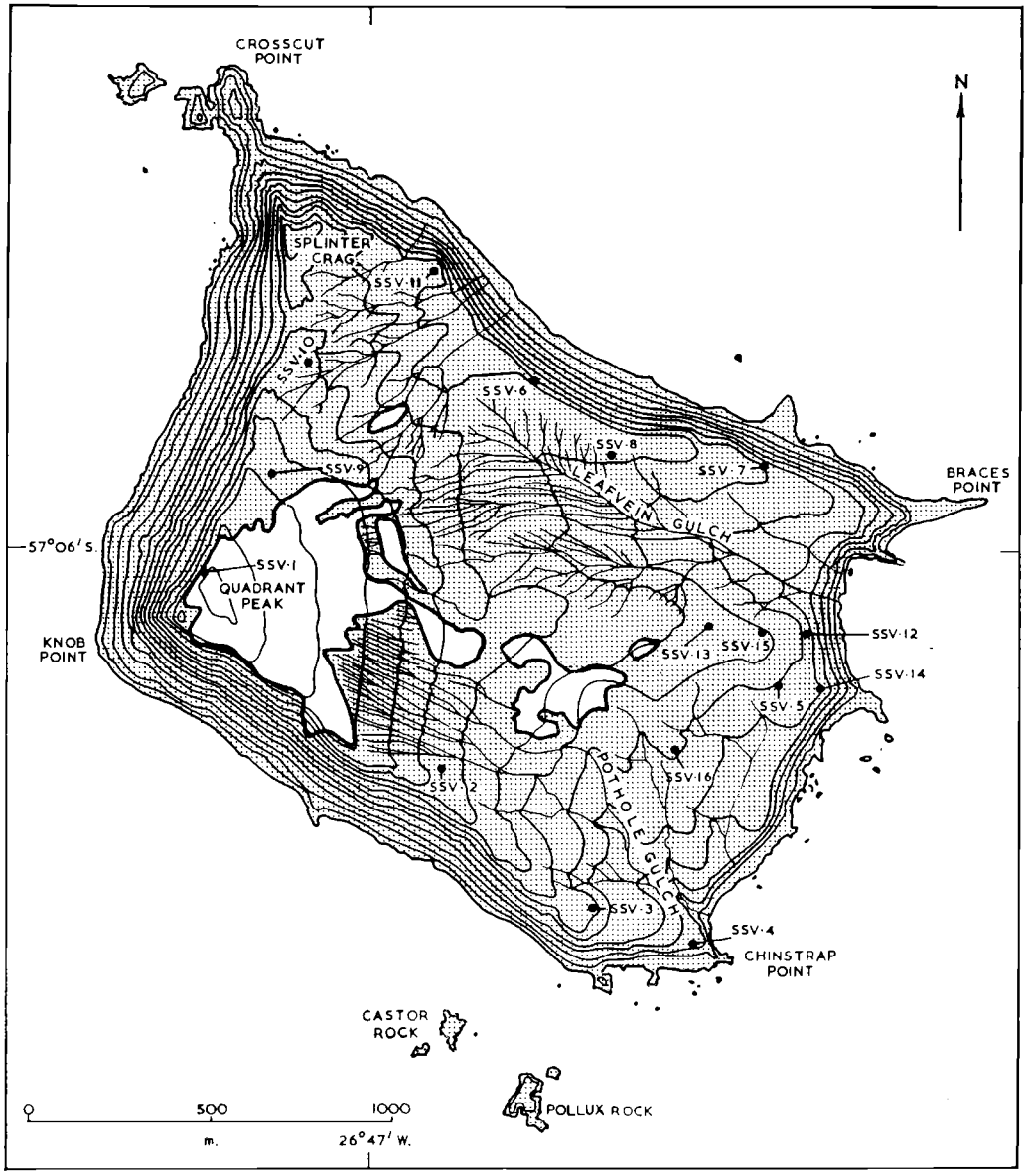

Copyright American Geophysical Union

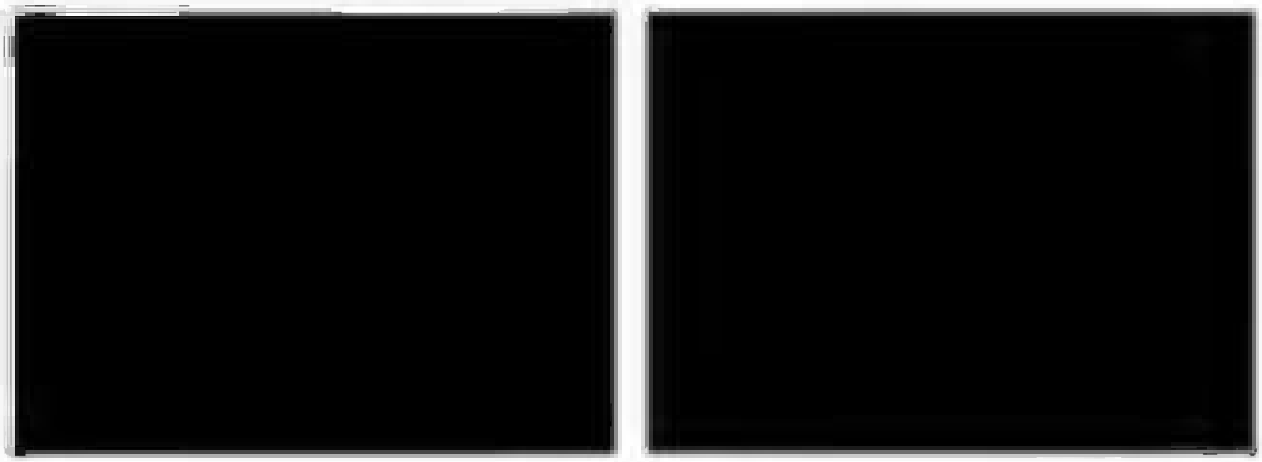

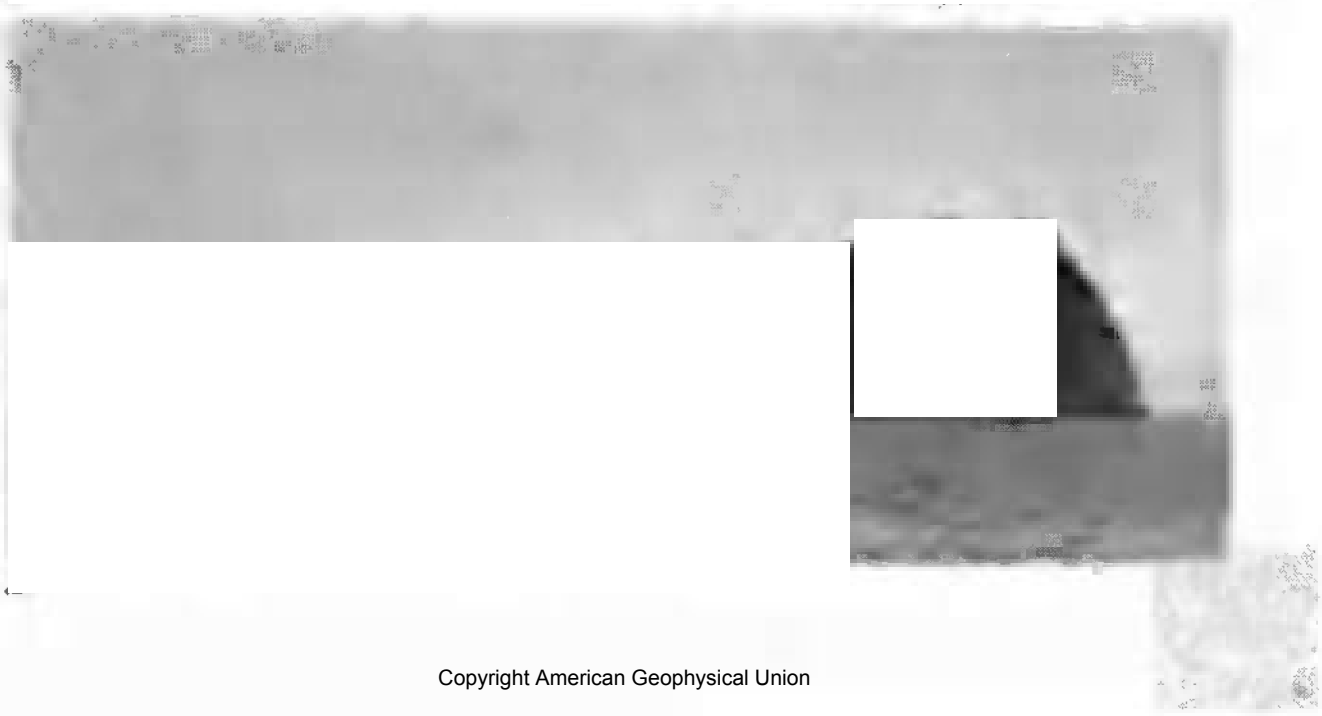

Copyright American Geophysical Union

TABLE E.5.1. Representative Chemical Analyses and CIPW Norms of Volcanic Rocks From Vindication Island

	1	2	3
SiO_2	50.24	51.55	54.87
TiO_2	0.49	0.50	0.95
Al_2O_3	19.00	17.64	16.70
Fe_2O_3*	9.16	9.55	11.16
MnO	0.17	0.18	0.23
MgO	6.89	6.83	3.68
CaO	12.49	12.27	9.77
Na_2O	1.39	1.73	2.83
K_2O	0.09	0.10	0.18
P_2O_5	0.03	0.01	0.05
LOI	0.00	0.00	0.00
Total	99.95	100.36	100.42
Q	2.97	3.46	8.47
or	0.53	0.59	1.06
ab	11.76	14.64	23.94
an	45.34	40.08	32.34
di	13.43	16.98	13.27
hy	22.52	21.15	16.51
mt	1.58	1.65	1.93
il	0.93	0.95	1.80
ap	0.07	0.02	0.12
Ba	46	46	90
Ce	<5	<5	<5
Co	32	33	23
Cr	86	81	42
Cu	91	112	37
La	<2	<2	<2
Nb	<1	<1	<1
Ni	20	20	11
Pb	2	5	3
Rb	4	<1	4
Sr	99	99	115
Th	<1	4	<1
U	<1	<1	<1
V	190	226	322
Y	11	12	23
Zn	58	66	83
Zr	32	32	55

All analyses were made by XRF. For further details, see Table E.1.1 footnote.

*Total Fe expressed as Fe_2O_3.

1. SSV.1.2. Basalt, Quadrant Peak.
2. SSV.12.1. Basalt, 500 m south-southwest of Braces Point.
3. SSV.8.1. Basaltic andesite, north of Leafvein Gulch.

olivine and magnetite. Cristobalite occurs in the groundmass of some of the lavas. The pyroclastic rocks include some palagonite or sideromelane tuffs. Chemically, the lavas are conspicuously low in alkalis and related trace elements (Table E.5.1).

Chronologic Data

No radiometric ages have been determined, but it seems unlikely that the lavas are older than about 1 Ma.

Extent of Knowledge

Most of the high cliffs are completely inaccessible, and much of the surface is covered with loose debris. Within these constraints the existing rock collection probably provides a reasonable coverage of the island. Although further sampling from the lower eastern slopes and coastal promontory would be possible, it is doubtful whether it would add much to our knowledge of the island.

Bibliography

Baker, 1978
Holdgate and Baker, 1979
Kemp and Nelson, 1931

Copyright American Geophysical Union

E.6. CANDLEMAS ISLAND

Type of volcano: An eroded stratovolcano (southern Candlemas Island) with an attached complex of scoria cones and lava flows (in the north).

Location: 57°05′S, 26°43′W.

Height above sea level: 550 m.

Evidence of Holocene activity: Steam emission, geysers, and hot pools have been observed on several occasions this century. Reports of glowing lava in 1953–1954 [*Holdgate,* 1963] are questionable. The lavas of northern Candlemas Island are very young, but it has not proved practicable to demonstrate which, if any, have formed since the island was discovered in 1775.

Author of report: P.E. Baker.

Date of report: 1986.

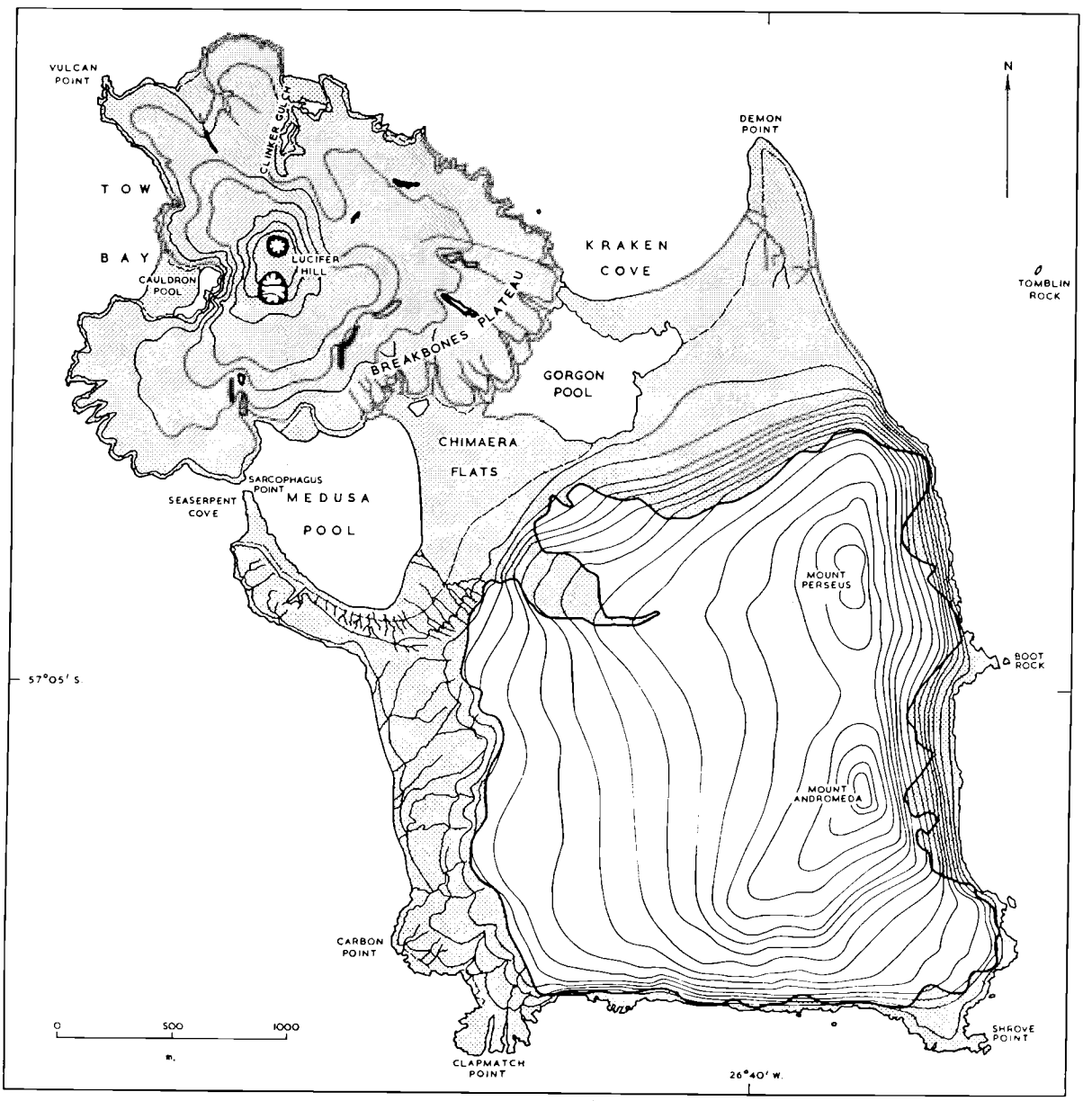

Copyright American Geophysical Union

Copyright American Geophysical Union

TABLE E.6.1. Representative Chemical Analyses and CIPW Norms of Volcanic Rock From Candlemas Island

	1	2	3
SiO_2	50.37	56.86	65.17
TiO_2	0.69	0.83	0.90
Al_2O_3	18.65	16.75	13.67
Fe_2O_3*	10.46	9.89	8.87
MnO	0.18	0.19	0.18
MgO	5.78	3.34	1.50
CaO	11.55	9.02	5.58
Na_2O	1.82	3.09	3.88
K_2O	0.05	0.26	0.45
P_2O_5	0.02	0.07	0.11
LOI	0.10	0.00	0.00
Total	99.67	100.30	100.31
Q	3.33	10.99	23.85
or	0.30	1.54	2.66
ab	15.40	26.14	32.83
an	42.58	31.07	18.56
di	12.05	11.09	7.20
hy	21.85	15.15	10.94
mt	1.81	1.71	1.52
il	1.31	1.58	1.71
ap	0.05	0.17	0.26
Ba	66	104	170
Ce	<5	<5	<5
Co	33	21	16
Cr	54	35	14
Cu	114	114	70
La	--	6	8
Nb	<1	2	1
Ni	20	9	2
Pb	2	7	6
Rb	2	4	8
Sr	116	116	104
Th	1	1	4
U	<1	<1	<1
V	293	216	92
Y	13	23	37
Zn	74	67	81
Zr	37	59	94

All analyses were made by XRF. For further details, see Table E.1.1 footnote. Dash, not detected.

*Total Fe expressed as Fe_2O_3.

1. SSC.35.1. Basalt, southern Candlemas Island.
2. SSC.36.1. Basaltic andesite, southern Candlemas Island.
3. SSC.29.1. Aphyric dacite lava flow, northern Candlemas Island.

Bibliography

Baker, 1978
Holdgate, 1963
Holdgate and Baker, 1979
Kemp and Nelson, 1931
Larsen, 1908
Morrell, 1832
Tomblin, 1979

Copyright American Geophysical Union

E.7. MOUNT MICHAEL, SAUNDERS ISLAND

Type of volcano: Stratovolcano with lava platform and parasitic cones.

Location: Central part of the South Sandwich Islands (57°47′S, 26°27′W).

Height above sea level: 990 m.

Evidence of Holocene activity: Repeated reports of vapor emission from the main summit crater since 1820 (similar activity has been reported as recently as 1964); patchy distribution of basaltic cinders on the flanks of Mount Michael and Blackstone Plain. There is some evidence of changes in Ashen Hills since 1820 [*Holdgate and Baker*, 1979].

Author of report: P.E. Baker.

Date of report: 1986.

Fig. E.7.1. (*a*) Sketch map of Saunders Island, showing the 1964 sample localities [after *Baker*, 1978; *Holdgate and Baker*, 1979]. Stippled areas depict rock outcrop; the remainder is ice- or snow-covered ground. Regarding form lines, see Figure E.2.1. caption.

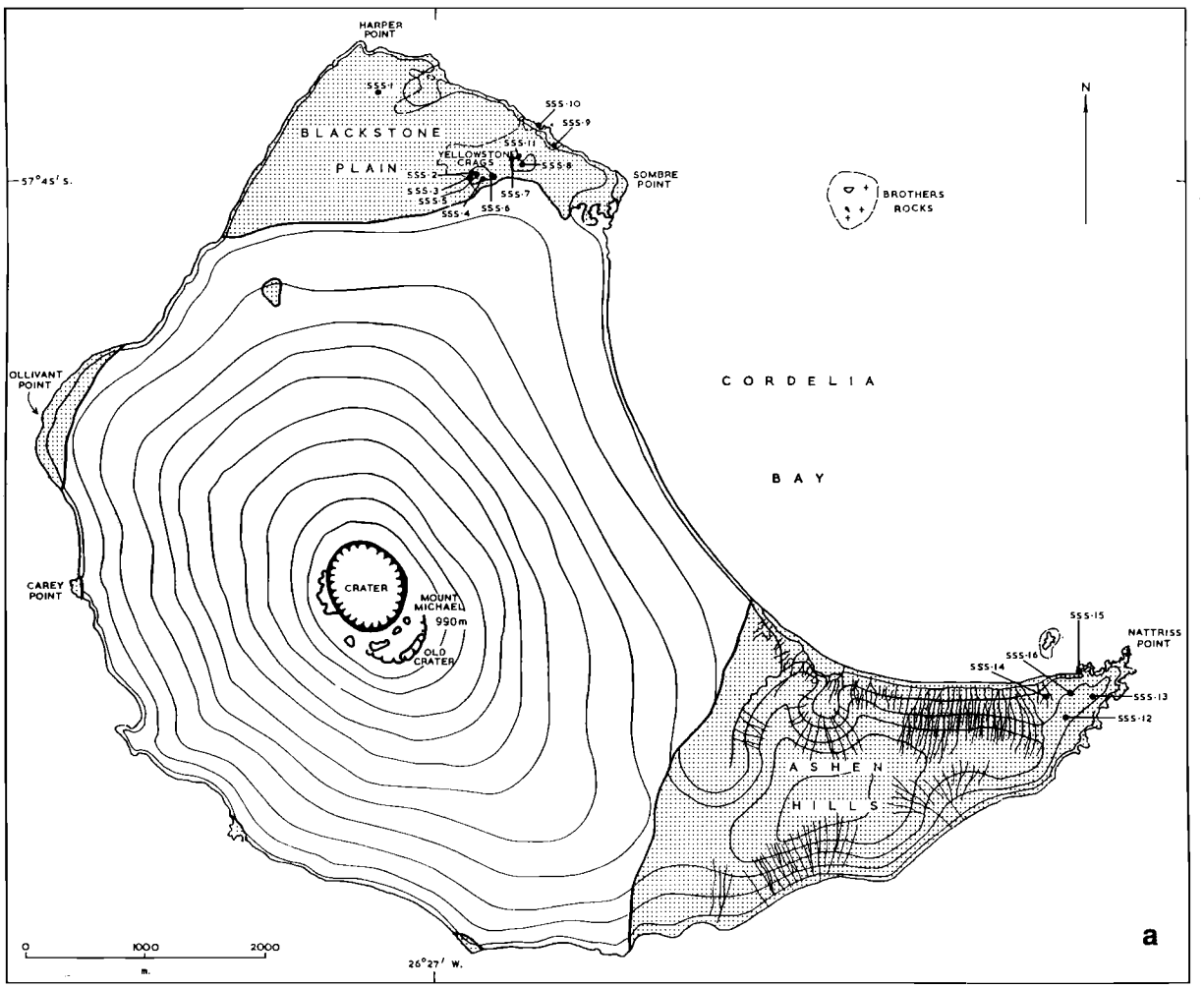

Copyright American Geophysical Union

Copyright American Geophysical Union

Form and Structure

Saunders Island is dominated by Mount Michael (Figures E.7.1*a* and E.7.1*b*), a near-symmetrical and largely ice-covered stratovolcano with a distinct 700-m-diameter summit crater, with the remnant of a somma rim to the southeast. The ice which cloaks the mountain extends to sea level around much of the island, including the length of Cordelia Bay. Blackstone Plain, in the north, is an ice-free plateau of dark basaltic lava between 30 and 50 m above sea level (Figure E.7.2). It is probably the product of a recent flank eruption of Mount Michael which extended out into the sea, partially enveloping the former sea stacks of Yellowstone Crags. Many of the original surface features are preserved, and the flow is partly covered by a light sprinkling of basaltic cinders. A group of secondary volcanic cones forms the so-called Ashen Hills in the southeast of the island, terminating in the headland at Nattriss Point. This part of the island appears to have been constructed around four craters and is composed of loosely consolidated ash and lapilli cut by numerous small erosion gulleys. Nattriss Point itself is a lava platform situated at a lower level. Mount Michael is essentially in a constructional stage, and unlike many of the other stratovolcanoes of the South Sandwich Islands, marine erosion has as yet made little inroad into the main part of the cone. About 35% of the volume of the island is probably represented by tephra.

Petrologic Characteristics

Saunders Island is composed of aphyric, vitrophyric, and porphyritic basalts and basaltic andesites. The basalt of Blackstone Plain is a porphyritic lava with conspicuous phenocrysts of plagioclase, olivine, and augite. The glassy tuffs at Yellowstone Crags also include blocks of dolerite and gabbro. Chemically, the basalts are distinguished by their low contents of alkalis and incompatible trace elements (Table E.7.1).

Chronologic Data

No radiometric age determinations have been made on lavas from Saunders Island, but in view of its constructional stage it seems probable that the entire island is younger than 1 Ma. There has possibly been some activity in the Ashen Hills region since 1820, and on numerous occasions a plume of vapor has been reported issuing from the summit crater of Mount Michael [e.g., *Holdgate and Baker,* 1979] (Figure E.7.3).

Extent of Knowledge

Although 80% of the island is ice covered, fairly comprehensive rock collections have been made from the main ice-free areas of Blackstone Plain and Ashen Hills. Some additional information could be derived from sampling the few small rocky outcrops along the west coast of the island, but landing on these would be difficult.

TABLE E.7.1. Representative Chemical Analyses and CIPW Norms of Volcanic Rocks From Saunders Island

	1	2	3
SiO_2	50.71	52.65	53.26
TiO_2	0.90	1.00	1.03
Al_2O_3	16.94	15.08	15.07
Fe_2O_3*	10.76	11.86	11.98
MnO	0.19	0.20	0.20
MgO	6.77	6.02	5.36
CaO	11.34	10.54	10.05
Na_2O	2.15	2.18	2.43
K_2O	0.39	0.35	0.39
P_2O_5	0.09	0.10	0.11
LOI	0.00	0.00	0.00
Total	100.24	99.98	99.88
Q	0.81	5.20	5.95
or	2.31	2.07	2.31
ab	18.19	18.44	20.56
an	35.42	30.33	29.07
di	16.63	17.62	16.68
hy	22.16	21.08	20.00
mt	1.86	2.04	2.06
il	1.71	1.90	1.96
ap	0.21	0.24	0.26
Ba	122	116	128
Ce	15	<5	22
Co	37	34	32
Cr	193	96	77
Cu	166	95	250
La	<2	9	<2
Nb	<1	<1	1
Ni	64	20	22
Pb	10	5	6
Rb	10	10	12
Sr	132	120	123
Th	4	<1	1
U	<1	<1	<1
V	308	356	375
Y	23	24	25
Zn	76	85	90
Zr	59	60	62

All analyses were made by XRF. For further details, see Table E.1.1 footnote.

*Total Fe expressed as Fe_2O_3.

1. SSS.1.3. Basalt, Blackstone Plain.
2. SSS.15.1. Basalt, Nattriss Point.
3. SSS.5.2. Basaltic andesite, block in tuff, Yellowstone Crags.

Bibliography

Baker, 1978
Holdgate, 1963
Holdgate and Baker, 1979
Larsen, 1908

Copyright American Geophysical Union

E.8. MONTAGU ISLAND

Type of volcano: One or more stratovolcanoes with parasitic cones and possibly domes.
Location: South central part of the South Sandwich Islands (58°25′S, 26°20′W).
Height above sea level: 1370 m.
Evidence of Holocene activity: None.
Author of report: P.E. Baker.
Date of report: 1986.

Form and Structure

Montagu Island, the largest of the South Sandwich Islands, is about 90% ice covered. It has a rectangular outline (Figure E.8.1), apart from the conspicuous projection of Mount Oceanite in the southeast, and measures about 19 km north-south by 20 km east-west. The highest peak (Mount Belinda) is more or less in the center of the island, rising above a broad ice plateau which is about 1000 m above sea level. Little is known about the major structure of the island, and it is not clear whether it has been built from one or more stratovolcanoes. Around much of the island the glaciers extend to the sea and form vertical ice cliffs, broken here and there by rocky buttresses and promontories. Mount

Fig. E.8.1. Sketch map of Montagu Island, showing the 1964 sample localities [after *Baker*, 1978; *Holdgate and Baker*, 1979]. Stippled areas depict rock outcrop; the remainder is ice- or snow-covered ground. Regarding form lines, see Figure E.2.1 caption.

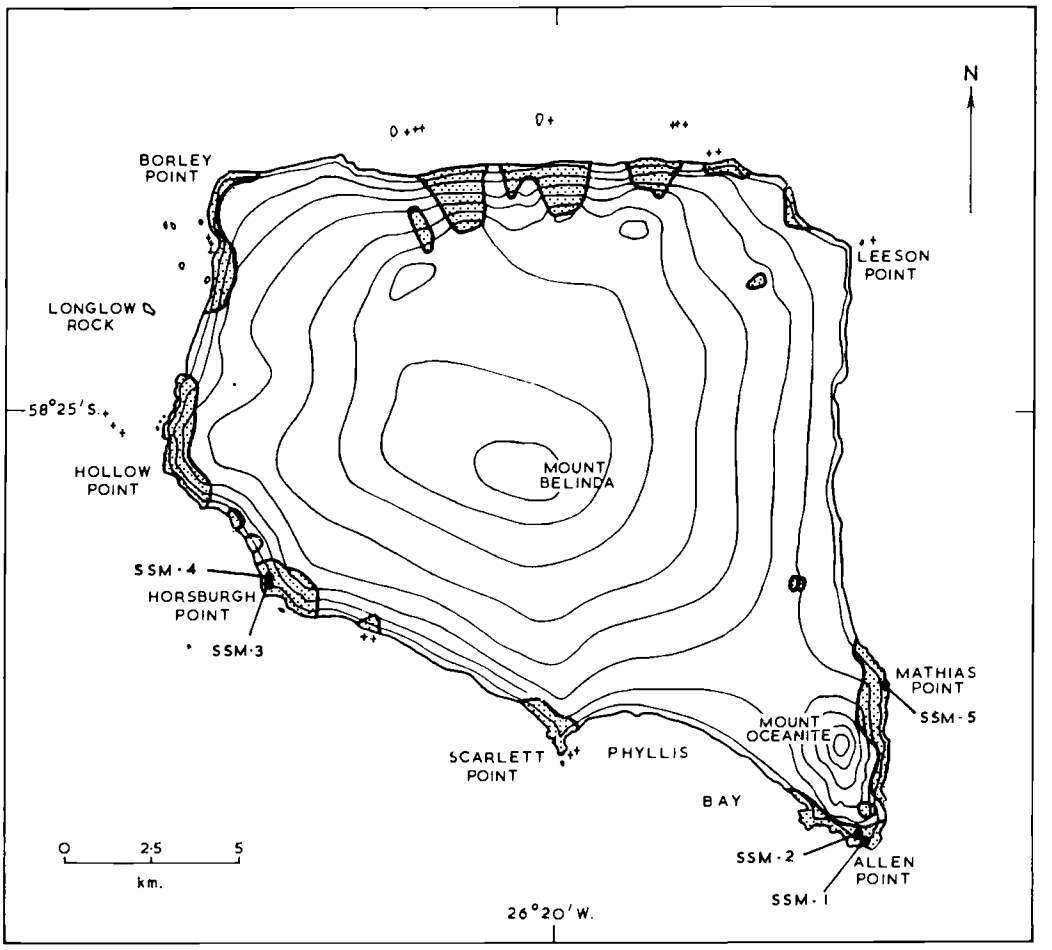

Copyright American Geophysical Union

TABLE E.8.1. Representative Chemical Analyses and CIPW Norms of Volcanic Rocks From Montagu Island

	1	2
SiO_2	48.96	53.12
TiO_2	0.43	0.69
Al_2O_3	15.60	18.19
Fe_2O_3*	9.69	10.41
MnO	0.16	0.19
MgO	10.83	4.20
CaO	13.24	10.71
Na_2O	1.30	2.36
K_2O	0.09	0.24
P_2O_5	0.02	0.06
LOI	0.00	0.00
Total	100.32	100.17
Q	0.00	6.47
or	0.53	1.42
ab	11.00	19.97
an	36.47	38.34
di	23.51	12.02
hy	17.75	17.79
ol	7.67	--
mt	1.67	1.80
il	0.82	1.31
ap	0.05	0.14
Ba	59	82
Ce	<5	8
Co	56	27
Cr	239	35
Cu	60	79
La	<2	<2
Nb	<1	<1
Ni	65	5
Pb	6	6
Rb	4	5
Sr	103	134
Th	<1	1
U	<1	<1
V	222	244
Y	9	17
Zn	55	73
Zr	27	43

All analyses were made by XRF. For further details, see Table E.1.1 footnote. Dash, not present.

*Total Fe expressed as Fe_2O_3.

1. SSM.1.3. Basalt (oceanite), Allen Point.
2. SSM.3.1. Basaltic andesite, Horsburgh Point.

Oceanite is a conspicuous isolated peak about 900 m high, with heavily crevassed slopes. Although it has a dome-like form, it is probably a steep cone with its crater obscured by ice and snow. Lava flows emitted from Mount Oceanite crop out in the headlands of Allen Point and Mathias Point. There are a number of parasitic cones on the higher part of the island; one occurs above Horsburgh Point and another inland from Leeson Point.

Petrologic Characteristics

Samples from around the southeast headland, at Allen Point and Mathias Point, are conspicuously porphyritic basalts. They were referred to as oceanites in the field on account of the abundance of phenocrysts of olivine and clinopyroxene. In fact, plagioclase almost matches the ferromagnesian minerals in abundance but tends to form smaller crystals. Porphyritic basalts dominated by plagioclase phenocrysts occur at Horsburgh Point, where there are also vitric tuffs. Chemically, the basalts are distinguished by low contents of Na_2O, K_2O, and incompatible elements (Table E.8.1).

Chronologic Data

The main part of the island appears to have been constructed by lavas and pyroclastics emitted from Mount Belinda and perhaps also from other unidentified volcanoes. These were probably followed by flows from a number of older secondary centers along the northern side of the present island and by Mount Oceanite and its associated lava flows; oceanite dikes intruded into these flows represent a later stage in this phase of activity. Probably the most recent event has been the development of parasitic cones around the periphery of the central plateau. A K-Ar age on a basalt from Horsburgh Point gave an age of 1.0 ± 0.3 Ma [*Baker et al.*, 1977]. There is no record of any historic volcanic or fumarolic activity.

Extent of Knowledge

Rock samples have been collected only from Horsburgh Point and the coast around Mount Oceanite. Under favorable conditions, landings would be possible at some other localities, but for the most part, rock outcrops would be accessible only with great difficulty. A comprehensive geologic study is precluded by the extensive ice cover.

Bibliography

Baker, 1978
Baker et al., 1977
Holdgate, 1963
Holdgate and Baker, 1979
Kemp and Nelson, 1931
Larsen, 1908

Copyright American Geophysical Union

E.9. BRISTOL ISLAND

Type of volcano: Stratovolcano complex.

Location: South central part of the South Sandwich Islands chain (59°02′S, 26°35′W).

Height above sea level: 1100 m.

Evidence of Holocene activity: A steaming crater was observed on the west side of the island in 1962, and recent cinders on the ice in 1964. Eruptions were witnessed in 1935 and 1956 [*Holdgate and Baker,* 1979].

Author of report: P.E. Baker.

Date of report: 1986.

Fig. E.9.1. (*a*) Sketch map of Bristol Island and Freezland Rock (inset), showing the 1964 sample localities [after *Baker,* 1978; *Holdgate and Baker,* 1979]. Stippled areas depict rock outcrop; the remainder is ice- or snow-covered ground. Regarding form lines, see Figure E.2.1 caption. (*b*) Sketch of Bristol Island and off-lying stacks, viewed from the north.

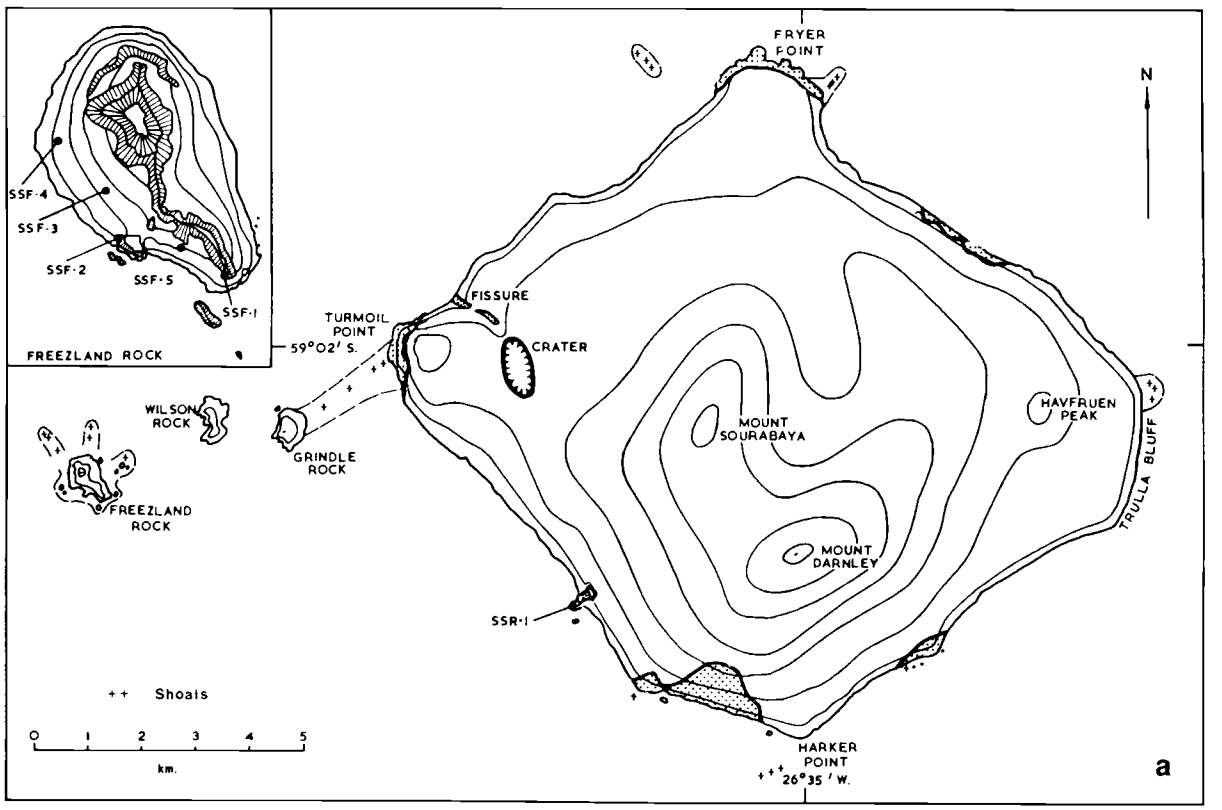

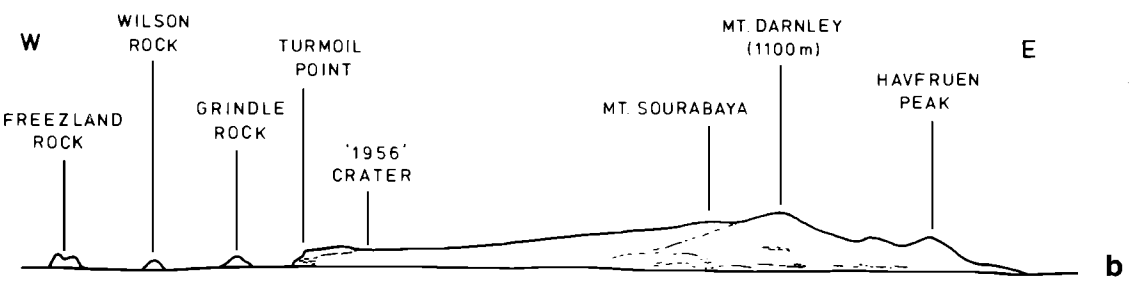

Copyright American Geophysical Union

Copyright American Geophysical Union

TABLE E.9.1. Representative Chemical Analyses and CIPW Norms of Volcanic Rocks From Bristol Island and Freezland Rock

	1	2
SiO_2	49.22	59.85
TiO_2	0.57	0.70
Al_2O_3	19.30	16.68
Fe_2O_3*	10.59	7.90
MnO	0.18	0.13
MgO	5.82	2.61
CaO	12.36	6.67
Na_2O	1.76	3.81
K_2O	0.12	1.08
P_2O_5	0.05	0.16
LOI	0.00	0.66
Total	99.97	100.25
Q	0.81	12.83
or	0.71	6.38
ab	14.89	32.24
an	44.41	25.23
di	13.70	5.72
hy	21.50	13.43
mt	1.83	1.36
il	1.08	1.33
ap	0.12	0.38
Ba	65	223
Ce	16	24
Co	35	19
Cr	43	20
Cu	107	77
La	8	<2
Nb	<1	<1
Ni	15	10
Pb	5	7
Rb	4	19
Sr	148	167
Th	<1	<1
U	<1	<1
V	238	116
Y	14	34
Zn	69	73
Zr	40	103

All analyses were made by XRF. For further details, see Table E.1.1 footnote.

*Total Fe expressed as Fe_2O_3.

1. SSR.1.1. Basalt, mid-southwestern coast of Bristol Island.
2. SSF.1.3. Andesite dike, Freezland Rock.

Bibliography

Baker, 1978
Baker et al., 1977
Holdgate, 1963
Holdgate and Baker, 1979
Hydrographic Department, 1948
Secretaria de Marina, 1958

Copyright American Geophysical Union

E.10. BELLINGSHAUSEN ISLAND

Type of volcano: Small stratovolcano.

Location: Southern Thule (59°26′S, 27°05′W).

Height above sea level: 253 m.

Evidence of Holocene activity: No historic eruptions are documented, but there is persistent and extensive fumarolic activity around the southern and eastern side of the crater rim.

Author of report: P.E. Baker.

Date of report: 1986.

Fig. E.10.1. Sketch map of Bellingshausen Island, showing the 1964 sample localities [after *Baker*, 1978; *Holdgate and Baker*, 1979]. Stippled areas depict rock outcrop, and unshaded areas denote ice- and snow-covered ground; solid black shading represents fumarolic areas. The dashed line defines the margin of the rough lava area. Regarding form lines, see Figure E.2.1 caption.

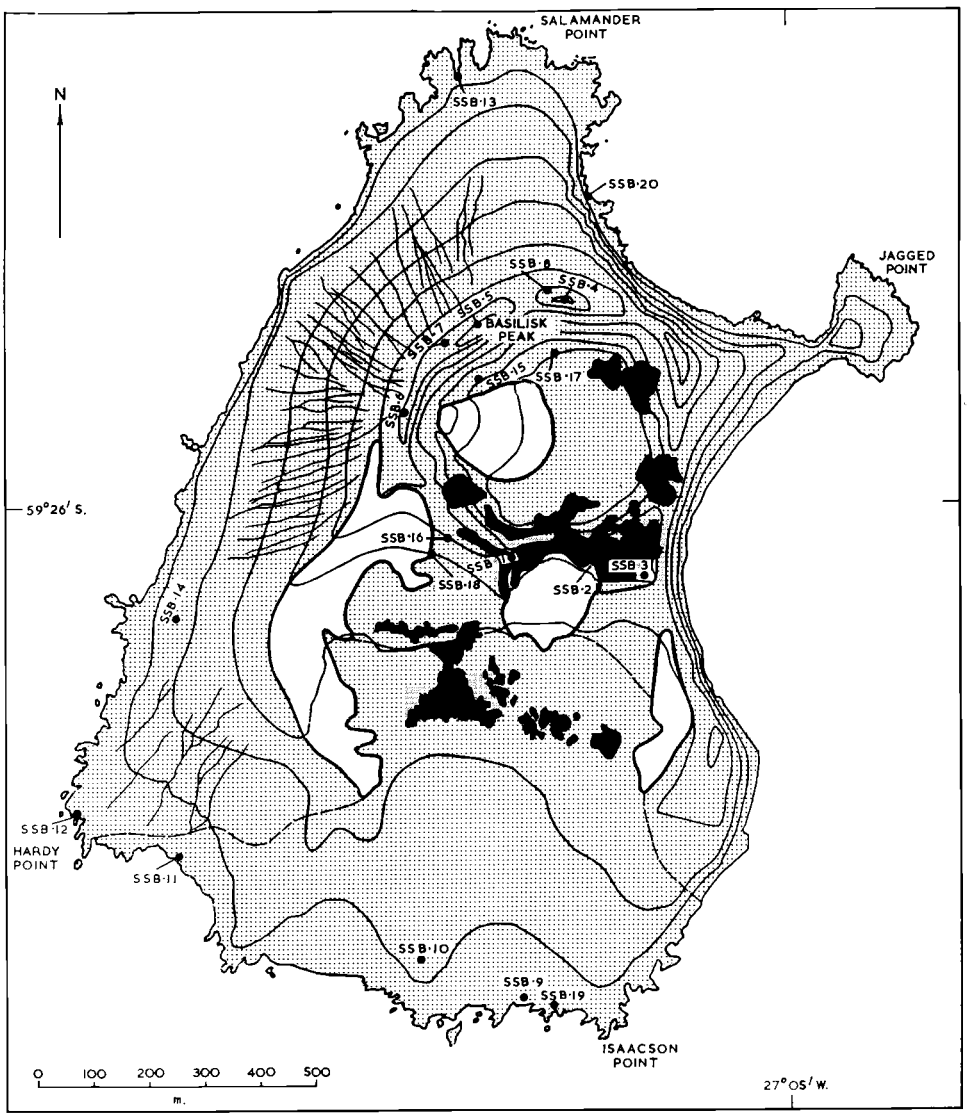

Copyright American Geophysical Union

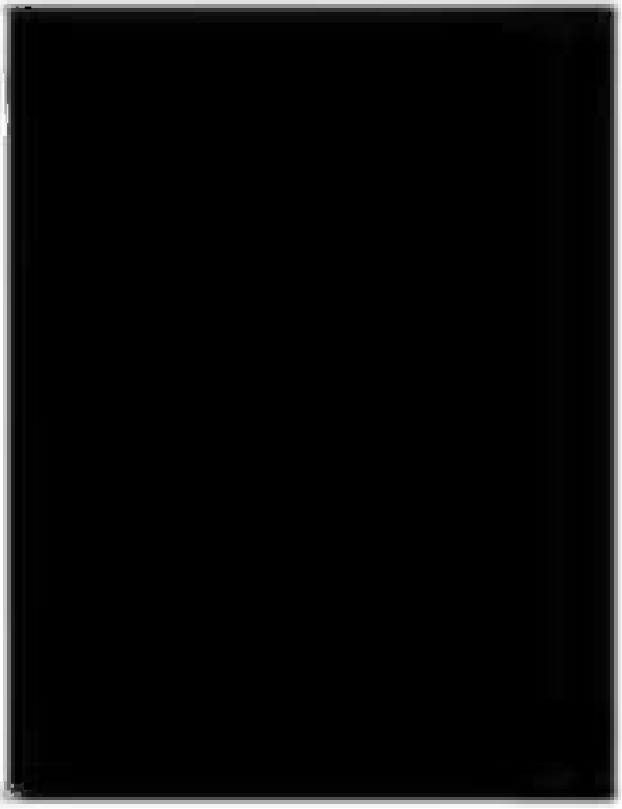

Copyright American Geophysical Union

TABLE E.10.1. Representative Chemical Analyses and CIPW Norms of Volcanic Rocks From Bellingshausen Island

	1	2
SiO_2	54.64	56.60
TiO_2	0.80	0.96
Al_2O_3	15.97	15.23
Fe_2O_3*	11.72	11.98
MnO	0.18	0.20
MgO	3.82	3.19
CaO	9.37	8.23
Na_2O	2.93	3.05
K_2O	0.45	0.55
P_2O_5	0.10	0.12
LOI	0.00	0.00
Total	99.98	100.11
Q	7.20	10.82
or	2.66	3.25
ab	24.79	25.81
an	29.10	26.25
di	14.06	11.67
hy	17.37	17.10
mt	2.02	2.06
il	1.52	1.82
ap	0.24	0.28
Ba	132	156
Ce	18	<5
Co	34	23
Cr	35	21
Cu	84	165
La	8	10
Nb	2	1
Ni	18	6
Pb	5	7
Rb	10	14
Sr	140	131
Th	3	1
U	<1	<1
V	253	232
Y	24	29
Zn	82	98
Zr	66	87

All analyses were made by XRF. For further details, see Table E.1.1 footnote.

*Total Fe expressed as Fe_2O_3.

1.SSB.15.4. Basaltic andesite, crater wall below Basilisk Peak.

2. SSB.19.1 Basaltic andesite, 100 m east of Isaacson Point.

Bibliography

Baker, 1978
Holdgate, 1963
Holdgate and Baker, 1979
Kemp and Nelson, 1931

Copyright American Geophysical Union

E.11. COOK ISLAND

Type of volcano: Stratovolcano complex.
Location: Central island of Southern Thule (59°28′S, 27°12′W).
Height above sea level: 1075 m (Mount Harmer).
Evidence of Holocene activity: None.
Author of report: P.E. Baker.
Date of report: 1986.

Form and Structure

Cook Island is approximately rectangular in outline and is almost completely surrounded by precipitous cliffs (Figure E.11.1); the interior is covered by ice. The two highest peaks, Mount Harmer and Mount Holdgate, rise from a system of ridges around the northern and eastern edges of the island. Broken glaciers plunge seaward from the high ridges, but there are also many rock outcrops in the cliffs beneath the ice. Somewhat gentler slopes grade westward from the central ice field. *Kemp and Nelson* [1931] suggested that Cook Island may be the remnant of a larger island which originally included neighboring Thule Island. They thought that the material forming both islands had been derived from

Fig. E.11.1. Sketch map of Cook Island, showing the 1964 sample locality at Reef Point [after *Baker*, 1978; *Holdgate and Baker*, 1979]. Stippled areas depict rock outcrop; the remainder is ice- or snow-covered ground. Regarding form lines, see Figure E.2.1 caption.

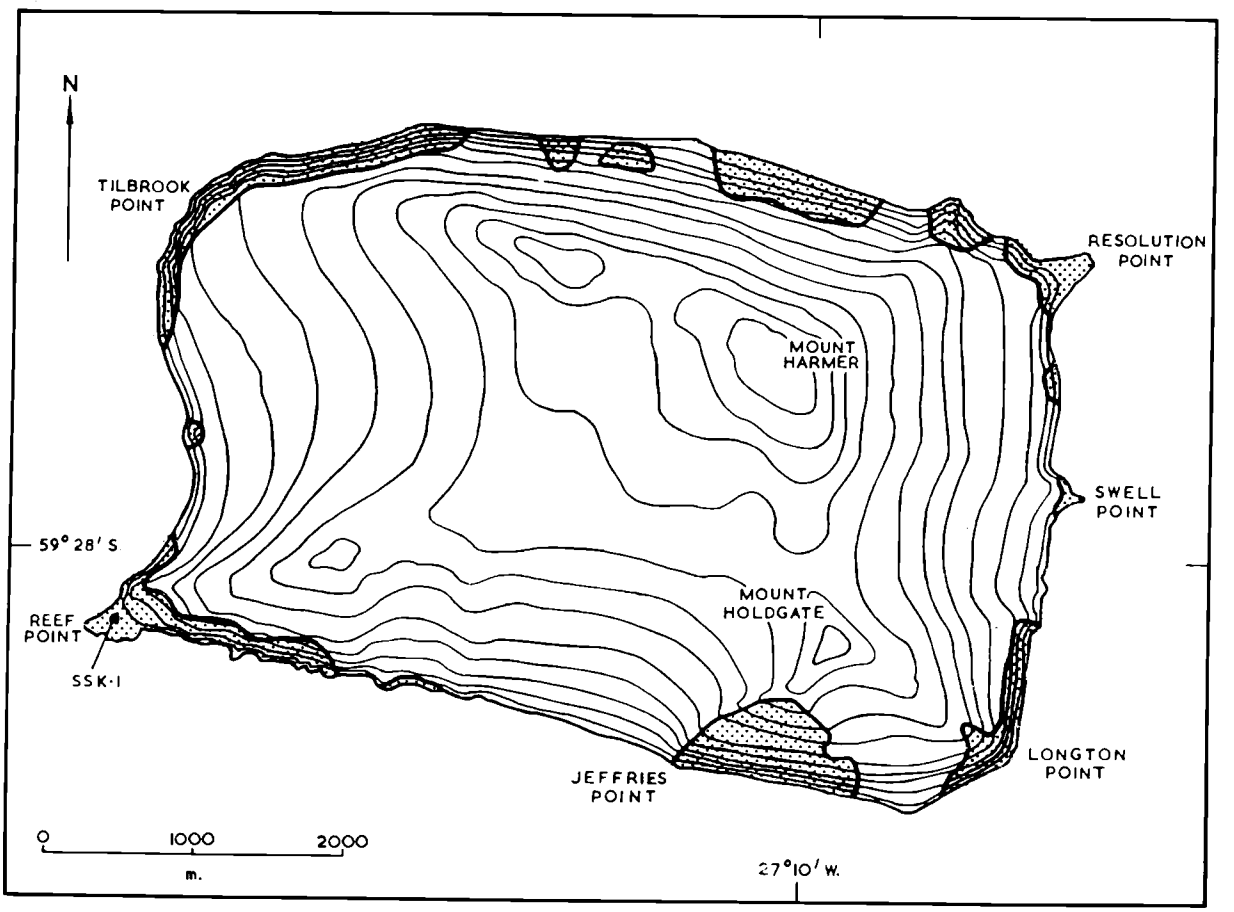

Copyright American Geophysical Union

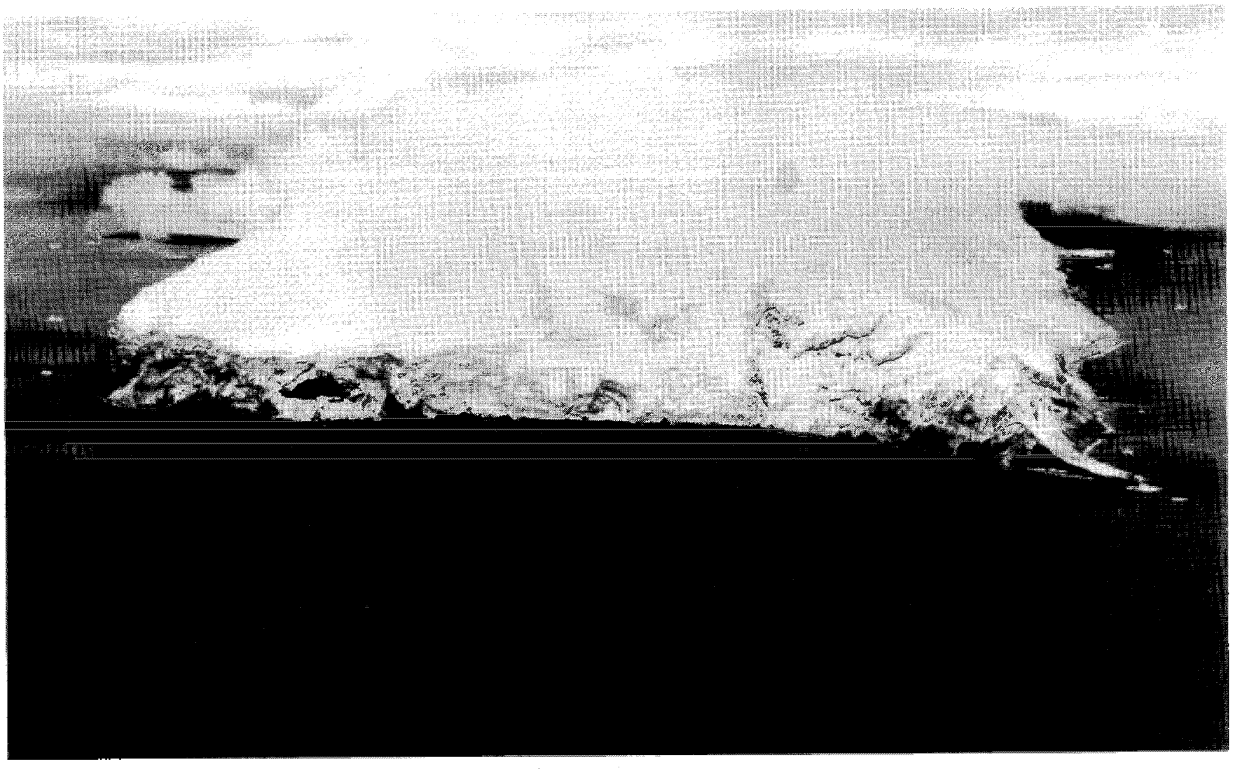

Fig. E.11.2. Oblique air photograph of Cook Island from the west; Reef Point is the low headland at right. Bellingshausen Island, partly obscured by cloud, can be seen at top left. (Photograph by P.E. Baker.)

TABLE E.11.1. Representative Chemical Analyses and CIPW Norms of Volcanic Rocks From Cook Island

	1	2
SiO_2	50.82	66.21
TiO_2	0.51	0.70
Al_2O_3	19.00	13.35
Fe_2O_3*	9.35	8.74
MnO	0.16	0.18
MgO	5.92	0.84
CaO	11.37	4.24
Na_2O	2.37	4.20
K_2O	0.23	1.58
P_2O_5	0.05	0.16
LOI	0.00	0.00
Total	99.78	100.20
Q	0.93	22.34
or	1.36	9.34
ab	20.05	35.54
an	40.53	12.91
di	12.79	6.15
hy	20.60	9.94
mt	1.61	1.51
il	0.97	1.33
ap	0.12	0.38

TABLE E.11.1. (continued)

	1	2
Ba	100	351
Ce	<5	15
Co	34	8
Cr	29	13
Cu	87	74
La	<2	10
Nb	<1	4
Ni	18	<2
Pb	8	11
Rb	4	37
Sr	149	119
Th	<1	5
U	<1	<1
V	179	35
Y	14	55
Zn	63	107
Zr	35	185

All analyses were made by XRF. For further details, see Table E.1.1 footnote.

*Total Fe expressed as Fe_2O_3.

1. SSK.1.2. Basalt, Reef Point.
2. SSK.1.3. Aphyric dacite, Reef Point.

Copyright American Geophysical Union

a large crater located in the present Douglas Strait. However, there is little to support this view, and recent observations indicate that the lavas and pyroclastic rocks were derived from a source within Cook Island itself.

Petrologic Characteristics

The only samples come from Reef Point, a 25-m-high promontory extending from the southwest corner of the island (Figure E.11.2). The point is composed of a dark, almost aphyric dacite with sparse crystals of plagioclase. A dike exposed in the high ground behind Reef Point is a dark, partly glassy aphyric andesite. A loose block of lava, presumably fallen from the country rock cut by the dike, is a strongly porphyritic basalt with phenocrysts of plagioclase, olivine, and augite. Chemically, the Reef Point dacite is a rock with 66% SiO_2, high iron, and the highest K_2O content recorded in the entire South Sandwich Islands (1.58%) (Table E.11.1). The andesite dike has 60% SiO_2, high total iron, and more than 1% K_2O.

Chronologic Data

No radiometric dates are available for Cook Island, and there is no evidence of recent volcanic or fumarolic activity.

Extent of Knowledge

Cook Island is at least 90% ice covered, and the only known landing was made at Reef Point in 1964. Under favorable conditions, landings might be possible at headlands along the east coast, but access to the interior of the island, and to other coastal exposures, would be exceedingly difficult.

Bibliography

Baker, 1978
Holdgate, 1963
Holdgate and Baker, 1979
Kemp and Nelson, 1931

Copyright American Geophysical Union

E.12. THULE ISLAND

Type of volcano: Stratovolcano.

Location: Westernmost island of Southern Thule (59°27′S, 27°22′W).

Height above sea level: 725 m (Mount Larsen).

Evidence of Holocene activity: In 1962, steam was reported rising from the water-filled summit crater, and ash was observed on the surface of the ice in the southwestern part of the island [*Holdgate,* 1963].

Author of report: P.E. Baker.

Date of report: 1986.

Form and Structure

Thule Island is an irregularly shaped, roughly triangular island about 5 km east-west (Figure E.12.1). It appears to be a single stratovolcano, composed of lava flows, scoria, agglomerates, and tuffs, with a broad summit plateau containing a small active crater slightly east of center. The highest point of the island, Mount Larsen, is on the eastern edge of this plateau, from which cliffs fall steeply to Douglas Strait. Ice-covered slopes descend more gently in other directions but end abruptly in rock or ice cliffs around the coast. Since the highest cliffs occur along the eastern, more protected side of the island, it is possible that they have formed as a result of caldera collapse in Douglas Strait. A most conspicuous promontory terminates at Hewison Point, in the southeast (Figure E.12.2); it is a lava platform with a serrated coastline about 1 km long by 0.4 km across and 10–30 m above sea level. It is believed to be a relatively recent lava flow emitted from a parasitic center above Ferguson Bay. Beach Point, another promontory in the northeast, consists of a boulder beach surrounding a low rocky ridge.

Fig. E.12.1. Sketch map of Thule Island, showing the 1964 sample localities [after *Baker,* 1978; *Holdgate and Baker,* 1979]. Stippled areas depict rock outcrop; the remainder is ice- or snow-covered ground. Regarding form lines, see Figure E.2.1 caption.

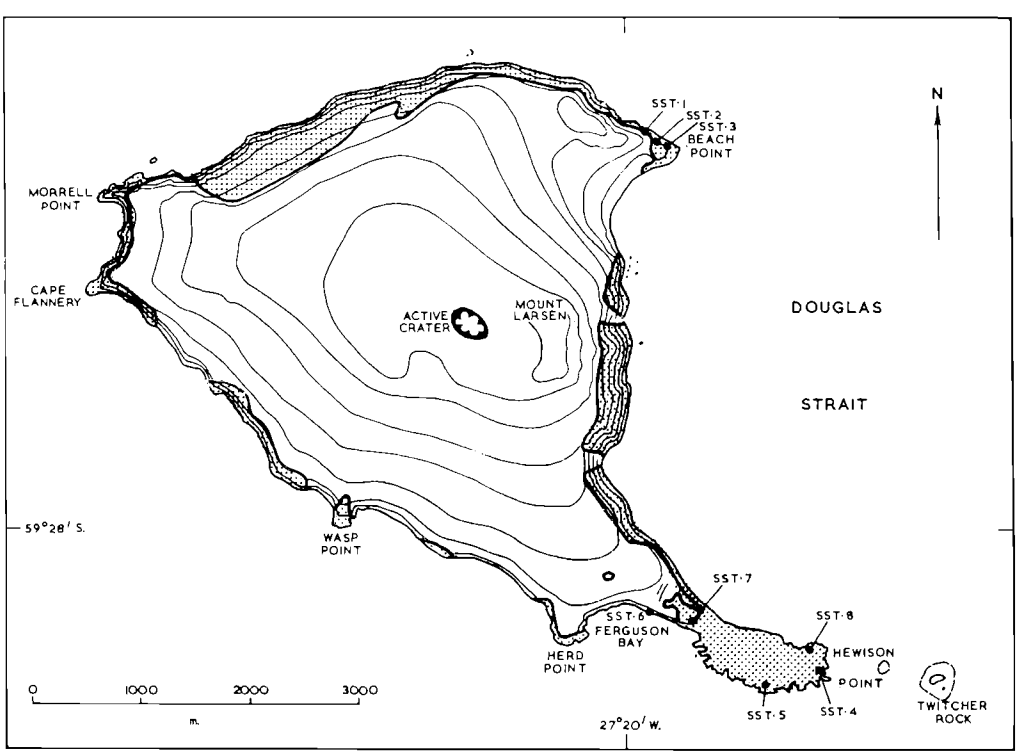

Copyright American Geophysical Union

Copyright American Geophysical Union

Petrologic Characteristics

The Hewison Point lava is an aphyric andesite with high total iron and relatively high K_2O (1.04%) (Table E.12.1) compared with other lavas from the South Sandwich Islands. *Tyrrell* [1945] described an aphyric dacite (or rhyodacite) collected from Beach Point.

Chronologic Data

No radiometric dates are available for Thule Island. It is possible that part of the island dates back to about 1 Ma, but the Hewison Point lava is relatively young, and the summit crater is known to be active [*Holdgate,* 1963].

Extent of Knowledge

Landings have been made relatively frequently on Thule Island but apparently have been confined to Beach Point and Hewison Point; the interior is largely ice covered and unknown. In favorable weather conditions, landings might be possible at some of the other headlands around the island.

Bibliography

Baker, 1978
Holdgate, 1963
Holdgate and Baker, 1979
Kemp and Nelson, 1931
Tyrrell, 1945

BIBLIOGRAPHY

Baker, P.E., Comparative volcanology and petrology of the Atlantic island-arcs, *Bull. Volcanol., 32,* 189–206, 1968.

Baker, P.E., The South Sandwich Islands, III, Petrology of the volcanic rocks, *Br. Antarct. Surv. Sci. Rep.,* no. 93, 34 pp., 1978.

Baker, P.E., F. Buckley, and D.C. Rex, Cenozoic volcanism in the Antarctic, *Philos. Trans. R. Soc. London, Ser. B, 279,* 131–142, 1977.

Barker, P.F., A spreading centre in the east Scotia Sea, *Earth Planet. Sci. Lett., 15,* 123–132, 1972.

Barker, P.F., and I.A. Hill, Back-arc extension in the Scotia Sea, *Philos. Trans. R. Soc. London, Ser. A., 300,* 249–262, 1981.

Barker, P.F., I.A. Hill, S.D. Weaver, and R.J. Pankhurst, The origin of the eastern South Scotia Ridge as an intraoceanic island arc, in *Antarctic Geoscience,* edited by C. Craddock, pp. 203–211, University of Wisconsin Press, Madison, 1982.

Barker, P.F., et al., An early Miocene Ridge Crest–Trench collision on the South Scotia Ridge near 36°W, *Tectonophysics, 102,* 315–332, 1984.

Dalziel, I.W.D., and D.H. Elliot, The Scotia arc and Antarctic margin, in *The Ocean Basins and Margins,* vol. 1, *The South Atlantic,* edited by A.E.M. Nairn and F.G. Stehli, pp. 171–246, Plenum, New York, 1973.

Fanning, E., *Voyages Round the World, With Sketches of Voyages to the South Seas, North and South Pacific Oceans, China etc. Under the Command and Agency of the Author,* O. Rich, London, 1834.

Filchner, W., *Zum sechsten Erdteil: die zweite deutsche Südpolar-Expedition,* 410 pp., Ullstein, Berlin, 1923.

Forsyth, D.W., Fault plane solutions and tectonics of the South Atlantic and Scotia Sea, *J. Geophys. Res., 80,* 1429–1443, 1975.

Gass, I.G., P.G. Harris, and M.W. Holdgate, Pumice eruption in the area of the South Sandwich Islands, *Geol. Mag., 100,* 321–330, 1963.

Hawkesworth, C.J., R.K. O'Nions, R.J. Pankhurst, P.J. Hamilton, and N.M. Evensen, A geochemical study of island-arc and back-arc tholeiites from the Scotia Sea, *Earth Planet. Sci. Lett., 36,* 253–262, 1977.

Holdgate, M.W., Observations in the South Sandwich Islands, 1962, *Polar Rec., 11,* 394–405, 1963.

Holdgate, M.W., and P.E. Baker, The South Sandwich Islands, I, General description, *Br. Antarct. Surv. Sci. Rep.,* no. 91, 76 pp., 1979.

Hydrographic Department, *The Antarctic Pilot,* 2nd ed., The Admiralty, London, 1948.

Jakeš, P., and J. Gill, Rare earth elements and the island arc tholeiitic series, *Earth Planet. Sci. Lett., 9,* 17–28, 1970.

Kemp, S., and A.L. Nelson, The South Sandwich Islands, *Discovery Rep., 3,* 133–198, 1931.

Larsen, C.A., Original report on an exploring expedition with the steam yacht *Undine* round part of South Georgia and to the South Sandwich Islands, from 5 to 21 November 1908, *Doc. SPRI MS 101/97,* 10 pp., Scott Polar Res. Inst., Cambridge, England, 1908.

Morrell, B., *A Narrative of Four Voyages to the South Sea, North and South Pacific Ocean, Chinese Sea, Ethiopic and Southern Atlantic Ocean, Indian and Antarctic Ocean, From the Year 1822–1831,* Harper, New York, 1832.

Secretaria de Marina, *Derrotero Argentino, V, Antártida y archipielagos subantárticos Argentinos,* Buenos Aires, Argentina, 1958.

Tomblin, J.F., The South Sandwich Islands, II, The geology of Candlemas Island, *Br. Antarct. Surv. Sci. Rep.,* no. 92, 33 pp., 1979.

Tyrrell, G.W., Report on rocks from West Antarctica and the Scotia arc, *Discovery Rep., 23,* 37–102, 1945.

Copyright American Geophysical Union

Copyright American Geophysical Union

Summary

W.J. Verwoerd, L. Chevallier, and J.W. Thomson

Frontispiece. "Ice and Fire" on Marion Island: blue ice grotto and 20-m ice cliff formed by melting back of small ice cap at western end of summit plateau, as a result of black aa lava (right foreground) erupted from a radial fissure sometime during 1980. (Photograph by G. Kerley, 1981.)

Introduction

This section describes a widely scattered group of oceanic islands on the Antarctic plate (see map inside front cover and Table F.I). Six individual volcanic islands (see individual volcano descriptions (IVD's) F.1–F.3, F.6, and F.7) and three archipelagoes (Îles Crozet, Îles Kerguelen, and the McDonald Islands; see IVD's F.4, F.5, and F.6) lie between Antarctica and the Southwest and Southeast Indian Ocean ridges, i.e., from about 0° to 90°E (Figure F.I). The Balleny Islands and Scott Island (see IVD's F.9 and F.10) are located 250–300 km northeast and northwest, respectively, of Victoria Land, Antarctica, between 160°E and 180°. Peter I Island (see IVD F.11) is an isolated island in the Bellingshausen Sea, at 90°W and 400 km north of the Eights Coast of Antarctica. Although Gaussberg (see IVD F.8), on the Antarctic continent itself, is not an oceanic island volcano, it is compositionally unlike any other volcano on the Antarctic plate, and it is included here because it cannot be grouped conveniently with any of the volcanoes described in the other sections.

All the islands are uninhabited except by temporary scientific personnel. Bouvetøya is under Norwegian jurisdiction and is occasionally visited by Norwegian and South African ships, mainly for meteorological purposes. Marion and Prince Edward islands are South African territory; a meteorological station, manned throughout the year by a team of 12–14 people, has been maintained on the former since 1948. The only way to reach these two islands is by relief ship from Cape Town during April and September each year. A decision not to construct a landing strip for aircraft on Marion Island was made in 1987 after a thorough environmental impact assessment. Access to Prince Edward Island is strictly controlled for reasons of nature conservation. Heard Island, belonging to Australia, supported a research base between 1947 and 1955. Several of the other islands are part of the Terres Australes et Antarctiques Françaises (TAAF); a manned meteorological station (Port-aux-Français) was established on Îles Kerguelen in 1949, and another (Alfred Faure) on Île de la Possession (in the Crozet

Copyright American Geophysical Union

TABLE F.I. Oceanic Island Volcanoes of the Antarctic Plate

Volcano (IVD)	Analyzed Rock Compositions	K-Ar Indicated Age Range*
1. Big Ben, Heard Island (F.6) (53°06′S, 73°30′E)	Basanite, alkali basalt, trachybasalt, trachyandesite, trachyte	Pleistocene–Present
2. Marion Island (F.2) (46°54′S, 37°45′E)	Alkali basalt, hawaiite, mugearite, benmoreite	Pleistocene–Present
3. Saint Paul Island (F.7) (38°43′S, 77°33′E)	Aluminous tholeiitic basalt	Pleistocene–Present
4. McDonald Islands (F.6) (53°02′S, 72°36′E)	Phonolite	Pleistocene–Holocene (?)**
5. Prince Edward Island (F.3) (46°38′S, 37°57′E)	Alkali basalt, ankaramite, hawaiite, trachybasalt, trachyte	Pleistocene–Holocene (?)
6. Amsterdam Island (F.7) (37°50′S, 77°30′E)	Transitional tholeiite	Pleistocene–Holocene (?)
7. Bouvetøya (F.1) (54°25′S, 3°21′E)	Transitional alkali basalt, hawaiite, mugearite, benmoreite, trachyte, alkali rhyolite (comendite)	Pleistocene–Holocene (?)
8. Île aux Cochons, Crozet group (F.4) (46°06′S, 50°14′E)	Alkali basalt	Pleistocene–Holocene (?)
9. Rallier du Baty fissure eruption, Île Kerguelen (F.5) (49°37′S, 68°52′E)	Trachyte	Pleistocene–Holocene (?)
10. Gaussberg, Antarctica (F.8) (66°47′S, 89°18′E)	Olivine leucitite	Pleistocene
11. Île de la Possession, Crozet group (F.4) (46°25′S, 51°38′E)	Alkali basalt, ankaramite, basanite, trachybasalt, trachyphonolite	Pliocene–Holocene (?)
12. Île de l'Est, Crozet group (F.4) (46°26′S, 52°12′E)	Alkali basalt, oceanite, ankaramite, hawaiite	Miocene–Holocene (?)
13. Mont Ross stratovolcano, Île Kerguelen (F.5) (49°31′S, 69°30′E)	Alkali basalt, hawaiite, mugearite, *ne*-trachyte, phonolite	Pliocene–Holocene (?)
14. Balleny Islands (F.9) (66°57′S, 163°30′E)	Basanite, hawaiite	(Miocene–Present)
15. Peter I Island (F.11) (68°51′S, 90°35′W)	Basalt, trachyte	Miocene–Holocene (?)
16. Courbet shield volcano, Île Kerguelen (F.5) (49°15′S, 70°00′E)	Basanite, *ne*-basalt, basalt, andesite, trachyte, alkali rhyolite	Miocene
17. Île des Pingouins, Crozet group (F.4) (46°30′S, 50°24′E)	?	Miocene
18. Scott Island (F.10) (67°30′S, 180°00′)	*ne*-mugearite, phonolite	?

*Listed approximately in order of increasing age. "Present" means historically active; age range in parentheses is inferred from magnetic anomalies and paleontologic data.

**Holocene (?) notation is based on occurrence of samples too young to be dated by K-Ar (<0.2 Ma), and/or fumarolic activity, and/or geomorphologic evidence such as poorly vegetated lava flows and well-preserved scoria cones.

Copyright American Geophysical Union

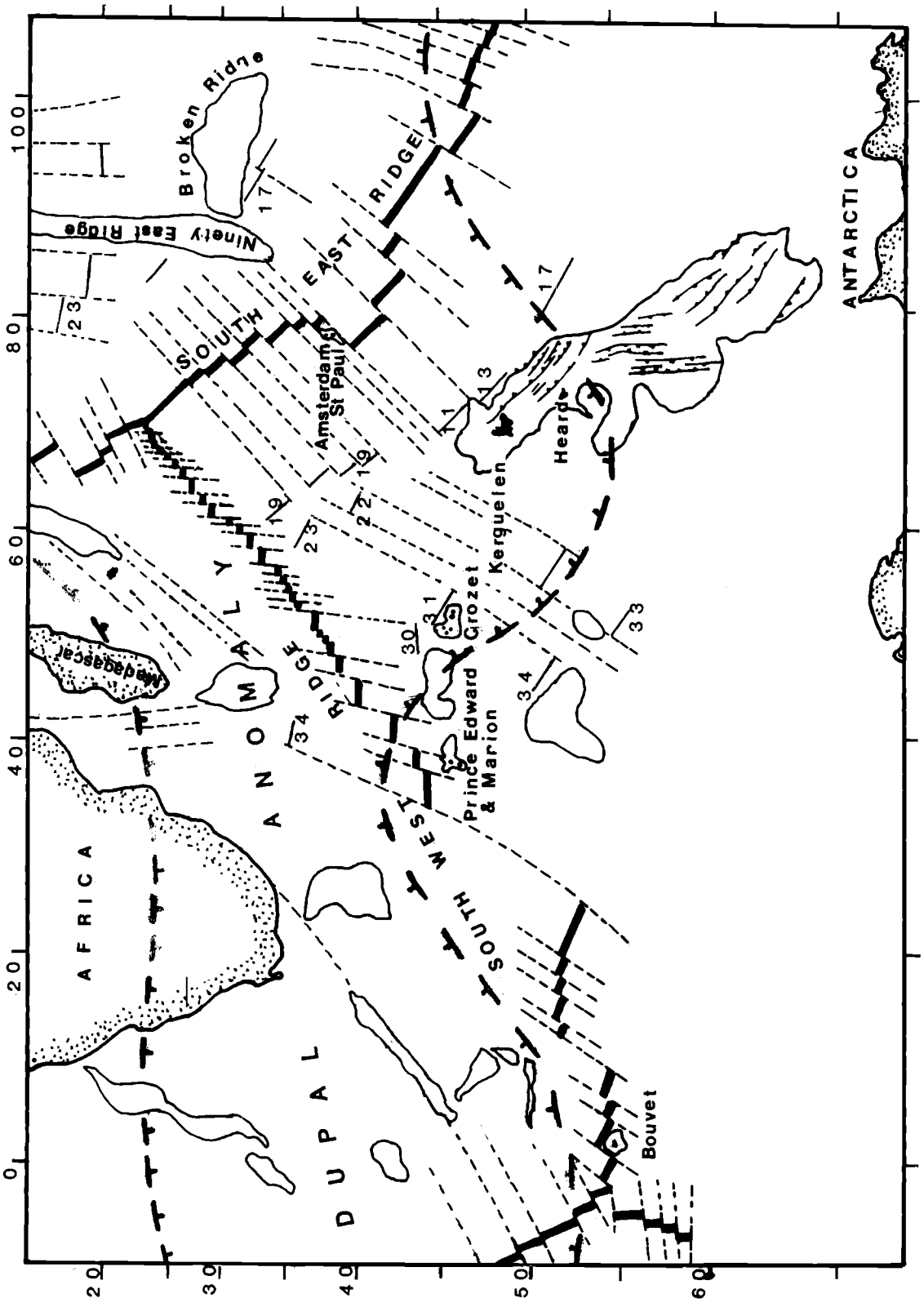

Fig. F.I. Oceanic volcanic islands of the southern Indian and Atlantic oceans. Also shown are mid-ocean ridge crests and associated transforms, numbered magnetic anomalies, aseismic submarine plateaus and associated faults, and approximate boundaries of the Dupal anomaly (spiked line) as delineated by $^{87}Sr/^{86}Sr = 0.7040$ [*Hart*, 1984].

Copyright American Geophysical Union

group) in 1964; Amsterdam Island also has a base (La Roche Godon). These stations are normally visited twice per year by ship from Réunion. A crayfish factory and harbor were constructed on Saint Paul Island in 1928 and 1938, respectively, but are no longer in operation. During the nineteenth and early twentieth centuries these islands often harbored shipwrecked sailors and seal hunters. No scientific stations have been established on the Balleny Islands, Scott Island, or Peter I Island because heavy pack ice in summer makes yearly access to them difficult or impossible. Few landings have been made on any of these remote southern islands; Scott Island has not been investigated geologically since 1902.

Extent of Knowledge

Saint Paul and Amsterdam islands were probably the first to be discovered. They were reported by Antonie van Diemen in 1633 but may have been sighted earlier by Magellan returning to Europe in 1522 and by a Dutch vessel, the *Zeewolf*, in 1617. Captain François Lozier-Bouvet discovered the island named after him in 1739 on a quest for the "great southern continent." The discovery of Marion and Prince Edward islands (the latter named by Captain Cook after the fourth son of King George III) is usually credited to the French explorer Nicolas Marion-Dufresne in 1772, although the Dutch skipper Barent Ham reported two islands named Dina and Maerseveen in the same general area in 1663. Îles Crozet, named after Marion-Dufresne's lieutenant, were sighted a few days after Marion and Prince Edward islands, on the same ill-fated voyage that ended with Marion-Dufresne's death in New Zealand. In the same year, 1772, Yves Kerguelen-Tremarec first set foot on Îles Kerguelen. Although Peter I Island was seen for the first time in 1821, by Captain von Bellingshausen, no landing was made until 1929. Heard Island was apparently not sighted before 1833, and the first sighting of the Balleny Islands was made a few years later, in February 1839. Scott Island was discovered in December 1902 by Lieutenant William Colbeck of *Morning*, the relief ship for Captain Scott's expedition.

Apart from reports resulting from the famous *Challenger* (1874), *Valdivia* (1898), *Gauss* (1901–1903), *Discovery II* (1929), and *Bougainville* (1939) expeditions, as well as pioneering work by E. Aubert de la Rüe on Îles Kerguelen in 1928–1931, geological research on most of these islands did not start in earnest until the 1960s.

Physical Volcanology

Marion and Heard islands are active volcanoes which last erupted in 1980 and 1987, respectively. Fumarolic activity is known on Bouvetøya, Île de la Possession, Îles Kerguelen, and Saint Paul Island. Evidence of very recent eruptions is also present on Amsterdam and Prince Edward islands and Île aux Cochons, and there were reported sightings of volcanic activity in the Balleny Islands during the nineteenth century. The other islands described in this section show varying degrees of erosion, but a renewal of eruptive activity is nowhere excluded.

The volcanic islands of the Antarctic plate have certain morphological characteristics in common. With few exceptions (e.g., Mont Ross, on Îles Kerguelen (see IVD F.5), and Big Ben, on Heard Island (see IVD F.6), with its 10°–20° slope) they are basaltic shield volcanoes that have undergone various degrees of subsidence by faulting and of erosion by glaciers and the sea. Most were built in two or more stages. Holocene activity of a uniform Strombolian type is recognizable on every major island in the Indian Ocean described here, and it is clearly demarcated from the earlier stages by unconformable relationships.

Petrology and Geochemistry

The most primitive lavas in these oceanic islands are the altered tholeiites of Saint Paul Island (see IVD F.7) and the transitional basalts forming the older basement of Îles Kerguelen (see IVD F.5), Île de l'Est (see IVD F.4), and Amsterdam Island (see IVD F.7). The basement is intruded by plutonic bodies (gabbro, pyroxenite, and diorite) and metamorphosed to the epidote-zeolite facies. The shield-building phase on these islands was dominated by an alkali basalt–hawaiite–trachybasalt crystal fractionation sequence. On Bouvetøya (see IVD F.1), Îles Kerguelen, and Saint Paul Island the ultimate products are oversaturated (soda rhyolite or comendite), but an undersaturated trend, leading to trachyte and phonolite, is also present

Copyright American Geophysical Union

on Îles Kerguelen, McDonald Island (see IVD F.6), Île de la Possession (see IVD F.4), and Scott Island (see IVD F.10). Related to these two trends are the volcano-plutonic ring complexes of Îles Kerguelen, with their fayalite-syenites and alkali granites (Péninsule Rallier du Baty) and olivine gabbro/nepheline-syenite association (Montagnes Vertes). The Holocene Strombolian products consist, without exception, of alkali basalts.

Isotopic studies by *Collerson and McCulloch* [1983] indicate that the leucitite from Gaussberg was derived from an enriched mantle source. Other isotopic studies by *Dosso et al.* [1979] and *Dosso and Murthy* [1980] have shown conclusively that the Kerguelen archipelago is not a continental fragment but that its igneous rocks were derived from an enriched mantle source. *Dupré and Allègre* [1983] demonstrated that most islands, as well as ocean floor basalts of the southern Indian and Atlantic oceans, have a characteristically enriched Pb-Sr isotopic signature. *Hart* [1984] proposed that this domain forms part of a globe-encircling isotopic anomaly centered on latitude 30°S (termed the Dupal anomaly (Figure F.I)) and argued that it has been in existence for billions of years. Geochemical characteristics of Dupal hotspots are high $^{87}Sr/^{86}Sr$ (>0.7040), high Ba/Nb (8–22), and high La/Nb (0.75–1.25), whereas non-Dupal hotspots (including Marion and Prince Edward islands and Bouvetøya) have low $^{87}Sr/^{86}Sr$ (<0.7040), low Ba/Nb (<9), and low La/Nb (<0.6) [*le Roex*, 1986]. No agreement has been reached on the causes for these differences. *White* [1985] questioned the validity of a systematic geographic distribution and considered it more likely that five or more distinct classes of oceanic basalt (based on Sr, Nd, and Pb isotope ratios) represent different mantle reservoirs that evolved via a limited number of processes. Indeed, *Mukasa et al.* [1987] found that the Dupal signature is not restricted to the southern hemisphere, or to mid-ocean ridge basalt (MORB) and ocean island basalt (OIB), since it also characterizes subduction-related lavas of the Philippine island arc. In addition, *Duncan et al.* [1986] showed that both Dupal and non-Dupal mantle reservoirs have been tapped at a single island of the Marquesas group. It is thus perhaps premature to describe a large section of the mantle beneath Tristan da Cunha, Îles Crozet, Îles Kerguelen, and Amsterdam Island as geochemically anomalous.

Comparative Geochronology

An important question is whether volcanic activity on these oceanic islands is synchronous or not. In broad outline this is apparently true: none are extinct, and Holocene activity has been recognized or inferred on all of them (except Îles des Apôtres and Île des Pingouins (see IVD F.4) and Scott Island (see IVD F.10), which are unimportant on account of their small size). Holocene flows have not been reliably dated, but there is good correlation between raised beaches on most islands in the Indian Ocean; the last one, at 3 m, could be attributed to the climatic optimum of 5500 years B.P. A major unconformity coincides with the retreat of glaciers about 11,000 years B.P.; it is marked by moraine and striated pavements on the larger islands (Marion Island, Île de la Possession, Île de l'Est, and Îles Kerguelen). On the basis of variations in vegetation cover of lava flows, palynology, and ^{14}C dates on swamps, eruptive activity can be considered essentially continuous, at a slow rate, since that time.

Detailed correlation of Tertiary and Pleistocene events is not possible, owing to inaccessibility or the altered character of basal units, limited sampling, and limited resolution of the K-Ar method of dating. No radiometric ages have been determined for the volcanic rocks on the Balleny Islands and Scott Island, and only one date (12.8 ± 1.5 Ma) has been obtained from Peter I Island. However, all the available K-Ar dates for the Indian Ocean islands and Bouvetøya are compared on a correlation chart (Figure F.II). Îles Kerguelen are more deeply dissected (perhaps older) than the others, the earliest date being 39 Ma on a gabbroic plug. Flood basalts are thought to have started in the Eocene and continued until the end of the Miocene (5–6 Ma). It would be interesting if lavas from the other aseismic plateaus (e.g., Marion Island, Del Cano) could be dated and compared with those of Îles Kerguelen. Pliocene and early Pleistocene dates have been obtained on the volcanic basements of Île de la Possession, Île de l'Est, and Îles des Apôtres (see IVD F.4), Heard Island(?) (see IVD F.6), and Îles Kerguelen (see IVD F.5), followed by an unconformity at about 1 Ma. It seems likely that Bouvetøya, Marion and Prince Edward islands, and Île aux Cochons are younger islands that may have originated about this time, because they present no evidence of an older basement; the positions of Amsterdam and Saint Paul islands in this sequence

Copyright American Geophysical Union

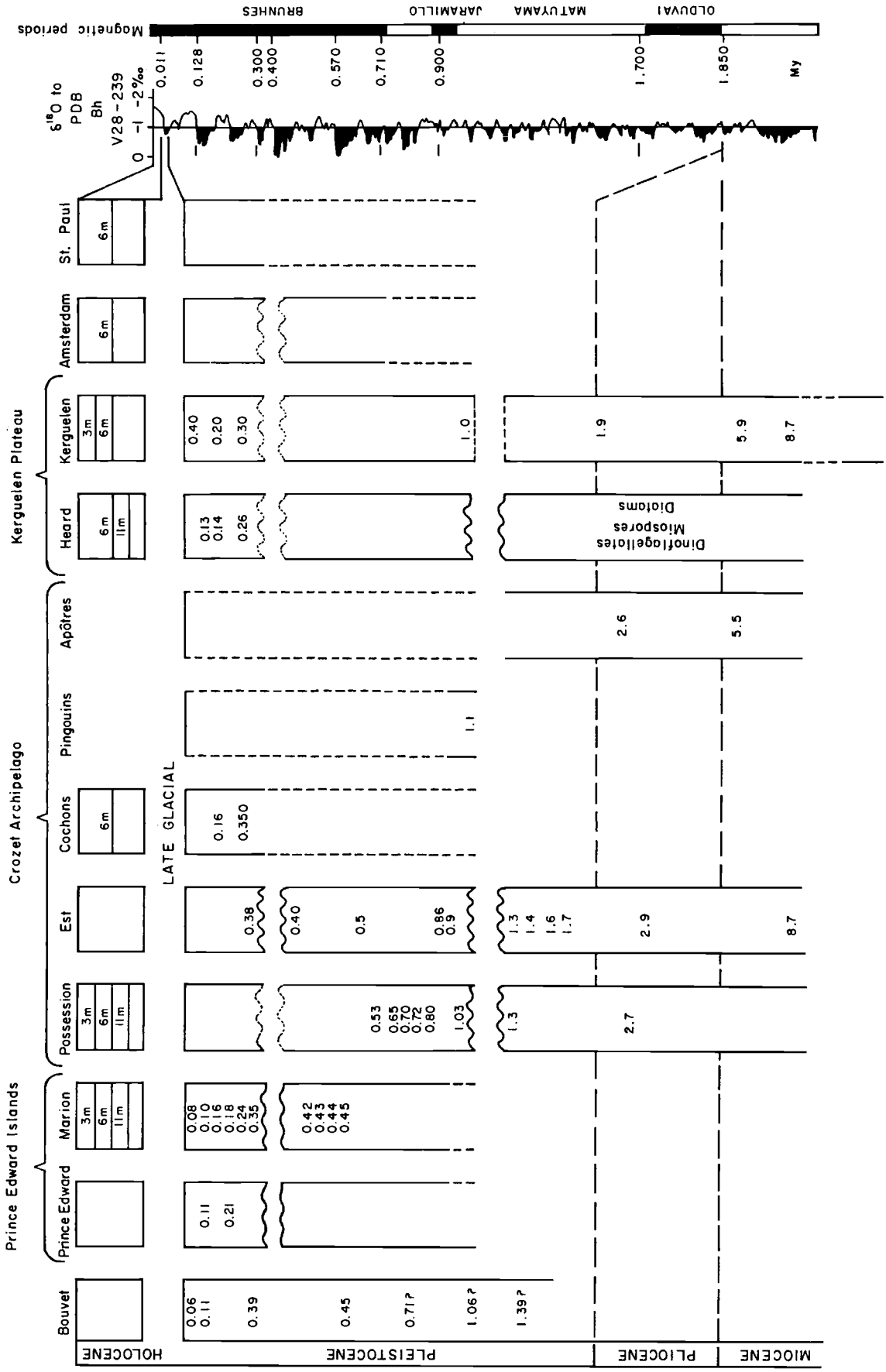

Fig. F.II. Comparative geochronology of southern Indian and Atlantic ocean islands. Figures are K-Ar dates (Ma) of lavas (Miocene-Pleistocene) and heights in meters of raised beach terraces (Holocene). The last two columns on the right are glacial cycles based on oxygen isotope measurements of a Pacific deep-sea sediment borehole core [*Shackleton and Opdyke*, 1976] and the corresponding geomagnetic polarity time scale. Data are from *Prestvik and Winsnes* [1981] for Bouvetøya; *McDougall* [1971, and personal communication, 1985] for Marion and Prince Edward islands; *Cantagrel et al.* [1980], *Chevallier et al.* [1983], and Cantagrel (personal communication, 1985) for Îles Crozet; *Stephenson* [1964], *Clarke et al.* [1983], and *Quilty et al.* [1983] for Heard Island; *Giret and Lameyre* [1983] and *Nougier et al.* [1983] for Îles Kerguelen; and *Nougier* [1982] for Amsterdam and Saint Paul islands.

Copyright American Geophysical Union

are uncertain owing to the lack of data. Another widespread unconformity, perhaps related to a common tectonic event, occurred on most of the islands around 0.38–0.40 Ma. It seems that volcanic activity continued more or less without interruption during the last 300,000 years of the Pleistocene epoch on Marion and Prince Edward islands, Îles aux Cochons, Heard Island, Îles Kerguelen, and perhaps Bouvetøya but came to an end on Île de la Possession and Île de l'Est before the onset of the last glacial period.

Tectonic Relationships

A currently popular theory holds that volcanically active oceanic islands or "hotspots" mark the sites of fixed mantle plumes that can be used as a frame of reference for measuring the movement of lithospheric plates over them. The plume theory explains the alkaline geochemical composition of OIB by derivation from deeper mantle sources than MORB, but its application is not without difficulties.

The southern Indian and Atlantic oceans lack well-defined linear island and seamount chains that can be interpreted as hotspot tracks by analogy with Hawaii and the Emperor seamounts of the Pacific plate. Bathymetric features in the Atlantic Ocean floor correspond reasonably well with postulated hotspot tracks based on relative motions of the African and South American plates determined by matching magnetic anomalies, but the relative ages of these features are not well constrained. *Morgan* [1983] pointed out that magnetic anomalies are much better mapped in the Atlantic than in the Indian Ocean and that errors in the plate tectonic reconstruction of the Indian Ocean are expected to yield mismatch of hotspot tracks. *Duncan* [1978, 1981] attempted to trace these tracks in the area under review, and *Hartnady and le Roex* [1985] revised the position of the Bouvetøya track. According to these authors, Bouvetøya, Marion Island, and Îles Kerguelen are the longest continually active hotspots and produced subparallel aseismic lineaments: Madagascar Ridge in the case of Marion Island and Ninetyeast Ridge in the case of Îles Kerguelen and Heard Island. Hotspots which began more recently (Îles Crozet, Ob seamount, Gaussberg) exhibit shorter lineaments consistent with absolute motion of the African plate. The model also predicts that the Antarctic plate is barely moving over the hotspot network [*Duncan*, 1981]. It appears to have been slow enough to allow extensive volcanism at Îles Kerguelen over the last 39 m.y. According to *Duncan* [1978] the hotspot that generated Ninetyeast Ridge is now located beneath Heard Island. Slow northwestward movement of the Antarctic plate should have left a hotspot track between Heard Island and Îles Kerguelen. Indeed, a line of three seamounts was recently discovered in this position [*Coffin et al.*, 1986]. Amsterdam and Saint Paul islands, 1200 km north of Îles Kerguelen, do not seem to fit into either the hotspot track or the fracture zone patterns. They are situated at the mid-ocean ridge crest 80 km north-south of one another and have been interpreted rather speculatively as the terminus of an asthenospheric channel or "pipeline" that feeds the ridge horizontally from the Îles Kerguelen hotspot [*Morgan*, 1978]. Gaussberg volcano, in Antarctica, although geochemically distinct from Kerguelen Plateau volcanic rocks, lies on an extension of the Kerguelen-Heard trend and the trend of submarine plateaus, but such a hotspot track will be difficult to reconcile with previously determined Antarctic plate motions. The existence of hotspot tracks is plausible only if linear features become progressively younger in the direction of inferred plate movement; unfortunately, this has been demonstrated in just one instance in the Indian Ocean, namely, Ninetyeast Ridge [*Duncan*, 1978].

In an alternative approach, linear bathymetric features like Agulhas Ridge, Ninetyeast Ridge, and part of Madagascar Ridge are ascribed to voluminous eruptions along "leaky" fracture zones. This is in accordance with *Sykes'* [1978] explanation of intraplate alkaline volcanism on the continents. Pairs of aseismic plateaus like Kerguelen/Broken Ridge in the east and Madagascar Ridge/Del Cano in the west are symmetrical with respect to the ridge axes. *Goslin and Patriat* [1984] proposed that these volcanic plateaus formed at different times on the mid-ocean ridge and migrated to intraplate positions with seafloor spreading. It implies that the plateaus are built of MORB and that the association of some of them with OIB appearing as hotspots is fortuitous. *Chevallier and Vatin-Perignon* [1982] suggested that volcanism on Réunion resulted from the reactivation of a 60 Ma extinct paleorift. The importance of structural control was also emphasized for Îles Kerguelen by *Giret*

Copyright American Geophysical Union

[1983], for Marion and Prince Edward islands by *Chevallier* [1986], and for Îles Comores by *Nougier et al.* [1986]. The alkaline nature of the volcanism and the systematic orientation of the fractures imply that the structural control is deep seated and regional, i.e., intimately connected with plate tectonics, but these authors do not find it necessary to postulate plume-like sources decoupled from the lithosphere.

Both theories agree that the volcanic islands of the southern Indian and Atlantic oceans belong to an intraplate tectonic setting and are clearly distinguishable from subduction-related volcanism.

Copyright American Geophysical Union

F.1. BOUVETØYA

Type of volcano: Ice-capped shield volcano surmounted by a 3.5-km-wide caldera.

Location: South Atlantic Ocean (54°25′S, 3°21′E), about 2600 km south-southwest of Cape Town.

Height above sea level: ~780 m.

Estimated volume: 2000 km^3 (25 km^3 above sea level) [*Imsland et al.*, 1977].

Evidence of Holocene activity: Fumaroles occur near the caldera.

Author of report: W.J. Verwoerd.

Date of report: July 1987.

Form and Structure

Bouvetøya is a solitary island with an area of 55 km^2, of which 95% is covered by ice (Figure F.1.1). It is asymmetric as a result of marine erosion, with precipitous cliffs in the west and a breach of the caldera in the northwest (Figure F.1.2). The ice cap and probably the underlying lava flows dip 8° eastward from the top of the caldera rim. Gently dipping (15°–17°) lava flows and pyroclastic deposits close to the volcanic center are exposed along the steep southwestern coast as a result of vigorous wave action under the influence of westerly winds. These low dips are more characteristic of a volcanic shield than a stratovolcano. A 3- to 4-km-wide wave-cut shelf surrounds the island.

Bouvetøya is built of two formations: a lower, hydrothermally altered sequence of mainly pyroclastic (partly hyaloclastite) rocks and an upper formation of predominantly subaerial basaltic lava flows [*Prestvik and Winsnes*, 1981]. The transition is believed to represent the time when the structure became rigid enough to prevent seawater from entering the vents. Both basic and silicic dikes can be seen on the west coast. The only evidence of possible late-stage parasitic eruptions is the columnar-jointed extrusive rhyolite dome at Cape (Kapp) Valdivia and a small rhyolite flow on Lars Island (Larsøya). The 3.5-km-wide amphitheater known as "Wilhelmplatået" is the result of caldera collapse, but it is not known whether the breach in the north is mainly due to volcanism, slope failure, glacial action, or marine erosion.

Controversy surrounds the interpretation of a new beach (Westwindstranda) and raised platform (Nyrøysa) behind it. This feature was formed at the foot of a steep recess in the cliffs of the northwest coast sometime between 1955 and 1958 (inclusive). *Baker and Tomblin* [1964] originally described it as the result of the extrusion of a small volume of highly viscous lava (later termed benmoreite), accompanied by the uplift of a larger volume of older lava and pyroclastics. *Baker* [1967] elaborated on this, describing the chaotic assemblage as a carapace of older volcanic rocks carried along and fragmented during the ascent of the benmoreite magma, which was just able to break through as small dome-like protrusions and short blocky flows, probably preceded by an explosive phase which scattered vesicular blocks of benmoreite onto the surface. *Lunde* [1965] interpreted the structure of the flow as giant broken pillows, and thus the result of a submarine eruption. *Verwoerd et al.* [1976] regarded the "domes" as huge blocks embedded in debris and found no indications of recently solidified lava; they interpreted the platform as an avalanche deposit. *Furnes and Løvlie* [1978] rejected this on the basis of the constant magnetic polarity found in different blocks and proposed that the eruption started subglacially but ended as a subaerial block lava. Finally, *Prestvik and Winsnes* [1981] obtained K-Ar dates of 0.45–0.5 Ma for the benmoreite, thus discrediting the recent eruption. They also found that the internal structure of the platform retained much of its original stratigraphy, concluding that it came down the slope as a landslide rather than an avalanche, in accordance with the magnetic measurements.

Petrologic Characteristics

Bouvetøya volcano is located among the western rift mountains off the Southwest Indian Ridge, in the general vicinity of the triple junction between the African, South American, and Antarctic plates. The island has been regarded as the surface expression of a mantle plume which caused the breakup of the Gondwanaland supercontinent, and for this reason the petrology and geochemistry of its lavas have attracted considerable attention. These lavas also provide an ideal opportunity for testing crystal fractionation models uncomplicated by sialic crust.

There is general agreement that the Bouvetøya rocks represent a mildly alkaline (i.e., transitional) suite between tholeiitic and alkaline. (The "tholeiites" reported by *O'Nions and Pankhurst* [1974] were shown to be hydrothermally altered hawaiites by *Prestvik and Winsnes* [1981].) The series extends from basic to intermediate to acid. Representative analyses (Table F.1.1) are from *Verwoerd et al.* [1976] and *le Roex and Erlank* [1982], and their terminology will be used. *Imsland et al.* [1977], *Prestvik and Winsnes* [1981], and *Prestvik* [1982*a*] prefer

Copyright American Geophysical Union

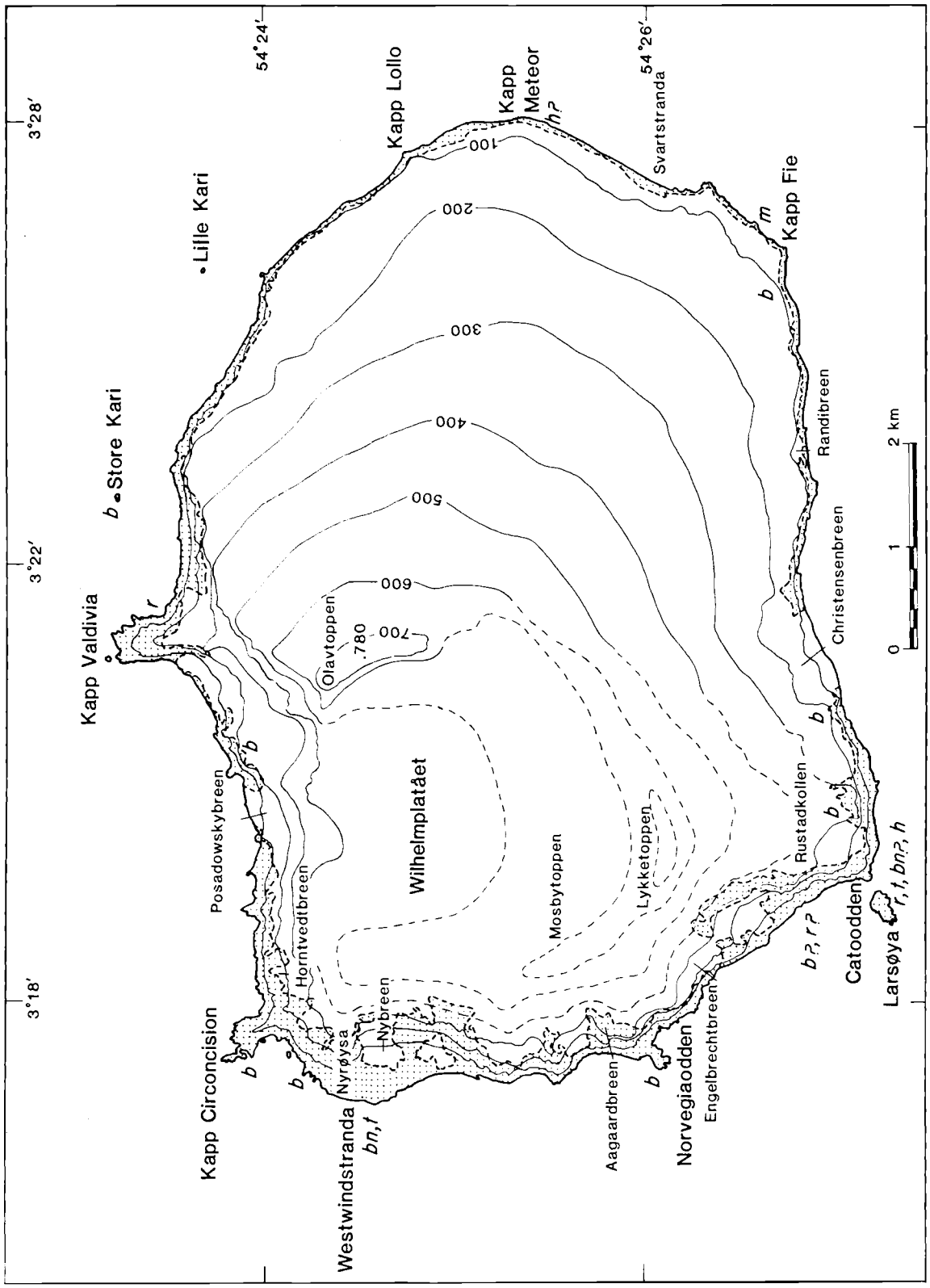

Fig. F.1.1. Sketch map of Bouvetøya showing the distribution of exposed rock (stippled areas): b, transitional basalt; h, hawaiite; m, mugearite; bn, benmoreite; t, trachyte; r, rhyolite.

Copyright American Geophysical Union

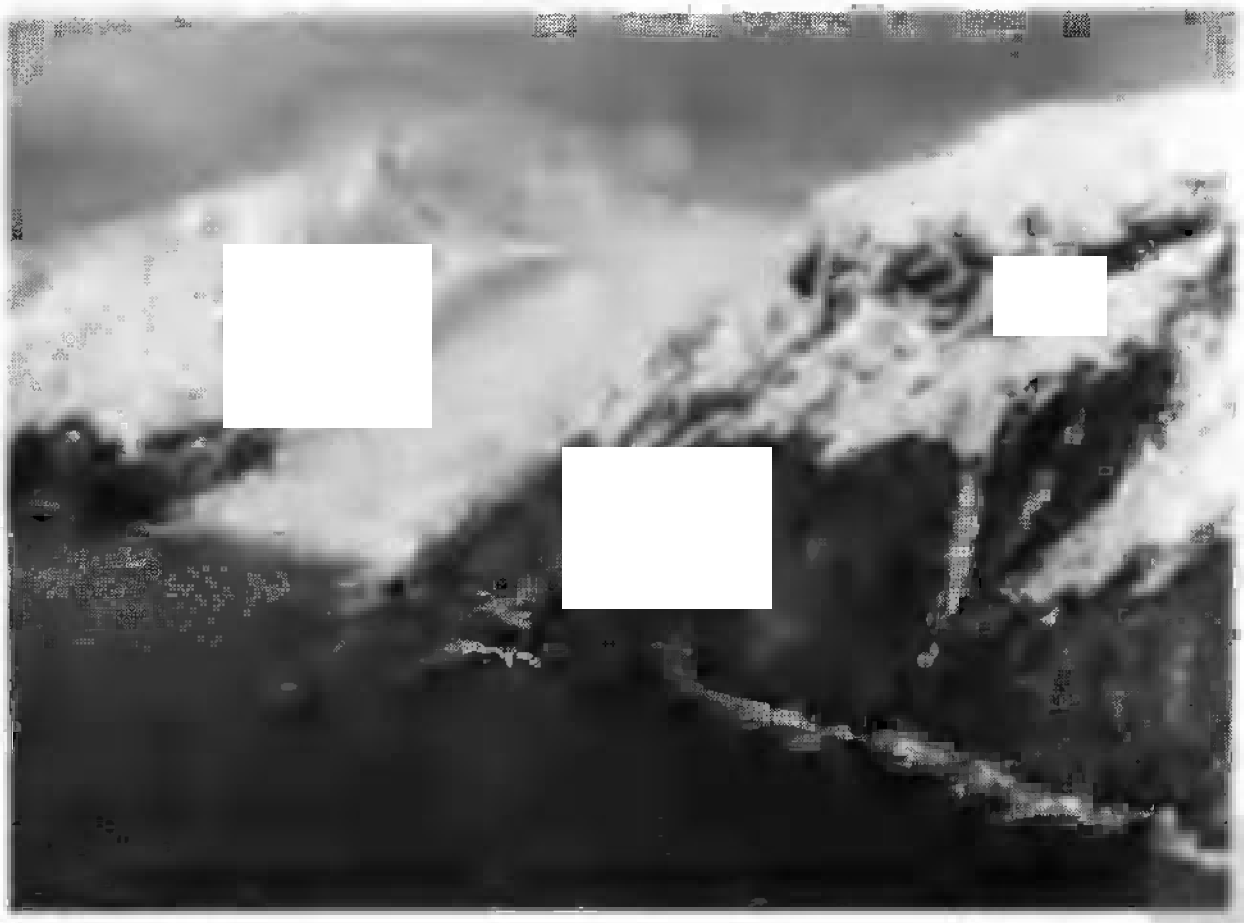

Copyright American Geophysical Union

TABLE F.1.1. Representative Chemical Analyses and CIPW Norms of Volcanic Rocks From Bouvetøya

	1	2	3	4
SiO_2	50.13	54.37	60.59	69.56
TiO_2	3.50	1.95	1.10	0.30
Al_2O_3	15.38	15.55	15.65	13.29
Fe_2O_3	3.39	2.89	1.63	1.84
FeO	8.92	8.35	7.29	2.70
MnO	0.19	0.21	0.28	0.12
MgO	4.30	2.17	0.99	0.09
CaO	8.72	5.98	4.32	0.76
Na_2O	3.36	4.32	4.42	5.33
K_2O	1.31	2.25	2.98	4.85
P_2O_5	0.49	0.65	0.32	0.01
H_2O^+	0.27	0.76	0.30	--
H_2O^-	0.06	0.29	0.05	0.02
CO_2	--	0.56	--	0.29
Total	100.02	100.30	99.92	99.16
Q	0.20	2.62	9.77	17.60
or	7.80	13.47	17.67	29.01
ab	28.60	37.06	35.57	41.90
an	23.06	16.64	14.14	--
ac	--	--	--	2.17
ns	--	--	--	0.31
di	14.26	7.80	4.59	3.33
hy	15.38	14.43	11.28	5.09
mt	2.96	2.74	2.17	--
il	6.61	3.72	2.07	0.56
ap	1.16	1.56	0.76	0.02
An%	44.6	31.0	28.4	--
Ba	250	439	584	298
Ce	50	89	106	175
Co	44	18	5	4
Cr	20	7	6	4
Eu	3.14	4.55	4.64	3.09
Ga	23	26	28	31
La	32.3	51.8	65.7	104
Lu	0.4	0.6	0.7	1.1
Nb	44	69	95	155
Ni	21	--	4	9
Rb	20	40	56	105
Sc	28	14.7	13.8	1.3
Sm	10	15	16	23
Sr	434	413	315	14.5
Tb	1.4	2.2	2.6	4.2
Th	2.9	5.8	8.6	16.2
U	0.9	1.6	2.0	4.8
V	278	47	9	3
Y	38	52	59	90
Yb	2.9	4.8	5.5	9.2
Zr	281	466	638	1188

All major oxides analyzed by XRF, from *Verwoerd et al.* [1976]; trace-element data from *le Roex and Erlank* [1982]. Dashes, not determined (elements) or not present (norms).

1. WJ2B. Hawaiite, plagioclase-phyric, Rustadkollen.
2. WJ1B. Mugearite, aphyric, Cape (Kapp) Fie.
3. WJ5B. Benmoreite, plagioclase, and clinopyroxene-phyric, Nyrøysa.
4. WJ18B. Rhyolite, anorthoclase-phyric, Lars Island (Larsøya).

Copyright American Geophysical Union

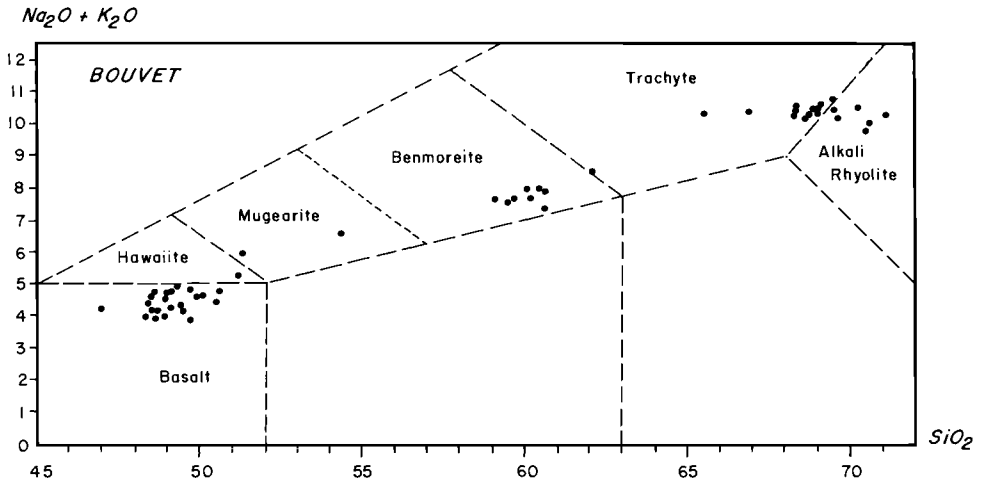

Fig. F.1.3. Alkali versus silica plot for analyzed samples of volcanic rocks from Bouvetøya; subdivisions after *Le Maitre* [1984].

explain the geochemical trends, but this conclusion is largely based on Rb values for the hawaiites that are suspect. In all three calculations the fractionating phases are feldspar, clinopyroxene, olivine, and opaque oxides in similar proportions but with different compositions, with plagioclase dominant.

Ratios between incompatible trace elements remain more or less unaffected by crystal fractionation and can be used to characterize the source area of a parental magma. Radiogenic isotope ratios are even more sensitive indicators. The Bouvetøya "hotspot" carries the following signature: low Zr/Nb (6.4), Y/Nb (0.88), and $^{143}Nd/^{144}Nd$ (0.51282–0.51285) ratios and high Zr/Y (7.5), $^{87}Sr/^{86}Sr$ (0.70265–0.70376), and La_n/Yb_n (6.8) ratios [*O'Nions and Pankhurst,* 1974; *O'Nions et al.,* 1977; *le Roex and Erlank,* 1982]. These values indicate a mantle source that is less depleted in lithophile elements with respect to bulk earth, and probably deeper than that of normal mid-ocean ridge basalt. This is compatible with the idea of a hot rising mantle plume whose geochemical influence has been detected in dredged basalts from the ridges east and west of Bouvetøya over a distance of some 800 km [*le Roex et al.,* 1983].

Chronologic Data

The age of the oceanic crust beneath Bouvetøya has been estimated at 4.5–5.0 Ma, which is a maximum for the edifice [*Prestvik and Winsnes,* 1981]. On the basis of normal magnetic polarity, *Verwoerd et al.* [1976] thought that an age in excess of 1 Ma is unlikely. However, *Prestvik and Winsnes* [1981] reported an apparently reliable K-Ar determination of 1.39 ± 0.2 Ma for an aphyric hawaiite above Nyrøysa, and 1.06 ± 0.3 Ma for a fresh porphyritic hawaiite at 200 m elevation above Cato-odden. According to the geochronologic results, the benmoreite and rhyolite samples are much younger. *Løvlie and Furnes* [1978] tentatively inferred an age of 2000 years for a flow at Cape (Kapp) Meteor by determining the virtual paleomagnetic south pole and assuming a standard westward drift of the pole. Present-day activity is evidenced by fumaroles.

Extent of Knowledge

Captain François Lozier-Bouvet discovered the island that was named after him in 1739 on a quest for the "great southern continent." The existence and geographic position of Bouvetøya remained in doubt for the next 159 years [*Baker,* 1967]. In 1898, members of the German *Valdivia* expedition determined its coordinates but did not land. Preliminary petrologic information was obtained from a few dredged samples [*Reinisch,* 1905]. The island was annexed by Norway in December 1927 during the first of the two *Norvegia* expeditions, 1927–1928 and 1928–1929. These were undertaken primarily to examine the feasibility of a whaling base on Bouvetøya but with scientific objectives as well. Among other achievements the intrepid aviator Riiser-Larsen flew over the caldera in 1929. Although there was no geologist attached to the *Norvegia* expeditions, *Holtedahl* [1929] subsequently gave the first geological account of Bouvetøya, based on photographs and reports. Petrographic descriptions of rock specimens collected by the two biologists were only published much later by *Broch* [1946], *Imsland et al.* [1977], and *Prestvik* [1982*b*].

South African meteorological reconnaissance visits to Bouvetøya took place in 1955, 1964, and 1966; the last of these expeditions experienced 5 days of exceptionally good

Copyright American Geophysical Union

weather and produced a new map. The results of geological observations and petrographic work on the lavas were published by *Baker and Tomblin* [1964], *Lunde* [1965], *Baker* [1967], *Verwoerd et al.* [1976], *Imsland et al.* [1977], *Prestvik* [1982*b*], and *le Roex and Erlank* [1982]. The most extensive scientific program yet undertaken on Bouvetøya was that of the Norwegian Antarctic Research Expeditions of 1976–1977 and 1978–1979, the latter involving 24 scientists. The main purpose was to operate a manned upper air meteorological station during the period January to March 1979 as a contribution to the Global Weather Experiment. In contrast to previous visits that seldom lasted for more than a few hours, five men were left ashore for 3 months. Results that are of importance to volcanology include paleomagnetic measurements [*Løvlie and Furnes,* 1978], glaciology [*Orheim,* 1981], a comprehensive geological account [*Prestvik and Winsnes,* 1981], micro-earthquake studies [*Bungum et al.,* 1981], and improved topographic and hydrographic maps.

Bouvetøya was declared a nature reserve by Norwegian Royal Decree in 1971.

Bibliography

Baker, 1965, 1967
Baker and Tomblin, 1964
Broch, 1946
Bungum et al., 1981
Furnes and Løvlie, 1978
Helle, 1981
Holtedahl, 1929
Imsland et al., 1977
Kristoffersen and Bungum, 1982
le Roex and Erlank, 1982
Løvlie and Furnes, 1978
Lunde, 1965
O'Nions and Pankhurst, 1974
O'Nions et al., 1977
Orheim, 1981
Prestvik, 1982*a, b*
Prestvik and Winsnes, 1981
Reinisch, 1905
Verwoerd et al., 1976

Copyright American Geophysical Union

F.2. MARION ISLAND

Type of volcano: Basaltic shield volcano with a subsidiary shield built upon its western flank; no caldera or pit crater.

Location: Southern Indian Ocean (46°54′S, 37°45′E). Approximately 2300 km southeast of Cape Town and 2300 km north of the Lützow-Holm Bay region, Antarctica. Marion and Prince Edward islands are known as the Prince Edward Islands group.

Height above sea level: 1230 m.

Evidence of Holocene activity: About 150 Strombolian cones, smaller scoria cones, and Surtseyan tuff cones with associated aa and pahoehoe flows. The only known historic eruption occurred in 1980 [*Verwoerd et al.*, 1981], when 5,000,000 m^3 of lava poured from a 9-km en echelon fissure that opened up from coast to summit on the western side.

Author of report: W.J. Verwoerd.

Date of report: July 1987.

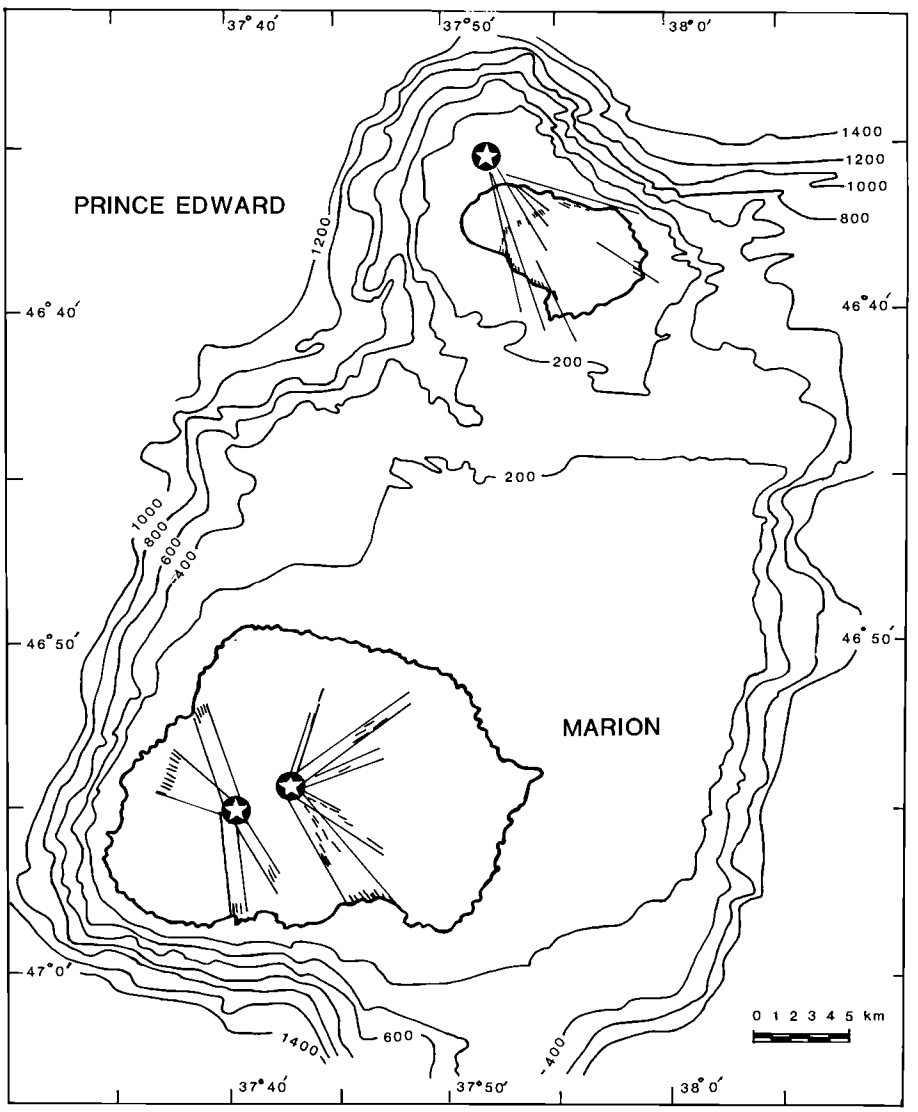

Fig. F.2.1. Radiating dike swarms and structural centers of the Marion and Prince Edward islands shield volcanoes. Isobaths at 200-m intervals outline the submarine plateau around Marion Island.

Copyright American Geophysical Union

Form and Structure

Marion Island has a low, dome-like profile with slopes varying from 4.5° to 9°. The island has an area of about 290 km², and it emerges from a flat-topped submarine plateau 200 m below sea level (Figure F.2.1). The shape of this platform is determined by steep N20°E and east-west-trending boundary scarps parallel to the ocean floor transform faults and ridge axis, respectively. These directions are also reflected in a prominent subaerial escarpment adjoining a narrow coastal plain parallel to the western and southern coastlines, suggesting that lithospheric fractures have been reactivated during and after the shield-building phase [*Chevallier*, 1986]. By extrapolating radial dikes and fissures, two centers of eruption (4 km apart) have been identified in the summit area. These centers have no obvious topographic expression but are nevertheless considered to represent a double feeding system. The existence of two coalescing shields is reflected by the outline of the island, which can be generalized as two overlapping semicircles of unequal diameter (Figure F.2.2*a*), and has been confirmed by petrographic and stratigraphic differences as well as K-Ar dating.

The island slope is not an even surface but is divided into radially distributed highlands and lowlands. Previously described as "sector grabens" due to faulting [*Verwoerd*, 1971], most valleys have been reinterpreted as the result of landsliding due to slope instability [*Chevallier*, 1986]. The most prominent graben-like structure, the Santa Rosa Valley, was probably influenced by intrusion of magma into an arcuate rift zone which is marked by a concentration of scoria cones and fissures, including the two main eruptive centers.

Striated pavements and moraine [*Hall*, 1978] testify to the fact that the island was glaciated prior to the outflow of the Holocene aa and pahoehoe lavas. The latter can be clearly distinguished by their black color and primary constructional features from the Pleistocene gray lava succession of the shield-building phase (Figures F.2.3 and F.2.4). Intercalated with the gray lavas are red scoriaceous deposits, lenticular hyaloclastite remnants of tuff cones, sedimentary layers with fluvioglacial outwash characteristics, and a broken-up, contorted lava embedded in hyaloclastite and interpreted as the result of an intraglacial eruption. Local unconformities can be used to subdivide the eastern and western shields into three and two stratigraphic

Fig. F.2.2. (*a*) Simplified geologic map of Marion Island showing the western coastal plain, radial distribution of Holocene volcanic cones, and the relationship between the main and subsidiary shields. (*b*) Stratigraphic cross sections of the main and subsidiary shields of Marion Island, showing glacial intercalations and unconformities between units predominantly built of lava. Numbers are K-Ar ages in millions of years.

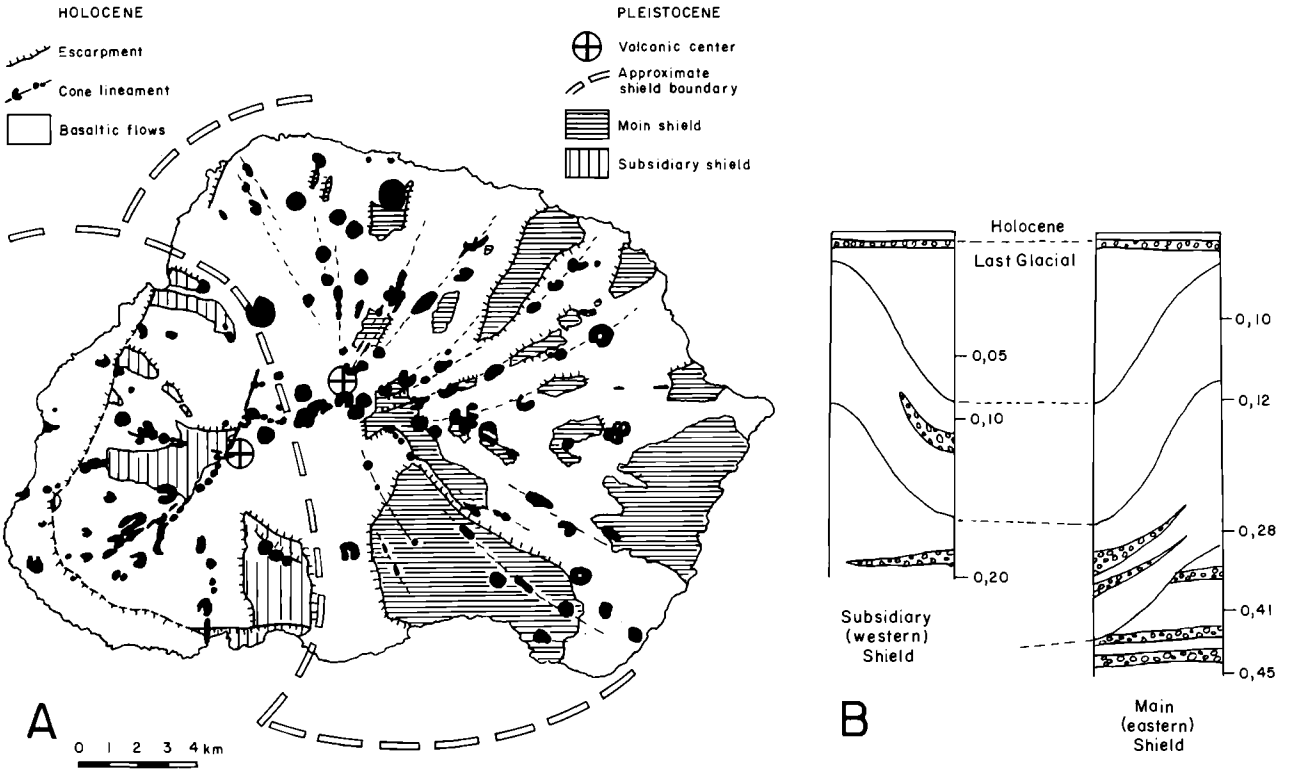

Copyright American Geophysical Union

Copyright American Geophysical Union

TABLE F.2.1. Representative Chemical Analyses and CIPW Norms of Volcanic Rocks From Marion Island

	Pleistocene								
	1	2	3	4	5	6	7	8	9
SiO_2	45.21	46.02	46.46	46.54	46.63	47.10	47.23	50.68	55.33
TiO_2	3.11	3.60	3.17	3.64	2.52	3.29	3.54	2.46	1.50
Al_2O_3	14.67	18.62	16.32	17.78	13.07	15.79	15.42	17.27	17.06
Cr_2O_3	0.03	--	--	--	0.09	--	--	--	--
Fe_2O_3	3.77	4.64	3.79	5.61	5.03	3.31	4.02	4.34	2.30
FeO	8.79	6.91	8.12	6.30	6.46	8.87	8.92	6.77	6.30
MnO	0.16	0.16	0.17	0.17	0.17	0.16	0.21	0.18	0.21
MgO	9.02	4.39	6.90	4.32	10.88	6.18	5.01	4.12	2.60
CaO	10.01	11.38	9.78	10.64	10.24	10.22	8.13	6.77	5.06
Na_2O	3.19	3.36	3.79	3.80	3.11	3.79	4.49	5.05	5.81
K_2O	0.49	0.90	1.28	1.21	0.24	1.02	1.64	1.61	2.17
P_2O_5	0.31	0.43	0.57	0.54	0.30	0.46	0.62	0.83	0.66
H_2O^+	0.17	0.12	0.28	0.31	0.34	0.24	0.34	0.17	0.23
H_2O^-	0.08	0.05	0.23	0.17	0.25	0.12	0.04	0.17	0.11
Total	99.01	100.58	100.86	101.03	99.33	100.55	99.61	100.42	99.34
or	2.90	5.35	7.58	7.12	1.41	6.02	9.70	9.58	12.81
ab	23.17	24.05	23.07	25.16	25.55	25.94	31.06	40.73	49.18
an	24.24	33.05	23.74	27.89	21.01	23.06	17.75	19.69	14.06
ne	2.09	2.38	4.88	3.80	0.41	3.31	3.73	1.09	--
di	18.75	16.53	16.91	17.12	22.24	19.82	12.57	6.95	5.57
hy	--	--	--	--	--	--	--	--	5.54
ol	15.25	4.62	10.97	4.52	17.40	8.77	10.15	10.53	3.82
mt	6.69	7.39	6.78	7.46	5.83	6.95	7.94	5.74	4.35
il	5.91	6.83	6.03	6.92	4.79	6.25	7.55	4.66	2.85
ap	0.74	1.01	1.35	1.29	0.70	1.09	3.23	1.96	1.56
As	235	--	--	--	100	--	--	425	735
Ba	176	115	149	280	153	202	--	509	594
Ce	52	43	63	66	51	57	--	116	136
Co	55	70	51	44	49	48	--	26	18
Cr	237	--	--	--	489	--	--	67	104
Hg	425	--	--	--	60	--	--	340	53
La	22	13	23	20	16	20	--	54	64
Nb	30	25	36	34	24	31	48	63	80
Nd	29	26	33	33	28	36	--	57	66
Ni	144	26	80	26	251	55	--	5	3
Rb	17	17	20	20	11	17	24	37	46
Sc	28	22	25	23	29	25	--	13	13
Sr	530	646	584	652	450	529	698	844	715
Th	3	--	--	--	3	--	--	10	13
U	-2	--	--	--	-2	--	--	6	7
Y	33	31	34	35	32	33	45	50	67
Zr	198	188	267	247	185	221	292	378	520

Samples 1–9 analyzed by XRF at Department of Geology, University of Stellenbosch; FeO determined by titration; H_2O^+ calculated from loss on ignition. Major oxide analyses of samples 10–13 performed at National Institute for Metallurgy, Johannesburg, by standard gravimetric, volumetric, and flame photometric procedures, and trace-element analyses at Department of Geochemistry, University of Cape Town [*Verwoerd,* 1971]. Dashes, not determined (elements) or not present (norms).

1. LC51. Basalt (Type I), top of Triegaardt Bay cliff.
2. LC67. Basalt (Type III), north of Triegaardt Bay.
3. LC120. Basalt (Type II), Black Haglet Valley.
4. LC160. Feldspar-phyric basalt (Type III), top of Triegaardt Bay cliff.
5. LC31. Basalt (Type I), eastern cliff of Santa Rosa Valley.
6. LC171. Basalt (Type II), west of Long Ridge.
7. 81WV10. Trachybasalt (Type IV), eastern cliff of Santa Rosa Valley.
8. LC58. Trachybasalt (Type IV), Ship's Cove.
9. LC23. Trachyandesite (Type IV), base of Goodhope Bay.

Copyright American Geophysical Union

TABLE F.2.1. (continued)

	Holocene			
	10	11	12	13
SiO_2	45.97	46.79	47.64	48.78
TiO_2	3.60	2.57	3.29	3.62
Al_2O_3	17.91	13.37	15.96	16.58
Cr_2O_3	--	--	--	--
Fe_2O_3	3.27	1.69	1.94	3.89
FeO	8.93	9.29	9.73	8.00
MnO	0.14	0.16	0.18	0.22
MgO	4.94	11.49	5.61	4.80
CaO	9.67	10.23	10.65	8.13
Na_2O	3.30	3.02	3.54	3.70
K_2O	1.38	0.98	1.31	1.75
P_2O_5	0.43	0.30	0.52	0.65
H_2O^+	0.49	0.25	0.30	0.26
H_2O^-	0.01	0.07	0.02	0.03
Total	100.04	100.21	100.69	100.41
or	8.15	5.79	7.74	10.34
ab	23.82	17.42	23.53	31.31
an	29.98	20.03	23.82	23.46
ne	2.22	4.41	3.48	4.15
di	12.39	23.16	20.97	10.22
hy	--	--	--	5.13
ol	10.40	21.05	9.73	5.64
mt	4.74	2.45	3.65	5.64
il	6.85	4.88	6.25	6.88
ap	1.02	0.71	1.23	1.54
As	--	--	220	--
Ba	358	203	326	395
Ce	--	--	71	--
Co	--	--	45	--
Cr	--	--	100	--
Hg	--	--	261	--
La	--	--	32	--
Nb	44	29	47	54
Nd	--	--	36	--
Ni	22	292	46	22
Rb	23	16	25	32
Sc	--	--	26	--
Sr	692	447	694	679
Th	--	--	6	--
U	--	--	5	--
Y	34	27	42	38
Zr	275	205	279	363

10. WJM42. Basalt (Type III), west of Gordon's Hill.
11. WJM62. Basalt (Type I), flow from Santa Rosa Hill.
12. 81WV3. Basalt (Type II), 1980 eruption, Kaalkoppie.
13. WJM67. Trachybasalt (Type IV), Fred's Hill.

Copyright American Geophysical Union

units, respectively (Figure F.2.2*b*). A small permanent ice cap is still present on the summit plateau.

Petrologic Characteristics

The lavas (both Pleistocene and Holocene) belong to a typical alkaline oceanic island basalt suite, showing a limited range of differentiation between 45% and 55% SiO_2 (Table F.2.1). On the alkali versus silica plot (Figure F.2.5) they are overwhelmingly basalt and trachybasalt, with very subordinate trachyandesite. In view of their sodic character the terms alkali basalt, hawaiite, mugearite, and benmoreite are preferred; tholeiite has not been found. The trend on an AFM diagram (Figure F.2.6) is the same as that of the Crozet archipelago if the trachyte samples from Prince Edward Island are included.

The alkali basalts and hawaiites have been subdivided further on textural grounds; this subdivision clearly has evolutionary significance as shown by normative (Figure F.2.7) and trace-element (Figures F.2.8 and F.2.9) variation diagrams, as well as stratigraphic position. Type I has a microdoleritic groundmass with olivine (Fo_{78-82}), clinopyroxene (En_{42-44}), and plagioclase (An_{70}) phenocrysts. Type II has a basaltic groundmass with fewer (3–15%) phenocrysts of olivine (Fo_{71}) and plagioclase (An_{67}); microphenocrysts constitute up to 50% of the rock and include rare clinopyroxene (En_{41}). Type III is a porphyritic plagioclase-rich basalt (An_{82}) with subordinate olivine (Fo_{60}) and clinopyroxene (En_{37}); it is a cumulative rock, distinct from the liquid line of descent. Type IV is aphyric with a fluidal texture; laths of plagioclase (An_{47}) predominate over olivine (Fo_{51}) and clinopyroxene (En_{34}).

Types I and II basalt erupted form both centers during the shield-building and Holocene phases. They probably originated at different depths in closely related magma chambers. Type IV is restricted to the main shield and Type

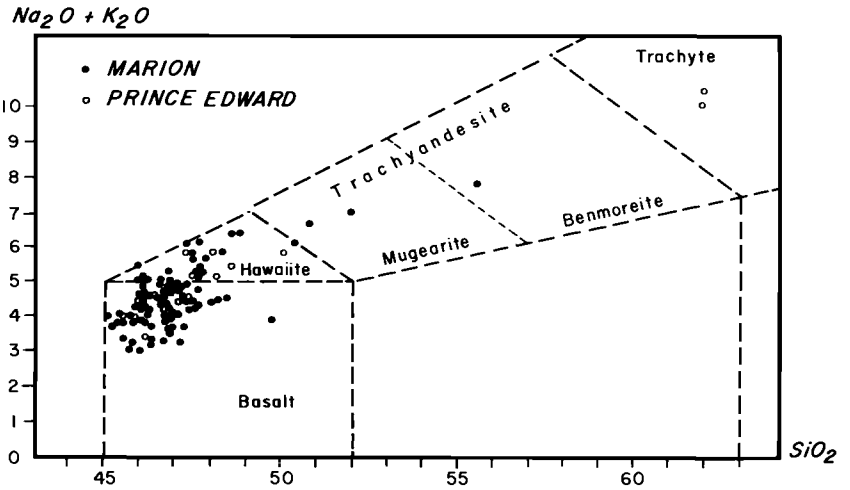

Fig. F.2.5. Alkali versus silica plot for volcanic rocks from Marion and Prince Edward islands; subdivisions after *Le Maitre* [1984].

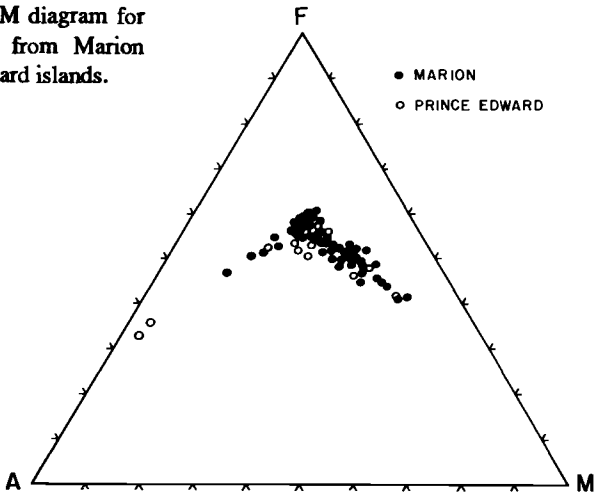

Fig. F.2.6. AFM diagram for analyzed lavas from Marion and Prince Edward islands.

Copyright American Geophysical Union

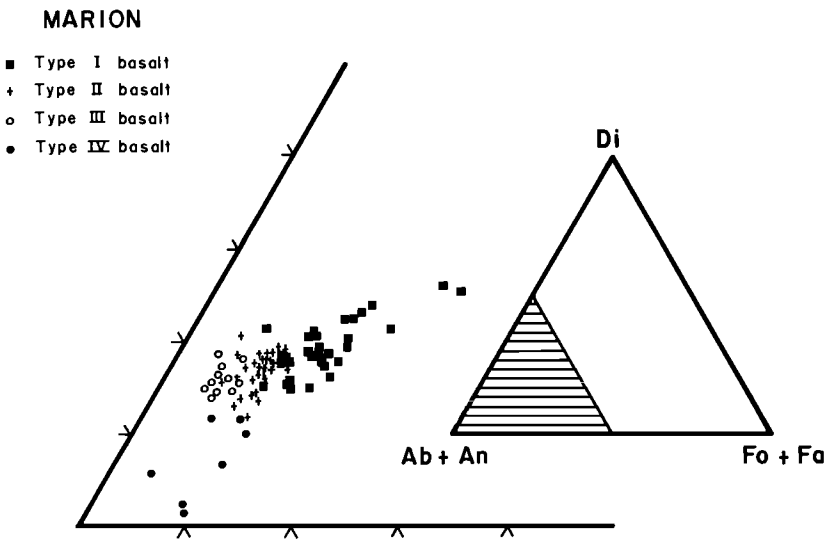

Fig. F.2.7. Normative plagioclase-diopside-olivine diagram for Type I to Type IV Marion Island basalts.

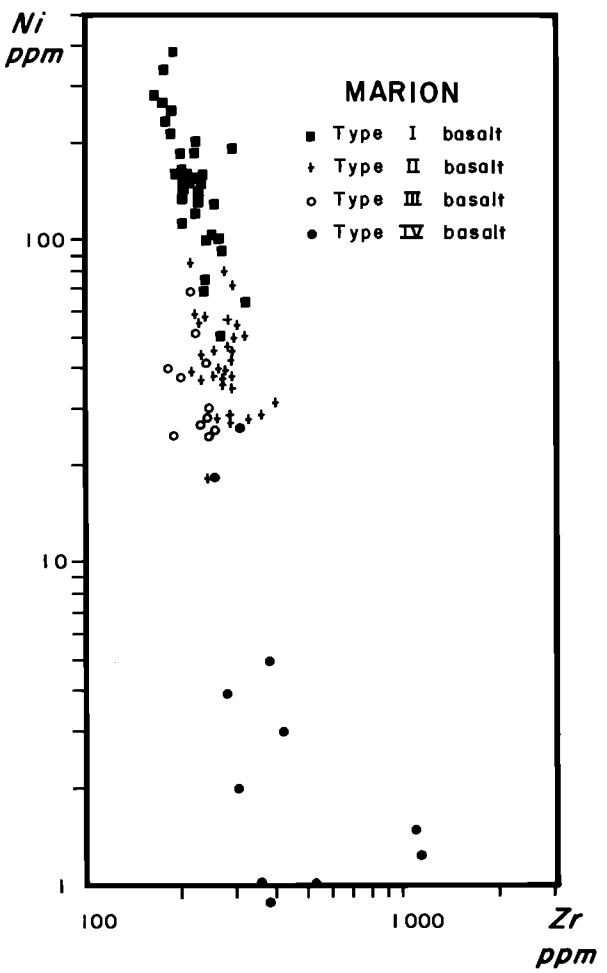

Fig. F.2.8. Ni-Zr variation diagram for Type I to Type IV Marion Island basalts.

III to the western shield; they may represent brief interruptions of the normal evolutionary process. Pb and Sr isotope ratios (Figure F.2.10) indicate that the Marion Island lavas are derived from a mantle source not as highly enriched in incompatible elements as that of Îles Kerguelen, but moderately enriched compared to mid-ocean ridge basalt.

Chronologic Data

The Marion Island plateau was built on 50-m.y.-old seafloor, the age of which is based on the extrapolated position of Anomaly 21 beneath Marion Island, according to the magnetic survey of *Bergh and Norton* [1976]. The volcanic shields are generally assumed to be much younger.

The first K-Ar dates of Marion Island lavas [*McDougall*, 1971] confirmed the distinction between the younger (Holocene) and older (Pleistocene) sequences, but samples were restricted to the northeastern sector of the island. Subsequently, stratigraphically controlled sections of the two Pleistocene shields were sampled at Triegaardt Bay, the eastern sidewall of the Santa Rosa Valley, and between Ship's Cove and Katedraalkrans. K-Ar determinations on these samples by McDougall (unpublished data, 1985) unequivocally show that the main (eastern) shield is the older one and was built above sea level from 0.45 ± 0.02 to 0.36 ± 0.01 Ma. A subsidiary shield came into being on its western slope at ~0.20 ± 0.01 Ma. This late Pleistocene time interval encompassed three glacial maxima and four interstadials according to oxygen isotope measurements (Figure F.II), but the resolution of the K-Ar method does not allow detailed correlations of glacial deposits to be made. The most recent glaciation (0.116–0.013 Ma) left moraine and striated pavements on Marion Island, terminating the shield-building phase.

Copyright American Geophysical Union

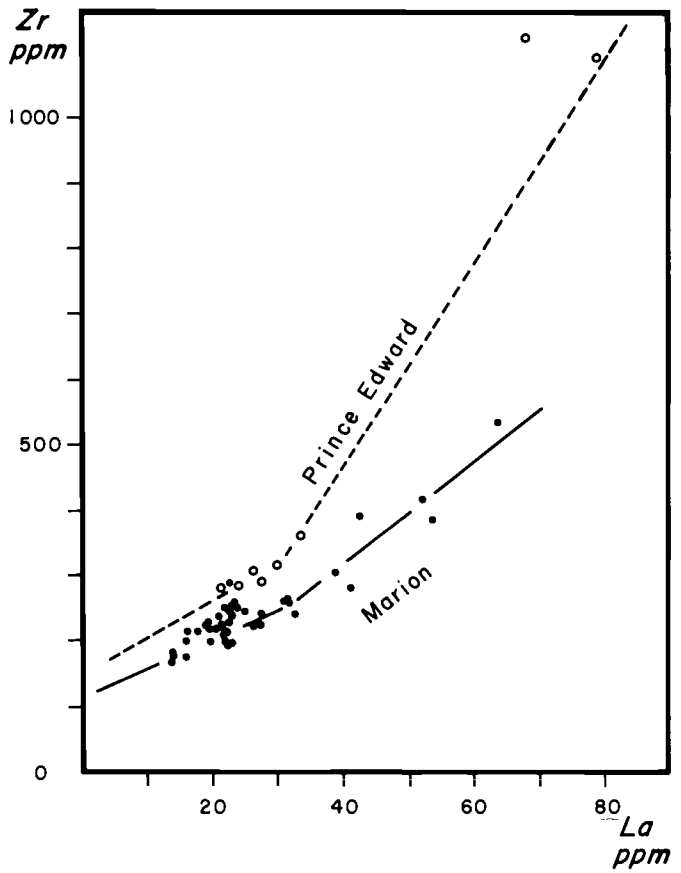

Fig. F.2.9. Zr-La variation diagram for analyzed lavas from Marion and Prince Edward islands.

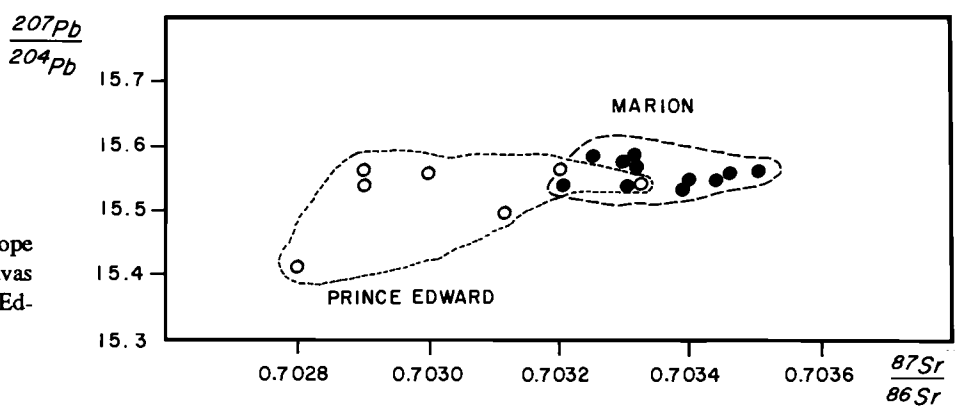

Fig. F.2.10. Pb-Sr isotope variation diagram for lavas from Marion and Prince Edward islands.

The younger black lavas of Marion Island have not been reliably dated, apart from the 1980 flow. Relative dating on the basis of superposition, vegetation, and other criteria has led to a threefold grouping (Figure F.2.3) and the general impression that the rate of volcanism was constant over a considerable length of time. Minimum ages of 4020 ± 55 and 3180 ± 120 years have been fixed for flows in two of the older groups by radiocarbon dating of swamps on them [*Verwoerd,* 1971]. A maximum age for the oldest of the Holocene flows would be 10,000 years (end of Pleistocene). On the assumption that the 150 scoria cones represent approximately the same number of events, the average interval between eruptions on Marion Island can therefore be estimated at 27 to 66 years, giving a particularly low rate of activity.

Extent of Knowledge

The discovery of Marion and Prince Edward islands is usually credited to the French explorer Nicolas Marion-

Copyright American Geophysical Union

Dufresne in 1772, although the Dutch skipper Barent Ham reported two islands named Dina and Maerseveen in the same general area in 1663. Captains Marion-Dufresne in 1772, Cook in 1776, and Ross in 1840 and the *Gauss* expedition of 1901 were all unable to land because of adverse weather conditions. The principal volcanic features of Marion Island were recognized by the naturalists aboard H.M.S. *Challenger* in 1873. Basalts collected by the geologist J.Y. Buchanan were described by *Renard* [1889*a*], and two analyses were subsequently published by *Lacroix* [1923]. Three basalt samples collected by the *Bougainville* expedition of 1939 were found to be identical to the previous rock collections [*Lacroix*, 1940]. Isolated samples collected on behalf of the South African Geological Survey in 1949 again proved to be alkali basalts [*Abbott*, 1963]. The first effort to map and describe the geology of Marion and Prince Edward islands was carried out in 1965–1966 [*Verwoerd*, 1971]. *McDougall* [1971] provided K-Ar dates of the lavas, and *Snape and Retief* [1971] reported paleomagnetic results. *Hall* [1978, 1980] subsequently studied the products of Quaternary glaciation on the island. The unexpected volcanic eruption of 1980 (which was more extensive than initially reported by *Verwoerd et al.* [1981]) triggered a new series of studies [*Chevallier*, 1986; *Verwoerd and Chevallier*, 1987] that are still in progress.

Bibliography

Abbott, 1963
Bergh and Norton, 1976
Chevallier, 1986
Hall, 1978, 1980
Lacroix, 1923, 1940
McDougall, 1971
Renard, 1889*a*
Snape and Retief, 1971
Verwoerd, 1971
Verwoerd and Chevallier, 1987
Verwoerd et al., 1981

Copyright American Geophysical Union

F.3. PRINCE EDWARD ISLAND

Type of volcano: Basaltic shield volcano, four fifths of which subsided below sea level.

Location: Southern Indian Ocean (46°38′S, 37°57′E), 22 km north-northeast of Marion Island.

Height above sea level: 672 m.

Evidence of Holocene activity: About 15 scoria cones and four associated aa lava flows, as well as four Surtseyan tuff cones on a coastal plain. No historic eruptions have been recorded.

Author of report: W.J. Verwoerd.

Date of report: July 1987.

Form and Structure

Prince Edward Island rises from the northern edge of the Marion Island submarine plateau (Figure F.2.1). It is a small island (44 km^2) with an asymmetric profile and a trapezoid shape (Figure F.3.1). It has a western coastal plain, a 400-m escarpment, and an eastward slope (or planèze) of about 6°. A radial dike swarm converges to an extrapolated volcanic center a short distance offshore to the northwest. Block faulting took place along the regional tectonic directions (N20°E and east-west), on a much larger scale than at Marion Island, and it is responsible for the disappearance of the major subaerial portion of the shield, which must have had an original diameter of about 20 km.

As in the case of Marion Island, the bulk of Prince Edward Island consists of a Pleistocene succession of thin

Fig. F.3.1. Geologic sketch map of Prince Edward Island.

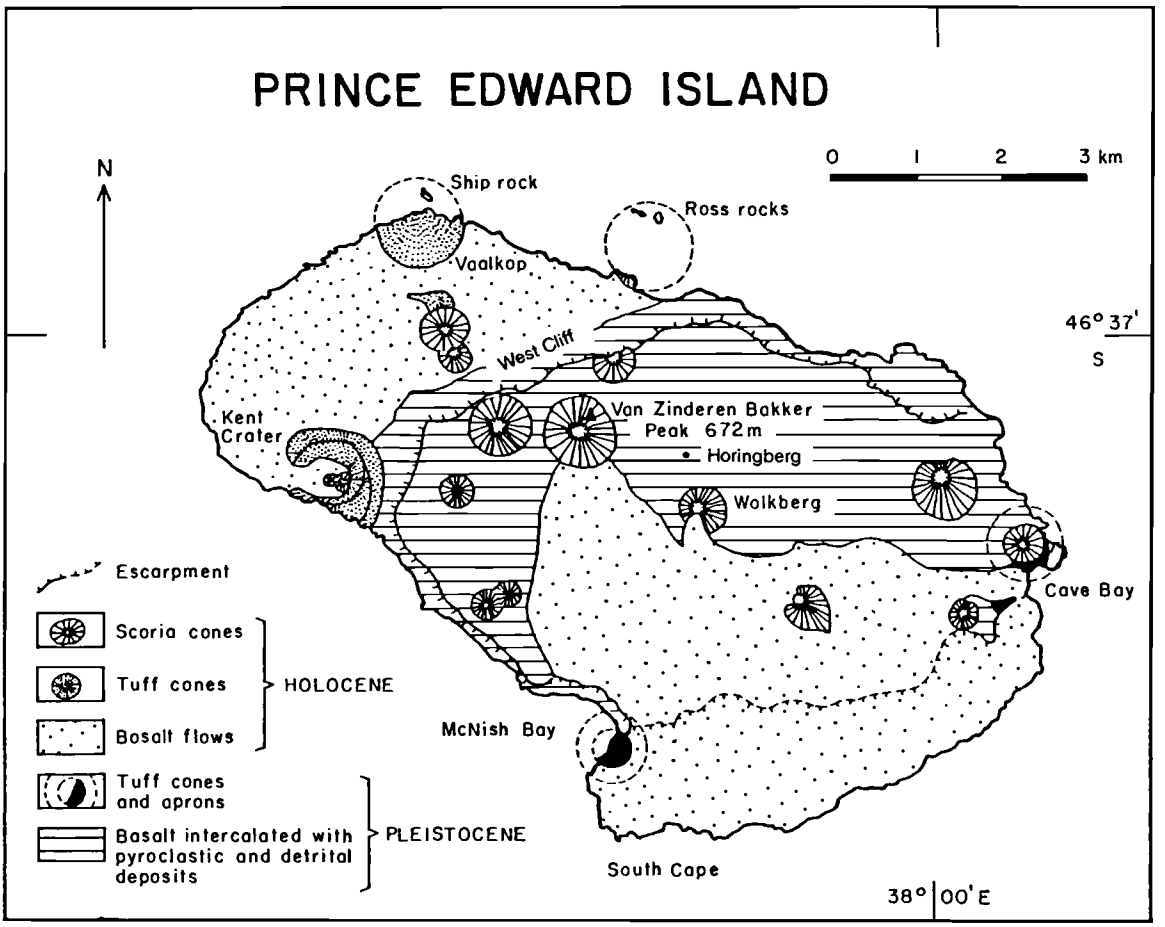

Copyright American Geophysical Union

Copyright American Geophysical Union

TABLE F.3.1. Representative Chemical Analyses and CIPW Norms of Volcanic Rocks From Prince Edward Island

	Pleistocene				Holocene	
	1	2	3	4	5	6
SiO_2	45.85	45.92	48.60	61.73	47.63	48.11
TiO_2	3.53	4.36	3.31	0.50	3.77	3.52
Al_2O_3	12.99	14.88	16.72	17.34	15.74	16.64
Cr_2O_3	0.04	0.02	--	--	0.01	--
Fe_2O_3	6.38	3.65	4.25	2.49	6.24	1.75
FeO	6.44	9.59	7.32	3.24	6.21	10.08
MnO	0.16	0.17	0.18	0.17	0.16	0.10
MgO	10.54	6.25	5.42	0.69	5.53	5.72
CaO	9.28	9.47	7.57	2.03	8.71	8.13
Na_2O	3.40	3.91	3.55	6.60	4.23	3.54
K_2O	0.63	0.68	1.75	3.55	1.04	1.53
P_2O_5	0.56	0.59	0.77	0.15	0.72	0.90
H_2O^+	0.17	0.16	0.31	0.23	0.21	0.16
H_2O^-	0.11	0.07	0.10	0.09	0.18	0.08
Total	100.08	99.72	99.85	98.81	100.38	100.26
Q	--	--	--	2.76	--	--
or	3.73	4.02	10.34	20.98	6.16	9.12
ab	26.02	30.53	30.04	55.85	34.12	29.95
an	18.32	21.05	24.52	7.21	20.88	24.99
ne	1.49	1.37	2.23	0.06	0.91	1.06
di	19.16	17.57	6.42	1.61	14.10	7.77
hy	--	--	10.47	6.26	--	3.50
ol	16.47	7.85	3.41	8.96	8.04	13.45
mt	7.29	8.49	6.16	2.90	7.64	2.54
il	6.70	8.28	6.29	0.94	7.16	6.69
ap	1.31	1.41	1.82	0.36	1.71	2.13
As	270	330	--	737	225	--
Ba	151	161	342	615	200	325
Ce	64	74	--	163	85	--
Co	63	40	--	12	42	--
Cr	340	69	--	92	78	--
Hg	39	110	--	78	102	--
La	24	26	--	80	33	--
Nb	33	35	51	108	47	45
Nd	40	43	--	70	49	--
Ni	191	50	31	2	31	36
Rb	19	20	28	70	26	23
Sc	26	26	--	4	22	--
Sr	634	708	825	446	895	951
Th	4	7	--	--	8	--
U	-2	4	--	--	6	--
Y	40	47	51	62	51	45
Zr	291	308	436	1107	363	389

Samples 1, 2, 4, and 5 analyzed by XRF at Department of Geology, University of Stellenbosch; FeO determined by titration; H_2O^+ calculated from loss on ignition. Major oxide analyses of samples 3 and 6 performed at National Institute for Metallurgy, Johannesburg, by standard gravimetric, volumetric, and flame photometric procedures, and trace element analyses at Department of Geochemistry, University of Cape Town [*Verwoerd,* 1971]. Dashes, not determined (elements) or not present (norms).

1. LC43. Basalt (Type I), base of McNish Bay.
2. LC38. Basalt (Type II), West Cliff.
3. WJE11. Trachybasalt (Type IV), Cave Bay.
4. LC46. Trachyte, east of Horingberg.
5. LC42. Basalt (Type II), dike, McNish Bay.
6. WJE33. Basalt (Type II), Wolkberg.

Copyright American Geophysical Union

F.4. ÎLES CROZET

Type of volcano: Stratovolcanoes or remnants thereof; many parasitic scoria cones.

Location: Southwestern Indian Ocean: Île de l'Est, 46°26′S, 52°12′E; Île de la Possession, 46°25′S, 51°38′E; Île aux Cochons, 46°06′S, 50°14′E; Île des Pingouins, 46°30′S, 50°24′E; Îles des Apôtres, 45°58′S, 50°26′E.

Height above sea level: Île de l'Est, 1090 m; Île de la Possession, 934 m; Île aux Cochons, 775 m; Île des Pingouins, 360 m; Île des Apôtres, 289 m.

Evidence of Holocene activity: No historic eruptions have been recorded, but Recent or near-Recent volcanism prior to the Flandrian transgression (5500 years) occurred on Île aux Cochons and Île de la Possession [*Chevallier et al.*, 1983], and there is a possibility that all the islands are volcanically active.

Authors of report: J. Nougier and J.W. Thomson.

Date of report: June 1987.

Form and Structure

Îles Crozet lie on a submarine plateau located on the eastern flank of the southwest Indian Ocean ridge, at the boundary between magnetic anomalies 30 and 31 (Figures F.I and F.4.1). The archipelago includes an eastern group of volcanic islands (Île de l'Est and Île de la Possession) and a western group (Île des Pingouins, Île aux Cochons, and Îles des Apôtres). The plateau, as outlined by the 2000-m isobath, is covered by thick well-bedded sediments and is aseismic. From the magnetic anomalies identified on the northern flank of the Crozet plateau and on neighboring Crozet Bank (anomalies 29, and 31 and 33, respectively), it is possible that the plateau formed ~54 m.y. ago [*Goslin et al.*, 1981*a*, *b*].

Île de l'Est (Figure F.4.2) represents a glacially eroded stratovolcano, the original center of the volcano coinciding with the present center of the island. A number of scoria cones and red scoriaceous massifs are scattered on the eastern flank of the volcano (Figure F.4.2). The 1000-m-thick sequence of agglomerates and subordinate lava flows rests unconformably on a metamorphosed gabbroic complex (pyroxenite, monzogabbro, and monzodiorite), which was intruded at 8.75 Ma [*Chevallier et al.*, 1983]. A dense network of dikes and cone sheets, approximately convergent on the center of the island, cuts the plutonic complex and acted as feeders to the younger volcanic units (units II, III, and IV) [*Lameyre and Nougier*, 1982]. Unit II has a basal conglomerate followed by a thick sequence of agglomerates and thin basaltic lava flows; Unit

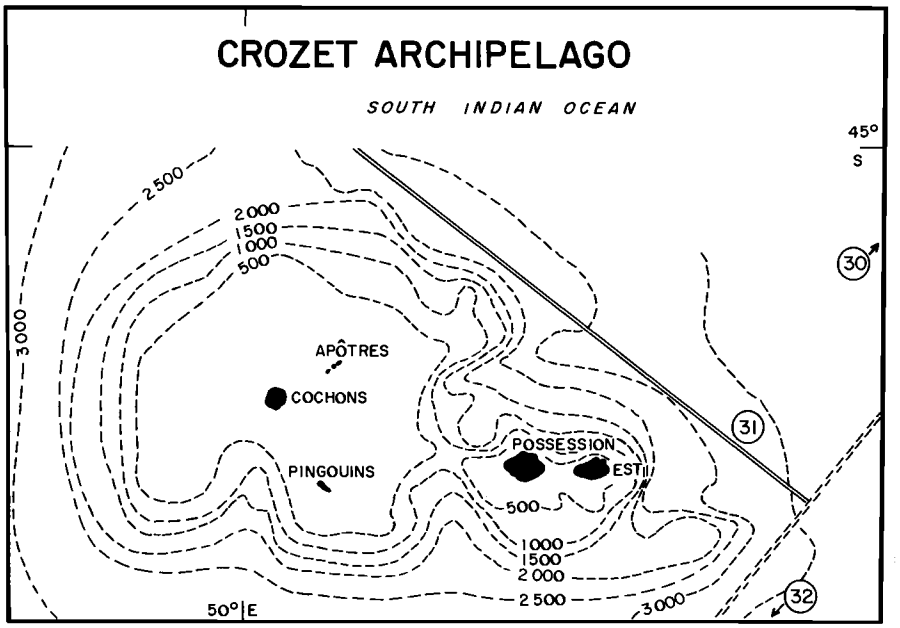

Fig. F.4.1. Sketch map of Îles Crozet, showing the relative positions of the volcanic islands. Bathymetry after *Berthois et al.* [1969], and magnetic anomalies (encircled numbers) after *Schlich* [1975]. The isobaths are at 500-m intervals.

Copyright American Geophysical Union

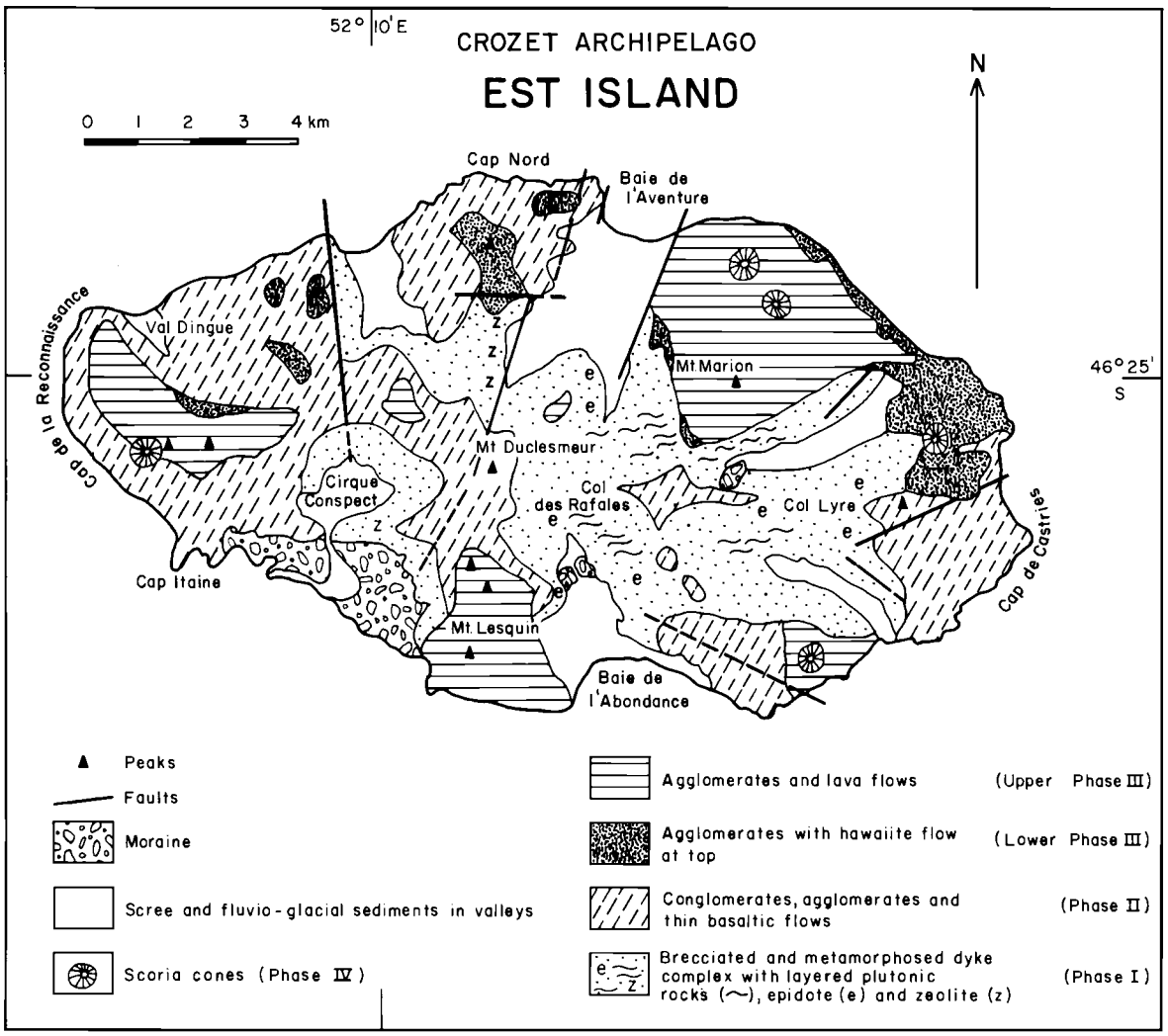

Fig. F.4.2. Geologic sketch map of Île de l'Est.

III, which transgresses units I and II, is another thick agglomerate sequence interbedded with oceanite to hawaiite lava flows; Unit IV consists of a number of scoria cones representing a late phase of Strombolian volcanic activity on the island.

The Île de la Possession stratovolcano developed during at least five phases of volcanic activity [*Chevallier et al.*, 1983], the volcanic center being located at the western side of the island (Figure F.4.3). Prominent block faulting, marine erosion, and uplift have modified the overall shape of the volcano. The oldest rocks (Phase I), a sequence of palagonitized hyaloclastites with an interbedded marine fossiliferous bed rich in pectens and mussels, crop out only on the western side of the island, whereas the earliest subaerial rocks (Phase II) are exposed in valley bottoms on the eastern flank of the volcano. These early subaerial deposits correspond to the development of a subaerial stratovolcano that now forms the island basement. They are represented by thick basalt lava flows interbedded with volcaniclastic rocks which become increasingly abundant toward the top of the succession. A series of ring dikes and cone sheets intruded the subaerial rocks toward the end of Phase II activity.

Phase III volcanic rocks were deposited on the eroded surface of the Phase II stratovolcano. They include a basal conglomerate followed by volcaniclastic rocks interbedded with thin lava flows and sills; the sills become more numerous upward. The lavas were fed by a series of radial dikes centered on the western side of the island. Phase IV volcanic activity culminated in the eruption of 10-m-thick plateau basalts from a rift system which trends 135°. These basalts and the associated dike swarm (one dike every 10 m)

Copyright American Geophysical Union

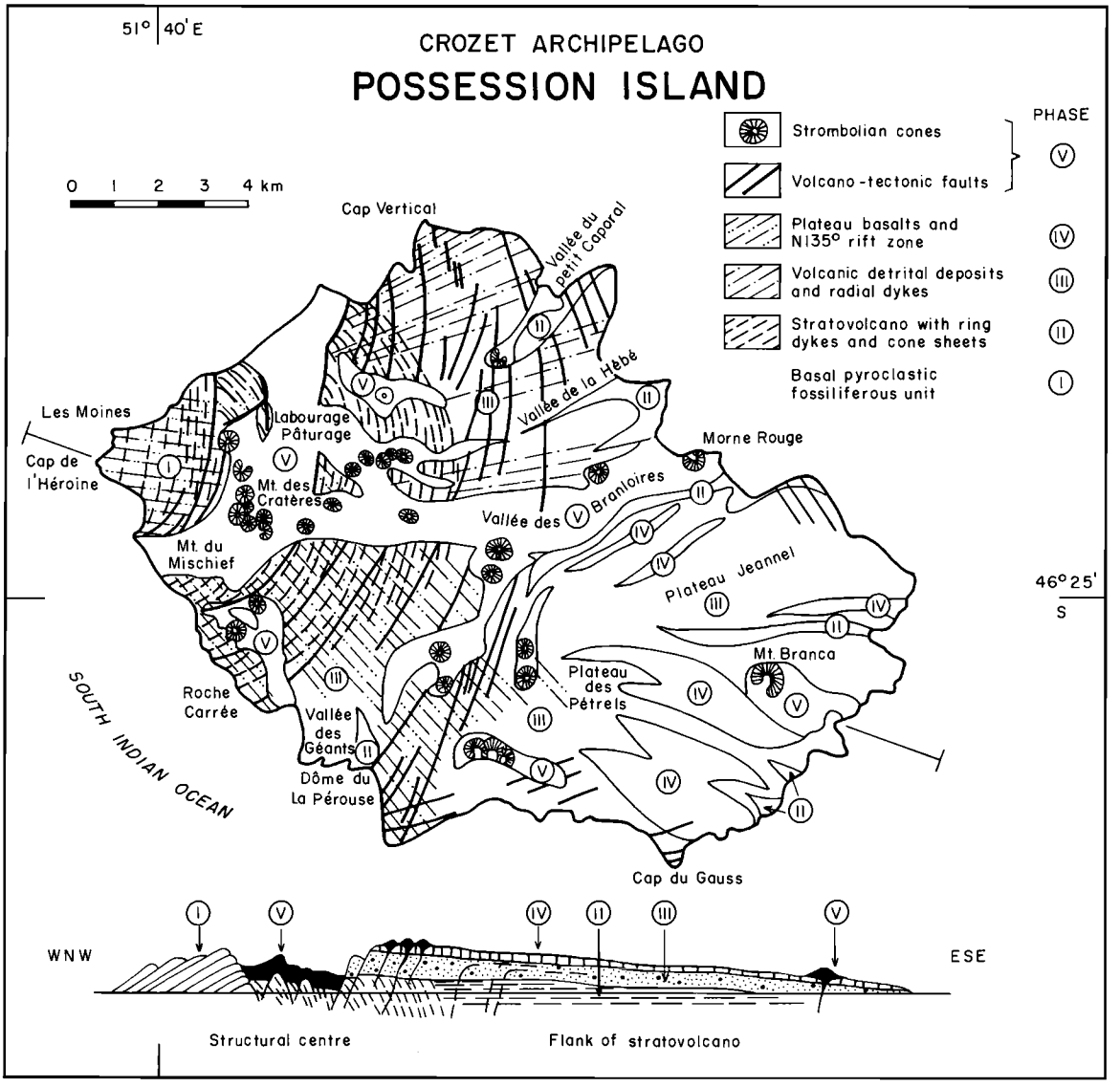

Fig. F.4.3. Geologic sketch map of Île de la Possession [after *Chevallier et al.*, 1983].

reflect a major extensional zone in the oceanic crust at that time. Phase IV was followed by a glacial period. Phase V is represented by a number of Strombolian scoria cones and some lava flows. Although widely distributed over the island, the scoria cones and associated dikes are located along a series of north-south or 40°-trending fractures centered on the original stratovolcano.

Île aux Cochons is a single stratovolcano formed during two phases of volcanic activity; both phases had the same focus near the present center of the island. Phase I is represented by ~400 m of phreatomagmatic breccias interbedded with 1-m-thick lava flows, now exposed in cliff faces formed by block faulting along 70° and 160° trends. Phase II followed block faulting and produced lava flows radiating from the central crater on the island, and more than 60 scoria cones located along a system of radial fractures trending 40°, 70°, 100°, and 160° (Figure F.4.4). There is a summit caldera on the island, and some of the littoral cones (<5500 years B.P.) are maar-type structures with hyaloclastite deposits.

Île des Pingouins, located 35 km south-southeast of Île aux Cochons, is a remnant of another volcano. Vertical sea cliffs show well-stratified exposures of hyaloclastites followed by coarse breccias and lava flows at the summit.

Îles des Apôtres, situated 15 km northeast of Île aux Cochons, has 14 islets in the group, all aligned along a 70°

Copyright American Geophysical Union

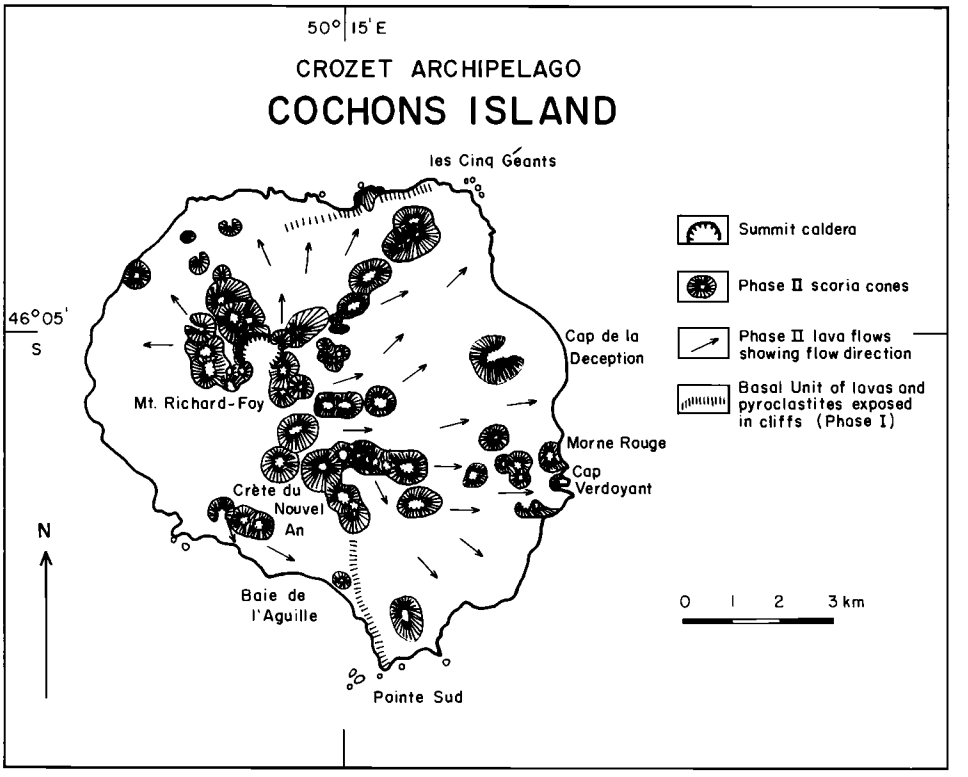

Fig. F.4.4. Geologic sketch map of Île aux Cochons [after *Boudon and Nougier*, 1982].

trend. Downfaulting has reduced the size of the volcano, and only a remnant of it is now visible. Volcanic deposits include coarse breccias and piles of lava flows separated by scoriaceous horizons.

Petrologic Characteristics

In spite of lithological variations between the islands in the archipelago, Île de l'Est and Île de la Possession represent a single volcano-structural area and petrographic province which had a parental alkalic magma [*Chevallier et al.*, 1983] (Figure F.4.5). Île de l'Est is the only island known to have an exposed basal plutonic complex (8.75 Ma). Feeder dikes on Île de l'Est and Île de la Possession have a 110°–135° trend which can be correlated with the 120° trend of magnetic anomaly 31, identified on the northeast side of the Crozet plateau.

The Île de l'Est lavas include oceanites, ankaramites, olivine basalts, feldspar-phyric basalts (An_{60}) and hawaiites; all analyzed samples have normative *ne* (Table F.4.1). Fractionation trends suggest that the lavas were generated either by loss of chromite, olivine, and low Ti-clinopyroxene from an alkali basalt parent magma under low-pressure conditions or by differential partial melting of the mantle.

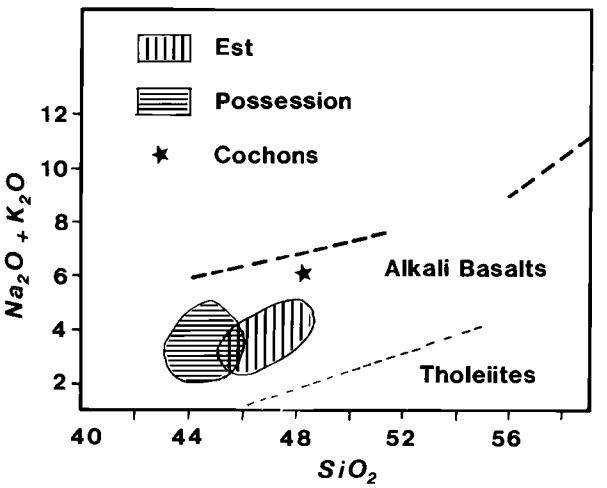

Fig. F.4.5. Alkali versus silica plot for the Îles Crozet volcanic rocks.

The Île de la Possession volcanic rocks are dominated by a suite of alkali basalts and their derivatives [*Chevallier et al.*, 1983] (Table F.4.2). The rocks of Phase I and Phase II include glassy (submarine) and porphyritic (subaerial)

Copyright American Geophysical Union

TABLE F.4.1. Representative Chemical Analyses and CIPW Norms of Volcanic Rocks From Île de l'Est and Île aux Cochons

	1	2	3	4
SiO_2	45.81	46.58	47.07	48.40
TiO_2	1.89	2.56	3.10	2.00
Al_2O_3	8.96	12.14	14.50	17.10
Fe_2O_3	2.35	4.00	3.64	4.55
FeO	8.60	7.75	8.07	7.20
MnO	0.16	0.16	0.16	0.19
MgO	18.89	11.50	6.86	5.10
CaO	10.72	11.64	11.98	9.00
Na_2O	1.66	2.24	2.80	3.80
K_2O	0.70	1.00	1.34	2.10
P_2O_5	0.26	0.39	0.47	0.59
H_2O^+	--	--	--	0.30
H_2O^-	--	--	--	0.30
Total	100.00	100.00	100.00	100.63
or	4.14	5.92	7.93	12.42
ab	10.71	17.61	19.54	25.84
an	14.91	20.10	23.00	23.35
ne	1.80	0.72	2.24	3.40
di	29.22	28.16	27.11	14.44
ol	31.67	15.98	7.99	8.80
mt	3.41	5.80	5.28	6.60
il	3.59	4.87	5.89	3.80
ap	0.62	0.92	1.11	1.40
Ba	186	255	300	--
Cr	1028	443	105	--
Cu	61	91	109	--
Ni	387	211	82	--
Pb	0.5	2	1	--
Rb	16	25	31	--
Sr	302	442	548	--
Th	3	6	8	--

Dashes, not determined.
1. Oceanite, Île de l'Est [*Gunn et al.*, 1970].
2. Ankaramite, average of seven analyses, Île de l'Est [*Gunn et al.*, 1970].
3. Alkali basalt, average of two analyses, Île de l'Est [*Gunn et al.*, 1970].
4. Basalt, Île aux Cochons [*Bellair*, 1963].

picritic olivine basalts, basanite dikes and a pale-colored felsic tristanite dike. All the early volcanic rocks were hydrothermally altered following emplacement of Phase II ring dikes. Rocks of Phase III and Phase IV represent an inverted petrologic sequence with differentiated lavas (feldspar-phyric basalts, An_{40}) preceding cumulate rocks (ankaramitic olivine basalts with augite, olivine, and plagioclase (An_{65}) phenocrysts). The nepheline-phonolite plug at Dôme du La Pérouse was emplaced early during Phase III. Phase V rocks range from felsic basalt flows, with phenocrysts of augite (some zoned aegerine-augite) and plagioclase (An_{40-50}), to intrusive phonolites with phenocrysts of zoned sanidine and anorthoclase, aegerine-augite, aegerine, brown hornblende, sphene, and glomeroporphyritic nepheline.

Chronologic Data

The oldest volcanic rocks occur on Île de l'Est and Île de la Possession, where the first cycle (Phase I and Phase II) of volcanic activity took place between 9 and 1.3 Ma [*Chevallier et al.*, 1983]. A second cycle (Phase III and Phase IV, 1–0.5 Ma) produced outpourings of lava and pyroclastic rocks on all islands in the archipelago, and a third cycle (Phase V, 0.2 Ma? to present) was responsible for the numerous small scoria cones on Île de la Possession and Île aux Cochons and for the more limited number of scoria cones on Île de l'Est [*Chevallier et al.*, 1983]. This third resurgence of volcanic activity is characteristic of the volcanic activity which has affected the other southern Indian Ocean volcanoes in the past 10,000 years. Although there are no records of historical activity on either Île de l'Est or Île de la Possession, it is possible that both islands are still volcanically active.

K-Ar age determinations for the volcanic rocks of Île de l'Est (Nougier, unpublished data, 1980) are summarized below:

Strombolian activity (Unit IV)	0.1? Ma
Unit III lavas	0.5–0.4 Ma
Unit II lavas	1.6–0.9 Ma
Gabbroic plutonic complex	8.75 Ma

The dated volcanic record of Île de la Possession (Table F.4.3) ranges from 8.1 to 0.53 Ma [*Chevallier et al.*, 1983]. The Strombolian eruptions have not been dated, but they represent Recent or near-Recent volcanism prior to 5500 years B. P. [*Chevallier et al.*, 1983].

Extent of Knowledge

Early geological observations of Îles Crozet were made by members of the Deutsche Südpolar Expedition of 1901–1903 [*Reinisch*, 1908*c*], the British, Australian and New Zealand Antarctic Research Expedition of 1929 [*Tyrrell*, 1937*b*], and the *Bougainville* expedition of 1939 [*Lacroix*, 1940]. Modern investigations began after the establishment of a scientific station on Île de la Possession in 1964 [*Gunn et al.*, 1972; *Chevallier*, 1981; *Chevallier and Nougier*, 1981; *Boudon and Nougier*, 1982; *Lameyre and Nougier*, 1982; *Chevallier et al.*, 1983].

Copyright American Geophysical Union

TABLE F.4.2. Representative Chemical Analyses and CIPW Norms of Volcanic Rocks From Île de la Possession

	1	2	3	4	5
SiO_2	42.00	43.85	45.90	57.50	63.00
TiO_2	2.90	2.20	2.50	1.30	0.04
Al_2O_3	12.90	10.05	13.00	19.50	19.10
Fe_2O_3	9.85	5.22	4.41	3.58	2.50
FeO	2.75	5.21	6.66	1.01	--
MnO	0.20	0.16	2.50	0.23	0.15
MgO	10.80	15.00	11.50	1.10	0.40
CaO	12.40	13.50	12.20	3.50	1.10
Na_2O	2.30	1.50	2.00	6.80	6.60
K_2O	0.55	0.35	0.18	4.80	5.70
H_2O^+	2.04	1.62	0.37	0.26	0.90
H_2O^-	0.73	0.35	0.10	0.02	0.10
Total	99.42	99.01	100.02	99.60	99.95
or	3.37	2.13	7.13	28.59	34.07
ab	11.09	9.24	12.37	41.17	56.37
an	24.02	20.23	23.02	8.52	5.52
ne	4.89	2.07	2.50	9.05	--
di	30.82	38.15	29.87	5.98	--
wo	--	--	--	--	--
hy	--	--	--	--	0.64
ol	9.57	16.07	13.92	--	0.26
hm	9.40	--	--	3.44	2.53
mt	1.14	7.80	6.42	0.24	--
il	5.70	4.31	4.77	2.49	0.32

Dashes, not determined (elements) or not present (norms).
1. R.9286. Olivine basalt flow, Phase II [*Chevallier et al.*, 1983].
2. R.9416. Picritic basalt, Phase II [*Chevallier et al.*, 1983].
3. R.9251. Ankaramite flow, Phase IV [*Chevallier et al.*, 1983].
4. Ne-phonolite dyke, Jeannel Plateau, Phase V [*Chevallier et al.*, 1983].
5. R.9252. Ne-phonolite plug, Dôme du La Pérouse, Phase III [*Chevallier et al.*, 1983].

TABLE F.4.3. K-Ar Age Determinations for Volcanic Rocks From Île de la Possession

Sample	Rock Type	Age, Ma
R.9417	Ankaramite, Phase IV	0.53 ± 0.09
R.9418	Ankaramite, Phase IV	0.65 ± 0.15
R.9251	Ankaramite, Phase IV	0.70 ± 0.15
R.9419	Olivine basalt sill, Phase III	0.72 ± 0.11
R.9253	Feldspar-phyric basalt sill, Phase III	0.80 ± 0.20
R.9252	Phonolite plug, Phase III	1.03 ± 0.04
R.9255	Basanite ring dike, Phase II	1.30 ± 0.40
R.9416	Picritic basalt, Phase II	2.70 ± 0.80
R.9286	Olivine basalt, Phase II	8.10 ± 0.60

All data from *Chevallier et al.* [1983, Table 1].

Bibliography

Bellair, 1963, 1964
Berthois et al., 1969
Boudon and Nougier, 1982
Cantagrel et al., 1980
Chevallier, 1981
Chevallier and Nougier, 1981
Chevallier et al., 1983
Dreux and Remy, 1963
Goslin et al., 1981*a*, *b*
Gunn et al., 1970, 1972
Lacroix, 1940
Lameyre and Nougier, 1982
Reinisch, 1908*c*, 1909
Schlich, 1975
Tyrrell, 1937b

Copyright American Geophysical Union

F.5. ÎLES KERGUELEN

Type of volcano: Four basaltic shield volcanoes overlie a basement of older plutonic rocks and partly synchronous volcano-plutonic complexes. Younger stratovolcanoes (mainly pyroclastic rocks) are associated with numerous parasitic scoria cones.

Location: On the submarine Kerguelen Plateau, southern Indian Ocean (~49°22′S, 69°30′E).

Height above sea level: 1840 m (Mont Ross).

Estimated volume: 3600 km^3 (for flood basalts above sea level).

Evidence of Holocene activity: Fresh appearance of lava lobes peripheral to the volcano-pluton of Péninsule Rallier du Baty, and fumarolic activity and hot springs at a height of 300–650 m along the western margin of this pluton [*Nougier*, 1972*a*].

Authors of report: J. Nougier and J.W. Thomson.

Date of report: June 1988.

Form and Structure

Îles Kerguelen comprise a large island, 6500 km^2 in area, surrounded by about 400 small islands; ~600 km^2 is covered by ice. The main island is built of subhorizontal plateau basalts and pyroclastic rocks, representing the outpourings from four separate shield volcanoes, and a complex of plutonic rocks (Figure F.5.1*a*). The plutonic complexes form a series of intersecting alkaline ring complexes (including alkali-granite, nepheline-syenite, and biotite-gabbro), and there are a number of older tholeiitic to transitional sills and massifs [*Giret and Lameyre*, 1983]. The volcano-plutonic complexes in southeastern Îles Kerguelen are associated with trachyphonolitic domes and phonolitic spines, cupolas, and dikes [*Nougier et al.*, 1983].

Plateau basalts in the central and southern part of Îles Kerguelen are almost 1000 m thick, individual flows being 3–10 m thick. The flows are interbedded with red cinders, pyroclastic rocks, and rare fossiliferous marine horizons of Tertiary age [*Fletcher*, 1938]. Silicified tree trunks and lignite beds occur locally in the lava sequences in the north, east, and southeast of Îles Kerguelen [*Aubert de la Rüe and Dixon*, 1932; *Nougier*, 1970]. The flows usually have shallow dips of 1°–5°, but 40°–60° dips occur where emplacement of the ring complexes has caused upwarping [*Nougier*, 1963, 1966].

The younger volcanic features include the stratovolcano at Mont Ross, a predominantly pyroclastic cone (15 km in diameter) which is cut by feeder dikes and has been breached in the east by a 5-km-wide caldera; it has numerous Strombolian parasitic cones on its flanks. Mont Richards (or Societé de Geógraphie) and Mont Guynemer, shown as Quaternary volcanoes on earlier maps, have been shown to be plutonic complexes. A geothermal field on Péninsule Rallier du Baty has been related to a series of Holocene trachytic eruptive centers under an ice cap [*Ballestracci and Nougier*, 1984].

It has been suggested that there is a rift structure to the west of the archipelago which provided some tectonic control on magmatism in these islands [*Giret and Lameyre*, 1983]. Block faulting about northeast-southwest and northwest-southeast trends has occurred, and a system of ring fractures is centered on the Mont Ross volcano (Figure F.5.1*b*).

Petrologic Characteristics

The plateau basalts range in composition from transitional tholeiites (basal series) to the younger alkali olivine basalts and rhyolitic, trachytic, and phonolitic differentiates [*Watkins et al.*, 1974] (Figure F.5.1*a* and Table F.5.1). *Nougier* [1972*b*] concluded that the differentiated alkaline lavas can be divided into a *ne*-rich and strongly undersaturated series (phonolites and *ne*-bearing trachytes) and a silica-saturated series, including numerous alkali trachytes, peralkaline trachytes, and soda rhyolites.

The commonest lithologies of the plateau basalts are aphyric hawaiites (andesine microlites, small prisms of clinopyroxene, and abundant titanomagnetite) and mugearites (oligoclase, clinopyroxene, Fe-Ti oxides, and apatite) with flow textures. Other textural varieties include pilotaxitic, porphyritic, doleritic, vesicular, and scoriaceous rocks. Phenocrysts in the porphyritic rocks are plagioclase (An_{50-55}), clinopyroxene, and/or olivine. The older basalts are strongly zeolitized; the youngest rocks are basanites.

The differentiated alkaline lavas range from alkali trachytes (K-feldspar crystals and rare olivine phenocrysts in a flow-banded feldspathic groundmass of K-feldspar, clinopyroxene, and Fe-Ti oxides) through quartz-rich trachytes (microporphyritic rocks with a groundmass of K-feldspar and small crystals of soda amphibole, clinopyroxene, and quartz) to spherulitic rhyolites containing a few phenocrysts of oligoclase.

Copyright American Geophysical Union

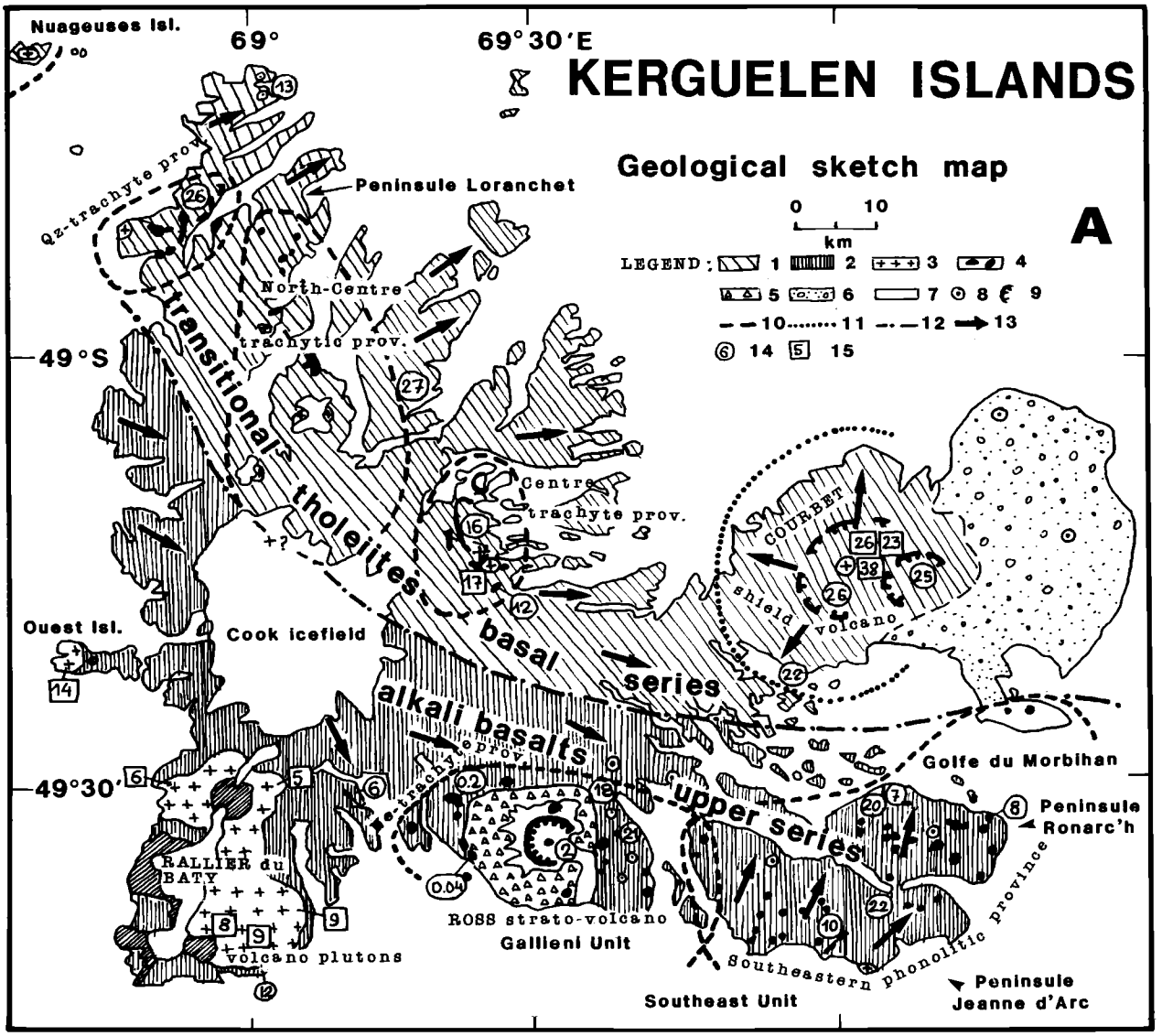

Fig. F.5.1. (*a*) Geologic sketch map of Îles Kerguelen: 1, transitional tholeiite basal series; 2, alkali basalt upper series; 3, volcano-plutonic complexes; 4, differentiated lavas and intrusions; 5, pyroclastic rocks of Mont Ross stratovolcano; 6, fluvioglacial deposits and moraine; 7, ice; 8, isolated volcanic plug or parasitic cone; 9, caldera structures; dashed lines, limit of petrographic province; dotted lines, limit of Courbet shield volcano; dash-dotted line, hypothetical limit between transitional tholeiites and alkali series; arrows, main lava flow directions; encircled numbers, K-Ar dates of volcanic rocks; numbers in squares, K-Ar dates of plutonic rocks. (*b*) Fracture network and fault systems, Îles Kerguelen.

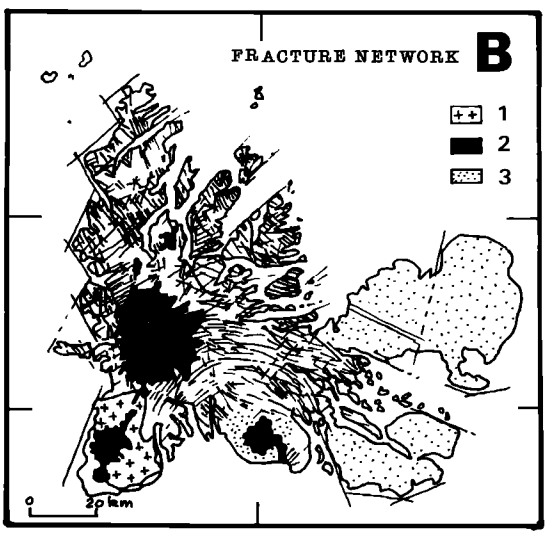

Copyright American Geophysical Union

TABLE F.5.1. Representative Chemical Analyses and CIPW Norms of Volcanic and Plutonic Rocks From Îles Kerguelen

	1	2	3	4	5	6	7	8	9	10
SiO_2	45.50	45.75	46.80	49.00	54.55	57.86	60.30	61.40	65.22	71.57
TiO_2	3.20	3.26	3.50	2.12	0.50	0.40	0.25	0.00	0.60	0.30
Al_2O_3	16.50	12.46	16.90	16.46	21.45	18.48	18.29	18.50	15.82	14.76
Fe_2O_3	4.68	2.00	5.70	2.00	2.29	1.98	2.86	3.28	2.76	1.63
FeO	8.40	8.93	7.39	10.49	1.45	3.27	2.61	1.01	1.46	1.38
MnO	0.19	0.21	0.15	0.17	0.13	0.07	0.18	0.18	0.12	0.05
MgO	6.90	10.75	4.60	7.14	0.47	0.94	0.24	0.03	0.48	0.46
CaO	8.30	9.85	6.10	10.36	1.10	0..51	1.71	0.70	0.61	0.74
Na_2O	2.80	3.53	3.50	2.54	9.20	5.77	6.72	8.00	5.80	4.15
K_2O	1.10	2.20	1.85	0.48	6.50	5.05	6.13	5.60	5.79	4.96
P_2O_5	--	1.06	--	0.23	--	0.40	--	--	--	0.27
H_2O^+	1.00	--	1.54	--	0.87	3.80	0.37	0.85	--	--
H_2O^-	0.69	--	1.11	--	0.16	1.30	0.17	0.28	0.71	--
Total	99.16	100.00	99.14	100.00	99.07	99.80	99.83	99.83	99.37	100.00
Q	--	--	--	--	--	1.89	--	--	8.11	26.46
or	6.68	13.01	11.34	2.81	39.38	31.53	36.52	33.56	34.71	29.26
ab	24.28	11.24	30.66	21.26	19.23	51.48	44.45	50.01	49.66	34.98
an	29.92	11.63	25.80	31.74	--	0.19	1.60	--	--	2.08
ne	--	10.08	--	--	30.63	--	6.91	7.94	--	--
di	9.92	24.89	4.45	14.65	4.62	--	5.75	0.99	2.38	--
wo	--	--	--	--	--	--	0.12	0.99	--	--
ac	--	--	--	--	3.43	--	--	3.39	--	--
hy	6.47	--	9.83	15.23	--	6.53	--	--	0.11	11.93
ol	9.54	17.75	2.46	6.96	0.06	--	--	--	--	--
mt	6.96	2.90	8.57	2.87	1.68	3.03	4.18	3.12	3.40	2.36
il	6.24	6.19	6.89	3.99	0.97	0.80	0.48	--	1.16	0.57
ap	--	2.51	--	0.54	--	1.00	--	--	0.44	0.64
cor	--	--	--	--	--	3.63	--	--	0.02	1.78
Ba	--	651	--	--	--	--	--	--	<125	--
Co	--	--	--	--	--	--	--	--	27	--
Cr	--	--	--	143	--	--	--	--	<24	--
Cu	--	--	--	82	--	--	--	--	<18	--
Nd	--	43	--	28	--	--	--	--	66	--
Ni	--	--	--	100	--	--	--	--	<19	--
Pb	--	--	--	1	--	--	--	--	--	--
Rb	--	67	--	18	--	271	--	--	64	57
Sm	--	8	--	6	--	--	--	--	13	--
Sr	--	1081	--	560	--	1535	--	--	765	404
Th	--	--	--	2	--	--	--	--	--	--
V	--	--	--	--	--	--	--	--	<10	--

Dashes, not determined (elements) or not present (norms).

1. K72. Alkali olivine basalt flow, Gallieni unit [*Nougier et al.*, 1983].
2. Average of 14 analyses. Basanite, eastern Îles Kerguelen [*Watkins et al.*, 1974; *Dosso and Murthy*, 1980].
3. K138. Alkali basalt flow, Southeast unit, Péninsule Ronarc'h [*Nougier et al.*, 1983].
4. Average of nine analyses. Transitional tholeiites of basal series, northern Îles Kerguelen [*Watkins et al.*, 1974; *Dosso and Murthy*, 1980].
5. K107. Differentiated phonolite flow, Southeast unit, Péninsule Ronarc'h [*Nougier et al.*, 1983].
6. Average of two analyses. Alkali trachyte, central Îles Kerguelen [*Nougier*, 1970].
7. Average of seven analyses. Trachyphonolite, southern Gallieni unit (analyst, J. Nougier).
8. K24. Differentiated *ne*-trachyte flow, Gallieni unit [*Nougier et al.*, 1983].
9. Average of 43 analyses. Syenite from volcano-plutonic complexes, Péninsule Rallier du Baty [*Lameyre et al.*, 1981].
10. Average of 13 analyses. Rhyolite and rhyotrachyte from northern Îles Kerguelen [*Nougier*, 1970].

Copyright American Geophysical Union

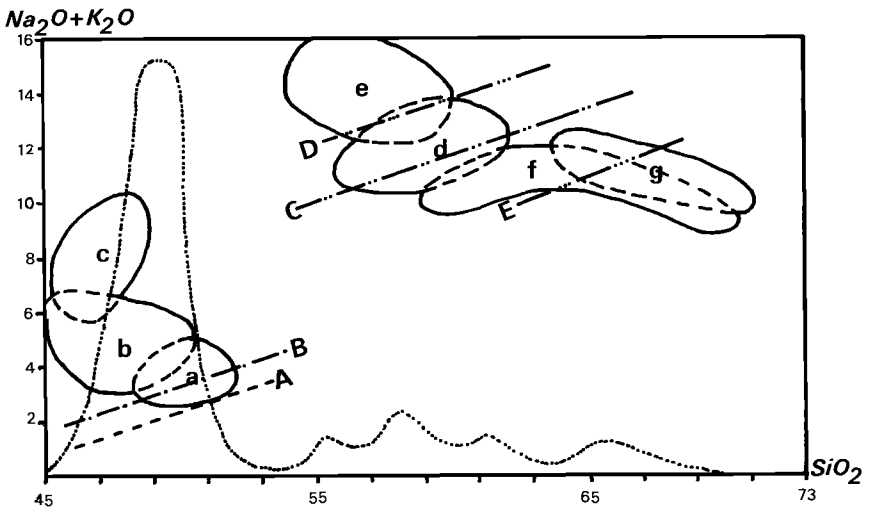

Fig. F.5.2. Alkali versus silica plot for volcanic and plutonic rocks of Îles Kerguelen. A, tholeiite/transitional tholeiite limit; B, transitional tholeiite/alkali basalt limit; C, *ne*-trachyte/*Q*-trachyte limit; D, *ne*-trachyte/phonolite limit; E, *Q*-trachyte/rhyolite (or syenite/granite) limit; a, transitional tholeiite basal series and metabasalts of Péninsule Rallier du Baty; b, alkali basalts (Gallieni unit); c, alkali basalts and basanites (Southeast unit); d, trachyphonolites of central area; e, phonolites, southeastern area; f, *Q*-trachytes and rhyolites of northern province; g, syenites and granites of ring complexes, Péninsule Rallier du Baty. Dotted curve, frequency distribution of rock types.

Detailed work on the upper series of the alkali basalts in southeastern Îles Kerguelen (Figure F.5.1*a*) has revealed morphological, lithological, and geochemical differences between two adjacent shield volcanoes (the Gallieni and Southeast units of *Nougier et al.* [1983]). Alkali versus silica plots (Figure F.5.2) show that the Gallieni unit has lower alkalis than the Southeast unit, and differences in their differentiation trends are shown by SiO_2, Al_2O_3, Na_2O, and TiO_2, possibly reflecting differences in their parental magmas [*Nougier et al.*, 1983].

Watkins et al. [1974] suggested a geographic migration of differentiating magmatism from oversaturated and saturated lavas in the northwest of the archipelago to undersaturated lavas in the southeast. *Nougier et al.* [1983] confirmed these spatial geochemical variations, since they found that saturated intrusive and extrusive rocks occur along the western coast, intermediate rocks occur in the central part of the island, and undersaturated rocks are restricted to the southeast. There are, however, exceptions to this distribution, and there is no simple chronologic-spatial migration scheme.

The plutonic complexes of Îles Kerguelen have been divided into three mineralogical and geochemical groups: (1) tholeiitic to transitional sills and massifs associated with the older shield volcanoes in the north of the archipelago [*Giret and Beaux*, 1984], (2) silica-oversaturated alkaline ring complexes, forming a western magmatic province, and (3) silica-undersaturated alkaline intrusive rocks which are synchronous with group 2 but occur only in the central and eastern part of Îles Kerguelen [*Giret and Lameyre*, 1983]. The boundary between groups 2 and 3 trends north-northwest to south-southeast.

The alkaline ring complexes of Péninsule Rallier du Baty [*Lameyre et al.*, 1976, 1981; *Dosso et al.*, 1979; *Dosso and Murthy*, 1980; *Giret et al.*, 1980; *Giret and Lameyre*, 1983] form a massif of quartz-rich alkali syenite with less common alkali granite and peralkaline granite, cut by dike-like differentiates of *ne*-rich monzonites and tonalites [*Nougier*, 1972*b*]. Other plutons in the archipelago include diorite [*Nougier*, 1970], nepheline-syenite [*Lacroix*, 1924], essexite, monzonite, and gabbro [*Aubert de la Rüe*, 1956, 1962].

The younger stratovolcanoes were associated with weak outpourings of undersaturated, alkaline, and largely *ne*-rich rocks [*Nougier*, 1972*b*] represented by basanite, limburgite, and tephrite [*Edwards*, 1938]. These lavas and the plateau basalts contain numerous xenoliths of eucrite, dunite, peridotite, pyroxenite, and amphibolite [*Lacroix*, 1924; *Aubert de la Rüe*, 1932; *Edwards*, 1938; *Talbot et al.*, 1963].

A Nd isotope study of the Iles Kerguelen rocks [*Dosso and Murthy*, 1980] (Figure F.5.3) has shown that the basalts have higher $^{87}Sr/^{86}Sr$ and lower $^{143}Nd/^{144}Nd$ values than the bulk earth. *Dosso and Murthy* [1980] concluded that the syenites, granites, gabbros, and basalts of Îles Kerguelen had a common "enriched-mantle" source (higher Rb/Sr and lower Sm/Nd than the bulk earth) which lay above a mantle plume. They suggested that isotopic variability in these

Copyright American Geophysical Union

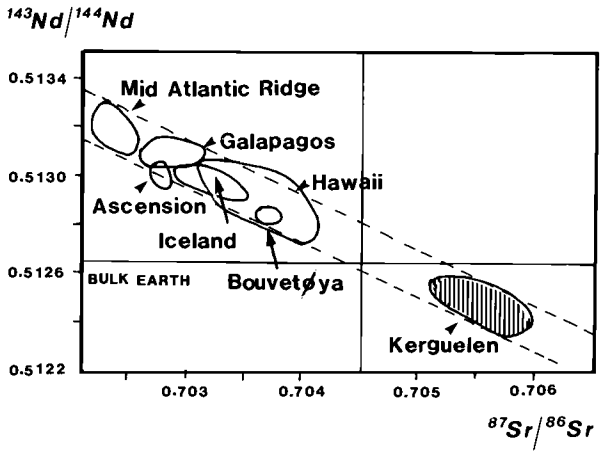

Fig. F.5.3. Nd-Sr plot of basalts from Îles Kerguelen [after *Dosso and Murthy*, 1980].

rocks may represent either heterogeneities in plume sources or the effects of plume material mixing with depleted upper mantle sources in variable proportions. Geochemical and geophysical studies have shown that sialic affinities are lacking [*Dosso et al.*, 1979; *Dosso and Murthy*, 1980; *Goslin and Patriat*, 1984; *Hartnady and le Roex*, 1985; *Recq and Charvis*, 1986] and there is therefore no evidence for the earlier interpretation that Îles Kerguelen represented a continental fragment.

Chronologic Data

The K-Ar age determinations obtained by *Nougier* [1972*a*] and *Nougier et al.* [1983] are shown in Table F.5.2. These results and other data [*Giret and Lameyre*, 1983] indicate that the older series of transitional tholeiitic basalts was emplaced between 40 and 25 Ma and that the main alkali basalt volcanism occurred at 23–17 Ma, with local recurrences between 6 and 2 Ma in the Mont Ross area. Dates for the differentiated lavas range from 26 Ma in northwestern Îles Kerguelen (rhyolites and quartz trachytes) to 12 Ma in the central part (alkali trachytes) and 8 Ma in the southeast of the archipelago (phonolites). The Mont Ross stratovolcano dates from about 2 Ma, and the Strombolian parasitic cones date from 1 Ma; younger differentiated extrusive rocks and sills (1.9–0.2 Ma) occur around the edge of the Mont Ross stratovolcano.

Giret and Lameyre [1983] recognized two main plutonic episodes on Île Kerguelen. The oldest, represented by tholeiitic to transitional intrusions [*Giret and Beaux*, 1984], began at least 40 m.y. ago, and a second event, beginning at 26 Ma, produced the alkaline intrusions which were responsible for resetting the isotopic ages of the older basalts. *Nougier et al.* [1983] noted that the volcanic activity had been rhythmic, with long periods of quiescence (about 10,000 years on average), as indicated by the presence of basal breccias, angular unconformities, conglomerates, and lignite beds.

TABLE F. 5.2. K-Ar Age Determinations of Volcanic Rocks From Îles Kerguelen

Lithology	Location	Age, Ma	Source
Ne-trachyte flow (differentiated)	SW of Mont Ross	0.04 ± 0.02	1
Ne-trachyte flow (differentiated)	NW of Mont Ross	0.2 ± 0.05	1
Ne-trachyte flow (differentiated)	E of Mont Ross	0.2 ± 0.05	1
Ne-trachyte flow (differentiated)	NW of Mont Ross	0.3 ± 0.08	1
Basalt flow	Parasitic cone, Mont Ross	1.0 ± 0.07	2
Trachyte flow	Periphery of Mont Ross stratovolcano	1.92 ± 0.08	2
Plateau basalt	Southern part of main island	5.9 ± 0.2	2
Phonolite	Péninsule Ronarc'h	6.6 ± 0.2	1
Nephelinite flow	Péninsule Ronarc'h	7.4 ± 0.2	1
Phonolite	Péninsule Jeanne d'Arc	8.4 ± 1.1	2
Phonolite	Péninsule Ronarc'h	8.4 ± 0.2	1
Syenite from volcano-pluton	Péninsule Rallier du Baty	8.7 ± 0.9	2
Phonolite	Péninsule Jeanne d'Arc	10.2 ± 0.3	1
Basalt near edge of pluton	Péninsule Jeanne d'Arc	11.5 ± 0.2	2
Basalt plug	Péninsule Loranchet	13.3 ± 0.2	2
Trachytic sill	Central province	15.6 ± 0.2	2
Trachybasalt	Gallieni unit	17.7 ± 0.5	1
Alkali basalt	Southeast unit	20.0 ± 0.6	1
Olivine alkali basalt	Gallieni unit	21.0 ± 0.6	1
Basalt	Golfe du Morbihan	21.9 ± 2.5	2
Alkali basalt	Péninsule Jeanne d'Arc	21.9 ± 0.5	1
Rhyolite dike in basalts	Péninsule Loranchet	25.9 ± 2.4	2
Basalt	Île Foch	27–30	2

Sources are (1) *Nougier et al.* [1983] and (2) *Nougier* [1972*a*].

Copyright American Geophysical Union

Extent of Knowledge

Îles Kerguelen were discovered by Yves de Kerguelen-Tremarec on February 12, 1772, and several expeditions visited the islands subsequently (Captain Cook in 1776, Sir James Clarke Ross in 1840 [*MacCormick,* 1842], and HMS *Challenger* in 1874 [*Renard,* 1889*a*]). During the nineteenth century, sealers inhabited the coastal area, showing interest in the lignite beds.

Early geological observations were made by members of German expeditions in 1898 and 1902 [*Philippi,* 1908*a*; *Reinisch,* 1908*a*, 1909] and French expeditions in 1908–1909 and 1913–1914 [*Lacroix,* 1924]. *Aubert de la Rüe* [1932] mapped the main volcanic provinces in 1928–1929 and 1931.

France established a manned weather station on the main island in 1950, and scientific work began in 1957. Much detailed geological research has been undertaken since the early 1960s [*Nougier,* 1972*a, b*; *Giret et al.,* 1980; *Giret and Lameyre,* 1983; *Nougier et al.,* 1983].

Bibliography

Aubert de la Rüe, 1932, 1956, 1962
Aubert de la Rüe and Dixon, 1932
Bauer and Berthois, 1962*a, b*
Bellair and Nougier, 1964
Dosso and Murthy, 1980
Dosso et al., 1979
Edwards, 1938
Fletcher, 1938
Giret and Beaux, 1984
Giret and Lameyre, 1983
Giret et al., 1980, 1984
Girod and Nougier, 1972
Goslin and Patriat, 1984
Hartnady and le Roex, 1985
Kovtoun et al., 1967
Lacroix, 1924
Lameyre et al., 1976, 1981
MacCormick, 1842
Nougier, 1963, 1966, 1970, 1972*a, b*
Nougier et al., 1983
Philippi, 1908*a*
Recq and Charvis, 1986
Reinisch, 1908*a*, 1909
Renard, 1889*a*
Talbot et al., 1963
Watkins et al., 1974

Copyright American Geophysical Union

F.6. HEARD AND MCDONALD ISLANDS

Type of volcano: Heard Island is a composite volcano composed of a Holocene(?) Newer Lava succession with subordinate pyroclastics above an exposed basement of Eocene-Pleistocene(?) age.

Location: Heard Island (53°06′S, 73°30′E) is located 440 km southeast of Îles Kerguelen and 60 km east of the McDonald Islands (53°02′S, 72°36′E), on the Kerguelen Plateau in the southern Indian Ocean.

Height above sea level: 2745 m.

Evidence of Holocene activity: Heard Island is currently active; the cone at Mawson Peak contained a small lava lake within a cylindrical vent in 1986. The Big Ben volcanic cone is largely Holocene.

Author of report: J. Barling.

Date of report: September 1987.

Form and Structure

Heard Island is 85–90% covered by permanent snow and ice (Figure F.6.1); very little is known about its internal structure and the relative proportions of lava and pyroclastic rocks. The Holocene(?) Newer Lavas are built up on a basement of Eocene-Oligocene Laurens Peninsula Limestone and Pleistocene(?) Drygalski Formation. The Laurens Peninsula Limestone consists of thinly bedded limestones with intercalated thin tuffaceous shales intruded by concordant doleritic sills. These are unconformably overlain by the Drygalski Formation, which is composed of interbedded volcaniclastic deposits and basalt flows and small basaltic and trachytic intrusions. The dominant constructional feature of the island is the Big Ben cone (2745 m), approximately 20 km in diameter at sea level (Figure F.6.2). A smaller secondary cone, Mount Dixon (706 m), and two other peaks form the Laurens Peninsula to the northwest. Small coastal parasitic scoria cones are concentrated on the northern side of the island. The lower apron of Big Ben slopes at ~10°, but above 1000 m the slope steepens sharply to 20°, suggesting an increased proportion of pyroclastic deposits in the central part of the cone. The summit region forms a broad plateau at about 2000 m, on which stands Mawson Peak, the assumed site of volcanic activity in 1985 [*Williams and Duhamel,* 1986]. The morphology of the plateau suggests an older caldera, about 5 km across, that is breached to the southwest. The small coastal cones show varied degrees of erosion from deeply dissected (Rogers Head) to almost untouched (Macey Cone) structures. The information in this account is derived largely from *Lambeth* [1952] and *Stephenson* [1964].

The McDonald Islands (McDonald Island, Flat Island, and Meyer Rock) reach a maximum elevation of only 186 m and are therefore free of snow and ice. McDonald Island, the largest of the group (1 km^2), consists of a laminated tuff plateau intruded by phonolitic dikes and domes [*Clarke et al.,* 1983, also unpublished data, 1980]; thin phonolitic flows are found on Flat Island. Limestone clasts found in the tuff indicate that, like Heard Island, the McDonald Islands are underlain by limestone.

Petrologic Characteristics

The igneous rocks of Heard and McDonald Islands form a highly potassic suite. Available samples of the New Lavas (collected by Stephenson, Clarke, and the Blunt-Vining Expedition) indicate that Big Ben and its parasitic cones are built solely of highly porphyritic basalts with limburgitic and ankaramitic affinities. The three modal variants recognized show no systematic distribution pattern: (1) olivine-pyroxene basalt (alkali olivine basalt–trachybasalt) with olivine as the predominant phenocryst and pyroxenes zoned from Cr-diopside to salite; (2) olivine-pyroxene basanite, distinguished from the olivine-pyroxene basalt by higher Ca, Ti/Al, and Fe and lower Si and containing subequal abundances of the two phenocryst phases, the pyroxenes being characterized by pronounced Ca-Ti "salite" rims; (3) olivine-pyroxene-plagioclase trachybasalts.

More evolved members of the suite, trachyandesites (with phenocrysts of olivine, diopsidic to salitic pyroxene, green Fe-salite cored pyroxene, and Fe-Ti oxide) and trachytes (ferrosalite-kaersutite-plagioclase), are confined to the Laurens Peninsula and the dissected remains of a smaller cone around Cave Bay, while phonolites (pyroxene–K-feldspar–kaersutite ± biotite ± sphene) are present on the McDonald Islands. Representative chemical and modal analyses of these rocks are given in Tables F.6.1 and F.6.2, and an alkali versus silica plot is shown in Figure F.6.3.

The relatively altered lavas and intrusions of the underlying Pleistocene(?) and Tertiary successions are chemically most similar to the olivine-pyroxene-plagioclase trachybasalt.

Copyright American Geophysical Union

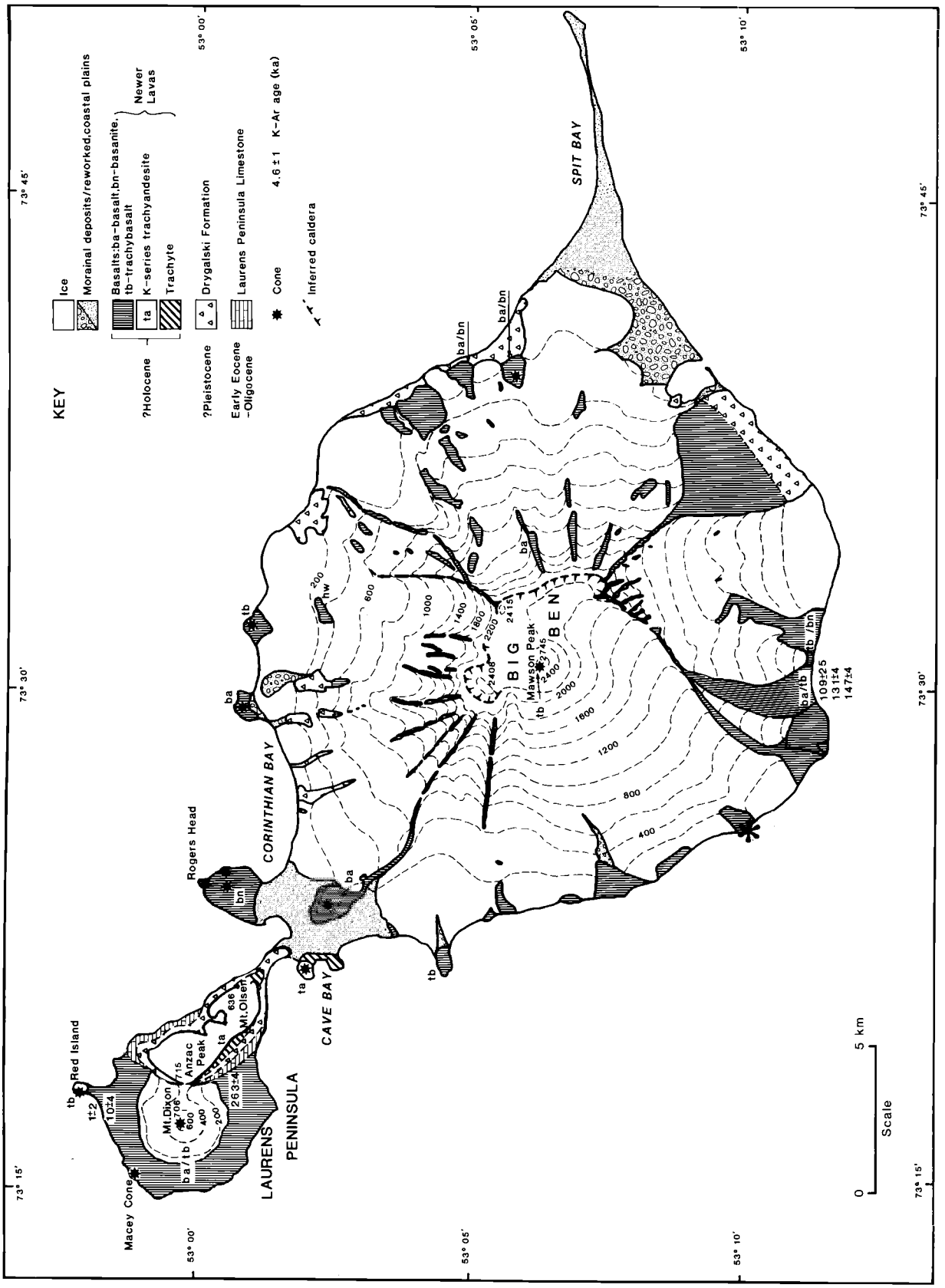

Fig. F.6.1. Geologic sketch map of Heard Island. The contour interval is 200 m.

Copyright American Geophysical Union

Copyright American Geophysical Union

TABLE F.6.1. (continued)

	1[a,c]	2[b,d,e]	3[a]	4[b,d]	5[b,d,e]	6[b,d]
or	8.87	9.93	12.18	21.04	35.40	37.53
ab	1.99	10.17	22.25	29.20	27.87	35.85
an	10.38	8.06	13.41	16.11	0.00	2.93
ne	5.61	6.00	--	1.55	21.82	11.66
ac	--	--	--	--	2.28	--
di	40.63	28.18	20.94	11.67	7.60	6.74
hy	--	--	3.04	--	--	--
ol	20.70	27.52	17.31	9.73	2.57	1.89
mt	2.78	2.97	2.74	2.44	0.18	1.54
il	7.41	5.98	6.87	6.11	1.75	1.41
ap	1.66	1.23	1.30	2.18	0.57	0.50
an%	83.89	44.22	37.60	35.56	0.00	7.57
Ba	500	482	--	720	204	696
Ce	--	74.23	--	--	100.09	--
Cr	916	696	--	16	16	3
Cu	47	80	--	30	13	5
Rb	36	40	--	72	156	159
Dy	--	4.68	--	--	3.14	--
Er	--	1.93	--	--	1.60	--
Eu	--	2.44	--	--	1.62	--
Gd	--	6.59	--	--	3.35	--
La	--	34.69	--	--	58.62	--
Lu	--	0.200	--	--	0.264	--
Nb	47	38	--	107	120	127
Nd	--	36.42	--	--	32.41	--
Ni	397	533	--	11	13	2
Pb	4	3	--	11	32	16
Sm	--	7.64	--	--	5.33	--
Sr	779	589	--	1146	771	790
Th	8	5	--	11	30	22
U	0	0	--	1	4	3
V	280	266	--	214	46	10
Y	20	20	--	42	16	31
Yb	--	1.30	--	--	1.65	--
Zn	112	110	--	149	87	99
Zr	196	246	--	791	1228	1130

Dashes, not determined (elements) or not present (norms).
[a]Major oxides analyzed by XRF except for Na_2O (flame photometry) and FeO (volumetrically) [*Stephenson*, 1972].
[b]Major oxides analyzed by XRF (Clarke, unpublished data, 1980).
[c]Trace elements analyzed by XRF (Barling and McCall, unpublished data, 1986).
[d]Trace elements analyzed by XRF (Barling and McCabe, unpublished data, 1985).
[e]REE analyzed by isotope dilution mass spectroscopy (Barling, unpublished data, 1986).
1. H9. Basanite, south flank of Big Ben, Heard Island.
2. 65085. Basalt, south flank of Big Ben, Heard Island.
3. H66. Trachybasalt, northeast coast of Heard Island.
4. 65005. Trachyandesite, Cave Bay, Heard Island.
5. 65125. Phonolite, McDonald Island.
6. 65042. Trachyte (phonolitic), Mount Olsen, Heard Island.

Copyright American Geophysical Union

TABLE F.6.2. Representative Modal Analyses of Lavas From Heard and McDonald Islands

	1	2	3	4	5	6
Phenocrysts, %						
Olivine	19.0	25.3	10.0	1.3	--	--
Pyroxene	29.7	7.0	2.6	2.7	2.0	1.5
Plagioclase	--	0	1.7	0	--	7.5
Fe-Ti oxide	0	0	0	2.3	--	0.5
Kaersutite	--	--	--	--	2.3	0.5
K-feldspar	--	--	--	--	14.0	--
Biotite	--	--	--	--	1.7	--
Sphene	--	--	--	--	0.7	--
Matrix	--	36.3	--	56.7	79.3	--
Glass	21.3	--	30.0	--	--	--
Groundmass, %						
Olivine	0	0	0.7	0	--	--
Pyroxene	16.7	10.0	13.0	8.7	0	9.5
Plagioclase	--	7.7	29.0	19.0*	--	77.0*
Fe-Ti oxide	13.3	13.7	13.0	9.3	--	3.5
Kaersutite	--	--	--	--	0	0
K-feldspar	--	--	--	--	0	--
Biotite	--	--	--	--	0	--
Sphene	--	--	--	--	0	--
Total	100.0	100.0	100.0	100.0	100.0	100.0
% Phenocrysts	48.7	32.3	14.3	6.3	20.7	10.0

Analyses by J. Barling (unpublished data, 1986). Dashes, not present.
*Includes alkali feldspar in fine-grained groundmass.
1. H9. Basanite, south flank of Big Ben, Heard Island.
2. 65085. Basalt, south flank of Big Ben, Heard Island.
3. H66. Trachybasalt, northeast coast of Heard Island.
4. 65005. Trachyandesite, Cave Bay, Heard Island.
5. 65125. Phonolite, McDonald Island.
6. 65042. Trachyte (phonolitic), Mount Olsen, Heard Island.

Chronologic Data

K-Ar dates obtained from six samples of the Newer Lavas range from 1000 ± 2000 years to 266,000 ± 4000 years. Because most lavas are highly porphyritic, these ages are viewed as maxima [*Clarke et al.*, 1983]. None of the Tertiary and Pleistocene(?) lavas and intrusions have been found suitable for K-Ar dating. K-Ar dates are also available for three McDonald Island samples; these give ages ranging from 36,000 ± 3000 years to 79,000 ± 3000 years.

Extent of Knowledge

Early sightings of Heard Island were reported in 1833, 1849, and 1853, the last by Captain Heard, after whom the island was named. The first landing was made in 1855, and from then until the 1930s the island was used as a base by sealers. The earliest geological work [*Renard*, 1889*b*] resulted from the *Challenger* Expedition in 1873. Visits by the German *Gauss* Expedition in 1902, by Aubert de la Rüe in 1929, and by the British, Australian and New Zealand Antarctic Expedition, also in 1929, resulted in a series of papers on the geology of the island [*Philippi*, 1908*b*; *Reinisch*, 1908*b*, 1909; *Aubert de la Rüe*, 1929*a*; *Mawson*, 1932, 1933; *Tyrrell*, 1937*a*]. Subsequently, an Australian National Antarctic Research Expedition (ANARE) station was established from 1947 to 1955, which enabled mapping to be undertaken by *Lambeth* [1952]. Petrologic and geochemical studies have been made by *Stephenson* [1972], *Clarke et al.* [1983], *Barling* [1986], *Barling et al.* [1988], and Clarke (unpublished data, 1980).

Copyright American Geophysical Union

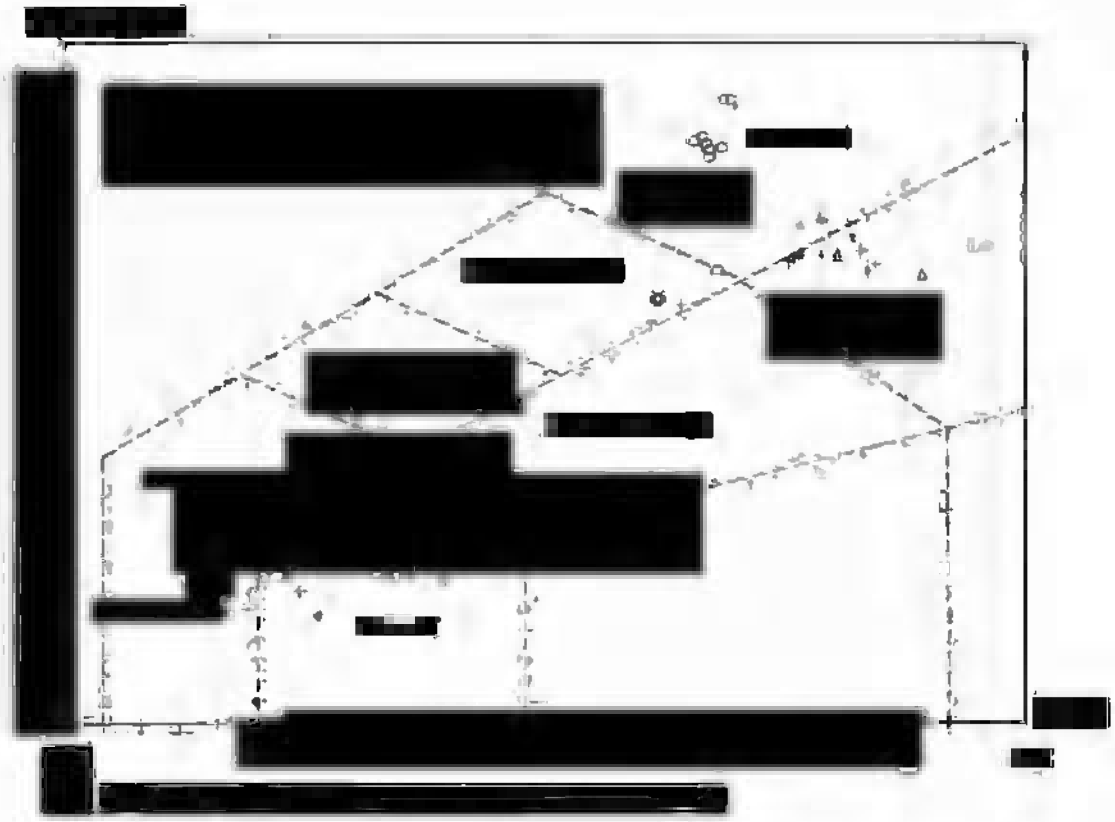

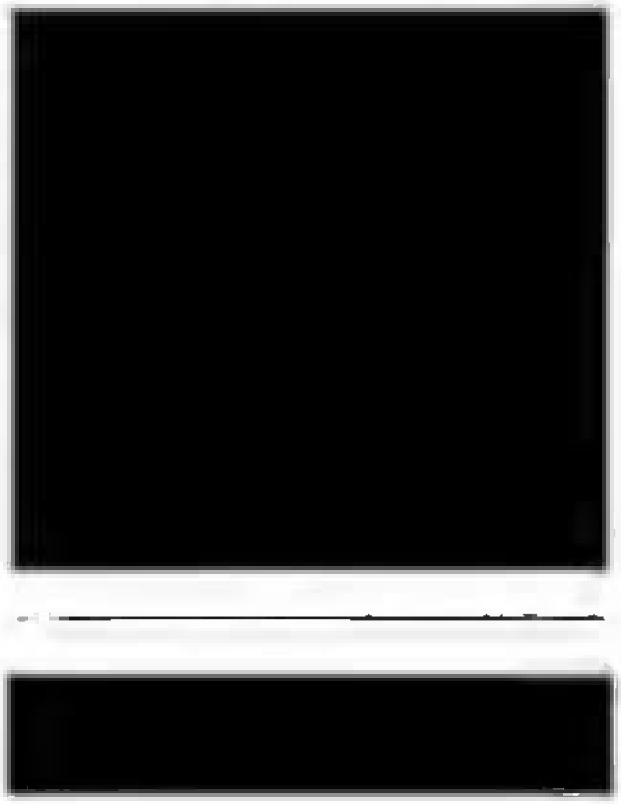

Copyright American Geophysical Union

Copyright American Geophysical Union

F.7. AMSTERDAM AND SAINT PAUL ISLANDS

Type of volcano: Stratovolcanoes built from migrating volcanic centers; numerous scoria cones on flanks.

Location: Amsterdam Island (37°50′S, 77°31′E) and Saint Paul Island (38°43′S, 77°32′E), southern Indian Ocean.

Height above sea level: Amsterdam Island, 881 m; Saint Paul Island, 268 m.

Evidence of Holocene activity: In 1793, smoke and fresh ash were observed on a parasitic cone near the southwestern corner of Saint Paul Island; fumaroles were recorded in 1792, 1793, 1854, 1857, 1874, 1903, 1928–1931 [*Neumann van Padang*, 1963, p. 63] and 1972. There is evidence of recent aa activity (probably 100 years ago) near the scientific station at Dumas, Amsterdam Island [*Nougier*, 1982].

Authors of report: J. Nougier and J. W. Thomson.

Date of report: June 1987.

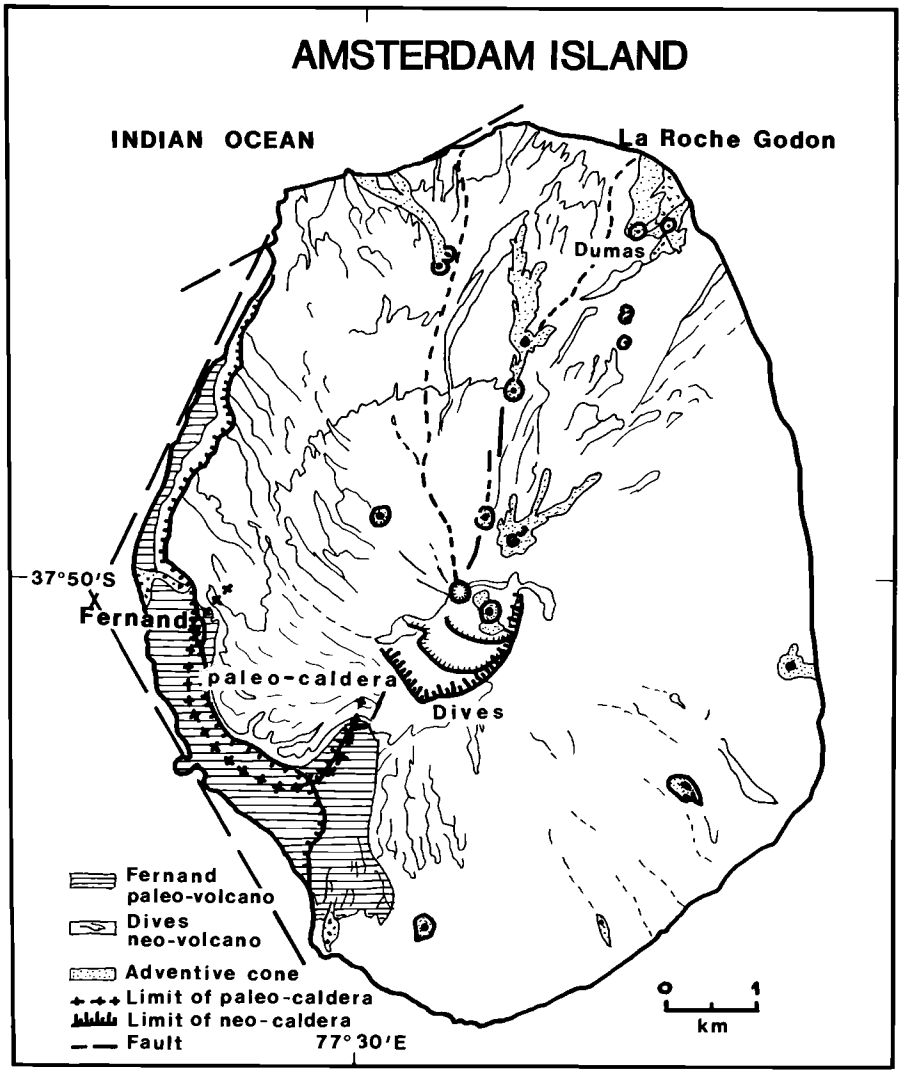

Fig. F.7.1. Sketch map of Amsterdam Island showing the location of the younger eruptive center and its relationship to the older volcanic rocks.

Copyright American Geophysical Union

Form and Structure

Amsterdam and Saint Paul islands are ice-free, subantarctic volcanic islands. On Amsterdam Island, only 5% of an older volcano is still visible, centered around a paleocaldera at the western side of the island (Figure F.7.1). Boulder deposits and breccias intruded by dikes form the basal unit of this volcano, followed by an upper series of lavas without dikes. A younger eruptive center is located 2 km east-northeast of the earlier one. Its elliptical terraced caldera contained a lava lake from which there were three phases of lava outflows. About 25 scoria cones, distributed along a number of radial fractures on the flanks of the volcano, mark a late stage in the history of this volcanic island.

Saint Paul Island has the remnants of an older tuff cone preserved beneath a younger volcano. The older deposits (yellow, graded palagonite tuffs cut by dikes and a comendite intrusion) are exposed by faults on the northeastern flank of the younger volcano (Figure F.7.2). The younger volcano has a central crater 1800 m in diameter and 300 m in height, from which were erupted numerous thin lava flows interlayered with cinders and scoria. There are a number of peripheral scoria cones related to a set of radial fissures, and geothermal areas are located on the crater rim. The crater is now breached, following late-stage faulting.

Petrologic Characteristics

The volcanic rocks on Amsterdam Island are transitional tholeiites trending toward an alkaline series (Figure F.7.3 and Table F.7.1); there are no differentiation products. Most of the lavas from the older volcano are porphyritic basalts (plagioclase (An_{60-65}), clinopyroxene, and some olivine phenocrysts) but aphyric basalt flows occur in the middle of the sequence. The younger volcano produced markedly feldspar-phyric lavas (An_{60-80}) which became laterally aphyric, and the scoria cones emitted glassy lavas [*Nougier*, 1982].

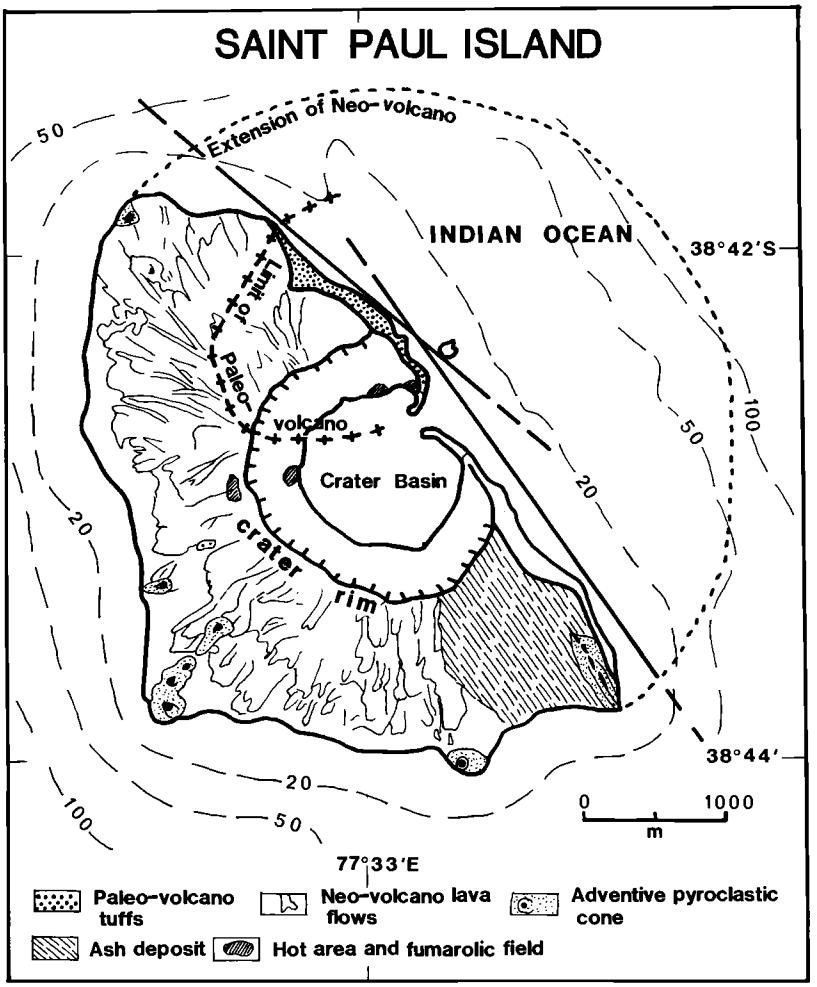

Fig. F.7.2. Geologic sketch map of Saint Paul Island.

Copyright American Geophysical Union

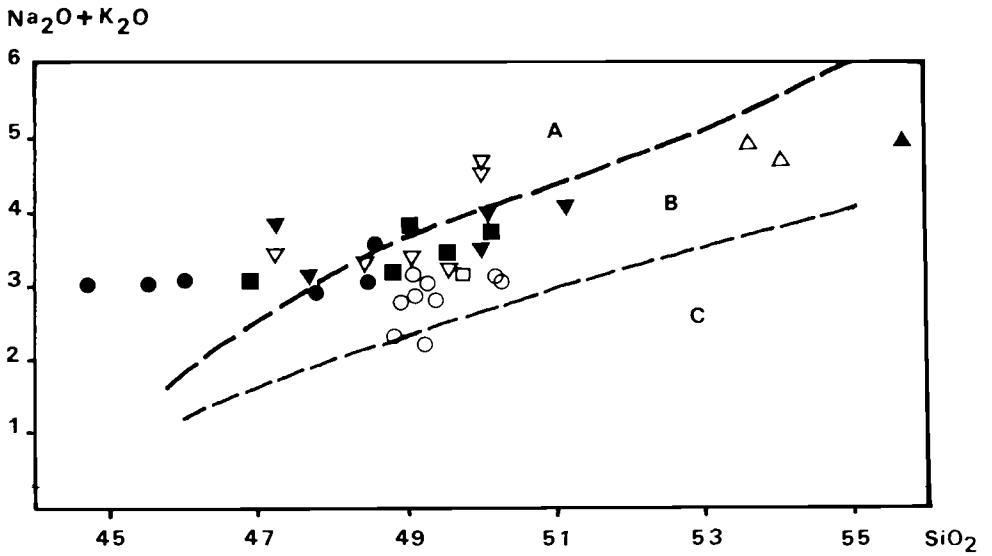

Fig. F.7.3. Alkali versus silica plot for volcanic rocks from Amsterdam and Saint Paul islands [after *Nougier*, 1982, Figure 92.4]. Solid symbols represent data from *Nougier* [1982], and open symbols data from *Gunn et al.* [1971, 1975] and *Girod et al.* [1971]: squares, paleovolcano, Amsterdam Island; circles, Dives volcano, Amsterdam Island; upright triangles, tuffs from paleovolcano, Saint Paul Island; inverted triangles, younger volcano, Saint Paul Island. A, field of alkali basalts; B, field of hypersthene tholeiites; C, field of pigeonite tholeiites [after *Kuno*, 1959].

The older tuff cone on Saint Paul Island has a tholeiitic basalt composition (Table F.7.1), and the feldspar-phyric basalt lavas (zoned plagioclase (An_{82-57}) and clinopyroxene phenocrysts) from the younger volcano are all aluminous tholeiitic rocks; the upper aphyric lavas are enriched in fayalitic olivine [*Nougier*, 1982].

Chronologic Data

K-Ar date determinations and paleomagnetism give a range of 0.7 Ma to present for the volcanic rocks on Amsterdam Island and 0.5–0.04 Ma for those on Saint Paul Island [*Watkins et al.*, 1975].

Extent of Knowledge

Amsterdam Island was sighted on March 18, 1522, by Captain Magellan and was named by Captain Van Diemen in July 1633; it was claimed for France in July 1843. In spite of its early discovery, scientific observations on this island and Saint Paul Island were not made until the period between 1857 and 1901, when early expeditions yielded some geological data [*Hochstetter*, 1866; *Philippi*, 1909] and the first volcanologic studies [*Vélain*, 1878]. More recent investigations have included petrologic [*Girod et al.*, 1971; *Gunn et al.*, 1971, 1975], paleomagnetic [*Watkins and Nougier*, 1973], and isotopic work [*Hedge et al.*, 1973; *Watkins et al.*, 1975].

Saint Paul Island is uninhabited, but a scientific station has been maintained on Amsterdam Island since December 1949.

Bibliography

Girod et al., 1971
Gunn et al., 1971, 1975
Hedge et al., 1973
Hochstetter, 1866
Nougier, 1982
Philippi, 1909
Vélain, 1878
Watkins and Nougier, 1973
Watkins et al., 1975

Copyright American Geophysical Union

TABLE F.7.1. Representative Chemical Analyses and CIPW Norms of Volcanic Rocks From Amsterdam and Saint Paul Islands

	1	2	3	4	5	6	7	8
SiO_2	46.00	48.47	49.00	49.50	49.80	50.10	55.66	72.46
TiO_2	1.75	1.75	2.22	1.78	2.62	2.23	1.84	--
Al_2O_3	19.85	15.69	16.70	19.20	14.00	14.90	15.08	14.28
Fe_2O_3	2.39	4.35	2.25	3.51	4.32	6.23	8.78	2.55
FeO	6.44	6.55	9.52	3.81	11.07	5.51	2.90	2.10
MnO	0.11	0.19	0.27	0.12	0.22	0.20	0.21	--
MgO	4.13	6.46	4.90	4.37	4.00	4.87	4.12	0.15
CaO	12.45	12.71	11.01	11.23	9.20	10.35	4.04	0.84
Na_2O	2.43	2.48	2.88	2.73	3.38	3.14	3.70	2.67
K_2O	0.68	0.65	0.85	0.68	0.90	0.74	1.14	4.29
H_2O^-	2.72	0.68	0.09	3.21	0.02	0.47	1.90	1.52
Total	98.95	99.98	99.69	100.14	99.63	98.70	99.37	100.86
Q	--	--	--	3.73	0.76	4.72	15.36	37.96
C	--	--	--	--	--	--	0.41	3.73
or	4.18	3.87	5.05	4.15	5.34	4.45	6.92	25.54
ab	21.34	21.11	24.44	23.80	28.68	27.01	32.08	22.72
an	42.81	29.93	30.21	39.28	20.42	24.77	20.58	4.20
di	17.49	26.95	20.40	14.35	21.20	21.67	--	--
hy	0.42	6.33	6.02	5.95	12.32	3.88	10.57	2.14
ol	6.71	2.11	6.38	--	--	--	--	--
hm	--	--	--	--	--	--	5.69	--
mt	3.60	6.35	3.28	5.25	6.29	9.19	4.82	3.72
il	3.46	3.35	4.23	3.49	5.00	4.31	3.59	--
Ba	165	179	70	106	180	144	204	--
Co	24	<10	40	29	45	40	35	--
Cr	82	85	140	147	80	109	66	--
Cu	78	50	100	101	55	55	26	--
Ni	48	55	60	58	50	60	60	--
Sr	321	333	260	266	230	264	140	--
V	<10	288	320	300	380	283	135	--

Dashes, not determined (elements) or not present (norms).

1. High-Al basalt from Dives lava lake, younger volcano, Amsterdam Island [*Nougier*, 1982].
2. Feldspar-phyric basalt, younger volcano, northwest cliffs of Amsterdam Island [*Nougier*, 1982].
3. Olivine basalt from older volcano, at 600 m above sea level, Amsterdam Island [*Nougier*, 1982].
4. High-Al basalt from base of older volcano, Amsterdam Island [*Nougier*, 1982].
5. Aphyric low-Al basalt from the southeastern crater rim of the younger volcano, Saint Paul Island [*Nougier*, 1982].
6. Feldspar-phyric tholeiitic basalt from base of younger volcano, Saint Paul Island [*Nougier*, 1982].
7. Average analyses of two palagonitized tholeiitic tuffs from older volcano, Saint Paul Island [*Nougier*, 1982].
8. Average analyses of three comendite intrusions cutting older volcano, Saint Paul Island [*Vélain*, 1878].

Copyright American Geophysical Union

F.8. GAUSSBERG

Type of volcano: Talus-covered leucitite cone with a few bedrock exposures.

Location: On Wilhelm II Coast, East Antarctica (66°47′S, 89°18′E).

Height above sea level: 370 m.

Evidence of Holocene activity: None.

Author of report: R.J. Tingey.

Date of report: 1984.

Fig. F.8.1. Geologic map of Gaussberg.

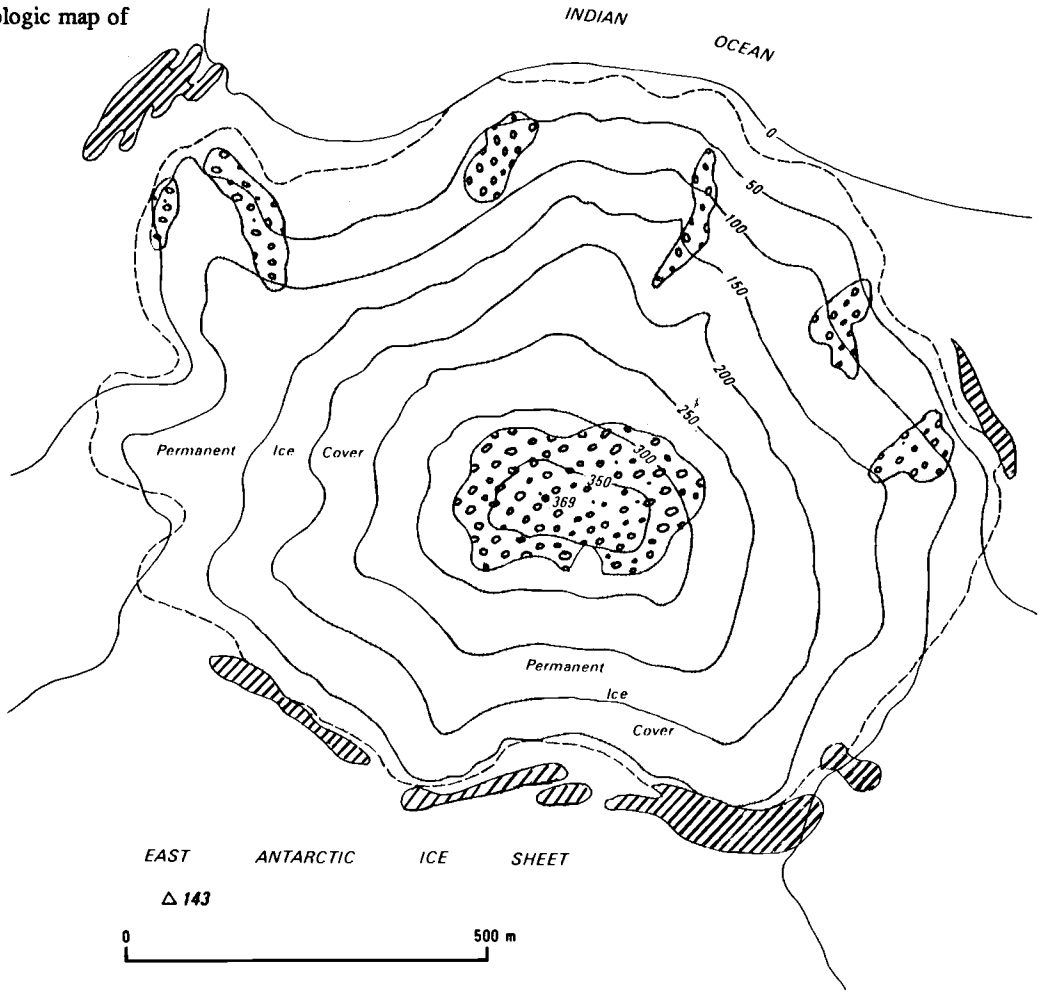

Bedrock outcrops. Pillow-structured Leucitite. (Exact limits not well defined.)

Moraines.

Edge of main rock mass.

NOTE. Most of Gaussberg is covered by leucitite scree but main bedrock outcrops are indicated on the map. Others occur within the scree but are too small to be mapped at this scale.

Contours and spot heights in metres.

Copyright American Geophysical Union

Copyright American Geophysical Union

TABLE F.8.1. Mean Chemical Composition and CIPW Norms of Leucitite Lavas From Gaussberg

	Mean*
SiO_2	50.9
TiO_2	3.42
Al_2O_3	9.86
Fe_2O_3	2.46
FeO	3.78
MnO	0.09
MgO	7.95
CaO	4.63
Na_2O	1.65
K_2O	11.61
P_2O_5	1.48
H_2O^+	1.17
H_2O^-	0.05
CO_2	0.05
SO_3	0.11
F	0.33
Cl	0.06
Total	99.60
or	51.90
lc	1.52
hl	0.10
th	0.20
ac	7.12
ns	1.10
ks	4.10
di	10.40
ol	11.60
il	6.50
ap	3.51
fr	0.41
cc	0.11
z	0.20
As	3.0
Ba	5550
Ce	337
Cr	306
Cu	29
Ga	18
La	210
Nb	90
Ni	233
Pb	40
Rb	315
Sn	2
Sr	1808
Th	30
U	2.5
V	106
Y	18
Zn	79
Zr	1004

*Mean of 11 analyses of leucitite. Major oxides analyzed by XRF; trace elements analyzed by instrumental neutron activation analysis [*Sheraton and Cundari*, 1980, Table 5].

mm diameter) are present in a fresh yellow-brown glassy matrix which is generally full of quench crystal growth toward the pillow cores. This groundmass contains very fine grained leucite, diopside, reddish-brown phlogopite, ilmenite, and chromite. There is relatively little chemical or petrographic variation in the rock sample. Crustal xenoliths are abundant, cognate inclusions (olivine + diopside + leucite ± phlogopite) less common, and mantle xenoliths (lherzolite) rare.

Gaussberg lies at the southern end of an aseismic submarine topographic feature, the Kerguelen Plateau. *Tingey et al.* [1983] concluded that the leucitite has few chemical, chronologic, and petrologic characteristics common to other volcanic piles (Heard Island and Îles Kerguelen) on the Kerguelen Plateau. Isotopic studies by *Collerson and McCulloch* [1983], which indicate that the Gaussberg leucitite probably derived from an enriched mantle source, support this observation. On present evidence there is little justification for the suggestion [*Duncan*, 1981] that the Kerguelen Plateau is a hotspot trace.

Chronologic Data

K-Ar and fission track geochronologic data indicate that Gaussberg accumulated about 55,000 years B.P., when the Antarctic ice sheet was more extensive than at present [*Tingey et al.*, 1983]. Previous K-Ar dates of 20 Ma [*Ravich and Krylov*, 1964] and 9 Ma [*Soloviev*, 1972] are thought to be erroneous, probably because of the incomplete outgassing of radiogenic argon at the time of eruption [*Tingey et al.*, 1983].

Extent of Knowledge

Gaussberg was discovered in 1901 by the Imperial German Antarctic Expedition, led by E. von Drygalski. His party was beset for a year in the sea ice a few kilometers away, and they mapped Gaussberg in detail. Mawson's Australasian Antarctic Expedition visited the volcano in 1912 [*Nockolds*, 1940], and in 1956 a party from the Soviet Antarctic Expedition base at Mirnyy worked there [*Vyalov and Sobolev*, 1959]. An Australian National Antarctic Research Expedition party visited Gaussberg in 1977 [*Sheraton and Cundari*, 1980; *Tingey et al.*, 1983] and again in 1981 [*Collerson and McCulloch*, 1983].

Bibliography

Collerson and McCulloch, 1983
Duncan, 1981
Nockolds, 1940
Ravich and Krylov, 1964
Sheraton and Cundari, 1980
Soloviev, 1972
Tingey et al., 1983
Vyalov and Sobolev, 1959

Copyright American Geophysical Union

F.9. BALLENY ISLANDS

Type of volcano: Basaltic lava flows and pyroclastic deposits, cinder cones, and plugs surmounting a submarine volcanic ridge.

Location: Southern Pacific Ocean, 250 km northwest of Cape Adare, (66°16′–67°38′S, 162°15′–164°44′E).

Height above sea level: 2179 m.

Evidence of Holocene activity: Eruption columns reportedly observed in 1839 and 1899 [*Quartermain*, 1964].

Authors of report: A.C. Wright and P.R. Kyle.

Date of report: October 1986.

Form and Structure

The Balleny Islands (Figures F.9.1 and F.9.2), a chain of volcanic islands 160 km long, are located at the southern end of a submarine ridge system that extends north to New Zealand but which is offset by the Indian-Antarctic ridge system. Volcanism in the Balleny Islands area is thought to be related to the Balleny Fracture Zone [*Falconer*, 1972; *Kyle and Cole*, 1974].

There are three large islands in the group (Young, Buckle, and Sturge, of which Sturge is the largest (approximately 300 km^2) and highest), three small islands (Row, Borradaile, and Sabrina), and several rocks and offshore stacks. The islands are characterized by steep cliffs and ice caps, and all are volcanic in origin, comprising interbedded tuff, agglomerate scoria, and lava flows. Several of the small islets may be volcanic necks or plugs [*Hatherton et al.*, 1965].

Petrologic Characteristics

Petrographic studies indicate the presence of olivine trachybasalt and minor olivine-augite basalts [*Mawson*, 1950; *Kyle*, 1976]. Sugary quartz xenoliths are present in lavas on Sabrina Island [*Waterhouse*, 1965]. A total of five geochemical analyses [*Mawson*, 1950; *Kempe*, 1973; *Johnson et al.*, 1982] indicate that these rocks range from basanite (four samples) to hawaiite (one sample) (Table F.9.1). In general, the lavas have a chemistry similar to that of the Hallett volcanic province (see section A.I) but are

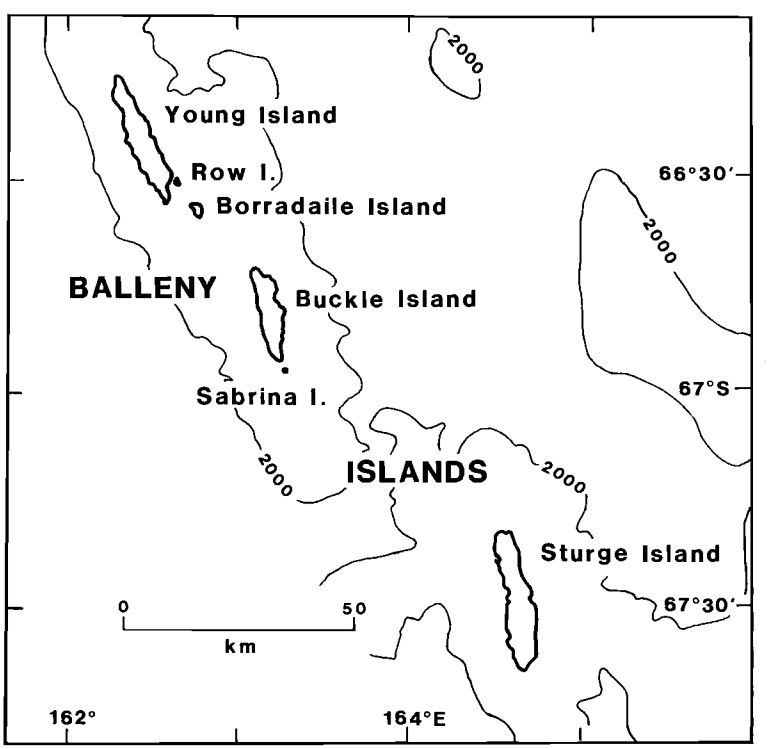

Fig. F.9.1. Sketch map of the Balleny Islands [after *Johnson et al.*, 1982].

Copyright American Geophysical Union

Copyright American Geophysical Union

TABLE F.9.1. Representative Chemical Analyses and CIPW Norms of Volcanic Rocks From the Balleny Islands and From Nearby Dredge Samples

	1	2	3	4	5
SiO_2	44.34	44.74	44.99	45.06	47.73
TiO_2	2.52	3.00	2.70	2.69	2.39
Al_2O_3	15.20	16.34	15.51	18.76	16.87
Fe_2O_3	4.15	3.72	3.43	0.23	2.52
FeO	6.38	7.72	7.27	9.94	8.87
MnO	0.18	0.19	0.19	0.29	0.18
MgO	10.74	7.53	9.29	7.33	5.80
CaO	10.27	10.60	9.63	9.72	8.64
Na_2O	3.41	3.86	4.32	4.19	4.90
K_2O	1.28	1.28	1.13	1.57	1.99
P_2O_5	0.60	0.63	0.70	0.65	0.65
H_2O^+	0.52	0.31	0.32	0.12	0.14
H_2O^-	0.60	0.04	0.01	0.02	0.02
Total	100.19	99.96	99.45	100.45	100.57
or	7.56	7.56	6.68	9.28	11.76
ab	13.43	15.33	17.59	11.00	20.61
an	22.39	23.48	19.59	27.74	18.16
ne	8.36	9.39	10.28	13.25	11.30
di-wo	10.29	10.44	9.52	6.78	8.54
di-fs	1.32	2.47	1.88	2.83	3.44
di-en	7.89	7.14	6.79	3.70	4.76
fo	13.22	8.14	11.45	10.20	6.78
fa	2.43	3.11	3.50	8.60	5.40
mt	6.02	5.39	4.97	0.33	3.65
il	4.79	5.70	5.13	5.11	4.54
ap	1.39	1.46	1.62	1.51	1.51
cc	--	--	0.30	--	--
Others	1.12	0.35	0.36	0.24	0.29
Ba	275	279	450	540	540
Cr	362	196	200	--	--
Cu	78	56	--	--	--
Ni	258	106	200	--	--
Rb	31	32	14	--	--
Sr	621	688	800	--	--
V	197	227	300	--	--
Y	--	--	50	--	--
Zn	72	79	--	--	--
Zr	--	--	350	--	--

Dashes, not determined (elements) or not present (norms).

1. 24591. Basanite, dredge sample from ~3 km northeast of Sabrina Island [*Johnson et al.*, 1982].
2. 24583. Basanite, ~1 km north of southernmost end of Sabrina Island [*Johnson et al.*, 1982].
3. 2200. Basanite, dredge sample from 67°09.5′S, 163°27.7′E, at a depth of 512–532 m [*Kempe*, 1973].
4. Basanite, Borradaile Island [*Mawson*, 1950].
5. *Ne*-hawaiite, Buckle Island [*Mawson*, 1950].

Copyright American Geophysical Union

F.10. SCOTT ISLAND

Type of volcano: Phonolitic cone surmounting a submarine plateau.

Location: Northern Ross Sea (67°30′S, 180°00′).

Height above sea level: ~100 m.

Evidence of Holocene activity: None.

Authors of report: A.C. Wright and P.R. Kyle.

Date of report: October 1986.

Form and Structure

Scott Island is the subaerial peak of a submarine plateau (Scott plateau) which is some 145 km long by 30 km wide, at a depth of 300 m (Figure F.10.1). The flat-topped island is bounded by 100-m-high cliffs and is ~3 km across. The north-south trend of the Scott plateau is oblique to the typical northwest-southeast and northeast-southwest structures of the Ross Sea [*Johnson et al.*, 1982, Figure 2].

Petrologic Characteristics

Chemical analyses of five samples from the vicinity of Scott Island [*Prior*, 1907; *Johnson et al.*, 1982] indicate the presence of *ne*-mugearite (one sample) and phonolite (four samples) (Table F.10.1). These rocks show a well-defined trend of alkali enrichment relative to silica and have probably evolved by fractional crystallization from basanite or alkali basalt; the most silica-rich sample is also peralkaline.

Chronologic Data

No radiometric ages have been determined, but Scott Island is probably of late Cenozoic age.

Extent of Knowledge

Apart from a single phonolite sample collected in December 1902 during the *Morning* Expedition of Captain W. Colbeck [*Prior*, 1907], no geological investigations have been carried out on Scott Island. There are four dredge samples from the vicinity, and a seismic reflection profile crosses the Scott plateau [*Johnson et al.*, 1982; *Campsie et al.*, 1983]. Petrographic descriptions and major-element analyses have been determined on all samples, and there are partial trace-element analyses for the dredge samples [*Prior*, 1907; *Johnson et al.*, 1982].

Bibliography

Campsie et al., 1983
Ferrar, 1907
Johnson et al., 1982
Prior, 1907

Fig. F.10.1. Sketch map of Scott Island. Inset map shows its location in relation to the Balleny Islands.

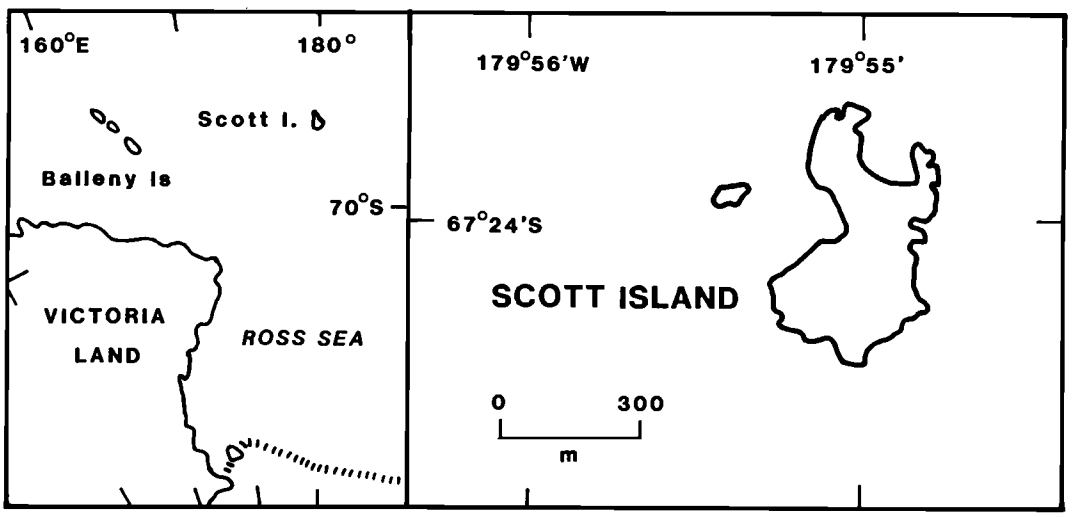

Copyright American Geophysical Union

TABLE F.10.1. Representative Chemical Analyses and CIPW Norms of Volcanic Rocks From Scott Island

	1	2	3	4	5
SiO_2	50.93	55.93	57.14	57.28	58.76
TiO_2	1.53	0.64	0.24	0.21	0.11
Al_2O_3	17.81	19.61	18.76	18.81	18.68
Fe_2O_3	2.26	1.75	1.84	2.21	3.01
FeO	7.84	6.32	5.88	5.36	2.51
MnO	0.31	0.13	0.36	0.29	0.27
MgO	2.18	0.50	0.12	0.09	0.10
CaO	5.80	3.53	2.59	2.71	1.63
Na_2O	6.39	7.75	8.79	8.74	9.14
K_2O	2.44	3.67	3.63	3.59	3.97
P_2O_5	0.63	0.12	0.13	0.15	0.07
H_2O^-	0.25	0.10	0.13	0.14	0.45
LOI	1.63	0.19*	0.39	0.42	1.30
Total	100.00	100.24	100.00	100.00	100.00
or	14.4	21.7	21.4	21.2	23.5
ab	34.5	39.5	43.5	44.6	47.5
an	12.7	7.9	1.0	1.5	--
ne	10.6	14.1	16.7	15.9	14.3
ac	--	--	--	--	3.0
di	10.1	7.7	9.8	9.7	9.7
ol	8.1	5.0	3.6	2.5	--
mt	3.3	2.5	2.7	3.2	2.9
il	2.9	1.2	0.4	0.4	0.2
ap	1.5	0.3	0.3	0.3	0.2
Ba	670	--	920	1160	880
Co	13	--	--	--	--
Cr	6	--	6	8	5
Ga	21	--	23	21	21
Ni	6.5	--	8.5	7	7
Rb	51	--	97	95	89
V	50	--	tr	10	tr

Dashes, not determined (elements) or not present (norms). tr, trace. LOI, loss on ignition.

*H_2O.

1. E27-34C. *ne*-mugearite, dredge sample [*Campsie et al.*, 1983].
2. Phonolite [*Prior*, 1907].
3. E27-34B. Phonolite, dredge sample [*Campsie et al.*, 1983].
4. E27-34D. Phonolite, dredge sample [*Campsie et al.*, 1983].
5. E27-34A. Phonolite, dredge sample [*Campsie et al.*, 1983].

Copyright American Geophysical Union

F.11. PETER I ISLAND

Type of volcano: Shield-like ocean island volcano (seamount) consisting of lava flows and subordinate volcanic breccia of basalt and less mafic rocks.

Location: Northern Bellingshausen Sea (68°51′S, 90°35′W).

Height above sea level: 1750 m.

Evidence of Holocene activity: The unmodified volcano form indicates a late Cenozoic age. The elevation of the volcanic peak was given as 1219 m by Bellingshausen in 1821, 1752 m in 1960 [*Bastien and Craddock,* 1976*a*], and 1640 m in 1987 [*Norsk Polarinstitutt,* 1988]. Although it was suggested that the differences in elevation could be an indication of intervening activity [*Bastien and Craddock,* 1976*a*], it is more likely that they reflect inaccuracies in the earlier measurements.

Author of report: P.D. Rowley.

Date of report: August 1986 (minor amendments, May 1989).

Form and Structure

Peter I Island (Figure F.11.1), measuring 19 km north-south and 11 km east-west, is the upper part of an oceanic shield volcano [*Craddock et al.,* 1964; *Bastien and Craddock,* 1976*a*]. It is a mainly ice-covered island characterized by an abrupt coastline which makes landing difficult. The base of the island, which is circular in plan view and about 64 km in diameter, is ~2000 fathoms (3660 m) below sea level; the submerged slope of the volcano averages 10°–15°. The summit contains a small, circular crater ~100 m in diameter. The crater and volcanic morphology of the island prove that it is a major volcano, here called Peter I Island volcano. The rocks on the island consist mostly of lava flows (between 0.5 and 12 m thick) and minor volcanic breccia of olivine-phyric basalt and intermediate-composition rock types; the flows vary from dense to highly vesicular rock types. Pahoehoe lava surfaces were seen, but no pillows. Dikes and intrusive plugs of basalt cut the volcanic sequence in places.

Petrologic Characteristics

Bastien and Craddock [1976*a*] refer to the rocks of Peter I Island as principally ocean island basalt and subordinate andesite, trachyandesite, trachyte, and perhaps benmoreite. Only a few of the basalts and trachytes (in the sense of *Le Bas et al.* [1986]) have been chemically analyzed (Table F.11.1).

The basalt samples are dark gray to reddish-brown, hypocrystalline to holocrystalline, and nonporphyritic to porphyritic. Olivine is the most common phenocryst, followed by minor plagioclase and clinopyroxene (Table F.11.2). The chemical composition of the basalt (Table F.11.1) indicates that it falls near the boundary between the fields of alkaline and subalkaline rocks of *Irvine and Baragar* [1971] and that it is silica saturated. Andesite, collected only by *Broch* [1927], is aphanitic and contains phenocrysts of plagioclase and subordinate olivine, basaltic hornblende, green diopsidic augite, and brown basaltic augite. No andesite has been chemically analyzed. The most silicic rock is "trachyandesite" consisting of light pinkish-gray to light gray aphanitic rock containing phenocrysts of plagioclase and basaltic hornblende; alkali feldspar occurs as rims on the plagioclase phenocrysts. Two chemical analyses (Table F.11.1) show that this rock is trachyte (in the sense of *Le Bas et al.* [1986]) containing normative *Q* and *hy* and that it falls in the field of alkaline rocks, near the boundary with subalkaline rocks [*Irvine and Baragar,* 1971].

The chemical composition of the analyzed rocks from Peter I Island reflects their unique evolution in an oceanic setting. There is a bimodal distribution to the chemical analyses, but without additional analyses it is not possible to verify whether the andesite observed on the island would fall on a line connecting the two clusters. Nonetheless, the basalt falls in the tholeiitic field of *Irvine and Baragar* [1971]; it is also relatively low in alkalis on a total alkali versus silica diagram.

Chronologic Data

A single K-Ar whole-rock date of 12.8 ± 1.5 Ma was reported by *Bastien and Craddock* [1976*a*] for an olivine-phyric basalt lava flow near sea level. The unmodified volcanic form of the higher parts of the island, however, argues that parts of the volcano may be considerably younger, probably Holocene or historic.

Extent of Knowledge

Peter I Island was discovered (but not landed upon) by Captain Thaddeus von Bellingshausen on January 10, 1821, while commanding the Russian ships *Vostok* and *Mirnyy* [*Bastien and Craddock,* 1976*a*]. Since then, the island has been subjected only to the briefest of reconnaissance

Copyright American Geophysical Union

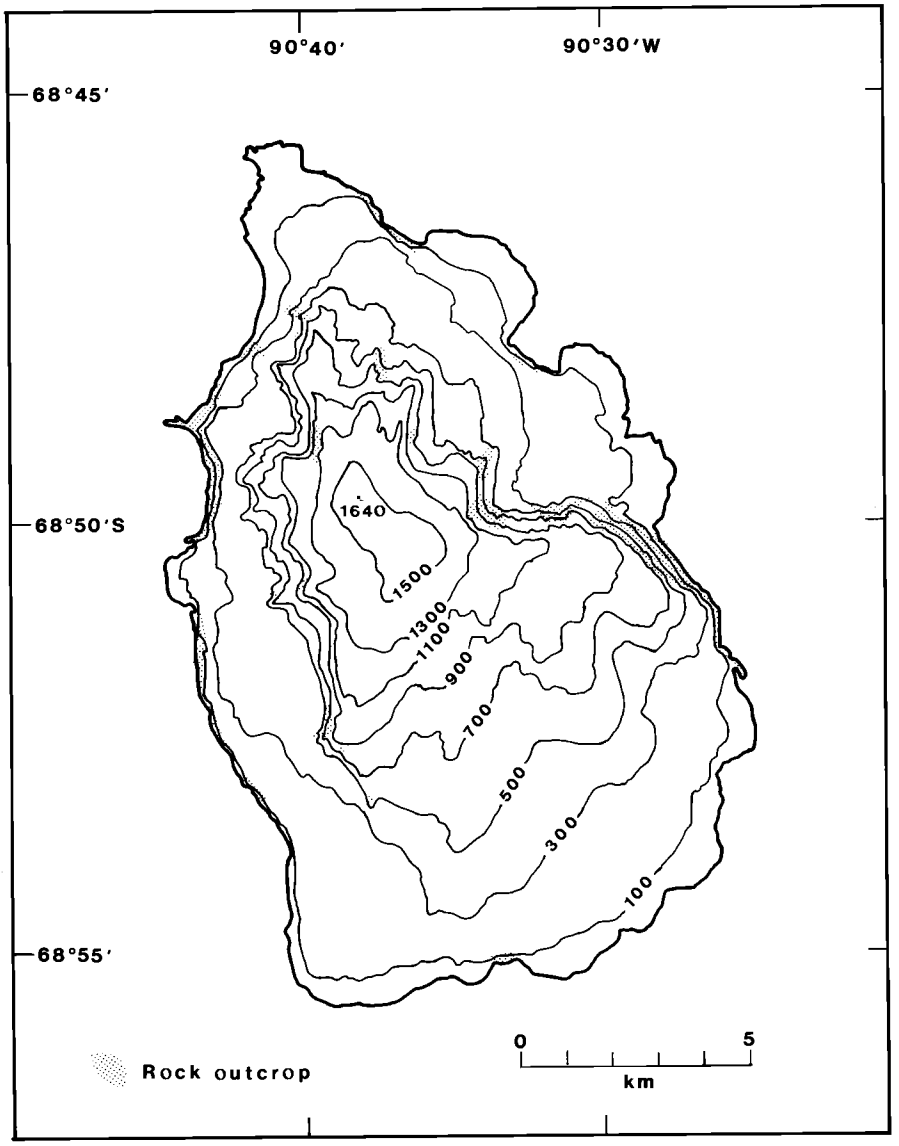

Fig. F.11.1. Topographic map of Peter I Island [after *Norsk Polarinstitutt,* 1988].

geologic studies, including several landings of only a few hours or a few days duration. This is due in part to its location far from regular shipping lanes and also because pack ice commonly renders it inaccessible in the summer. In January 1927 the Norwegian vessel *Odd I* circumnavigated the island, but pack ice prevented any landing from being made; dredge hauls provided specimens for the petrographic and chemical study by *Broch* [1927]. The first landing on the island was on February 2, 1929, by a party from the *Norvegia,* commanded by Nils Larsen; a brief mention of the geology was given by *Holtedahl* [1929]. The most detailed description of the geology [*Bastien and Craddock,* 1976*a*] is based on a landing and 2.5-hour study in February 1960 by a field party from the U.S.S. *Burton Island* [*Bastien and Craddock,* 1976*b*]. A Norwegian expedition worked on the island for about 10 days in January and February 1987. Although surveying was one of the main goals of the expedition, samples of rock were collected at five localities (Prestvik, personal communication, 1989) (note added in proof, May 1989).

Bibliography

Bastien and Craddock, 1976*a, b*
Broch, 1927
Craddock et al., 1964
Holtedahl, 1929

Copyright American Geophysical Union

TABLE F.11.1. Representative Chemical Analyses and CIPW Norms of Lava Flows From Peter I Island

	1	2	3	4	5
SiO_2	47.64	48.46	48.88	61.13	62.31
TiO_2	2.89	2.94	3.25	0.51	0.72
Al_2O_3	12.79	12.90	12.46	18.49	17.28
Fe_2O_3	3.25	2.52	3.77	4.77	2.65
FeO	8.96	10.93	8.09	0.58	1.67
MnO	0.18	0.17	0.15	0.01	0.05
MgO	10.64	8.39	8.64	1.09	1.41
CaO	8.25	8.63	8.70	2.51	2.42
Na_2O	2.64	2.42	3.08	6.31	6.72
K_2O	1.10	1.21	1.55	3.10	3.58
P_2O_5	0.51	--	0.59	0.25	0.29
H_2O^+	1.01	0.40	0.15	0.03	0.11
H_2O^-	--	0.09	0.67	0.43	0.30
CO_2	--	0.36	--	1.25	--
BaO	0.05	--	0.06	--	0.06
Cl	0.09	--	0.14	--	0.34
S	0.02	--	0.01	--	0.03
Total	100.02	99.42	100.19	100.46	99.94
Q	--	--	--	8.44	3.45
or	6.58	7.29	9.24	18.91	21.36
ab	22.60	20.87	26.28	55.11	57.41
an	20.03	21.16	15.73	3.11	6.47
cc	--	--	--	3.74	--
di	14.72	16.44	19.44	--	3.12
hy	12.95	19.02	9.05	6.05	2.91
ol	11.68	5.80	7.22	--	--
mt	4.77	3.72	5.51	3.01	3.25
il	5.55	5.69	6.22	1.00	1.38
ap	1.13	--	1.30	0.56	0.64

Dashes, not determined (elements) or not present (norms). All analyses by wet chemical methods.

1. B-2. Basalt, from *Broch* [1927].
2. PI-5. Basalt, from *Craddock et al.* [1964, Table 1].
3. B-3. Basalt, from *Broch* [1927].
4. PI-14. Trachyte, from *Bastien and Craddock* [1976*a*, Table 5].
5. B-5. Trachyte, from *Broch* [1927].

TABLE F.11.2. Modal Analyses of Basalt Lava Flows, Peter I Island

Minerals	PI-1	PI-3	PI-5	PI-7
Olivine	17.2	11.4	9.8	9.8
Plagioclase	38.2	34.6	25.3	30.6
Pyroxene				
Matrix	30.0	34.4	41.6	38.4
Phenocrysts	0.2	0	0	3.2
Fe-Ti oxides	14.4	19.6	23.4	18.0

Values for olivine and plagioclase include both phenocryst and matrix minerals. All analyses are from *Bastien and Craddock* [1976*a*, Table 2].

Copyright American Geophysical Union

BIBLIOGRAPHY

Abbott, D., The petrology of some Marion Island basalts, *Ann. Geol. Surv. S. Afr., 2,* 89–100, 1963.

Aubert de la Rüe, E., Contribution a l'étude géologique de l'Île Heard, *C.R. Acad. Sci. Paris, 189,* 129–131, 1929*a*.

Aubert de la Rüe, E., Un voyage d'exploration dans les miers australes, Île Heard, Archipel de Kerguelen, Île Saint-Paul, *Rev. Geogr. Phys. Geol. Dyn., 2,* 97–146, 1929*b*.

Aubert de la Rüe, E., Note préliminaire sur la géologie et la pétrographie des Îles Kerguelen, *C.R. Assoc. Fr. Avan. Sci., 1929,* 387–390, 1930*a*.

Aubert de la Rüe, E., La constitution géologique de l'archipel de Kerguelen, *Bull. Soc. Oceanogr. Fr.,* no. 51, 941–942, 1930*b*.

Aubert de la Rüe, E., Etude géologique et prospection minière dans l'archipel de Kerguelen, *Bull. Soc. Geol. Normandie, 35,* 34–47, 1931*a*.

Aubert de la Rüe, E., Sur l'extension des roches éruptives grenues dans l'archipel de Kerguelen, *C.R. Acad. Sci. Paris, 193,* 863–866, 1931*b*.

Aubert de la Rüe, E., Sur la présence d'une flore fossile tertiaire dans l'archipel de Kerguelen, *C.R. Acad. Sci. Paris, 193,* 1102–1104, 1931*c*.

Aubert de la Rüe, E., Etude géologique et géographique de l'archipel de Kerguelen, *Rev. Geogr. Phys. Geol. Dyn., 5,* 1–231, 1932.

Aubert de la Rüe, E., Sur de récentes observations intéressant de la géologie des Îles Kerguelen, *C.R. Acad. Sci. Paris, 230,* 765–767, 1950*a*.

Aubert de la Rüe, E., Notes sur une récente reconnaissance dans l'Est des Îles Kerguelen, *C.R. Somm. Seances Soc. Geol. Fr.,* no. 231, 32–37, 1950*b*.

Aubert de la Rüe, E., Sur les différentes séries de laves et les roches intrusives associées dans la péninsule Courbet (archipel de Kerguelen), *Bull. Volcanol., Ser. 2, 18,* 133–137, 1956.

Aubert de la Rüe, E., Les dépôts sédimentaires quaternaires et actuels de l'archipel de Kerguelen, *Bull. Soc. Geol. Fr., Ser. 6, 8,* 123–130, 1958.

Aubert de la Rüe, E., Remarques sur les liaisons possibles entre plutons et volcans dans quelques territoires français d'Outre-Mer, *Rev. Geogr. Phys. Geol. Dyn., Ser. 2, 3,* 109–112, 1960.

Aubert de la Rüe, E., Une reconnaissance géologique dans la péninsule Courbet, archipel de Kerguelen, *Bull. Soc. Geol. Fr., Ser. 7, 4,* 826–836, 1962.

Aubert de la Rüe, E., and G. Deflandre, Sur un calcaire à micro-organismes enclavé dans un basalte du val Studer, archipel de Kerguelen, *Bull. Mus. Natl. Hist. Nat., Ser. 2, 33,* 123–127, 1961.

Aubert de la Rüe, E., and H. N. Dixon, Sur quelques mousses fossiles des Îles Kerguelen, *Rev. Bryol. Lichen., 5,* 29–30, 1932.

Aubert de la Rüe, E., J. Nougier, and J. Delépine, Bibliographie: Les sciences naturelles dans les îles australes françaises de leur découverte, *CNFRA,* no. 16, 61 pp., 1966.

Bailey, D.K., and R. MacDonald, Petrochemical variations among mildly peralkaline (comendite) obsidians from the oceans and continents, *Contrib. Mineral. Petrol., 28,* 340–351, 1970.

Baker, P.E., The recent eruption on Bouvetøya with a note on magma-type, *Proc. Geol. Soc. London,* no. 1625, 144–145, 1965.

Baker, P.E., Historical and geological notes on Bouvetøya, *Br. Antarct. Surv. Bull.,* no. 13, 71–84, 1967.

Baker, P.E., Islands of the South Atlantic, in *The Ocean Basins and Margins,* vol. I, *The South Atlantic,* edited by A.E.M. Nairn and F.G. Stehli, pp. 493–553, Plenum, New York, 1973.

Baker, P.E., and J.F. Tomblin, A recent eruption on Bouvetøya, South Atlantic Ocean, *Nature, 203,* 1056–1057, 1964.

Balleny, J., New land in the southern ocean, *Literary World, 2,* 185–187, 1839.

Ballestracci, R., and J. Nougier, Detection by infrared thermography and modelling of an ice-capped geothermal system in Kerguelen archipelago, *J. Volcanol. Geotherm. Res., 20,* 85–99, 1984.

Ballestracci, R., J. Nougier, and Y. Benderitter, Mise en évidence d'une zone electriquement conductive dans les basaltes des plateaux des Îles Kerguelen (TAAF), *C.R. Acad. Sci. Paris, 296,* 833–838, 1983.

Barling, J., Geochemistry of the newer lavas, Heard Island, southern Indian Ocean, *Int. Volc. Congr. N.Z. Abstr.,* p. 134, 1986.

Barling, J., S.L. Goldstein, G.E. Wheller, and I.A. Nicholls, Heard Island: An example of large isotopic variations on a small oceanic island, *Chem. Geol., 70,* 46, 1988.

Bastien, T.W., and C. Craddock, The geology of Peter I Island, in *Initial Rep. Deep Sea Drill. Proj., 35,* 341–357, 1976*a*.

Bastien, T.W., and C. Craddock, Igneous rocks of Peter I Island, *Antarct. J. U.S., 11*(4), 267–269, 1976*b*.

Bauer, A., and L. Berthois, Manifestations ultimes liées à l'activité volcanique dans l'Île de Kerguelen, *C.R. Acad. Sci. Paris, 250,* 742–743, 1962*a*.

Bauer, A., and L. Berthois, Activité volcanique dans l'Île de Kerguelen, *CNFRA,* no. 2, 79–105, 1962*b*.

Bellair, P., Niveaux marins anciens aux Îles Crozet et Kerguelen, *C.R. Acad. Sci. Paris, 256,* 2643–2645, 1963.

Bellair, P., Recent data on Crozet islands, in *Antarctic Geology,* edited by R.J. Adie, pp. 3–7, North-Holland, Amsterdam, 1964.

Bellair, P., Le volcanisme des îles australes de l'océan Indien, *C.R. Acad. Sci. Paris, 262,* 1054–1057, 1966.

Bellair, P., and J. Nougier, The volcanism of presqu'île Rallier du Baty, in *Antarctic Geology,* edited by R.J. Adie, pp. 8–13, North-Holland, Amsterdam, 1964.

Copyright American Geophysical Union

Bellair, P., J.P. Carron, J. Nougier, and J. Trichet, Niveaux intercalaires dans les strates de basaltes des plateaux de l'archipel de Kerguelen, *Geol. Rundsch., 55,* 342–354, 1965.

Bergh, H.W., and I.O. Norton, Prince Edward Fracture Zone and the evolution of the Mozambique Basin, *J. Geophys. Res., 81,* 5221–5239, 1976.

Berninghausen, W.H., and M. Neumann van Padang, *Antarctica,* vol. 10, *Catalogue of Active Volcanoes of the World,* I.A.V.C.E.I., Rome, 1960.

Berthois, L., R. Schlich, and P. Patriat, Carte bathymétrique du Sud de l'Océan Indien, no. 26, 8 pp., 4 maps, Inst. de Phys. du Globe, Paris,1969.

Boudon, G., and J. Nougier, Etude volcanologique preliminaire du groupe occidental de l'archipel Crozet (TAAF), Océan Indien Austral, *C.R. Acad. Sci. Paris, Ser. 2, 295,* 895–899, 1982.

Broch, O.A., Gesteine von der Peter I Insel, West Antarktis, *Avh. Nor. Vidensk. Akad. Oslo, Mat. Naturvidensk. Kl., 9,* 1–41, 1927.

Broch, O.A., Lavas of Bouvet Island, Two Contributions to Antarctic Petrography, *Sci. Results Norw. Antarct. Exped., 1927-1928,* no. 25, 3–26, 1946.

Budd, G.M., The ANARE 1963 expedition to Heard Island, *ANARE Rep., Ser. A, 1,* 53, 1964.

Bungum, H., Y. Kristoffersen, and A.K. Nilsen, The seismicity of the Bouvetøya region, *Skr. Nor. Polarinst., 175,* 71–78, 1981.

Burge, W.E., and D.C. Parker, Infrared survey in Antarctica: Imagery analysis, *Rep. 1160-9-f,* 53 pp., Willow Run Lab., Univ. of Mich., Ann Arbor, 1969.

Campsie, J., E.R. Neumann, and G.L. Johnson, Dredged volcanic rocks from the southern oceans: The Eltanin collection, *N. Z. J. Geol. Geophys., 26,* 31–45, 1983.

Cantagrel, J.M., J. Lameyre, and J. Nougier, Volcanologie et géochronologie d'une île volcanique, Île de l'Est (archipel Crozet), *Int. Geol. Cong., 26th, Paris, I,* 27, 1980.

Cheminée, J.L., and J. Nougier, Distribution of uranium, thorium and potassium in the volcanic suites of Îles Kerguelen, in *Antarctic Geology and Geophysics,* edited by R.J. Adie, pp. 817–823, Universitetsforlaget, Oslo, 1972.

Chevallier, L., Carte géologique de l'Île de la Possession, 1: 50 000, avec notice (TAAF), *CNFRA,* no. 50, 16 pp., 1981.

Chevallier, L., Tectonics of Marion and Prince Edward volcanoes (Indian Ocean): Result of regional control and edifice dynamics, *Tectonophysics, 124,* 155–175, 1986.

Chevallier, L., and J. Nougier, Première étude volcano-structurale de l'Île de la Possession, Îles Crozet (TAAF), Océan Indien Austral, *C.R. Acad. Sci. Paris, 292,* 363–368, 1981.

Chevallier, L., and N. Vatin-Perignon, Volcano-structural evolution of Piton des Neiges, Reunion Island, Indian Ocean, *Bull. Volcanol., 45,* 285–298, 1982.

Chevallier, L., and W.J. Verwoerd, A numerical model for the mechanical behavior of intraplate volcanoes, *J. Geophys. Res., 93,* 4182–4198, 1988.

Chevallier, L., J. Nougier, and J.M. Cantagrel, Volcanology of Possession Island, Crozet archipelago (TAAF), in *Antarctic Earth Science,* edited by R.L. Oliver, P.R. James, and J.B. Jago, pp. 652–658, Cambridge University Press, New York,, 1983.

Clarke, I., Report on geology, in Expedition to the Australian Territory of Heard and McDonald Islands 1980, *Tech Rep., 31,* pp. 46–51, Div. of Natl. Mapp., Canberra, 1982.

Clarke, I., I. McDougall, and D. J. Whitford, Volcanic evolution of Heard and McDonald islands, southern Indian Ocean, in *Antarctic Earth Science,* edited by R.L. Oliver, P.R. James, and J.B. Jago, pp. 631–635, Cambridge University Press, New York, 1983.

Coffin, M.F., H.L. Davies, and W.F. Haxby, Structure of the Kerguelen Plateau province from Seasat altimetry and seismic reflection data, *Nature, 324,* 134–136, 1986.

Collerson, K.D., and M.T. McCulloch, Nd and Sr isotope geochemistry of leucite-bearing lavas from Gaussberg, East Antarctica, in *Antarctic Earth Science,* edited by R.L. Oliver, P.R. James, and J.B. Jago, pp. 676–680, Cambridge University Press, New York, 1983.

Cookson, I.C., Plant microfossils from the lignites of Kerguelen archipelago, *Rep. B.A.N.Z. Antarct. Res. Exped., Ser. A, 2,* 127–142, 1947.

Corbiac, H. de, L'achèvement de la carte de reconnaissance des Îles Kerguelen, *TAAF,* no. 36, 3–6, 1966.

Courtney, R.C., and M. Recq, Anomalous heat flow near the Crozet Plateau and mantle convection, *Earth Planet. Sci. Lett., 79,* 373–384, 1986.

Craddock, C., T.W. Bastien, and R.H. Rutford, Geology of the Jones Mountains area, in *Antarctic Geology,* edited by R.J. Adie, pp. 171–187, North-Holland, Amsterdam, 1964.

Dickey, J.S., Jr., F.A. Frey, S.R. Hart, and E.B. Watson, Geochemistry and petrology of dredged samples from the Bouvet triple junction, South Atlantic, *Geochim. Cosmochim. Acta, 41,* 1105–1118, 1977.

Dosso, L., Données isotopiques (Sr, Pb) sur le volcanisme et le plutonisme des Îles Kerguelen: Le problème de la contamination crustale, thèse 3ième cycle, 72 pp., Univ. Rennes, France, 1977.

Dosso, L., and V.R. Murthy, A Nd-isotopic study of Kerguelen islands: Inferences on enriched oceanic mantle sources, *Earth Planet. Sci. Lett., 48,* 268–276, 1980.

Dosso, L., P. Vidal, J.M. Cantagrel, J. Lameyre, A. Marot, and S. Zimine, "Kerguelen: Continental fragment or oceanic island?": Petrology and isotopic geochemistry evidence, *Earth Planet. Sci. Lett., 43,* 46–60, 1979.

Dreux, P., and J.M. Remy, Les manifestations volcaniques de l'Île de la Possession (archipel Crozet), *C.R. Acad. Sci. Paris, 257,* 2517–2518, 1963.

Dreux, P., Y. Frenot, P. Jouventin, L. Massé, and O. Verdier, First scientific expedition to Île des Pingouins, archipel Crozet, *Polar Rec., 24*(150), 235–238, 1988.

Drygalski, E. von, Geographie von Heard Insel, *Dtsch. Sudpolar Exped. 1901–1903, 2, Geogr. Geol.,* 223–239, 1908.

Copyright American Geophysical Union

Duncan, R.A., Geochronology of basaltic rocks from the Ninetyeast Ridge and continental dispersion in the eastern Indian Ocean, *J. Volcanol. Geotherm. Res., 4,* 283–305, 1978.

Duncan, R.A., Hot spots in the southern oceans—an absolute frame of reference for the motion of Gondwana continents, *Tectonophysics, 74,* 29–42, 1981.

Duncan, R.A., M.T. McCulloch, H.G. Barsczus, and D.R. Nelson, Plume versus lithospheric sources for melts at Ua Pou, Marquesas islands, *Nature, 322,* 534–538, 1986.

Dupré, B., and C.J. Allègre, Pb-Sr isotope variation in Indian Ocean basalts and mixing phenomena, *Nature, 303,* 142–146, 1983.

Edwards, A.B., Tertiary lavas from the Kerguelen archipelago, *Rep. B.A.N.Z. Antarct. Res. Exped., Ser. A, 2,* 72–100, 1938.

Falconer, R.K.H., The Indian-Antarctic-Pacific triple junction, *Earth Planet. Sci. Lett., 17,* 151–158, 1972.

Ferrar, H.T., Report on the field-geology of the region explored during the "Discovery" Antarctic Expedition, 1901–1904, *Natl. Antarct. Exped. 1901–1904, Natl. Hist., 1,* Geol., 1–100, 1907.

Fleming, C.A., A new species of fossil *Chlamys* from the Drygalski Agglomerate of Heard Island, Indian Ocean, *J. Geol. Soc. Aust., 4,* 13–19, 1957.

Fletcher, H.O., Marine Tertiary fossils and a description of a Recent *Mytilus* from Kerguelen island, *Rep. B.A.N.Z. Antarct. Res. Exped., Ser. A, 2,* 101–116, 1938.

Furnes, H., and R. Løvlie, An eruptional model for recent lava flow on Bouvetøya, South Atlantic Ocean, *Skr. Nor. Polarinst., 169,* 103–109, 1978.

Gautier, I., D. Weis, A. Giret, and P. Vidal, The basalts of Kerguelen Islands, *Terra Cognita, 7,* 11, 1987.

Gesellschaft für Erdkunde, Wiedererwachen der vulkanischen Tätigkeit auf der Heard Insel, *Z. Ges. Erdk. Berlin,* 529, 1910.

Giret, A., Genèse de roches feldspathoïdiques par la déstabilisation des amphiboles: Massif des Montagnes Vertes, Kerguelen (TAAF), *C.R. Acad. Sci. Paris, 289,* 379–382, 1979.

Giret, A., Le plutonisme océanique intraplaque: Exemple de l'archipel Kerguelen, thèse Doctorat d'etat, 290 pp., Univ. Pierre et Marie Curie, Paris, 1983.

Giret, A., and J.F. Beaux, Le pluton du Val Gabbro (Îles Kerguelen), un complexe tholéiitique témoin de l'activité de la paléo-ride Est-Indienne, *C.R. Acad. Sci. Paris, Ser. 2, 299,* 965–970, 1984.

Giret, A., and J. Lameyre, Mise en place et évolution magmatique des complexes plutoniques de la caldéra de Courbet, Îles Kerguelen (TAAF), *Bull. Soc. Geol. Fr., Ser. 7, 22,* 437–446, 1980.

Giret A., and J. Lameyre, A study of Kerguelen plutonism: Petrology and geochronology, geological implications, in *Antarctic Earth Science,* edited by R.L. Oliver, P.R. James, and J.B. Jago, pp. 646–651, Cambridge University Press, New York, 1983.

Giret, A., J. Lameyre, A. Marot, J. Nougier, and S. Zimine, Carte géologique au 1:50 000 de la péninsule Rallier du Baty, Îles Kerguelen (TAAF), *CNFRA,* no. 45, 12 pp., 1980.

Giret, A., J.M. Cantagrel, and J. Nougier, Nouvelles données sur les complexes volcano-plutoniques des Îles Kerguelen (TAAF), *C.R. Acad. Sci. Paris, 293,* 191–194, 1981.

Giret, A., M.M. Ghomshei, J.L. Cheminée, and J. Nougier, Comportement de l'uranium et du thorium dans les laves alcalines des Îles Kerguelen (Océan Indien, TAAF), *C.R. Acad. Sci. Paris, Ser. 2, 299,* 239–244, 1984.

Girod, M., and J. Nougier, Volcanism of the sub-Antarctic islands, in *Antarctic Geology and Geophysics,* edited by R.J. Adie, pp. 777–788, Universitetsforlaget, Oslo, 1972.

Girod, M., G. Camus, and Y. Vialette, Sur la présence de tholeiites à l'Île St. Paul (Océan Indien), *Contrib. Mineral. Petrol., 33,* 108–117, 1971.

Goslin, J., and P. Patriat, Absolute and relative plate motions and hypotheses on the origin of five aseismic ridges in the Indian Ocean, *Tectonophysics, 101,* 221–224, 1984.

Goslin, J., M. Recq, and R. Schlich, Structure profonde du plateau de Madagascar: Relations avec le plateau de Crozet, *Tectonophysics, 76,* 75–97, 1981*a*.

Goslin, J., M. Recq, and R. Schlich, Mise en place et évolution des plateaux sousmarins de Madagascar et de Crozet, *Bull. Soc. Geol. Fr., Ser. 7, 23,* 609–618, 1981*b*.

Gunn, B.M., R. Coy-yll, N.D. Watkins, E.C. Abranson, and J. Nougier, Geochemistry of an oceanite-ankaramite-basalt suite from East Island, Crozet archipelago, *Contrib. Mineral. Petrol., 28,* 319–339, 1970.

Gunn, B.M., E.C. Abranson, J. Nougier, N.D. Watkins, and A. Hajash, Amsterdam Island, an isolated volcano in the southern Indian Ocean, *Contrib. Mineral. Petrol., 32,* 79–92, 1971.

Gunn, B.M., E.C. Abranson, N.D. Watkins, and J. Nougier, Petrology and geochemistry of Îles Crozet: A summary, in *Antarctic Geology and Geophysics,* edited by R.J. Adie, pp. 825–829, Universitetsforlaget, Oslo, 1972.

Gunn, B.M., N.D. Watkins, W. Trzcienski, and J. Nougier, The Amsterdam—St. Paul volcanic province and the formation of low–Al tholeiitic andesites, *Lithos, 8,* 137–149, 1975.

Hall, K., Evidence for Quaternary glaciation of Marion Island (sub-Antarctic) and some implications, in *Antarctic Glacial History and World Paleoenvironments,* edited by E.M. van Zinderen Bakker, pp. 137-147, A.A. Balkema, Rotterdam, 1978.

Hall, K., Late glacial ice cover and palaeotemperatures on sub-Antarctic Marion Island, *Palaeogeogr. Palaeoclimatol. Palaeoecol., 29,* 243–259, 1980.

Hamelin, B., B. Dupré, and J.C. Allègre, Pb-Sr-Nd isotopic data of Indian Ocean ridges: New evidence of large-scale mapping of mantle heterogeneities, *Earth Planet. Sci. Lett., 76,* 288–298, 1985.

Hart, S.R., A large-scale isotope anomaly in the southern hemisphere mantle, *Nature, 309,* 753–757, 1984.

Hartnady, C.J.H., and A.P. le Roex, Southern ocean hotspot tracks and the Cenozoic absolute motion of the African,

Copyright American Geophysical Union

Antarctic and South American plates, *Earth Planet. Sci. Lett.*, *75*, 245–257, 1985.

Hatherton, T., E.W. Dawson, and F.C. Kinsky, Balleny Islands reconnaissance expedition, 1964, *N. Z. J. Geol. Geophys.*, *8*, 164–179, 1965.

Hedge, C., N. D. Watkins, R. Hildreth, and W. Doering, $^{87}Sr/^{86}Sr$ ratios in basalts from islands in the Indian Ocean, *Earth Planet. Sci. Lett.*, *21*, 29–34, 1973.

Helle, S.G., New map of Bouvetøya, *Skr. Nor. Polarinst.*, *175*, 7–9, 1981.

Hinks, A.R., Bouvet Island, *Geogr. J.*, *72*, 537–546, 1928.

Hochstetter, F. von, *Geologische Betrachtungen während der Reise der Osterreichischen Fregatte "Novara" um die Erde*, vol. 2, 58 pp., Gerold, Vienna, 1866.

Holtedahl, O., On the geology and physiography of some Antarctic and sub-Antarctic islands, with notes on the character and origin of fjords and strandflats of some northern lands, etc., *Sci. Results Norw. Antarct. Exped. 1927–1928*, no. 3, 1–172, 1929.

Houtz, R.E., D.E. Hayes, and R.G. Markl, Kerguelen Plateau bathymetry, sediment distribution and crustal structure, *Mar. Geol.*, *25*, 95–130, 1977.

Huang, T.C., N.D. Watkins, and D.M. Shaw, Atmospherically transported volcanic glass in deep-sea sediments: Volcanism in sub-antarctic latitudes of the South Pacific during late Pliocene and Pleistocene time, *Geol. Soc. Am. Bull.*, *86*, 1305–1315, 1975.

Imsland, P., J.G. Larsen, T. Prestvik, and E.M. Sigmond, The geology and petrology of Bouvetøya, South Atlantic Ocean, *Lithos*, *10*, 213–234, 1977.

Irvine, T.N., and W.R.A. Baragar, A guide to the chemical classification of the common volcanic rocks, *Can. J. Earth Sci.*, *8*, 523–548, 1971.

Irving, E., P.J. Stephenson, and A. Major, Magnetism in Heard Island rocks, *J. Geophys. Res.*, *70*, 3421–3427, 1965.

Ivanac, J.F., Geological observations on Heard Island, *Rec. Bur. Miner. Resour. Aust.*, *1948/38*, 1948.

Jeremine E., and A. Sandrea, Contribution à la lithologie de l'archipel volcanique de Kerguelen—Péninsule Courbet, *Bull. Volcanol., Ser. 2*, *19*, 179–193, 1958.

Johnson, G.L., P.R. Kyle, J.R. Vanney, and J. Campsie, Geology of Scott and Balleny islands, Ross Sea, Antarctica and morphology of adjacent seafloor, *N. Z. J. Geol. Geophys.*, *25*, 427–436, 1982.

Jones, A.G.E., Scott Island and its discovery, *Antarctic*, *6*, 437–440, 1973.

Kempe, D.R.C., Rocks from Antarctica: The Discovery collection in the British Museum (Natural History), *Bull. Br. Mus. Nat. Hist., Mineral.*, *2*, 337–376, 1973.

Kovtoun, A.A, O.M. Raspopov, V.A. Troitskaya, G. Laurent, B.N. Kazak, R. Schlich, and J. Nougier, Recherches magnétotelluriques dans la région de Port-aux-Français (Kerguelen), *CNFRA*, *21*, 107–112, 1967.

Kristoffersen, Y., and H. Bungum, A micro-earthquake survey of Bouvet Island, South Atlantic, *Tectonophysics*, *81*, T1–T5, 1982.

Kuno, H., Origin of Cenozoic petrographic provinces of Japan and surrounding areas, *Bull. Volcanol.*, *20*, 37–76, 1959.

Kyle, P.R., Geology, mineralogy, and geochemistry of the Late Cenozoic McMurdo Volcanic Group, Victoria Land, Antarctica, Ph.D. thesis, 444 pp., Victoria Univ. of Wellington, New Zealand, 1976.

Kyle, P.R., and J.W. Cole, Structural control of volcanism in the McMurdo Volcanic Group, Antarctica, *Bull. Volcanol.*, *38*, 16–25, 1974.

Lacroix, A., Sur l'existence de roches néphéliniques grenues dans l'archipel de Kerguelen, *C.R. Acad. Sci. Paris*, *160*, 187–190, 1915*a*.

Lacroix, A., Les zéolites et les produits siliceux des basaltes de l'archipel de Kerguelen, *Bull. Soc. Fr. Mineral.*, *38*, 134–136, 1915*b*.

Lacroix, A., *Minéralogie de Madagascar*, vol. III, pp. 239–240, Société d'Editions Géographiques, Maritimes et Coloniales, Paris, 1923.

Lacroix, A., Les roches éruptives grenues de l'archipel de Kerguelen, *C.R. Acad. Sci. Paris*, *179*(3), 113–119, 1924.

Lacroix, A., Les laves des volcans inactifs des archipels Marion et Crozet, *Mem. Mus. Natl. Hist.*, *14*, 47–62, 1940.

Lambeth, A.J., Heard Island, geography and glaciology, *J. Proc. R. Soc. N.S.W.*, *84*, 92–98, 1951.

Lambeth, A.J., A geological account of Heard Island, *J. Proc. R. Soc. N.S.W.*, *86*, 14–19, 1952.

Lameyre, J., and J. Nougier, Geology of Île de l'Est, Crozet archipelago (TAAF), in *Antarctic Geoscience*, edited by C. Craddock, pp. 767–770, University of Wisconsin Press, Madison, 1982.

Lameyre J., A. Marot, S. Zimine, J.M. Cantagrel, L. Dosso, and P. Vidal, Chronological evolution of the Kerguelen islands syenite-granite ring complex, *Nature*, *263*, 306–307, 1976.

Lameyre, J., A. Marot, S. Zimine, J.M. Cantagrel, L. Dosso, P. Vidal, A. Giret, J. Joron, and M. Treuil, Etude géologique du complexe plutonique de la péninsule Rallier du Baty, Îles Kerguelen, *CNFRA*, no. 49, 176 pp. 1981.

Le Bas, M.J., R.W. Le Maitre, A. Streckeisen, and B. Zanettin, A chemical classification of volcanic rocks based on the total alkali-silica diagram, *J. Petrol.*, *27*, 745–750, 1986.

Le Maitre, R.W., A proposal by the I.U.G.S. Subcommission on the Systematics of Igneous Rocks for a chemical classification of volcanic rocks based on the total alkali silica (TAS) diagram, *Aust. J. Earth Sci.*, *31*, 243–255, 1984.

le Roex, A.P., Geochemical correlation between southern African kimberlites and South Atlantic hotspots, *Nature*, *324*, 243–245, 1986.

le Roex, A.P., and A.J. Erlank, Quantitative evolution of fractional crystallisation in Bouvet Island lavas, *J. Volcanol. Geotherm. Res.*, *13*, 309–338, 1982.

Copyright American Geophysical Union

le Roex, A.P., H.J.B. Dick, A.J. Erlank, A.M. Reid, F.A. Frey, and S.R. Hart, Geochemistry, mineralogy and petrogenesis of lavas erupted along the southwest Indian Ridge between the Bouvet triple junction and 11 degrees east, *J. Petrol., 24,* 267–318, 1983.

Løvlie, R., and H. Furnes, Paleomagnetism and morphology of lava(s) at Cape Meteor, Bouvetøya, *Skr. Nor. Polarinst., 169,* 93–101, 1978.

Lunde, T., Fra et besøk pa Bouvetøya, *Arbok Nor. Polarinst., 1963,* 197–203, 1965.

Luyendyk, B.P., and W. Rennick, Tectonic history of aseismic ridges in the eastern Indian Ocean, *Geol. Soc. Am. Bull., 88,* 1347–1356, 1977.

MacCormick, R., Geological remarks on Kerguelen's Land, *Tasmanian J., 1,* 27–34, 1842.

Mahoney, J.J., J.D. MacDougall, G.W. Lugmair, and K. Gopalan, Kerguelen hotspot source for Rajmahal traps and Ninetyeast Ridge?, *Nature, 303,* 385-389, 1983.

Marot, A., and S. Zimine, Géologie du complexe plutonique dans la péninsule Rallier du Baty, Îles Kerguelen, *CNFRA,* no. 49, 15–114, 1981.

Mawson, D., The B.A.N.Z. Antarctic Research Expedition 1929–31, *Geogr. J., 80,* 105–106, 1932.

Mawson, D., The geology and glaciation of some islands of the southern ocean and the newly discovered Antarctic mainland, *Q. J. Geol. Soc. London, 89,* 113–115, 1933.

Mawson, D., Basaltic lavas of the Balleny Islands, ANARE report, *Trans. R. Soc. Aust., 73,* 223–231, 1950.

McDougall, I., Geochronology, in *Marion and Prince Edward Islands,* edited by E.M. van Zinderen Bakker, J.M. Winterbottom, and R.A. Dyer, pp. 72–77, A.A. Balkema, Cape Town, 1971.

Mechkova, Ju. I., Pollens et spores des lignites des Îles Kerguelen, *TAAF,* no. 46, 11–21, 1969.

Morgan W.J., Rodriguez, Darwin, Amsterdam, ..., a second type of hotspot island, *J. Geophys. Res., 83,* 5355–5360, 1978.

Morgan, W. J., Hotspot tracks and the early rifting of the Atlantic, *Tectonophysics, 94,* 123–129, 1983.

Mukasa, S.B., R. McCabe, and J.B. Gill, Pb-isotopic compositions of volcanic rocks in the west and east Philippine island arcs: Presence of the Dupal isotopic anomaly, *Earth Planet. Sci. Lett., 84,* 153–164, 1987.

Nativel, P., and J. Nougier, Les facies zeolitiques des basaltes des plateaux des Îles Kerguelen (TAAF): Implications volcanologiques, *Bull. Soc. Geol. Fr., 25(6),* 957–962, 1983.

Neumann van Padang, M., Arabia and the Indian Ocean, *Catalogue of Active Volcanoes of the World,* vol. 16, I.A.V.C.E.I., Rome, 1963.

Nockolds, S.R., Petrology of rocks from Queen Mary land, *Rep. Aust. Antarct. Exped., 1911–1914, Ser. A IV,* part 2, 15–86, 1940.

Norsk Polarinstitutt, Peter I Øy, topographic map, scale 1: 50,000, Oslo, 1988.

Nougier, J., Les phases volcaniques successives de la péninsule Rallier du Baty (archipel de Kerguelen), *C.R. Acad. Sci. Paris, 256,* 4054–4056, 1963.

Nougier, J., Etude des formations de Porte-Jeanne d'Arc (archipel de Kerguelen), *CNFRA,* no. 11, 31–55, 1965.

Nougier, J., Esquisse géologique de la péninsule Rallier du Baty, archipel de Kerguelen, Terres Australes et Antarctique Françaises, *Bull. Soc. Geol. Fr., Ser. 7, 8,* 567–576, 1966.

Nougier, J., Contribution à l'étude géologique et géomorphologique des Îles Kerguelen (TAAF), *CNFRA,* no. 27, (vol. 1, 440 pp.; vol. 2, 246 pp. plus map at 1:200 000), 1970.

Nougier, J., Geochronology of the volcanic activity on Îles Kerguelen, in *Antarctic Geology and Geophysics,* edited by R.J. Adie, pp. 803–808, Universitetsforlaget, Oslo, 1972*a*.

Nougier, J., Volcanic associations in Îles Kerguelen, in *Antarctic Geology and Geophysics,* edited by R.J. Adie, pp. 809–815, Universitetsforlaget, Oslo, 1972*b*.

Nougier, J., Volcanism of Saint Paul and Amsterdam islands (TAAF): Some aspects of volcanism along plate margins, in *Antarctic Geoscience,* edited by C. Craddock, pp. 755–765, University of Wisconsin Press, Madison, 1982.

Nougier, J., and J. Lameyre, Les nordmarkites des Îles Kerguelen (TAAF) dans leur cadre structural: Problème de leur origine et de celle de certaines roches plutoniques alcalines en domaines océaniques, *Bull. Soc. Geol. Fr., Ser. 7, 15*(3 and 4), 306–311, 1973.

Nougier, J., and C. Plessard, Sur une inversion du champ magnetique terrestre aux Îles Kerguelen au cours du Miocène, *C.R. Acad. Sci. Paris, Ser. B, 267,* 1249–1252, 1968.

Nougier, J., R. Ballestracci, and B. Blavoux, Les manifestations post-volcaniques dans les îles australes françaises (TAAF): Zones fumerolliennes et sources thermominérales, *C.R. Acad. Sci. Paris, 295,* 389–392, 1981.

Nougier, J., J.M. Cantagrel, and D. Pawlowski, Chronospatial evolution of the volcanic activity from southeastern Kerguelen (TAAF), in *Antarctic Earth Science,* edited by R.L. Oliver, P.R. James, and J.B. Jago, pp. 640–645, Cambridge University Press, New York, 1983.

Nougier, J., J.M. Cantagrel, and J.P. Karch, The Comores archipelago in the western Indian Ocean: Volcanology, geochronology and geodynamic setting, *J. Afr. Earth Sci., 5(2),* 135–145, 1986.

O'Nions, R.K., and R.J. Pankhurst, Petrogenetic significance of isotope and trace element variations in volcanic rocks from the Mid-Atlantic Ridge, *J. Petrol., 15,* 603–634, 1974.

O'Nions, R.K., P.J. Hamilton, and N.M. Evensen, Variations in $^{143}Nd/^{144}Nd$ and $^{87}Sr/^{86}Sr$ ratios in oceanic basalts, *Earth Planet. Sci. Lett., 34,* 13–22, 1977.

Orheim, O., The glaciers of Bouvetøya, *Skr. Nor. Polarinst., 175,* 79–84, 1981.

Copyright American Geophysical Union

Patriat, P., J. Segoufin, R. Schlich, J. Goslin, J.M. Auzende, P. Beuzard, J. Bonnin, and J.L. Olivet, Les mouvements relatifs de l'Inde, de l'Afrique et de l'Eurasie, *Bull. Soc. Geol. Fr., 7,* 363–373, 1982.

Philippi, E., Geologische Beobachtungen auf Kerguelen, *Dtsch. Sudpolar Exped. 1901–1903, 2,* 187–207, 1908*a*.

Philippi, E., Geologie der Heard Insel, *Dtsch. Sudpolar Exped. 1901–1903, 2,* 241–250, 1908*b*.

Philippi, E., Geologie von St. Paul, *Dtsch. Sudpolar Exped. 1901–1903, 2,* 370–376, 1909.

Prestvik, T., Trace element geochemistry of volcanic rocks from Bouvetøya, South Atlantic, in *Antarctic Geoscience,* edited by C. Craddock, pp. 771–774, University of Wisconsin Press, Madison, 1982*a*.

Prestvik, T., The geology, volcanic activity and age of Bouvetøya, South Atlantic, *Norw. Antarct. Res. Exped. 1978/79 Publ. 58,* 115–123, 1982*b*. (Also published as *Rev. Univ. Açores Ser. Cien. Nat.,* no. 3, 115, 1982.)

Prestvik, T., and T.S. Winsnes, Geology of Bouvetøya, South Atlantic, *Skr. Nor. Polarinst., 175,* 41–69, 1981.

Prior, G.T., Report on the rock specimens collected during the "Discovery" Antarctic Expedition, 1901–1904, *Nat. Antarct. Exped. 1901–1904, Nat. Hist. 1, Geol.,* 101–140, 1907.

Quartermain, L.B., The Balleny Islands: A descriptive and historical outline, compiled for the use of the New Zealand Antarctic Research Expedition Balleny Islands Reconnaissance Party 1963–1964, 42 pp., Antarct. Div. New Zealand Dep. of Sci. and Ind. Res., Wellington, 1964.

Quilty, P.G., S. Shafik, A. McMinn, H. Brady, and I. Clarke, Microfossil evidence for the age and environment of deposition of sediments on Heard and McDonald islands, in *Antarctic Earth Science,* edited by R.L. Oliver, P.R. James, and J.B. Jago, pp. 636–639, Cambridge University Press, New York, 1983.

Ramsay, D.C., J.B. Colwell, M.F. Coffin, H.M.J. Stagg, C.J. Pigram, H.L. Davies, P.J. Hill, and N.A. Johnson, Geophysical investigations of Heard-Kerguelen Plateau, (abstract), *Eos Trans. AGU, 66,* 374, 1985.

Ravich, M.G., and A.Y. Krylov, Absolute ages of rocks from East Antarctica, in *Antarctic Geology,* edited by R.J. Adie, pp. 579–589, North-Holland, Amsterdam, 1964.

Recq, M., and P. Charvis, A seismic refraction survey in the Kerguelen Isles, southern Indian Ocean, *Geophys. J. R. Astron. Soc., 84,* 529–559, 1986.

Reddy, V.V., K.V. Subbarao, G.R. Reddy, J. Matsuda, and R. Hekinian, Geochemistry of volcanics from the Ninetyeast Ridge and its vicinity in the Indian Ocean, *Mar. Geol., 26,* 99–117, 1978.

Reinisch, R., Petrographie, II, Gesteine von der Bouvet-Insel, von Kerguelen, St. Paul und Neu-Amsterdam, *Wiss. Ergeb. Dtsch. Tiefsee Exped. Dampfer "Valdivia" 1898–1899), 10,* 49–75, 1905.

Reinisch, R., Petrographische Beschreibung der Kerguelen-Gesteine, *Dtsch. Sudpolar Exped. 1901–1903, 2,* 211–222, 1908*a*.

Reinisch, R., Gesteine der Heard Insel, *Dtsch. Sudpolar Exped. 1901–1903, 2,* 251–263, 1908*b*.

Reinisch, R., Gesteine von der Possession-Insel (Crozetgruppe), *Dtsch. Sudpolar Exped. 1901–1903, 2,* 325–333, 1908*c*.

Reinisch, R., Gesteine von St. Paul und Neu-Amsterdam, Anhang, Chemische Beziehungen der Basalte von St. Paul, Neu-Amsterdam, Kerguelen, Heard und Possession Inseln, *Dtsch. Sudpolar Exped. 1901–1903, 2,* 385–398, 1909.

Renard, A.F., Notes on the rocks of Kerguelen Island, *Rep. Sci. Results HMS "Challenger" Phys. Chem., 2,* 107–141, 1889*a*.

Renard, A.F., Report on Petrology of Oceanic Islands, *Rep. Sci. Results HMS "Challenger" Phys. Chem., 2,* 142, 1889*b*.

Sachse, W., Das Wiederauffinden der Bouvet-Insel durch die Deutsche Tiefsee-Expedition, *Wiss. Ergeb. Dtsch. Tiefsee Exped. Dampfter "Valdivia" 1898–1899, 10,* 1–34, 1905.

Schlich, R., Structure et âge de l'Océan Indien Occidental, *Mem. Soc. Geol. Fr., 6,* 103 pp., 1975.

Schlich, R., and P. Patriat, Anomalies magnétiques de la branche est de la dorsale medio-indiènne entre les îles Amsterdam et Kerguelen, *C.R. Acad. Sci. Paris, 272,* 773, 1971.

Shackleton, N.J., and N.D. Opdyke, Oxygen isotope and paleomagnetic stratigraphy of Pacific core V28-239, late Pliocene to latest Pleistocene, in *Investigation of Late Quaternary Paleogeography and Paleoclimatology,* Mem. 145, edited by R.M. Cline and J.D. Hays, pp. 449–464, Geological Society of America, Boulder, Colo., 1976.

Sheraton, J.W., and A. Cundari, Leucitites from Gaussberg, Antarctica, *Contrib. Mineral. Petrol., 71,* 417–427, 1980.

Snape, C., and J.A. Retief, Paleomagnetic study of some recent lavas, in *Marion and Prince Edward Islands,* edited by E.M. van Zinderen Bakker, J.M. Winterbottom, and R.A. Dyer, pp. 63–71, A.A. Balkema. Cape Town, 1971.

Soloviev, D.S., Platform magnetic formations of East Antarctica, in *Antarctic Geology and Geophysics,* edited by R.J. Adie, pp. 793–801, Universitetsforlaget, Oslo, 1972.

Stephenson, P.J., Some geological observations on Heard Island, in *Antarctic Geology,* edited by R.J. Adie, pp. 14-24, North Holland, Amsterdam, 1964.

Stephenson, P.J., Geochemistry of some Heard Island igneous rocks, in *Antarctic Geology and Geophysics,* edited by R.J. Adie, pp. 793–801, Universitetsforlaget, Oslo, 1972.

Storey, M., A.D. Saunders, J. Tarney, P. Leat, M.F. Thirlwall, R.N. Thompson, M.A. Menzies, and G.F. Marriner, Geochemical evidence for plume-mantle interactions beneath Kerguelen and Heard islands, Indian Ocean, *Nature, 336,* 371–373, 1988.

Studer, T., Geologische Beobachtungen auf Kerguelensland, *Z. Dtsch. Geol. Ges.., 30,* 327–350, 1878.

Studer, T., Geologie von Kerguelen, in *Forschungsreise SMS*

Copyright American Geophysical Union

"Gazelle" III, in den Jahren 1874 bis 1876, 56–86, Berlin, 1889.

Sun, S.S., and G.N. Hanson, Origin of Ross Island basanitoids and limitations upon the heterogeneity of mantle sources for alkali basalts and nephelinites, *Contrib. Mineral. Petrol., 52,* 77–106, 1975.

Sykes, L.R., Intraplate seismicity, reactivation of pre-existing zones of weakness, alkaline magmatism and other tectonism postdating continental fragmentation, *Rev. Geophys., 16,* 621–688, 1978.

Talbot, J.L., B.E. Hobbs, H.G. Wilshire, and T.R. Sweatman, Xenoliths and xenocrysts from lavas of the Kerguelen archipelago, *Am. Mineral., 48,* 159–179, 1963.

Tingey, R.J., I. McDougall, and A.J.W. Gleadow, The age and mode of formation of Gaussberg, Antarctica, *J. Geol. Soc. Aust., 30,* 241–246, 1983.

Tyrrell, G.W., The petrology of Heard Island, *Rep. B.A.N.Z. Antarct. Res. Exped., Ser. A., 2,* 29–56, 1937*a*.

Tyrrell, G.W., The petrology of Possession Island (Crozet Islands), *Rep. B.A.N.Z. Antarct. Res. Exped., Ser. A, 2,* 59–68, 1937*b*.

Vallon, M., Bilan de Masse et fluctuations recentes du Glacier Ampere (Îles Kerguelen, TAAF), *Z. Gletscherkd. Glazialgeol., 13,* 57–85, 1977.

Vélain, C., *Description Géologique de la presq'île d'Aden, de l'île de la Réunion, des îles St. Paul et Amsterdam,* 356 pp., A. Hennuyer, Paris, 1878.

Verwoerd, W.J., Geology, in *Marion and Prince Edward Islands,* edited by E.M. van Zinderen Bakker, J.M. Winterbottom, and R.A. Dyer, pp. 40–62, A.A. Balkema, Cape Town, 1971.

Verwoerd, W.J., Islands on the mid-ocean ridge between Africa and Antarctica (abstract), *Eos Trans. AGU, 53,* 168–170, 1972.

Verwoerd, W.J., and L. Chevallier, Contrasting types of Surtseyan tuff cones on Marion and Prince Edward islands, southwest Indian Ocean, *Bull. Volcanol., 49,* 399–417, 1987.

Verwoerd, W.J., A.J. Erlank, and E.J.D. Kable, Geology and geochemistry of Bouvet Island, in *Proceedings of the International Symposium on Andean and Antarctic Volcanology Problems,* edited by O. González-Ferrán, pp. 203–237, I.A.V.C.E.I., Rome, 1976.

Verwoerd, W.J., S. Russell, and A. Berruti, 1980 volcanic eruption reported on Marion Island, *Earth Planet. Sci. Lett., 54,* 153–156, 1981.

Vyalov, O.S., and V.S. Sobolev, Gaussberg, Antarctica, *Int. Geol. Rev., Engl. Transl., 1,* 30–40, 1959.

Waterhouse, B.C., Western Ross Sea–Balleny Ridge expedition: January–March 1965, open file report, New Zealand Geol. Surv., Wellington, 1965.

Watkins, N.D., and J. Nougier, Excursion and secular variation of the Brunhes epoch geomagnetic field in the Indian Ocean region, *J. Geophys. Res., 78,* 6060–6068, 1973.

Watkins, N.D., B.M. Gunn, J. Nougier, and A.K. Baksi, Kerguelen: Continental fragment or oceanic island?, *Geol. Soc. Am. Bull., 85,* 201–212, 1974.

Watkins, N.D., I. McDougall, and J. Nougier, Paleomagnetism and potassium-argon age of St. Paul Island, southeastern Indian Ocean; contrasts in geomagnetic secular variation during the Brunhes epoch, *Earth Planet. Sci. Lett., 24,* 377–384, 1975.

Weis, D., J.-F. Beaux, and A. Giret, The two plutonic alkaline trends of Kerguelen Islands, *Terra Cognita, 7,* 12, 1988.

Werth, E., Aufbau und Gestaltung von Kerguelen, *Dtsch. Sudpolar Exped. 1901–1903, 2,* 89–183, 1908.

White, W.M., Sources of oceanic basalts: Radiogenic isotopic evidence, *Geology, 13,* 115–118, 1985.

Whitford, D.J., and R.A. Duncan, Origin of the Ninetyeast Ridge: Trace-element and Sr isotope evidence, *Year Book Carnegie Inst. Washington, 1977–78,* 606–613, 1979.

Williams, R., and G. Duhamel, Volcanic activity on Heard Island, *Polar Rec., 23,* 88–90, 1986.

Winsnes, T.S., Besøk pa Bouvetøya i 1958 og 1966, *Arbok Nor. Polarinst., 1965,* 143–149, 1966.

Copyright American Geophysical Union

Copyright American Geophysical Union

Summary

J.A. Gamble and J.W. Thomson

Frontispiece. The eroded core of Carnley Volcano, Auckland Islands. View is from Adams Island looking north. High ground on the skyline consists of basaltic lava flows. These rest on Miocene conglomerates, sandstones, carbonates, and tuffs which are exposed at sea level on Masked Island (center), Camp Cove (center left), and Musgrave Peninsula (spit of land protruding from extreme right). Eroded granitoid (Cretaceous) basement is also exposed on Musgrave Peninsula, and a gabbro intrusion (coeval with the basalts) forms the prominent headlands in the middle background. (Photograph by J.A. Gamble.)

Introduction

Except for Macquarie Island these remote and relatively inaccessible volcanic islands are all located on the Campbell Plateau (Figure G.I and Table G.I), a vast area (~800,000 km^2) of shallow epicontinental ocean that has geological and structural links to the continental mass of New Zealand. Macquarie Island, located to the southwest of Campbell Plateau, is the exposed part of the Macquarie Ridge, which formed as a result of oblique compression between the Indian-Australian and Pacific plates [*Williamson*, 1988].

Antipodes Island (see IVD G.1) is composed of a sequence of coalesced scoria cones and tuff cones, and the Auckland Islands (see IVD G.2) and Campbell Island (see IVD G.3) are intraplate shield volcanoes. Basement to the Auckland Islands volcanoes is the late Cretaceous granitoid exposed in the heart of Carnley Harbour [*Gamble and Adams*, 1985], whereas the volcanic rocks of Campbell Island are underlain by a sequence of late Mesozoic sedimentary rocks that rest unconformably on schist of presumed lower Paleozoic age [*Adams et al.*, 1979]. No pre-Cenozoic basement has been observed on Antipodes Island. Macquarie Island (see IVD G.4), an ophiolite complex, is a rare example of uplifted oceanic crust.

Extent of Knowledge

Although Captain Cook must have sailed close to the Antipodes Islands on his voyage to Antarctica in 1773, it was Captain Waterhouse of *Reliance* who discovered the islands in March 1800, naming them the Penantipodes Islands because of their location near the antipodes of London. By 1803 a sealing industry was flourishing on Antipodes Island, and the quest for fresh sealing and whaling grounds led to the discovery of the Auckland Islands in August 1806 by Captain Bristow of *Ocean* and of Campbell and Macquarie islands by Captain Hasselborough of *Perseverance;* Campbell Island was named after the owner of the vessel, and Macquarie Island after the governor of New South Wales. By 1820 the sealing industry had

Copyright American Geophysical Union

Copyright American Geophysical Union

the islands are free of any substantial permanent snow and ice, and they support tussock grassland, shrubland and herbfield, and some tree growth. None of the islands, however, are inhabited, although Auckland Island was settled briefly by Maoris and British colonists between 1842 and 1852 and Campbell Island was leased for sheep farming between 1895 and 1931. Macquarie and Campbell islands have manned scientific stations, established during the 1911–1914 Australasian Antarctic Expedition and in 1941, respectively. Macquarie Island was declared a wildlife sanctuary in 1933 and became a nature reserve in 1978; Campbell Island was made a fauna and flora reserve in 1954 and a nature reserve in 1983.

Petrology and Geochemistry

Volcanic rocks from the Auckland Islands (see IVD G.2) and Campbell Island (see IVD G.3) are identical petrographically and geochemically [*Gamble and Morris*, 1984; *Morris*, 1984; *Gamble and Adams*, 1985; *Gamble et al.*, 1986; *McDonough et al.*, 1986; *Weaver et al.*, 1986]. They vary from strongly to sparsely porphyritic ankaramitic lavas fed from fissure dike systems which are centered on the deeply eroded cores of the volcanoes. Their compositions vary from mildly alkaline to transitional basalts (<5% normative *ne* to *hy*-normative) with lesser volumes of intermediate and felsic lavas (mugearites, benmoreites, trachytes, and rhyolites).

The Antipodes Islands (see IVD G.1), built up of a series of coalesced scoria and tuff cones with only minor lava flows and associated intrusive rocks, differ in this respect from the effusive, flow-dominated volcanism of Campbell Island and the Auckland Islands. Petrographically, the rocks vary from strongly porphyritic ankaramites rich in olivine and clinopyroxene to aphyric glassy basalts. Kaersutite occurs as resorbed phenocrysts in a number of lavas, and some tephra layers are rich in euhedral clinopyroxene megacrysts. All the rocks from the Antipodes Islands are strongly undersaturated compared with the rocks from Auckland and Campbell islands, and they vary from basanite to *ne*-hawaiite. They contain relatively high contents of large ion lithophile, high field strength, and light rare earth elements when compared to the Auckland and Campbell islands rocks of similar Mg number. Trace-element ratios and isotopic ratios, however, are broadly similar, leading *Gamble et al.* [1986], *McDonough et al.* [1986], and *Weaver et al.* [1986] to speculate on a relatively homogeneous upper mantle source with variable degrees of partial melting to explain the chemical differences in the rock types.

The mafic extrusive and intrusive rocks on Macquarie Island (see IVD G.4) form part of an ophiolite complex which probably generated at the Australian-Antarctic spreading ridge [*Christodoulou et al.*, 1984]. The extrusive rocks are predominantly pillow lava flows with compositions which range from typical ocean floor basalts to varieties relatively enriched in some incompatible trace elements [*Griffin and Varne*, 1980].

Geochronology

The volcanic islands on the Campbell Plateau range in age from about 18 Ma (Auckland Islands (Adams and Gamble, unpublished data)) to <1 Ma (Antipodes Island [*Cullen*, 1969]). By correlating seafloor spreading magnetic anomaly 7 across Macquarie Island, *Williamson* [1988] has suggested that the original oceanic crust of the island was formed at the Indian-Antarctic accreting mid-oceanic ridge around the time of anomaly 7 (27 Ma). However, paleontological evidence obtained from the sedimentary rocks intercalated with the lavas on Macquarie Island, and K-Ar dates of 11.5–9.7 Ma [*Duncan and Varne*, 1988] for the lavas indicate a younger age, possibly reflecting later metamorphic or igneous episodes after the original oceanic crust formed [*Williamson*, 1988]. There are no records of historical volcanic activity on any of these islands.

Copyright American Geophysical Union

G.1. ANTIPODES ISLANDS

Type of volcano: Intraplate basaltic scoria and tuff cones.

Location: Campbell Plateau, 750 km southwest of New Zealand (49°41′S, 178°46′E).

Height above sea level: ~300 m.

Evidence of Holocene activity: Well-preserved scoria cones.

Authors of report: J.A. Gamble and C.J. Adams.

Date of report: September 1986.

Form and Structure

The Antipodes Islands (Figure G.1.1) are the smallest, most remote, and least well known of New Zealand's subantarctic islands. They consist of Antipodes Island (~4 km wide), Bollons Island (~1 km wide), and numerous small islets and sea stacks.

No pre-Cenozoic basement is exposed on the islands, and the volcanic rocks are predominantly pyroclastic, with minor volumes of lava flows and intrusive rocks. The most recent volcanic activity was centered on the steep cone forming Mount Galloway and Mount Waterhouse. Marine erosion has exposed 200-m-high cliff sections through tuff cones at Perpendicular Head and Albatross Point.

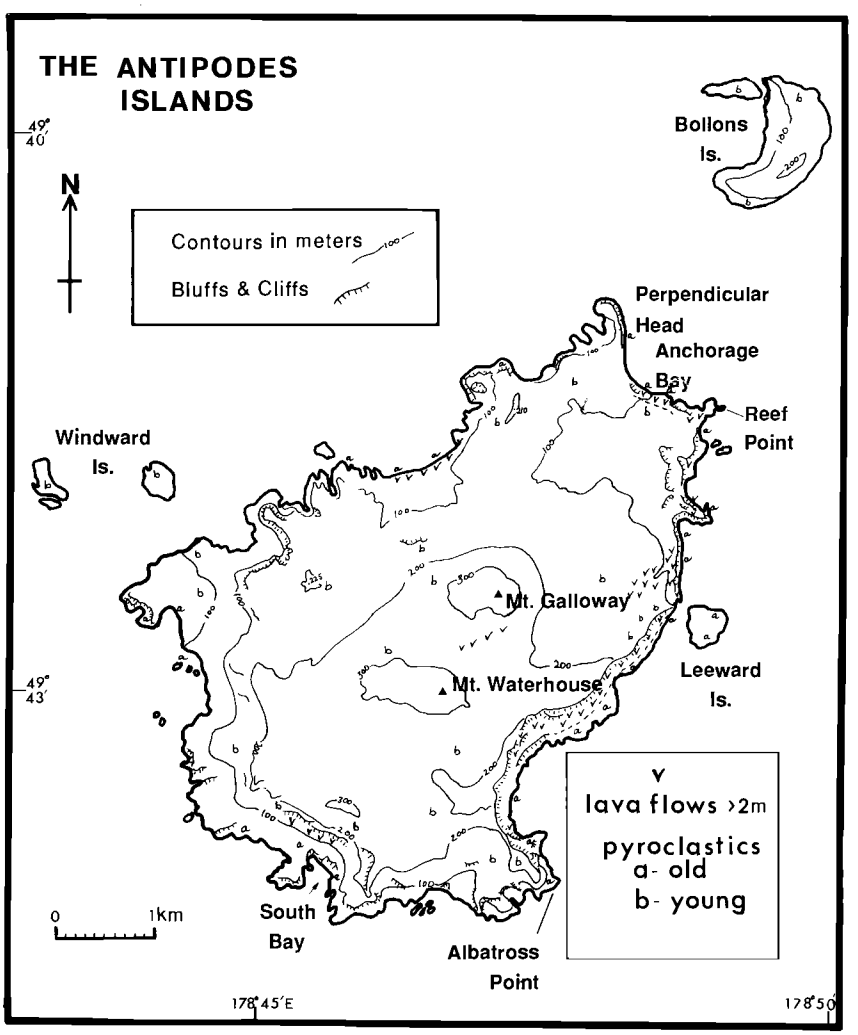

Fig. G.1.1 Geologic sketch map of the Antipodes Islands. Geology is from Adams (unpublished field notes, 1985).

Copyright American Geophysical Union

TABLE G.1.1. Representative Chemical Analyses of Volcanic Rocks From Antipodes Island

	1	2	3	4
SiO_2	41.89	42.11	42.39	47.51
TiO_2	4.15	3.92	2.95	2.28
Al_2O_3	11.32	12.97	8.47	16.59
Fe_2O_3	2.69	2.38	2.46	1.86
FeO	13.46	11.91	12.30	9.30
MnO	0.19	0.20	0.17	0.20
MgO	9.48	7.95	15.35	3.23
CaO	11.45	10.94	12.41	7.43
Na_2O	2.32	4.85	1.49	6.62
K_2O	0.75	1.57	0.25	2.22
P_2O_5	0.52	1.19	0.31	1.19
LOI	1.00	--	1.20	1.1
Total	99.22	100.00	99.75	99.53
Ba	209	494	110	617
Ce	70	156	39	205
Cr	301	124	659	11
Cu	58	64	51	37
Ga	21	21	12	26
La	25	83	16	112
Nb	45	100	23	135
Ni	138	117	283	19
Pb	4	5	1	7
Rb	17	45	4	63
Sc	29	19	36	10
Sr	517	1181	335	1413
Th	4	11	3	16
V	366	244	319	89
Y	29	38	21	41
Zn	126	178	115	201
Zr	228	393	136	571
Zr/Nb	5.07	3.93	5.91	4.23
$\frac{100.Mg}{Mg + Fe}$	55.7	54.34	69.0	38.2
$\frac{100.An}{An + Ab}$	64.8	72.4	74.4	28.0

All analyses by XRF except Fe_2O_3 and FeO (by titration) and LOI (gravimetric). Dash, not determined; LOI, loss on ignition.

1. 81/7. Basanite lava flow, Reef Point, north end of Antipodes Island (analyst, J.A. Gamble).
2. 81/15. Basanite lava flow, west of South Bay (analyst, J.A. Gamble).
3. 81/10. Ankaramite lava flow, east side of Anchorage Bay (analyst, J.A. Gamble).
4. 81/11. *Ne*-hawaiite-benmoreite lava flow, east side of Anchorage Bay (analyst, J.A. Gamble).

Petrologic Characteristics

The majority of the lavas are fine grained and glassy, variably porphyritic, mafic rocks; phenocrysts are olivine, clinopyroxene, Fe-Ti oxides, and plagioclase. Kaersutite occurs as resorbed megacrysts in some lava flows, and clinopyroxene megacrysts have been recovered from some of the tephra. Representative chemical analyses are shown in Table G.1.1, and microprobe data are given by *Gamble et al.* [1986].

Chronologic Data

Many youthful volcanic landforms are preserved on the islands, and the available whole-rock age determinations [*Cullen*, 1969] have yielded dates of < 1 Ma (0.25 ± 0.2 and 0.50 ± 0.4 Ma). Reconnaissance work on the new samples (Adams, unpublished data, 1985) confirms this young age.

Extent of Knowledge

Antipodes Island is the least accessible of New Zealand's subantarctic islands. There is but one favorable landing beach, at the north end of the island, and much of the island is covered with dense scrub and tussock grass. Geological descriptions of the Antipodes Islands have been given by *Hector* [1870, 1896], *Speight and Finlayson* [1909], *Cullen* [1969], *Wareham and Johns* [1975], and *Gamble et al.* [1986].

Bibliography

Cullen, 1969
Gamble and Morris, 1984
Gamble et al., 1986
Hector, 1870, 1896
McDonough et al., 1986
Speight and Finlayson, 1909
Wareham and Johns, 1975

Copyright American Geophysical Union

G.2. AUCKLAND ISLANDS

Type of volcano: Intraplate basaltic shield.

Location: Campbell Plateau, 400 km south of New Zealand (50°50′S, 166°E).

Height above sea level: 680 m on Adams Island.

Evidence of Holocene activity: None.

Authors of report: J.A. Gamble and C.J. Adams.

Date of report: September 1986.

Form and Structure

The Auckland Islands are a group of subantarctic islands which lie 400 km to the south of New Zealand. There are four main islands: Auckland Island (the largest), Adams Island, Disappointment Island, and Enderby Island, together with numerous small islets and sea stacks (Figure G.2.1). Their topographic expression and the available K-Ar age data [*Adams,* 1980] (Figure G.2.2) suggest that the islands are composed of two coalesced volcanic shields, Carnley Volcano in the south and the younger Ross Volcano to the north [*Fleming,* 1959; *Wright,* 1966].

Most of the islands consist of laterally discontinuous lava flows 5–10 m in thickness with occasional, more extensive flows reaching 20–30 m in thickness. Around Carnley Harbour the flows on Circular Head, McClure Head, and the Fleming Plateau dip gently at 5°–7° to the northwest; flows on Adams Island dip to the southwest at 5°–8°, and those on Mount D'Urville are virtually horizontal. These dips appear to be reasonably consistent with a volcanic edifice (Carnley Volcano) centered on Carnley Harbour. In the northwest part of the island group, a generalized dip of lava flows to the east [*Wright,* 1966, p. 74] is consistent with an offshore locus for the main eruptive center, possibly near Disappointment Island [see *Fleming,* 1959; *Wright,* 1966; *Adams,* 1980]. *Wright* [1966] measured and sampled several gully sections along this coastline, and petrographic studies [*Wright,* 1966, 1967] show that the rocks are more or less porphyritic basalts interbedded with scoria, tuffs, and agglomerate, with minor volumes of evolved lavas (mostly trachytes and rhyolites). The lava flows exposed on the northern parts of Auckland and Enderby islands would have erupted on the distal flanks of the shield and, accordingly, should give relatively young ages [*Adams,* 1980] (Figure G.2.2). No rock from the lower parts of the Ross Volcano (at the base of the western cliffs) has been dated radiometrically, and furthermore, no base to its volcanic succession has been recorded.

In the north-facing slopes and cliffs of Adams Island (Carnley Volcano) more than 40 flow units can be traced from sea level through 680 m of section. Flow tops and bottoms are typically rubbly and vesicular, and vesicle cylinders and pipe vesicles have been observed in the basal parts of many lava flows. Localized centers of explosive activity have been recognized within the lower part of the lava succession (e.g., toward the western end of Adams Island, adjacent to Victoria Passage) and are characterized by an abundance of well-bedded lapilli layers, commonly containing bombs, and scoria. Stratigraphic relationships show that the scoria cones have been overwhelmed by the more extensive and voluminous lava flows. Minor volumes of rhyolite and trachyte occur sporadically in the lower parts of the shield. Their restricted but frequently thick outcrop pattern suggests that they formed domes or stumpy flows. They have not been recorded from the higher parts of the succession on Adams Island and Fleming Plateau.

In the central part of Carnley Harbour the basal pyroclastic sedimentary and flow rocks are cut by a north-south-trending dike swarm which peters out vertically, implying that the dikes probably acted as feeders to the lava flows. Where they cut the basement granite on Musgrave Peninsula, heat fusion of the granite and back-veining of the dike rock occurred.

At Circular Head and McClure Head a coarse-grained olivine-biotite-gabbro cuts the lower part of the lava flow and pyroclastic sequence. The gabbro is heterogeneous, locally layered, and cut by felsic veins which form intrusion breccias. It is also cut by the dike swarm which, here, is less intense than that observed in Camp Cove and on Masked Island, lying directly to the south along strike. This relationship tends to confirm the radiometric dating of *Denison and Coombs* [1977], which suggested that gabbro emplacement was contemporaneous with shield building.

Petrologic Characteristics

The volcanic and intrusive rocks are composed predominantly of basic lava flows and dikes which range from strongly to sparsely porphyritic in nature. Phenocryst phases include olivine, clinopyroxene, and plagioclase. Plagioclase becomes predominant in more evolved compositions, and in the trachytes and rhyolites, sodic plagioclase and sanidine are the sole phenocryst phases.

Detailed petrographic descriptions [*Wright,* 1966, 1967, 1968] indicate that the rocks of Ross Volcano are similar to those of Carnley Volcano. Chemical analyses (Table G.2.1) show that the basic rocks of Carnley Volcano are mildly alkaline, ranging from *ne*-normative to *hy*-normative and from basalt to hawaiite. Trace-element abundances show a systematic variation in Ni, Cr, Sr, and Ba that is consistent with

Copyright American Geophysical Union

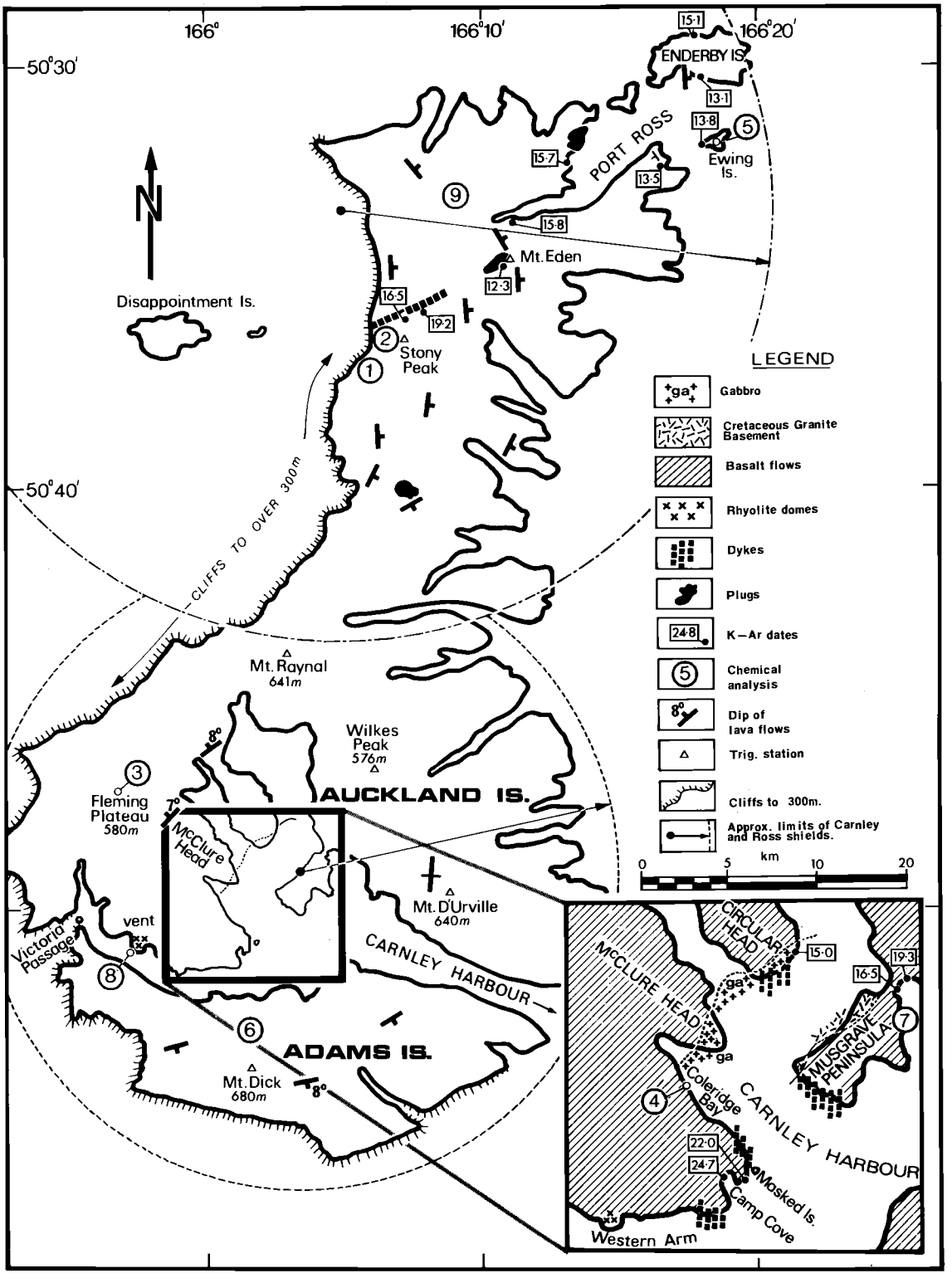

Fig. G.2.1. Geologic map of the Auckland Islands. Circles enclose the approximate areas of the coalesced Ross (dot-dashed circle) and Carnley (dashed circle) shield volcanoes. Solid circles indicate loci of circles in the central part of Carnley Harbour, coincident with the dike swarm, and off the west coast of Auckland Island. Encircled numbers indicate the locations of representative chemical analyses (Table G.2.1). K-Ar age data (from *Denison and Coombs* [1977] and *Adams* [1980]), shown as numbers in squares, are adjacent to their collection site.

Copyright American Geophysical Union

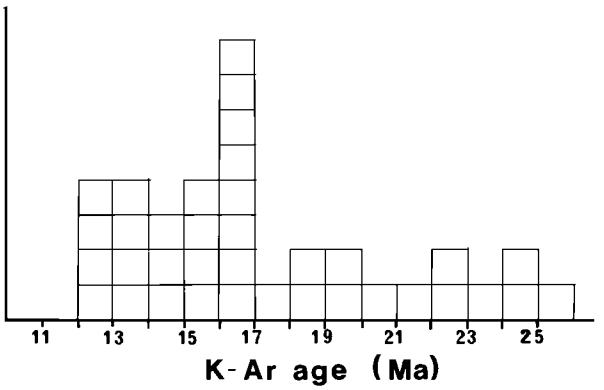

Fig. G.2.2. Histogram of available K-Ar ages for Tertiary volcanic rocks from the Auckland Islands (data from *Adams* [1983, and unpublished data, 1984]); an average date of 15 Ma for the gabbro is from *Denison and Coombs* [1977].

fractionation of olivine, plagioclase, and clinopyroxene, the principal phenocryst minerals. Evolved rocks represent a minor proportion of each volcano and are separated from the bulk of the lavas by a compositional hiatus. Both *ne*- and *Q*-normative evolved compositions are represented in the Ross Shield [*Wright,* 1970], but only *Q*-normative compositions are reported from Carnley Volcano. Compositions range from trachyte to rhyolite, and all are enriched in the incompatible elements La, Ce, Rb, Th, Zr, Nb, Ba, Y, and Sc and depleted in Ni, Cr, Cu, and Sr.

Chronologic Data

The chronologic data available are taken from *Adams* [1980] and *Denison and Coombs* [1977] (Figure G.2.2). The dated samples were collected from the hearth of Carnley Volcano (i.e., the oldest rocks) and from the peripheral flanks of Ross Volcano (representing the youngest rocks). Consequently, a span of ages could be anticipated. New K-Ar dating on superior samples collected by Gamble and Adams (see *Gamble and Adams* [1985] for brief sample descriptions) suggests a range from early to late Miocene (18–12 Ma) for the Auckland Islands.

Extent of Knowledge

A dense covering of scrub (0–300 m above sea level) effectively obliterates outcrop on the lower slopes of the islands, and it is succeeded above 300 m by peat bog and tussock grass. Accessible exposed rocks (20% of the volcanoes) are confined to coastal and cliff sections.

Current knowledge is based on the records and reports of a number of scientific expeditions to the islands since the turn of the century [*Speight and Finlayson,* 1909; *Wright,* 1966; *Adams,* 1980; *Gamble et al.,* 1982, 1986; *Gamble and Morris,* 1984; *Gamble and Adams,* 1985; *Ritchie and Turnbull,* 1985; *McDonough et al.,* 1986; *Weaver et al.,* 1986].

Bibliography

Adams, 1980
Denison and Coombs, 1977
Fleming, 1959
Gamble and Adams, 1985
Gamble and Morris, 1984
Gamble et al., 1982, 1986
McDonough et al., 1986
Ritchie and Turnbull, 1985
Speight and Finlayson, 1909
Weaver et al., 1986
Wright, 1966, 1967, 1968, 1970, 1971

Copyright American Geophysical Union

TABLE G.2.1. Representative Chemical Analyses of Volcanic Rocks From Carnley and Ross Volcanoes

	1	2	3	4	5	6	7	8	9
SiO_2	41.20	44.00	45.85	46.34	47.00	52.73	66.23	72.06	73.30
TiO_2	4.60	2.80	3.12	2.75	2.50	2.18	0.54	0.40	0.58
Al_2O_3	14.20	13.80	14.59	11.88	11.90	16.43	14.59	14.46	14.20
Fe_2O_3	3.30	2.08	3.43	3.18	3.30	4.34	1.60	1.38	0.33
FeO	11.50	10.42	9.40	8.99	8.20	5.50	4.52	0.28	1.66
MnO	0.16	0.38	0.19	0.15	0.13	0.13	0.06	0.01	0.02
MgO	9.20	11.10	7.95	8.93	11.10	2.80	0.37	0.08	0.05
CaO	11.00	11.40	9.60	9.77	9.10	6.45	0.69	1.24	0.24
Na_2O	2.10	2.10	2.74	2.78	2.50	3.59	3.08	3.87	4.40
K_2O	0.75	0.38	1.04	0.80	0.90	2.53	5.12	5.09	4.80
P_2O_5	0.34	0.33	0.59	0.47	0.50	0.79	0.11	0.05	0.06
LOI	1.4*	1.10*	1.39	3.52	3.15*	2.33	2.40	0.70*	0.68*
Total	99.85	99.99	99.89	99.56	100.28	99.80	99.31	99.62	100.47
Ba	--	--	322	206	--	513	765	754	--
Ce	--	--	82	56	--	131	181	224	--
Cr	--	--	222	305	--	9	2	<2	--
Cu	--	--	65	64	--	14	4	2	--
Ga	--	--	21	19	--	26	29	28	--
La	--	--	37	24	--	63	86	113	--
Nb	--	--	61	42	--	74	105	106	--
Ni	--	--	149	201	--	11	29	2	--
Pb	--	--	<2	2	--	12	22	25	--
Rb	--	--	21	13	--	77	182	196	--
Sc	--	--	22	24	--	14	13	10	--
Sr	--	--	698	508	--	583	161	227	--
Th	--	--	6	5	--	12	24	24	--
V	--	--	268	222	--	158	3	<2	--
Y	--	--	33	29	--	43	59	64	--
Zn	--	--	114	121	--	123	160	148	--
Zr	--	--	229	183	--	392	631	590	--
Zr/Nb	--	--	3.75	4.36	--	5.30	6.01	5.57	--
$\frac{100.Mg}{Mg+Fe}$	57.2	65.5	57.2	61.3	67.6	38.5	11.6	10.0	5.09
$\frac{100.An}{An+Ab}$	72.9	65.4	51.3	42.7	46.8	41.2	9.4	15.1	2.10

Analyses 1, 2, 5, and 9 by wet chemical methods; analyses 3, 4, 6, 7, and 8 by XRF except Fe_2O_3 and FeO (by titration) and LOI (gravimetric). LOI, loss on ignition. Dashes, not determined.

*H_2O.

1. Olivine basalt flow (sea level), western cliffs, Ross Volcano [*Wright,* 1970, 1971].
2. Olivine basalt flow (440 m), western cliffs, Ross Volcano [*Wright,* 1970, 1971].
3. Olivine basalt flow, topmost lava flow (580 m) on Fleming Plateau, Carnley Volcano (analyst, J.A. Gamble).
4. Olivine basalt flow, west side of Coleridge Bay (sea level), Carnley Volcano (analyst, J.A. Gamble).
5. Olivine basalt flow (sea level), Ewing Island, Ross Volcano [*Wright,* 1970, 1971].
6. Olivine hawaiite flow at 520 m, Adams Island, Carnley Volcano (analyst, J.A. Gamble).
7. Trachyte flow (sea level), Tagua Bay, Musgrave Peninsula, Carnley Volcano (analyst, J.A. Gamble).
8. Rhyolite dome (sea level), western arm, Carnley Harbour, Carnley Volcano (analyst, J.A. Gamble).
9. Rhyolite (350 m), Hooker Saddle Suite, Ross Volcano [*Wright,* 1970, 1971].

Copyright American Geophysical Union

G.3. CAMPBELL ISLAND

Type of volcano: Shield volcano comprising approximately 200 m of Miocene volcaniclastic breccia overlain by approximately 300 m of volcanic flows; minor high-level intrusions. Erosion about the primary vent system has revealed pyroclastic and flow sequences and a secondary center of igneous activity.

Location: 750 km south of New Zealand (52°30′S, 169°10′E).

Height above sea level: 569 m (above Perseverance Harbour).

Evidence of Holocene activity: None.

Authors of report: P.A. Morris and J.A. Gamble.

Date of report: September 1986.

Form and Structure

Pyroclastic rocks and lava flows have been derived from a vent system to the west of Campbell Island, in present-day Northwest Bay. The western half of the original volcanic shield has been removed by erosion. Glacial erosion has accentuated fluvial erosion about the vent system, exposing a secondary center of igneous activity at the head of Perseverance Harbour, namely, Beeman Hill and its associated high-level intrusions at Lion Rock and at Shoal, De La Vire, and Boyack points (Figure G.3.1). Intrusions at Menhir and Dent Island are related spatially to the Northwest Bay center. Numerous dikes intrude sedimentary rocks at the head of Perseverance Harbour and in the cliffs to the east of Northwest Bay.

Petrologic Characteristics

The majority of flows are porphyritic hawaiites, comprising phenocrysts of olivine and plagioclase (subordinate titansalite) in a groundmass of feldspar, opaque oxide, clinopyroxene, and minor olivine. Rare trachyte

Fig. G.3.1. Geologic sketch map of Campbell Island.

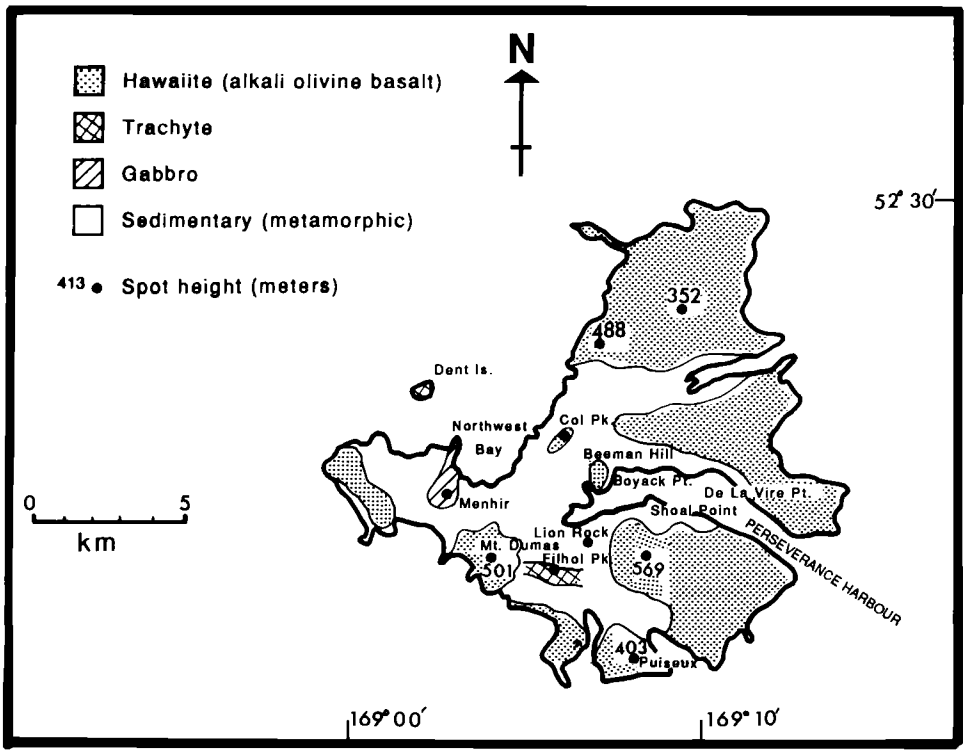

Copyright American Geophysical Union

TABLE G.3.1. Representative Chemical Analyses of Volcanic Rocks From Campbell Island

	1	2	3	4
SiO_2	46.86	47.63	55.10	63.73
TiO_2	3.00	3.51	1.68	0.53
Al_2O_3	12.85	17.61	16.61	17.00
Fe_2O_3	2.15	2.01	1.70	0.89
FeO	10.76	10.03	8.51	4.43
MnO	0.19	0.16	0.22	0.10
MgO	10.95	4.27	1.87	0.43
CaO	9.72	9.36	5.30	2.17
Na_2O	2.14	3.73	5.87	5.34
K_2O	0.89	0.91	2.43	5.27
P_2O_5	0.48	0.78	0.71	0.11
Total	100.00	100.00	100.00	100.00
Ba	251	297	611	825
Ce	73	79	150	255
Cr	350	10	--	4
La	38	35	70	142
Nb	50	50	105	80
Ni	265	30	4	4
Rb	23	23	66	84
Sr	542	634	488	117
Th	6	--	12	16
V	238	241	58	9
Y	28	36	55	45
Zr	192	203	545	845
Zr/Nb	3.8	4.1	5.2	10.6
$\frac{100.Mg}{Mg+Fe}$	64.5	43.2	28.1	14.7
$\frac{100.An}{An+Ab}$	55.8	47.5	19.7	13.2

All analyses by XRF except Fe_2O_3 and FeO (by titration) and LOI (gravimetric). Dashes, not determined.

1. 39796. Alkali basalt, southwest side of Puiseux Peak [*Morris*, 1984].
2. 36168. Hawaiite, northeast side of Mount Dumas [*Morris*, 1984].
3. 19891. Benmoreite, Lion Rock [*Morris*, 1984].
4. 26172. Trachyte, Dent Island [*Morris*, 1984].

(ferroaugite + feldspar) and rhyolite (feldspar, quartz, aegirine, arfvedsonite, and glass) flows crop out at the top of the flow sequence on Filhol Peak and 1 km northwest of Col Peak, respectively. Intrusive rocks include hawaiite (Beeman Hill, Lion Rock, Boyack, Shoal, and De La Vire points, and most of the dikes), mugearite, benmoreite (Lion Rock only), and trachyte (Dent Island). Menhir is an alkaline to transitional gabbro consisting of early-formed olivine, clinopyroxene, and feldspar, with late-stage pockets of clinopyroxene, feldspar, apatite, biotite, and minor quartz + orthopyroxene. Representative chemical analyses of some of these rocks are given in Table G.3.1.

Chronologic Data

K-Ar dating [*Adams et al.*, 1979] shows that lava flow and high-level intrusive activity occurred over approximately 1.5 m.y. of the upper Miocene (8.0–6.5 Ma), although one flow of alkali olivine basalt directly overlying volcaniclastic breccia on Puiseux Peak gives an earlier date of 11.1 Ma. The Menhir gabbro (16 Ma) predates the earliest volcanic activity by 5 m.y.

Extent of Knowledge

Detailed mapping was carried out by *Oliver et al.* [1950], and the petrology of the volcanic flows and intrusive rocks has been described by *Morris* [1976, 1984]. Apart from the work of *Oliver et al.* [1950], there are no published data on the volcaniclastic breccia.

Bibliography

Adams et al., 1979
Morris, 1976, 1984
Oliver et al., 1950

Copyright American Geophysical Union

G.4. MACQUARIE ISLAND

Type of volcano: Uplifted oceanic crust/ophiolite complex.

Location: On the Macquarie Ridge, ~1500 km south-southeast of Tasmania (54°37′S, 158°54′E) and ~1100 km south-southwest of New Zealand (Figure G.I).

Height above sea level: 433 m (Mount Hamilton).

Evidence of Holocene activity: None.

Authors of report: R. Varne and J.W. Thomson.

Date of report: June 1988.

Form and Structure

Macquarie Island (Figure G.4.1), which is unique among islands of the major ocean basins in being composed of oceanic crust, marks the tectonic emergence above sea level of part of the Macquarie Ridge [*Varne et al.*, 1969]. The island is about 35 km long but less than 6 km wide, elongated north-northwest along the axis of the Macquarie Ridge. It is topped by an elevated and undulating lake-studded plateau, which is best developed in the northern part of the island, cut off seaward by steep cliffs. A marked coastal platform with relic sea stacks occurs in places at the base of the cliffs; this has its greatest development at Handspike Point (Figure G.4.1), where it is 1 km wide and rises to an elevation of about 15 m above sea level [*Mawson*, 1943].

Marine, glacial, and other subaerial erosional processes may all have played a part in shaping Macquarie Island from the ridge as it rose. Some terraces in the northern part of the island may be relics of periglacial activity [*Löffler et al.*, 1983], but others are associated with raised beach deposits that were apparently lifted to their present position by neotectonic processes [*Varne et al.*, 1969; *Selkirk et al.*, 1983; *Ledingham and Peterson*, 1984]. It could be that the summit plateau was largely cut by marine erosion, either before renewed compression along the Macquarie Ridge uplifted the island to its present position or when sea levels were higher in the past [*Varne*, 1989].

The landscape has been modified by recent faulting. *Ledingham and Peterson* [1984] described recent lineaments and fault lines: some displace young topographic features and are associated with topographic depressions and lakes. These young lineaments and fault lines follow generally northerly trends (Figure G.4.1).

The northern part of the island is formed mainly of intrusive igneous rocks, including peridotites, gabbros, and sheeted dolerite dike complexes, whereas most of the southern part is formed of extrusive volcanic rocks and associated sedimentary rocks (Figure G.4.1). The contact zone follows a topographic depression between Bauer Bay and Sandy Bay and corresponds in part with a northwest-trending fault zone marked by mylonites and flaser gabbros and invaded by gabbroic veins [*Varne et al.*, 1969].

The extrusive volcanic rocks are basaltic. Pillow lavas are common, and volcanic breccias, hyaloclastites, and massive lavas are also present [*Mawson*, 1943; *Varne and Rubenach*, 1972; *Christodoulou et al.*, 1984; *Crohn*, 1986]. Thin lenses of volcaniclastic sedimentary rocks, ranging from mudstone to conglomerate, are associated with volcanic sequences which contain massive lavas, as at Mawson Point. Calcareous oozes occur between pillows and are widely distributed, although not abundant. They indicate that volcanic activity took place in a submarine setting, but the water depths at the time of deposition are unknown.

Two strike directions are commonly found in the volcanic and sedimentary rocks. South of Mawson Point and near Green Gorge the dominant strike trends are westerly, but elsewhere they lie in the northwest quadrant. Dips range from shallow to steep and are variable even in areas of constant strike. Tilting may have occurred first about near-horizontal axes parallel to dike–bedding plane intersections, with variations in strike due to later rotation about vertical axes [*Varne and Rubenach*, 1972; *Williamson*, 1978].

Petrologic Characteristics

Basalts and dolerites range from coarsely porphyritic to aphyric and from almost wholly crystalline to almost wholly glassy. Euhedral to subhedral plagioclase (An_{87-70}) is the most abundant phenocryst phase, followed by olivine (Fo_{89-95}), rare clinopyroxene ($Ca_{45}Mg_{50}Fe_5$-$Ca_{38}Mg_{50}Fe_{12}$), and tiny euhedra of Cr-spinel [*Mawson*, 1943; *Varne and Rubenach*, 1972; *Griffin and Varne*, 1980; *Cameron et al.*, 1980]. At North Head, Mawson Point, and Pyramid Peak the rocks are relatively fresh, but elsewhere there is widespread metamorphism and alteration. *Griffin* [1982] described a section from the south of the island where the volcanic succession is about 1.4 km thick and passes from zeolite facies assemblages through to lower greenschist facies assemblages. Metamorphism tends to be of higher grade in the dolerite dike swarms, locally ranging up to amphibolite facies.

Gabbros and peridotites are restricted to the northern third of the island. The peridotites are serpentinized; most were originally harzburgitic assemblages of olivine, orthopyroxene, and Cr-rich spinel. A layered gabbro complex contains troctolite, olivine gabbro, and dunite, and massive gabbros also occur [*Varne and Rubenach*, 1972; *Christodoulou et al.*, 1984; *Crohn*, 1986]. Mineral

Copyright American Geophysical Union

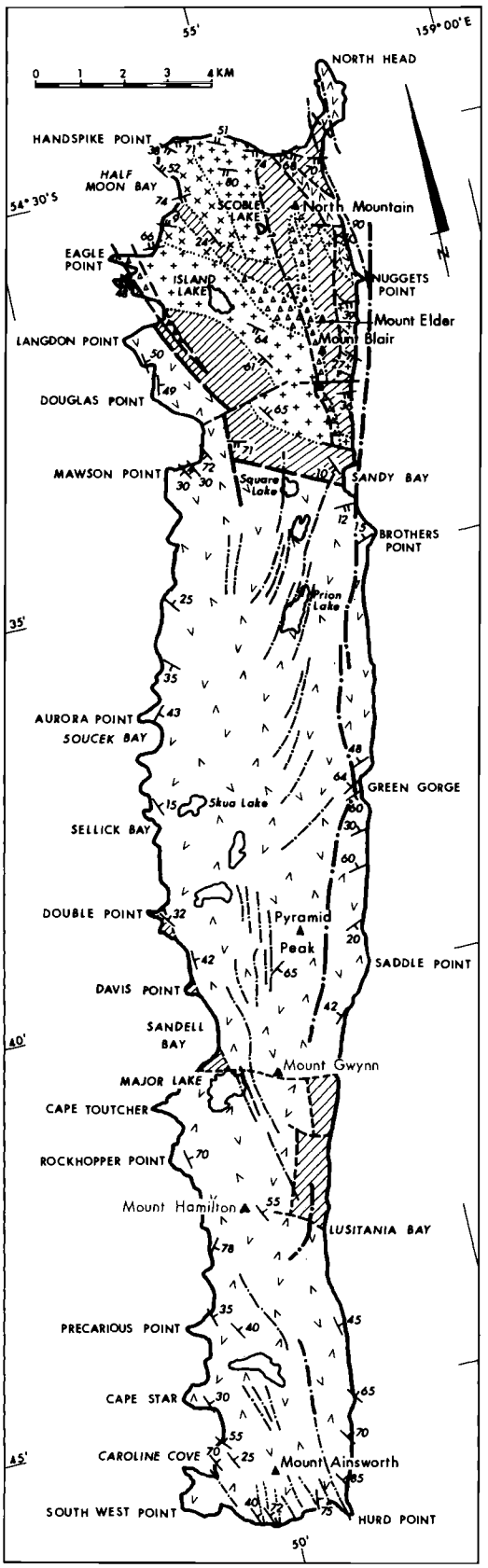

compositions of the gabbros closely resemble the phenocryst compositions of the basalts and dolerites, demonstrating that the igneous rocks of Macquarie Island are genetically related [*Griffin and Varne,* 1980].

Chemical and normative analyses of Macquarie Island basalts, glasses, and dolerites (Tables G.4.1 and G.4.2 and *Griffin and Varne* [1980, Figure 4]) show that they range from *ol*- and *hy*-bearing varieties to those that are mildly *ne*-bearing and rare *Q*-bearing. Mg/(Mg+Fe) values range from about 0.72 to 0.51. The analyzed samples shown in Table G.4.2 were selected to include compositions with high Ni and Cr contents and high Mg/(Mg+Fe) values, ranging from *ol*- and *hy*-normative varieties with low Nb contents to *ne*-normative compositions with high Nb contents. In general, the Macquarie Island basalts and dolerites resemble ocean floor basalts from the mid-Atlantic Ridge near 36°N and 45°N [*Griffin and Varne,* 1980]. Jenner (personal communication, 1987) reported that the Sr and Nd isotopic compositions of Macquarie Island glasses and little-altered rocks fall within the range defined by southwest Pacific ocean floor and volcanic island basalts.

Chronologic Data

Poorly preserved coccoliths recovered from oozes interstitial to the pillow lavas at North Head indicate that these samples are of early or middle Miocene age [*Quilty et al.,* 1973]. Radiometric dates for basalts range from 11.5 to 9.7 Ma, broadly compatible with the ages indicated by the fossils but younger than those suggested by the nearby seafloor spreading anomaly pattern, west of the Macquarie Ridge [*Duncan and Varne,* 1988].

Extent of Knowledge

Geological investigations of Macquarie Island began during the Australasian Antarctic Expedition of 1911–1914

Fig. G.4.1. (opposite) Interpretive geological map of Macquarie Island with superficial deposits omitted (compiled from mapping by *Varne et al.* [1969], *Varne and Rubenach* [1972], *Griffin* [1982], *Christodoulou et al.* [1984], *Crohn* [1986], and *Lees* [1987]). There is little outcrop inland on Macquarie Island, and the map is therefore more reliable along the coast; maps by *Crohn* [1986] and *Lees* [1987] show areas of the northern part of the island where outcrop is good. The structural lineaments are from *Ledingham and Peterson* [1984]. Open triangles, serpentinized periodotite bodies; crosses, layered gabbro complex; pluses, other gabbro bodies; diagonal lines, dolerite dike swarms; random v, extrusive volcanic rocks and associated sedimentary rocks; heavy dashed lines, gradational or uncertain geological contacts; heavy dash-dotted lines, minor structural lineaments; single tick, strike of lavas; double tick, strike of dikes.

Copyright American Geophysical Union

TABLE G.4.1. Summary of Major Element Analyses of Lavas and Dikes From Macquarie Island

	Means and Standard Deviations			Ranges	
	Lavas (68)	Dikes (29)	Combined	Lavas	Dikes
SiO_2	49.53 ± 1.10	49.96 ± 1.29	49.66 ± 1.17	46.35 – 52.95	46.92 – 52.25
TiO_2	1.36 ± 0.37	1.41 ± 0.41	1.38 ± 0.38	0.61 – 2.13	0.61 – 2.61
Al_2O_3	17.95 ± 1.90	16.58 ± 1.85	17.54 ± 1.98	14.22 – 23.33	14.22 – 21.80
FeO	7.78 ± 1.31	8.60 ± 1.74	8.02 ± 1.49	5.33 – 10.79	4.44 – 11.76
MgO	7.68 ± 0.99	8.08 ± 1.52	7.80 ± 1.18	6.19 – 11.17	6.43 – 14.14
MnO	0.15 ± 0.03	0.16 ± 0.04	0.15 ± 0.03	0.09 – 0.22	0.06 – 0.20
CaO	11.27 ± 1.18	11.42 ± 1.03	11.31 ± 1.13	7.77 – 13.17	9.54 – 13.62
Na_2O	3.18 ± 0.52	3.07 ± 0.67	3.13 ± 0.57	0.10 – 1.60	0.08 – 1.23
K_2O	0.68 ± 0.41	0.38 ± 0.34	0.59 ± 0.41	0.04 – 2.06	0.07 – 1.23
P_2O_5	0.26 ± 0.12	0.23 ± 0.14	0.25 ± 0.12	0.06 – 0.95	0.07 – 0.82

All data from *Griffin* [1982].

[*Mawson,* 1943], when L.R. Blake produced the first geological map of the island. More recent geological and geophysical studies are described by *Varne et al.* [1969], *Varne and Rubenach* [1972], *Williamson and Rubenach* [1972], *Williamson* [1974], *Butler et al.* [1976], *Griffin and Varne* [1980], *Christodoulou et al.* [1984], *Ledingham and Peterson* [1984], *Crohn* [1986], *Lees* [1987], *Duncan and Varne* [1988], and *Williamson* [1988]; some rare earth element data are quoted by *Jakeš and Gill* [1970]. *Selkirk et al.* [1986] prepared a useful annotated bibliography of Macquarie Island. Two groups of outlying islands (Judge and Clerk Islands, and Bishop and Clerk Islands) were visited in February 1976, and new geological collections were made [*Lugg et al.*, 1978].

Bibliography

Butler et al., 1976
Christodoulou et al., 1984
Coleman, 1971
Crohn, 1986
Duncan and Varne, 1988
Griffin, 1982
Griffin and Varne, 1980
Hobart "Mercury," 1969
Jakeš and Gill, 1970
Ledingham and Peterson, 1984
Lees, 1987
Lugg et al., 1978
Mawson, 1943
Quilty et al., 1973
Selkirk et al., 1986
Varne, 1989
Varne and Rubenach, 1972; 1973
Varne et al., 1969
Williamson, 1974, 1978, 1988
Williamson and Rubenach, 1972
Wilson, 1963

Copyright American Geophysical Union

TABLE G.4.2. Representative Chemical Analyses of Lavas and a Dike From Macquarie Island

	1	2	3	4	5	6
SiO_2	46.60	46.69	47.19	49.05	49.15	50.06
TiO_2	0.78	1.25	0.68	1.33	1.08	1.14
Al_2O_3	19.79	15.81	19.44	17.28	16.95	16.43
Fe_2O_3	2.73	3.86	3.01	--	3.45	--
FeO	4.36	4.84	3.20	7.89	4.27	8.53
MnO	0.10	0.14	0.09	--	0.13	--
MgO	8.19	10.33	7.71	8.41	9.25	8.72
CaO	12.49	10.33	11.93	12.53	10.23	12.38
Na_2O	2.34	2.78	2.79	2.92	2.73	2.41
K_2O	0.09	0.38	0.58	0.59	0.64	0.19
P_2O_5	0.12	0.27	0.09	--	0.20	--
LOI	2.19	3.39	3.18	--	2.69	--
Total	99.78	100.01	99.89	100.10	101.24	99.86
or	0.53	0.47	3.43	3.49	3.78	1.12
ab	20.56	23.52	22.01	18.41	23.10	20.39
an	42.83	30.43	38.81	32.30	32.11	33.45
ne	--	--	0.87	3.41	--	--
di	14.59	15.06	15.60	24.29	13.70	22.80
hy	1.80	7.97	--	--	12.61	7.95
ol	11.65	10.33	10.13	15.57	5.27	11.97
mt	3.96	5.60	4.36	--	5.00	--
il	1.48	2.37	1.29	2.53	2.05	2.17
ap	0.28	0.63	0.21	--	0.46	--
Cr	523	514	663	--	652	--
Nb	8	30	3	--	16	--
Ni	207	199	164	--	158	--
Rb	0	7	3	--	16	--
Sr	171	232	322	--	219	--
Y	18	27	11	--	28	--
Zr	46	84	27	--	69	--

Sample numbers are those of the Department of Geology, University of Tasmania. Analyses 1–3 and 5 by XRF; analyses 4 and 6 by electron microprobe [*Griffin,* 1982]. LOI, loss on ignition; dashes, not determined.

1. 60779. Porphyritic dike cutting pillow lavas, creek mouth, southwest of Mount Hamilton.
2. 38188. Lava.
3. 60798. Plagioclasephyric pillow lava, 250 m north of Mount Gwynn.
4. 60706. Glass from hyaloclastite breccia, 1 km west of Pyramid Peak.
5. 60794. Pillow lava, Aurora Point.
6. 40428. Glass.

Copyright American Geophysical Union

BIBLIOGRAPHY

Adams, C.J., Age of the Auckland Island volcanoes, *N. Z. Dep. Sci. Ind. Res. Rep., INS-R-281,* 24 pp., 1980.

Adams, C.J., Age of the volcanoes and granite basement of the Auckland Islands, southwest Pacific, *N. Z. J. Geol. Geophys., 26,* 227–237, 1983.

Adams, C.J., P.A. Morris, and J.M. Beggs, Age and correlation of volcanic rocks of Campbell Island and metamorphic basement of the Campbell Plateau, south-west Pacific, *N. Z. J. Geol. Geophys., 22,* 679–691, 1979.

Butler, R.F., S.K. Banerjee, and T.H. Stout, Magnetic properties of oceanic pillow basalts: Evidence from Macquarie Island, *Geophys. J. R. Astron. Soc., 47,* 179–196, 1976.

Cameron, W.E., E.G. Nisbet, and V.J. Dietrich, Petrographic dissimilarities between ophiolitic and ocean-floor basalts, in *Ophiolites, Proceedings of the International Ophiolite Symposium, Nicosia, 1979,* edited by A. Panayiotou, pp. 182–192, Ministry of Agriculture and Natural Resources, Geological Survey Department, Nicosia, Cyprus, 1980.

Chilton, C., The subantarctic islands of New Zealand and the history of their scientific investigation, in *The Subantarctic Islands of New Zealand,* vol. I, edited by C. Chilton, pp. xiv–xxxv, Government Printer, Wellington, 1909.

Christodoulou, C., B.J. Griffin, and J. Foden, Geology of Macquarie Island, *ANARE Res. Notes, 21,* 15 pp., 1984.

Coleman, R.G., Plate tectonic emplacement of upper mantle peridotites along continental edges, *J. Geophys. Res., 76,* 1212–1222, 1971.

Crohn, P.W., Geology and geomorphology of Macquarie Island with special emphasis on heavy metal trace element distribution, *ANARE Res. Notes, 39,* 28 pp., 1986.

Cullen, D.J., Quaternary volcanism at the Antipodes Islands: Its bearing on the structural interpretation of the southwest Pacific, *J. Geophys. Res., 74,* 4213–4220, 1969.

Davey, F.J., and D.A. Christoffel, Magnetic anomalies across Campbell Plateau, New Zealand, *Earth Planet. Sci. Lett., 41,* 14–20, 1978.

Denison, R.E., and D.S. Coombs, Radiometric ages for some rocks from Snares and Auckland Islands, Campbell Plateau, *Earth Planet. Sci. Lett., 34,* 23–29, 1977.

Duncan, R.A., and R. Varne, The age and distribution of the igneous rocks of Macquarie Island, *Pap. Proc. R. Soc. Tasmania, 122,* 45–50, 1988.

Filhol, H., Mission de l'Île Campbell, *Recueil de memoires, rapports et documents relatif a l'observation du passage de Vénus sur le soleil du 9 Décembre 1874,* Académie des Sciences, Paris, 1885.

Fleming, C.A., Auckland Islands, *Lex. Stratigr. Int., 6,* 34–35, 1959.

Fleming, C.A., Campbell Island geology, Preliminary Report of the Campbell Island Expedition 1975–76, pp. 44–46, Dep. of Lands and Survey, Wellington, New Zealand, 1980.

Gamble, J.A., and C.J. Adams, Volcanic geology of Carnley Volcano, Auckland Islands, *N. Z. J. Geol. Geophys., 28,* 43–54, 1985.

Gamble J.A., and P.A. Morris, Cenozoic and Recent volcanism on the Campbell Plateau: Geochemistry of volcanic rocks and an assessment of the sub continental mantle (abstract), in *Proceedings of the Seventh Australian Geological Convention, Sydney, 1984,* pp. 181–182, Geological Society of Australia, Sydney, 1984.

Gamble, J.A., C. J. Adams, D.D. Ritchie, and I.M. Turnbull, Report of Carnley Harbour Party: Auckland Island Expedition, 1982, Preliminary Report of Auckland Islands Expedition, 20 pp., Dep. of Lands and Survey, Wellington, New Zealand, 1982.

Gamble, J.A., P.A. Morris, and C.J. Adams, The geology, petrology and geochemistry of Cenozoic volcanic rocks from the Campbell Plateau and Chatham Rise, in *Late Cenozoic Volcanism in New Zealand, Bull. 12,* edited by I.E.M. Smith, pp. 344–365, Royal Society of New Zealand, Wellington, 1986.

Griffin, B.J., Igneous and metamorphic petrology of lavas and dykes of the Macquarie Island Ophiolite Complex, Ph.D. thesis, University of Tasmania, Hobart, 1982.

Griffin, B.J., and R. Varne, The Macquarie Island ophiolite complex: Mid-Tertiary oceanic lithosphere from a major ocean basin, *Chem. Geol., 30,* 285–308, 1980.

Hector, J., Notes on the geology of the outlying islands of New Zealand: With extracts from official reports, *Trans. N.Z. Inst., 2,* 176–186, 1870.

Hector, J., Note on the geology of the outlying islands of New Zealand, *Trans. N.Z. Inst., 28,* 736–738, 1896.

Hobart "Mercury," Is Macquarie Island oceanic crust?, Aug. 20, 1969. (Reproduced in *Antarctic, 5,* 359–360, 1969.)

Jakeš, P., and J. Gill, Rare earth elements and the island arc tholeiite series, *Earth Planet. Sci. Lett., 9,* 17–28, 1970.

Ledingham, R., and J.A. Peterson, Raised beach deposits and the distribution of structural lineaments on Macquarie Island, *Pap. Proc. R. Soc. Tasmania, 118,* 223–225, 1984.

Lees, T.R., Report on geological observations, Macquarie Island, December 1986 to January 1987, Antarctic Division, Dep. of Science and Technology, Kingston, Tasmania, 1987.

Löffler, E., M.E. Sullivan, and A.N. Gillison, Periglacial landforms on Macquarie Island, Subantarctic, *Z. Geomorphol., 27,* 223–236, 1983.

Lugg, D.J., G.W. Johnston, and B.J. Griffin, Outlying islands of Macquarie Island, *Geogr. J., 144,* 277–287, 1978.

Marshall, P., and R. Browne, The geology of Campbell

Copyright American Geophysical Union

Island and The Snares, in *The Subantarctic Islands of New Zealand,* vol. II, edited by C. Chilton, pp. 680–704, Government Printer, Wellington, 1909.

Mawson, D., Macquarie Island, its geography and geology, in *Australasian Antarctic Expedition 1911–1914, Sci. Rep. Sect. A:5,* Government Printing Office, Sydney, 1943.

McDonough, W.F., M.T. McColloch, R.A. Duncan, J.A. Gamble, I. McDougall, P.A. Morris, and R.M. Briggs, Geochemical and isotopic systematics of Cenozoic intraplate basalts from continental and oceanic regions in the South Pacific, paper presented at *Int. Volcanol. Congr.,* Hamilton, New Zealand, 1986.

Morris, P.A., The igneous geology of Campbell Island, southwest Pacific Ocean, B.Sc. thesis, University of Otago, New Zealand, 1976.

Morris, P.A., Petrology of the Campbell Island Volcanics, southwest Pacific Ocean, *J. Volcanol. Geotherm. Res., 21,* 119–148, 1984.

Oliver, R.L., H.J. Finlay, and C.A. Fleming, Geology of Campbell Island, *Cape Exped. Ser. Bull., 3,* 7–60, 1950.

Quilty, P.G., M. Rubenach, and J.A. Wilcoxon, Miocene ooze from Macquarie Island, *Search, 4,* 163–164, 1973.

Ritchie, D.D., and I.M. Turnbull, Cenozoic sedimentary rocks at Carnley Harbour, Auckland Islands, Campbell Plateau, *N. Z. J. Geol. Geophys., 28,* 23–41, 1985.

Selkirk, D.R., P.M. Selkirk, and K. Griffin, Palynological evidence for Holocene environmental change and uplift on Wireless Hill, Macquarie Island, *Proc. Linn. Soc. N. S. W., 107,* 1–17, 1983.

Selkirk, D.R., P.M. Selkirk, and R.D. Seppelt, An annotated bibliography of Macquarie Island, *ANARE Res. Notes, 38,* 134 pp., 1986.

Speight, R., and A.M. Finlayson, Physiography and geology of the Auckland, Bounty and Antipodes Islands, in *The Subantarctic Islands of New Zealand,* vol. II, edited by C. Chilton, pp. 704–744, Government Printer, Wellington, 1909.

Varne, R., Macquarie Island, in *Geology and Mineral Resources of Tasmania, Spec. Publ. 15,* edited by C.F. Burrett and E.L. Martin, pp. 398–402, Geological Society of Australia, Sydney, 1989.

Varne, R., and M.J. Rubenach, Geology of Macquarie Island and its relationship to oceanic crust, in *Antarctic Oceanology II: The Australian-New Zealand Sector, Antarct. Res. Ser.,* vol. 19, edited by D.E. Hayes, pp. 251–266, AGU, Washington, D.C., 1972.

Varne, R., and M.J. Rubenach, Geology of Macquarie Island in relation to tectonic environment, in *Western Pacific: Island Arcs, Marginal Seas, Geochemistry,* edited by P.J. Coleman, pp. 535–541, University of Western Australia Press, Nedlands, 1973.

Varne, R., R.D. Gee, and P.G.J. Quilty, Macquarie Island and the cause of oceanic linear magnetic anomalies, *Science, 166,* 230–233, 1969.

Wareham, J., and P.M. Johns, The University of Canterbury Antipodes Island Expedition of 1969, *J. R. Soc. N. Z., 5,* 103–131, 1975.

Weaver, S.D., D.S. Coombs, J.A. Gamble, I.L. Gibson, R.J. Pankhurst, and R.J. Sewell, Late Cenozoic intraplate volcanism in southern, continental New Zealand, papers presented at Int. Volcanol. Congr., Hamilton, New Zealand, 1986.

Williamson, P., Recent studies of Macquarie Island and the Macquarie Ridge complex, *Bull. Aust.. Soc. Explor. Geophys., 5,* 19–22, 1974.

Williamson, P., The palaeomagnetism of outcropping oceanic crust on Macquarie Island, *J. Geol. Soc. Aust., 27,* 387–394, 1978.

Williamson, P., Origin, structural and tectonic history of the Macquarie Island region, *Pap. Proc. R. Soc. Tasmania, 122,* 27–43, 1988.

Williamson, P., and M. Rubenach, Preliminary report on geophysical studies on Macquarie Island, in *Antarctic Oceanology II: The Australian-New Zealand Sector, Antarctic Res. Ser.,* vol. 19, edited by D.E. Hayes, pp. 243–249, AGU, Washington, D.C., 1972.

Wilson, J.T., A resumé of the geology of islands in the main ocean basins, vol. 2, Pacific Ocean, *Toronto Univ. Inst. Earth Sci. Rep., no. 4,* 166 pp., 1963.

Wright, J.B., Contributions to the volcanic succession and petrology of the Auckland Islands, New Zealand, I, West coast section through the Ross Volcano, *Trans. R. Soc. N. Z., 3,* 215–229, 1966.

Wright, J.B., Contributions to the volcanic succession and petrology of the Auckland Islands, New Zealand, II, Upper parts of the Ross Volcano, *Trans. R. Soc. N. Z., 5,* 71–87, 1967.

Wright, J.B., Contributions to the volcanic succession and petrology of the Auckland Islands, New Zealand, III, Minor intrusives on the Ross Volcano, *Trans. R. Soc. N. Z., 6,* 1–11, 1968.

Wright, J.B., Contributions to the volcanic succession and petrology of the Auckland Islands, New Zealand, IV, Chemical analyses from the lower half of the Ross Volcano, *Trans. R. Soc. N. Z., 8,* 109–115, 1970.

Wright, J.B., Contributions to the volcanic succession and petrology of the Auckland Islands, New Zealand, V, Chemical analyses from the upper parts of the Ross Volcano, *J. R. Soc. N. Z., 1,* 175–183, 1971.

Copyright American Geophysical Union

INDEX

Bold type indicates the first page of a major entry (individual volcano description); italic type indicates reference to a map or photograph (with or without a text reference on the same page); regular type indicates a text or table reference. Where a range is given, the intervening pages can contain either text or figure references.

Abbott Peak, *104*, 105
Abel Nunatak, 308, *342*, **344**
Adams Island, 465, 470, *471*, 473
Adare Peninsula, 2, 9, 11, 20, 21, *26*, *27*–30, **32**, *38*, 46
Agulhas Ridge, 403
Åkerlundh Nunatak, *350*, 351
Albatross Point, 468, *468*
Alexander Island, 11, 14, **256**, 259, **277**, 297
Aleyone Cone, 60, *61*, 63
Allen Point, *382*, 364, 383
Ames Range, *149*, 159, 161, *162*, 165, 175, 196, 197, 199, **216**, 229, 234, *240*, 250
Amsterdam Island, 5, 7, 8, 9, 398–403, **442**
Amundsen Sea, *2*, 235, 239
Anchorage Bay, 468, 469
Andersson Island, *339*, 341
Antarctic Peninsula, *2*, 4, *13*–15, *258*, 259, *260*, 346
Antarctic plate, 1, *2*, 10, 14, 15, **396**
Antarctic Sound, **339**
Antipodes Island, 465, 466, 469
Antipodes Islands, 3, 5, 8, *466*, 467, **468**
Anvers Island, *304*, 307–309, **334**
Arctowski Nunatak, 349, *350*, 351
Argo Point, 306, 309, **352**
Ashen Hills, 363, *379*, *380*, 381
Astrolabe Island, *334*, 336
Auckland Island, 4, 8, 467, 471
Auckland Islands, 3, 4, 8, 9, *464*, 465, *466*, 467, **470**
Aurora Point, *477*, 479
Aurora Trachyte Formation, 114
Aviator Glacier, *48*, 50, 51, 58, *65*, 68, *76*, *79*

Bahía Bouquet Formation, 334
Baily Head, *316*, 318
Baker Rocks, 49, 73, 78
Bakutis Coast, 169, 180
Balleny Fracture Zone, 449
Balleny Islands, 8, *12*, 19, 397, 398, 400, 401, **449**, *452*
Balleny volcanic province, 19
Basilisk Peak, *387*–389
Bauer Bay, 476
Beach Point, *393*, 395
Beacon Supergroup, 50, 69, 70
Beak Island, *342*, 343
Beaufort Island, *20*, 22, 81, *83*, *85*, *90*, 92, **94**
Beeman Hill, *474*, 475
Beethoven Peninsula, 259, 262–265, **273**, 280
Behrendt Mountains, 294, *296*
Bellingshausen Island, 5, 7, *360*–365, **387**, *391*
Bellingshausen Sea, *2*, 11, 160, *258*, 397, 454
Bellingshausen volcanic province, 7, 257, *258*, 260, 261
Benes Peak, *242*
Bentley Subglacial Trench, *2*, 11
Bernacchi Head, 91, *91*
Bibby Point, 308, *345*, 347
Big Ben, 4, 6, 398, 400, *436*–439
Birthday Bluffs, *128*, 129
Bishop and Clerk Islands, 478
Black Haglet Valley, 413, 414
Black Hill, 135
Black Island, 23, 81, *82*–*85*, 87, *103*, **113**, *121*
Blackstone Plain, 363, *379*, *380*, 381
Bollons Island, *468*
Bomb Peak, *104*–106
Borchgrevink Glacier, *26*, 49, 50, *53*, *54*, 59
Borradaile Island, *449*–451
Bouvetøya, 5, 7–9, 397, 398, *399*, 400–403, **405**, *406*
Bowers structure, *20*
Bowyer Butte, 161, 244, *244*, *245*–247
Boyack Point, *474*, 475
Boyd Ridge, *180*, 181
Brabant Island, *304*, 306–309, **334**
Braces Point, 373, *374*, 375
Brandau Vent, 132, 133
Brandenberger Bluff, *226*, *229*–231, 233
Bransfield Island, 316, *334*
Bransfield Strait, 303, *304*–309, 312, 313, 320, **334**
Bridgeman Island, 5, *304*, 307–309, 312, **313**, 322
Bristol Island, 5, *362*–365, **384**
Broken Ridge, *399*, 403
Brown Bluff, 340, *339*–341
Brown Peninsula, 23, 81, *82*, 84, *85*, 87, **113**, *120*, *121*
Brown Valley, *216*, *217*
Bruce Nunatak, 349, *350*, 351
Bryan Coast, *258*
Bucher Rim, 172, 173
Buckle Island, 5, *449*–451
Bull Nunatak, 349–351
Burtis Island, *186*
Buttress Hill, *339*
Byrd Subglacial Basin, *2*, 11, *12*

Cadwalader Beach, *94*–96
Cain Nunatak, 308, *342*, **344**
Campbell Glacier, *48*, 69, *72*, *73*, *76*, *79*
Campbell Island, 3, 4, 8, 9, 466, 465–467, **474**
Campbell Plateau, 3, *12*–15, 465–468, 470
Camp Cove, *464*, 470, *471*
Candlemas Island, 5, 9, *362*–365, **376**
Cape Adare, *20*, *32*–35
Cape Arkona, *440*
Cape Barne, *104*–106
Cape Bird, *82*, 85, 91, *97*, 114
Cape Burd, *339*, 341
Cape Cockburn, *334*
Cape Crossfire, *53*, 56, 59
Cape Crozier, 85, *99*–102
Cape Fie, 406–408
Cape Hallett, *36*, 39
Cape McCormick, *32*–34
Cape Melville, *325*, 326
Cape Meteor, *406*, 409
Cape Phillips, *40*–42
Cape Purvis, *339*, 340
Cape Roget, *32*–35
Cape Royds, *104*–106
Cape Valdivia, 405, *406*

Cape Washington, 49, *72*, 73, 75–77, 83
Cape Wheatstone, *36*–38
Carlson Island, *345*
Carnley Harbour, 465, 470, *471*, 473
Carnley Volcano, *464*, 470, 472, 473
Castor Nunatak, 349, *350*
Casy Island, *334*
Cato-odden, *406*, 409
Cave Bay (Heard Island), 435, *436*, 438, 439
Cave Bay (Prince Edward Island), *420*–422
Chabrier Rock, *327*, 328
Chalcedony Island, 129
Chancellor Ridge, *131*, 133
Chang Peak, 199, *203*, *205*, 208–211
Cheyenne Crater, 135
Christensen Nunatak, 349, *350*, 351
Cinder Hill, 97
Cinder Spur, *327*–330
Circular Head, 470, *471*
Claude Point, 307, *334*, *335*
Cockburn Island, *345*
Coleman Glacier, 216, *217*
Coleman Nunatak, 152, 155, *244*–247, 250, 252
Coleridge Bay, *471*, 473
Collins Point, 316, 319
Col Peak, *474*, 475
Cook Island, 9, *362*–365, **390**, *394*
Cordelia Bay, *379*, 381
Corry Island, *342*
Cosmonaut Glacier, 51, 80
Cotter Cliffs, *27*, *36*–39
Coulman caldera, 43, *44*, 45
Coulman Island, *2*, 9, 21, *26*, 27–30, *37*, *42*, **43**, *66*
Courbet shield volcano, 398, *430*
Cousins Rock, *244*
Cox Bluff, *175*, *177*, 178
Crary Mountains, *149*, 159, 161, *162*, 167, **180**, *189*, 205, 222
Crater Bay, *366*, 367
Crater Cirque, 38
Crosscut Point, *373*, 374
Cross Hill, *316*, *317*, 319, 321
Crozet Archipelago, see Îles Crozet
Cruzen Island, 4, *148*, *149*, *162*, *248*–250

Dad's Nose, 129
Dailey Islands, 132
Dallman Nunatak, 349, *350*
Daniell Peninsula, 21, *26*, *27*–30, *37*, **40**, 49
Davis Island, *334*, 336
Deacon Peak, *322*
Debussy Heights, 259, **268**
Deception Island, *2*, 4–6, 9, *302*, 303, *304*, 306–309, 311, 312, **316**
Deception Plateau, *65*, 66
De La Vire Point, *474*, 475
Del Cano, *401*, 403
Dellbridge Islands, 104–106
Dent Island, *474*, 475
Disappointment Island, 470, *471*
Discovery graben, 83
Discovery subprovince, 83–87
Dives volcano, *442*, 444, 445
Dome C, 169, 174
Dôme du La Pérouse, *425*, 427, 428
Donald Nunatak, 349, *350*, 351
Dorrel Rock, 9, 168, 234–238, 245
Douglas Strait, 363, 392–*394*
Downshire Cliffs, *32*, 35
Drake Passage, *304*
Dry Valleys, see Taylor Valley and Wright Valley
Duclaux Point, *334*, 336
Dundee Island, *339*, 340
Dupal anomaly, *399*, 401
Duse Bay, *342*

Eady Ice Piedmont, *128*
Eagle Island, *342*, 343
Eagle's Bluff, 50, 54, 58, 59
East Antarctic Shield, *2*, *13*
Edinburgh Hill, 308, *331*, *332*
Edisto Inlet, *36*–38
Edmonson Point, 49, 51, *72*, *73*, *76*–78
Edwards Spur, 225, *226*, 227
Egg Island, *342*, 343
Eights Coast, *258*, 397
Elgar Uplands, 257, 262, *268*–271
Ellsworth Land, 11, **256**
Ellsworth Mountains, 11, *12*, *13*, 259
Enderby Island, 470, *471*
Engberg Bluff, 54, 58
English Coast, *258*, 280, 283
Erebus volcanic province, 19, 20, 25, **81**, 83
Espenschied Nunatak, *280*, 283, 284
Evans Névé, *48*, *60*, *79*
Evensen Nunatak, 349, *350*, 351
Ewing Island, *471*, 473
Executive Committee Range, *149*, 157, 161, *162*, 163, 189, 190, 193, 195, 196, *198*, 199, 202–204, 208, 222, *242*

Fang Glacier, *103*
Fang Ridge, *103*, 105–107
Ferguson Bay, *393*, 394
Filchner Ice Shelf, *2*
Filhol Peak, *474*, 475
Finger Point, *371*, 372
Flat Island, 435
Fleming Plateau, 470, *471*, 473
Flood Range, *149*, 159, 161, *162*, 175, *216*, 218, 221, 222, 224–*226*, 229, 233, 234, *240*
Foch Island, see Île Foch
Football Saddle, *36*, 39
Fosdick Mountains, *148*, 152, 153, 155, *162*, 167, **251**
Foster Crater, 88, *131*–133
Foyn Island, *32*, 46
Frame Ridge, *113*, 114
Franklin Island, *20*, 22, *83*, *90*, **91**
Fred's Hill, *413*, 415
Freezland Rock, *362*, 363, 365, *384*, 385, 386
Fryer Point, *384*, 385

Gallieni unit, *430*–433
Gandalf Ridge, *85*, 87, 88, *124*, 125–127
Gardiner Ridge, *217*, 218
Gaussberg, *2*, 7, 9,10, 397, 398, 401, 403, **446**
George VI Sound, *258*, 260, *277*, 279
Gerlache Strait, 336
Gill Bluff, *169*–*171*
Gleaner Heights, *331*–333
Gluck Peak, 265, *273*–276
Goddard Hill, *316*, 321
Golfe du Morbihan, *430*, 433
Gondwanaland, 15, 259, *260*, 405
Goodhope Bay, *413*, 414
Gordon's Hill, *413*, 415
Gourdon Glacier, *345*, 347
Graham Land, *2*, 7, 8, 10, 14, 15, **302**
Grant Island, *162*, 218, 234, *248*–250
Gray Nunatak, *350*, 351
Green Gorge, 476, *477*
Greenwich Island, 312, **331**
Grindle Rock, *384*, 385

Haag Nunataks, *13*, *258*, 259
Hades Terrace, 49, 80
Hallett Fracture, 28
Hallett Peninsula, *2*, 4, 9, 21, 26–30, **36**, 41
Hallett volcanic province, 7, 8, 11, 19, 20, 24, 25, **26**, 32, 35, *37*, 47, 66, 449
Handspike Point, 476, *477*
Hanson Peak, 32–34
Hardy Point, *387*, *388*
Harker Point, *384*, 385
Harry Island, *334*
Havfruen Peak, *384*, *385*
Heald Island, *131*, 133
Heaps Rock, *221*–223
Heard Island, 4–10, 15, 398, *399*–403, **435**, 448
Hedin Nunatak, *164*, *165*, 235–238
Heftye Island, *32*, 46
Henry Nunataks, 259, 260, 262, 264, 265, **294**, *296*
Hertha Nunatak, 349, *350*
Hewison Point, 363, *393*–395
Hidden Lake, *345*, 347
Hillary Fault, 123

Hobbs Coast, *149*, 161, 212, 216, 234, **244**, **248**
Hodgson Nunatak, *290*–293
Hollick-Kenyon Peninsula, *258*, 265
Holmes Bluff, 161, *244*–246
Hooker Saddle Suite, 473
Hooper Crags, *131*–133
Hoopers Shoulder, 103, *104*
Hope Bay, 343
Horingberg, *420*, 422
Hornpipe Heights, 259, 260, *268*, 270, **271**
Horsburgh Point, 365, *382*, 383
Howchin Glacier, *131*, 133
Hudson Mountains, *12*, 257, 259, *258*–265, **289**
Hunt Island, *334*, 336
Hurricane Ridge, *24*, *125*, 127
Hut Point Peninsula, 9, 20, 23, 81–87, *103*, 105, **109**
Hutt Peak, *221*–224

Île aux Cochons, 5, 398, 400–403, 423, 425, *426*, 427
Île de la Possession, 397, 398, 400–403, *423*–428, *425*
Île de l'Est, 398, 400–403, 423, *424*, 426, 427
Île des Apôtres, 401, 402, *423*, 425
Île des Pingouins, 398, 401, 402, *423*, 425
Île Foch, 433
Îles Crozet, 7, 15, 397–*399*, 400–403, 416, **423**
Îles Kerguelen, 1, 5, 7–11, 15, 397–*399*, 400–403, 417, **429**, 448
Inaccessible Island, 106
Inman Nunatak, 289–*291*
Inott Point, 308, *331*, *332*
Irving Point, *371*, 372
Isaacson Point, *387*–389

Jagged Point, *387*–389
James Ross Island, *2*, 4, 9, *304*, 306, 307, 309, 340, 342, 343, **345**
James Ross Island Volcanic Group, 307, 342, 349, 352
Jason Peninsula, *352*
Jeannel Plateau, 428
Jonassen Island, *339*, 341
Jones Mountains, 4, 245, 257, 259–262, **286**
Judge and Clerk Islands, 478

Kapp Fie, see Cape Fie
Kapp Meteor, see Cape Meteor
Kapp Valdivia, see Cape Valdivia
Katedraalkrans, 417
Kempe Glacier, *131*–133
Kent Crater, *420*, *421*
Kenyon Peninsula, see Hollick-Kenyon Peninsula
Kerguelen Archipelago, see Îles Kerguelen
Kerguelen Plateau, 9, 403, 429, 435, 448
King George Island, *304*, 307–309, 322, **325**, **327**
Kirkpatrick Basalt Group, 70
Knezevich Rock, 172, 173
Knob Point, *373*, *374*
Knoll, The, *99*, 101
Koerner Bluff, *221*–234
Koettlitz Glacier, *82*, *113*, *120*, 124, *131*, 132
Kohler Dome, 225, *226*
Kohler Range, *148*, 161, *162*, 176, 235–238, 247
Kouperov Peak, 9, 150, 161, 234, *244*–246
Kraków Peninsula, 308, 326, **327**
Kyle Cone, *99*, 101

Lafarge Rocks, *334*
Laguna Hill, see Cross Hill
Lake Morning, *124*
Larsen Nunatak, 349, *350*, 351
Lars Island, 405, *406*, 408
Larsøya, see Lars Island
Lauff Island, *186*
Laurens Peninsula, 435, *436*
Lavris Peak, *198*, *199*
Leafvein Gulch, *373*, 375
Lee Arch, 83
Leeson Point, *382*, 383
Leister Peak, 235, 236, *237*, 238
Leskov Island, 5, 361–**366**
Liège Island, *334*
Lindenberg Island, 349, *350*
Lion Rock, *474*, 475
Lions Rump, *327*, 328, 330
Livingston Island, 304, 312, **331**
Local Suite, 5, 22, 50, **79**
Lockyer Island, *345*
Long Ridge, *413*, 414
Loranchet Peninsula, see Péninsule Loranchet
Lovill Bluff, 185, *186*, 187
Low Head, *327*, 328
Lucifer Hill, 363, *376*, 377

Macey Cone, 435, *436*
Macquarie Island, 3, 8, *12*, 465, *466*, 467, **476**
Macquarie Ridge, 465, *466*, 476
Madagascar Ridge, 403
Maher Island, *186*
Main Crater, *104*, 105
Maish Nunatak, 289, *290*, 292
Malta Plateau, 9, 21, 48–52, **53**, 77, *79*
Mandible Cirque, *40*, *41*
Marie Byrd Land, 1, 3–5, 7–11, *13*, 14, 15, **146**, 258, 260, 261, 289
Mariner Glacier, *54*, 56–*61*, *79*
Marion Island, 5, 7, *396*–404, **411**, 420, 421
Martins Head, *327*–330
Masked Island, *464*, 470, 471
Mason Spur, 9, 23, 81, *85*–88, 126, **128**
Mathewson Point, *248*
Mathias Point, *382*, 383
Mawson Peak, 435, *436*, *440*, *441*
Mawson Point, 476, *477*
McClure Head, 470, *471*
McDonald Island, 7, 9, 401, 439
McDonald Islands, 397, 398, **435**
McMurdo Sound, 11, *20*, *83*–*85*, *104*, 113, 134
McMurdo Volcanic Group, **18**, *20*, 24, 25, 30, 49, 50, 59, 70, 77, 78, 84, 103, 112, *131*
McNish Bay, *420*, 422
Meander Glacier, *53*, 54
Mefford Knoll, *226*, 230–232
Melania Basalt Formation, 114
Melbourne volcanic province, 7, 19–*20*, 25, **48**, 72, 77
Melville Peak, 307, 308, **325**
Menhir and Dent Island, *474*
Merrem Peak, *226*, 229–232
Merrick Mountains, 259, 261, 262, **296**
Metchnikoff Point, *334*
Meyer Rock, 435
Meyers Nunatak, *290*, *291*
Miers Valley, *131*–133
Minna Bluff, 23, 81, *82*, 84–87, *103*, **117**
Möll Spur, 169, *170*, 172, 173
Montagnes Vertes, 401
Montagu Island, *362*–365, **382**
Mont Guynemer, 429
Mont Richards, 429
Mont Ross, 398, 400, 429, *430*, 433
Morbihan Gulf, see Golfe du Morbihan
Morrison Bluff, 235, *237*
Moubray Bay, *26*, *27*
Moubray Glacier, *26*, 27
Mount Alberts, *53*, 54
Mount Aldaz, 239–*242*, 247
Mount Andromeda, 363, *376*, 377
Mount Andrus, 5, 9, *148*, 151, 167, 174, 175, 193, 216–220, *222*, 250
Mount Atlas, *60*
Mount Aurora, *85*, *113*, 114
Mount Belinda, *382*, 383
Mount Benkert, *280*, 283, *284*, 285
Mount Berlin, 2, 4, 5, 9, *148*, 150, 151, 157, *162*, 165, 174, 175, 221, *226*, **229**, 250
Mount Bird, 2, 4, 9, 22, 81–*85*, 92, **97**
Mount Brewster, *40*, 41
Mount Bursey, 9, *148*, 151, 165, 167, 174, 196, 197, 199, *216*, 218, **221**, 226, 229, 233, 250

Mount Cis, *104*, 105
Mount Colburn, **248**
Mount Combs, 260, *280*, 281
Mount Cumming, 147, *148*, 151, 167, **195**, 202, 218
Mount Curry, 363, **368**
Mount Darnley, 363, *384*
Mount Discovery, 2, 4, 9, 23, 81–*85*, 87, *103*, 113, 117, **120**, 124, *125*, 128
Mount Dixon, 435, *436*
Mount Dromedary, 132, 133
Mount Dumas, *474*, 475
Mount D'Urville, 470, *471*
Mount Early, 2, 4, 11, 19, 20, 24, 25, **138**
Mount Erebus, 2–7, 9, 10, 15, 18, 19, *20*, 22, 24, 25, 81–87, **103**, 110, 203, 204
Mount Flint, 9, *148*, 151, 157, 159, 162, 163, 167, **212**, *217*, 218, 235, *239*, *240*
Mount Frakes, 2, 9, 10, *148*, 151, 159, *180*–183, 189, 225
Mount Galla, *242*, 243
Mount Galloway, *468*
Mount Guynemer, see Mont Guynemer
Mount Gwynn, *477*, 479
Mount Haddington, 308, *345*, 346
Mount Hamilton, 476, *477*, 479
Mount Hampton, 2, 9, 10, *148*, 151, 158, 159, 183, **189**, *195*–197, 205, 212, 213
Mount Harcourt, *36*, *38*, 39, 41
Mount Harmer, *390*
Mount Hartigan, 9, 147, *148*, 151, *195*, 196, *198*, **199**, 208
Mount Heine, *113*, 115
Mount Hodson, 363, **371**
Mount Holdgate, *390*
Mount Kauffman, 5, 9, *148*, 151, *216*–220
Mount Kirkwood, *316*, 318, 321
Mount Kosciusko, 9, *148*, 151, *216*–220
Mount Larsen, *393*
Mount Manthe, 261, 289–293
Mount McCann, 261, *280*, 283, 285
Mount McCarthy, *79*, 80
Mount Melania, *113*, 114, 115
Mount Melbourne, 2, 4, 5, 7, 9, *20*, 22, 24, 25, 48–52, 54, **72**, *79*, 84
Mount Michael, 362, 363, **379**
Mount Morning, 2, 4, 5, 9, 23, 81–88, *103*, *121*, **124**
Mount Moses, 261, 289, *290*, 292
Mount Moulton, 9, *148*, 151, **225**, 229, 233, 252
Mount Murchison, *48*, *66*, *79*
Mount Murphy, 4, 9, 147, *148*, 151–155, 158, 160, *162*, **164**, *176*, 187, 204, 218, 235, *237*, 245, 247
Mount Nickens, 289, *290*, 292, 293
Mount Noice, 65–68
Mount Obiglio, *248*, 249
Mount Oceanite, *382*, 383
Mount Olsen, *436*, 438, 439
Mount Overlord, 9, 21, 48–52, **65**, 71, 72, 77, *79*
Mount Parry, *334*, 336
Mount Perkins, *251*, 252
Mount Perseus, *376*, 377
Mount Petinos, *248*, 249
Mount Petras, *148*, 152, 155, 161, 163, 234, **239**, 247
Mount Phillips, *53*, 54, 57, *79*
Mount Pinafore, *256*, 259, **268**, 297
Mount Pleiones, 51, *60*, *61*, 63
Mount Plymouth, 308, *331*–333
Mount Pond, *316*, *317*, 321
Mount Poster Formation, 294
Mount Prior, *53*
Mount Rees, *180*, 181
Mount Richards, see Mont Richards
Mount Ross, see Mont Ross
Mount Saltonstall, 136
Mount Sidley, 2–4, 9, 10, *146*, *148*–151, 159, 163, 165, 175, 189, 190, 202, **203**
Mount Siple, 2–5, *148*, 150–153, 155, 160, *162*, 167, **185**
Mount Steere, 9, *148*, 151, 167, *180*–183
Mount Takahe, 4, 5, 9, *148*, 150, 151, 157–160, *162*, 165, **169**, *176*, 225, 232, 247, 250
Mount Terra Nova, *99*, 101, 102
Mount Terror, 2, 4, 9, 22, 81–*85*, **99**
Mount Thornton, *280*, 283, 285
Mount Waesche, 5, 9, *148*, 151, 160, *162*, 163, 189, 193, 196, 199, 202–*205*, **208**, 233
Mount Waterhouse, *468*
Mount Wise, *113*, 114
Murdoch Nunatak, 349, *350*
Musgrave Peninsula, *464*, 470, *471*, 473
Mussorgsky Peaks, *273*–276

Nameless Glacier, *32*, *33*
Nathan Hills, 49, 50, 80
Nattriss Point, *379*–381
Neptune Glacier, *277*, 279
Neptunes Bellows, *316*–318
New Zealand–Campbell Plateau Block, *12*, *13*, 14
Ninetyeast Ridge, *399*, 403
Northeast Cape, *117*
North Head, 476, *477*
Northwest Bay, *474*
Nubian Basalt Formation, 114
Nyrøysa, 405, *406*, 408

Oakley Glacier, 58
Ob Seamount, 403
Observation Hill, *109*–111
Oceana Nunatak, 349, *350*, 351
Oeschger Bluff, 169, *170*, 172, 173
Oscar Point ridge, *72*, 73, *76*, 77

Pacific-Antarctic Ridge, *12*
Pacific plate, **464**
Palisade Nunatak, *345*–347
Palmer Land, 2, 11, 14, **256**
Pampa Island, see Hunt Island
Pankratz Bay, 185, *186*
Parasite Cone, 50, *65*, 68
Patton Bluff, 161, 167, *244*–246
Paulet Island, 5, 306, 308, **337**
Penantipodes Islands, 465
Pendulum Cove, *316*, 321
Penguin Island, 5, 308, 312, **322**
Péninsule Jeanne d'Arc, *430*, 433
Péninsule Loranchet, *430*, 433
Péninsule Rallier du Baty, 398, 401, 429, *430*–433
Péninsule Ronarc'h, *430*, 431, 433
Perpendicular Head, *468*
Perserverance Harbour, *474*
Persson Island, *345*
Peter I Island, 2, 4, 5, 8, 9, *258*, 397, 398, 400, 401, **454**
Petrel Crater, *322*, 323
Pipecleaner Glacier, *131*, 132
Pleiades, The, 5, 9, 21, 48–52, **60**, 73, 77, *79*
Port Foster, *316*, 317, 321
Posadowskybreen, *406*, 407
Possession Island, 28, 30, *32*, *33*, 46
Possession Islands, 9, 21, *26*, *32*, 33, 42, **46**
Post Office Hill, *99*, 101
Prahl Crags, *225*–227
Prince Edward Island, 5, 7, 9, 397–404, 411, 416, **420**
Prince Gustav Channel, 306, 309, **342**, 344
Protector Shoal, 5, 9, *362*–364, **370**
Puiseux Peak, *474*, 475
Pyramid Peak, 476–479
Pyramid Trough, *131*, 133

Quadrant Peak, *373*–375

Radian Glacier, *131*, 132
Rainbow Ridge, *113*–116
Rallier du Baty, see Péninsule Rallier du Baty
Ramp, The, *54*
Random Hills, 72, 75
Redcastle Ridge, *36*, 39
Red Island, *342*, 343
Reef Point (Antipodes Island), *468*, 469
Reef Point (Cook Island), 364, *390*–392
Rennick fault, *20*, 25, 123

Reynolds Ridge, 167, **212**, 235, *239*
Richmond Peak, 176, *177*
Ridley Beach, *32*–35
Riviera Ridge, *85*, 87, 88, *124*–127
Roaring Valley, *131*–133
Roberts Cliff, *36*, 39
Robertson Bay, *26*, 29, *32*–35
Rogers Head, 435, *436*
Ronarc'h Peninsula, see Péninsule Ronarc'h
Ronne Ice Shelf, 2, *258*
Roper Point, *169, 170,* 172, 173
Rosamel Island, 308, *339*, 341
Rosenberg Glacier, 216, *217,* 218
Ross Embayment, 1, 4, 8, 9, 11, 14, 15, **18**, 49, 83, 88, 136
Ross Ice Shelf, 2, 19, *20*, 81, *82*, 96, 113, 117, *120*
Ross Island, 2, *12, 20, 83*–86, *90*, 97, 99, 103–105, 109, *121*
Ross Sea, 1, 2, 3, 11, *13*–15, 19, 20, 22, 24–*26,* 28, *32*, 34, 84, **89**, 94, 160, 452
Ross Shield, 472
Ross Volcano, 470–473
Rothschild Island, 259, 260, 262, **266**
Row Island, *449, 450*
Royal Society Range, 5, 23, 81, 84, *85*, 88, 124, *125*, **131**
Ruppert Coast, *149*, 248
Rustadkollen, *406*, 408
Rücker Ridge, *131*, 133
Rydberg Peninsula, 259, 261, 262, **280**, 283

Sabrina Island, *449*, 451
Saint Paul Island, 5, 7–9, 398, *399*–403, **442**
Salamander Point, *387, 388*
Salmon Cliff, *36*–39
Sandy Bay, 476, *477*
San Fernando Hill, 308
Santa Rosa Hill, *413*, 415
Santa Rosa valley, 412–414, 417
Saunders Island, 5, *362*–365, **379**
Scotia Ridge, 361
Scott Glacier, 19, 136, 138
Scott Island, 8, 9, 19, 397, 398, 400, 401, **452**
Seabee Hook, *36*, 39
Seal Nunataks, 5, *304*, 306, 307, 309, 312, **349**, 352
Seven Buttresses, *339*–341
Seward Mountains, 257
Seymour Island, *345*, 348
Shamrock Hill, *371*, 372
Sharp Peak, 308, *331*, 332
Shell Glacier, *97*
Shepard Island, 4, 9, *148*, 152, 155, *162*, 218, 234, 245, *248*–250
Shepherd Dome, 289–*291*
Sheridan Bluff, 4, 19, 20, 24, **136**, 139
Shetland Plate, *2*
Shibuya Peak, 152, 155, *244*–247, 252
Shield Nunatak, 4, 49, *72*, 73, *76*–78
Ship's Cove, *413*, 414, 417
Shoal Point, *474*, 475
Sims Island, *281, 283*
Siple Island, *12, 162, 186*
Siren Rock, *290*, 292
Snow Nunataks, 259, 261, 262, *280*, 281, **283**
Sollas Glacier, *134,* 135
South Bay, *468*, 469
South Sandwich Islands, 1, 3, 4, 6–8, 11, 14, 15, **360**
South Shetland Islands, 1, 2, 7, 8, 10, 14, 15, **302**
Southeast Cape, *117*
Southeast Indian Rise, *12*
Southern Thule, 362, 387, 390, 393
Southwest Indian Ridge, 405
Spitz Ridge, *175, 177*
Starbuck Crater, *221*–224
Stauffer Bluff, 169, 170, 172, 173
Stench Point, *368*, 369
Sturge Island, 449, 450
St. Paul Island, see Saint Paul Island
Sulphur Point, 365, *371*, 372
Surprise Cone, 129
Surprise Hills, 70
Syrstad Rock, *221*, 222

Tabarin Peninsula, 308, **339**, 342
Table Nunatak, 265
Tagua Bay, 473
Tail Island, *342*, 343
Taygete Cone, *60*–63
Taylor Glacier, *134,* 135
Taylor Valley, 23, *81*, 84, 85, **134**
Teeters Nunatak, 261, 289, *290*
Telefon Bay, *316,* 319, 321
Telefon Ridge, *316*–318
Ternyck Needle, *327*–329
Terra Nova Bay, *48*, 72, *79*
Terrapin Hill, 308
Terror rift, *2, 20*, 24, *83,* 84
The Knoll, see Knoll, The
The Pleiades, see Pleiades, The
Three Sisters Cones, 103, *104*
Thule Island, 5, *362*–364, 387, 390, **393**
Thurston Island, *13, 258*–260
Toney Mountain, 2, 3, 5, 9, *148*, 150, 151, 160–162, 165, 168, **175**, 208, 237
Topping Cone, *99*, 101
Tower Island, *334*
Trachyte Hill Formation, *97*, 114
Trafalgar Glacier, 53, *79*
Transantarctic Mountains, *2*, 11, 12, 14, 19, 24, 25, 28, 49, 52, 62, 72, *73*, 77, *85*, 88, 132, 134, 135
Traversay Islands, 366
TriCones, 129
Triegaardt Bay, *413*, 414, 417
Trinity Peninsula, **344**
Trousers Rock, *377*
Tryggve Point, *104*–106
Tucker Glacier, *26, 36*–38, *40*, 41
Tuff Bluff, *113,* 114
Turks Head, *104*, 105
Turmoil Point, *384*, 385
Tur Peak, *53*, 54, 56, 57
Turret Point, 322
Turtle Peak, *164, 165,* 168, 235–238
Twitcher Rock, *393, 394*

Usas Escarpment, *148, 149,* 161, *162*, **239**

Vauréal Peak, *327*, 328, 330
Vega Island, 342, *345, 346*
Velie Nunatak, *290*, 293
Victoria Land, 19, *20*, 24, 26, 28, *79*, *90*
Victoria Passage, 470, *471*
Victory Mountains, *26*, 53
Vindication Island, *362*–365, **373**
Visokoi Island, 5, 362–365, **371**
Vortex Island, *342*
Vulcan Hills, 9, 22, *48*, 49, 51, 52, **69**, *79*
Vulcan Nunatak, *251*

Waitabit Cliffs, *277*–279
Walcott Glacier, *131,* 132
Walgreen Coast, *149*, 234, **235**, *258*
Webber Nunatak, 5, 289–*291*
Webb Névé, 80
Weddell Sea, 2, 11, 14, *258, 304, 350*
Wedemeyer Rocks, *226*, 230, 231
West Antarctic rift system, 2, 3, 11, 14, 15, 160
West Cliff, *420*, 422
West Ice Shelf, 447
Westwindstranda, 405, *406*
Whalers Bay, *316*, 321
White Island, 9, 23, 81, *83*–*85*, *103*, **113**, 114, *121*
Whitmore Mountains, *13*, 259
Whitney Peak, *189*–*194*, 212, 213
Wilhelm II Coast, 446
Wilhelmplatået, 405–*407*
Willows Nunatak, 49
Wilson Rock, *384*, 385
Wold Nunatak, 289, 291
Wolkberg, *420,* 422
Wood Bay, *48, 72, 79*
Wordie Point, *371*, 372
Worley Point, *248*–250
Wright Valley, 23, 81, 84, *85*, **134**

Yankee Harbour, 332
Yellowstone Crags, *379*–381
Young Island, *449, 450*

Zavodovski Island, 5, 361, *362*–365, **368**

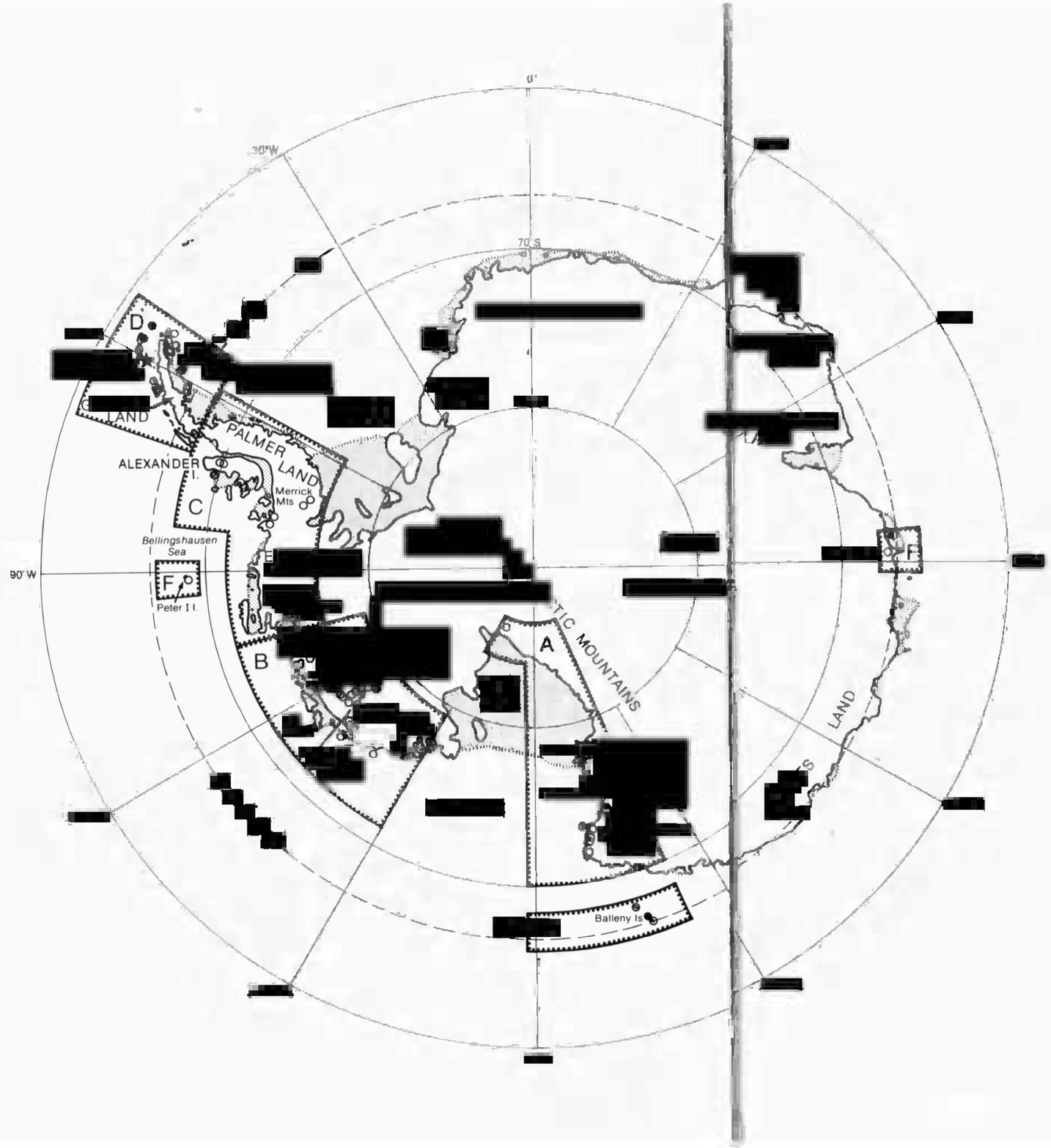
0°
30°W
70°S
90°W
D
C
PALMER LAND
ALEXANDER I.
Merrick Mts
Bellingshausen Sea
F
Peter I I.
B
A
TIC MOUNTAINS
LAND
Balleny Is